

# Journal of Polymer Science

PART A: GENERAL PAPERS

Volume 2, 1964

Editors: H. MARK · C. G. OVERBERGER · R. S. STEIN

Editorial Board: R. M. FUOSS · J. J. HERMANS · H. W. MELVILLE · G. SMETS

N. G. GAYLORD, Book Review Editor

Advisory Board:	T. ALFREY, JR. <i>Midland, Mich.</i>	J. FURUKAWA <i>Kyoto</i>	A. PETERLIN <i>Durham, N. C.</i>
	W. O. BAKER <i>Murray Hill, N. J.</i>	G. GEE <i>Manchester</i>	C. C. PRICE <i>Philadelphia, Pa.</i>
	H. BENOIT <i>Strasbourg</i>	A. KATCHALSKY <i>Rehovoth</i>	CH. SADRON <i>Strasbourg</i>
	C. J. BEVINGTON <i>Birmingham</i>	H. D. KEITH <i>Murray Hill, N. J.</i>	G. V. SCHULZ <i>Mainz</i>
	J. W. BREITENBACH <i>Vienna</i>	A. KELLER <i>Bristol</i>	H. M. SPURLIN <i>Wilmington, Del.</i>
	A. M. BUECHE <i>Schenectady, N. Y.</i>	G. M. KLINE <i>Washington, D. C.</i>	A. J. STAVERMAN <i>Delft</i>
	C. W. BUNN <i>Welwyn Garden City</i>	O. KRATKY <i>Graz</i>	J. K. STILLE <i>Iowa City, Iowa</i>
	G. M. BURNETT <i>Aberdeen</i>	M. MAGAT <i>Paris</i>	W. H. STOCKMAYER <i>Hanover, N. H.</i>
	F. S. DAINTON <i>Leeds</i>	C. S. MARVEL <i>Tucson, Ariz.</i>	M. SZWARC <i>Syracuse, N. Y.</i>
	P. DEBYE <i>Ithaca, N. Y.</i>	G. NATTA <i>Milano</i>	A. V. TOBOLSKY <i>Princeton, N. J.</i>
	F. EIRICH <i>Brooklyn, N. Y.</i>	S. OKAMURA <i>Kyoto</i>	K. UEBERREITER <i>Berlin</i>
	P. J. FLORY <i>Stanford, Calif.</i>		K. WOLF <i>Ludwigshafen</i>

INTERSCIENCE PUBLISHERS

Copyright © 1964, by John Wiley & Sons, Inc.

Statement of ownership, management, and circulation (Act of October 23, 1962: Section 4369, Title 39 United States Code)

1. Date of filing: September 28, 1964
2. Title of Publication: JOURNAL OF POLYMER SCIENCE
3. Frequency of issue: monthly
4. Location of known office of publication: 20th and Northampton Streets, Easton, Pennsylvania 18043
5. Location of headquarters of general business offices of publisher: 605 Third Avenue, New York, New York 10016
6. The names and addresses of publisher, editor, and managing editor:

*Publisher:* Eric S. Proskauer, John Wiley & Sons, Inc., 605 Third Avenue, New York, New York 10016

*Editor:* Herman Mark, Polytechnic Institute of Brooklyn, 333 Jay Street, Brooklyn 1, New York  
*Managing Editor:* None

7. Owner: John Wiley & Sons, Inc., 605 Third Avenue, New York, New York 10016  
Stockholders owning or holding 1 per cent or more of total amount of John Wiley & Sons, Inc., stock as of September 30, 1964:

Cynthia W. Darby, 23 Farrington St., Newburgh, N. Y.; Maurits Dekker, 511 West 232nd St., Bronx, N. Y.; Rozetta S. Dekker, 511 West 232nd St., Bronx, N. Y.; Julia W. Gilbert, Box 1191, Carmel, Calif.; Edward P. Hamilton, c/o John Wiley & Sons, Inc., 605 Third Ave., New York 16, N. Y.; Elizabeth W. Hamilton, c/o John Wiley & Sons, Inc., 605 Third Ave., New York 16, N. Y.; W. Bradford Wiley and Francis Lobdell, Trustees of Elizabeth W. Hamilton Trust, dated 12/23/52, c/o John Wiley & Sons, Inc., 605 Third Ave., New York 16, N. Y.; I. M. Kolthoff, University of Minnesota, School of Chemistry, Minneapolis, Minn.; Willy Levinger, 336 Central Park West, New York, N. Y.; R. R. Pennywitt, Box 211, Mantaloking, N. J.; R. C. Runyon, Jr., 130 East End Ave., New York 28, N. Y.; Francis Lobdell and William J. Seawright, Trustees f/b/o Deborah Elizabeth Wiley, u/a dated 6/2/58, c/o John Wiley & Sons, Inc., 605 Third Ave., New York 16, N. Y.; Kate R. Q. Wiley, 1192 Park Ave., New York 28, N. Y.; Edward P. Hamilton, Trustee f/b/o Kate R. Q. Wiley, u/a dated 6/6/38, c/o John Wiley & Sons, Inc., 605 Third Ave., New York 16, N. Y.; Francis Lobdell and William J. Seawright, Trustees f/b/o Peter Booth Wiley, u/a dated 6/2/58, c/o John Wiley & Sons, Inc., 605 Third Ave., New York 16, N. Y.; K. R. Q. Wiley, E. P. Hamilton and Cynthia W. Darby, Executors of the will of W. O. Wiley, c/o E. P. Hamilton, 605 Third Ave., New York 16, N. Y.; Francis Lobdell and William J. Seawright, Trustees f/b/o William Bradford Wiley, 2nd, u/a dated 6/2/58, c/o John Wiley & Sons, Inc., 605 Third Ave., New York 16, N. Y.; Adele E. Windheim, 8 Dundee Rd., Larchmont, N. Y.; W. Bradford Wiley and E. P. Hamilton, Trustees for Edward P. Hamilton Foundation, u/a dated 12/23/57, c/o John Wiley & Sons, Inc., 605 Third Ave., New York 16, N. Y.; Reing & Co., P. O. Box 491, Church St. Station, New York 8, N. Y.; Eric S. Proskauer and Charles H. Lieb, as Trustees u/a dated 11/27/62, 220 Central Park South, New York 19, N. Y.

8. Known bondholders, mortgagees, and other security holders owning or holding 1 per cent or more of total amount of bonds, mortgages, or other securities: None

9. Paragraphs 7 and 8 include, in cases where the stockholder or security holder appears upon the books of the company as trustee or in any other fiduciary relation, the name of the person or corporation for whom such trustee is acting, also the statements in the two paragraphs show the affiant's full knowledge and belief as to the circumstances and conditions under which stockholders and security holders who do not appear upon the books of the company as trustees, hold stock and securities in a capacity other than that of a bona fide owner. Names and addresses of individuals who are stockholders of a corporation which itself is a stockholder or holder of bonds, mortgages or other securities of the publishing corporation have been included in paragraphs 7 and 8 when the interests of such individuals are equivalent to 1 per cent or more of the total amount of the stock or securities of the publishing corporation.

10. This item must be complete for all publications except those which do not carry advertising other than the publishers own and which are named in Sections 132.231, 132.232, and 132.233, Postal Manual (Sections 4355a, 4355b, and 4356 of Title 39, United States Code)

I certify that the statements made by me above are correct and complete:

Eric S. Proskauer  
Publisher

# CONTENTS

Vol. 2, Issue Nos. 1-12

## *Journal of Polymer Science*

### *Part A: General Papers*

ISSUE No. 1, JANUARY

ELIZABETH DYER and RICHARD J. HAMMOND: Thermal Degradation of <i>N</i> -Substituted Polycarbamates. . . . .	1
ROBERT L. MERKER and MARY JANE SCOTT: Preparation and Properties of Poly(tetramethyl- <i>p</i> -Silphenylene-Siloxane). . . . .	15
ROBERT L. MERKER, MARY JANE SCOTT, and G. G. HABERLAND: Random and Block Copolymers of Poly(tetramethyl- <i>p</i> -Silphenylene-Siloxane) and Polydimethylsiloxane. . . . .	31
L. W. BREED, R. L. ELLIOTT, and A. F. FERRIS: Preparation and Polymerization of 1,5-Diamino-2,4-alkylenetrissilazanes. . . . .	45
W. BURLANT, J. HINSCH, and C. TAYLOR: Crosslinking and Degradation in $\gamma$ -Irradiated Poly- <i>n</i> -alkyl Acrylates. . . . .	57
CONSTANTINE C. PETROPOULOS: Kinetics of the Photopolymerization of Tetraethylene Glycol Dimethacrylate in the Bulk with the Use of Desyl Aryl Sulfides as Photoinitiators. . . . .	69
JOSEPH H. FLYNN and WILLIAM L. MORROW: Photolysis of Cellulose in a Vacuum with 2537 A. Light. . . . .	81
JOSEPH H. FLYNN and WILLIAM L. MORROW: Effects of Deuteration and Temperature upon the Photolysis of Cellulose in a Vacuum with 2537 A. Light. . . . .	91
MOSHE KREISEL, URI GARBATSKI, and DAVID H. KOHN: Copolymerization of Styrene. I. Copolymerization with Styrene Derivatives Containing Nitrile Groups in the Side-Chain. . . . .	105
W. G. CREWETHER: Mean Square Length of Random Polypeptide Chains and the Length of Protein Fibers. . . . .	123
W. G. CREWETHER: Crosslinkages in Wool Fibers and Their Relationship to the Two-Stage Supercontraction of Wool Fibers in Solutions of LiBr. . . . .	131
W. G. CREWETHER: Covalent Acid-Labile Crosslinkages in Wool. . . . .	149
CARL J. STACY and RAYMOND L. ARNETT: A Scattered-Light Study of Linear Polyethylenes. . . . .	167
PAUL W. MORGAN and STEPHANIE L. KWOLEK: Low Temperature Solution Polycondensation of Piperazine Polyamides. . . . .	181

PAUL W. MORGAN and STEPHANIE L. KWOLEK: Amine Acid-Acceptors for the Preparation of Piperazine Polyamides by Low-Temperature Solution Polycondensation.....	209
R. SALOVEY and W. A. YAGER: Electron Spin Resonance of Irradiated Solution-Crystallized Polyethylene.....	219
R. I. C. MICHIE and S. M. NEALE: Effect of Copper on the Autoxidation of Cellulose Suspended in Sodium Hydroxide Solution.....	225
SADAO TORIKAI: Main-Chain Degradation and Thermal Stabilization of Polyoxymethylene by Ionizing Radiation.....	239
NAOYA YODA and IKUO MATSUBARA: Studies on Structure and Properties of Aromatic Polyamides. I. Structural Elucidation of Poly( <i>m</i> -xylylene Adipamide).....	253
CHARLES J. FOX: Polymers Containing the 2,5-Diphenylthiazolo-[5,4-d]thiazole Moiety.....	267
GERARD KRAUS and G. A. MOCZVIGEMBA: Chain Entanglements and Elastic Behavior of Polybutadiene Networks.....	277
SYDNEY BLUESTONE and MARJORIE J. VOLD: Monte-Carlo Calculations of the Dimensions of Coiling Type Polymers in Solutions of Finite Concentration.....	289
MILTON KERKER, JOSIP P. KRATOHVIL, and EGON MATIJEVIĆ: Calibration of Light-Scattering Instruments. II. The Volume Content.....	303
HIDEHIKO KOBAYASHI, KIICHIRO SASAGURI, YOSHISATO FUJISAKI, and TOSHIHIKO AMANO: Effect of Molecular Weight and Its Distribution on Stretching of Polyacrylonitrile Gel.....	313
H. K. FRENSDORFF: Diffusion and Sorption of Vapors in Ethylene-Propylene Copolymers. I. Equilibrium Sorption.....	333
H. K. FRENSDORFF: Diffusion and Sorption of Vapors in Ethylene-Propylene Copolymers. II. Diffusion.....	341
RICHARD S. BERGER and E. A. YOUNGMAN: Emulsion Polymerization of Vinyl Monomers by Transition Metal Compounds.....	357
J. P. KENNEDY, L. S. MINCKLER, JR., and R. M. THOMAS: Cationic Polymerization of 3-Methylbutene-1. I. Polymerizations at Moderately Low Temperatures.....	367
J. P. KENNEDY: Cationic Polymerizations of 3-Methylbutene-1. II. Polymerizations at Extremely Low Temperatures.....	381
J. C. SIEGLE, L. T. MUUS, TUNG-PO LIN, and H. A. LARSEN: The Molecular Structure of Perfluorocarbon Polymers. II. Pyrolysis of Polytetrafluoroethylene.....	391
J. K. STILLE and B. M. CULBERTSON: Cyclopolymerization of Diepoxides.....	405
M. BAER: Anionic Block Polymerization. II. Preparation and Properties of Block Copolymers.....	417
P. W. MORGAN: Linear Condensation Polymers from Phenolphthalein and Related Compounds.....	437
SABURO OKAJIMA and KIMIO INOUE: X-Ray Diffraction and Infrared	

Spectra Studies on the Fine Structure of Rayon Improved by High Temperature Steaming . . . . .	461
H. Q. SMITH and F. L. SCOTT: Polymers from Sulfamide. I. Preparation . . . . .	481
R. A. FLORENTINE, G. BARTH-WEHRENALP, I. MOCKRIN, I. POPOFF, and R. RIORDAN: Polymers from Sulfamide. II. Evaluation and Structure . . . . .	489
RICHARD BECKERBAUER AND HENRY E. BAUMGARTEN: Preparations and Reactions of <i>p</i> -Cyanostyrene-Styrene Copolymers . . . . .	503

## ISSUE NO. 2, FEBRUARY

MAURICE MORTON, M. A. DEISZ, and E. E. BOSTICK: Base-Catalyzed Solution Polymerization of Octamethylcyclotetrasiloxane . . . . .	513
MAURICE MORTON and E. E. BOSTICK: Anionic Polymerization of Octamethylcyclotetrasiloxane in Tetrahydrofuran Solution . . . . .	523
A. J. HAVLIK and THOR L. SMITH: Crosslinked and Noncrosslinked Diisocyanate-Linked Elastomers Containing Substituted Urea Groups . . . . .	539
R. H. HANSEN, C. A. RUSSELL, T. DE BENEDICTIS, W. M. MARTIN, and J. V. PASCALE: Inhibition of the Copper-Catalyzed Oxidation of Polypropylene . . . . .	587
DAVID L. TAYLOR: An Evaluation of Column Thermal Diffusion As a Means of Polymer Characterization . . . . .	611
MASAO HORIO and RIKIZO IMAMURA: Crystallographic Study of Xylan from Wood . . . . .	627
D. W. BEHNKEN: Estimation of Copolymer Reactivity Ratios: An Example of Nonlinear Estimation . . . . .	645
S. KRIMM and S. ENOMOTO: Infrared Studies of Conformational Changes in Polyvinyl Chloride . . . . .	669
A. KISHIMOTO and K. MATSUMOTO: Effect of Film Thickness upon the Sorption of Organic Vapors in Polymers Slightly above their Glass Transition Temperatures . . . . .	679
NEVILLE SUE RAPP and JOHN D. INGHAM: Polymer Degradation. I. Column Elution Fractionation and Thermal Degradation of Polyoxypropylene Glycol-Toluene Diisocyanate (PPG-TDI) Polymers . . . . .	689
JOHN N. LOMONTE and GEORGE A. TIRPAK: Detection of Ethylene Homopolymer in Ethylene-Propylene Copolymers . . . . .	705
J. L. MATEO and IRVING COHEN: Emulsion Polymerization of Styrene in Coacervating and Noncoacervating Soap-Electrolyte Systems . . . . .	711
A. CIFERRI and K. J. SMITH, JR.: Phase Changes in Fibrous Macromolecular Systems and Associated Elasticity. Model Phase Diagrams . . . . .	731
C. G. OVERBERGER, H. KAYE, and G. WALSH: Synthesis of Crystalline Polyvinylcyclobutane and Polyvinylcycloheptane . . . . .	755

ALEXANDRE BLUMSTEIN: Photoelastic Properties of Tightly Cross-linked Networks.....	769
JESSE C. H. HWA: Mechanism of Film Formation from Latices. Phenomenon of Flocculation.....	785
J. T. GRUVER and GERARD KRAUS: Rheological Properties of Polybutadienes Prepared by <i>n</i> -Butyllithium Initiation.....	797
J. T. DUDEK and F. BUCHE: Polymer-Solvent Interaction Parameters and Creep Behavior of Ethylene-Propylene Rubbers....	811
RICHARD BECKERBAUER and HENRY E. BAUMGARTEN: Some Reactions of <i>p</i> -Vinylacetophenone-Styrene Copolymers.....	823
J. C. MOORE: Gel Permeation Chromatography. I. A New Method for Molecular Weight Distribution of High Polymers..	835
F. E. BAILEY, JR., R. D. LUNDBERG, and R. W. CALLARD: Some Factors Affecting the Molecular Association of Poly(ethylene Oxide) and Poly(acrylic Acid) in Aqueous Solution.....	845
AKIYOSHI WADA and SHICHIBEI KOZAWA: Instrument for the Studies of Differential Flow Dichroism of Polymer Solutions....	853
B. LIONEL FUNT and FREDERICK D. WILLIAMS: Electroinitiated Anionic Polymerization of Acrylonitrile.....	865
YOSHIO IWAKURA, MUNENORI SAKAMOTO, and YASUHIRA AWATA: Polyurethane Sulfides Containing a Cyclohexane Ring in the Polymer Chain.....	881
RIICHIRO CHUJO, SHIROH SATOH, and EIICHI NAGAI: High Resolution NMR Study of Vinylidene Chloride-Vinyl Chloride Copolymer.	895
A. IKEGAMI: Hydration and Ion Binding of Polyelectrolytes.....	907
D. G. LEGRAND: Rheo-Optical Properties of Polymers. V.....	923
D. G. LEGRAND: Rheo-Optical Properties of Polymers. VI. Dynamic Birefringence.....	931
E. H. DARUWALLA and R. T. SHET: Studies in the Kinetics of Removal of Water from Cellulosic Fibers.....	943
T. K. KWEI and W. M. ARNHEIM: Linear Free Energy Relationship in the Diffusion of Gases Through Polymer Films.....	957
TSUNEO YOSHINO and KENJI FUJISAWA: Compositions in Equilibrium Two Phases of Polymer-Solvent Mixture Systems.....	965
RONALD L. OTT: Mechanism of the Mechanical Degradation of Cellulose.....	973
N. GRASSIE and J. R. MACCALLUM: Thermal and Photochemical Degradation of Poly ( <i>n</i> -butyl Methacrylate).....	983
A. T. DiBENEDETTO and D. R. PAUL: An Interpretation of Gaseous Diffusion Through Polymers Using Fluctuation Theory.....	1001
C. G. OVERBERGER and E. SARLO: Copolymerization of Diethyl Phosphonoalkyl Acrylates.....	1017
Book Review	
The Effect of Ionizing Radiation on High Polymers, T. S. NIKITINA, E. V. ZHURAVSKAYA, and A. S. KUZMINSKY. Reviewed by D. S. BALLANTINE.....	1023

## Erratum

- ALEXANDER MELLER: Some Considerations on the Kinetics of the Acid Hydrolysis of Poly- and Olig-saccharides (article in *J. Polymer Sci.*, **C2**, 97-107, 1963) . . . . . 1024

## ISSUE No. 3, MARCH

- K. J. SMITH, JR., A. CIFERRI, and J. J. HERMANS: Anisotropic Elasticity of Composite Molecular Networks Formed from Non-Gaussian Chains . . . . . 1025
- P. R. BLAKEY and R. P. SHELDON: Cold-Drawing of Acetone-Crystallized Polyethylene Terephthalate . . . . . 1043
- DAVID W. THOMSON and GERHARD F. L. EHLERS: Aromatic Polysulfonates: Preparation and Properties . . . . . 1051
- A. M. KOTLIAR: Evaluation of Molecular Weight Averages Resulting from Random Chain Scission Process for Wide Distribution as in Polyolefins . . . . . 1057
- G. DELZENNE, W. DEWINTER, S. TOPPET, and G. SMETS: Photosensitized Polymerization of Acrylic Monomers. II. Kinetics of Polymerization in the Presence of Oxygen . . . . . 1069
- ROBERT M. VALLETTA, FELIX J. GERMINO, ROBERT E. LANG, and RAYMOND J. MOSHY: Amylose V Complexes: Low Molecular Weight Primary Alcohols . . . . . 1085
- A. A. MILLER: Free Volumes in Polystyrene and Polyisobutylene . . . . . 1095
- KEI MATSUZAKI, TAKEHIKO OKAMOTO, AKIRA ISHIDA, and HIROSHI SOBUE: Polymerization of Butyl Esters of Methacrylic Acid and Hydrolysis of the Polymers . . . . . 1105
- H. L. FRISCH: Multicomponent Non-Fickian Diffusion through Inhomogeneous Polymer Membranes . . . . . 1115
- J. L. LUNDBERG: Molecular Weight Distributions in Equilibrium Polymerizations . . . . . 1121
- A. H. FRAZER and F. T. WALLENBERGER: Aliphatic Polyhydrazides: A New Low Temperature Solution Polymerization . . . . . 1137
- A. H. FRAZER and F. T. WALLENBERGER: Aromatic Polyhydrazides: A New Class of Highly Bonded, Stiff Polymers . . . . . 1147
- A. H. FRAZER, W. SWEENEY, and F. T. WALLENBERGER: Poly(1,3,4-Oxadiazoles): A New Class of Polymers by Cyclodehydration of Polyhydrazides . . . . . 1157
- A. H. FRAZER and F. T. WALLENBERGER: Poly(1,3,4-Oxadiazole)-Fibers: New Fibers with Superior High Temperature Resistance 1171
- A. H. FRAZER and F. T. WALLENBERGER: Poly(1,3,4-Oxadiazolidine) 1181
- RICHARD M. McCURDY and JULIANNE H. PRAGER: Thiaalkyl Polyacrylates: The Influence of Sulfur in the Side Chain . . . . . 1185
- PETER KOVACIC, FRED W. KOCH, and CHARLES E. STEPHAN: Water Cocatalysts in the Polymerization of Benzene by Ferric Chloride 1193

JAMES C. SPITSBERGEN and HAROLD C. BEACHELL: Light-Scattering Study of the Oxidative Degradation of Polystyrene . . . . .	1205
JAMES A. BITTLES, A. K. CHAUDHURI, and SIDNEY W. BENSON: Clay-Catalyzed Reactions of Olefins. I. Polymerization of Styrene . . . . .	1221
ROBERT RABINOWITZ, RUTH MARCUS, and JOSEPH PELLON: Free Radical Homopolymerization and Copolymerization of Vinyl Phosphines, Oxides, and Sulfides . . . . .	1233
ROBERT RABINOWITZ, RUTH MARCUS, and JOSEPH PELLON: Synthesis, Polymerization, and Copolymerization of Diphenyl- <i>p</i> -Styrylphosphine, Phosphine Oxide, and Phosphine Sulfide . . . . .	1241
EDWARD H. HILL and JOHN R. CALDWELL: Polysulfones of Norbornene and Derivatives . . . . .	1251
H. SOTOBAYASHI and K. UEBERREITER: Molecular Weight Dependence of the Second Virial Coefficient. Solutions of Styrene Dimers up to High Polymers and Other Systems . . . . .	1257
LLOYD J. FORRESTAL and WILLIAM G. HODGSON: Electron Spin Resonance Studies of Irradiated Polypropylene . . . . .	1275
HENRI J. R. MAGET: Product Distribution of Consecutive Competitive Second-Order Reactions . . . . .	1281
I. HEBER: Die sekundäre Keimbildung bei Polyäthylen-Sphärolithen . . . . .	1291
GEORGE A. MORTIMER and WILLIAM F. HAMNER: Density of Polyethylene . . . . .	1301
JULIAN L. DAVIS: An Elementary Theory of Nonlinear Viscoelasticity . . . . .	1311
MARVIN CHARTON and ANTHONY J. CAPATO: Nature of the Price-Alfrey $q$ and $\epsilon$ Parameters . . . . .	1321
J. P. DE VILLIERS and J. R. PARRISH: Rapid Characterization of Ion-Exchange Resins by NMR . . . . .	1331
D. MEJZLER: Random Degradation of Chain Polymers Accompanied by Partial Dissolution of the Degraded Material . . . . .	1341
SAMUEL F. REED and M. G. BALDWIN: Polymerization Studies on Allylic Compounds. Part II . . . . .	1355
MIHIR KUMAR SAHA, PREMAMOY GHOSH, and SANTI R. PALIT: Determination of Halogen in Copolymers by Dye-Partition Technique and Calculation of $r$ , Therefrom . . . . .	1365
A. M. KOTLIAR: Critical Analysis of Molecular Weight Distributions Derived from Fractionation Data. I. Column Elution . . . . .	1373
SONJA KRAUSE and ELIZABETH COHN-GINSBERG: Branching in High Conversion Poly(methyl Methacrylate) . . . . .	1393
MINORU IMOTO, TAKAYUKI OTSU, KAZUICHI TSUDA, and TOSHIO ITO: Vinyl Polymerization. LXXIII. Polymerization and Copolymerization of Bornyl or Isobornyl Methacrylate . . . . .	1407
AKIRA KISHIMOTO: Diffusion and Viscosity of Polyvinyl Acetate-Diluent Systems . . . . .	1421
J. P. KENNEDY, L. S. MINCKLER, JR., G. G. WANLESS, and R. M.	



THOMAS: Intramolecular Hydride Shift Polymerization by Cationic Mechanism. I. Introduction and Structure Analysis of Poly-3-methylbutene-1 . . . . .	1441
E. KENEALLY, J. GARD, and G. ADLER: Temperature Dependence of Birefringence in Irradiated Polyethylene . . . . .	1463
T. GUHA, M. BISWAS, R. S. KONAR, and S. R. PALIT: Role of Organic Diluents in Sol-Phase Polymerization . . . . .	1471
R. S. KONAR, T. GUHA, and S. R. PALIT: Role of Organic Diluents in a Precipitative Aqueous Polymerization . . . . .	1481
J. K. STILLE and T. ANYOS: A Novel Diels-Alder Polymerization . . . . .	1487
MARY E. CARTER and O. K. CARLSON: Catalytic Polymerization of Glycine Ethyl Ester . . . . .	1493
TOMONOBU MANABE: Molecular Weight Distribution and Viscosity of Multichain Polymers in $\epsilon$ -Caprolactam Polymerization . . . . .	1501
SHIGEMITSU TSUNAWAKI and CHARLES C. PRICE: Preparation of Poly(arylene Sulfides) . . . . .	1511
HIROSHI SOBUE, KENKICHI MURAKAMI, and HIROYUKI HOSHINO: Determination of Molecular Weights of Polymers by Procedure X in Stress Relaxation . . . . .	1523

## Book Review

An Introduction to Polymer Chemistry, W. R. MOORE. Reviewed by ROBERT W. LENZ . . . . .	1535
---	------

## ISSUE No. 4, APRIL

Editorial . . . . .	1537
S. TOPPET, G. DELZENNE, and G. SMETS: Photosensitized Polymerization of Acrylic Monomers. III. Kinetics of Polymerization of Acrylamide in the Absence of Oxygen . . . . .	1539
HENRY S. MAKOWSKI, BENJAMIN K. C. SHIM, and ZIGMOND W. WILCHINSKY: 1,5-Hexadiene Polymers. I. Structure and Properties of Poly-1,5-Hexadiene . . . . .	1549
TOSHIHIRO TAKATA, IWAO HIROI, and MASAKAZU TANIYAMA: Coloration in Acrylonitrile Polymers . . . . .	1567
DOV KATZ and ARTHUR V. TOBOLSKY: Rubber Elasticity in Highly Crosslinked Polyesters . . . . .	1587
DOV KATZ and ARTHUR V. TOBOLSKY: Rubber Elasticity in Highly Crosslinked Polyethyl Acrylate . . . . .	1595
MITSUO TASUMI, TAKEHIKO SHIMANOUCI, HIROSHI TANAKA, and SAKUJI IKEDA: Stereoregulated Polydeuteroethylene. II. Infrared Spectra and Normal Vibration Analysis . . . . .	1607
J. B. YANNAS: Fractionation of Chemically Heterogeneous Latex Particles by Centrifugation . . . . .	1633
HOWARD C. HAAS and NORMAN W. SCHULER: $\alpha$ -Trifluoromethyl Vinyl Acetate . . . . .	1641

JOE W. HIGHTOWER and P. H. EMMETT: Nitrogen Adsorption Isotherms on Polyolefins.....	1647
H. P. SCHREIBER and M. H. WALDMAN: Effect of Temperature on Molecular Weight Measurements in Polyethylene.....	1655
J. JAFFEE et J.-M. LOUZE: Les Polymeres à l'Interface Eau-Air.....	1669
M. BERGER and IRVING KUNTZ: The Distinction between Terminal and Penultimate Copolymerization Models.....	1687
D. T. TURNER: Radiolysis of Polyisobutene. Part I. Yields of Fractures, Double Bonds, and Gas.....	1699
G. M. C. HIGGINS and D. T. TURNER: Radiolysis of Polyisobutene. Part II. Infrared and Ultraviolet Absorption Spectra.....	1713
D. T. TURNER: Radiolysis of Polyisobutene. Part III. Effect of Additives.....	1721
RANJIT S. KONAR and SANTI R. PALIT: Permanganate-Oxalic Acid as a Redox Initiator of Acrylonitrile Polymerization in Aqueous Media. Part III. Kinetics and DP.....	1731
KENSUKE OKUDA: Structures of Vinylidene Chloride-Vinyl Chloride Copolymers.....	1749
ALFRED H. FRYE, RAYMOND W. HORST, and MARKO A. PALIOBAGIS: The Chemistry of Poly(vinyl Chloride) Stabilization. III. Organotin Stabilizers Having Radioactively Tagged Alkyl Groups..	1765
ALFRED H. FRYE, RAYMOND W. HORST, and MARKO A. PALIOBAGIS: The Chemistry of Poly(vinyl Chloride) Stabilization. IV. Organotin Stabilizers Having Radioactively Tagged Tin Atoms..	1785
ALFRED H. FRYE, RAYMOND W. HORST, and MARKO A. PALIOBAGIS: The Chemistry of Poly(vinyl Chloride) Stabilization. V. Organotin Stabilizers Having Radioactively Tagged Y Groups.....	1801
FERDINAND C. STEHLING: Stereochemical Configurations of Polypropenes by High Resolution Nuclear Magnetic Resonance.....	1815
A. H. FRAZER and F. T. WALLEMBERGER: Metal Chelates of Polyhydrazides.....	1825
WILLIAM E. DICK, JR., and ROY L. WHISTLER: Polyesters and Polyurethanes of Dihydroxymethylxylitol and Glucitol.....	1833
G. P. BROWN and S. AFTERGUT: Bis(imidazolato)-Metal Polymers...	1839
JAMES A. BITTLES, A. K. CHAUDHURI, and SIDNEY W. BENSON: Clay-Catalyzed Reactions of Olefins. II. Catalyst Acidity and Mechanism.....	1847
DEAN E. LEY and W. FRANK FOWLER, JR.: Emulsion Copolymerization of Some Halogenated Olefins. I. Vinyl Chloride in Ternary Copolymerizations.....	1863
T. K. KWEI and W. N. ARNHEIM: Solubility of Nonpolar Gases in Polymers: Some New Considerations.....	1873
J. C. LEYTE and M. MANDEL: Potentiometric Behavior of Poly-methacrylic Acid.....	1879
J. C. BEVINGTON and B. W. MALPASS: Reactivities of Esters of Methacrylic Acid. Part I. Relative Reactivities of Esters toward the Benzoyloxy Radical.....	1893

S. BROWNSTEIN and D. M. WILES: Proton Resonance Spectra and Tacticities of Some Poly(methyl Vinyl Ethers) . . . . .	1901
RAFFAELE SABIA and F. R. EIRICH: Viscoelastic Behavior of Plasticized Polyvinyl Chloride at Large Deformations. III. The Effect of Filler . . . . .	1909
A. RAVVE and C. FITKO: Polymer Formation through Diazonium Coupling . . . . .	1925
JULIANNE H. PRAGER, RICHARD M. MCCURDY, and GEORGE B. RATHMANN: $\omega$ -Cyanothiaalkyl Polyacrylates: A New Class of Synthetic Rubbers . . . . .	1941
NOBUTAMI KASAI and MASAO KAKUDO: Fine Texture in Necking Portions of Cold-Drawn Polyethylene . . . . .	1955
YONEHO TABATA, HIROSHI SHIBANO, and HIROSHI SOBUE: Copolymerization of Tetrafluoroethylene with Ethylene Induced by Ionizing Radiation . . . . .	1977
A. V. TOBOLSKY and N. TAKAHASHI: Elemental Sulfur as a Plasticizer for Polysulfide Polymers and Other Polymers . . . . .	1987
R. A. WESSLING: Transformation of Mechanical Model Representations of Viscoelasticity to Operator Equations . . . . .	2001

## Book Reviews

Orbitals in Atoms and Molecules. CHR. K. JØRGENSEN. Reviewed by H. L. FRISCH . . . . .	2011
Crystallography and Crystal Perfection. G. N. RAMACHANDRAN. Reviewed by L. G. ROLDAN . . . . .	2012
Organic Reactions, Vol. XIII. A. C. COPE. Reviewed by JAY K. KOCHI . . . . .	2012
The Chemistry of Wood. B. L. BROWNING. Reviewed by R. H. MARCHESSAULT . . . . .	2013
Progress in Physical Organic Chemistry. S. G. COHEN, A. STREITWIESER, JR., and R. W. TAFT. Reviewed by HERBERT MORAWETZ . . . . .	2014
Polymer Single Crystals (Polymer Reviews, Vol. 5), P. H. Geil. Reviewed by ROBERT L. MILLER . . . . .	2015

## ISSUE No. 5, MAY

M. FREEMAN and P. P. MANNING: Molecular Weight of Poly(vinyl Chloride) . . . . .	2017
B. R. JENNINGS and H. G. JERRARD: The Use of Syton 2X Colloidal Silica as a Calibration Medium for Light-Scattering Photometers . . . . .	2025
R. SALOVEY and J. V. PASCALE: Analysis of the Gases Evolved from Irradiated Polyethylene . . . . .	2041
K. P. PAOLETTI and F. W. BILLMEYER, JR.: Absolute Propagation Rate Constants for the Radical Polymerization of Substituted Styrenes . . . . .	2049

R. I. C. MICHIE and S. M. NEALE: Kinetic Study of the Autoxidation of Cellulose Suspended in Sodium Hydroxide Solution . . . . .	2063
R. B. FOX, L. G. ISAACS, S. STOKES, and R. E. KAGARISE: Photo-degradation of Poly(methyl Acrylate) . . . . .	2085
J. P. KENNEDY, L. S. MINCKLER, JR., G. WANLESS, and R. M. THOMAS: Intramolecular Hydride Shift Polymerization by Cationic Mechanism. II. Spectroscopic Analysis of Poly-3-methylbutene-1 . . . . .	2093
CHARLES J. KIBLER, ALAN BELL, and JAMES G. SMITH: Polyesters of 1,4-Cyclohexanedimethanol . . . . .	2115
L. D. LOAN: The Reaction between Dicumyl Peroxide and Butyl Rubbers . . . . .	2127
W. BURLANT and J. HINSCH: Radiation-Initiated Copolymerization of Styrene with Unsaturated Esters . . . . .	2135
F. J. BALTA CALLEJA and A. KELLER: On the Relation between Long Spacings, Molecular Length, and Orientation in Long Chain Compounds with Reference to the Possibility of Chain Folding. Part I. Oligomeric Amides . . . . .	2151
F. J. BALTA CALLEJA and A. KELLER: On the Relation between Long Spacings, Molecular Length, and Orientation in Long Chain Compounds with Reference to the Possibility of Chain Folding. Part II. Poly(ethylene Oxide)s . . . . .	2171
F. L. HIRSCHFELD and G. M. J. SCHMIDT: Topochemical Control of Solid-State Polymerization . . . . .	2181
W. P. SHYLUK: Poly(1,2-dimethyl-5-vinylpyridinium Methyl Sulfate). Part I. Polymerization Studies . . . . .	2191
HISASHI UEDA: Electron Spin Resonance Studies of Irradiated Single Crystals of Methacrylamide . . . . .	2207
A. E. NEWKIRK, A. S. HAY, and R. S. McDONALD: Thermal Degradation of Poly( <i>m</i> -diethynylene Benzene) . . . . .	2217
YONEHO TAEATA, KENKICHI ISHIGURE, and HIROSHI SOBUE: Radiation-Induced Copolymerization of Tetrafluoroethylene with Propylene at Low Temperature . . . . .	2235
P. P. SPIEGELMAN and G. PARRAVANO: Heterophase Polymerization of 4-Vinylpyridine and Butyllithium . . . . .	2245
V. S. NANDA: Theoretical Consideration of Linear Condensation Polymerization in a Dispersed Medium . . . . .	2275
H. ARIMOTO: $\alpha$ - $\gamma$ Transition of Nylon 6 . . . . .	2283
HOWARD C. HAAS and HELEN HUSEK: The Polymerizing System: Vinyl Acetate-Diphenyl . . . . .	2297
D. L. FLOWERS, W. A. HEWETT, and R. D. MULLINEAUX: Fractionation of Polymers of Higher $\alpha$ -Olefins . . . . .	2305
K. FUJII, T. MOCHIZUKI, S. IMOTO, J. UKIDA, and M. MATSUMOTO: Investigation of the Stereoregularity of Poly(vinyl Alcohol) . . . . .	2327
SABURO ISHIKAWA, TOSHIO KURITA, and EIKICHI SUZUKI: Negative Spherulite of Poly- $\gamma$ -Methyl-L-Glutamate and Effect of Aging Polymer Solution on Spherulite Growth . . . . .	2349

G. V. VINOGRADOV and A. YA. MALKIN: Temperature-Independent Viscosity Characteristics of Polymer Systems . . . . .	2357
ALEXANDER MELLER: Some Considerations of the Kinetics of the Acid Hydrolysis of Poly- and Oligosaccharides. II. The Trisaccharides, Isomaltotriitol, Panitol, and Isomaltotriose . . . . .	2373
JESSE, C. H. HWA, WILLIAM A. FLEMING, and LEON MILLER: Acrylic Anhydrides and Polymers Derived Therefrom . . . . .	2385
R. E. MOSER, H. KAMOGAWA, H. HARTMANN, and H. G. CASSIDY: Electron Exchange Polymers. XX. Preparation and Polymerization of Vinylbis (1-ethoxyethyl)hydroquinone . . . . .	2401
H. KAMOGAWA and H. G. CASSIDY: Electron Exchange Polymers. XXI. Polymerization Behavior of 2,5-Dimethoxystyrene . . . . .	2409
G. SMETS and W. VAN RILLAER: Decomposition of Asymmetric Peranhydrides . . . . .	2417
W. VAN RILLAER and G. SMETS: Graft Copolymerization with Peranhydride Side Groups . . . . .	2423
KOJI KAWASAKI and YOSHIYASU SEKITA: Sorption and Diffusion of Water Vapor by Nylon 6 . . . . .	2437
YONEHO TABATA, KENKICHI ISHIGURE, KEICHI OSHIMA, and HIROSHI SOBUE: Copolymerization of Tetrafluoroethylene with Isobutene Induced by Ionizing Radiation . . . . .	2445
W. C. SEARS: $\gamma$ -Radiation-Induced Changes in the Structure of Polyethylenes . . . . .	2455
RICHARD G. SCHWEIGER: Synthetic Polysaccharides. I. Methyl Mono- and Methyl Di- <i>O</i> -allyl- $\alpha$ -D-Glucosides and Their Polymerization . . . . .	2471
C. G. OVERBERGER and MARTIN TOBKES: Polymerization Behavior of Aziridines and 1,2-Epoxides . . . . .	2481
EDWARD SCHONFELD: A Series of Poly(methylene Acetals) Derived from Aliphatic Aldehydes . . . . .	2489

## Book Review

Quantum Mechanics, Vols. I and II. A. MESSIAH. Reviewed by ERNEST M. LOEBEL . . . . .	2495
---	------

## ISSUE NO. 6, JUNE

Editorial . . . . .	2497
AVROM A. BLUMBERG, SIDNEY S. POLLACK, and C. A. J. HOEVE: A Poly(ethylene Oxide)-Mercuric Chloride Complex . . . . .	2499
RICHARD H. WILEY, N. T. LIPSCOMB, C. F. PARRISH, and J. E. GUILLET: Kinetics of the $\gamma$ -Radiation-Induced Polymerization of Ethylene in Alkyl Chlorides . . . . .	2503
M. C. SHEN and A. V. TOBOLSKY: Rubber Elasticity of Preswollen Polymer Networks: Lightly Crosslinked Vinyl-Divinyl Systems . . . . .	2513

C. S. MARVEL, J. C. HILL, J. C. COWAN, J. P. FRIEDRICH, and J. L. O'DONNELL: Preparation and Polymerization of Vinyl Esters of Cyclic and Polychloro Fatty Acids.....	2523
R. H. MICHEL: Cationic Polymerization of 9-Vinylnanthracene.....	2533
MANFRED J. R. CANTOW, ROGER S. PORTER, and JULIAN F. JOHNSON: Thermoelectric Determination of Polymer Molecular Weights...	2547
P. DAS GUPTA and ROY L. WHISTLER: Preparation and Polymerization of 1,2-Epoxypropyl 2,3,4,6-Tetra- <i>O</i> -acetyl- $\beta$ -D-glucopyranoside.....	2555
L. PLUMMER and C. S. MARVEL: Polybenzimidazoles. III.....	2559
KATSUMI HAYASHI and C. S. MARVEL: $\alpha,\omega$ -Glycols and Dicarboxylic Acids from Butadiene, Isoprene, and Styrene and Some Derived Block Polymers, Esters, and Urethans.....	2571
ROY L. WHISTLER and PAUL A. SEIB: Ring-Opening Polymerization of a Sugar Episulfide.....	2595
YOSHIO IWAKURA, KEIKICHI UNO, and YOSHIO IMAI: Polyphenylenebenzimidazoles.....	2605
G. ADLER and W. REAMS: Polymerization in Solid Solutions of Acrylamide in Propionamide.....	2617
F. BORSA and G. LANZI: Nuclear Magnetic Absorption in Polystyrene-Styrene Systems.....	2623
G. E. MYERS, and J. R. DAGON: Distribution of Molecular Weight and of Branching in High Molecular Weight Polymers from Bisphenol A and Epichlorohydrin.....	2631
YONEHO TABATA, YOSHIO HASIZUME, and HIROSHI SOBUE: Radiation-Induced Copolymerization of Acrylonitrile with Methyl Methacrylate.....	2647
J. L. GARDON: Free Radical-Catalyzed Reaction of the Acrylamidomethyl Ether of Cotton.....	2657
J. F. KLEBE: Poly(xylylenylpiperazine), A Novel Polyamine.....	2673
LEO REICH and SALVATORE S. STIVALA: Copolymerizations in Electron-Donor Solvents and Organolithium Catalysts.....	2685
STEPHANIE L. KWOLEK and PAUL W. MORGAN: Preparation of Polyamides, Polyurethanes, Polysulfonamides, and Polyesters by Low Temperature Solution Polycondensation.....	2693
FELIX J. GERMINO, R. J. MOSHY, and ROBERT M. VALLETTA: Amylose V Complexes. II. Lower Molecular Weight Ketones.....	2705
GLENN R. SVOBODA: Redox Polymerization of Unsaturated Polyester Resins. I. Effect of Metal Species on Polymerization Rates in the Presence of a Variety of Peroxides and Hydroperoxides.....	2713
GLENN R. SVOBODA: Redox Polymerization of Unsaturated Polyester Resins. II. Effect of Copromoter Metals on the Redox Polymerization Activity of Vanadium Chelates.....	2721
GLENN R. SVOBODA: Redox Polymerization of Unsaturated Polyester Resins. III. Catalytic Properties of Tertiary Amine <i>N</i> -	

Oxides. Redox Polymerization with the System, Dimethylaniline <i>N</i> -Oxide and Vanadyl Acetyl Acetonate.....	2729
GEORGE E. HAM: General Relationships among Monomers in Copolymerization.....	2735
A. V. TOBOLSKY, D. KATZ, M. TAKAHASHI, and R. SCHAFFHAUSER: Rubber Elasticity in Highly Crosslinked Systems: Crosslinked Styrene, Methyl Methacrylate, Ethyl Acrylate, and Octyl Acrylate.....	2749
BERNHARD WUNDERLICH, EDWARD A. JAMES, and TSAO-WEN SHU: Crystallization of Polyethylene from <i>o</i> -Xylene.....	2759
A. PACKTER: Association of Organic Quaternary Ammonium Cations with Polyacrylates. Conductivity and Viscosity Measurements	2771
I. M. PAUSHKIN and S. A. NIZOVA: Preparation of Polyconjugated Systems by New Reaction of Dihydrohalogen Polymerization	2783
HERBERT A. POHL and RICHARD P. CHARTOFF: Carriers and Unpaired Spins in Some Organic Semiconductors.....	2787
PREMAMOY GHOSH, ASISH RANJAN MUKHERJEE, and SANTI R. PALIT: Incorporation of Hydroxyl Endgroups in Vinyl Polymer. Part I. Initiation of Hydrogen Peroxide Systems.....	2807
PREMAMOY GHOSH, ASISH R. MUKHERJEE, and SANTI R. PALIT: Incorporation of Hydroxyl Endgroups in Vinyl Polymer. Part II. Aqueous Polymerization of Methyl Methacrylate Initiated by Salts or Complexes of Some Metals in Their Higher Oxidation States.....	2817
IRVING KUNTZ: Polymerization of Isoprene with Normal, Iso-, Secondary and Tertiary Butyllithium.....	2827
GEORGE ODIAN and BRUCE S. BERNSTEIN: Radiation Crosslinking of Polyethylene-Polyfunctional Monomer Mixtures.....	2835
PH. TEYSSIÉ and A. C. KORN-GIRARD: Synthesis of New Monomers and Polymers. IV. Synthesis and Properties of Polydiphenyldiacetylenes.....	2849
LIENG-HUANG LEE: Mechanisms of Thermal Degradation of Phenolic Condensation Polymers. I. Studies on the Thermal Stability of Polycarbonate.....	2859
J. A. LAMB and K. E. WEALE: Some Graft Copolymerizations at High Pressure.....	2875
M. MANDEL and J. C. LEYTE: Interaction of Poly(methacrylic Acid) and Bivalent Counterions. I.....	2883
TAKAYUKI OTSU, TOSHIO ITO, and MINORU IMOTO: Vinyl Polymerization. LXXIX. Effect of the Alkyl Group on the Radical Polymerization of Alkyl Methacrylates.....	2901
MINORU TSUDA: Some Aspects of the Photosensitivity of Poly(vinyl Cinnamate).....	2907
R. FERNANDEZ PRINI and A. E. LAGOS: Tracer Diffusion, Electrical Conductivity, and Viscosity of Aqueous Solutions of Polystyrenesulfonates.....	2917

K. HAYASHI, H. OCHI, and S. OKAMURA: Radiation-Induced Post Polymerization of Trioxane in the Solid State . . . . .	2929
H. G. THIELKE and F. W. BILLMEYER, JR.: Origins of X-Ray Line Broadening in Polyethylene Single Crystals . . . . .	2947
LEON SEGAL: Comparison of the Effects of Allylamine and <i>n</i> -Propylamine on Cellulose . . . . .	2951
G. BONERA, A. CHERICO, and A. RIGAMONTI: Effects of Swelling on Proton Relaxation in Vinyl Polymers . . . . .	2963

## Erratum

F. E. BAILEY, JR., R. D. LUNDBERG, and R. W. CALLARD: Some Factors Affecting the Molecular Association of Poly(ethylene Oxide) and Poly(acrylic Acid) in Aqueous Solution (article in <i>J. Polymer Sci.</i> , <b>A2</b> , 845-851, 1964) . . . . .	2975
---	------

## ISSUE NO. 7, JULY

R. N. HAWARD, B. WRIGHT, G. R. WILLIAMSON, and G. THACKRAY: Effect of Blending on the Molecular Weight Distribution of Polymers . . . . .	2977
NOBUYUKI ASHIKARI, TAKAYUKI KANEMITSU, KAZUO YANAGISAWA, KISAKU NAKAGAWA, HIROSHI OKAMOTO, SHŌGO KOBAYASHI, and ATSUO NISHIOKA: Copolymerization of Propylene and Styrene . . . . .	3009
D. H. DAWES and C. A. WINKLER: Polymerization of Butadiene in the Presence of Triethylaluminum and <i>n</i> -Butyl Titanate . . . . .	3029
L. D. LOAN: Peroxide Crosslinking of Ethylene-Propylene Rubber . . . . .	3053
R. SALOVEY, D. L. MALM, A. L. BEACH, and J. P. LUONGO: Irradiation of Polyethylene Crystals: Gas Evolution Studies . . . . .	3067
W. R. KRIGBAUM and J. D. WOODS: Thermodynamic Parameters for Isotactic and Atactic Poly-1-pentene . . . . .	3075
UMBERTO BIANCHI: Temperature Coefficient of Unperturbed Dimensions from Solution Properties . . . . .	3083
A. CIFERRI: Temperature Coefficient of Unperturbed Polymer Dimensions from Thermoelastic Properties . . . . .	3089
HIDEO SAWADA: Thermochemistry of Polymerization. Part I. Thermochemical Aspects of Copolymerization . . . . .	3095
R. D. BURKHART and J. A. FAUCHER: Some Considerations on Non-stationary-State Kinetics of Vinyl Polymerization . . . . .	3103
JOSEPH GREEN, NATHAN MAYES, and MURRAY S. COHEN: Carborane Polymers. I. Polyesters . . . . .	3113
JOSEPH GREEN, NATHAN MAYES, ANATOLE P. KOTLOBY, and MURRAY S. COHEN: Carborane Polymers. II. Cyclic Polymeric Formals . . . . .	3135
RAYMOND M. FUOSS, IVAL O. SALYER, and HARRY S. WILSON: Evaluation of Rate Constants from Thermogravimetric Data . . . . .	3147



RICHARD H. WILEY and ROLLA M. DYER: Analytical and Preparative Vapor-Phase Chromatographic Separation of Divinylbenzene Mixtures. . . . .	3153
A. BONDI: Packing Density of Polymer Melts near the Glass Transition Temperature. . . . .	3159
M. H. GEORGE: Polymerization of Styrene in <i>N,N</i> -Dimethylformamide and <i>N,N</i> -Dimethylacetamide. . . . .	3169
CARL R. KRÜGER and EUGENE G. ROCHOW: Polyorganosilazanes. . . . .	3179
J. H. BRADBURY, W. F. FORBES, J. D. LEEDER, and G. W. WEST: Proton Magnetic Resonance Study of Sorption of Water and Alcohols by Wool. . . . .	3191
M. LAZÁR and J. PAVLINEC: Graft Copolymerization with Styrene and Methyl Methacrylate in Very Viscous Medium. . . . .	3197
JAMES A. BITTLES, A. K. CHAUDHURI, and SIDNEY W. BENSON: Clay-Catalyzed Reactions of Olefins. III. Kinetics of Polymerization of Styrene. . . . .	3203
HARVEY SCOTT, ROBERT E. FROST, ROGER F. BELT, and D. E. O'REILLY: Stereoregular Diene Polymerization with Inorganic Catalysts. I. <i>cis</i> 1,4-Polymerization of 1,3-Butadiene with a Cobaltous Chloride-Aluminum Chloride Complex. . . . .	3233
D. E. O'REILLY, CHARLES P. POOLE, JR., ROGER F. BELT, and HARVEY SCOTT: Stereoregular Diene Polymerization with Inorganic Catalysts. II. Magnetic Resonance Optical and X-Ray Study of Catalysts Containing Cobalt. . . . .	3257
G. LEFEBVRE and F. DAWANS: 1,3-Cyclohexadiene Polymers. Part I. Preparation and Aromatization of Poly-1,3-cyclohexadiene. . . . .	3277
F. DAWANS: 1,3-Cyclohexadiene Polymers. Part II. Copolymerization of 1,3-Cyclohexadiene and Isoprene. . . . .	3297
STEFAN POLOWIŃSKI, ELIGIA TURSKA, and JERZY KROH: Investigations on the Radiation-Produced Peroxide of Poly(methyl Methacrylate) and Its Copolymers. . . . .	3305
MAURICE MORTON and L. J. FETTERS: Homogeneous Anionic Polymerization. V. Association Phenomena in Organolithium Polymerization. . . . .	3311
RICHARD H. WILEY and PETER JÄGER: $\gamma$ -Irradiation- and Radical-Initiated Polymerization of <i>N,N</i> -Dimethylethylsulfonamide. . . . .	3327
H. SOBUE, T. URYU, K. MATSUZAKI, and Y. TABATA: Stereoregularity of Polymethacrylonitrile. . . . .	3333
HIROSHI SOBUE, KEI MATSUZAKI, and SHINTARO NAKANO: Stereospecific Polymerization of Menthyl Methacrylate. . . . .	3339
EISHUN TSUCHIDA, CHUNG-NAN SHIH, ISAO SHINOHARA, and SHU KAMBARA: Synthesis of a Polymer Chain Having Conjugated Unsaturated Bonds by Dehydrohalogenation of Polyhalogen-Containing Polymers. . . . .	3347
NIICHIRO TOKURA, MINORU MATSUDA, and KOJI ARAKAWA: Polymerization in Liquid Sulfur Dioxide. Part XVIII. Poly-	

merization of <i>p</i> -Isopropylstyrene and Its Copolymerization with Styrene in Liquid Sulfur Dioxide . . . . .	3355
---	------

## ISSUE No. 8, AUGUST

EMIL OTT . . . . .	3365
JOGINDER LAL and JAMES E. McGRATH: Stereoregular Polymerization of Vinyl Alkyl Ethers with Metal Sulfate-Sulfuric Acid Complex Catalysts . . . . .	3369
YOSHIO IWAKURA, KEIKICHI UNO, and KIYOSHI ICHIKAWA: Cyclopolymerization of $\alpha,\omega$ -Polymethylene Diisocyanates . . . . .	3387
YOSHIO TANAKA and HIROSHI KAKIUCHI: Study of Epoxy Compounds. Part VI. Curing Reactions of Epoxy Resin and Acid Anhydride with Amine, Acid, Alcohol, and Phenol as Catalysts . . . . .	3405
MILOSLAV KUČERA and EDUARD SPOUSTA: Kinetics of Polymerization of Molten Trioxane . . . . .	3431
MILOSLAV KUČERA and EDUARD SPOUSTA: Initiation of the Bulk Polymerization of Trioxane . . . . .	3443
HIROSHI OKAMOTO: A Method of Estimating Molecular Weight Distributions of Polymer Fractions . . . . .	3451
SADAO TORIKAI: Some Aspects of Thermal Decomposition of Polyoxymethylene and Irradiated Polyoxymethylene . . . . .	3461
MURRAY GOODMAN and AKIHIRO ABE: Coupled Vinyl and Acetal Ring-Opening Polymerization . . . . .	3471
AKIHIRO ABE and MURRAY GOODMAN: Optically Active Polymers: Cyclopolymerization of the Divinylacetal of ( <i>R</i> ) (+)-3,7-Dimethyloctanal . . . . .	3491
MITSUO ASAHINA and MITSUO ONOZUKA: Thermal Decomposition of Model Compounds of Polyvinyl Chloride. I. Gaseous Thermal Decomposition of Model Compounds Having Secondary and Tertiary Chlorine . . . . .	3505
MITSUO ASAHINA and MITSUO ONOZUKA: Thermal Decomposition of Model Compounds of Polyvinyl Chloride. II. Gaseous Thermal Decomposition of Unsaturated Chain End Model Compounds . . . . .	3515
S. ENOMOTO and M. ASAHINA: Lattice Modes of Polyethylene . . . . .	3523
ICHIRO SAKURADA, AKIO NAKAJIMA, and KYOICHIRO SHIBATANI: Dilute Solution Properties of Partly Urethanized Polyvinyl Alcohol . . . . .	3545
RICHARD L. BALLMAN and ROBERT H. M. SIMON: The Influence of Molecular Weight Distribution on Some Properties of Polystyrene Melt . . . . .	3557
CYNTHIA KOLB WHITNEY and R. L. HAMILTON: Stress Relaxation in Fibers: Effect of Water and Temperature . . . . .	3577
A. T. DIBENEDETTO: Viscosity of Amorphous Polymers . . . . .	3585
HIROYOSHI KAMOGAWA, JOEL MARIE LARKIN, KYOJI TÔEI, and	

HAROLD G. CASSIDY: Electron Exchange Polymers. XXII. Preparation and Properties of Poly-2-vinylphenothiazine. . . . .	3603
E. A. S. CAVELL, I. T. GILSON, B. R. JENNINGS, and H. G. JERRARD: Determination of a Mark-Houwink Type Relationship for Poly- <i>N-tert</i> -butylacrylamide in Methanol. . . . .	3615
FRANCIS E. BROWN and GEORGE E. HAM: General Conclusions about the Copolymerization of Ethylene with Other Monomers by Free Radical Catalysis. . . . .	3623
GEORGE E. HAM: Proof of Validity of Expanded Copolymerization Equations. . . . .	3633
YONEHO TABATA, HIROKIMI KITANO, and HIROSHI SOBUE: Radiation-Induced Polymerization of 2-Methyl-5-vinylpyridine. . . . .	3639
YONEHO TABATA, YOSHIO HASHIZUME, and HIROSHI SOBUE: Radiation-Induced Copolymerization of Acrylonitrile with Styrene. . . . .	3649
MATAHUMI ISHIBASHI: CH <sub>2</sub> Rocking Vibrations of Polyethylene Oxybenzoate. . . . .	3657
MATAHUMI ISHIBASHI: CH <sub>2</sub> Rocking Vibrations of Linear Oligomers of Poly( <i>p</i> -ethylene Oxybenzoate) Having Hydroxyl and Carboxylic Acid Endgroups. . . . .	3665
HENRY E. HARRIS and J. G. PRITCHARD: Determination of 1,2-Glycol Units in Polyvinyl Alcohol. . . . .	3673
TAKAYUKI FUENO and JUNJI FURUKAWA: Probability Theory of Asymmetric Chain Growth in Polymerization. . . . .	3681
BERNHARD WUNDERLICH and TAMIO ARAKAWA: Polyethylene Crystallized from the Melt under Elevated Pressure. . . . .	3697
PHILLIP H. GEIL, FRANKLIN R. ANDERSON, BERNHARD WUNDERLICH, and TAMIO ARAKAWA: Morphology of Polyethylene Crystallized from the Melt Under Pressure. . . . .	3707
C. E. BROCKWAY: Efficiency and Frequency of Grafting of Methyl Methacrylate to Granular Corn Starch. . . . .	3721
C. E. BROCKWAY: Extractability of Homopolymer of Methyl Methacrylate from Its Graft Copolymers with Starch. . . . .	3733
KENICHI FUKUI and TOKIO YAMABE: Statistical Theory of the Polymerization of Polyepoxide Monomers. . . . .	3743
P. R. SAUNDERS: Dilute Solution Properties of Polyamides in Formic Acid. Part I. Repression of Polyelectrolyte Effects by Means of Excess Counterions. . . . .	3755
P. R. SAUNDERS: The Unperturbed Dimensions of Nylon 66. . . . .	3765
M. MANDEL and J. C. LEYTE: Interaction of Polymethacrylic Acid and Bivalent Counterion. II. . . . .	3771
CLARENCE J. WOLF and A. C. STEWART: Radiation Chemistry of Iodine-Octamethylcyclotetrasiloxane Solutions. . . . .	3781
HANS SCHOTT: Elastic Effects and Extrudate Distortions in Capillary Flow of Molten Polyethylene Resins. . . . .	3791
A. G. PITTMAN and R. E. LUNDIN: Synthesis and Polymerization of 1-(Perfluoroacyl)aziridines. . . . .	3803

## Book Review

- Polymerization of Aldehydes and Oxides (Polymer Reviews, Vol. 3), J. FURUKAWA and T. SAEGUSA. Reviewed by ARTHUR M. SCHILLER. . . . . 3811

## Errata

- ELIZABETH DYER and RICHARD J. HAMMOND: Thermal Degradation of *N*-Substituted Polycarbamates (article in *J. Polymer Sci.*, **A2**, 1-14, 1964) . . . . . 3812
- D. W. BEHNKEN: Estimation of Copolymer Reactivity Ratios: An Example of Nonlinear Estimation (article in *J. Polymer Sci.*, **A2**, 645-668, 1964) . . . . . 3812

## ISSUE NO. 9, SEPTEMBER

- P. H. GEIL: Polymer Deformation. II. Drawing of Polyethylene Single Crystals . . . . . 3813
- P. H. GEIL: Polymer Deformation. III. Annealing of Drawn Polyethylene Single Crystals and Fibers . . . . . 3835
- P. H. GEIL: Polymer Deformation. IV. Drawing of Nylon 6 and Polyoxymethylene Crystals . . . . . 3857
- J. K. STILLE and J. R. WILLIAMSON: Polyquinoxalines . . . . . 3867
- MINORU MATSUDA, SUSUMU ABE, and NICHIRO TOKURA: Polymerization in Liquid Sulfur Dioxide. Part XIX. Effects of Aniline and Its Derivatives on the Radical Polymerization of Acrylonitrile in Liquid Sulfur Dioxide . . . . . 3877
- HERBERT N. FRIEDLANDER: Influence of Catalyst Depletion or Deactivation on Polymerization Kinetics . . . . . 3885
- G. C. ROBINSON: Polymerization of Carbon-Nitrogen Double Bond in Carbodiimides . . . . . 3901
- EDMUND F. JORDAN, JR., and ARTHUR N. WRIGLEY: Homopolymerization of *N*-Allylacetamide and *N*-Allylstearamide . . . . . 3909
- J. L. LUNDBERG: Diffusivities and Solubilities of Methane in Linear Polyethylene Melts . . . . . 3925
- H. SPEDDING and J. O. WARWICKER: Effect of Chemical Reagents on the Fine Structure of Cellulose. Part I. Action of Diazomethane . . . . . 3933
- N. G. McCrum: Inadequacies in Time-Temperature Equivalence . . . . . 3951
- R. C. MEHROTRA and V. S. GUPTA: Studies in Condensed Phosphates. Part VI. Paper Chromatographic Studies of Condensed Phosphates . . . . . 3959
- R. C. MEHROTRA and V. S. GUPTA: Studies in Condensed Phosphates. Part VII. Metachromatic Reactions of Sodium Polymetaphosphate and Its Derivatives . . . . . 3963
- N. G. GAYLORD and I. KÖSSLER, M. ŠTOLKA, and J. VODEHNAL: Cyclo- and Cyclized Diene Polymers. I. Polymerization of

Conjugated Dienes to Ladder Cyclo-polymers with Complex Catalysts.....	3969
M. ŠTOLKA, J. VODEHNAL, and I. KÖSSLER: Cyclo- and Cyclized Diene Polymers. II. Infrared Study of the Cyclization of <i>cis</i> -1,4, <i>trans</i> -1,4 and 3,4-Polyisoprenes.....	3987
H. KÄMMERER and M. HARRIS: A Contribution to the Preparation of Phenolic Polynuclear Compounds with Sulfonyl Bridges.....	4003
JAMES B. GANCI and FREDERICK A. BETTELHEIM: Polymerization of Chlorinated Diphenylsiloxanes.....	4011
J. H. GOLDEN and E. A. HAZELL: Degradation of Poly-3,3-bis(chloromethyl)-oxacyclobutane (Penton).....	4017
A. H. FRAZER: Thermal Stability of the Copolymer of Sulfur Dioxide and <i>cis</i> , <i>cis</i> -1,5-Cyclooctadiene.....	4031
R. VAN LEEMPUT and R. STEIN: Experimental Data on Dilute Polymer Solutions. Hydrodynamic Properties and Statistical Coil Dimensions of Poly( <i>n</i> -butyl Methacrylate). Part II.....	4039
H. A. ENDE and V. STANNETT: Density Gradient Centrifugation of a Graft Copolymer.....	4047
H. A. ENDE and J. J. HERMANS: Analysis of Copolymers by Means of Density Gradient Centrifugation. II. Comparison with Kinetic Requirements.....	4053
W. BANKS, A. SHARPLES, and J. N. HAY: The Effect of Simultaneously Occurring Processes on the Course of Polymer Crystallization.....	4059
J. P. BERRY: Fracture Processes in Polymeric Materials. V. Dependence of the Ultimate Properties of Poly(methyl Methacrylate) on Molecular Weight.....	4069
YONEHO TABATA, KIYOSHI HARA, and HIROSHI SOBUE: Radiation-Induced Polymerization of Acrylonitrile in Liquid Ethylene.....	4077
H. R. ALLCOCK: X-Ray-Induced Polymerization of Diphenylvinylphosphine Oxide.....	4087
PETER HEDVIG: Radiation-Induced Electrical Conductivities in Polyamide Copolymers.....	4097
JOSEPH PELLON, ROBERT L. KUGEL, RUTH MARCUS, and ROBERT RABINOWITZ: Free Radical Polymerization and Copolymerization of Bicyclo-(2.2.1)-hepta(2.5)-diene (Norbornadiene).....	4105
C. G. OVERBERGER, F. S. DIACHKOVSKY, and P. A. JAROVITZKY: Kinetic Study of the Polymerization of $\alpha$ - <i>d</i> -Styrene and/or Styrene by Homogeneous Catalysis. Part I.....	4113
JOSEPH V. KOLESKE and SHELDON F. KURATH: Configuration and Hydrodynamic Properties of Fully Acetylated Guaran.....	4123
O. C. DERMER and W. A. AMES: Kinetics of Ring-Scission Copolymerization.....	4151
ROGER P. KAMBOUR: Refractive Indices and Compositions of Crazes in Several Glassy Polymers.....	4159

ROGER P. KAMBOUR: Refractive Index and Composition of Poly-(methyl Methacrylate) Fracture Surface Layers . . . . .	4165
GEORGE E. HAM: Generality of Product Probability Values in Unifying and Predicting Relationships Among Monomers in Copolymerization . . . . .	4169
GEORGE E. HAM: Calculation of Copolymerization Reactivity Parameters From Product Probabilities . . . . .	4181
GEORGE E. HAM: Penultimate Unit Effects in Terpolymerization . . . . .	4191
KENNETH F. O'DRISCOLL: Prediction of Ionic Copolymerization Reactivity Ratios . . . . .	4201
FRANK R. MAYO: On Correlation of Data on Copolymerization . . . . .	4207
RICHARD L. HANSEN: Kinetics and Mechanism of the Trialkylboron-Catalyzed Polymerization of Methyl Methacrylate in the Presence of Oxygen . . . . .	4215
B. D. PHILLIPS, T. L. HANLON, and A. V. TOBOLSKY: Ionic Copolymerization of Styrene and <i>p</i> -Methylstyrene . . . . .	4231
GEORGE A. MORTIMER and LLOYD C. ARNOLD: Free-Radical Polymerization of Olefins . . . . .	4247

## Book Review

Newer Methods of Polymer Characterization. B. KE. Reviewed by W. R. SORENSON . . . . .	4255
--	------

## Notes

The Application of Schofield's Equation to the Uptake of Electrolytes by a Cation Exchange Resin . . . . .	4257
--	------

## Errata

DAVID L. TAYLOR: An Evaluation of Column Thermal Diffusion as a Means of Polymer Characterization (article in <i>J. Polymer Sci.</i> , <b>A2</b> , 611-625, 1964) . . . . .	4260
C. G. OVERBERGER and MARTIN TOBKES: Polymerization Behavior of Aziridines with 1,2-Epoxides (article in <i>J. Polymer Sci.</i> , <b>A2</b> , 2481-2487, 1964) . . . . .	4260

## ISSUE NO. 10, OCTOBER

W. MARCONI, A. MAZZEI, S. CUCINELLA, and M. CESARI: Stereospecific Polymerization of 2-Substituted-1,3-butadienes. I. Crystalline Polymers of 2- <i>tert</i> -Butyl-1,3-butadiene . . . . .	4261
MINORU MATSUDA, KOICHI OHSHIMA, and NIICHIRO TOKURA: Polymerization in Liquid Sulfur Dioxide. Part XXI. Effect of Liquid Sulfur Dioxide Concentration on Cationic Copolymerization of Styrene with Methyl Acrylate in Liquid Sulfur Dioxide . . . . .	4271

MINORU MATSUDA and NIICHIRO TOKURA: Polymerization in Liquid Sulfur Dioxide. Part XXII. Comparison of Retarding Effects of Bases on the Radical Polymerization of Acrylonitrile in Liquid Sulfur Dioxide.....	4281
T. C. TRANTER: Isomorphism in Copolyamides Containing the <i>p</i> -Phenylene Linkage.....	4289
A. M. KOTLIAR: A Critical Evaluation of Mathematical Molecular Weight Distribution Models Proposed for Real Polymer Distributions. I. Effects of a Low Molecular Weight Cut-Off Value...	4303
A. M. KOTLIAR: A Critical Evaluation of Mathematical Molecular Weight Distribution Models Proposed for Real Polymer Distributions. II. Effects of a High Molecular Weight Cut-off Value...	4329
H. D. KEITH: On the Relation between Different Morphological Forms in High Polymers.....	4339
MATAHUMI ISHIBASHI: Polyether-Ester Copolymer Prepared from <i>p</i> - $\gamma$ -Hydroxypropoxy Benzoate and Bis- $\beta$ -hydroxyethyl Terephthalate.....	4361
B. MUKHERJI and W. PRINS: Applicability of Polymer Network Theories to Gels Obtained by Crosslinking a Polymer in Solution	4367
W. R. KRIGBAUM and R.-J. ROE: Diffraction Study of Crystallite Orientation in a Stretched Polychloroprene Vulcanizate.....	4391
J. M. WILBUR, JR., and C. S. MARVEL: Homopolymers and Terpolymers of 5,7-Dimethyl-1,6-octadiene.....	4415
K. C. TSOU, H. E. HOYT, and B. D. HALPERN: Epoxidation of Poly-2-methyl-6-allyl-1,4-phenylene Oxide and Copolymer of 2-Methyl-6-allyl-4-bromophenol and 2,6-Dimethyl-4-bromophenol	4425
PREMAMOY GHOSH, SUBHASH CHANDER CHADHA, ASISH R. MUKHERJEE, and SANTI R. PALIT: Endgroup Studies in Persulfate-Initiated Vinyl Polymer by Dye Techniques. Part I. Initiation by Persulfate Alone.....	4433
PREMAMOY GHOSH, SUBHASH CHANDER CHADHA, and SANTI R. PALIT: End group Studies in Persulfate-Initiated Vinyl Polymer by Dye Technique. Part II. Initiation by Redox Persulfate Systems.....	4441
G. E. MYERS and J. R. DAGON: Some Calculations of Intrinsic Viscosity and Molecular Weight Distribution for Trifunctional, Randomly Branched Polymers.....	4453
A. D. KETLEY and R. J. ENRIG: Polymers Containing the Cyclopentyl and Cyclohexyl Groups.....	4461
F. LYNN HAMB and ANTHONY WINSTON: Copolymerization of 4-Cyclopentene-1,3-dione with Acrylonitrile and Methyl Methacrylate.....	4475
N. Lakshminarayanaiah and V. Subrahmanyam: Measurement of Membrane Potentials and Test of Theories.....	4491
R. ST. J. MANLEY: Chain Folding in Amylose Crystals.....	4503
B. R. JENNINGS and H. G. JERRARD: Molecular Configuration and	

Hydrodynamic Behavior of Poly- <i>N-tert</i> -butylacrylamide in Methanol . . . . .	4517
T. ALTARES, JR., D. P. WYMAN, and V. R. ALLEN: Synthesis of Low Molecular Weight Polystyrene by Anionic Techniques and Intrinsic Viscosity-Molecular Weight Relations Over a Broad Range in Molecular Weight . . . . .	4533
D. P. WYMAN, V. R. ALLEN, and T. ALTARES, JR.: Reaction of Polystyryllithium with Carbon Dioxide . . . . .	4545
M. L. MILLER and J. SKOGMAN: Polymerization of <i>tert</i> -Butyl Crotonate . . . . .	4551
JOGINDER LAL and G. S. TRICK: Glass Transformation Temperatures of Poly(vinyl Alkyl Ethers) and Poly(vinyl Alkyl Sulfides) . . . . .	4559
TATSUYA IMOTO and TSUTOMU MATSUBARA: Polymerization of Acetaldehyde. Part V. Polyaldol Condensation of Acetaldehyde by Alkali Metal Amalgam as Catalyst. II . . . . .	4573
V. S. NANDA and R. K. JAIN: A Study of the Statistical Character of Anionic Polymers . . . . .	4583
O. VOGL: Polymerization of Higher Aldehydes. III. Elastomeric Polyacetaldehyde . . . . .	4591
O. VOGL: Polymerization of Higher Aldehydes. IV. Crystalline Isotactic Polyaldehydes: Anionic and Cationic Polymerization . . . . .	4607
O. VOGL: Polymerization of Higher Aldehydes. V. End-Capped Crystalline Isotactic Polyaldehydes: Characterization and Properties . . . . .	4621
O. VOGL and W. M. D. BRYANT: Polymerization of Higher Aldehydes. VI. Mechanism of Aldehyde Polymerization . . . . .	4633
HIROYOSHI KAMOGAWA, YUEH-HUA CHEN GIZA, and HAROLD G. CASSIDY: Electron Transfer Polymers. XXIII. Interactions of the Quinhydrone Type in Polyvinylhydroquinone Solutions . . . . .	4647
ULRICH P. STRAUSS and SHNEIOR LIFSON: On the Theory of Divalent Ion Binding by Polyelectrolytes . . . . .	4661
W. R. LICHT and D. E. KLINE: Effect of Gamma Radiation on the Specific Volume of Polytetrafluoroethylene from $-80^{\circ}\text{C}$ . to $+40^{\circ}\text{C}$ . . . . .	4673
JOSEPH S. YUDELSON and RANDALL E. MACK: Association Phenomena in Carboxyl-Containing Polymers . . . . .	4683
R. C. WEATHERWAX and HAROLD TARKOW: Adsorption of Poly(vinyl-Acetate- $\text{C}^{14}$ ) on Smooth, Geometrically Simple Surfaces . . . . .	4697

#### Book Review

Grundriss der Makromolekularen Chemie. B. VOLLMERT. Reviewed by NORBERT M. BIKALES . . . . .	4705
--	------



## Erratum

- P. W. MORGAN: Linear Condensation Polymers from Phenolphthalein and Related Compounds (article in *J. Polymer Sci.*, **A2**, 437-459, 1964)..... 4707

## ISSUE No. 11, NOVEMBER

- B. S. WILDI and J. E. KATON: Synthesis and Electrical Conductivity Measurements on Semiconducting Organic Polymers Derived from Nitriles..... 4709
- J. B. YANNAS and I. E. ISGUR: Chemically Heterogeneous Populations of Copolymer Latex Particles. Preparation, Fractionation, and Characterization..... 4719
- C. A. AUFDERMARSH, JR. and R. PARISER: *cis*-Polychloroprene..... 4727
- RAYMOND C. FERGUSON: Infrared and Nuclear Magnetic Resonance Studies of the Microstructures of Polychloroprenes..... 4735
- BEN-AMI FEIT, JOSEPH WALLACH, and ALBERT ZILKHA: Anionic Polymerization and Oligomerization of Methacrylonitrile by Alkali Metal Alkoxides..... 4743
- F. J. GERMINO and R. M. VALLETTA: Amylose V Complexes from Dimethyl Sulfoxide Solutions..... 4757
- R. M. VALLETTA and F. J. GERMINO: Amylose V Complexes from 2-Aminoethanol Solutions..... 4765
- H. C. BEACHELL and C. P. NGOC SON: Thermal Degradation of Ethylene Bis(*N*-phenylcarbamate)..... 4773
- J. H. GOLDEN, B. L. HAMMANT, and E. A. HAZELL: Degradation of Polycarbonates. IV. Effect of Molecular Weight on Flexural Properties..... 4787
- WOLFGANG WRASIDLO and HAROLD H. LEVINE: Polybenzimidazoles. I. Reaction Mechanism and Kinetics..... 4795
- WILLIAM E. GIBBS: Copolymerization of Divinylbenzene with Monovinyl Monomers..... 4809
- WILLIAM E. GIBBS: Mechanism of Alternating Inter-Intramolecular Propagation. II. General Kinetics..... 4815
- G. SMETS, P. HOUS, and N. DEVAL: Cyclopolymerization. IV. Structure of Polymethacrylic Anhydride and Kinetics of Polymerization of Methacrylic Anhydride..... 4825
- G. SMETS, N. DEVAL, and P. HOUS: Cyclopolymerization. V. Copolymerization of Acrylic and Methacrylic Anhydrides with Vinyl Monomers..... 4835
- LEON SEGAL and F. V. EGGERTON: Study of the Hexamethylenediamine-Cellulose Complex..... 4845
- J. R. SCHAEFGEN and R. ZBINDEN: An Infrared Study of Polyhydroxymethylene and Deuterated Polyhydroxymethylene..... 4865
- L. H. TUNG: Comparison of Polyethylene Molecular Weights Determined by Light-Scattering Measurements in 1-Chloronaphthalene and 1,2,3,4-Tetrahydronaphthalene..... 4875

RICHARD E. ROBERTSON and ROBERT J. BUENKER: Some Elastic Moduli of Bisphenol A Polycarbonate. . . . .	4889
EUGENE C. WINSLOW and ALBERT A. MANNING: Salicylaldehyde-Formaldehyde Polymers and Their Metallic Chelates. . . . .	4903
E. J. MEEHAN, I. M. KOLTHOFF, and P. R. SINHA: Apparent Transfer Constants of Mercaptans in Emulsion Polymerization. II. Effect of Reactions Other than Polymer Chain Transfer. . . . .	4911
W. JACK HILLEND and HAROLD A. SWENSON: Electron Radiation of Aqueous Methyl Cellulose Solutions. . . . .	4921
JAN HERMANS, JR.: On the Deformation of Networks of Very Stiff Random Chains Existing in Certain Colloidal Gels. . . . .	4931
J. D. INGHAM and N. S. RAPP: Polymer Degradation. II. Mechanism of Thermal Degradation of Polyoxypropylene Glycol-Toluene 2,4-Diisocyanate Polymer (POPG-TDI) and a Block Polyether Glycol-TDI Polymer. . . . .	4941
R. C. GIBERSON: Diffusion of Oxygen in Gamma-Irradiated Polyethylene. . . . .	4965
HENRY S. MAKOWSKI, BENJAMIN K. C. SHIM, and ZIGMOND W. WILCHINSKY: 1,5-Hexadiene Polymers. II. Copolymers of Ethylene and 1,5-Hexadiene. . . . .	4973
GERHARD F. L. EHLERS and JAMES D. RAY: Synthesis and Characterization of Poly- <i>s</i> -Triazinyleneimides. . . . .	4989
F. DAWANS, B. REICHEL, and C. S. MARVEL: 2,7-Disubstituted 1,3,6,8-Tetraazopyrene and Related Polymers. . . . .	5005
J. J. STRATTA, F. P. REDING, and J. A. FAUCHER: Glass Transitions of Polyoxetanes. . . . .	5017

### Book Review

Foreign-Language and English Dictionaries in the Physical Sciences and Engineering, a Selected Bibliography 1952 to 1963, TIBOR W. MARTON. Reviewed by E. H. IMMERGUT. . . . .	5025
--	------

### Errata

RICHARD H. WILEY, W. H. RIVERA, T. H. CRAWFORD, and N. F. BRAY: Poly(bicyclo[2.2.1]heptadiene-2,5) (article in <i>J. Polymer Sci.</i> , <b>61</b> , S38-S40, 1962). . . . .	5027
MIHIR KUMAR SAHA, PREMAMOY GHOSH, and SANTI R. PALIT: Determination of Halogen in Copolymers by Dye-Partition Technique and Calculation of $r_1$ Therefrom (article in <i>J. Polymer Sci.</i> , <b>A2</b> , 1365-1372 1964). . . . .	5027
RAYMOND M. FUOSS, IVAL O. SALYER, and HARRY S. WILSON: Evaluation of Rate Constants from Thermogravimetric Data (article in <i>J. Polymer Sci.</i> , <b>A2</b> , 3147-3151, 1964). . . . .	5027
FRANCIS E. BROWN and GEORGE E. HAM: General Conclusions about the Copolymerization of Ethylene and Other Monomers by	

Free Radical Catalysis (article in <i>J. Polymer Sci.</i> , <b>A2</b> , 3623-3632, 1964) . . . . .	5028
--	------

## ISSUE NO. 12, DECEMBER

J. P. KENNEDY, J. J. ELLIOTT, and W. NÄEGELE: Intramolecular Hydride Shift Polymerization by Cationic Mechanism. IV. Cationic Isomerization Polymerization of Vinylcyclohexane . . . . .	5029
UMBERTO BIANCHI and ENRICO PEDEMONTE: Rubber Elasticity: Thermodynamic Properties of Deformed Networks . . . . .	5039
R. A. MALZAHN, J. H. GRIFFITH, C. S. MARVEL, GLEN W. HEDRICK, J. B. LEWIS, CAROLYN R. MOBLEY, and F. C. MAGNE: Polymers and Copolymers of Vinyl Pinolate and Some Reactions with Isocyanates . . . . .	5047
MACIEJ BERO, MARCELI LACZKOWSKI, and HENRYK PSTROCKI: Investigations on the Continuous Copolymerization of Acrylonitrile with Methyl Methacrylate in a Heterogeneous System . . . . .	5057
J. M. CRISSMAN, J. A. SAUER, and A. E. WOODWARD: Dynamic Mechanical Behavior of Some High Polymers at Temperatures from 6°K.: Polyethylene, Nylon 66, Polypropylene, Poly(vinyl Chloride), Poly( <i>d,l</i> -propylene Oxide), Polybutene-1, Poly(4-Methylpentene-1), Poly(methyl Methacrylate), Poly(ethyl Methacrylate), Poly-4-methylpentene-1 and Poly(isobutyl Methacrylate) . . . . .	5075
H. YASUDO and M. F. REFOJO: Graft Copolymerization of Vinylpyrrolidone onto Polydimethylsiloxane . . . . .	5093
JEAN-CLAUDE BAUWENS: Processus de l'Écoulement visqueux des hauts Polymères . . . . .	5099
G. M. BURNETT, J. N. HAY and J. D. B. SMITH: Study of Cross-link Formation by Partial Conversion Properties. I. Copolymerization of Poly(ethylene Fumarate) and Styrene . . . . .	5111
W. DE WINTER and C. S. MARVEL: Synthesis and Cyclopolymerization of 4,4-Dimethyl-1,6-heptadiene-3,5-dione . . . . .	5123
F. D. OTTO and G. PARRAVANO: Polymerization of Styrene with $TiCl_3-Al(C_2H_5)_3$ and $VCl_3-Al(C_2H_5)_3$ Catalysts . . . . .	5131
STEPHANIE L. KWOLEK: Study of the Preparations of a Piperazine Polyurea and Polyamide by Low Temperature Solution Polymerization . . . . .	5149
R. JEFFRIES: Deuteration of Proteins and Polyamides in Deuterium Oxide Vapor . . . . .	5161
J. P. KENNEDY: Cationic Isomerization Polymerization of $\beta$ -Methylstyrene and Allylbenzene . . . . .	5171
D. PATTERSON: Heats of Mixing of Polymers with Ester and Ether Solvents . . . . .	5177
G. SMETS, X. VAN DER BORGH, and G. VAN HAEREN: Electrochemical Transformations of Polymeric Acid Solutions. I. Crossed Kolbe Synthesis . . . . .	5187

MARIO RAGAZZINI, MARIO MODENA, ENZO GALLINELLA and GUIDO-BALDO CEVIDALLI: Preparation and Structure of Some Carbon Monoxide-Formaldehyde Copolymers. . . . .	5203
R. E. BARKER, JR.: Kishi Lag Times for O <sub>2</sub> Adsorption onto Irradiated Poly(Bisphenol-A Carbonate) and Poly(methyl Methacrylate) . . . . .	5213
SHIROH SATOH: Undecoupled and Decoupled High Resolution Nuclear Magnetic Resonance Study of Poly(vinyl Chloride) . . . . .	5221
JAMES R. KUPPERS: Conformation of Styrene-Maleic Acid Copolymer in Aqueous HCl Solutions . . . . .	5239
R. C. SOVISH and W. BOETTCHER: Polymerization of 2-Nitroolefins	5247
R. B. BEEVERS: Dependence of the Glass Transition Temperature of Polyacrylonitrile on Molecular Weight . . . . .	5257
EARL D. HOLLY: Interaction Parameters and Heats of Dilution for Ethylene-Propylene Rubber in Various Solvents. . . . .	5267
W. E. Gibbs and R. J. McHENRY: Copolymerization of Nonconjugated Diolefins: General Composition Relationships . . . . .	5277
J. C. LEYTE: Polyelectrolytes in Salt Solutions . . . . .	5287
VERNON L. BELL: Polymerization of Conjugated Trienes . . . . .	5291
VERNON L. BELL: Post-Modification of Conjugated Triene Polymers Via the Diels-Alder Reaction . . . . .	5305
E. B. JONES and C. S. MARVEL: $\alpha,\omega$ -Glycols from Isobutylene and Some Derived Block Copolymers . . . . .	5313
JOHN F. VOEKS: Cohesive Energy Density and Internal Pressure of High Polymers . . . . .	5319
H. G. SPENCER and O. L. HUNT: Kinetics of Sorption of Water Vapor by Hydrophilic Polymers. Potassium and Lithium Forms of Poly(vinyl Methyl Ether-Maleic Acid) . . . . .	5327
E. G. BRAME, JR., R. S. SUDOL, and O. VOGL: Polymerization of Higher Aldehydes. VII. Tacticity of Elastomeric Polyacetaldehyde . . . . .	5337
R. H. WILEY and GIOVANNI DEVENUTO: Kinetics of the Polymerization of Divinylbenzene Isomers . . . . .	5347

## Notes

S. ENOMOTO, M. KOGURO, and M. ASAHINA: Infrared Studies of Chain Conformations in Polyvinyl Chloride . . . . .	5355
J. PRESTON, J. K. LAWSON, JR.: A Convenient Preparation for Ethylenesulfonic Acid . . . . .	5364
Author Index Volume 2 . . . . .	5367
Subject Index Volume 2 . . . . .	5382

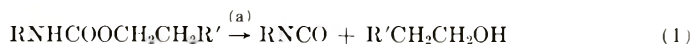
## Thermal Degradation of *N*-Substituted Polycarbamates

ELIZABETH DYER and RICHARD J. HAMMOND,\* *Department of Chemistry, University of Delaware, Newark, Delaware*

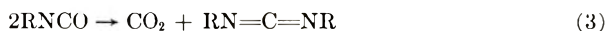
### Synopsis

*N*-substituted polycarbamates of relatively low molecular weight have been prepared from the condensation of 1,6-hexanebischloroformate with *N*-substituted diamines, both aliphatic and aromatic. The initial rates of thermal degradation of these polymers and of unsubstituted analogs have been determined at 230–285°C. by following the evolution of carbon dioxide. The results showed that the more thermally stable polymers were those derived from the substituted aliphatic diamines, having the formula  $[-N(R)-X-N(R)-COO(CH_2)_6OCO-]_n$ , where X is  $(CH_2)_5$  or  $(CH_2)_6$ . When R was  $-CH_3$  and  $-C_6H_5$ , the overall  $E_A$  was 31 and 46 kcal./mole, respectively. The polymers derived from aromatic diamines, where X was 4,4'- $C_6H_4CH_2C_6H_4$ , showed low values for  $E_A$ , approximately 15 kcal./mole, regardless of whether R was H or alkyl. This low thermal stability was shown to be caused by amine endgroups. Some evidence as to modes of thermal degradation was obtained from a study of volatile products.

Previous investigations<sup>1-4</sup> on the thermal degradation of mono-*N*-substituted carbamates showed that the decomposition proceeded by two general paths:



Subsequent pyrolysis of isocyanate formed by path (a) gave carbodiimide and carbon dioxide:

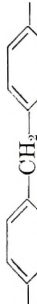


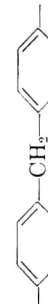


Polythiolcarbamates also yielded products<sup>5</sup> derived from both types of breakdown.

In the di-*N*-substituted carbamates ( $RR'NCOOR''$ ), degradation by path (a) is excluded. The products from a monomeric compound of this type consisted solely of amine, olefin, and carbon dioxide.<sup>4</sup> In addition, the *N*-disubstituted carbamate had a much greater thermal stability than the mono-*N*-substituted analog.<sup>4</sup> The patent literature reports<sup>6,7</sup> that *N*-substituted polycarbamates (polyurethans) are more stable to heat than

\* From the Ph.D. dissertation, University of Delaware, of Richard J. Hammond, Armstrong Cork Co. Research Fellow, 1960-1962.

TABLE I  
 Properties of Polyurethans  $[-\text{N}-\text{X}-\text{N}-\text{CO}(\text{CH}_2)_6\text{OC}-]_n$ , from Diamines and 1,6-Hexanebischloroformate

No.	X	R	Melt temp., °C. <sup>a</sup>	Solubility <sup>b</sup>	$[\eta]^c$	Mol. wt. <sup>d</sup>	D.P.	Yield, %
I	(CH <sub>2</sub> ) <sub>6</sub>	H	150-153	C, D	0.65			87
II	(CH <sub>2</sub> ) <sub>6</sub>	H	172-176	C, D	0.48	8000 (E)	30	91
III	(CH <sub>2</sub> ) <sub>6</sub>	CH <sub>3</sub>	-50	A, C, D		2000 (B)	6	88
IV	(CH <sub>2</sub> ) <sub>6</sub>	C <sub>6</sub> H <sub>5</sub>	0-5	A (sl.), C, D	0.22			43
V <sup>e</sup>		H	203-207	C, D	0.60			95
VI		H	95-07	A (sl.), C, D	0.09			86
VII		CH <sub>3</sub>	68-73	A, C, D	0.37	2500 (B) 1900 (E)	6	31
VIII		m-C <sub>6</sub> H <sub>5</sub>	< -50	A, C, D		1700 (B)	4	10

<sup>a</sup> Temperature of initial softening.

<sup>b</sup> Solubility in acetone (A), *m*-cresol (C), dimethylformamide (D).

<sup>c</sup> Intrinsic viscosity in *m*-cresol at 25°C.

<sup>d</sup> As determined by (E) endgroup analysis by acetylation; (B) by boiling point elevation in acetone.

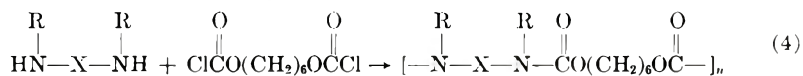
<sup>e</sup> Compound prepared earlier<sup>2</sup> by isocyanate method (dec. 229-231°C.).

the unsubstituted polymers, although little quantitative work has been done. Hence, it was of interest to study in some detail the effect of *N*-substitution on the thermal degradation of a variety of polyurethans.

## RESULTS AND DISCUSSION

### Preparation and Properties of *N*-Substituted Polyurethans

Polyurethans having substituents on nitrogen have been prepared from bischloroformates and substituted diamines.<sup>6-9</sup> In the current work representative *N*-substituted polyurethans were obtained by the interfacial condensation of 1,6-hexanebischloroformate (*a*) with an aliphatic diamine (1,6-hexanediamine and its *N,N'*-dimethyl and diphenyl derivatives) and (*b*) with an aromatic diamine (4,4'-methylenedianiline and its *N,N'*-dimethyl and di-*n*-butyl derivatives). Unsubstituted polyurethans were prepared in the same way for comparison.



The properties of these polymers are shown in Table I.

The polymers had the expected compositions, as shown by the analyses of Table II. The yields (Table I) are for products that had been reprecipitated to remove traces of unreacted monomers. The intrinsic viscosities of polymers I and II were lower than those of the comparable polymers from 1,4-butanediamine and 1,4-butanebischloroformate (reported<sup>10</sup> to be 0.76-1.1), while the intrinsic viscosity of polymer V was slightly higher than those of the comparable polymers from methylenebis(4-phenyl isocyanate) and 1,4-butanediol (reported<sup>11</sup> as 0.40). The *N*-substituted polymers were of lower molecular weights than the unsubstituted ones,

TABLE II  
Analysis of Carbamates and Polycarbamates

No.	Calculated			Found		
	C, %	H, %	N, %	C, %	H, %	N, %
I	57.32	8.88	10.28	58.16	9.14	10.28
II	58.30	9.18	9.71	58.58	8.98	9.94
III	61.12	9.62	7.91	60.49	9.78	7.94
IV	71.20	7.81	6.38	70.81	8.00	6.52
V <sup>a</sup>	68.45	6.56	7.60	68.09	6.47	7.82
VI	69.67	7.12	7.07	69.54	7.04	7.01
VII	69.67	7.12	7.07	69.10	7.18	7.07
VIII	72.46	8.38	5.82	72.93	8.61	5.81
X	64.78	11.05	7.78	64.47	10.82	7.52
XI	71.34	8.42	6.16	72.03	8.47	6.30
XIII	76.22	8.41	4.08	76.26	8.74	4.38
XIV	78.32	5.88	4.81	78.01	5.62	4.77
XV	79.94	10.78	2.83	79.50	10.62	3.03

<sup>a</sup> Analytical data on this compound made previously<sup>2</sup> by a different synthesis are incorrect. The found values should have been: C, 68.31%; H, 6.52%; N, 7.61%.

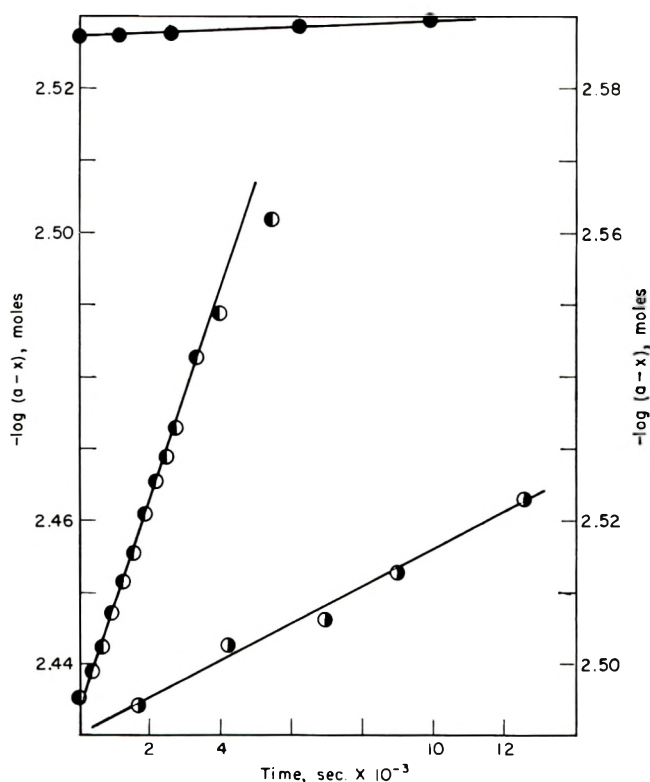


Fig. 1. A first-order plot of the rate of decarboxylation of (right ordinate) poly[*O*-hexamethylene-*N*-hexamethylenedicarbamate], II, (○) at 250.3°C.; (left ordinate) poly[*O*-hexamethylene-*N*-(*N*-phenyl)hexamethylenedicarbamate], IV, (●) at 245.5°C. and (●) at 274.4°C.

and were in the range of the rubbery polymers prepared by Frazer and Goldberg<sup>9</sup> from the bischloroformate of polytetramethylene ether glycol and *N*-substituted aromatic amines.

The lower melting points of the *N*-substituted polymers (III, IV, VII, and VIII) may be attributed both to the low molecular weights and to the loss of hydrogen bonding due to the presence of substituted nitrogen atoms. The latter effect has been well shown with polyamides.<sup>12</sup> A slight apparent anomaly is that polymer IV, with phenyl groups on nitrogen, melts higher than polymer III, with methyl on nitrogen. This can be explained by reference to a Stuart model of polymer IV, which shows that the phenyl groups are perpendicular to the backbone of the polymer chain. Unlike the relatively small methyl groups, the phenyl groups are capable of interaction, resulting in an increase in chain order and in melting point.

### Pyrolysis of Polyurethans

**Rate Data.** The pyrolysis of polyurethans has not been previously studied in detail except for the determination of the products from one polymer.<sup>2</sup> Hence three examples of unsubstituted polyurethans (I, II,



TABLE III  
Initial Rates of Carbon Dioxide Evolution from Pyrolysis of Polyurethans,

$$\left[ \begin{array}{c} \text{R} \quad \text{R} \quad \text{O} \quad \text{O} \\ | \quad | \quad || \quad || \\ -\text{N}-\text{X}-\text{N}-\text{CO}(\text{CH}_2)_m\text{OC}- \end{array} \right]_n$$

No.	X	R	<i>m</i>	Temp., °C. <sup>a</sup>	10 <sup>5</sup> × <i>k</i> <sub>1</sub> , sec. <sup>-1</sup>	<i>E</i> <sub>A</sub> , kcal./ mole <sup>b</sup>
I	(CH <sub>2</sub> ) <sub>3</sub>	H	6	232.3	0.13	26
				246.7	0.34	
				256.8	1.5	
				265.6	3.6	
				274.3	5.7	
II	(CH <sub>2</sub> ) <sub>6</sub>	H	6	249.1	2.2	29
				258.3	3.4	
				267.1	5.2	
III	(CH <sub>2</sub> ) <sub>6</sub>	CH <sub>3</sub>	6	246.8	5.6 <sup>c</sup>	31
				257.0	7.1	
IV	(CH <sub>2</sub> ) <sub>6</sub>	C <sub>6</sub> H <sub>5</sub>	6	266.7	15 <sup>c</sup>	46
				253.5	0.054	
				265.2	0.14	
				272.7	0.22	
V	C <sub>6</sub> H <sub>4</sub> CH <sub>2</sub> C <sub>6</sub> H <sub>4</sub>	H	6	284.7	0.60	15
				246.6	2.0	
				258.0	2.6 <sup>c</sup>	
VII	C <sub>6</sub> H <sub>4</sub> CH <sub>2</sub> C <sub>6</sub> H <sub>4</sub>	CH <sub>3</sub>	6	267.2	3.5 <sup>c</sup>	15
				249.7	6.9 <sup>c</sup>	
				258.1	8.7	
VIII	C <sub>6</sub> H <sub>4</sub> CH <sub>2</sub> C <sub>6</sub> H <sub>4</sub>	<i>n</i> -C <sub>4</sub> H <sub>9</sub>	6	267.2	11.3 <sup>c</sup>	14
				249.2	5.2	
				257.2	6.4 <sup>d</sup>	
IX	C <sub>6</sub> H <sub>4</sub> CH <sub>2</sub> C <sub>6</sub> H <sub>4</sub> <sup>e</sup>	H	10	266.7	8.2 <sup>d</sup>	34
				262.4	1.1	
				277.7	2.5	
				289.6	4.6	

<sup>a</sup> Maximum deviation ±0.25°C.

<sup>b</sup> Approximate value for overall changes forming CO<sub>2</sub>.

<sup>c</sup> Duplicate analyses gave identical *k*<sub>1</sub> values.

<sup>d</sup> Estimated maximum deviation of duplicates ±3%.

<sup>e</sup> Polymer with no amine endgroups.<sup>11</sup>

V, and IX) were pyrolyzed for comparison with the substituted polyurethans (III, IV, VII, and VIII). Approximate initial rates of decomposition (Table III) were obtained by following the rate of evolution of carbon dioxide. The evolution of carbon dioxide followed first-order rate curves to 8–14% conversion (except for polymer V, to 38% conversion). Typical graphs are given in Figure 1 and Figure 2.

A comparison of the energies of activation for formation of carbon dioxide from compounds I, II, III, and IV in Table III shows that the *N*-substituted polyurethans III and IV have greater thermal stability than the unsubstituted polymers I and II. This is notable in the case of the *N*-phenyl derivative (IV). The previously studied monomeric models,<sup>4</sup>

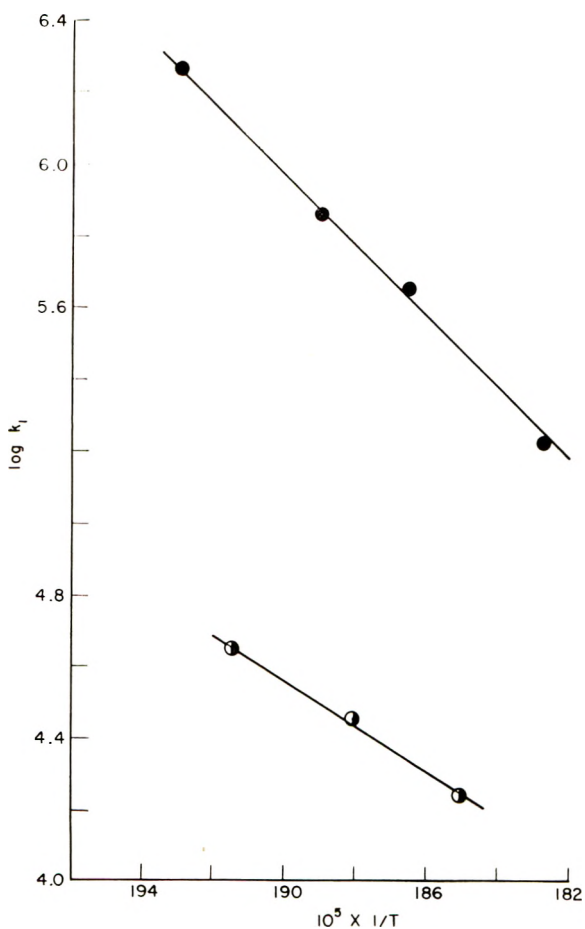


Fig. 2. Plot of  $\log k$  vs. the reciprocal of absolute temperature for (●) poly[*O*-hexamethylene-*N*(*N*-phenyl)hexamethylenedicarbamate], IV and (◐) poly[*O*-hexamethylene-*N*-hexamethylenedicarbamate], II.

*O*-hexadecyl-*N*-1-naphthylcarbamate and its *N*-1-propyl substitution product, had somewhat higher values for activation energy  $E_A$  (34 and 62 kcal./mole, respectively).

Polymers V, VII, and VIII, having aromatic units in the chain, had surprisingly low energies of activation, regardless of substitution on nitrogen. This low stability was found to be caused by amine endgroups. Polymers V and VII were shown by titration in nonaqueous medium to contain 0.36 and 0.35 mole of basic endgroups per molecule, whereas polymer II contained only 0.04 mole.\* Previous work<sup>3</sup> has shown that primary and secondary aromatic amines are powerful accelerating agents for the thermal decomposition of monomeric aromatic carbamates. For example, the addition of 50 mole-% of aniline to benzyl carbanilate reduced the half-life of a 6.0-g. sample from 7.1 hr. to 1.9 hr. at 248°C.<sup>3</sup>

\* Why the aliphatic polymers were so low in amine endgroups is not known, and will be studied further.

TABLE IV  
 Products from Pyrolysis of Polycarbamates  $\left[ \text{N}-\text{X}-\text{N} \begin{array}{c} \text{O} \\ || \\ \text{C}(\text{CH}_2)_6\text{OC} \end{array} \right]_n$  and Biscarbamates at 280°C.

No.	X	R	Time, hr.	CO <sub>2</sub> , % <sup>a</sup>	Alc., % <sup>b</sup>	Other volatiles, % <sup>c</sup>	Material balance, wt.-% <sup>d</sup>
Polymers							
II	(CH <sub>2</sub> ) <sub>6</sub>	H	14	75	76	NH <sub>2</sub> (CH <sub>2</sub> ) <sub>6</sub> NH <sub>2</sub> , trace	88
III	(CH <sub>2</sub> ) <sub>6</sub>	CH <sub>3</sub>	26	72		CH <sub>2</sub> =CHCH <sub>2</sub> CH <sub>2</sub> CH=CH <sub>2</sub> , 65 CH <sub>3</sub> NH(CH <sub>2</sub> ) <sub>6</sub> NHCH <sub>3</sub> , 20	86
V <sup>e</sup>	C <sub>6</sub> H <sub>4</sub> CH <sub>2</sub> C <sub>6</sub> H <sub>4</sub>	H	4.2	74	Trace	CH <sub>2</sub> =CH(CH <sub>2</sub> ) <sub>4</sub> OH, 32 NH <sub>2</sub> C <sub>6</sub> H <sub>4</sub> CH <sub>2</sub> C <sub>6</sub> H <sub>4</sub> NH <sub>2</sub> , 8 Cyclic carbamate, f 4.5	99
VII	C <sub>6</sub> H <sub>11</sub> CH <sub>2</sub> C <sub>6</sub> H <sub>11</sub>	CH <sub>3</sub>	5.0	63			98
Monomeric Biscarbamates							
X	[CH <sub>3</sub> (CH <sub>2</sub> ) <sub>6</sub> OCONH(CH <sub>2</sub> ) <sub>2</sub> ] <sub>2</sub>		23 <sup>g</sup>	5.3	22		94
XI	[CH <sub>3</sub> (CH <sub>2</sub> ) <sub>3</sub> OCONH <sub>2</sub> ] <sub>2</sub> CH <sub>2</sub>		3.1	51	28	CH <sub>2</sub> =CH(CH <sub>2</sub> ) <sub>3</sub> CH <sub>3</sub> , trace	99

<sup>a</sup> Calculated as mole-% of -C=O in sample.

<sup>b</sup> Mole-% of alcohol moiety, HO(CH<sub>2</sub>)<sub>6</sub>OH for polymers, C<sub>6</sub>H<sub>13</sub>OH for biscarbamates.

<sup>c</sup> Mole-% of theory for each product.

<sup>d</sup> Total wt.-% of sample, as CO<sub>2</sub>, volatiles, and residue.

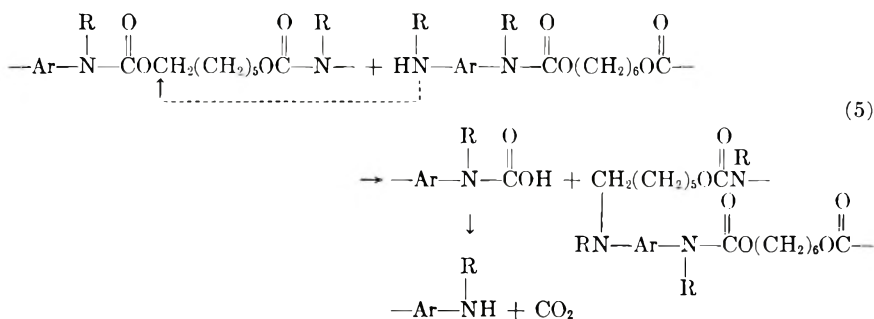
<sup>e</sup> Data of Dyer and Newborn.<sup>2</sup>

<sup>f</sup> Cyclo-O,O'-hexamethylenebis(N-methyl-4-phenylcarbamate).

<sup>g</sup> At 255°C.

Further evidence that the amine endgroup is responsible for the instability of polymers V, VII, and VIII is that polymer IX, analogous to V, but prepared in such a way as to exclude amine endgroups, had an  $E_A$  of 34 kcal./mole. This polymer, made from the diisocyanate and diol<sup>11</sup> by melt polymerization, had been treated with methanol after the reaction, and therefore could have only carbamate or hydroxyl endgroups.

Previous work<sup>3</sup> has shown that in pyrolysis of *N*-aryl monomeric carbamates a prominent location of the attack by amines is the alkyl carbon attached to the ester oxygen atom. This is unlike the aminolysis observed in solution.<sup>13-15</sup> By analogy, the accelerating action of a terminal amine group on the pyrolysis of the aromatic polycarbamates V, VII, and VIII may be assumed to proceed as shown in eq. (5):

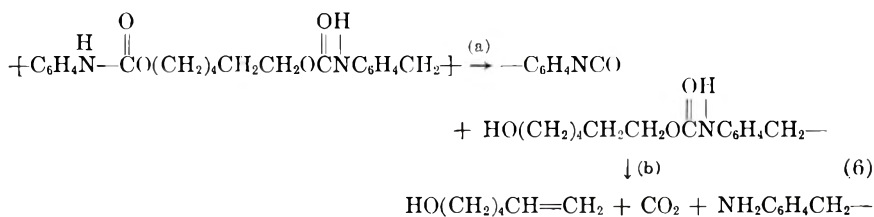


**Products of Pyrolysis.** In Table IV are shown the products from pyrolysis at 280°C. of two unsubstituted polycarbamates (II and V), of their *N*-methyl derivatives (III and VII), and of two monomeric bis-carbamates (X and XI). Quantitative determinations were made of carbon dioxide and of volatile products.

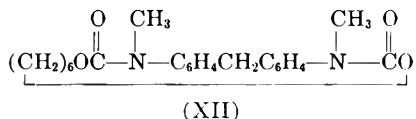
A comparison of the amounts of carbon dioxide and of other products shows that the proportion of saturated alcohol was relatively high for compounds II, X, and XI. Hence these compounds decompose to a large extent by the isocyanate path (a). These compounds did not yield secondary amines. This is in accord with the previous results on pyrolysis of *n*-butyl and neopentyl biscarbamates derived from methylenebis(4-phenyl isocyanate),<sup>2</sup> but contrary to the behavior of *O*-1-hexadecyl-*N*-1-naphthylcarbamate,<sup>4</sup> which gave large amounts of secondary amines.

Polymer III, which cannot give isocyanate and alcohol, decomposed to yield olefin and secondary amine, the same type of products as obtained from the monomeric model.<sup>4</sup> These products are explainable by a simple intramolecular displacement reaction involving a six-centered transition state.<sup>4</sup>

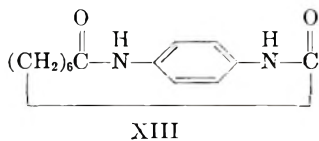
Polymer V, the aromatic analog of polymer II, yielded as major product (in addition to carbon dioxide) 1-hexene-6-ol. The formation of this substance indicates cleavage by both paths (a) and (b):



Polymer VII, also an aromatic polyurethan, yielded a small amount of a monomeric cyclic carbamate, XII. (Other products were unidentified complex residues.)

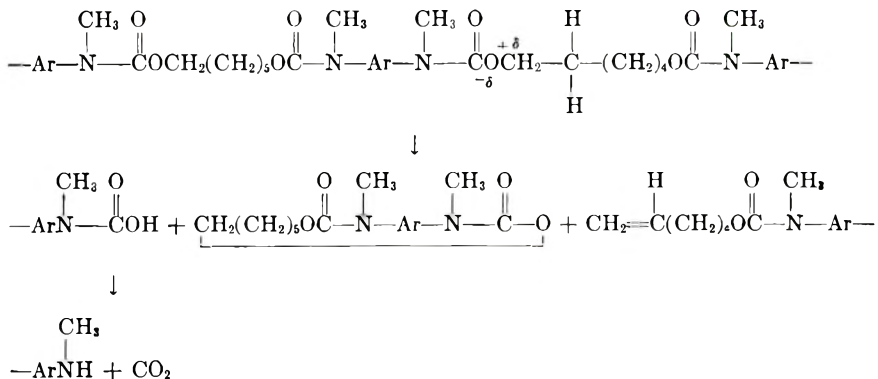


This structure is supported by analyses, molecular weight data, and infrared and nuclear magnetic resonance spectra (described below). Cyclic carbamates containing one carbamate unit are well known,<sup>16,17</sup> but examples with more than one unit are scarce. Rings of 13 or 16 atoms in which there was one carbamate and one allophanate group have been described.<sup>18</sup> A cyclic diamide, XIII, somewhat analogous to the cyclic carbamate XII, is known.<sup>19</sup> The melting point of XIII (320°C.)



is considerably higher than that of XII (256–258°C.), perhaps due to the lack of hydrogen bonding and greater flexibility in the latter compound.

The formation of the cyclic carbamate XII from polymer VII may be accounted for by alkyl-oxygen cleavage in two locations:



XII

In accord with this theory is the fact that an alkyl-oxygen cleavage is necessary to explain the formation of the olefinic alcohol, 1-hexene-6-ol, obtained from polymer V.

## EXPERIMENTAL

### Preparation of Hexane-1,6-Bischloroformate

The preparation was carried out as follows.<sup>20</sup> In a flask fitted with a Dry Ice condenser, mechanical stirrer, thermometer, and solids addition capsule was placed 300 ml. (417.6 g., 4.22 moles) of freshly distilled phosgene. After cooling to 0–5°C., the addition capsule, containing 94.4 g. (0.80 mole) of 1,6-hexanediol was manipulated in such a manner that addition of the diol did not cause the reaction temperature to exceed 5°C. Stirring at 0–5°C. was continued for 2 hr. after addition had been completed. The mixture was allowed to come to room temperature and the excess phosgene removed by gentle heating under reduced pressure. The residual liquid was run through a short column of alumina and dried with 5A Linde molecular sieves. Distillation gave 150.8 g. (78% yield) of colorless product, b.p. 108–110°C./0.6 mm. The purity was checked by treating a 1.0 g. sample with dry ammonia in toluene to give the known hexane 1,6-biscarbamate,<sup>21</sup> m.p. 186–188°C., in 98% yield (after recrystallization from water).

### Preparation of Polycarbamates

The general method was the interfacial polycondensation of 0.05 mole of redistilled diamine, dissolved in 150 ml. of water containing 0.01 mole of sodium carbonate and 1.5 g. of Duponol ME, with 0.05 mole of a solution of hexane-1,6-bischloroformate in 150 ml. of benzene in a home blender according to the procedure of Wittbecker and Katz.<sup>22</sup> In the case of water-insoluble diamines, a solution of 0.05 mole of the diamine in 50 ml. of benzene was used with the other reactants, except that the amount of benzene for the chloroformate was reduced to 100 ml. The polymers were separated by filtration or by evaporation of the reaction solution. Purification was accomplished by reprecipitation from an organic solvent with water and from an organic solvent with an organic nonsolvent. Properties are given in Table I and results of analyses in Table II.

Poly(*O*-hexamethylene-*N*-pentamethylenedicarbamate), I, and poly(*O*-hexamethylene-*N*-hexamethylenedicarbamate), II, were separated by filtration and reprecipitated once from dimethylformamide with water and twice from dimethylformamide with acetone.

Poly[*O*-hexamethylene-*N*-(*N*-methyl)-hexamethylenedicarbamate], III, was prepared from *N,N'*-dimethyl-1,6-hexanediamine.<sup>23</sup> The product was obtained as a yellow viscous mass by evaporation of the reaction solution to dryness at 50°C. and precipitation of the residue from acetone by water, then from acetone by *n*-hexane (twice).

Poly[*O*-hexamethylene-*N*-(*N*-phenyl)-hexamethylenedicarbamate], IV, poly[*O*-hexamethylene methylenebis(3-methyl-4-phenylcarbamate)], VI, poly[*O*-hexamethylene methylenebis(*N*-methyl-4-phenylcarbamate)], VII, poly[*O*-hexamethylene methylenebis(*N*-butyl-4-phenylcarbamate)], VIII, were prepared from the following water-insoluble diamines: *N,N'*-diphenyl-1,6-hexanediamine,<sup>24</sup> 4,4'-diamino-3,3'-dimethyldiphenyl-

methane,<sup>25</sup> *N,N'*-dimethyl-4,4'-diaminodiphenylmethane,<sup>25</sup> and *N,N'*-di-*n*-butyl-4,4'-diaminodiphenylmethane,<sup>25</sup> respectively. Products, isolated and purified in the same way as polymer III, were polymer IV, as a white rubbery liquid, polymer VI, as a tan powder, polymer VII, as a white, flexible solid, and polymer VIII as a viscous brown oil.

Poly[*O*-hexamethylene methylenebis(4-phenylcarbamate)], V, prepared from 4,4'-methylenedianiline, was purified by solution in dimethylformamide and precipitated first with water, then twice with methanol. The product was a tan powder.

### Preparation of Biscarbamates

**a. *O,O'*-Dihexamethylene *N,N'*-Hexamethylene Dicarbamate (X).** A solution of 16.5 g. (0.1 mole) of freshly distilled 1-hexylchloroformate, 7.9 g. (0.1 mole) of pyridine, and 75 ml. of benzene was slowly stirred while a solution of 5.8 g. (0.05 mole) of 1,6-hexanediamine in 75 ml. of benzene was added over a 30-min. period. Stirring was continued for an additional 30 min. and the solution washed with two 100-ml. portions of water. The benzene solution was evaporated to dryness and the residue recrystallized from ether. The white crystalline biscarbamate, m.p. 94–96°C., was obtained in 34% yield.

**b. *O,O'*-Dihexamethylene Methylenebis(4-Phenylcarbamate) (XI).** A solution of 9.4 g. (0.047 mole) of 4,4'-methylenedianiline in 50 ml. of benzene was added to a solution of 10.6 g. (0.10 mole) of sodium carbonate, 1.5 g. of Duponol M.E. Detergent and 150 ml. of water. The mixture was stirred at high speed and a solution of 16.5 g. (0.10 mole) of 1-hexylchloroformate in 100 ml. of benzene was rapidly added. After 15 min. of stirring, the organic phase was separated, evaporated to dryness, and the residue extracted for 24 hr. with *n*-hexane. The extract yielded 7.0 g. (34%) of white crystalline biscarbamate melting at 108–100°C.

**Cyclo-*O,O'*-hexamethylene Methylenebis(*N*-methyl-4-phenylcarbamate) (XII).** This white crystalline compound, m.p. 256–258°C., was obtained by pyrolysis of polymer VII. It was soluble in chloroform, acetone and *n*-pentane. The infrared spectrum showed carbonyl absorption at 1720 cm.<sup>-1</sup> and no —NH or —OH absorption. The NMR spectrum (Fig. 3) indicates four CH<sub>2</sub> groups of the same kind (peak 1), two identical CH<sub>3</sub> groups (peak 2), three CH<sub>2</sub> groups where splitting indicates different neighbors (peak 3) and eight aromatic protons (peak 4). A Varian Associates Model A-60 instrument was used with deuteriochloroform as the solvent.

ANAL. Calc. for C<sub>23</sub>H<sub>28</sub>N<sub>2</sub>O<sub>4</sub>: C, 69.67%; H, 7.12%; N, 7.06%; molecular weight, 396. Found: C, 69.89%; H, 7.04%; N, 7.19%; molecular weight (Rast in camphor) 394.

### Preparation of Di-*N*-substituted Carbamates

These new compounds were synthesized for comparison.

**a. *O*-Ethyl *N*-1-Hexyl-*N*-1-Naphthylcarbamate (XIII).** A solution of 11.4 g. (0.50 mole) of *N*-1-hexyl-1-naphthylamine, 27.3 g. (0.252 mole)

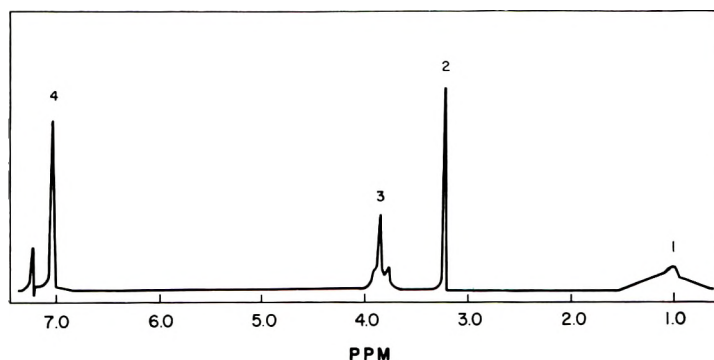


Fig. 3. Nuclear magnetic resonance spectrum of cyclo-*O,O'*-hexamethylene methylenebis-(*N*-methyl-4-phenylcarbamate).

of freshly distilled ethyl chloroformate, and 50 ml. of dry dioxane was refluxed for 18 hr. After removal of solvent, fractionation yielded 9.0 g. (84% yield) of product, b.p. 183–185°C./2 mm.

**b. *O*-Ethyl *N*-Phenyl-*N*-1-Naphthylcarbamate (XIV).** A mixture of 21.9 g. (0.10 mole) of *N*-phenyl-1-naphthylamine and 5.45 g. (0.05 mole) of ethyl chloroformate was heated at 100°C. for 80 hr. Acetone was added, the precipitate removed, and the acetone extract evaporated. The residue was extracted with *n*-pentane for 72 hr. The pentane extract was distilled giving a fraction boiling at 165–175°C./0.35 mm., which was recrystallized from *n*-pentane. The crystalline product, m.p. 105–107°C., was obtained in 90% yield (13.0 g.).

**c. *O*-Hexadecyl *N*-1-Hexyl-*N*-1-Naphthylcarbamate (XV).** This compound was prepared in 8% yield by the alkylation procedure of Dannley and Lukin.<sup>26</sup> It boiled at 269–272°C./1.5 mm.

### Pyrolysis Procedure

A 1.0-g. sample of the carbamate was heated in a 2.5 × 30 cm. Pyrex tube that had been dried for 30 min. at operating temperature. The tube was fitted with an inlet tube for dry, oxygen-free nitrogen and an exit tube leading to a microtrap cooled in Dry Ice and acetone, followed by Ascarite-filled absorption tubes. The heating bath was an insulated cylindrical aluminum block, 8 in. high and 6 in. in diameter, drilled to contain the reaction tube, a thermometer, twelve 50-w. cartridge heaters, and a Fenwal bimetallic thermoregulator. The heaters, operated through a relay-controlled Variac and the regulator, kept the temperature in the reaction tube constant to ±0.25°C.

Weights of carbon dioxide were obtained periodically. When the reaction was stopped, the residue in the pyrolysis tube was weighed, but not investigated further. Sublimate on the walls of the reaction vessel was collected, and products in the cold trap were determined quantitatively, chiefly by vapor-phase chromatography with the use of the peak enhancement technique. A 10-ft. silicone oil column proved satisfactory in the separation of 1-hexene-6-ol and 1,5-hexadiene. A flow rate of 40 ml./min.



of helium through a Wilkens Instrument and Research, Inc. Aerograph-Master A-100 gave the best results for these compounds. It was necessary, however, to use the Perkin-Elmer vapor fractometer Model 154 with a column of dotriacontane on glass beads for the identification of the two aliphatic diamines (1,6-hexanediamine and its *N,N'*-dimethyl derivative). Peak areas were used as a measure of relative concentrations.

### Titration for Amine Endgroups

Titrations for amine endgroups were done on polymers II, V, and VII, 0.1*N* perchloric acid in glacial acetic acid being used as titrant and methyl violet as indicator.<sup>27</sup> The polymers were dissolved by heating in glacial acetic acid at 70°C. and cooling before titration. A control analysis on the model biscarbamate XI showed that no degradation occurred under these conditions, and a control analysis on *N,N'*-dimethyl-4,4'-methylenedianiline showed that no acetylation of the amine occurred and that the accuracy of the method was within 0.2%. On polymer samples the precision was better than 2%.

For calculation of the amine group content, the observed molecular weights of polymers II and VII (8000 and 2500, respectively) were used. Polymer V, for which only the intrinsic viscosity is known, was assumed to have a molecular weight of 10,000. The values found for Moles of NH<sub>2</sub> per mole of polymer were II, 0.04; V, 0.36; VII, 0.35.

The authors are indebted to the Armstrong Cork Company for a fellowship in support of this research, and to Drs. L. H. Dunlap, J. A. Parker, and H. C. Beachell for helpful discussions.

### References

1. Fletcher, M. A., M. W. Lakin, and S. G. P. Plant, *J. Chem. Soc.*, **1953**, 3898.
2. Dyer, E., and G. E. Newborn, *J. Am. Chem. Soc.*, **80**, 5495 (1958).
3. Dyer, E., and G. C. Wright, *J. Am. Chem. Soc.*, **81**, 2138 (1959).
4. Dyer, E., and R. E. Read, *J. Org. Chem.*, **26**, 4388 (1961).
5. Dyer, E., and D. W. Osborne, *J. Polymer Sci.*, **47**, 349 (1960).
6. Goldberg, E. J., U. S. Pat. 2,927,098 (1960).
7. Cluff, E. F., U. S. Pat. 2,913,496 (1959).
8. Katz, M., U. S. Pat. 2,929,802 (1960).
9. Frazer, A. H., and E. J. Goldberg, U. S. Pat. 2,888,440 (1959).
10. Jones, W. D., and S. B. McFarlane, U. S. Pat. 2,660,574 (1953).
11. Dyer, E., and D. W. Osborne, *J. Polymer Sci.*, **47**, 369 (1960).
12. Biggs, B. S., C. J. Frosch, and R. H. Erickson, *Ind. Eng. Chem.*, **38**, 1016 (1946).
13. Dyer, E., and G. W. Bartels, *J. Am. Chem. Soc.*, **76**, 591 (1954).
14. Reilly, C. B., *Univ. Microfilms*, Publ. No. 24799 (1957).
15. Mukaiyama, T., and Y. Hoshino, *J. Am. Chem. Soc.*, **78**, 1946 (1956).
16. Hall, H. K., Jr. and A. K. Schneider, *J. Am. Chem. Soc.*, **80**, 6409 (1958).
17. Delaby, R., R. Damiens, and G. d'Huyteza, *Compt. Rend.*, **239**, 674 (1954).
18. Viard, M. J., U. S. Pat. 2,703,810 (1955).
19. Stetter, H., and L. Marx-Moll, *Ber.*, **91**, 677 (1952).
20. Hoshino, T., and I. Ichikizaki, *Chem. High Polymer (Japan)*, **2**, 328 (1945).
21. Baird, W., P. Gaubert, and A. Lowe, Brit. Pat. 614,295 (1948).
22. Wittbecker, E. L., and M. Katz, *J. Polymer Sci.*, **40**, 374 (1959).
23. Shashoua, V. E., and W. M. Eareckson, *J. Polymer Sci.*, **40**, 345 (1959).
24. Billman, J. H., and L. R. Caswell, *J. Org. Chem.*, **16**, 1041 (1951).

25. Wagner, E. C., *J. Am. Chem. Soc.*, **56**, 1944 (1934).  
 26. Dannley, R. L., and M. Lukin, *J. Org. Chem.*, **22**, 268 (1953).  
 27. Siggia, S., *Quantitative Analysis via Functional Groups*, 2nd Ed., Wiley, New York, 1954, p. 105.

### Résumé

Des polycarbamates *N*-substitués, de poids moléculaire relativement bas, ont été préparés par condensation du 1,6-hexanebischloroformite avec des diamines *N*-substituées, aussi bien aliphatiques qu'aromatiques. Les vitesses de dégradation thermique de ces polymères et de polymères analogues non-substitués ont été déterminées à 230–285°C en suivant le dégagement d'anhydride carbonique. Les résultats montrent que les polymères les plus stables thermiquement sont ceux dérivés des diamines aliphatiques substituées, de formule  $[-N(R)-X-N(R)-COO(CH_2)_6OCO-]_n$ , où X est  $(CH_2)_5$  ou  $(CH_2)_6$ . Lorsque R est  $-CH_3$  et  $-C_6H_5$ ,  $E_A$  est de 31 et 46 kcal/mole. Les polymères dérivés des diamines aromatiques, où X est 4,4'- $C_6H_4CH_2C_6H_5$ , présentent de faibles valeurs de  $E_A$ , de l'ordre de 15 kcal/mole, que R soit H ou un groupement alcoyle. Cette faible stabilité thermique est causée par les groupes amine terminaux. On a pu mettre en évidence les différents processus de dégradation thermique, à partir d'une étude des produits volatils.

### Zusammenfassung

Verhältnismässig niedermolekulare *N*-substituierte Polycarbamate wurden durch Kondensation von 1,6-Hexanbischloroformiat mit aliphatischen und aromatischen *N*-substituierten Diaminen dargestellt. Die Geschwindigkeit des thermischen Abbaus dieser Polymeren und von unsubstituierten Analogen wurde durch Messung der Kohlendioxydentwicklung bei 230–285°C bestimmt. Die Ergebnisse zeigten, dass die von substituierten aliphatischen Diaminen abgeleiteten Polymeren mit der Formel  $[-N(R)-X-N(R)-COO(CH_2)_6OCO-]_n$ , wo X  $(CH_2)_5$  oder  $(CH_2)_6$  bedeutet, die thermisch stabileren waren. Für R gleich  $-CH_3$  und  $-C_6H_5$  betrug die Bruttoaktivierungsenergie  $E_A$  31 bzw. 46 kcal/Mol. Die von aromatischen Diaminen abgeleiteten Polymeren mit X gleich 4,4'- $C_6H_4CH_2C_6H_5$  zeigten unabhängig davon, ob R gleich H oder Alkyl war, niedrige Werte für  $E_A$ , etwa bei 15 kcal/Mol. Diese geringe thermische Stabilität konnte auf die Aminoendgruppen zurückgeführt werden. Einige Hinweise auf den Mechanismus des thermischen Abbaus wurden durch eine Untersuchung der flüchtigen Produkte erhalten.

Received September 19, 1962

Revised October 31, 1962

## Preparation and Properties of Poly(tetramethyl-*p*-Silphenylene-Siloxane)

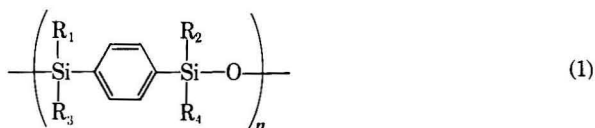
ROBERT L. MERKER and MARY JANE SCOTT, *Mellon Institute,  
Pittsburgh, Pennsylvania\**

### Synopsis

Improved methods for the synthesis of *p*-bis(dimethylhydroxysilyl)benzene are described. This useful monomer was prepared from *p*-bis(dimethylhydrogensilyl)benzene which was obtained in 60–70% yields from *p*-dibromobenzene and dimethylchlorosilane by use of an *in situ* Grignard technique. The great reluctance due to steric factors of the *p*-silphenylene-siloxane configuration to form cyclic structures has been amply demonstrated. The condensation polymerization of *p*-bis(dimethylhydroxysilyl)benzene in benzene solution has yielded high molecular weight, crystalline poly(tetramethyl-*p*-silphenylene-siloxanes). The heat of fusion  $\Delta H_u$  of the tetramethyl-*p*-silphenylene-siloxane was found to be 4350 cal./unit. The modified Staudinger equation relating intrinsic viscosity and weight-average molecular weight was applicable over a range of 70,000–400,000. These results are summarized in the relationship,  $[\eta] = 1.12 \times 10^{-4} M_w^{0.75}$ . Tetramethyl-*p*-silphenylene-siloxanes were found to be more stable than dimethylsiloxanes both to atmospheric oxidation and degradation through volatile formation in the temperature range 200–305°C.

### INTRODUCTION

In the search for new and useful silicone polymers the *p*-silphenylene-siloxanes possessing the structure,



have recently received considerable attention. However, to date no reproducible method for the preparation of truly high molecular weight polymers has been reported, nor are published methods of synthesizing possible monomers entirely satisfactory. The condensation of trisubstituted silanes with benzene in the presence of aluminum trichloride or boron trichloride has been accomplished yielding mixtures of isomeric derivatives.<sup>1-3</sup> Sveda has obtained *p*-bis(diphenylchlorosilyl)benzene and *p*-bis(dimethylchlorosilyl)benzene by means of a Grignard reaction with *p*-dibromobenzene and the appropriate chlorosilane and also reports the

\* Multiple Fellowship on Silicones sustained by the Dow Corning Corporation and Corning Glass Works.

preparation of poly(tetramethyl-*p*-silphenylene-siloxane).<sup>4,5</sup> However, no information concerning yields, reproducible methods of polymerization, molecular weight, thermal stability, etc., was revealed. Gainer<sup>6</sup> describes the preparation of *p*-bis(dichloromethylsilyl)benzene by a di-Grignard reaction and reports a yield of 10%.

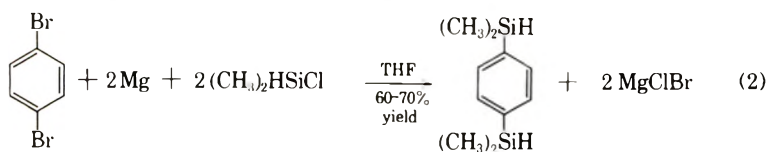
A recent publication of Breed<sup>7</sup> and associates reports 30–40% yields of *p*-bis(diethoxymethylsilyl)benzene by means of a di-Grignard reaction in which chlorodiethoxymethylsilane and *p*-dibromobenzene in tetrahydrofuran solution were added concomitantly to the magnesium. When diethoxydimethylsilane was substituted for chlorodiethoxymethylsilane in the above reaction, a yield of 19.7% *p*-bis(ethoxydimethylsilyl)benzene was obtained. The method developed by Breed and co-workers closely approximates the synthetic methods developed in this laboratory and used over the past four years for the preparation of *p*-silphenylene intermediates.

Price<sup>8</sup> has carried out crystallographic studies on poly(tetramethyl-*p*-silphenylene-siloxane) of about 50,000 molecular weight, the highest heretofore reported. No details of monomer preparation or methods of polymerization were disclosed.

This paper presents improved methods for the synthesis of intermediates convertible to monomers which on polymerization yield linear polymers having the structure shown in (1), where R<sub>1</sub>, R<sub>2</sub>, R<sub>3</sub>, and R<sub>4</sub> are methyl (CH<sub>3</sub>) groups and discusses the polymerization of these monomers and the properties of the resulting high molecular weight crystalline homopolymer. A second paper<sup>9</sup> describes both random and block copolymers of tetramethyl-*p*-silphenylene-siloxane and dimethylsiloxane.

### In Situ Grignard Preparation of *p*-Bis(dimethylhydrogensilyl)benzene

The general method for the synthesis of the above intermediate involves the formation of the Grignard reagent in the presence of the chlorosilane.



The addition of *p*-dibromobenzene in tetrahydrofuran solution to the magnesium shavings dispersed in a solution of dimethylchlorosilane in tetrahydrofuran tends to minimize undesirable Grignard side reactions, since Grignard formation and subsequent coupling with the chlorosilane occur in sequence throughout the reaction. Dimethylchlorosilane is preferable to dimethyldichlorosilane or dimethyldiethoxysilane, since the latter two silanes yield considerable amounts of polycoupled *p*-silphenylenes, i.e., (CH<sub>3</sub>)<sub>3</sub>XSi[*p*-C<sub>6</sub>H<sub>4</sub>Si(CH<sub>3</sub>)<sub>2</sub>]<sub>*n*</sub>X, where X is Cl or OCH<sub>2</sub>CH<sub>3</sub>. Dimethylchlorosilane also offers another distinct advantage, since the magnesium salts can be removed from the Grignard reaction mixture through water

washing techniques prior to distillation without the formation of polymeric *p*-silphenylene-siloxanes.

The yields of *p*-bis(dimethylhydrogensilyl)benzene were somewhat reduced because the dimethylchlorosilane employed contained some trichlorosilane as well as smaller amounts of other chlorosilanes which could not be removed by distillation. A better indication of the value of this *in situ* technique can be seen in yields as high as 86% in the preparation of *p*-bis(trimethylsilyl)benzene in which the more easily purified trimethylchlorosilane was used.

### Monomers

Cyclic structures of tetramethyl-*p*-silphenylene-siloxane would be convenient monomer units to which existing polymerization techniques could be easily applied. McKay<sup>10</sup> has described the preparation of  $[(\text{CH}_3)_2\text{Si}-p\text{-C}_6\text{H}_4\text{-Si}(\text{CH}_3)_2\text{O}]_2$  in low yield through the trifluoroacetic acid-catalyzed condensation of  $\text{HO}(\text{CH}_3)_2\text{Si}-p\text{-C}_6\text{H}_4\text{-Si}(\text{CH}_3)_2\text{OH}$  in dilute benzene solution. Repeated attempts in this laboratory to obtain reasonable yields of cyclic tetramethyl-*p*-silphenylene-siloxanes through the hydrolysis of *p*-bis-(dimethylhydrogensilyl)benzene or condensation of *p*-bis(dimethylhydroxysilyl)benzene in dilute solution were not successful. The predominant products in both cases, even in extremely dilute solution (ca. 2 wt.-%) were linear polymers of low molecular weight (2000-7000). Only one of these experiments is described in the experimental section because of the negative nature of the results.

Thermal cracking of these low molecular weight polymers yielded the dimer and trimer cyclics in the presence of lithium hydroxide and largely the dimer cyclic in the presence of sodium hydroxide. Overall yields of cyclics based on the amount of polymer were extremely low, so that in spite of the fact that these cyclics could be easily polymerized to very high molecular weight polymers, this general approach was not felt to be satisfactory.

The dilute solution conversion of *p*-bis(dimethylhydroxysilyl)benzene to linear polymer demonstrates the strong preference shown by this group for intermolecular hydroxyl condensation rather than intramolecular hydroxyl condensation. Also, the linear polymers so formed show extreme reluctance to yield cyclic siloxanes under the influence of high temperatures and alkali metal catalysts. This is in sharp contrast to the behavior of typical dialkyldihalosilanes which yield almost exclusively cyclic dialkylsiloxanes on hydrolysis in dilute solution. Polydialkylsiloxanes, under the influence of heat and alkali metal catalysts, can be converted almost quantitatively to cyclic dialkylsiloxanes. One might, therefore, suggest that the steric factors which contribute to the strong reluctance of the *p*-silphenylene-siloxane configuration to form cyclic structures should also give rise to linear polymers manifesting an extremely high degree of thermal stability, since intramolecular unzipping of polymer chains to yield cyclics and polymers of lower molecular weight is definitely impeded.

This attribute of *p*-silphenylene-siloxane polymers necessitated the search for a monomer other than the cyclic dimer or trimer. However, eventually, through modification of a procedure developed by Hyde and associates<sup>11</sup> for the polymerization of  $\text{HO}[(\text{CH}_3)_2\text{SiO}]_n\text{H}$ , it was found possible to achieve high molecular weight polymers through the condensation polymerization of *p*-bis(dimethylhydroxysilyl)benzene.

Either of two methods has been employed for the preparation of *p*-(bisdimethylhydroxysilyl)benzene from *p*-bis(dimethylhydroxysilyl)benzene. In the first, the initial step involved the preparation of *p*-bis(dimethyl-ethoxysilyl)benzene from *p*-bis(dimethylhydroxysilyl)benzene in the conventional way by refluxing in absolute ethanol and employing sodium ethoxide as catalyst. This reaction mixture was then hydrolyzed in aqueous pyridine solution to give a 74% yield of product.

In the second procedure, the reaction products from the *p*-bis(dimethyl-ethoxysilyl)benzene preparation were hydrolyzed in 90% methanol which contained 15 wt.-% sodium hydroxide. This mixture was then neutralized with excess potassium phosphate solution and an 85% yield of product isolated.

## EXPERIMENTAL

### Materials

Tetrahydrofuran used in this work was dried by distillation from lithium aluminum hydride. J. T. Baker magnesium turnings and Eastman *p*-dibromobenzene were used without further purification. Dimethylchlorosilane and trimethylchlorosilane obtained from the Dow Corning Corporation were redistilled. The potassium phosphate used was monobasic (crystal), from J. T. Baker.

### *In Situ* Grignard Reactions

**Preparation of *p*-Bis(dimethylhydroxysilyl)benzene.** To 36.5 g. magnesium (1.5 g.-atom) and 212.5 g. dimethylchlorosilane (2.25 moles) in 180 ml. of tetrahydrofuran in a three-necked flask was added dropwise a solution of 177 g. *p*-dibromobenzene (0.75 mole) in 300 ml. tetrahydrofuran. The reaction products were refluxed 1 hr., poured over crushed ice, washed with water, and dried over sodium sulfate. The solvents were removed and the mixture distilled. A 65.9% of theory yield 95.6 g. of *p*-bis(dimethylhydroxysilyl)benzene was obtained:  $n_D^{25}$  1.5007;  $d_4^{25}$  0.8832;  $R_D$  found 0.3332,  $R_D$  calc. for *p*-bis(dimethylhydroxysilyl)benzene 0.3316. The structure was confirmed by  $\text{H}^1$  NMR spectral analysis.

**Preparation of *p*-Bis(trimethylsilyl)benzene.** In a three-necked reaction flask were placed 10.3 g. (0.424 g.-atom) magnesium, 57.5 g. trimethylchlorosilane, and 75 ml. tetrahydrofuran. To this was added dropwise a solution of 50 g. (0.212 mole) of *p*-dibromobenzene in 75 ml. tetrahydrofuran. In the usual way, the reaction mixture was refluxed for 1 hr., poured over cracked ice, washed with water, and dried over an-

hydrous sodium sulfate. Removal of solvents revealed a crystalline product which was purified by two recrystallizations from absolute ethanol. A yield of 86%, 40.5 g. of *p*-bis(trimethylsilyl)benzene was obtained: m.p. 97–98°C. (uncorr.); cryoscopic molecular weight found 227, theory 222.

### Cyclic Monomers

#### Hydrolysis of *p*-Bis(dimethylhydrogensilyl)benzene in Aqueous Ethanol.

To a refluxing mixture of 17.7 g. water, 309 ml. absolute alcohol and 1 g. KOH was added dropwise 66.1 g. (0.34 mole)  $\text{H}(\text{CH}_3)_2\text{Si}-p\text{C}_6\text{H}_4-\text{Si}(\text{CH}_3)_2\text{H}$ . After the evolution of a theoretical volume of hydrogen and removal of most of the ethanol, a nearly quantitative yield of white powdery polymer was filtered off and recrystallized from 50% by volume absolute ethanol and hexane. The cryoscopic molecular weight as measured in benzene was about 2,200.

**Thermal Cracking.** In thermal cracking, 1 g. NaOH, 40 g. toluene, and 49 g. low molecular weight polymeric powders—the combined products of hydrolysis reactions employing various alcohols as solvents—were refluxed at 180–200°C. for 1 hr. while water was being removed through an azeotrope trap. Following removal of the toluene, thermal cracking (300–350°C.) at ultimate vacuum yielded 2 g. dimer cyclic (4%). This material was recrystallized three times from absolute ethanol, white cottony crystals: m.p. 208°C.; cryoscopic molecular weight found 420, theory 416.

Similar experiments with LiOH yielded a mixture of dimer and trimer cyclics; m.p. 128–129°C.; yield 10–30%; cryoscopic molecular weight found 550, theory for trimer 624. Based on the melting point and molecular weight data, this material is probably largely trimer. Structures of the above compounds were also confirmed by their  $H^1$  NMR spectra.

#### Preparation of *p*-Bis(dimethylhydroxysilyl)benzene

To 5 g. of refluxing absolute ethanol which contained a small pellet of metallic sodium was added dropwise 5 g. of *p*-bis(dimethylhydrogensilyl)benzene. The reaction mixture was neutralized with glacial acetic acid then added to a solution of 14 ml. pyridine and 4 ml. water. After five days the mixture was diluted with benzene and washed with water. The solvents were removed and the residue recrystallized from hexane-tetrahydrofuran, yielding 4.3 g. of product (74% of theory) m.p. 139°C.

To 200 ml. refluxing absolute ethanol which contained a small piece of sodium, 194 g. (1 mole) *p*-bis(dimethylhydrogensilyl)benzene was added dropwise. After the evolution of hydrogen had ceased, the reaction products were poured with constant stirring into a mixture of 116 g. NaOH, 700 ml.  $\text{CH}_3\text{OH}$ , and 77 ml.  $\text{H}_2\text{O}$ . To this was added a solution of 116 g. NaOH in 777 ml.  $\text{H}_2\text{O}$ . After standing 30 min., this mixture was poured with constant stirring into a solution of 1030 g.  $\text{KH}_2\text{PO}_4$  in excess ice and water. The precipitate which immediately formed was removed by filtra-

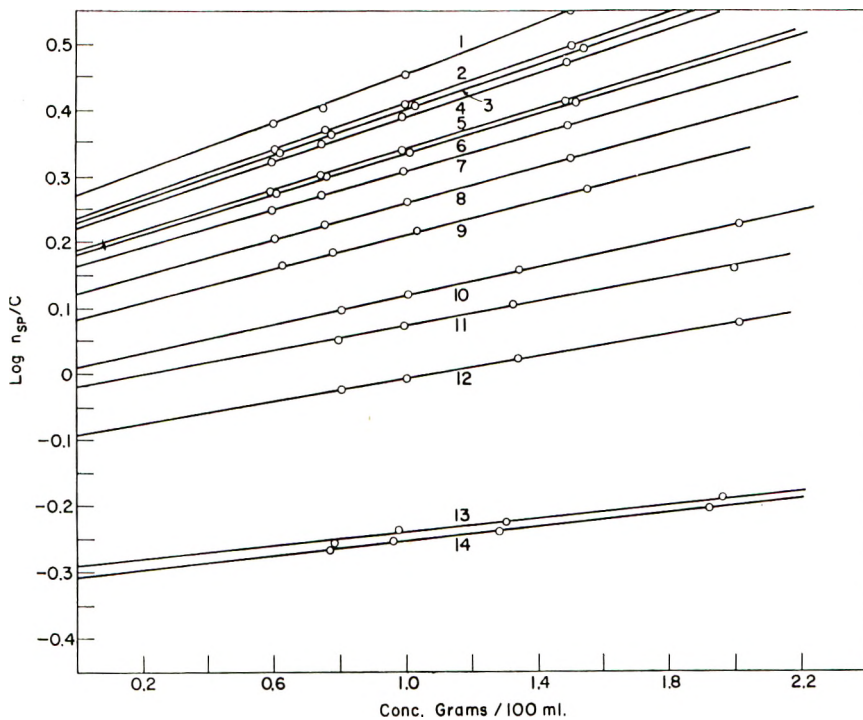
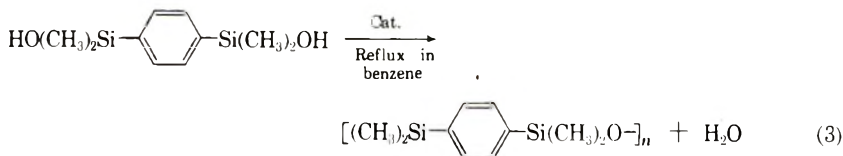


Fig. 1. Viscometric data for tetramethyl-*p*-silphenylene-siloxane polymer fractions. (Fraction numbers correspond to those of Table I.)

tion, dissolved in tetrahydrofuran, and washed with water. Evaporation of solvents revealed 220 g. crude products which were recrystallized from a mixture of hexane and tetrahydrofuran, giving a final yield of 191.6 g., 85% of theory.

### Methods of Polymerization

**1. From  $\text{HO}(\text{CH}_3)_2\text{Si}-p\text{-C}_6\text{H}_4\text{-Si}(\text{CH}_3)_2\text{OH}$ .** Because of the greater accessibility of the monomer species, the most convenient route to high molecular weight polymer is by refluxing 66% by weight of *p*-bis(dimethylhydroxylsilyl)benzene in benzene with 1 wt.-% (based on diol) of the catalyst, *n*-hexylamine 2-ethylhexoate.<sup>11</sup>



The water is removed azeotropically as formed. After 5 hr. reflux and removal of solvent a very tough, fiber-forming, high molecular weight polymer is the result. All subsequent studies conducted have employed polymers prepared by this method.



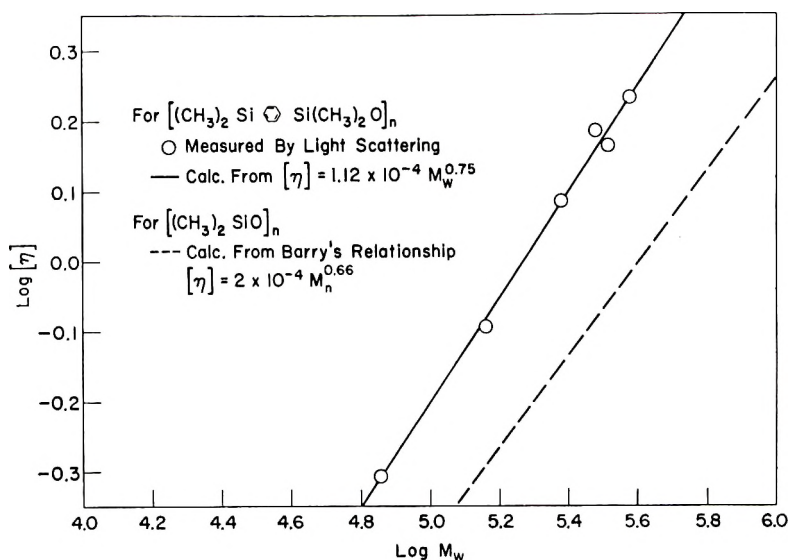


Fig. 2. Intrinsic viscosity-molecular weight relationship.

**2. From cyclics,  $[(\text{CH}_3)_2\text{Si-p-C}_6\text{H}_4\text{-Si}(\text{CH}_3)_2\text{O-}]_2$  or  $[(\text{CH}_3)_2\text{Si-p-C}_6\text{H}_4\text{-Si}(\text{CH}_3)_2\text{O-}]_3$ .** A mixture of dimer and trimer cyclics obtained by thermal cracking of the corresponding low molecular weight polymers along with a toluene solution of potassium dimethylsilanolate<sup>12</sup> (0.01 wt.-%  $\text{K}_2\text{O}$  based on cyclics) was introduced into a polymerization tube. After exhausting the toluene, the tube was sealed under vacuum and heated at  $180^\circ\text{C}$ . Within 15 min. a great increase in viscosity could be observed, and after 5 hr. a very strong, fiber-forming polymer, soluble in benzene, was removed from the tube.

## PROPERTIES OF HIGH MOLECULAR WEIGHT POLYMER

### Intrinsic Viscosity-Molecular Weight Relationship

The fractionation of high molecular weight poly(tetramethyl-*p*-silphenylene-siloxane) obtained by method No. 1 above was accomplished at  $35^\circ\text{C}$ . by the addition of 99% methanol/1% water by volume to a 2.9 wt.-% polymer solution in benzene. The percentage of water employed was found to be very critical in insuring the separation of a polymer-benzene phase rather than a crystalline polymer phase. Solid precipitates must be avoided in the fractionation of crystalline polymers since not only equilibrium solubility but rate of crystallization determines selection of molecules for the newly formed phase. Because of these opposing tendencies, it has been reported<sup>13</sup> that intermediate fractions may even exceed in molecular weight those removed earlier. Fractionation data obtained by this procedure are presented in Table I.

Solutions of approximately  $1\frac{1}{2}$ -2% of each polymer fraction in dry

TABLE I  
Molecular Distribution Data for Poly(Tetramethyl-*p*-Silphenylene-Siloxane)

Fraction No.	Wt. polymer, g. <sup>a</sup>	Polymer, % based on 38.6 g. total	Cumulative % polymer	$[\eta]$ , dl./g.	Mol. wt. <sup>b</sup> $\times 10^{-5}$
1	2.4	6.2	100.0	1.86	4.31
2	5.7	14.8	93.8	1.71	3.89
3	4.4	11.4	79.0	1.69	3.80
4	1.8	4.7	67.6	1.66	3.71
5	2.9	7.5	62.9	1.53	3.31
6	3.2	8.3	55.4	1.52	3.27
7	1.8	4.7	47.1	1.46	3.12
8	2.5	6.5	42.4	1.32	2.72
9	3.2	8.3	35.9	1.22	2.45
10	1.9	4.9	27.6	1.03	1.97
11	2.3	5.8	22.7	0.962	1.77
12	2.0	5.2	16.9	0.807	1.41
13	2.0	5.2	11.7	0.508	0.758
14	2.5	6.5	6.5	0.495	0.722
Total	38.6				

<sup>a</sup> Total grams raw polymer fractionated = 40.0.

<sup>b</sup> Calculated from  $[\eta] = 1.12 \times 10^{-4} M_w^{0.75}$ .

filtered toluene were used for intrinsic viscosity determinations. The viscosity of each was measured in a Cannon-Ubbelohde dilution viscometer and measured again after each of three dilutions with known volumes of toluene. The temperature control was provided by a water bath at 25°C.  $\pm 0.2^\circ$ . From these measurements were calculated specific viscosities and from a plot of concentration (in grams/100 ml.) against  $\log \eta_{sp}/c$  the intrinsic viscosities were determined. This graph is shown in Figure 1 and the intrinsic viscosity values ranging from 1.86 to 0.495 are given in Table I.

The molecular weights of six fractions over a range of approximately 70,000 to 400,000 were then determined by light scattering. These data are listed in Table II. A plot of  $\log$  intrinsic viscosity  $[\eta]$ , for poly-(tetramethyl-*p*-silphenylene-siloxane) in toluene solution versus the  $\log$  of the weight-average molecular weight is shown in Figure 2.

TABLE II  
Molecular Weights Determined by Light Scattering of Fractions of Tetramethyl-*p*-Silphenylene-Siloxane Polymer

Fraction <sup>a</sup>	$[\eta]$	$M_w \times 10^{-5}$
2	1.71	3.75
5	1.53	3.03
7	1.46	3.27
9	1.22	2.39
12	0.807	1.45
14	0.495	0.716

<sup>a</sup> Corresponds to numbers used in Table I.

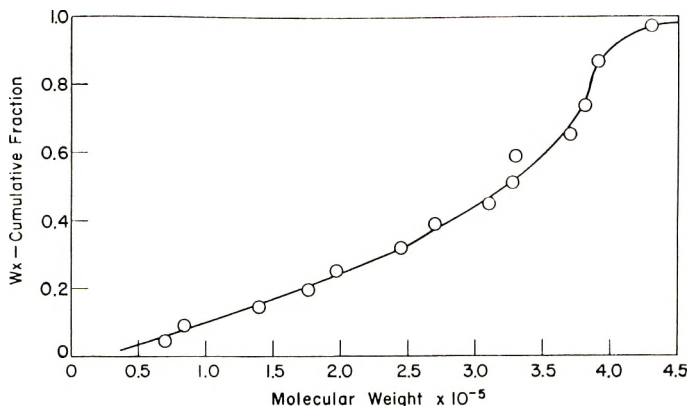


Fig. 3. Integral molecular weight distribution curve for  $[(\text{CH}_3)_2\text{Si-}p\text{-C}_6\text{H}_4\text{-Si}(\text{CH}_3)_2\text{O}]_n$ .

Since the data fall on a straight line, the modified version

$$[\eta] = K' M_w^a \quad (4)$$

of the Staudinger equation is clearly applicable over the molecular weight range investigated. From the slope of the straight line and its intercept on the ordinate axis,  $a$  and  $K'$  were found to be 0.75 and  $1.12 \times 10^{-4}$ , respectively, yielding the intrinsic viscosity-molecular weight relationship for poly(tetramethyl-*p*-silphenylene-siloxane)

$$[\eta] = 1.12 \times 10^{-4} M_w^{0.75} \quad (5)$$

Barry's<sup>14</sup> relationship, derived for polydimethylsiloxanes in toluene solution at 20°C.

$$[\eta] = 2 \times 10^{-4} M_n^{0.66} \quad (6)$$

is represented by the dashed line in Figure 2.

The integral molecular weight distribution curve, a plot of  $W_x$ , the cumulative fraction versus molecular weight is shown in Figure 3. The data plotted are from the same fractionation used to obtain the samples for the light-scattering measurements. It can be seen in Figure 3 that about 70% of the polymer prepared by the general method outlined in eq. (3) was above 250,000 in molecular weight, thus demonstrating the general utility of this method for the synthesis of high molecular weight poly-(tetramethyl-*p*-silphenylene-siloxane). The fractionation data were not considered to be sufficiently accurate to justify the differential molecular weight distribution plot.

### Heat of Fusion

To determine  $\Delta H_u$ , the method of Flory,<sup>15</sup> in which one observes the depression of the melting point by diluents was employed. It should be noted that the heat of fusion referred to is the heat required to melt one mole of crystalline units and not one mole of a semicrystalline polymer.

The latter value  $\Delta H_u^*$ , the latent heat of fusion, is dependent upon the degree of crystallinity which exists in a particular polymer sample. Calorimetric measurements yield  $\Delta H_u^*$  rather than the thermodynamically significant  $\Delta H_u$ .

Accordingly, varying known quantities of dibutyl phthalate were added to benzene solutions containing varying known amounts of a high molecular weight tetramethyl-*p*-silphenylene-siloxane polymer. Evaporation of the benzene from these samples yielded a series of crystalline, opaque polymer films approximately 0.004 cm. thick, whose melting points decreased with increasing dibutyl phthalate content. The volume fraction of dibutyl phthalate in each film was calculated from the known weights used and the densities of the constituents.

Melting points were determined by use of a polarizing microscope equipped with a heated stage. The stage was heated very slowly to within about 10°C. of the melting point, then raised to the melting temperature over a 2-hr. period. The temperature at which birefringence could no longer be observed as the sample was rotated in the polarized light was taken as the melting point. The temperature was determined by means of a thermocouple placed directly under the sample. The melting temperatures  $T_m$  of the mixtures and volume fractions  $v_1$  of dibutylphthalate are given in Table III. This method has been previously described by Evans<sup>16</sup> and associates and more recently by Conix<sup>17</sup> and van Kerpel.

TABLE III  
Melting Points  $T_m$  of Tetramethyl-*p*-Silphenylene-Siloxane Homopolymer and Dibutyl Phthalate Mixtures

$v_1$	$T_m$ , °C.
0	148.0
0.0471	145.0
0.1111	141.0
0.2143	134.5
0.3107	130.5
0.3991	126.0

The expression used to calculate  $\Delta H_u$  is given in eq. (7)

$$[(1/T_m) - (1/T_m^\circ)]/v_1 = (R/\Delta H_u)(V_2/V_1)[1-B(V_1v_1/RT_m)] \quad (7)$$

where  $\Delta H_u$  is the heat of fusion per polymer unit,  $T_m^\circ$  is the absolute melting temperature of pure polymer, and  $T_m$  is the absolute melting temperature of the polymer-diluent mixture.  $V_1$  and  $V_2$  represent the molar volumes of diluent and polymer, respectively,  $v_1$  is the volume fraction of diluent,  $R$  is the gas constant, and  $B$  is a diluent-polymer interaction parameter. A plot of  $[(1/T_m) - (1/T_m^\circ)]/v_1$  versus  $v_1/T_m$  to give a straight line as predicted in eq. (7) is shown in Figure 4.  $\Delta H_u$  was calculated from the intercept on the ordinate axis.  $\Delta S_u$  was calculated from the expression,

$$\Delta S_u = \Delta H_u/T_m^\circ \quad (8)$$

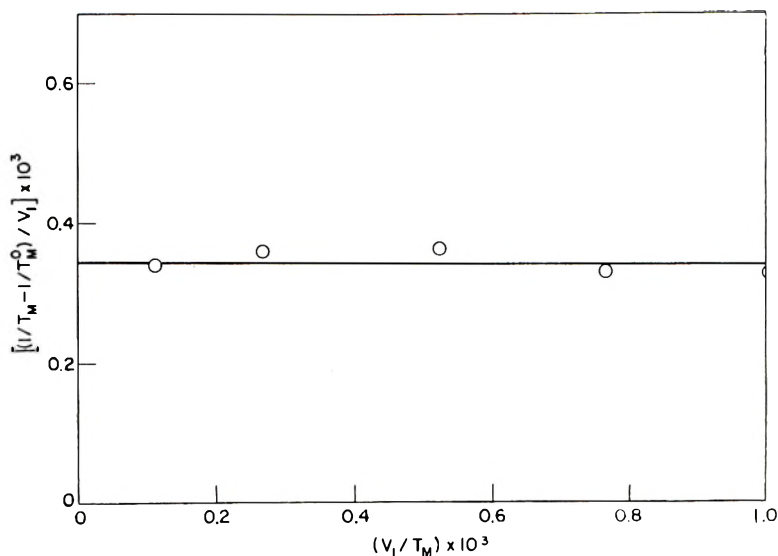


Fig. 4. Determination of the heat of fusion  $\Delta H_u$  for  $[(\text{CH}_3)_2\text{Si}-p\text{-C}_6\text{H}_4\text{-Si}(\text{CH}_3)_2\text{O}]_n$  in admixture with dibutyl phthalate.

and  $B$  was found from the slope of the straight line in Figure 4. The values obtained are shown in Table IV.

Since positive values of  $B$  are indicative of a poor solvent for a given solvent-polymer system and negative  $B$  values are manifested when a good solvent is employed, it can be seen from Table IV that dibutyl phthalate is a rather indifferent solvent for the tetramethyl-*p*-silphenylene-siloxane polymer.

### Thermal Stability

The thermal stability of poly(tetramethyl-*p*-silphenylene-siloxane) was compared to that of polydimethylsiloxane under rather severe conditions where oxidative and other degradative thermal processes could occur at appreciable rates. Polymer samples which had been previously purified to remove trace amounts of catalysts, residual monomers, etc., were introduced into small aluminum containers. The polymer film thickness was approximately 0.07 cm. The polymer films were then heated under atmospheric conditions in a Nouris dispatch oven to 200°C. and 255°C. and a Haskins electric furnace for 305°C.

TABLE IV  
Heat and Entropy of Fusion of Tetramethyl-*p*-Silphenylene-Siloxane Polymer and Energy of Interaction Constant with Dibutyl Phthalate

$T_m^0$ , °C.	$\Delta H_u$ , cal./unit	$\Delta S_u$ , cal./deg./unit	$\Delta S_u$ per bond, cal./deg.	$B$ , cal./cc.
148	4350	10.3	2.57	0.0

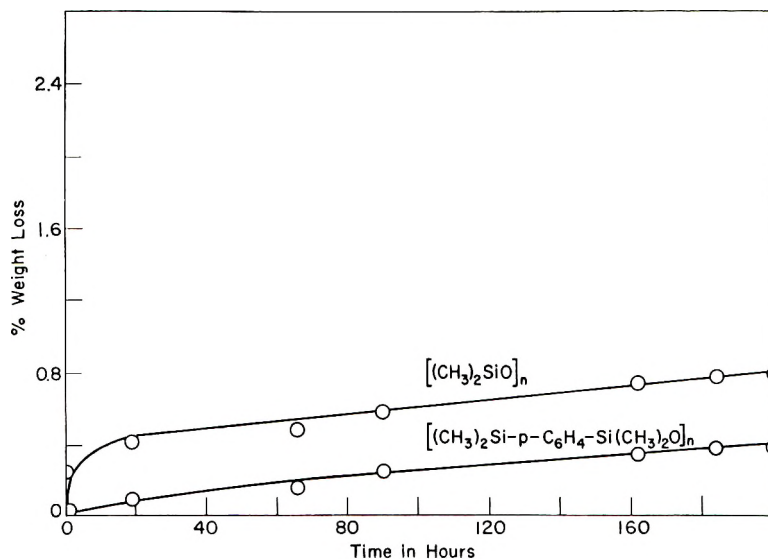


Fig. 5. Thermal stability at 200°C.

After 200 hr. at 200°C., both polymers were substantially unchanged. Solubility tests indicated that no gel formation had occurred in the tetramethyl-*p*-silphenylene-siloxane polymer. A small amount of gel in the dimethylpolysiloxane gum showed that some atmospheric oxidation of this polymer had occurred. That atmospheric oxidation of dimethylpolysiloxanes eventually leads to crosslinked gels has been amply demonstrated by Atkins<sup>18</sup> and associates and Andrianov and Sokolov.<sup>19</sup> While no change

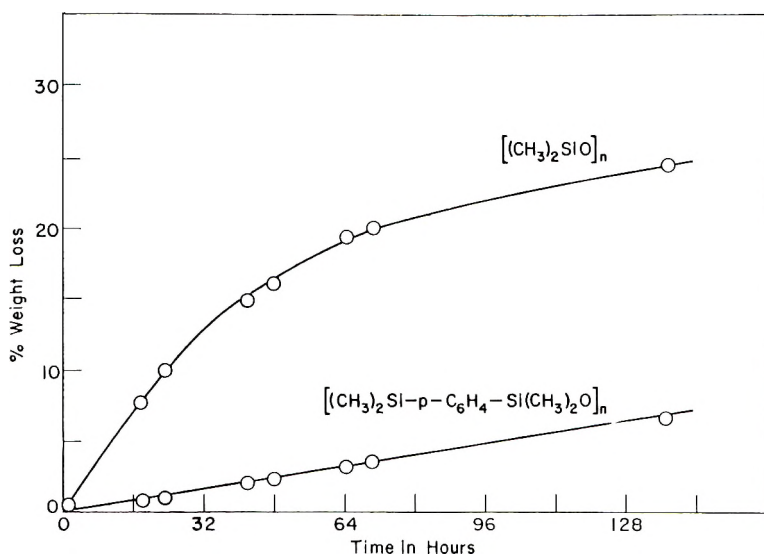


Fig. 6. Thermal stability at 255°C.

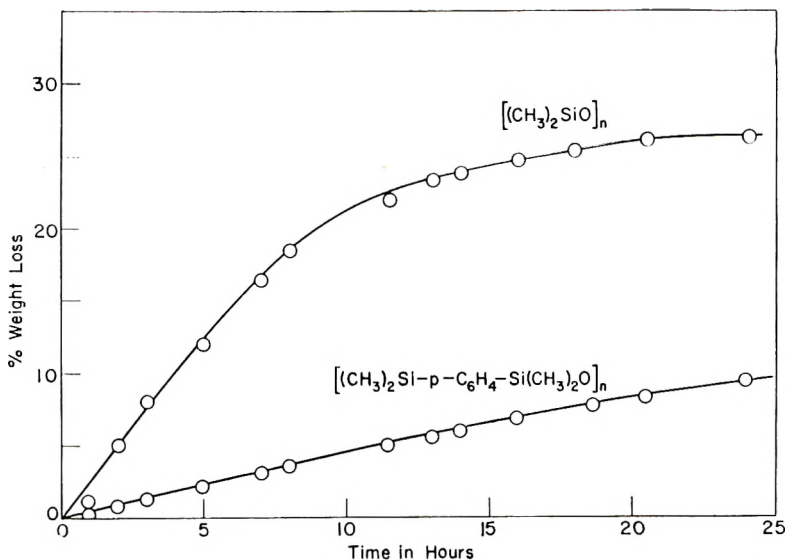
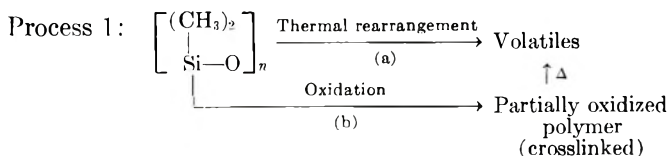


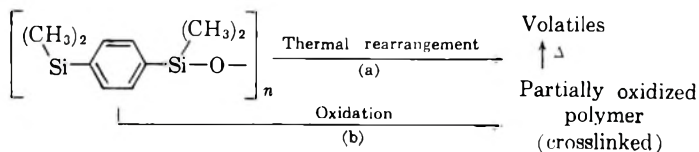
Fig. 7. Thermal stability at 305°C.

could be seen after 18 hr. heating at 255°C., the polymers were no longer soluble in benzene. The *p*-silphenylene polymer swelled to about twenty times its original volume, and the dimethylpolysiloxane to about double its original size in benzene, indicating the dimethylpolysiloxane was much more severely crosslinked than the *p*-silphenylene polymer. After 16 hr. at 305°C. the *p*-silphenylene polymer was slightly yellow in color but remained pliable. Dimethylpolysiloxane, though colorless, had decomposed into a hard splintery gel.

Comparative volatilities at the three temperatures are presented graphically in Figures 5-7. It is very evident that over the temperature range of 200-305°C. that the *p*-silphenylene-siloxane polymer has a much lower volatility loss than dimethylpolysiloxane. Thus, one can conclude that process 1, eq. (9), leading to the formation of volatiles occurs to a greater extent than process 2. In addition, the qualitative swelling measurements on samples of the two polymers which had been subjected to the 255°C. temperature for 18 hr.,



Process 2:



suggest that process 1b occurs at a much more rapid rate than 2b. Thus, it appears that the *p*-silphenylene-siloxane polymer is more stable to atmospheric oxidation at elevated temperatures than dimethylpolysiloxane. The low volatility loss at elevated temperatures observed for the *p*-silphenylene-siloxane polymer is attributable partially to the extreme reluctance, resulting from structural and steric factors, of this polymer to form volatile cyclic siloxanes, and partially to the stability and antioxidant effects of the *p*-phenylene configuration.

The *n*-hexylamine 2-ethylhexoate was obtained through the courtesy of Dr. Frank Hyde of Dow Corning.

The authors gratefully acknowledge the work of Frank E. Dickson of the Physical Measurements Department of Mellon Institute who under the direction of Dr. E. F. Cassassa performed the light-scattering measurements for molecular weight determination.

The authors are also indebted to Dr. C. A. Hoeve of the Fundamental Research Department of Mellon Institute who supplied the polarizing microscope equipped with a hot stage for use in this study.

### References

1. Barry, A. J., U. S. Pat. 2,557,931 (1951); Brit. Pat. 682,835 (1952).
2. Barry, A. J., D. E. Hook, and L. De Pree, U. S. Pat. 2,511,820 (1950); Brit. Pat. 635,645 (1950).
3. De Pre, L., A. J. Barry, and D. E. Hook, U. S. Pat. 2,580,159 (1951).
4. Sveda, M., U. S. Pat. 2,561,429 (1951).
5. Sveda, M., U. S. Pat. 2,562,000 (1951).
6. Gainer, G. C., U. S. Pat. 2,709,692 (1955).
7. Breed, L. W., W. J. Haggerty, Jr., and F. Baiocchi, *J. Org. Chem.*, **25**, 1633 (1960).
8. Price, F. P., *J. Polymer Sci.*, **37**, 71 (1959).
9. Merker, R. L., M. J. Scott, and G. G. Haberland, *J. Polymer Sci.*, **A2**, 31 (1964).
10. McKay, F., *Studies on Novel Linear and Cyclic Siloxanes*, Doctoral Dissertation Series, Publ. No. 19, 311 (1956).
11. Hyde, J. F., Fr. Pat. 1,263,448 (May 2, 1961).
12. Merker, R. L., and M. J. Scott, *J. Polymer Sci.*, **43**, 297 (1960).
13. Morey, D. R., and J. W. Tambllyn, *J. Phys. Chem.*, **50**, 12 (1946).
14. Barry, A. J., *J. Appl. Phys.*, **17**, 1020 (1946).
15. Flory, P. J., *Principles of Polymer Chemistry*, Cornell Univ. Press, Ithaca, N. Y., 1953.
16. Evans, R. D., H. R. Mighton, and P. J. Flory, *J. Chem. Phys.*, **15**, 685 (1947).
17. Conix, A., and R. Van Kerpel, *J. Polymer Sci.*, **40**, 521 (1959).
18. Atkins, D., C. Murphy, and C. Saunders, *Ind. Eng. Chem.*, **39**, 1395 (1947).
19. Andrianov, K. A., and N. N. Sokolov, *Khim. Prom.*, **1955**, No. 6, 329.

### Résumé

Des méthodes améliorées de synthèse du *p*-(bis-diméthylhydroxysilyl)-benzène sont décrites. Ce monomère important a été préparé à partir de *p*-(bis-diméthylhydrogène-silyl)-benzène obtenu à des rendements de 60 à 70% à partir de *p*-dibromobenzène et de diméthylchlorosilane au moyen d'une technique de Grignard *in situ*. La grande répulsion due à des facteurs stériques de la part de la configuration du *p*-silphénylène-siloxane pour former des structures cycliques, a été amplement démontrée. La polymérisation du *p*-(bis-diméthylhydroxysilyl)-benzène en solution benzénique donne lieu à des poids moléculaires élevés, des poly(tétraméthyl-*p*-silphénylène-siloxanes) cristallins. La



chaleur de fusion ( $\Delta H_u$ ) du tétraméthyl-*p*-silphénylène siloxane a été trouvée égale à 4350 Cal/unité. L'équation modifiée de Staudinger reliant la viscosité intrinsèque et le poids moléculaire moyen fut appliquée dans un domaine de 70.000 à 400.000. Ces résultats sont résumés dans la relation:  $[\eta] = 1.12 \times 10^{-4} M_w^{0.75}$ . Les tétraméthyl-*p*-silphénylène siloxanes ont été trouvés plus stables que les diméthylsiloxanes, aussi bien à l'égard de l'oxydation atmosphérique que de la dégradation par formation de produits volatiles dans un domaine de température de 200 à 305°C.

### Zusammenfassung

Verbesserte Syntheseverfahren für *p*-(Bisdimethylhydroxysilyl)benzol werden beschrieben. Dieses interessante Monomere wurde aus *p*-(Bisdimethylhydrogensilyl)benzol dargestellt, das in 60–70% Ausbeute aus *p*-Dibrombenzol und Dimethylchlorsilan nach einer *in-situ*-Grignard-syntheses erhalten worden war. Die durch sterische Faktoren bedingte geringe Neigung der *p*-Silphenylen-Siloxankonfiguration zur Bildung cyclischer Strukturen wurde klar nachgewiesen. Die Kondensationspolymerisation von *p*-(Bisdimethylhydroxysilyl)benzol in Benzollösung lieferte hochmolekulare, kristalline Poly(tetramethyl-*p*-silphenylensiloxane). Die Schmelzwärme ( $\Delta H_u$ ) von Tetramethyl-*p*-silphenylen-siloxan wurde zu 4350 cal/Einheit bestimmt. Die modifizierte Staudingerbeziehung zwischen Viskositätszahl und Gewichtsmittel des Molekulargewichts war im Bereich von 70000 bis 400000 anwendbar. Es ergibt sich die Gleichung  $[\eta] = 1,12 \times 10^{-4} M_w^{0.75}$ . Tetramethyl-*p*-silphenylen-siloxane sind gegen Oxydation durch Luft-sauerstoff und gegen Abbau unter Bildung flüchtiger Produkte im Temperaturbereich 200–305°C stabiler als Dimethylsiloxane.

Received June 11, 1962

Revised September 27, 1962

## Random and Block Copolymers of Poly(tetramethyl-*p*-Silphenylene-Siloxane) and Polydimethylsiloxane

ROBERT L. MERKER, MARY JANE SCOTT, and G. G.  
HABERLAND,\* *Mellon Institute, Pittsburgh, Pennsylvania*†

### Synopsis

High molecular weight block copolymers having the structure  $[(\text{CH}_3)_2\text{SiO}]_a[(\text{CH}_3)_2\text{Si}-p-\text{C}_6\text{H}_4-\text{Si}(\text{CH}_3)_2\text{O}]_b$  can be conveniently prepared from the copolymerization of hydroxy end-blocked dimethylpolysiloxanes and *p*-bis(dimethylhydroxysilyl)benzene by use of essentially nonequilibrating catalysts, such as tetramethylguanidine di-2-ethylhexoate or *n*-hexylamine 2-ethylhexoate. The values of *a* and *b* above may be altered by employing hydroxy-ended dimethylpolysiloxane of different degrees of polymerization or by preforming tetramethyl-*p*-silphenylene-siloxane units. If the length of a segment is maintained at a constant value in the copolymers decreasing the mole ratio *a/b* results in higher tensile strengths and higher melting points which are manifestations of increased degrees of crystallinity. If the mole ratio *a/b* is held constant, increasing the length of the *a* and *b* segments leads to higher melting points and higher tensile strengths again reflecting an increase in the degree of crystallinity. High molecular weight copolymers ( $[\eta]$  ranging from 1.0 to 2.1), possessing unstressed (unvulcanized) gum tensiles of 1000-2700 psi and elongations of 500-1000% can be readily obtained by the methods described.

### INTRODUCTION

The preparation and some of the properties of high molecular weight, crystalline tetramethyl-*p*-silphenylene-siloxane have been described in the first article of this series.<sup>1</sup> This present research concerns random and block copolymers of tetramethyl-*p*-silphenylene-siloxane and dimethylsiloxane.

### DISCUSSION

The physical properties of a copolymer composed of A units and B units are greatly influenced by the structural arrangement of these units. For the purpose of clarity of discussion, let us envision this for a simple case involving a copolymer consisting of equal molar quantities of monomer unit A and monomer unit B,

$$[(\text{A})_y(\text{B})_y]_z \quad (1)$$

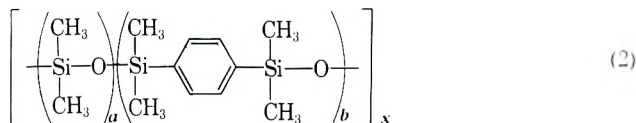
\* Present address, Dow Corning Corporation, Midland, Michigan.

† Multiple Fellowship on Silicones sustained by the Dow Corning Corporation and Corning Glass Works.

Here it can be seen that when  $y = 1$ , we have an alternating copolymer. For values of  $y$  greater than 1, providing that on the average the repeat sequence maintains its integrity, one obtains the so-called block copolymers. Copolymers which on the average possess no "repeat sequence" such as is found in alternating or block types, will be referred to as random copolymers.

It is rather evident that the various structural features possessed by units A and B which influence van der Waals effects, hydrogen bonding, dipole effects, crystallinity, etc., in each of the respective homopolymers will be altered to some extent in the copolymers depending not only on the molar quantities of the two units present, but also on the sequence in which the units appear in the copolymer chain. Thus in the above-mentioned hypothetical case for a copolymer consisting of equal numbers of A and B units, one could theoretically expect, if appropriate methods were available for their preparation, to obtain a whole series of copolymers with widely differing physical properties.

In considering the possible physical properties which would be manifested by the copolymers discussed in this paper which have the general structure,



the physical properties of the respective homopolymers are of prime importance. Thus, high molecular weight dimethylpolysiloxanes (A units) are typical ideal elastomers characterized by low gum tensiles, low surface tensions, etc., resulting from small intermolecular forces. Conversely, a homopolymer comprised of tetramethyl-*p*-silphenylene-siloxane (B) units is a tough, crystalline, fiber-forming polymer (m.p. 148°C.). Copolymers of the above structure might be expected to possess properties which are a compromise between the properties manifested by the homopolymers. Furthermore, it should be emphasized that at a given mole ratio of A units to B units ( $a/b$ ), one might obtain a series of copolymers of varying physical properties. For any particular copolymer of given composition,

$$a/b = \text{constant} \quad (3)$$

and consequently as  $a$  increases  $b$  must increase to satisfy the above expression. In other words, while  $a/b$  remains constant, the repeating sequences of A units and B units in the copolymer chain are each becoming longer.

Now, since the intermolecular interaction (van der Waals forces, crystallinity, etc.) of A units with A units and B units with B units can be modified

lizable at temperature  $T_1$ , the total number of B units as well as the sequence in which they occur must surely determine not only the maximum degree of crystallinity possible at temperature  $T_1$ , but also the temperature  $T_m$  at which the last crystallites melt. In the more general case, it might be said that as the numerical values of  $a$  and  $b$  increase, each distinct segment of the copolymer chain patterns its individual behavior more nearly after that of its corresponding homopolymer.

Since the homopolymers of dimethylsiloxane (A units) and tetramethyl-*p*-silphenylene-siloxane (B units) are not mutually compatible even above the melting point (148°C.) of the latter, it follows that copolymers composed of extremely long sequences of A units followed by extremely long sequences of B units conceivably could be composed of two amorphous phases above 148°C. and more nearly approximate in appearance and properties an intimate mixture of the two homopolymers. While preliminary experiments indicate that copolymers of this type have actually been prepared in this laboratory, the present discussion will be confined to copolymers which contain a single amorphous phase above their melting point. Copolymers falling into this category are comprised either of randomly distributed units or of moderately long to very short block sequences.

The very existence of these two classes of copolymers, one containing a single, amorphous phase above the melting temperature, the other, two amorphous phases above the melting temperature, is rather conclusive evidence that secondary intermolecular forces (van der Waals, etc.) are markedly affected by sequence length. The effect of sequence length on primary intermolecular interactions (crystallinity) will be discussed in the succeeding sections of this paper.

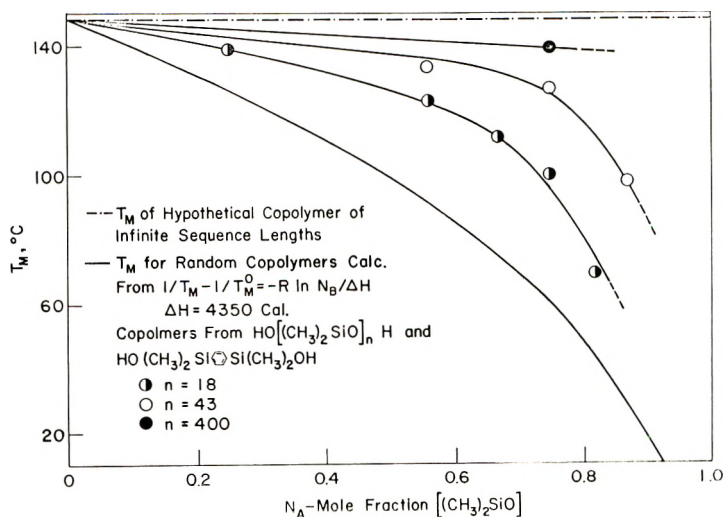


Fig. 1. The effect of sequence length on the melting point of block copolymers of the structure  $([(\text{CH}_3)_2\text{SiO}]_a[(\text{CH}_3)_2\text{Si}-p\text{-C}_6\text{H}_4-\text{Si}(\text{CH}_3)_2\text{O}]_b)_z$ .

## EXPERIMENTAL

### Monomers

High molecular weight copolymers were conveniently prepared from  $\text{HO}[(\text{CH}_3)_2\text{SiO}]_n\text{H}$  fluids, which were supplied by Dow Corning Corporation in degrees of polymerization of 18, 43, and 400 and *p*-bis(dimethylhydroxysilyl)benzene.<sup>1</sup> The hexamethylcyclotrisiloxane used in one copolymerization was also supplied by Dow Corning. The benzene used was Fisher, thiophene-free.

### Catalysts

Two essentially nonequilibrating condensation catalysts were successfully employed in preparing crystalline, block copolymers. One, *n*-hexylamine 2-ethylhexoate, was provided by Dr. Frank Hyde of Dow Corning.<sup>2</sup> The other, tetramethylguanidine di-2-ethylhexoate was prepared by mixing 14.4 g. of 2-ethylhexanoic acid and 5.6 g. tetramethylguanidine. Qualitative observation indicated that, under the reaction conditions employed, the copolymerizations catalyzed by the tetramethylguanidine di-2-ethylhexoate were the more rapid.

The use of these two silanol condensation catalysts essentially incapable of shuffling siloxane bonds of either the starting hydroxy-ended polydimethylsiloxanes of variable degrees of polymerization or those formed by the condensation reaction enabled experimental control of the average sequence lengths of the respective units.

### Procedure

The variations in experimental details of the polymerizations are summarized in Table I. All were conducted in essentially the following fashion. In a flask equipped with a reflux condenser and a benzene-filled azeotrope trap was placed a mixture of starting materials and the indicated per cent of catalyst which had been dissolved in benzene. The final mixture containing the catalyst was composed of 66% by weight monomers. At the conclusion of the polymerization and removal of the benzene, some of the copolymers were further heated in a vacuum oven. The reflux times, time in oven, and oven temperatures are given in Table I.

In the copolymerization (No. 7, Table I) in which hexamethylcyclotrisiloxane was used, the weight per cent of monomers and toluene was the same as that employed in benzene above. The toluene mixture was heated to dissolve as much of the monomers as possible, after which the catalyst was added. The procedure described above was then followed.

It is important to note that the *p*-bis(dimethylhydroxysilyl)-benzene was only moderately soluble in the initial reaction mixtures, and dissolved only as the reactions proceeded. From solubility measurements it was learned that for practically all of the combinations used, the initial concentration of OH groups from the hydroxy end-blocked dimethylsiloxane varied from approximately equal to approximately half of the initial con-

TABLE I  
High Molecular Weight Block Copolymers from  $\text{HO}[(\text{CH}_3)_2\text{SiO}]_n\text{H}$ , Monomer A, and  $\text{HO}[(\text{CH}_3)_2\text{Si}-p-\text{C}_6\text{H}_4-\text{Si}(\text{CH}_3)_2\text{OH}]_m$ , Monomer B,

No.	DP of Monomer A <sup>a</sup>	Silphenylene		Minimum avg. arrangement (a-b) <sup>b</sup>	Catalyst and concn., wt.-% <sup>c</sup>	Polymerization time, hr.	$[\eta]$ , dl./g.	Copolymer m.p., °C.
		Mole-%	Wt.-%					
1	18	75	90	18-54	1% A	6 (reflux) 16 (at 110°C.)	—	139
2	43	44	70	43-33.4	0.5% B	6.5 (reflux)	—	133
3	18	44	70	18-14	0.5% B	6.5 (reflux)	1.53	123
4	18	33	60	18-0	0.5% B	6.5 (reflux)	2.00	112
5	400	25	50	400-133	0.5% B	10 (reflux) <sup>d</sup>	3.10	139
6	43	25	50	43-14.3	0.5% B	6.5 (reflux)	—	126.5
7	—	25	50	Random	0.02% C <sup>b</sup>	8 (reflux)	—	—
8	18	25	50	18-6	1% A	7.5 (reflux) + 20 (at 110°C.)	1.17	—
9	18	25	50	18-6	0.5% B	6.5 (reflux)	2.11	100
10	18	18	40	18-4	0.5% B	6.5 (reflux)	1.91	69.5
11	18	13	30	18-2.5	0.5% B	6.5 (reflux)	1.29	<25
12	43	13	30	43-6	0.5% B	6.5 (reflux)	1.14	97.5
13 <sup>f</sup>	18	13	30	>18->2.5	0.5% B	6.5 (reflux)	0.955	—

<sup>a</sup> Values of  $n$  for  $\text{HO}[(\text{CH}_3)_2\text{SiO}]_n\text{H}$ .

<sup>b</sup> These values represent minimum average sequence arrangements. Actual values may be considerably higher but the ratio of the sequence numbers must remain unchanged.

<sup>c</sup> A represents *n*-hexylamine 2-ethylhexoate, B represents tetramethylguanidine di-2-ethylhexoate; percentages based on starting monomers.

<sup>d</sup> Used 100 ml. benzene initially to insure homogeneity.

<sup>e</sup> Potassium dimethylsilylanolate catalyst used with hexamethylcyclotrisiloxane as monomer A, toluene the solvent.

<sup>f</sup>  $\text{HO}[(\text{CH}_3)_2\text{Si}-p-\text{C}_6\text{H}_4-\text{Si}(\text{CH}_3)_2\text{OH}]_m$  allowed to polymerize 1 hr. before addition of  $\text{HO}[(\text{CH}_3)_2\text{SiO}]_n\text{H}$ .

centration of OH groups from the *p*-bis(dimethylhydroxysilyl) benzene in solution. However, the total concentration of OH groups available from the *p*-bis(dimethylhydroxysilyl)benzene varied from 4 to 55 times the concentration of OH groups from the hydroxy end-blocked dimethylsiloxane. Because of this and because of the lack of information concerning the actual rates of condensation of the two hydroxy end-blocked species or cross-condensation reaction rates, it is difficult at the present time, to approximate even crudely the average values of the repeat sequences obtained in the nonequilibrating catalyst systems. Needless to say, an accurate method for the determination of the length of repeat sequences would be a valuable aid in this study. For the present, the lack of such knowledge does not affect the validity of the experimental evidence or the general considerations and postulations under discussion.

In lieu of affixing reliable values to the repeat sequences of the crystalline copolymers the average block patterns cited throughout this discussion are minimum sequence arrangements based on the degrees of polymerization of the starting hydroxy-ended dimethylsiloxane fluids. It must be stressed that these values represent minimum average sequences and that the actual values are probably considerably higher. However, since, obviously, the molar ratio cannot change, the ratios of the sequence numbers must remain constant.

### Polymerization Efficiency

In general, at the conclusion of the polymerization, the polymers were dissolved in benzene and precipitated with methanol. In a sample experiment the initial yield of polymer was 100%. After redissolving in benzene and reprecipitation with methanol, 97.3% of the polymer was recovered, only 2.7% of the total being lost due to mechanical causes. None of the copolymer was of low enough molecular weight to be soluble in the methanol-benzene mixture.

### Rearrangement Experiments

Two samples of the strong, elastic, 50/50 (w/w) tetramethyl-*p*-silphenylene-siloxane/dimethylsiloxane copolymer (No. 9 in Table I) dissolved in benzene were placed in narrow-necked polymerization tubes. To one tube was added potassium dimethylsilanolate (0.02% by weight K<sub>2</sub>O based on polymer) an equilibration catalyst. After exhausting the solvent, both tubes were sealed and heated at 175°C. for 30 hr. Upon opening, examination of the contents revealed that while the blank had remained crystalline, the copolymer heated with the catalyst had become an amorphous copolymer having little or no gum tensile.

### Physical Measurements

Melting points of thin copolymer films cast from benzene were determined by use of a polarizing microscope equipped with a heated stage. The temperature at which birefringence could no longer be observed as the

sample was rotated in the polarized light was taken as the melting point. A thermocouple placed directly under the sample was used to determine the melting point.

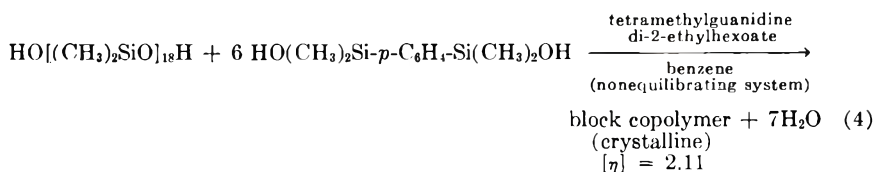
Viscosity measurements at three concentrations in toluene for each polymer sample selected were made in a Cannon-Ubbelohde dilution viscometer at  $25 \pm 0.1^\circ\text{C}$ . From these values the intrinsic viscosities were found and are given in Table I.

Films for tensile strength measurements were deposited by slow evaporation of benzene from a copolymer solution. In the case of the 70/30 tetramethyl-*p*-silphenylene-siloxane/dimethylsiloxane copolymer, it was necessary to heat the sample to melting, then allow it to cool to a satisfactory film. Tensile strength data are given in Tables II and III, and Figures 2-4. Test pieces of the copolymers were cut from the cast films with a standard A.S.T.M.  $\frac{1}{4} \times 1 \times \frac{3}{8}$  in. rubber die. An Instron tensile tester equipped with a recorder was used to obtain the stress-strain data. All rates of elongation and relaxation were 2 in./min. The specimens were elongated to rupture to determine rupture properties.

## RESULTS

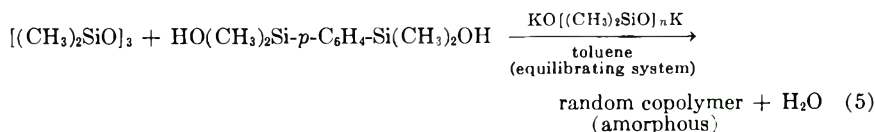
### Random Versus Block Configuration

As predicted earlier, rather dramatic differences in physical properties were observed between copolymers whose compositions were identical [ $a/b = \text{constant}$ , see eqs. (2) and (3)], but which differed in the arrangement of the units. In these copolymers, the dimethylsiloxane and tetramethyl-*p*-silphenylene-siloxane unit arrangements varied from completely random to ordered block arrangements possessing an average repeat sequence integrity. The block copolymer (No. 9 of Tables I and III) prepared by the process,



where the minimum value of  $a = 18$  and  $b = 6$  and  $a/b = 3$ , was a tough, elastic, crystalline copolymer (melting point =  $100^\circ\text{C}$ .) having an unvulcanized, unstressed gum tensile and elongation of 1840 psi and 750%, respectively.

A random copolymer obtained as shown in eq. (5) of identical



composition to the block copolymer of eq. (4), was a clear gum resembling in



TABLE II  
Effect of Sequence Length at Constant Mole Ratio in Block Copolymers of  $(\text{CH}_3)_2\text{SiO}$  (A units) and  $(\text{CH}_3)_2\text{Si}-p\text{-C}_6\text{H}_4\text{-Si}(\text{CH}_3)_2\text{O}$  (B units)

No. <sup>a</sup>	DP of Monomer A <sup>b</sup>	Stiphenylene		Minimum avg. arrangement (a-b)	$[\eta]$ , dl./g.	Tensile strength, psi		Elongation, %	Shore hardness
		Mole-%	Wt.-%			Unstressed <sup>e</sup>	Stressed <sup>d</sup>		
11	18	13	30	18-2.5	1.29	0	0	—	—
12	43	13	30	43-6	1.14	553	4525	717	47
13 <sup>e</sup>	18	13	30	>18->2.5	0.955	452	3460	667	45

<sup>a</sup> Numbers correspond to those shown in Table I.

<sup>b</sup> Values of  $n$  for  $\text{HO}[(\text{CH}_2)_2\text{SiO}]_n\text{H}$ .

<sup>c</sup> Tensile strength based on unstressed specimen dimensions.

<sup>d</sup> Tensile strength based on stressed specimen dimensions.

<sup>e</sup>  $\text{HO}(\text{CH}_3)_2\text{Si}-p\text{-C}_6\text{H}_4\text{-Si}(\text{CH}_3)_2\text{OH}$  allowed to polymerize 1 hr. before addition of hydroxy-ended dimethylpolysiloxane. Sequence values must be considerably larger than for those of copolymer No. 11.

TABLE III  
Effect of Increasing  $p$ -Stiphenylene Content in Block Copolymers of  $(\text{CH}_3)_2\text{SiO}$  (A units) and  $(\text{CH}_3)_2\text{Si}-p\text{-C}_6\text{H}_4\text{-Si}(\text{CH}_3)_2\text{O}$  (B units)

No. <sup>a</sup>	DP of Monomer A <sup>b</sup>	Stiphenylene		Minimum avg. arrangement (a-b)	$[\eta]$ , dl./g.	Tensile strength, psi		Elongation, %	Shore hardness
		Mole-%	Wt.-%			Unstressed <sup>e</sup>	Stressed <sup>d</sup>		
11	18	13	30	18-2.5	1.29	0	0	—	—
10	18	18	40	18-4	1.91	1137	12,100	962	50
9	18	25	50	18-6	2.11	1840	15,600	750	72
4	18	33	60	18-9	2.00	2085	15,500	643	86
3	18	44	70	18-14	1.53	2725	16,000	490	93

<sup>a</sup> Experiment numbers correspond to those used in Table I.

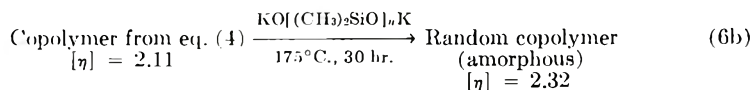
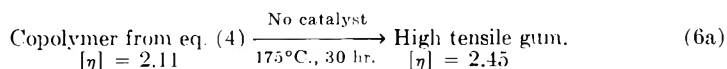
<sup>b</sup> Values of  $n$  for  $\text{HO}[(\text{CH}_2)_2\text{SiO}]_n\text{H}$ .

<sup>c</sup> Tensile strength based on unstressed specimen dimensions.

<sup>d</sup> Tensile strength based on stressed specimen dimensions.

appearance and properties high molecular weight polydimethylsiloxane. In addition to possessing essentially no gum tensile, the gum showed no birefringence under the polarizing microscope. Therefore this copolymer was adjudged to be amorphous at room temperature.

The rearrangement of the block copolymer of eq. (4) under equilibrating conditions to give the random copolymer of eq. (5) further verified the above observations.



As can be seen in eq. (6a), heating the block copolymer from eq. (4) in a sealed evacuated tube at 175°C. for 30 hr. resulted in a slight increase in molecular weight but the copolymer remained crystalline and hence retained its tensile strength. The same treatment in the presence of a rearranging catalyst, eq. (6b), also resulted in a slight increase in molecular weight, but in addition yielded amorphous random copolymer similar to copolymer of eq. (5).

#### Effect of Sequence Length at Constant Mole Ratio

Three block copolymers all composed of 70 wt.-%  $[(\text{CH}_3)_2\text{SiO}]$  and 30 wt.-%  $[(\text{CH}_3)_2\text{Si-}p\text{-C}_6\text{H}_4\text{-Si}(\text{CH}_3)_2\text{O}]$  ( $a/b$  is constant) provided an interesting example of variation in physical properties with differing sequence lengths. The copolymers were prepared under essentially nonequilibrating conditions as described in the experimental section. Their properties are summarized in Table II. The first one (No. 11, Table II) was prepared from hydroxy end-blocked dimethylpolysiloxane with a degree of polymerization of 18. A copolymer gum with little tensile strength was the result.

The second member of the series (No. 12) was the result of copolymerizing *p*-bis(dimethylhydroxysilyl)benzene with hydroxy end-blocked dimethylsiloxane of a degree of polymerization of 43. Thus, while  $a/b$  is the same for these two copolymers, it can be seen that the value of  $a$  was increased from a minimum of 18 (No. 11) to a minimum of 43 (No. 12) and it follows that the value of  $b$  must also have increased correspondingly from a minimum of 2.5 (No. 11) to a minimum of 6 (No. 12). From the melting point data in Table I and tensile strength data in Table II the longer sequence lengths present in copolymer No. 12 obviously permitted the formation of tetramethyl-*p*-silphenylene-siloxane crystallites.

The physical properties observed for copolymer No. 13 (Table II) substantiate this contention. Here, the values of  $a$  and  $b$  were increased by allowing the *p*-bis(dimethylhydroxysilyl)benzene to polymerize partially before the addition of the hydroxy end-blocked dimethylsiloxane (DP 18). The copolymer so prepared was elastic and possessed a tensile strength of

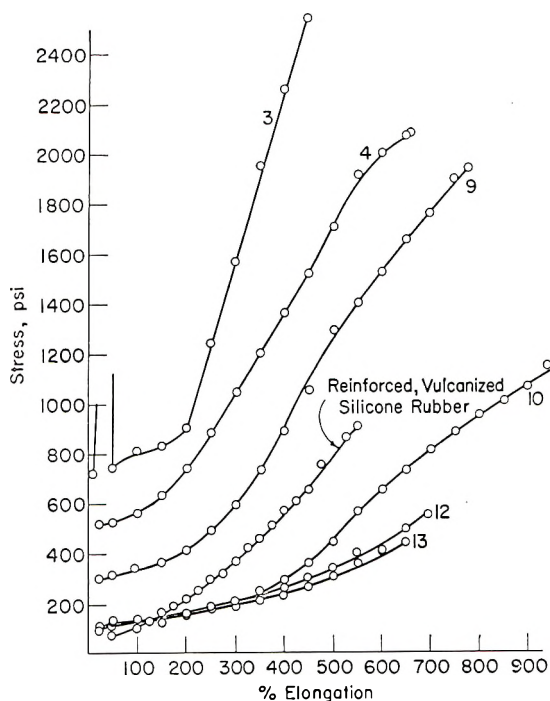


Fig. 2. Tensile strength (based on unstressed cross section).

452 psi, thus reflecting the great difference in physical properties between this copolymer and its counterpart prepared from the same hydroxy end-blocked dimethylsiloxane. When reasonably accurate methods of following the course of the polymerization either viscometrically or by measuring the water formed have been perfected, it will be possible to prepare high molecular weight copolymers of any desired arrangement from *p*-bis-(dimethylhydroxysilyl)benzene and one hydroxy end-blocked dimethylpolysiloxane of a low degree of polymerization.

#### Effect of *p*-Silphenylene Content

The series of copolymers outlined in Table III clearly illustrates the effect of increasing *p*-silphenylene content in copolymers of dimethylsiloxane (A units) and tetramethyl-*p*-silphenylene-siloxane (B units). These copolymers were all prepared under essentially nonrearranging conditions as outlined in the experimental section. As can be seen in Table III, increasing tetramethyl-*p*-silphenylene-siloxane content results in increasing tensile strengths but decreasing elongations. These effects are undoubtedly due to the increase in the number of microcrystalline regions in the copolymer which occurs as the molar content of tetramethyl-*p*-silphenylene-siloxane is increased.

In addition, an increase in *p*-silphenylene content also results in an in-

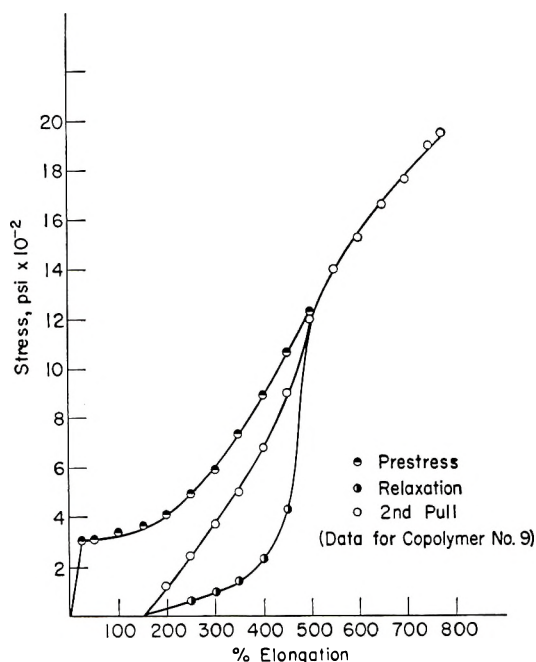


Fig. 3. Tensile strength (based on stressed cross section).

crease in the average length of the tetramethyl-*p*-silphenylene-siloxane sequences. This occurs because the same hydroxy end-blocked dimethylsiloxane was used to prepare all of the copolymers shown in Table III. Hence, the minimum sequence length of  $[(\text{CH}_3)_2\text{SiO}]$  (A units) was approximately the same for all of these copolymers. It necessarily follows that as the mole ratio of  $(a/b)$  was decreased, the average length of the B units (*p*-silphenylene) was increased. The enhanced effectiveness of the longer sequences of crystallizable units in the formation of microcrystalline regions was demonstrated in the preceding section of this paper where large variations in properties, obviously resulting from differences in degrees of crystallinity, were achieved by increasing the sequence length of the tetramethyl-*p*-silphenylene-siloxane segments while maintaining a constant mole ratio.

### Effect of Sequence Length on Melting Point

Since the value of  $\Delta H_u$  for the tetramethyl-*p*-silphenylene-siloxane unit is known,<sup>1</sup> the melting points for a series of hypothetical random copolymers formed from this unit and dimethylsiloxane can be calculated from the relationship<sup>3</sup>

$$(1/T_m) - (1/T_m^\circ) = (-R/\Delta H_u) \ln N_B \quad (7)$$

where  $N_B$  is equal to the mole fraction of *p*-silphenylene-siloxane units

(crystallizing units). It is probable that the melting points calculated from eq. (7) are considerably higher than the actual experimental values, however, since crystal growth leading to larger, higher melting crystallites would definitely be hindered in a direction parallel to the copolymer chain axis by the presence of the foreign dimethylsiloxy groups. In Figure 1 the calculated melting points for the random copolymers are plotted versus the mole fraction of the noncrystallizing unit  $[(\text{CH}_3)_2\text{SiO}]$ . Also plotted in Figure 1 are the experimental melting points (see Table I) obtained with the polarizing microscope for a series of block copolymers prepared from *p*-bis(dimethylhydroxysilyl)benzene and hydroxy end-blocked dimethylpolysiloxanes of different average degrees of polymerization. From Figure 1 it is immediately apparent that at any given composition, the block copolymers possessed higher melting points than those calculated for the random copolymers.

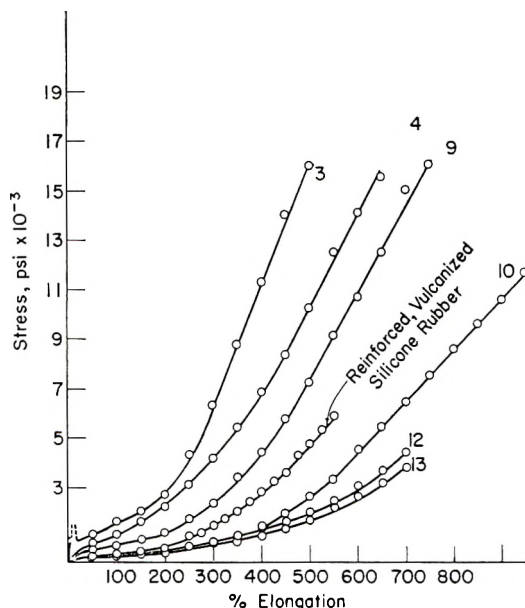


Fig. 4. Stress-strain behavior of crystalline block copolymer after prestressing.

Of even greater significance is the evident trend to higher melting copolymers with increasing average block sequence length. As emphasized earlier with the use of essentially nonequilibrating catalysts, the degree of polymerization of the hydroxy end-blocked dimethylpolysiloxane from which the copolymer was made determines the average sequence length of the block segments at any given copolymer composition. Higher degrees of polymerization of the hydroxy end-blocked dimethylpolysiloxane yield not only longer dimethylsiloxane segments but also longer tetramethyl-*p*-

silphenylene-siloxane segments in the resulting block copolymer. In Figure 1 the melting points of copolymers prepared from hydroxy end-blocked dimethylpolysiloxanes with a DP of 43 fall on a curve considerably above those made from hydroxy end-blocked dimethylpolysiloxane with a DP of 18. The one copolymer prepared from a hydroxy end-blocked dimethylpolysiloxane of DP 400 is in line with this trend.

The horizontal dashed line at the melting point (148°C.) of the tetramethyl-*p*-silphenylene-siloxane homopolymer represents the independence of melting point on composition as predicted by Flory<sup>3</sup> for hypothetical block copolymers of infinite sequence length and composed of crystallizing and noncrystallizing units.

Actually, the data shown in Figure 1 offer striking evidence in support of this contention. Of practical significance is the possibility of maintaining the desirable physical properties of such crystalline block copolymers at higher temperatures through the use of a higher melting crystallizing unit, by increasing the length of the block segments, or by a combination of these methods.

### Stress-Strain Behavior

In Figure 2 are shown stress-strain data obtained on elongating the unvulcanized block copolymer specimens directly to rupture. The sample numbers in this figure and in Figures 3 and 4 correspond to those used in Table I. A typical vulcanized silicone rubber (polydimethylsiloxane type) reinforced with silica is included for purposes of comparison. Figure 3 contains the same data presented in Figure 2 except that the tensile stress has been calculated on the dimensions of the stressed cross section. The stressed cross section was obtained by assuming that elongation took place under conditions of constant volume. Therefore, the stressed cross section equals  $(1/\alpha)$  times the original cross section or

$$\text{Tensile stress (stressed)} = \alpha[\text{Tensile stress (unstressed)}] \quad (8)$$

Figure 4 depicts the typical behavior exhibited by all the crystalline block copolymers examined on prestressing, relaxing, and subsequent stressing to rupture.

The curves of Figures 2-4 obtained for the crystalline block copolymers all show a rapid rise in tensile stress at low elongations followed by a rather sharp yield point, suggesting that randomly oriented microcrystalline regions were originally present. Beyond this yield point they show differing amounts of flow depending on the total amount of crystallinity present, i.e., *p*-silphenylene content and sequence length. This is then followed by another rapid rise in tensile stress indicating the presence of microcrystalline regions probably largely oriented in the direction of stress. How much, if any of such oriented crystallinity is stress induced (i.e., melts on removal of stress) is not known at the present time.

### References

1. Merker, R. L., and M. J. Scott, *J. Polymer Sci.*, **A2**, 15 (1964).
2. Hyde, J. F., *Fr. Pat.* 1,263,448 (May 2, 1961).
3. Flory, P. J., *J. Chem. Phys.*, **17**, 223 (1949); *ibid.*, **15**, 684 (1947).

### Résumé

On obtient aisément des copolymères en bloc ayant la structure  $[(\text{CH}_3)_2\text{SiO}]_a [(\text{CH}_3)_2\text{Si-}p\text{-C}_6\text{H}_4\text{-Si}(\text{CH}_3)_2\text{O}]_b)_n$ , en partant de diméthylpolysiloxanes portant des groupements hydroxyles terminaux et du *p*-(bis-diméthylhydroxylsilyl)benzène, et en employant essentiellement des catalyseurs non-équilibrants comme le tétraméthylguanidine-di-2-éthylhexoate ou le *n*-hexylamine-2-éthylhexoate. Les valeurs de *a* et de *b* peuvent être modifiées en employant des diméthylpolysiloxanes de différents degrés de polymérisation ou en formant au préalable des unités tétraméthyl-*p*-silphénylène-siloxane. Si la longueur des segments (*a*) est maintenue à une valeur constante, la diminution du rapport molaire *a/b* amène des forces d'extension et des points de fusion plus élevés, ce qui indique une augmentation des degrés de cristallinité. Si le rapport molaire *a/b* est maintenu constant, l'augmentation de la longueur des segments *a* et *b* entraîne des points de fusion et des forces d'extension plus élevés, reflétant ainsi de nouveau l'augmentation du degré de cristallinité. Les méthodes décrites permettent d'obtenir aisément des copolymères de poids moléculaire élevé ( $[\eta]$  entre 1 et 2.1) possédant des tensions de gommages nonvulcanisés de 1000–2700 psi et des élongations de 500–1000%.

### Zusammenfassung

Hochmolekulare Blockcopolymeren mit der Struktur  $[(\text{CH}_3)_2\text{SiO}]_a [(\text{CH}_3)_2\text{Si-}p\text{-C}_6\text{H}_4\text{-Si}(\text{CH}_3)_2\text{O}]_b)_n$  können durch Copolymerisation von Dimethylpolysiloxanen mit endständigen Hydroxylgruppen und *p*-(Bisdimethylhydroxylsilyl)-benzol mit im wesentlichen nichtgleichgewicht-einstellenden Katalysatoren wie Tetramethylguanidin-di-2-äthylhexoat oder *n*-Hexylamin-2-äthylhexoat leicht dargestellt werden. Die Werte von *a* und *n* können durch Verwendung von Dimethylpolysiloxan mit endständiger Hydroxylgruppe von verschiedenem Polymerisationsgrad oder durch Vorbildung von Tetramethyl-*p*-silphenylen-siloxan-bausteinen variiert werden. Bei konstanter (*a*)-Segmentlänge im Copolymeren führt eine Herabsetzung des Molverhältnisses *a/b* zu höherer Zugfestigkeit und zu höherem Schmelzpunkt, worin sich der grössere Kristallinitätsgrad äussert. Vergrößerung der Länge der *a*- und *b*-Segmente bei konstantem Molverhältnis *a/b* führt zu höheren Schmelzpunkten und höherer Zugfestigkeit, was wieder einer Zunahme des Kristallinitätsgrades entspricht. Hochmolekulare Copolymeren ( $[\eta]$  im Bereich von 1,0 bis 2,1) mit einer Zugfestigkeit als ungespannter (nicht vulkanisierter und füllstoffreier) Gummi von 1000 bis 2700 psi und Dehnungen von 500 bis 1000% kann nach den beschriebenen Methoden leicht erhalten werden.

Received June 11, 1962

Revised September 27, 1962

## Preparation and Polymerization of 1,5-Diamino-2,4-alkylenetrissilazanes

L. W. BREED, R. L. ELLIOTT, and A. F. FERRIS, *Midwest Research  
Institute, Kansas City, Missouri*

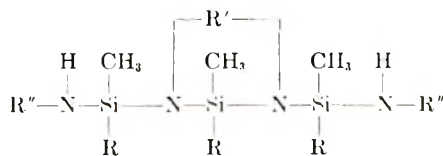
### Synopsis

1,5-Diamino-2,4-ethylenehexamethyltrissilazane and related compounds were prepared by treating the corresponding chlorosilane intermediates with ammonia or an amine. When these monomers were heated in xylene solution at 140°C. in the presence of ammonium sulfate, linear silicon-nitrogen polymers were obtained with molecular weights in the range of 7,500-15,000. Elemental analyses, infrared spectra, and the physical properties of the polymers support the proposed structure and polymerization route.

### INTRODUCTION

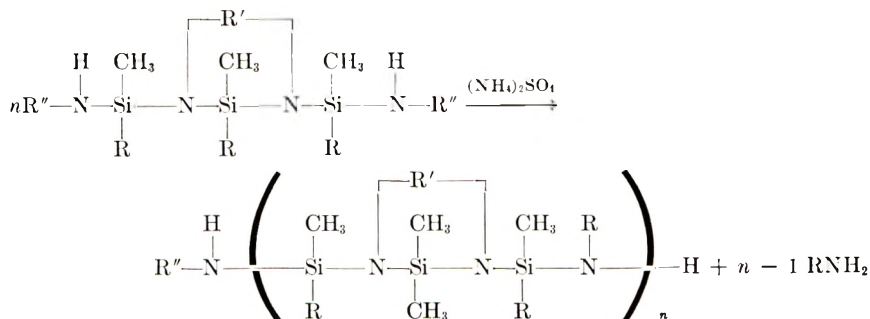
Although the hydrolysis of organosilicon dichlorides under suitable conditions can yield products containing substantial quantities of linear siloxanes, ammonolysis of the same materials gives almost exclusively small ring compounds. Also, the elimination of an amine in the thermal condensation of *N*-substituted diaminodiorganosilanes yields small ring cyclic compounds as the highest molecular weight portion of the product. Because of the ease of formation and stability of small ring silicon-nitrogen compounds, intermediate and even low molecular weight nitrogen analogues of the siloxanes have eluded preparation. Although a series of patents described the preparation of silazanes through the condensation of ammonia with various organosilicon halides,<sup>1-4</sup> no high molecular weight polymers containing alternately ordered silicon and nitrogen in a linear polymer chain have been characterized in the literature.

A preliminary communication on this work reported that long chain silicon-nitrogen polymers can be prepared in preference to ring structures if a monomer structure is selected that sterically prevents cyclizations during polymerization.<sup>5</sup> To meet this requirement, monomers were chosen that contained a trissilazane chain with an ethylene or propylene bridge between the 2- and 4-positions and terminal amino or substituted amino groups at the 1- and 5-positions.





Polymerization of these monomers has been effected with heat in the presence of catalytic quantities of an acid catalyst such as ammonium sulfate.

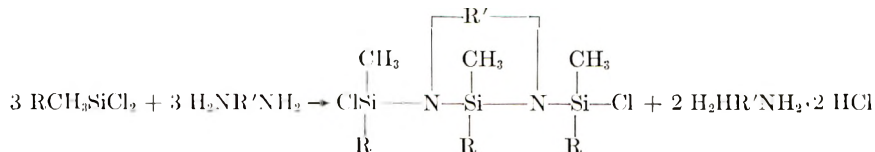


The formation of ammonia or amine in these reactions is analogous to the elimination of water between two silanol units in the formation of siloxane polymers. The conditions for the polymerization are similar to those for the transamination reaction commonly used for the preparation of silicon-nitrogen compounds in which a more volatile amine group is displaced by a less volatile amine group. The removal of amine from the system provides the driving force for the polymerization.

## RESULTS AND DISCUSSION

### Monomer Preparation

Monomer intermediates were prepared according to the procedure of Henglein<sup>6</sup> in a one-step procedure from alkylendiamines and diorganodihalosilanes:



The properties and elemental analyses for these intermediates are reported in Table I. The cyclic derivatives were obtained from the various combinations of ethylenediamine or 1,3-propylenediamine with dichlorodimethylsilane, dichloromethylphenylsilane, or dichloromethylvinylsilane. Ethylenediamine and dichlorodimethylsilane afforded no distillable products. The only products that could be isolated from the experiments in which dichlorodiphenylsilane was treated with various diamines, or on which *o*-phenylenediamine was added to several halogenosilanes, were the disubstituted amines (structure B, Table I) in low yields.

The chlorosilane intermediates were readily converted in good yield to the aminosilane monomers with ammonia or amines. The characteristics and elemental analyses of the monomers are shown in Table II. The char-

TABLE I  
Preparation and Properties of Chlorosilane Intermediates

Reactants		Product	Yield, % <sup>a</sup>	Boiling point, <sup>c</sup> °C./mm. Hg	Melting point, °C.	Molecular weight <sup>b</sup>		Analysis <sup>e</sup>			
Silane	Diamine					Calcd.	Found	N, %	Si, %	Calcd.	Found
Me <sub>2</sub> SiCl <sub>2</sub>	H <sub>2</sub> N(CH <sub>2</sub> ) <sub>2</sub> NH <sub>2</sub>	A	72	86/0.27	38	301	310	9.29	27.95	9.30	27.80
Me <sub>2</sub> SiCl <sub>2</sub>	H <sub>2</sub> N(CH <sub>2</sub> ) <sub>3</sub> NH <sub>2</sub>	A	54	83/0.1 100-104/0.3	—	—	—	8.88	26.71	9.02	26.59
Me <sub>2</sub> SiCl <sub>2</sub>	<i>o</i> -C <sub>6</sub> H <sub>4</sub> (NH <sub>2</sub> ) <sub>2</sub>	B <sup>d</sup>	6	—	116-18	—	—	9.52	19.43	9.37	19.66
MePhSiCl <sub>2</sub>	H <sub>2</sub> N(CH <sub>2</sub> ) <sub>2</sub> NH <sub>2</sub>	A	57	199-238/0.2-0.4 207/0.2	—	488	503	5.74	17.28	5.99	17.39
MePhSiCl <sub>2</sub>	H <sub>2</sub> N(CH <sub>2</sub> ) <sub>3</sub> NH <sub>2</sub>	A	52	205-225/0.1	—	502	514	5.59	16.80	5.77	16.73
Ph <sub>2</sub> SiCl <sub>2</sub>	<i>o</i> -C <sub>6</sub> H <sub>4</sub> (NH <sub>2</sub> ) <sub>2</sub>	B	4	—	187-90	542	535	5.17	10.37	4.94	10.65
Me(CH <sub>2</sub> ) <sub>2</sub> CH)SiCl <sub>2</sub>	H <sub>2</sub> N(CH <sub>2</sub> ) <sub>2</sub> NH <sub>2</sub>	A	42	104-120/0.2 95/0.2	—	—	—	8.30	24.97	8.25	25.11
MeHSiCl <sub>2</sub>	H <sub>2</sub> N(CH <sub>2</sub> ) <sub>2</sub> NH <sub>2</sub>	No distill- able product	—	—	—	—	—	—	—	—	—

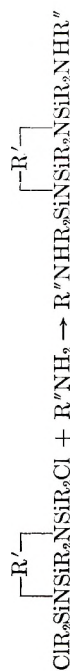
<sup>a</sup> Yields based on amine.

<sup>b</sup> All molecular weights were determined ebullioscopically.

<sup>c</sup> Analyses were determined by Spang Microanalytical Laboratory, Ann Arbor, Michigan, or by Galbraith Laboratories, Inc., Knoxville, Tennessee.

<sup>d</sup> A petroleum ether-soluble product, m.p. 165-70°, was isolated but not identified. Anal. Found: N, 11.11; Si, 15.06.

TABLE II  
Preparation of Aminosilane Monomers



Mono- mer	Reactants		Yield, %	Boiling Point, °C./mm.	Melting point, °C.	$n_D^{20}$	$d_{20}^{20}$	Analysis					
	Intermediate	Amine						Calcd.	Found				
I	$\text{ClMe}_2\text{SiNSiMe}_2\text{NSiMe}_2\text{Cl}$	$\text{NH}_3$	64	86/0.3	—	1.4620(25)	0.9530(25)	21.34 <sup>a</sup>	32.09	19.61	32.88	19.47	32.75
II		MeNH <sub>2</sub>	66	75-76/0.1	—	1.4582(26)	0.9304(26)	19.28	28.99	19.17	29.12	19.17	29.12
III		<i>n</i> -BuNH <sub>2</sub>	57	109/0.09	—	1.4566(28)	0.9108(28)	14.95	22.48	15.19	22.64	15.19	22.64
IV		PhNH <sub>2</sub>	58	—	41-44	—	—	13.51	20.31	13.25	20.14	13.34	20.08
V	$\text{ClMe}_2\text{SiNSiMe}_2\text{NSiMe}_2\text{Cl}$	NH <sub>3</sub>	52	74/0.2	—	1.4689(26)	0.9672(26)	20.26 <sup>a</sup>	30.46	19.60	27.58	19.52	27.44
VI		MeNH <sub>2</sub>	65	84/0.1	—	1.4671(26)	0.9542(26)	18.39	27.66	18.44	27.55	18.44	27.55
VII		<i>n</i> -BuNH <sub>2</sub>	51	123/0.1	—	1.4615(28)	0.9243(28)	14.41	21.67	14.27	21.50	14.27	21.50
VIII		PhNH <sub>2</sub>	90	—	41-44	—	—	13.07	19.65	12.81	19.64	12.81	19.64
IX	$\text{ClMePhSiNSiMePhNSiMePhCl}$	MeNH <sub>2</sub>	63	198/0.09 <sup>c</sup>	—	—	—	11.75	17.67	11.90	17.89	11.90	17.89
X		BuNH <sub>2</sub>	31	213/0.1	—	1.5431(28)	1.0434(28)	9.99	15.02	9.89	15.34	9.89	15.34
XI	$\text{ClMePhSiNSiMePhNSiMePhCl}$	MeNH <sub>2</sub>	64	190-230/0.2 <sup>c</sup>	—	—	—	11.42	17.17	11.25	17.38	11.25	17.38
XII	$\text{ClMe(CH}_2\text{)}_2\text{SiNSiMe(CH}_2\text{)}_2\text{NSiMe(CH}_2\text{)}_2\text{Cl}$	MeNH <sub>2</sub>	58	99-101/0.1	—	1.4848(28)	0.9676(28)	17.28	25.96	17.30	25.75	17.30	25.75

<sup>a</sup> The analyst reported that sample vials were under considerable pressure of ammonia. <sup>b</sup> Anal. Calcd.: C, 36.59%; H, 9.98%. Found: C, 38.27, 38.40%; H, 9.22, 9.36%. <sup>c</sup> Boiling point determined during a short path distillation. <sup>d</sup> Molecular weight: calcd., 477; found, 494. <sup>e</sup> Molecular weight: calcd., 491; found, 506.

acterization of the series was based on the analyses obtained from the methylamine and butylamine derivatives, which were easily purified by distillation, and the aniline derivative, which could be recrystallized. Although the ammonia derivatives could be distilled if the distillation was carried out rapidly in a short path apparatus at low pressures, they polymerized slowly at room temperature with the evolution of ammonia and failed to give satisfactory analyses for the monomeric compositions.

### Polymerization

In studies of the polymerization process, the effect of monomer structure on the rate of polymerization was assessed on the basis of the quantity of amine evolved when the compounds were heated 2 hr. in the presence of 1 or 5% ammonium sulfate (see Table III). The ammonia derivatives could not be used satisfactorily in these experiments because of their rapid loss of ammonia. As could have been predicted, the butylamine and methylamine compounds reacted more sluggishly and revealed the effect of substituents in other portions of the monomer molecule on the rate of condensation. The polymerization appeared to proceed considerably more rapidly in structures containing the ethylene bridge than in those with propylene bridge. Substitution of a phenyl group for a silicon-attached methyl group on each silicon atom of the monomer structure also led to a slower rate of polymerization. On the basis of these experiments no advantage was apparent in using monomers other than the simplest member of the series, 1,5-diamino-2,4-ethylene-1,1,3,3,5,5-hexamethylcyclotrisilazane, in the polymerization reaction.

The effect of several catalysts on the rate of amine evolution is shown in

TABLE III  
Effect of Structure on the Rate of Amine Evolution from 1,5-Bis(alkylamino)-2,4-alkylenetrisilazanes

Mono- mer	R	R'	R''	(NH <sub>4</sub> ) <sub>2</sub> SO <sub>4</sub> , wt.-%	Amine evolved after 2 hr. at 140°C., %*
II	CH <sub>3</sub>	(CH <sub>2</sub> ) <sub>2</sub>	CH <sub>3</sub>	5.5	108.2
VI	CH <sub>3</sub>	(CH <sub>2</sub> ) <sub>3</sub>	CH <sub>3</sub>	5.0	52.7
II	CH <sub>3</sub>	(CH <sub>2</sub> ) <sub>2</sub>	CH <sub>3</sub>	1.0	77.8
IX	C <sub>6</sub> H <sub>5</sub>	(CH <sub>2</sub> ) <sub>2</sub>	CH <sub>3</sub>	1.0	63.0
XI	C <sub>6</sub> H <sub>5</sub>	(CH <sub>2</sub> ) <sub>3</sub>	CH <sub>3</sub>	1.0	60.8
III	CH <sub>3</sub>	(CH <sub>2</sub> ) <sub>2</sub>	C <sub>4</sub> H <sub>9</sub>	1.0	19.5
VII	CH <sub>3</sub>	(CH <sub>2</sub> ) <sub>3</sub>	C <sub>4</sub> H <sub>9</sub>	1.0	4.6
X	C <sub>6</sub> H <sub>5</sub>	(CH <sub>2</sub> ) <sub>2</sub>	C <sub>4</sub> H <sub>9</sub>	1.0	14.9

\* Values uncorrected for ammonia content of catalyst.

Table IV. No catalyst more suitable than ammonium sulfate could be found for the polymerization reaction. Attempts to increase the solubility of the catalyst by the use of the sulfuric acid salts of aliphatic and aromatic amines failed to provide more effective materials. Although chlorotrimethylsilane and ammonium chloride have been reported to be effective in catalyzing the transamination reaction,<sup>7</sup> these compounds failed to catalyze the polymerization reaction.

TABLE IV  
Effect of Catalyst on the Rate of Amine Evolution from 1,5-bis(methylamino)-2,4-ethylenehexamethyltrisilazane

Catalyst <sup>a</sup>	Amine evolved after 2 hr. at 140°C., %
(NH <sub>4</sub> ) <sub>2</sub> SO <sub>4</sub>	78
(CH <sub>3</sub> NH <sub>2</sub> ) <sub>2</sub> · H <sub>2</sub> SO <sub>4</sub>	80
(C <sub>2</sub> H <sub>5</sub> NH <sub>2</sub> ) <sub>2</sub> · H <sub>2</sub> SO <sub>4</sub>	75
(C <sub>6</sub> H <sub>5</sub> NH <sub>2</sub> ) <sub>2</sub> · H <sub>2</sub> SO <sub>4</sub>	48
KHSO <sub>4</sub>	67
NH <sub>4</sub> Cl	11
(CH <sub>3</sub> ) <sub>3</sub> SiCl	4
No catalyst	7

<sup>a</sup> Catalyst level: 1 wt.-%.

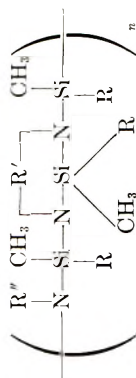
In most of the polymerization reactions, the monomers were dissolved in an equal volume of xylene. Although the reactions proceeded equally well in the absence of solvent, the solvent provided better temperature control. Pyridine, when used as a solvent was found to have a catalytic effect on the reaction (see Table VI). When the monomer was heated in boiling pyridine in the absence of any other catalyst, rapid ammonia evolution took place yielding a polymer with about the same degree of polymerization as when the same monomer was heated at the same temperature in xylene in the presence of ammonium sulfate. Boiling 4-picoline was as effective as pyridine, but tri-*n*-propylamine was ineffective.

### Polymer Characterization

The polymers were characterized by elemental analyses, infrared spectra, and molecular weight. These data, together with the physical properties of the polymers, indicated that polymerization had occurred primarily through chain extension. The polymers derived from 1,5-diamino-2,4-ethylenehexamethyltrisilazane (I) and 1,5-diamino-2,4-(1,3-propylene)-hexamethyltrisilazane (V) were soluble in organic solvents and were tacky, somewhat elastic, low-melting solids or viscous liquids. The polymers from the methylamine derivatives were less soluble and were viscous oils or brittle solids. The polymerization of the aniline and butylamine derivatives gave only low molecular weight oils.

The results of analyses for elements, which are shown in Table V, agree well with the calculated values, indicating that the molecular weights of the

TABLE V  
Analyses for Elements in Polymers



Monomer	R	R'	R''	Calcd.				Found			
				C, %	H, %	N, %	Si, %	C, %	H, %	N, %	Si, %
I	CH <sub>3</sub>	(CH <sub>2</sub> ) <sub>2</sub>	H	39.12	9.44	17.11	34.32	39.20	9.12	16.91	34.62
V	CH <sub>3</sub>	(CH <sub>2</sub> ) <sub>3</sub>	H	41.64	9.71	16.19	32.46	41.30	9.34	16.28	33.02
II	CH <sub>3</sub>	(CH <sub>2</sub> ) <sub>2</sub>	CH <sub>3</sub>	41.64	9.71	16.19	32.46	41.88	9.72	16.00	32.26
IX	C <sub>6</sub> H <sub>5</sub>	(CH <sub>2</sub> ) <sub>2</sub>	CH <sub>3</sub>	64.51	7.22	9.40	18.86	62.60	6.78	10.36	19.96

polymers were sufficiently high that the elemental content of the endgroups did not contribute significantly to the experimental values and that the polymerization had proceeded as postulated with no major contributing side reactions.

Additional evidence for a linear polymerization was obtained in a comparison of the infrared spectra of the monomers and polymers. The spectra of the monomers were consistent with their structure. In general only slight changes in the spectra were observed after a monomer was converted to a polymer, and essentially the same bands were presented in the spectra of polymer samples as were obtained from the corresponding monomers. An exception was a strong absorption band at about  $1180\text{ cm.}^{-1}$  found in several of the polymers, but absent in the monomers. The development of this band in the spectrum can be correlated with the formation of  $\text{--SiMe}_2\text{--NHSiMe}_2\text{--}$  groupings, absent in the monomers but present in the polymers. No such band was observed in the polymers containing the  $\text{--SiMe}_2\text{NMeSiMe}_2\text{--}$  group.

Other changes were observed in the NH region. Monomers I and V exhibited the two bands characteristic of primary amines in the  $3500\text{--}3300\text{ cm.}^{-1}$  region. The free secondary amino group was indicated by a single band in the same region of II and VI. Spectra of the polymers prepared from I and V contained only a single absorption band near  $3500\text{ cm.}^{-1}$ , reflecting the disappearance of the free amino group under polymerization conditions with the formation of the polysilazane structure. No bands were present in the NH region in the polymers prepared from II and VI. The infrared correlations are consistent with band assignments reported in the literature.<sup>8</sup>

### Molecular Weight

The molecular weight of many of the polymers were too high to assess with much confidence by the usual ebullioscopic methods. In addition to considerable foaming in the boiling polymer solution, the sizes of the boiling point elevation increments were sufficiently small to introduce considerable error in the determinations. From the polymer of I, values above 5000 were usually obtained, and the molecular weight was estimated to be in the neighborhood of 8000.

The relative degree of polymerizations of polymers prepared under various conditions could be compared, however, by the intrinsic viscosity of the polymer solutions in toluene. A polymer could be prepared from I with an intrinsic viscosity in toluene as high as 0.19. If the constants for the molecular weight-intrinsic viscosity relationship reported by Barry for siloxanes are used,<sup>9</sup> a molecular weight of about 15,000 can be calculated. A polymer from V had an intrinsic viscosity of 0.09 in toluene.

On the basis of intrinsic viscosity determinations, it was found that a polymerization temperature of  $140^\circ\text{C.}$  gave the highest degree of polymerization. Temperatures higher or lower than that value gave materials with lower intrinsic viscosities. The results of several experiments are reported in Table VI.

TABLE VI  
Intrinsic Viscosities of Experimental Polymer Solutions

Mono-mer	Temperature, °C.	Polymerization solvent	Catalyst	$[\eta]$	Solvent
I	120	Xylene	1% (NH <sub>4</sub> ) <sub>2</sub> SO <sub>4</sub>	0.13	Toluene
I	140	Xylene	1% (NH <sub>4</sub> ) <sub>2</sub> SO <sub>4</sub>	0.17	Toluene
I	160	Xylene	1% (NH <sub>4</sub> ) <sub>2</sub> SO <sub>4</sub>	0.14	Toluene
I	180	Xylene	1% (NH <sub>4</sub> ) <sub>2</sub> SO <sub>4</sub>	0.11	Toluene
I	120	Pyridine	None	0.13	Toluene
I	140	4-Picoline	None	0.11	Toluene
I	140	Tri- <i>n</i> -propylamine	None	0.01	Toluene

Attempts to advance the polymerization of these polymers by various physical and chemical methods were in most trials unsuccessful. When the polymer from I was treated with small quantities of CuCl<sub>2</sub> or water, the products exhibited a decrease in intrinsic viscosity. A sample of a polymer prepared from I having an intrinsic viscosity of 0.19 lost 7.5% of its weight after 19 hr. at 210°C. and a final intrinsic viscosity of 0.10 was observed. An exception was observed when a polymer based on II under the same heating conditions showed an increase in intrinsic viscosity from 0.05 to 0.13 (in xylene).

## EXPERIMENTAL

All amines were dried over KOH and distilled from sodium before use. Redistilled chlorosilanes were used.

### Chlorosilane Intermediates

The method for preparing 1,5-dichloro-2,4-ethylenehexamethyltrisilazane, which followed the procedure described by Henglein,<sup>8</sup> is typical of the preparation of compounds in this series. To a stirred, cooled mixture of 134 g. (1.05 mole) of dichlorodimethylsilane and 400 ml. toluene at 10°C. was added 60 g. (1.0 mole) of ethylenediamine dissolved in 200 ml. toluene. After the addition was complete (1 hr.), the mixture was refluxed 2 hr. and filtered. Additional filtration was required after about half of the toluene was distilled off. Fractional distillation of the devolatilized filtrate gave 73.6 g. (74% yield) of the product, boiling at 86°C. at 0.3 mm. Hg, melting point 38°C. The properties and analytical data for compounds in this series are given in Table I.

### Aminosilane Monomers

In a typical experiment, dry gaseous ammonia was bubbled through a mixture of 20.0 g. (0.067 mole) 1,5-dichloro-2,4-ethylenehexamethylcyclo-trisilazane in 350 ml. petroleum ether, which was cooled to 5°C. until the mixture was saturated with ammonia. When the product was warmed to 50°C. and filtered, 6.4 g. (90%) of the ammonium chloride was collected. Evaporation of the filtrate and distillation through a short path apparatus at 0.3 mm. Hg gave 1,5-diamino-2,4-ethylenehexamethyltrisilazane, boiling



at 86°C., in yields of 36–64%. Properties and analyses are reported in Table II. The compound was also prepared by the addition of the chlorosilane intermediate to a cooled solution of ammonia in petroleum ether.

The other aminosilane derivatives described in Table II were similarly prepared, but were purified by fractional distillation. The aniline derivatives were recrystallized from petroleum ether.

### Polymerization Studies

The data in Tables III and IV (the percentage of amine evolved after 2 hr. polymerization) were determined for methylamine derivatives with the use of a 15-ml. polymerization cell containing the monomer sample. The cell was immersed in a bath of boiling xylene and connected to a reflux condenser. A nitrogen purge tube was extended through the condenser to about 15 cm. above the surface of the monomer sample and the flow of nitrogen was adjusted to about 20 ml./min. The effluent nitrogen and amine from the polymerization cell were allowed to pass through an aliquot of 0.1*N* H<sub>2</sub>SO<sub>4</sub>, which was titrated at the conclusion of the experiment to determine the total amine evolved.

### Polymer Preparation and Characterization

Polymer samples were usually prepared by placing a 2.0 to 10.0 g. sample of the monomer dissolved in an equal volume of xylene in a 100-ml. thermowell flask and adding the appropriate quantity of catalyst. The polymers used in elemental analyses, infrared spectra, and molecular weight determinations were catalyzed with 0.5–1.0% ammonium sulfate and heated at 140°C. until ammonia or amine was no longer evolved. A slow stream of dry nitrogen was passed over the surface of the polymerizing mixture and the effluent gases were collected in a 0.1*N* H<sub>2</sub>SO<sub>4</sub> trap and titrated from time to time to determine the quantity of amine that had evolved. The resulting polymer solution was treated with additional solvent, filtered, and devolatilized under reduced pressure with the sample being finally heated to 100°C.

In a typical experiment, 8.5 g. of freshly distilled 1,5-diamino-2,4-ethylenhexamethyltrisilazane, 0.5 g. ammonium sulfate, and 10 ml. of xylene, heated at 140 ± 5°C., ceased to evolve significant amounts of ammonia after 6 hr. The cooled polymer solution was treated with 10 ml. benzene, filtered, and the solvent was evaporated leaving 7.7 g. (97% yield) of a soft tacky material. The analyses for this and related polymers are given in Table V. In the polymerization of the monomers, 90–105% of the expected amine was usually collected. The heating time for the polymers from V, II, and IX were 9, 19, and 19 hr., respectively.

This research was supported by the United States Army under Contract DA-23-072-ORD-1687 and monitored by Rock Island Arsenal, Rock Island, Illinois.

### References

1. Cheronis, N. D., U. S. Pat. 2,564,674 (1951).
2. Cheronis, N. D., and E. L. Gustus, U. S. Pat. 2,579,416 (1951).
3. Cheronis, N. D., and E. L. Gustus, U. S. Pat. 2,579,417 (1951).
4. Cheronis, N. D., and E. L. Gustus, U. S. Pat. 2,579,418 (1951).
5. Breed, L. W., R. L. Elliott, and A. F. Ferris, *J. Org. Chem.*, **27**, 1114 (1962).
6. Henglein, F. A., and K. Lienhard, *Makromol. Chem.*, **32**, 218 (1959).
7. Fessenden, R., and D. F. Crowe, *J. Org. Chem.*, **26**, 4638 (1961).
8. Smith, A. L., *Spectrochim. Acta*, **16**, 87 (1960).
9. Barry, A. J., *J. Appl. Phys.*, **17**, 1020 (1946).

### Résumé

On a préparé le 1,5-diamino-2,4-éthylène-hexaméthyltrisilazané et des composés analogues par traitement des intermédiaires chlorosilaniques correspondants avec de l'ammoniac ou une amine. Lorsqu'on chauffe ces monomères en solution dans le xylène à 140°C en présence de sulfate d'ammonium, obtient des polymères linéaires silicé-azote ayant des poids moléculaires d'environ 7.500 à 15.000. Les analyses élémentaires, les spectres infrarouges et les propriétés physiques des polymères confirment la structure proposée et le mode de polymérisation.

### Zusammenfassung

1,5-Diamino-2,4-äthylenhexamethyltrisilazan und verwandte Verbindungen wurden durch Behandlung der entsprechenden Chlorsilane mit Ammoniak oder einem Amin dargestellt. Beim Erhitzen dieser Monomeren in Xylollösung in Gegenwart von Ammonsulfat auf 140°C wurden lineare Silizium-Stickstoffpolymere mit Molekulargewichten von 7500 bis 15000 erhalten. Die vorgeschlagene Struktur und der angenommene Reaktionsweg werden durch Elementaranalyse, Infrarotspektren und die physikalischen Eigenschaften der Polymeren gestützt.

Received May 27, 1963

Revised July 18, 1963

## Crosslinking and Degradation in $\gamma$ -Irradiated Poly-*n*-alkyl Acrylates

W. BURLANT, J. HINSCH, and C. TAYLOR, *Scientific Laboratory, Ford Motor Company, Dearborn, Michigan*

### Synopsis

Polymers of methyl, ethyl, *n*-butyl, *n*-octyl, and *n*-cetyl acrylate were  $\gamma$ -irradiated *in vacuo*, and the effects of irradiation temperature ( $-196$  to  $56^{\circ}\text{C}.$ ) on energy yields for crosslinking and degradation estimated from gel fractions and swelling behavior of the gel. The extent of degradation is independent of polymer structure and reaction temperature, suggesting a molecular chain breaking process. Crosslinking, found to occur predominantly on the alkyl side chain, is independent of temperature above and below the polymer softening point, but is severalfold higher for irradiations above the softening point; these data seem to reflect the importance of segmental mobility of radiation produced polymer radicals in the crosslinking step.

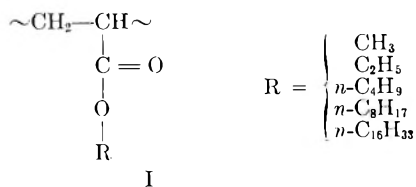
### INTRODUCTION

Polymers exposed to high energy electrons or  $\gamma$ -rays usually crosslink and/or degrade. While ionic and molecular processes explain some of the reported data, the most useful model postulates the radiation initiated formation of polymer free radicals capable of undergoing the competing reactions of crosslinking by bimolecular combination with another molecule or radical, chain cleavage by disproportionation, or H atom elimination to form an olefinic group with no accompanying change in polymer molecular weight. Consequently, one would expect radiation effects to be temperature sensitive since (1) the various competing reactions are temperature sensitive (2) the onset of segmental motion or chain mobility required for crosslink formation is marked in the region of the polymer glass transition  $T_g$  and, for some polymers, at the crystallite melting point.

The role of temperature in polymer irradiations has been studied only briefly, and the contribution to radiation damage of segmental diffusion and competing reactions is not yet clear. In most cases, cross-linking systems (polyethylene,<sup>1-3</sup> polyvinyl chloride,<sup>2</sup> polydimethylsiloxane,<sup>4</sup> rubber,<sup>5</sup> polystyrene,<sup>6</sup> *p*-substituted polystyrenes<sup>7</sup>) and those which degrade upon irradiation (polymethyl methacrylate,<sup>6</sup> polyisobutylene<sup>8</sup>) behave similarly: both exhibit slight temperature sensitivity at low radiation temperatures and somewhat greater dependence, i.e., more crosslinking or more degradation, when irradiations are above the polymer  $T_g$ . For some

*p*-substituted polystyrenes<sup>7</sup> crosslinking is observed below  $T_g$ , but degradation attributed to radical disproportionation predominates above this temperature; on the other hand, the copolymer of fluoroethylene and fluoropropylene degrades when irradiated at low temperatures, and crosslinks above  $T_g$ .<sup>9</sup>

The present paper describes in more detail than has previously been reported the temperature dependence of  $G_c$  (the number of crosslinks produced/100 e.v. absorbed) and  $G_d$  (the number of main chain bonds broken/100 e.v. absorbed) when poly-*n*-alkyl acrylates (I) are  $\gamma$ -irradiated *in vacuo*. This series is a



convenient one to study because  $T_g$  (which is the same as the brittle point  $T_b$  for the first four homologs) varies over a 100°C. range with a minimum change in chemical configuration. Furthermore, since the side chains of the cetyl homolog crystallize and melt at about 30°C.,  $T_g$  (around -80°C.) and  $T_b$  (33°C.) in this case are different enough<sup>10</sup> so that the influence of each on crosslinking and degradation might be estimated.

### APPROACH

Polyalkyl acrylates predominately crosslink when  $\gamma$ -irradiated, so that an insoluble (gel) fraction forms; simultaneous degradation also occurs. Based on the statistics of crosslinking and degradation, and the assumptions of (1) an initial most probable molecular weight distribution, i.e.,  $\bar{M}_w/\bar{M}_n = 2$  and (2) both bond-breaking and bond-making are independent, consecutive events (from Table II, the constancy of  $G_d$ , while  $G_c$  varies, over a wide range of reaction conditions in the present study substantiates the reasonableness of this assumption), Charlesby<sup>11a</sup> derives the following expression:

$$S + S^{1/2} = (1/q_0u_1)(1/R) + p_0/q_0 \quad (1)$$

where  $S$  is the soluble fraction of the irradiated polymer,  $q_0$  is the fraction of monomer units crosslinked by the radiation,  $u_1$  is the number-average degree of polymerization of the starting polymer,  $R$  is the radiation dose (in megarad), and  $p_0$  is the fraction of monomer units degraded by the radiation.  $S$  and  $R$  can be measured in the laboratory. A plot of  $S + S^{1/2}$  versus  $1/R$  should be a straight line with intercept  $p_0/q_0$  and slope of  $1/q_0u_1$ . If either  $u_1$  or  $q_0$  can be obtained, the absolute energy yields of crosslinking and degradation,  $G_c$  and  $G_d$ , then can be calculated according to eqs. (2) and (3):

$$G_c = 0.48 \times 10^6 q_0/w \quad (2)$$

$$G_c = 0.96 \times 10^6 p_0/w \quad (3)$$

where  $w$  is the molecular weight of the monomer unit.

If as is commonly the case, the starting molecular weight distribution is wide, radiation-initiated cleavage of only a few bonds per molecule will randomize the distribution, so that the initial broad distribution can be replaced by a random one of the same initial number-average molecular weight.

Usually, one measures  $\nu_1$  to obtain the ratio  $p_0/q_0$  in eq. (1), but this parameter could not be obtained for the high molecular weight, broad distribution, polyalkyl acrylates used.  $q_0$ , however, can be estimated from swelling data: The average molecular weight between crosslinks of the whole system (sol plus gel) is given by:

$$M_c = (w/q_0)(1/R) \quad (4)$$

The molecular weight between crosslinks of the gel portion alone  $M_{cg}$  related to  $M_c$ , is:<sup>11b</sup>

$$M_c/M_{cg} = (1 + S) \quad (5)$$

Since  $M_{cg}$  (therefore  $M_c$ ) can be obtained more or less conveniently from equilibrium swelling measurements on the isolated gel,  $q_0$  can be obtained from the slope of a plot of  $M_c$  versus  $1/R$ .

The relation between  $M_{cg}$  and equilibrium swelling,<sup>12</sup>

$$M_{cg} = \rho \bar{v} \left[ \frac{x/2 - x^{1/3}}{\ln(1-x) + x + \mu x^2} \right]$$

where  $\rho$  is polymer density in grams per cubic centimeter,  $\bar{v}$  is the molal volume of the swelling solvent, in cubic centimeters/gram mole,  $x = 1/V_0$ , where  $V_0$  is the volume swelling ratio, and  $\mu$  is the polymer-solvent interaction coefficient, requires a value for the polymer-solvent interaction coefficient. While this is often obtained osmotically or cryoscopically, it can be estimated from the second virial coefficient  $A_2$  derived from light-scattering data:<sup>13</sup> the slope of a plot of  $Kc/R_\theta$  vs.  $C$  (when  $\theta = 0$ , and where these symbols have their usual light-scattering significances) gives  $2A_2$ , and

$$A_2 = 1(1/2 - \mu)/V_1 d_2^2$$

where  $d_2$  is the density of the pure solvent and  $V_1$  is the molar volume of the solvent.

### Crosslinking in Sol and Gel

Equation (2) describes the overall  $G$  (crosslinking) in both sol and gel phases; this value is independent of the gel fraction. However, because the higher molecular weight fragments are selectively incorporated in the gel, more crosslinks accumulate in the latter phase, and the fraction of total crosslinks formed which end up in the gel increases as the gel fraction

increases.<sup>11</sup> The sol fraction dependences of the quantities  $G_c(\text{gel})$  and  $G_c(\text{sol})$ — $G$  values for crosslinks in the gel and sol separately—are given by

$$G_c(\text{gel}) = G_c(1 + S) \quad (6)$$

$$G_c(\text{sol}) = G_c(S) \quad (7)$$

From Table II, it is seen that at a sol fraction of 0.40, for example, the number of crosslinks in the gel is about 3.5 times that in the sol. For present purposes, the overall  $G$  values for crosslinking are employed.

### Errors

The irradiated polymer must warm up and swell in the extraction step, but the contribution to crosslinking and degradation of these experimental variables cannot be estimated. When comparing different polymers, the most significant source of error in accuracy in the derived  $G$  values is in estimation of  $\mu$ , where a variation in  $\mu$  of  $\pm 0.01$  introduces an error of  $\pm 10\%$  in  $G$ . Since experimental errors in volume swelling ratios and sol fractions are each about 8%, final  $G$  values are considered accurate to about  $\pm 25\%$ . The error in  $\Delta G$ -values, however, for a given polyacrylate is about  $\pm 15\%$ .

## EXPERIMENTAL

### Monomers

*n*-Hexadecyl acrylate was synthesized by ester interchange from *n*-hexadecyl alcohol and ethyl acrylate, according to described procedures.<sup>14</sup> The product, obtained in 43% yield, boiled at 142–144°C./1 mm. Other monomers were commercially available.

### Polymers

Monomers from which inhibitor was removed by washing with sodium hydroxide or sodium carbonate solution were polymerized in aqueous emulsion, with Lux soap and benzoyl peroxide according to the method reported<sup>14</sup> for the *n*-octyl homolog, to conversions of about 80%. The polymers were purified by reprecipitation from suitable solvents. For the methyl and ethyl polymers, the solvents were acetone and the nonsolvents, heptane and methyl alcohol, respectively; for the higher homologs, benzene was the solvent, and methyl alcohol the nonsolvent. Polymers were dried at 1 mm. at 50°C. for 15 hr.

ANAL. polyhexadecyl acrylate: Calcd. for  $(C_{19}H_{36}O_2)_n$ : C, 76.97%; H, 12.22%; Found: C, 76.86%; H, 11.92%.

### Interaction Coefficient, $\mu$

Light-scattering measurements were made at 25°C. with a Brice-Phoenix photometer with the 4360 Å. blue line as the light source. Scattered intensities of benzene solutions filtered through ultra-fine sintered glass were

measured at angles of 45°, 60°, 90°, 115°, and 135° to the primary beam for a series of five concentrations ranging from 0.003 g./ml. to 0.040 g./ml. Refractive index increments were determined on a Brice-Phoenix differential refractometer. In general, the best Zimm plots from  $Kc/R_\theta$  were obtained from values for angles above 45° and for concentrations less than 0.010 g./ml. Table I, which summarizes the light-scattering data, lists  $\mu$  values obtained from Zimm plots and indicates the broad molecular weight distribution of the starting polymers.

### Irradiations

Weighed polymer samples ( $0.5 \pm 0.0002$  g.) were sealed in air, or degassed in glass ampules and sealed *in vacuo*. Most  $\gamma$ -irradiations ( $\text{Co}^{60}$ ) were performed at temperatures ranging from  $-195$  to  $56^\circ\text{C}$ . Polyethyl acrylate and polybutyl acrylate spontaneously gelled at the latter temperature, perhaps because of peroxides not removed in the purification steps, and were not irradiated above  $33^\circ\text{C}$ . A single dose rate of  $5.0 \times 10^5$  rad./hr. ( $\pm 5\%$ ) was employed; total doses ranged from 1.0 to 25.0 Mrad. It was assumed that a dose of 1.0 Mrad corresponds to the absorption of  $62.5 \times 10^{18}$  e.v./g. of polymer.

TABLE I  
Light-Scattering Data for Poly-*n*-Alkyl Acrylates<sup>a</sup>

<i>n</i> -Alkyl group	$dn/dc, \times 10^2,$ cm. <sup>3</sup> /g.	$A_{21}, \times 10^5,$ cm. <sup>3</sup> g. <sup>-2</sup> g.-mole	$\mu$	Molecular weight $\times 10^{-6}$	
				$\bar{M}_w$	$\bar{M}_n^b$
CH <sub>3</sub>	2.21	0.8	0.49	4.6	—
C <sub>2</sub> H <sub>5</sub>	2.87	1.6	0.49	7.4	2.0
C <sub>4</sub> H <sub>9</sub>	2.83	0.8	0.49	11.5	2.0
C <sub>8</sub> H <sub>17</sub>	4.53	1.6	0.49	15.0	0.7
C <sub>16</sub> H <sub>33</sub>	4.98	0.5	0.49	22.2 <sup>c</sup>	1.4

<sup>a</sup> Solvent, benzene; temp., 25°; 4360 Å. light.

<sup>b</sup> Since  $q_0$  can be obtained, the initial  $\bar{M}_n$  was estimated from  $u_1$  using eq. (1).

<sup>c</sup> Using 5460 Å. as a check,  $\bar{M}_w$  was  $20.0 \times 10^6$ .

### Sol Fractions and Swelling Measurements

The irradiated samples were placed in thimbles comprised of three 200-mesh copper or Monel screens. Soluble polymer was quantitatively removed by hot benzene in 150 hr. in a Soxhlet extractor; duplicate runs using benzene at room temperature afforded identical values for the gel fraction. The gel fraction was dried to constant weight, *in vacuo*, at  $75^\circ\text{C}$ . and the equilibrium volume swelling ratio  $V_0$  obtained from weight swelling ratios in benzene at  $25^\circ\text{C}$ .

### Infrared Absorption Spectra of Polycetyl Acrylate

To explain some of the results obtained in this study, the effect of temperature on the degree of orientation in polycetyl acrylate was examined. This polymer strongly absorbs near 6.8 and 13.9  $\mu$ , assigned to methylene

scissoring and rocking vibrations, respectively. The dipole moment changes of both modes are in the same direction relative to the side chain axis, and both appear to reflect the degree of polymer orientation. Thus, while other absorption intensities are temperature independent, these two are reduced on heating and reversibly reappear on cooling. At 60°C. maximum decrease is observed after only a few minutes, but even at 55°C. (about 20°C. above  $T_b$ ) for 20 min. the intensities are not yet reduced to the limiting value. Maintaining the polymer at 40°C. for 1 hr. changes the intensities slightly. The data imply the existence of order in polycetyl acrylate at temperatures above  $T_b$ .

## RESULTS AND DISCUSSION

Figure 1 describes the sol fraction-dose relationships from which  $p_0/q_0$  was obtained according to eq. (1), and Figure 2 describes the dependence of  $M_c$  on  $1/R$  for gel fractions from which  $q_0$  was calculated from (4) and (5).  $G_c$ ,  $G_d$ ,  $G_c$  (sol), and  $G_c$  (gel) then were calculated according to eqs. (1)–(3), (6), and (7). Table II summarizes the  $G$  values and irradiation conditions.

TABLE II  
 $\gamma$ -Initiated Crosslinking and Degradation in Poly-*n*-alkyl Acrylates

<i>n</i> -Alkyl group	$T_b$ , °C. <sup>a</sup>	$p_0/q_0$	$G_c$	$G_d$	$G_c$ (sol) <sup>b</sup>	$G_c$ (gel) <sup>b</sup>	Irradiation temp., °C.
CH <sub>3</sub> <sup>c</sup>	0	—	—	—	—	—	—
C <sub>2</sub> H <sub>5</sub>	-20 <sup>d</sup>	0.45	0.075	0.07	0.03	0.11	0, 33
C <sub>4</sub> H <sub>9</sub>	-45	0.28	0.21	0.12	0.085	0.30	33
		0.40	0.11	0.09	0.045	0.16	-20
		0.64	0.10	0.12	0.04	0.14	-80
		0.70	0.07	0.10	0.03	0.10	-196
C <sub>8</sub> H <sub>17</sub>	-65	0.16	0.33	0.11	0.13	0.46	33
		0.26	0.33	0.17	0.13	0.46	-20
		0.52	0.15	0.15	0.06	0.21	-196, -80
C <sub>16</sub> H <sub>33</sub>	33	0.31	0.18	0.11	0.07	0.26	43, 56
		0.66	0.07	0.09	0.03	0.10	33
		0.73	0.06	0.09	0.025	0.09	-20
		0.87	0.06	0.10	0.02	0.08	-196, -80

<sup>a</sup> Data of Rehberg and Fisher;<sup>15</sup>  $T_g$  and  $T_b$  are identical for all but polycetyl acrylate, which has an estimated  $T_g$  of -80°C.

<sup>b</sup> Calcd. for  $S = 0.40$ .

<sup>c</sup> Polymethyl acrylate did not gel at doses up to 25.0 Mrad above and below its  $T_b$ .

<sup>d</sup> Polyethyl acrylate did not gel when irradiated at or below its  $T_b$ .

### Degradation

While the ratio  $p_0/q_0$  is sensitive to many factors, absolute energy yields for main chain degradation (Table II), seem to be independent of the degree of crosslinking, irradiation temperature, and chemical configuration of the monomer unit;  $G_d \cong 0.12$ . These data indicate that main chain breaking is not the result of competing reactions, and is not diffusion controlled.



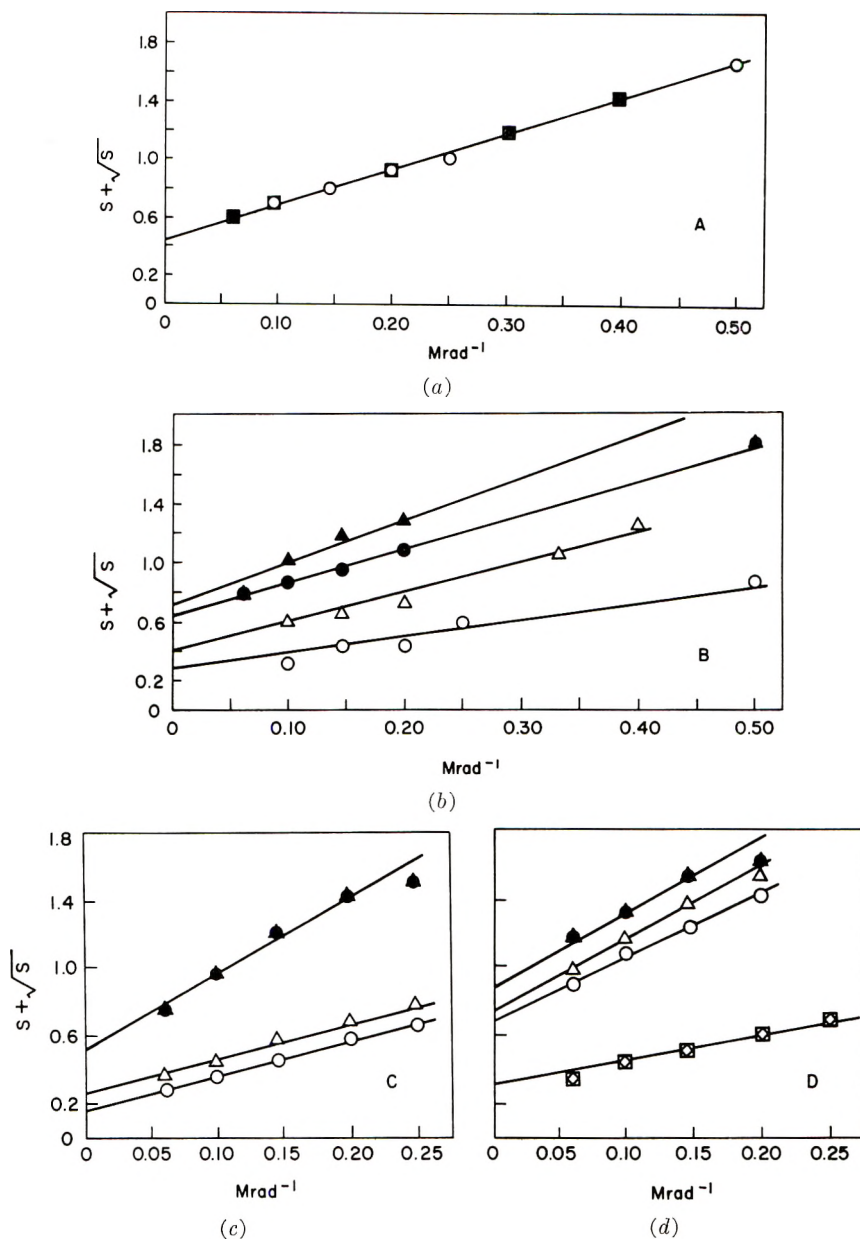


Fig. 1. Dependence of sol fraction on reciprocal radiation dose for polymers of (A) ethyl, (B) *n*-butyl, (C) *n*-octyl, and (D) *n*-cetyl acrylate; irradiation temperature ( $\diamond$ ) 56°C.; ( $\square$ ) 43°C.; ( $\circ$ ) 33°C.; ( $\blacksquare$ ) 0°C.; ( $\triangle$ ) -20°C.; ( $\bullet$ ) -80°C.; ( $\blacktriangle$ ) -196°C. Departure from linearity at low doses is attributed to the initially broad molecular weight distribution which randomizes in the early stages of the irradiation.

It appears that degradation follows a radiation event involving energies much in excess of thermal energies.

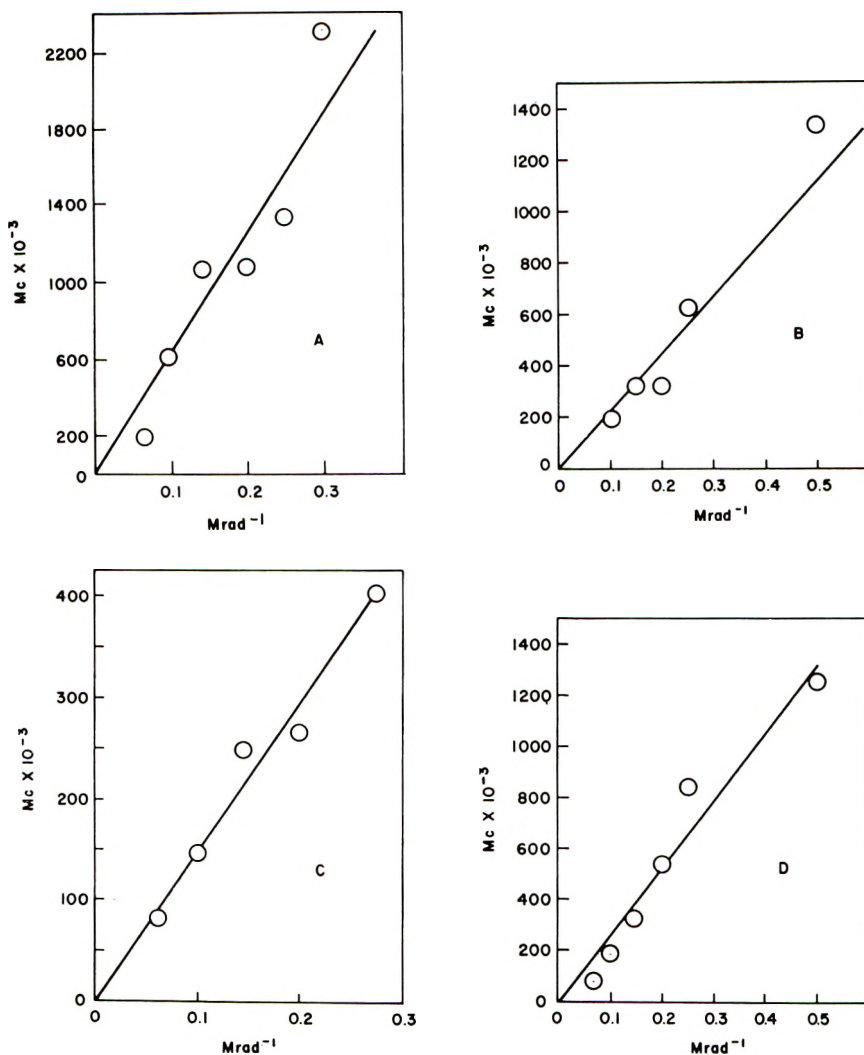


Fig. 2. Molecular weights between crosslinks of gel fractions as a function of reciprocal radiation dose for polymers of (A) ethyl, (B) *n*-butyl, (C) *n*-octyl, and (D) *n*-cetyl acrylate; each point represents an average value obtained for several irradiation temperatures above the polymer  $T_b$ .

In support of this conclusion, it is found that  $G_d$  does not change for room temperature irradiations in the presence of oxygen (a radical scavenger) and for irradiations *in vacuo* at  $-80^\circ\text{C}$ . (to freeze the radicals) followed by exposure to oxygen at the same low temperature. In accord with these data, Shultz and Bovey<sup>16</sup> find almost the identical energy yields for degradation ( $G = 0.16$ ) for polymers of methyl, *n*-butyl, isobutyl, and *tert*-butyl acrylate electron-irradiated in air.

The combined results of Shultz and Bovey<sup>16</sup> and the present work, suggesting the importance of a molecular chain breaking step, differ from the

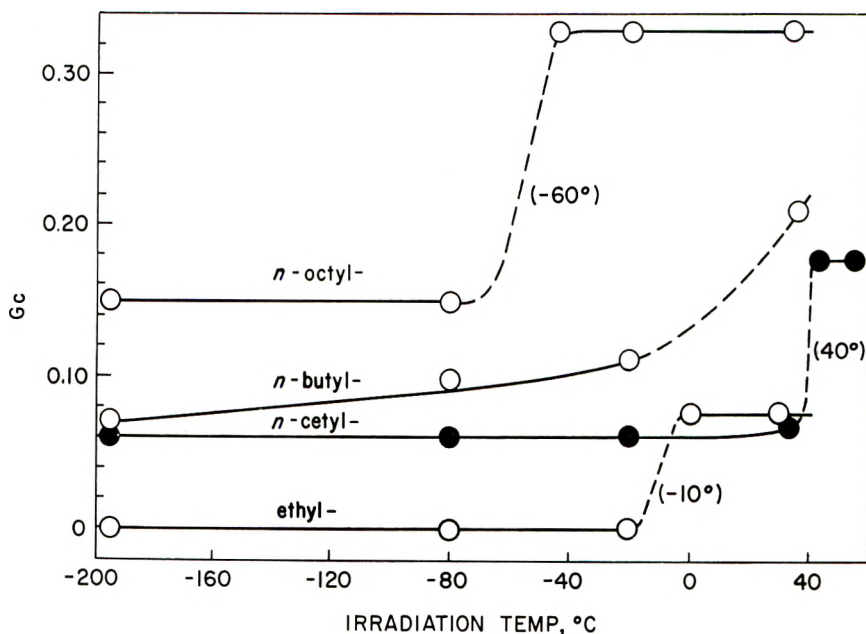


Fig. 3. Dependence of crosslinking efficiency on irradiation temperature; figures in parentheses indicate the approximate temperature at which the break in  $G_c$  occurs.

effects of temperature on radiation degradation in polyisobutylene<sup>8</sup> and polymethyl methacrylate,<sup>6</sup> where  $G_d$  increases about threefold over a 200°C. range, and from the changeover in mechanism above and below  $T_g$  for the *p*-substituted polystyrenes<sup>7</sup> and polyfluoroolefin<sup>9</sup> mentioned earlier. The occurrence of competing radical reactions explains the reported data.

### Crosslinking

Inspection of  $G_c$  values in Table II and Figure 3 reveals that (1) crosslinking efficiency is temperature independent below  $T_b$ , and greater, but again independent of temperature above this transition; in the case of polybutyl acrylate, for which incomplete data are available, the radiation results indicate a  $T_b$  about 30°C. higher than the reported one<sup>15</sup> of -45°C. (2) At a given temperature, crosslinking efficiency in the amorphous polymers increases as the length of the alkyl substituent increases. (3) Both above and below its  $T_b$ ,  $G_c$  for polycetyl acrylate, where side chain crystallinity occurs, is lower than expected on the basis of the behavior of the amorphous polymers, and is somewhere between the values for the butyl and ethyl homologs; within experimental error,  $G_c$  was the same for irradiations at 20° *in vacuo* and in the presence of oxygen.

These data are explained by assuming that under the relatively mild experimental conditions employed, crosslinking *in vacuo* occurs to the exclusion of competing reactions. Below  $T_b$ , when the polymer chains are rigid, radiation produced radicals either are generated in close proximity

or migrate along the polymer chain to sites favorable for cross-linking, i.e., where the carbon atoms of two chains are 3-4 Å. apart. If oxygen is present, polymeric peroxy radicals also capable of crosslinking may be produced, although no attempt was made to identify peroxidic structures. Crosslinking in the "locked" configuration thus is fixed by the geometry of the molecules in the glass, where a sufficient number of these positions exist to give the  $G_c$  noted for irradiations below the brittle point. It appears that radical sites stable for at least a few seconds also are formed in the glass on atoms not quite close enough for bond formation to occur—10 Å. apart, for example. As the reaction temperature is raised to  $T_b$ , the jump frequency of chain segments over a distance of several angstrom units increases sharply from essentially zero below  $T_b$  to an estimated 1 jump every few seconds at  $T_b$ ;<sup>17</sup> this extra mobility initiates production of a few more crosslinks. At the still higher temperatures employed in this study, or when the irradiated polymer is swollen with solvent in the extraction step, mobility and crosslinking may not increase because the presence of only a few crosslinks in the system greatly restricts segmental motion.

It is also concluded that crosslinking in the amorphous polymers both above and below  $T_b$  occurs predominantly on the hydrocarbon side chain. Thus, polymethyl acrylate never gels under the present experimental conditions, polyethyl acrylate gels only at elevated temperatures, and the higher homologs, excepting polycetyl acrylate, are progressively more radiation sensitive.

The anomalously low  $G_c$  for the cetyl polymer below  $T_b$  is attributed to immobility of radiation produced polymer radicals, now in the side chain crystallites. Even for irradiations at temperatures 20° above  $T_b$ , in the time scale of the present experiments, infrared spectra suggest sufficient order in the starting polymer so that radical motion may be limited. If a sample irradiated below  $T_b$  is annealed for several hours above its softening point, no change in crosslinking efficiency is noted, indicating that trapped "crosslinking radicals" in this polymer do not persist for long times. This behavior is different from that observed in high density polyethylene,<sup>1</sup> which occludes radicals capable of subsequent crosslinking when the polymer is heated to its amorphous state.

### References

1. Lawton, E., J. Balwit, and R. Powell, *J. Polymer Sci.*, **32**, 257 (1958).
2. Shen-Kan, I., A. Pravedinkov, and S. Medvedev, *Dok. Akad. Nauk. SSSR*, **122**, No. 2, 254 (1958).
3. Black, R., *Nature*, **178**, 305 (1956); *J. Appl. Chem.*, **8**, 159 (1958); A. Charlesby and W. Davison, *Chem. Ind. (London)*, **1957**, 232.
4. Miller, A., *J. Am. Chem. Soc.*, **82**, 3519 (1960).
5. Hayden, P., *Intern. J. Appl. Radiation Isotopes*, **8**, 65 (1960).
6. Wall, L., and D. Brown, *J. Phys. Chem.*, **61**, 129 (1957).
7. Burlant, W., V. Serment, and J. Neerman, *J. Polymer Sci.*, **58**, 491 (1962).
8. Alexander, P., R. Black, and A. Charlesby, *Proc. Roy. Soc. (London)*, **A232**, 31 (1955).
9. Bowers, G., and E. Lovejoy, *Ind. Eng. Chem., Prod. Res. Dev.*, **1**, No. 2, 89 (1962).

10. Riddle, E., *Monomeric Acrylic Esters*, Reinhold, New York, 1954, p. 59-62.
11. Charlesby, A., *Atomic Radiation and Polymers*, Pergamon, London, 1960 (a) p. 171; (b) *ibid.*, p. 145.
12. Flory, P., *Principles of Polymer Chemistry*, Cornell, New York, 1953, p. 579.
13. Stacey, K., *Light Scattering in Physical Chemistry*, Butterworths, London, 1956, p. 19, 23.
14. Rehberg, C., *Org. Syn.*, **26**, 18 (1946).
15. Rehberg, C., and C. Fisher, *J. Am. Chem. Soc.*, **66**, 1203 (1944).
16. Shultz, A., and F. Bovey, *J. Polymer Sci.*, **22**, 485 (1956).
17. Bucche, F., *J. Chem. Phys.*, **20**, No. 12, 1959 (1952).

### Résumé

Les polymères de l'acrylate de méthyle, d'éthyle, de *n*-butyle, *n*-octyle et de *n*-cétyle ont été irradiés par rayons-gamma sous vide; les effets de la température d'irradiation ( $-196$  à  $56^{\circ}$ ) sur les rendements énergétiques du point de vue du pontage et de la dégradation ont été estimés à partir des fractions de gel et du gonflement du polymère et de la température de réaction, suggérant un processus de rupture par chaîne moléculaire. Le pontage, qui a lieu principalement aux chaînons alcoyles latéraux, est indépendant de la température au-dessus et au-dessous du point de ramollissement du polymère, mais il est plusieurs fois plus prononcé pour des irradiations effectuées audessus du point de ramollissement. Ces données semblent montrer l'importance de la mobilité de segments des radicaux polymériques produits par radiation dans l'étape de pontage.

### Zusammenfassung

Polymere Methyl-, Äthyl-, *n*-Butyl-, *n*-Octyl und *n*-Cetylacrylat wurde im Vakuum  $\gamma$ -bestrahlt und der Einfluss der Bestrahlungstemperatur ( $-196^{\circ}$  bis  $56^{\circ}$ ) auf die Energieausbeute für Vernetzung und Abbau aus der Gelfraktion und dem Quellungsverhalten des Gels bestimmt. Das Ausmass des Abbaus ist von Polymerstruktur und Reaktionstemperatur unabhängig, was auf einen Bruchprozess für die Molekülketten hinweist. Vernetzung, die vornehmlich an den Alkylseitenketten eintritt, ist oberhalb und unterhalb des Polymererweichungspunktes von der Temperatur unabhängig, erweist sich jedoch für Bestrahlung oberhalb des Erweichungspunktes als einige Male höher. Diese Ergebnisse lassen die Bedeutung der Segmentbeweglichkeit der strahlungs-erzeugten Polymerradikale beim Vernetzungsschritt erkennen.

Received September 12, 1962

Revised October 8, 1962

## Kinetics of the Photopolymerization of Tetraethylene Glycol Dimethacrylate in the Bulk with the Use of Desyl Aryl Sulfides as Photoinitiators

CONSTANTINE C. PETROPOULOS, *The National Cash Register Company, Dayton, Ohio*

### Synopsis

Five desyl aryl sulfides were prepared for use as photoinitiators in the determination of the bulk polymerization rates of tetraethylene glycol dimethacrylate at 25°C. As a first approximation, the initial rates were first-order with respect to monomer and one half-order with respect to initiator. From this, approximate initial overall rate constants were determined. The data indicate that resonance stabilization of the dissociated radical seem to affect the polymerization rate. Complications arising from the auto catalytic gel effect were discussed.

### INTRODUCTION

It will be recalled that according to the simplest concept of free radical polymerization, initiator molecules (C) decompose to form free radicals (R) by a first-order law. Monomer (M) adds to a radical to form a new radical of similar activity, and many subsequent monomer molecules add by identical propagation steps, each first order in both monomer and radicals. Termination by either disproportionation or by combination involves two radicals. The steady-state treatment then leads to:

$$R_p = -d[M]/dt = k_2(k_d f/k_3)^{0.5}[M][C]^{0.5} \quad (1)$$

Subscripts 2 and 3 refer to the propagation and termination steps, respectively. The rate constant for the dissociation of the initiator is represented by  $k_d$  and the initiator efficiency is represented by  $f$ , the fraction of the total initiator radical effective in initiating a chain. The product  $k_d f$  is sometimes combined and is represented by  $k_1$ , the initiation rate constant. The constants in eq. (1) may be combined to give:

$$R_p = k[M][C]^{0.5} \quad (2)$$

where  $k$  represents the overall observed rate constant.

### Effect of Conversion on the Overall Rate

The concentration of the initiator usually does not change much during the course of the polymerization. Hence, if the initiator efficiency is

independent of the monomer concentration, first-order kinetics may be expected for the conversion of monomer to polymer. For example, the polymerization of styrene in toluene in the presence of benzoyl peroxide proceeds approximately as a first-order reaction according to the results of Schulz and Husemann.<sup>1</sup> Likewise, the benzoyl peroxide-initiated polymerization of *d*-*sec*-butyl  $\alpha$ -chloroacrylate and vinyl *l*- $\beta$ -phenylbutyrate in dioxane are quite accurately first-order up to high conversion.<sup>2</sup>

It is also known that the polymerization of certain monomers in the bulk or in concentrated solutions is accompanied by a marked deviation from first-order kinetics in the direction of an increase in the reaction rate termed autoacceleration. This effect is particularly pronounced with the benzoyl peroxide-initiated polymerization of methyl methacrylate<sup>3</sup> and with the photo-initiated polymerization of methyl methacrylate with benzoin or 2,2'-azobisisobutyronitrile.<sup>4</sup> It was shown that for the first 25% conversion, the rate was found to be first-order. The following equation was found to explain the results obtained to a first approximation:

$$\frac{-d(M)}{dt} = k_2(k_1/k_3)^{0.5}[M][C]^{0.5}[I]^{0.5} \quad (3)$$

where [I] is the light intensity and subscripts 1, 2, and 3, refer to the initiation, propagation, and termination rate constants, respectively.

At about 25% conversion a sharp increase in the rate is observed and simultaneously the average molecular weight of the polymer formed was observed to increase sharply. This increase in rate was attributed to the decrease in the termination rate constant. This is caused by an increase of viscosity of the medium at the gel point, where the large growing polymer radicals now become diffusion-controlled and cannot terminate as readily. The mobilities of the smaller monomer molecules however, have not as yet been affected.

Norrish and Smith,<sup>5</sup> in their investigation into the effect of diluents on the polymerization of methyl methacrylate, found they influenced the inception of the autoacceleration of the reaction rate. Monomer solvents which also acted as good solvents for the polymer delayed or even prevented the onset of rate acceleration. On the other hand, polymer precipitants, induced an early and marked autoacceleration. Bamford and Jenkins<sup>6</sup> have reported a similar autoacceleration in both the thermally catalyzed and photosensitized bulk polymerization of acrylonitrile. In this case the polymer is insoluble in its own monomer. Moreover, both they and Thomas and Pellon<sup>7</sup> have noted considerable deviation from the normal dependence of the rate of polymerization upon the square root of the initiator concentration. Such kinetic characteristics have been explained in terms of occlusion of free radicals by flocculated polymer. Under certain conditions, these occluded radicals become inaccessible to all but very small molecules. Biradical termination is hindered even at low degrees of occlusion.

### Effect of Crosslinking on the Overall Rate

In the copolymerization of methyl methacrylate with ethylene glycol dimethacrylate, Hayden and Melville<sup>8</sup> found that as the divinyl unit is increased, the inception of the autoacceleration rate occurs at an ever decreasing conversion to a point where the autoacceleration rate begins immediately. The polymerization also comes to a premature end before the monomer is completely exhausted.

At first, the viscosity of the solution increases rapidly causing the termination step to become diffusion controlled, thereby, decreasing the termination rate constant and increasing the overall rate. In the later stages, as the solution is transformed into a glass, both monomer and growing polymer radicals become immobilized causing the polymerization to end prematurely. The rate as noted by the other workers above also deviates from the normal square root dependence on the rate of initiation.

Because of the early inception of the autoaccelerated rate of these systems containing a difunctional monomer or a medium which precipitates the polymer, it is difficult to determine the initial rate. Also the range in which the rate obtained agrees with eq. (2) becomes ever so short.

In the work to be reported in this paper, the same difficulty arises. Here the photopolymerization of tetraethylene glycol dimethacrylate (TEGD) in the bulk at 25°C. was studied. Desyl aryl sulfides were used as initiators. Because of the difficulty in determining the initial rate and the short range in which the rates follow eq. (2), it is hoped that correlation with eq. (2) can be obtained at least at the very start of the polymerization as a first approximation. From this, it is hoped that the relative rates of polymerization of this monomer initiated by a few desyl aryl sulfides can be approximated. The purpose of this work is directed toward this end.

## EXPERIMENTAL

### Materials

The tetraethylene glycol dimethacrylate monomer was obtained from The Borden Company and used without further purification. The density of the monomer,  $d_4^{25}$  is 1.0740.

### Synthesis

The desyl aryl sulfide initiators were prepared in this laboratory. They are listed with their physical properties in Table I.

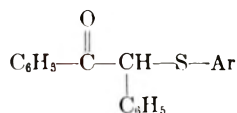
Desyl phenyl sulfide was prepared by the method of Schönberg and Islander<sup>9</sup> by reacting desyl chloride with thiophenol in alcoholic sodium ethoxide.

The other desyl aryl sulfides were prepared in the following manner.

Sodium methoxide (0.0086 mole) and the arylthiol compound (0.0086 mole) in 25 ml. of toluene were stirred vigorously with a magnetic stirrer while under reflux for 1 hr. Then 15 ml. of the solvent was stripped to



TABLE I



Ar	Abbreviation	M.P., °C.	M.P. (reported), °C.	Remarks
Phenyl	DPS	80.5-81.5	81 (83-84) <sup>a</sup>	Structure in agreement with I.R.
<i>o</i> -Tolyl	OTDS	111-112	115 <sup>b</sup>	Structure in agreement with I.R.
<i>p</i> -Tolyl	PTDS	91-92	79 <sup>b</sup>	Structure in agreement with I.R.
<i>p</i> -Anisyl	PADS	76-77		Structure in agreement with I.R. calculated: C, 75.4; H, 5.4; S, 9.6; found C, 75.0; H, 5.5; S, 9.5.
$\beta$ -Naphthyl	NDS	125-126		Structure in agreement with I.R. calculated: C, 81.3; H, 5.1; S, 9.0; found C, 81.0; H, 5.1; S, 9.2.

<sup>a</sup> Data of Schönberg and Islander.<sup>9</sup>

<sup>b</sup> Data of Schönberg et al.<sup>11</sup>

remove most of the methanol formed in the reaction. Desyl chloride (0.0086 mole) in 15 ml. of toluene was added to the mixture and the system was refluxed for 3 hr. The toluene solution was then extracted with two 20-ml. portions of water. The aqueous portions were combined and extracted once with fresh toluene. The organic layers were combined, dried with anhydrous calcium chloride, and the solvent stripped. The residue was then recrystallized from ligroin (b.p. 66-75°C.) or *n*-hexane.

In the preparation of  $\beta$ -naphthyl desyl sulfide some  $\beta$ -naphthyl disulfide was also obtained due to the air oxidation of the sodium salt of the thionaphthol. This was separated from the desyl sulfide derivative by fractional recrystallization from ethanol. The disulfide separates first. The  $\beta$ -naphthyldesyl sulfide was recovered from the filtrate and recrystallized from ligroin (b.p. 66-75°C.).

### Discussion of Experimental Method

The rate at which a polymerization reaction occurs can be followed in several ways. The usual methods involve following the change in some physical property of the system, i.e., volume, viscosity, etc. However, the present system (tetraethylene glycol dimethacrylate) presents difficulties of such a nature that these methods cannot be used, or are very difficult to use, since upon polymerization, a crosslinked gel is formed very quickly. This rapid gel formation and rapid insolubilization of the polymer quickly renders the dilatometric or viscometric methods difficult to use, therefore, the gravimetric procedure was used for following the polymerization.

It was found that under the experimental conditions employed, the polymerization of TEGD alone (no initiator) was negligible over the time

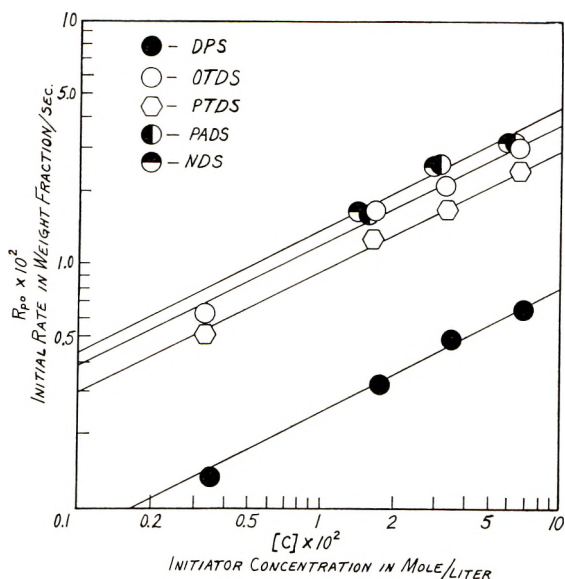


Fig. 1. Log-log plot of  $R_p$  vs.  $[C]$ : (DPS) initiated with desyl phenyl sulfide; (OTDS), initiated with *o*-tolyl desyl sulfide; (PTDS) initiated with *p*-tolyl desyl sulfide; (PADS) initiated with *p*-anisyl desyl sulfide; (NDS) initiated with  $\beta$ -naphthyl desyl sulfide. All lines drawn with a theoretical slope of 0.5.

interval studied. Only 0–2% polymer was formed after 6 min. of exposure and an average of (0.3%) polymer was obtained after a 1-min. exposure.

The light source employed for exposure was a Gates mercury arc lamp at a distance of 13 cm. from the sample. The voltage drop across the lamp was measured at  $\frac{1}{2}$ -hr. intervals throughout the working day and was found to be constant. Therefore, it was assumed that at a given distance and at a fixed spot under the shutter, the intensity of the light source remained constant.

After initial equilibrium has been reached, it was found that the temperature rise due to the light source at a given distance, at a given spot under the shutter was about 0.5°C. for a 30-sec. exposure and about 1°C. for a 1-min. exposure. It was assumed that a temperature variance of 1°C. could be neglected; the samples were nevertheless, thermostated at 25°C. before exposure.

The synchronized shutter employed enabled the exposure time to be controlled to within 0.2 sec.

### Polymerization Procedure

The solutions of the various desyl aryl sulfide initiators and monomer were prepared by weighing the components shortly before use. The reaction vessel used was a 30 ml. beaker containing a pad made up of two pieces of filter paper, about 2 cm.<sup>2</sup>, fastened together on one edge. A 100 mg. sample of monomer solution was weighed on the filter pad in a tared reaction

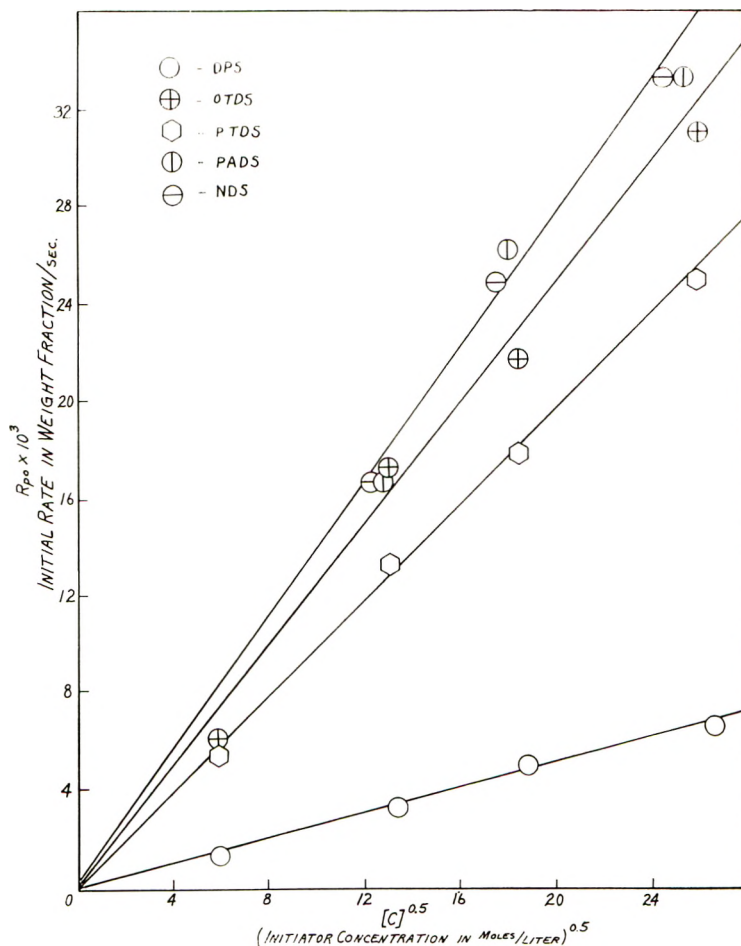


Fig. 2. Plot of  $R_{p0}$  vs.  $[C]^{0.5}$ : (DPS) initiated with desyl phenyl sulfide; (OTDS) initiated with *o*-tolyl desyl sulfide; (PTDS) initiated with *p*-tolyl desyl sulfide; (PADS) initiated with *p*-anisyl desyl sulfide; (NDS) initiated with  $\beta$ -naphthyl desyl sulfide.

vessel. By this method all of the monomer-initiator solution was retained within the area of the pad. The reaction vessel was placed in a constant temperature bath at 25°C.

After temperature equilibrium was reached, the reaction vessel was removed from the constant temperature bath and placed at a defined position under the shutter. After exposure to a Gates mercury lamp at a distance of about 13 cm., 2 ml. of a cold *n*-hexane solution was added and the reaction vessel was placed in an ice bath. The hexane was removed with a medicine dropper having a finely drawn capillary tip. The washing procedure was repeated twice with 3 ml. portions of cold *n*-hexane. The reaction vessel was dried on the outside, placed in a vacuum oven at approximately 100°C. for 1 hr. and allowed to stand at room temperature

for about  $1/2$  hr. before weighing. A blank correction of 0.3 mg. was applied.

## RESULTS AND DISCUSSION

Table I gives a list of the desyl aryl sulfides and their physical properties that were used as photoinitiators for studying the rates of photopolymerization of tetraethylene glycol dimethacrylate (TEGD) at 25°C.

Tables II-VI show the initial rates of polymerization with respect to initiator concentration. The ratio  $R_{p_0}/[C]^{0.5}$  in the last column of these tables is fairly constant implying a square root relationship of initial rates to initiator concentration. In Figure 1, a log-log plot of the initial rate versus the initiator concentration yields a straight line. A line drawn with a theoretical slope of 0.5 appears to be in good agreement with the points. A plot of the initial rate against the square root of the initiator concentration therefore, should give a straight line. This is shown in Figure 2. The straight line drawn appears to be in good agreement with the points. Since the line passes through the origin, thermal polymerization (if any) may be neglected.

TABLE II  
Initial Rates of Photopolymerization of TEGD with DPS at 25°C.

Initiator, wt.-%	Initial rate weight fraction/sec. $R_{p_0}$	Initiator concn. [C], mole/l.	$[C]^{0.5}$	$R_{p_0}/[C]^{0.5}$
2.0	0.0067	0.706	0.265	0.025
1.0	0.0050	0.0353	0.188	0.027
0.5	0.0032	0.0177	0.133	0.024
0.1	0.0014	0.0035	0.0594	0.023

TABLE III  
Initial Rates of Photopolymerization of TEGD with OTDS at 25°C.

Initiator, wt.-%	Initial rate weight fraction/sec. $R_{p_0}$	Initiator concn. [C], mole/l.	$[C]^{0.5}$	$R_{p_0}/[C]^{0.5}$
2.0	0.031	0.0674	0.259	0.12
1.0	0.022	0.0337	0.184	0.12
0.5	0.017	0.0169	0.130	0.13
0.1	0.0062	0.00337	0.0581	0.11

TABLE IV  
Initial Rates of Photopolymerization of TEGD with PTDS at 25°C.

Initiator, wt.-%	Initial rate weight fraction/sec. $R_{p_0}$	Initiator concn. [C], mole/l.	$[C]^{0.5}$	$R_{p_0}/[C]^{0.5}$
2.0	0.025	0.0674	0.259	0.097
1.0	0.018	0.0337	0.184	0.097
0.5	0.013	0.0169	0.130	0.10
0.1	0.0055	0.00337	0.0581	0.095

TABLE V  
Initial Rates of Photopolymerization of TEGD with PADS at 25°C.

Initiator, wt.-%	Initial rate weight fraction/sec. $R_{p_0}$	Initiator concn. [C], mole/l.	$[C]^{0.5}$	$R_{p_0}/[C]^{0.5}$
2.0	0.033	0.0642	0.253	0.13
1.0	0.026	0.0321	0.179	0.15
0.5	0.017	0.0161	0.127	0.13

TABLE VI  
Initial Rates of Photopolymerization of TEGD with NDS at 25°C.

Initiator, wt.-%	Initial rate weight fraction/sec. $R_{p_0}$	Initiator concn. [C], mole/l.	$[C]^{0.5}$	$R_{p_0}/[C]^{0.5}$
2.0	0.033	0.0606	0.246	0.14
1.0	0.025	0.0303	0.174	0.14
0.5	0.017	0.0152	0.123	0.14

The following equation describes the data:

$$R_{p_0} = \text{slope } [C]^{0.5} \quad (4)$$

where  $R_{p_0}$  is the initial rate in weight fraction per second. If it can be assumed that the initial rate is first-order with respect to monomer for a first approximation, and the light intensity remains constant, eq. (4) converts to:

$$R_{p_0} = kF_m^0 [C]^{0.5} \quad (5)$$

where  $F_m^0$  is the initial weight fraction of the monomer (initially equal to 1),  $k$  is the overall rate constant in (liter/mole)<sup>0.5</sup> per second. If eq. (5) is multiplied by the ratio  $d/M$  where  $d$  is the density of the monomer in grams per liter and  $M$  is the molecular weight of the monomer, eq. (5) then becomes equivalent to eq. (2) derived from theory which gives the rate of disappearance of the monomer in moles per liter per second.

Figure 3 shows the rate curve obtained for the conversion to polymer with time. The dotted line represents the theoretical first order curve. This is in agreement with the experimental curve up to about 5% conversion indicating that the first order assumption is reasonable for the initial rates as a first approximation.

Due to the early inception of the autoaccelerated rate, it was difficult to determine the initial rate accurately. However, from the data of Hayden and Melville,<sup>8</sup> it was shown that the initial rate of copolymerization of methyl methacrylate with ethylene glycol dimethacrylate at 22.5°C. was 3.4, 3.8, and 4.2%/hr. for 0.005, 0.05, and 0.22 mole fraction of the divinyl monomer, respectively. As the mole fraction of the divinyl monomer was increased, the inception of the accelerated rate occurred earlier. The value 4.2 represents the initial rate where the inception of the accelerated rate was practically instantaneous. The value for the initial rate for the polymerization of pure methyl methacrylate at 22.5°C. was given as 3.5%/hr.

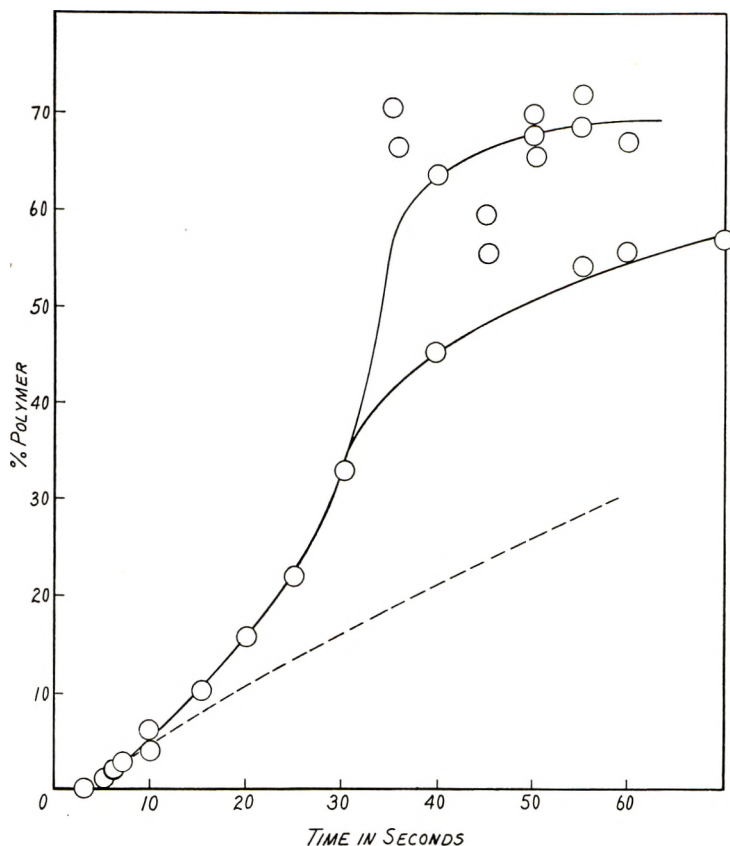


Fig. 3. Polymerization of tetraethylene glycol dimethacrylate initiated by 2% desyl phenyl sulfide at 25°C. Dotted line is the theoretical first-order curve calculated from the initial slope.

It appears reasonable in this work, therefore, to assume that the initial rates obtained experimentally do not differ too much from their actual values so that a first approximation can be obtained. For the benzoyl peroxide initiated copolymerization of methyl methacrylate and ethylene glycol dimethacrylate, Gordon and Roe<sup>10</sup> have shown that the initial rate varies with the square root of the initiator concentration before gelation sets in (about 2% conversion).

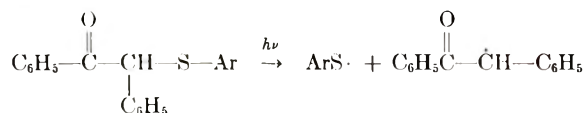
Another difficulty encountered, in addition to possible random errors, is the trapping of the monomer by the formation of a gel especially at higher conversions. This is evident from the scattering of points shown in Figures 3 and 4. This is probably caused by a continuation of polymerization by the trapped monomers and radicals in the gel during the drying process in the experimental rate determinations. As can be seen from Figure 3, at about 35% conversion, two different curves can be drawn to connect the experimental points. In this work, an attempt was made only to correlate the initial rates and as can be seen from Figure 3, the initial portion of the

curve is well defined. This is also true for other curves not shown here. Discussion here, however, does show the complications arising from the gel effect.

### CONCLUSION

The data indicate that the rates for initial polymerization (up to about 5% conversion) follow the rate law given by eq. (5) or (2). This indicates initially that upon irradiation with ultraviolet light, the initiator decomposes into radicals in a rate determining step, and a fast addition of these radicals to the monomer then initiates the chain. Termination proceeds through a bi-molecular process.

Evidence that these desyl aryl sulfides do dissociate into radicals upon irradiation, is given by Schönberg<sup>11</sup> and his co-workers, they proposed the following scheme:



These workers were able to isolate didesyl. In the cases in which Ar was phenyl, *o*-tolyl, *m*-tolyl, and *p*-tolyl, no thiophenol could be separated. However, in the case in which Ar was benzoyl, they succeeded in isolating both didesyl and dibenzoyl disulfide.

Since the monomer used with each of the desyl aryl sulfide initiators was the same in each case, the addition and termination reactions should also be the same.

It can be assumed that the propagation and termination rates in each case initially do not change significantly, the difference in the initial overall rates might be attributed to the relative rates of dissociation of the initiators.

It is not known whether the aryl thio radical, or the desyl radical, or both, are responsible for the initiation. From Table VII, the differences in the overall rate constants of desyl phenyl sulfide and the other substituted desyl aryl sulfides seem to indicate that resonance stabilization of the dissociated aryl thio radical might be important in increasing the rate of dissociation of the initiator.

TABLE VII  
The Overall Rate Constant for the Photopolymerization of TEGD with Various Desylaryl Sulfides at 25°C.

Initiator	Overall rate constant $k \times 10^2$ , (liter/mole) <sup>0.5</sup> /sec. <sup>1</sup>
DPS	2.6
OTDS	13.0
PTDS	9.9
PADS	14.0
NDS	14.0

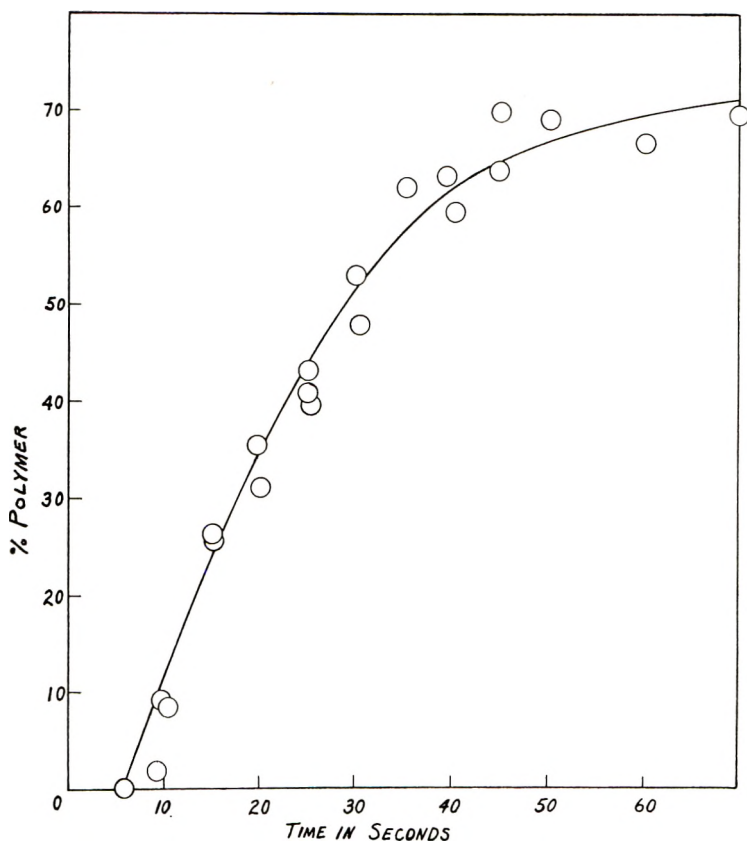


Fig. 4. Polymerization of tetraethylene glycol dimethacrylate initiated by 2% *o*-tolyl desyl sulfide at 25°C.

It is interesting to note that the rate of polymerization initiated by the *o*-tolyl derivative is slightly faster than that of the *p*-tolyl derivative. The effect of resonance stabilization should be the same in both derivatives. There may be a further enhancement of the dissociation rate of the *ortho* derivative due to steric factors. However, this difference is too small to come to any conclusions. It was just mentioned as a point of interest.

The author is indebted to the management of The National Cash Register Company of Dayton, Ohio, for permission to publish these results and to the members of these laboratories for discussion and assistance. The author wishes to thank Mr. T. Hoover, who first developed the technique used here for following the rates and Mr. J. Cartmell for his valuable assistance in the experimental determinations. The author also wishes to express his gratitude to the Air Force, Contract No. AF 33(616)-5510 under whose sponsorship the initiators were synthesized, and the Office of Naval Research, Contract No. 2848(00) under whose sponsorship the polymerization studies were carried out.



### References

1. Schulz, G. V., and E. Husemann, *Z. Physik. Chem.*, **B39**, 246 (1938).
2. Marvel, C. S., J. Dec, and H. G. Cooke, *J. Am. Chem. Soc.*, **62**, 3499 (1940).
3. Schulz, G. V., and G. Harborth, *Makromol. Chem.*, **1**, 106 (1947).
4. Naylor, M. A., and F. W. Billmeyer, Jr., *J. Am. Chem. Soc.*, **75**, 2181 (1953).
5. Norrish, R. G. W., and R. R. Smith, *Nature*, **150**, 336 (1942).
6. Bamford, C. H., and A. D. Jenkins, *Proc. Roy. Soc. (London)*, **A216**, 515 (1953).
7. Thomas, W. M., and J. J. Pellon, *J. Polymer Sci.*, **13**, 329 (1954).
8. Hayden, P., and H. Melville, *J. Polymer Sci.*, **43**, 201 (1960).
9. Schönberg, A., and Y. Islander, *J. Chem. Soc.*, **1942**, 90.
10. Gordon, M., and R. J. Roe, *J. Polymer Sci.*, **21**, 27 (1956).
11. Schönberg, A., et. al., *J. Am. Chem. Soc.*, **78**, 1224 (1956).

### Résumé

On a préparé cinq sulfures désyl-acryliques comme photo-initiateurs dans la détermination des vitesses de polymérisation en masse du diméthacrylate de tétraéthylène-glycol à 25°C. En première approximation les vitesses initiales sont d'ordre un en ce qui concerne le monomère et d'un ordre un-demi en ce qui concerne l'initiateur. A partir de ceci, on a déterminé des constantes approximatives de vitesses globales initiales. Les données indiquent que la stabilisation du radical dissocié par résonance semble affecter la vitesse de polymérisation. Des complications provenant de l'effet de gel auto-catalytique ont été discutées.

### Zusammenfassung

Fünf Desylarylsulfide wurden zur Verwendung als Photosensibilisatoren bei der Bestimmung der Polymerisationsgeschwindigkeit von Tetraäthylenglykoldimethacrylat bei 25°C dargestellt. In erster Näherung war die Anfangsgeschwindigkeit von erster Ordnung in bezug auf das Monomere und von der Ordnung ein halb in bezug auf den Starter. Daraus wurden angenäherte Brutto-Anfangsgeschwindigkeitskonstanten bestimmt. Die Ergebnisse zeigen, dass die Resonanzstabilisierung des dissoziierten Radikals auf die Polymerisationsgeschwindigkeit Einfluss zu besitzen scheint. Komplikationen durch den autokatalytischen Geleffekt werden diskutiert.

Received September 23, 1962

## Photolysis of Cellulose in a Vacuum with 2537 A. Light

JOSEPH H. FLYNN and WILLIAM L. MORROW, *Polymer Chemistry Section, National Bureau of Standards, Washington, D. C.*

### Synopsis

Cotton sliver, cotton linters, periodate-chlorite-oxidized cellulose, and several regenerated celluloses were photolyzed by 2537 A. ultraviolet light in a vacuum at 40°C. The changes in quantum yields of hydrogen, carbon monoxide, carbon dioxide, hydrocarbons, aldehyde groups, carboxyl groups, and chain scissions with respect to quanta of light absorbed and initial functional group concentration indicated that photolysis of alcohol groups plays a dominant role in the complex of interdependent primary and secondary reactions taking place. Periodate-chlorite-oxidized cellulose is much more susceptible to photochemical degradation than is unoxidized cellulose. Neutralization with very dilute sodium hydroxide solution reduced the quantum yields of the oxycellulose to values similar to those obtained with the unoxidized material.

### I. INTRODUCTION

Although the effects of ultraviolet light on cellulose have been a subject of investigation for many years, a detailed study of the stoichiometry and kinetics of the several reactions taking place upon irradiation has been attempted only recently.

The results from the irradiation of dried purified cotton sheets in a vacuum at 40°C. with monochromatic 2537 A. ultraviolet light were described in previous papers.<sup>1-3</sup> The rates of evolution of gaseous products as well as changes in degree of polymerization (D.P.) and carbonyl and carboxyl groups were obtained as a function of einsteins ( $Nh\nu$ ) of adsorbed radiation. The initial quantum yields were  $10^{-2}$  for hydrogen and  $10^{-3}$  for carbon monoxide plus carbon dioxide. A mechanism was proposed in which the alcohol groups were photolyzed to carbonyl groups with the liberation of hydrogen. Hydrogen had not been previously reported as a product, and alcohols were not believed to absorb at this wavelength.

In this paper, further speculation about the nature of the photochemical processes is based on analysis of the changes in the amounts and rates of formation of products that result from variation of the initial functional group content of the cellulose.

### II. EXPERIMENTAL

#### Preparation of Cellulose Sheets

The cellulose was hand beaten and formed into sheets in the manner described in a previous paper.<sup>3</sup> The cellulose used in many of these experi-

ments was acetate-grade cotton linters with an approximate degree of polymerization of 1700 (14.14% nitrogen content in ethyl acetate) and a Gaussian chain length distribution. These linters are further described as sample 8 by Timell.<sup>4,5</sup>

The periodate-chlorite-oxidized cellulose was prepared by soaking the cotton linters in 0.025*N* periodic acid solution at 25°C. for 2 hr., followed by treatment with 2% acidic NaClO<sub>2</sub> solution for 72 hr. and thorough washing with dilute acid and distilled water. Na<sup>+</sup> was introduced by washing with dilute NaOH solution. The alkali was removed by washing with distilled water.

The regenerated celluloses were prepared by dissolving cotton linters in cuprammonium solution or concentrated phosphoric acid. The cellulose was precipitated by dilution, and washed.

### Irradiation of Cellulose

The irradiation apparatus was essentially the same as that described in a previous publication except for one detail. Gases were removed as they were produced through a Dry Ice trap and diffusion pump into a chamber of measured volume. The irradiation chamber was maintained at a pressure of less than  $5 \times 10^{-5}$  mm. Hg to minimize reaction between the product gases and the substrate.

### Analysis of Products

The pressures of the evolved gases were measured in most cases by a McLeod gauge. Irregularities in the rate at higher pressures reported previously<sup>1</sup> were found to be the result of small explosions of the gaseous products initiated by a discharge gauge. Use of this gauge was discontinued.

Samples of gas were removed from time to time, and their composition determined by mass spectrometric analysis.

Irradiated samples were stored in air for several months and subsequently analyzed for changes in cuprammonium viscosity and carboxyl and aldehyde group content. These methods of analysis as well as methods of measurement of the intensity of absorbed radiation and other experimental details have been described in a previous publication.<sup>3</sup>

Chain scissions were calculated from change in viscosity-average D.P. from an equation whose derivation assumes an initial random molecular weight distribution and Lambert's law attenuation of the radiation by the absorbing media.<sup>2</sup> The absorption coefficient was assumed to be constant. This approximation is probably valid only at low einsteins of absorbed light.

## III. RESULTS AND DISCUSSION

The initial degrees of polymerization and the initial concentrations of the various functional groups (in equivalents/anhydroglucose unit) for the different types of celluloses used in these experiments are given in Table I.

The aldehyde (hemiacetal) and carboxyl groups are ordinarily present in concentrations a thousandfold smaller than the predominant functional groups, the primary and secondary alcohol groups, and the acetal or glucosidic linkages. The reducing groups in unmodified cellulose occur predominantly at the chain ends. However, they and the carboxyl groups may also occur at the 2, 3, and 6 carbon atoms in the anhydroglucose rings.

Tables II and III and Figure 1 present average or typical results of about forty experiments condensed into quantum yields as a function of total einsteins absorbed,  $Nh\nu$ , where  $N$  is Avogadro's number,  $h$  is Planck's constant, and  $\nu$  is the frequency of the 2537 Å. light.<sup>3</sup> The intensity of light at the surface of the cellulose sheets was calculated to be  $9.62 \times 10^{-9} Nh\nu/\text{cm.}^2$  sec. for most of these experiments. Intensities of  $6.49$  and  $13.4 \times 10^{-9} Nh\nu/\text{cm.}^2$  sec. were also employed for several of the experiments.

The quantum yields,  $\Phi$ , of gaseous products for the several varieties of cellulose are listed in Table II.

In Table III, the average quantum yields of chain scissions, gaseous products, and changes in carboxyl and aldehyde group content for celluloses irradiated with  $1.50 Nh\nu/\text{anhydroglucose unit}$  of 2537 Å. light at 40°C. are given. The quantum yields of chain scission and functional groups in Table III must be interpreted with the fact in mind that the cellulose may have been modified extensively by post-irradiation oxidation and by reaction of free radical and labile groups with the reagents used in the analysis.

Average values for the cumulative quantum yields of the various products for purified cotton sliver are plotted as a function of einsteins absorbed ( $Nh\nu/\text{anhydroglucose unit}$ ) in Figure 1.

A number of inferences may be drawn from the data presented in Figure 1 and Tables II and III.

The close stoichiometric correlation between quantum yields of hydrogen and aldehyde is again demonstrated. For  $3.2 Nh\nu/\text{anhydroglucose unit}$  of radiation, about 0.015 mole of hydrogen and equivalents of aldehyde are formed. This is far too great a quantity to be explained by photolysis of carboxyl or aldehyde groups initially present in the molecule. The only plausible source of this quantity of aldehyde and hydrogen is the photo-reduction of alcohol groups as was suggested in a previous article.<sup>3</sup> An analysis of the possible mechanisms for this reaction is postponed until pertinent data in a subsequent article are presented.<sup>6</sup>

A comparison of the initial concentrations of aldehyde and carboxyl groups in the various celluloses in Table I with the quantum yields of CO and CO<sub>2</sub> in Table III may be made. A sixfold increase in initial aldehyde groups results in only a twofold increase in quantum yield of carbon monoxide evolution. A thirtyfold increase in initial carboxyl groups gives only a threefold increase in carbon dioxide quantum yield. Thus, it appears that photolysis of aldehyde and carboxyl groups can be only partially responsible for the evolution of CO and CO<sub>2</sub>.

TABLE I  
Initial Functional Group Concentrations in the Celluloses

Cellulose	Cuam D.P.	Group concn., equivalents/anhydroglucose unit				
		Aldehyde	Carboxyl	Acetal	Primary alcohol	Secondary alcohol
Degummed cotton sliver (A)	1710	0.0006	0.0010	1.00	1.00	2.00
Degummed cotton sliver (B)	1910	0.0010	0.0014	1.00	1.00	2.00
Cotton linters (from T. Timell)	1300	0.0015	0.0007	1.00	1.00	2.00
Periodate-chlorite- oxidized cotton linters	570	0.0030	0.0198	1.00	1.00	1.98
Na <sup>+</sup> -Exchanged periodate-chlorite- oxidized cotton linters	570	0.0030	0.0198 (COONa)	1.00	1.00	1.98
Cuam-regenerated cotton linters	1020	0.0013	0.0009	1.00	1.00	2.00
H <sub>3</sub> PO <sub>4</sub> -regenerated cotton linters	300	0.0048	0.0008	0.99	1.00	2.00

TABLE II  
Quantum Yields of Gaseous Products

Cellulose	$Nh\nu$ range	Quantum Yield, moles/ $Nh\nu$			
		Hydrogen	Carbon monoxide	Carbon dioxide	Hydrocarbons
Cotton sliver A	0 <sup>a</sup>	0.0130	0.00071	0.00038	0.00000
Cotton linters	0 <sup>a</sup>	0.0102	0.00068	0.00047	0.00000
Cotton linters	0-0.0041	0.0063	0.00091	0.00054	0.00000
Cotton linters	0.0041-0.0082	0.0038	0.00155	0.00068	0.00000
Periodate-chlorite-oxidized cotton linters	0-0.0082	0.0066	0.00170	0.00164	0.00012
Periodate-chlorite-oxidized cotton linters, Na <sup>+</sup> washed	0-0.0032	0.0032	0.00081	0.00092	0.00000
Cuam-regenerated cotton linters	0-0.0082	~0.003	~0.0008	~0.0005	~0.0001
H <sub>2</sub> PO <sub>4</sub> -regenerated cotton linters	0-0.0082	0.0095	0.00150	0.00082	0.00005

<sup>a</sup> Zero indicates extrapolation of the quantum yield to  $Nh\nu \rightarrow 0$ .

TABLE III  
Quantum Yields at 1.50  $Nh\nu$ /anhydroglucose Unit

Cellulose	Chain Scissions	$\Delta$ Equiv. CHO	$\Delta$ Equiv. COOH	Quantum yield, moles or $\Delta$ equivalents/ $Nh\nu^a$				
				Moles H <sub>2</sub>	Moles CO	Moles CO <sub>2</sub>	Moles hydrocarbons	
Cotton sliver A	0.00107	0.00508	0.00254	0.00481	0.00064	0.00036	0.00000	
Cotton sliver B	0.00081	0.00506	0.00209	—	—	—	—	
Cotton linters	0.00096	0.00773	0.00217	0.00413	0.00101	0.00050	0.00000	
Oxidized linters	0.00297	0.00495	-0.00629	0.00363	0.00170	0.00164	0.00012	
Na <sup>+</sup> -washed oxidized linters	0.00128	0.00606	-0.00339	0.0032 <sup>b</sup>	0.00081 <sup>b</sup>	0.00092 <sup>b</sup>	0.00000 <sup>b</sup>	
Quam-regenerated linters	0.00069	0.00168	-0.00041	0.003	0.0008	0.0005	0.0001	
H <sub>3</sub> PO <sub>4</sub> -regenerated linters	0.00113	0.00410	0.00079	0.00945	0.00150	0.00082	0.00008	

<sup>a</sup>  $\Delta$  indicated change from initial functional group concentration (Table I). <sup>b</sup> Values for 0.78  $Nh\nu$ /anhydroglucose unit.

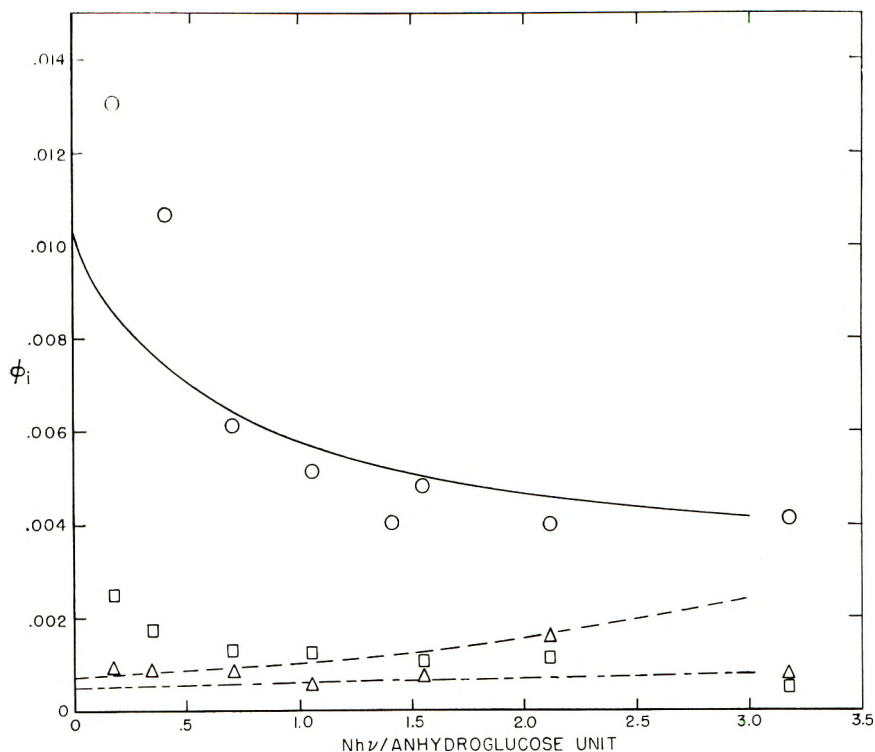


Fig. 1. Quantum yields  $\Phi$  as a function of einsteins absorbed ( $Nh\nu$ /anhydroglucose unit) for the products from the irradiation of cellulose (cotton linters) in a vacuum at 40°C. with 2357 Å. light: (○) aldehyde; (□) chain scission; (Δ) carboxyl; (—) hydrogen; (---) CO; (- - -) CO<sub>2</sub>.

Beélik<sup>7</sup> finds glucose (six carbon atoms) and arabinose (five carbon atoms) reducing units in equal amounts among the oligosaccharides formed during the irradiation of cellulose. The loss of the 1 carbon atom of an anhydroglucose unit in the form of CO or CO<sub>2</sub> during chain fracture would explain the presence of these reducing units as well as the stoichiometric correlation of CO and CO<sub>2</sub> evolution with chain scission rather than with initial carboxyl and aldehyde group concentration.

Beélik<sup>7</sup> has suggested that the absorption of ultraviolet light leading to the primary photochemical reaction takes place mainly at the glucosidic linkages which absorb weakly at 2660 Å. Such absorption might be responsible for much of the chain scission that occurs during and following photolysis.

### Photolysis of Oxycellulose

Periodic acid specifically oxidizes adjacent secondary alcohol groups to form aldehydes. Subsequent oxidation with chlorite converts the 2 and 3 carbon atoms of the anhydroglucose unit into carboxyl groups. Data in



Table I indicate that about 1% of the secondary alcohol groups were thus affected.

The tying-up of the carboxyl groups with  $\text{Na}^+$  resulted in the reduction of the quantum yield to a value near that for unoxidized cellulose. If the augmentation of the  $\text{CO}_2$  yield upon irradiation may be attributed to photo-decarboxylation, then it may be estimated that carboxyl groups contribute no more than 5–10% of the quantum yield of  $\text{CO}_2$  in the irradiation of unoxidized cellulose. However, the increase in  $\text{CO}_2$  yield in oxycellulose is not nearly large enough to account for the carboxyl group destruction. The yields of aldehyde, chain scission, and hydrogen and  $\text{CO}$  evolution are likewise increased, indicating an overall decreased photochemical stability of the oxidized cellulose.

Mass spectrometric analysis of the volatile gases indicates that one and three carbon atom hydrocarbons are present. Decarboxylation of the 2 and 3 positions followed by chain scission would result in three-carbon atom ( $\text{C}_4\text{—C}_5\text{—C}_6$ ) and one-carbon atom ( $\text{C}_1$ ) fragments. The mechanism by which these fragments could become completely hydrogenated is, to say the least, obscure.

The  $\text{Na}^+$ -washed cellulose does not give hydrocarbons upon irradiation.

This experiment clearly reveals the deleterious effects of free acid groups upon the photochemical stability of cellulosic materials. Oxidation renders cellulose much less stable to pyrolysis<sup>8</sup> as well as adding to its photochemical instability. More fragmentation of the anhydroglucose rings and less tar are obtained<sup>8</sup> when cotton cellulose oxidized with  $\text{NO}_2$  is pyrolyzed. Carboxyl groups, therefore, contribute to both the thermal and photochemical instability of cellulosic materials.

### Photolysis of Regenerated Cellulose

The irradiation of cuprammonium-regenerated cellulose resulted in low quantum yields in all categories. This may result from the presence of small amounts of water and unremoved copper ion.

The phosphoric-acid-regenerated cellulose, on the other hand, gave quantum yields higher than did its parent cellulose.

It appears that the differences in quantum yields among cotton sliver, cotton linters, and the regenerated celluloses are due to variations in physical properties rather than to variations in chemical constitution. Water vapor has been found to inhibit the photolysis at these wavelengths.<sup>9</sup> Therefore, water retentivity may be added to other properties such as amorphousness and molecular weight as possible sources of quantum yield variation.

### References

1. Flynn, J. H., *J. Phys. Chem.*, **60**, 1332 (1956).
2. Flynn, J. H., *J. Polymer Sci.*, **27**, 83 (1958).
3. Flynn, J. H., W. K. Wilson, and W. L. Morrow, *J. Res. Natl. Bur. Std.*, **60**, 229 (1958).

4. Timell, T., *Svensk Papperstidn.*, **58**, 234 (1955).
5. Bennett, C. F., and T. Timell, *Svensk Papperstidn.*, **59**, 73 (1956).
6. Flynn, J. H., and W. L. Morrow, *J. Polymer Sci.*, **A2**, 91 (1964).
7. Beélik, A., and J. K. Hamilton, *Das Papier*, **13**, 77 (1959).
8. Madorsky, S. L., V. E. Hart, and S. Straus, *J. Res. Natl. Bur. Std.*, **60**, 343 (1958).
9. Launer, H. F., and W. K. Wilson, *J. Am. Chem. Soc.*, **71**, 958 (1949).

### Résumé

On a photolysé, à la lumière ultraviolette à 2537 Å sous vide à 40°C, des linters de coton, de la cellulose oxydée au periodate et chlorite, et diverses celluloses régénérées. Les changements des rendements quantiques d'hydrogène, de CO, de CO<sub>2</sub>, d'hydrocarbures, de groupements aldéhydiques et carboxyliques et les cassures de chaînes comparées aux quanta de lumière absorbés et la concentration des groupements fonctionnels au début indiquaient que la photolyse des groupes joue un rôle primordial dans l'ensemble de réactions primaires et secondaires qui sont liées entr'elles. La cellulose oxydée au periodate et chlorite est beaucoup plus sensible à la dégradation photochimique que la cellulose non-oxydée. La neutralisation avec une solution très diluée de soude caustique réduit les rendements quantiques de l'oxycellulose à des valeurs semblables à celles obtenues avec le matériel non-oxydé.

### Zusammenfassung

Baumwoll-Sliver, Baumwoll-Linters, perjodat-chlorit-oxydierte Cellulose und verschiedene regenerierte Cellulosen wurden mit ultraviolettem Licht von 2537 Å im Vakuum bei 40°C photolysiert. Die Abhängigkeit der Quantenausbeute an Wasserstoff, Kohlenmonoxyd, Kohlendioxyd, Kohlenwasserstoffen, Aldehydgruppen, Karboxylgruppen und Kettenspaltungen von der Zahl der absorbierten Lichtquanten und der Ausgangskonzentration der funktionellen Gruppen zeigte, dass die Photolyse der Alkoholgruppen eine beherrschende Rolle im Komplex der stattfindenden, ineinandergreifenden Primär- und Sekundärreaktionen spielt. Perjodat-chlorit-oxydierte Cellulose ist gegen photochemischen Abbau viel empfindlicher als nichtoxydierte Cellulose. Neutralisation mit sehr verdünntem Natriumhydroxyd setzte die Quantenausbeute bei der Oxycellulose auf ähnliche Werte wie beim nichtoxydierten Material herab.

Received October 15, 1962

Revised December 7, 1962

## Effects of Deuteration and Temperature upon the Photolysis of Cellulose in a Vacuum with 2537 A. Light

JOSEPH H. FLYNN and WILLIAM L. MORROW, *Polymer Chemistry  
Section, National Bureau of Standards, Washington, D. C.*

### Synopsis

The effects of the exchange of deuterium for hydrogen in the hydroxyl groups on the composition of products and the kinetics of their formation during the irradiation of cellulose by 2537 A. in a vacuum at 77, 313, and 365°K. are described. About 50–70% of the total hydrogen evolved was HD. Little D<sub>2</sub> was formed. Total HD evolution was independent of temperature. Disproportionation, rather than atom abstraction or atom combination, was likely to be the dominant mechanism of hydrogen production. Much of the aldehyde group formation takes place during the photolysis and probably results directly from secondary photolysis or disproportionation of radicals. H<sub>2</sub>, CO, and CO<sub>2</sub> evolutions increase with temperature and result from both functional group photolysis and radical depropagation. Chain scission and carboxyl group formation take place to a large extent during the post-irradiative oxidation of long-lived oxygen-containing radicals.

### I. INTRODUCTION

The stoichiometry and kinetics of the photolysis of cellulose and chemically modified celluloses with 2537 A. ultraviolet light in a vacuum have been investigated recently.<sup>1–4</sup> The dominant reaction was the photolysis of alcohol groups resulting in the liberation of hydrogen and the formation of aldehyde groups on the cellulose chain.

The hydrogen in the hydroxyl groups of cellulose can be replaced by deuterium by exchange with heavy water.<sup>5</sup> About 60% of the hydroxyl hydrogens in cotton linters are exchangeable by deuterium. The accessibility of regenerated celluloses is somewhat higher—around 80%.

This investigation was undertaken to determine what effect these deuterium atoms would have upon the composition of the irradiation products and the kinetics of their formation at 77, 313, and 365°K.

### II. EXPERIMENTAL

The preparation and the irradiation of the cellulose sheets in a vacuum at constant temperature with 2537 A. ultraviolet light of measured intensity, and the measurement and analysis of evolved gases, chain scissions,

TABLE I  
Gaseous Products from the Irradiation of Heavy Water-Exchanged Cellulose with 2537 A. Light

Cellulose sample	Temp., °C.	Einsteins absorbed, Nhr/an- hydroglucose unit	Gaseous products, mole-%						hydro- carbons
			H <sub>2</sub>	HD	D <sub>2</sub>	Total hydrogen	CO	CO <sub>2</sub>	
Cotton linters	-196	0.00-0.65	24.4	65.1	0.7	90.2	4.8	4.8 <sup>a</sup>	0.2 <sup>a</sup>
Cotton linters	+40	0.00-1.03	~26	~38	~0.6	~65	~20	~14	—
Cotton linters	92	0.00-0.48	15.9	35.7	0.7	52.3	27.7	17.8	2.3 <sup>b</sup>
H <sub>2</sub> PO <sub>4</sub> -regenerated cotton linters	40	0.00-1.55	24.7	44.4	0.4	79.5	12.5	6.8	2.2 <sup>b</sup>
Periodate-chlorite- oxidized cotton linters	40	0.00-1.26	32.7	30.6	0.3	63.6	21.0	13.6	1.8 <sup>c</sup>

<sup>a</sup> CO<sub>2</sub> and hydrocarbons liberated upon warming to room temperature after irradiation.

<sup>b</sup> Deuterated hydrocarbons containing 1-4 carbon atoms.

<sup>c</sup> Mainly deuterated methanes and propanes.

carboxyl groups, and aldehyde groups are described in previous papers.<sup>3,4</sup>

Temperatures of 40 and 92°C. were maintained by circulating water from a constant temperature bath through the cold finger around which the cellulose sheet was wrapped. The cold finger was maintained at -196°C. by directly siphoning liquid nitrogen into it.

The deuterium exchange was accomplished by introducing the heavy water vapor (99.5% D<sub>2</sub>O) to the dried cellulose sheet in the evacuated irradiation apparatus. The sample was then dried under vacuum at 95°C. for one day. This cycle was repeated (about ten times) until no more exchange was observed. The deuterium content of the recovered water was measured by comparing its vapor pressure to that of pure water with a sensitive differential mercury manometer.

All photolyses described in this paper were performed at an intensity of  $9.62 \times 10^{-9} Nh\nu/cm.^2$  sec. upon well characterized acetate-grade cotton linters<sup>4</sup> or modifications of them. The pressure in the vessel during irradiation was maintained at less than  $5 \times 10^{-5}$  mm. Hg. The volatile products passed through a Dry Ice trap and diffusion pump into evacuated storage vessels where their pressure and volume were measured and samples withdrawn for analysis.

TABLE II  
Mole Percentages of H<sub>2</sub>, HD, and D<sub>2</sub> in Total Evolved Hydrogen

Cellulose sample	Temp., °C.	Einsteins absorbed, <i>Nhν</i> /an- hydroglucose unit	Mole-% of total hydrogen <sup>a</sup>			D/H
			H <sub>2</sub>	HD	D <sub>2</sub>	
Cotton linters	-196	0.00-0.65	27.1 (39.9)	72.1 (46.5)	0.8 (13.6)	0.584
Cotton linters	+40	0.00-1.03	~40 (48)	~59 (43)	~1 (9)	0.44
Cotton linters	92	0.00-0.48	30.4 (41.6)	68.3 (45.8)	1.3 (12.6)	0.550
Regenerated cotton linters	40	0.00-1.55	43.7 (51.2)	55.8 (40.7)	0.5 (8.1)	0.397
Periodate-chlorite- oxidized cotton linters	40	0.00-1.26	51.4 (57.0)	48.1 (37.0)	0.5 (6.0)	0.325

<sup>a</sup> Values in parentheses calculated assuming the random combination of H and D from a pool of composition given by the D/H ratio.

### III. RESULTS AND DISCUSSION

Results from the mass spectrometric analysis of gaseous products from the irradiation of various heavy-water-exchanged celluloses are given in Table I. Table II contains the percentages of H<sub>2</sub>, HD, and D<sub>2</sub> in the total evolved hydrogen and the total deuterium to hydrogen ratio of these products.

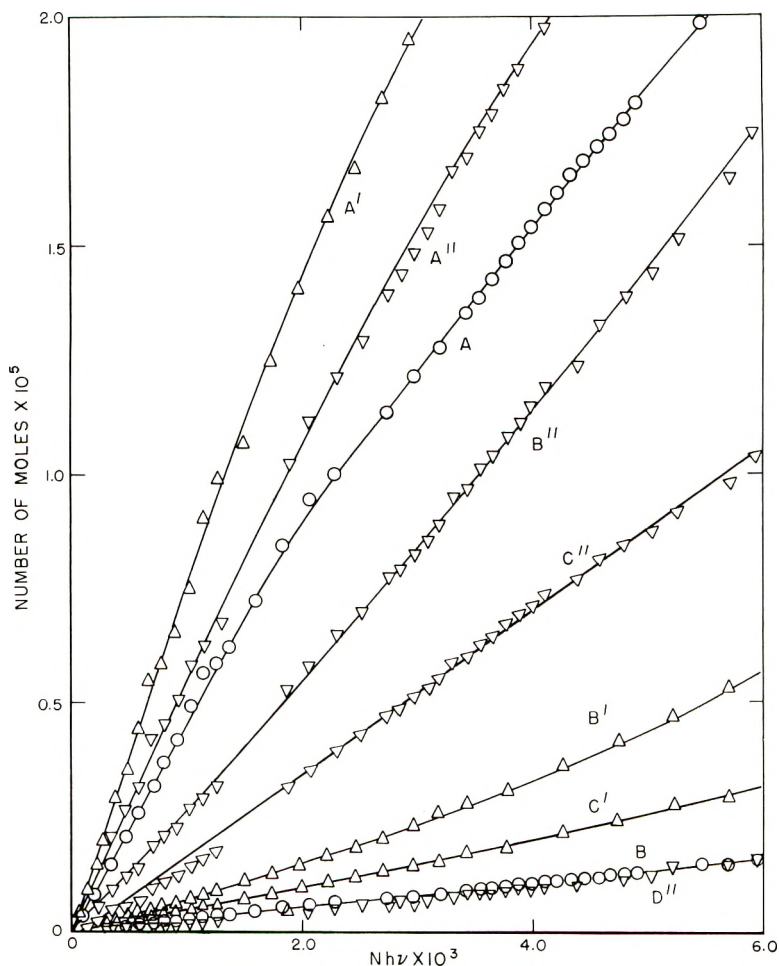


Fig. 1. Moles of gaseous products as a function of einsteins absorbed,  $9.62 \times 10^{-9}$   $Nh\nu/\text{cm}^2$  sec., 2537 Å. light, heavy water-exchanged celluloses: (A) total hydrogen at  $-196^\circ\text{C}$ .; (A') total hydrogen at  $+40^\circ\text{C}$ .; (A'') total hydrogen at  $+92^\circ\text{C}$ .; (B) CO at  $-196^\circ\text{C}$ .; (B') CO at  $+40^\circ\text{C}$ .; (B'') CO at  $+92^\circ\text{C}$ .; (C) CO<sub>2</sub> at  $40^\circ\text{C}$ .; (C') CO<sub>2</sub> at  $+92^\circ\text{C}$ .; (C'') CO<sub>2</sub> at  $+92^\circ\text{C}$ .; (D) Hydrocarbons at  $+92^\circ\text{C}$ . (No CO<sub>2</sub> evolved at  $-196^\circ\text{C}$ .; no hydrocarbons at  $-196^\circ\text{C}$ . and  $40^\circ\text{C}$ .)

Without at once becoming involved with the details of possible reaction mechanisms, one can draw several inferences from the H<sub>2</sub>-HD-D<sub>2</sub> distributions as to the types of reactions taking place.

The values calculated for random combination of H and D from pools of the experimental D/H ratios in Table II give values ten times as great as the experimental values for %D<sub>2</sub>. Therefore, hydrogen and deuterium atom combination may be ruled out as a mechanism for H<sub>2</sub>, HD, and D<sub>2</sub> production.

A purely random abstraction mechanism does not fit the data any better. If 67% of the hydroxyl hydrogens are exchanged by deuterium

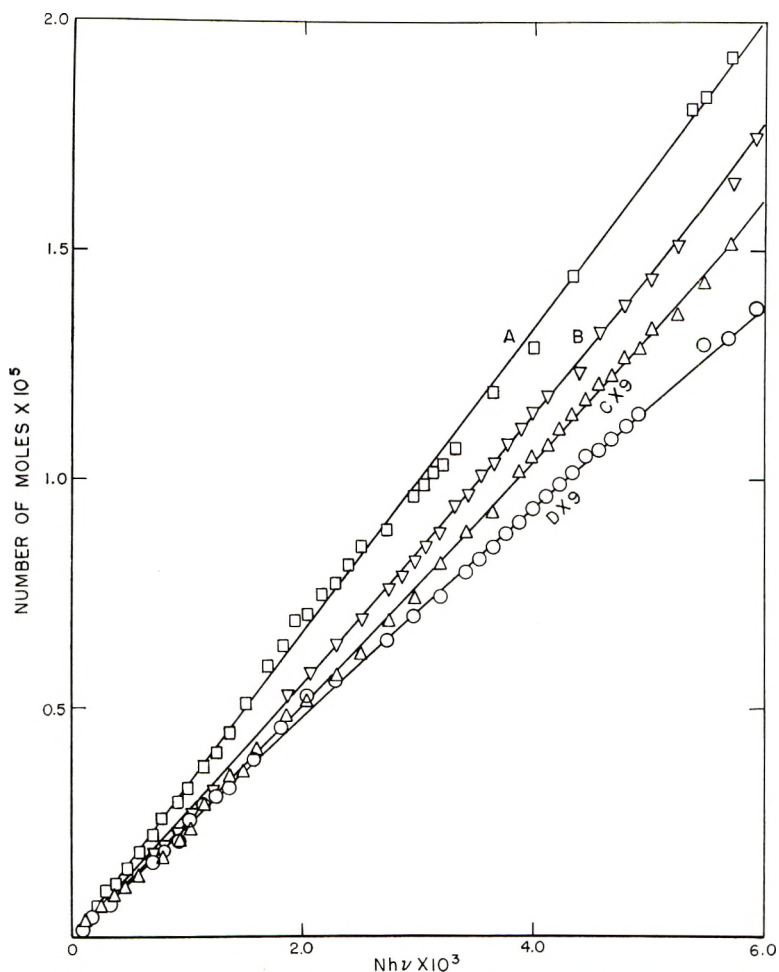


Fig. 2. Moles of CO evolved as a function of einsteins absorbed,  $9.62 \times 10^{-9} Nh\nu/\text{cm}^2 \text{ sec.}$ , 2537 Å. ultraviolet light: (A) cellulose at  $92^\circ\text{C.}$ ; (B) heavy water-exchanged cellulose at  $92^\circ\text{C.}$ ; (C) cellulose at  $-196^\circ\text{C.}$ ; (D) heavy water-exchanged cellulose at  $-196^\circ\text{C.}$

atoms and the resulting average  $\overline{[C_6H_7O_2(OH)(OD)_2]_x}$  is photolyzed to give D and H atoms at a 2/1 ratio and these abstract randomly from a pool of 8H and 2D, then values of 26.7%  $H_2$ , 60.0% HD, 13.3%  $D_2$ , and  $D/H = 0.734$  are obtained which do not fit the data in Table II. Two possible cases that will fit the data are evident. (1) Hydrogen and deuterium atoms are split from the hydroxyls, and these atoms abstract or disproportionate only hydrogen from the substrate to form  $H_2$  and HD. (2) Only H atoms are formed and these abstract or disproportionate D and H atoms from the substrate to form HD and  $H_2$ . The relative merits of these cases will be discussed later.

The effect of temperature on the evolution of gaseous products may be observed in Figure 1 for the irradiation of deuterium-exchanged cotton

linters. The temperature coefficients for CO and CO<sub>2</sub> evolution are much larger than those for hydrogen evolution. For CO evolution, the temperature coefficient calculated for initial rates, is about 6 kcal./mole in the 40–92°C. range and 0.2 kcal./mole for –196 to +40°C. The temperature coefficient for CO<sub>2</sub> evolution is also about 5.5 kcal./mole in the 40–92°C. range.

If there exists a direct primary or secondary photochemical reaction of zero activation energy which is responsible for part of these gases, then the remainder will have a temperature coefficient greater than the values given above. If the rate of CO evolution at –196°C. is subtracted from the rates of 40 and 92°C. to compensate for this component from the nonthermal process, the temperature coefficient for the remaining CO evolution is 8 kcal./mole.

In Figures 2 and 3, the moles of carbon monoxide and hydrogen, respectively, are plotted as a function of einsteins absorbed for deuterium-exchanged and nonexchanged cellulose at 196° and +92°C. In both cases gases are evolved from the deuterium-exchanged sample at a slightly lower rate.

In Table III, the average quantum yields of chain scissions, gaseous products, and changes in aldehyde and carboxyl group content are listed for the various cellulose samples at –196, +40, and +92°C. for 1.50  $Nh\nu$ /anhydroglucose unit.

It also may be noted in Table III that although the yields of CO and CO<sub>2</sub> evolved increase tenfold and fivefold, respectively, over the –196 to +92°C. temperature range, the number of chain scissions and the changes in carboxyl group content remain approximately constant. Chain fracture and change in carboxyl are rather insensitive to einsteins absorbed and do not extrapolate to the origin for zero  $Nh\nu$ . This can be observed in Figure 4.

The decrease in quantum yield of hydrogen at 92°C. compared to that at 40°C. is matched by a similar decrease in aldehyde group yield, again pointing to the interrelation of these products. However, the much greater decrease in yield of the aldehyde groups than in the yield of hydrogen at 92°C. suggests the thermal deactivation of the precursor of the aldehyde at these temperatures.

Although it was necessary to postulate photolysis of alcohol groups to explain the large amounts of aldehyde groups produced and the quantity of hydrogen evolved,<sup>3,4</sup> evidence for the photolysis of simple alcohols by 2537 Å. light has appeared only recently. (Sullivan and Koski<sup>6</sup> have identified a number of radicals from the ESR spectra of solid methanol irradiated with 2537 Å. light at 77°K.) The D/H ratio decreases with increasing einsteins absorbed as this photolysis is inhibited and side reactions producing hydrogen become more prominent. From the prevalence of deuterium in the hydrocarbons evolved during the irradiation, it appears that some of the hydrogen and deuterium, either in the atomic or molecular state, must be consumed or exchanged in the reduction



TABLE III  
Quantum Yields for Cotton Linters (Deuterated and Nondeuterated) Irradiated with 1.50  $Nh\nu$ /anhydroglucose unit of 2537 Å. Light at Several Temperatures

Cellulose	Temp., °C.	Quantum yield, moles or Δ equivalents/ $Nh\nu^a$							
		Chain scission	Δ equiv. CHO	Δ equiv. COOH	Moles hydrogen	Moles CO	Moles CO <sub>2</sub>	Moles hydrocarbon	
Cotton linters	-196	0.00063	0.00264	0.00076	0.00355	0.00029	0.00034	0.00001	
Heavy water-exchanged cotton linters	-196	0.00087	0.00267	0.00077	0.00328	0.00026	0.00029	0.00001	
Cotton linters	+40	0.00069	0.00565	0.00114	0.00480	0.00101	0.00050	0.00000	
Heavy water-exchanged cotton linters	+40	0.00110	0.00607	0.00088	0.00503	0.00123	0.00061	0.00000	
Cotton linters	+92	0.00039	0.00383	0.00085	0.00442	0.00315	0.00175	0.00030	
Heavy water-exchanged cotton linters	+92	0.00139	0.00169	0.00061	0.00419	0.00304	0.00168	0.00029	

<sup>a</sup> Δ indicates change from initial functional group concentration.

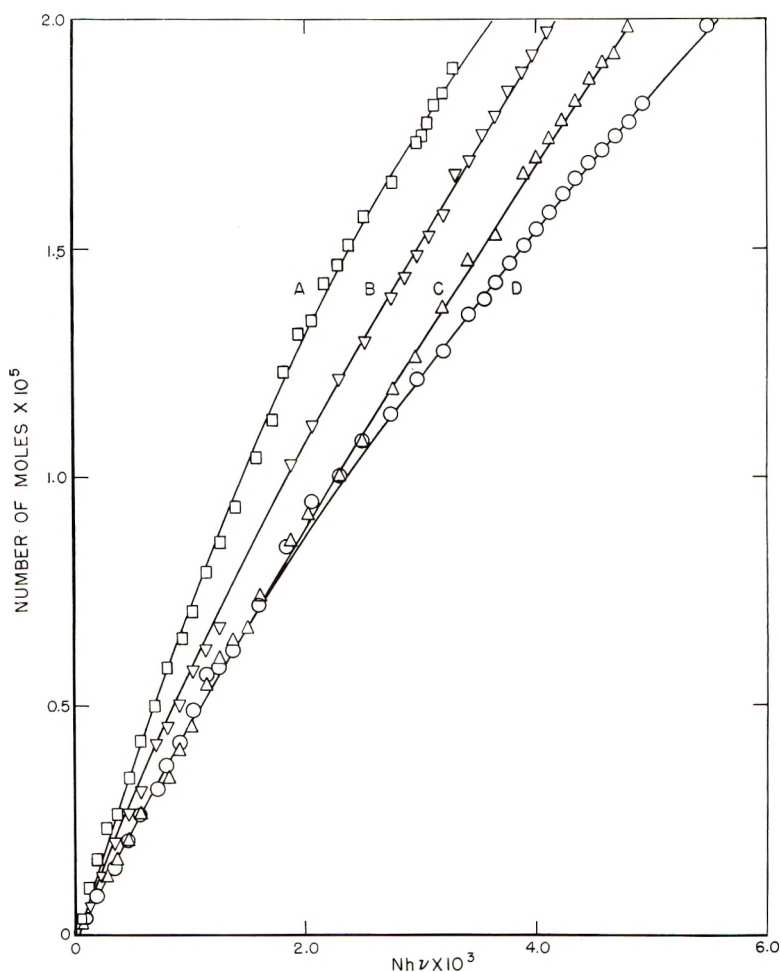


Fig. 3. Moles of total hydrogen evolved as a function of einsteins absorbed,  $9.62 \times 10^{-9} Nh\nu/\text{cm.}^2 \text{ sec.}$ , 2537 Å. ultraviolet light: (A) cellulose at  $92^\circ\text{C.}$ ; (B) heavy water-exchanged cellulose at  $92^\circ\text{C.}$ ; (C) cellulose at  $-196^\circ\text{C.}$ ; (D) heavy water-exchanged cellulose at  $-196^\circ\text{C.}$

reactions through which these hydrocarbons are formed. Unfortunately, the amounts of  $\text{H}_2\text{O}$ ,  $\text{HDO}$ , and  $\text{D}_2\text{O}$  evolved are not easily obtainable. Also, any water formed might exchange with the alcohol groups of the substrate despite the low pressures at which the irradiation was performed.

Hydrogen-deuterium exchange should take place to a greater extent in the less crystalline, more accessible, regenerated celluloses. Their low D/H values in Table II are in contradiction to this. However, changes in the physical modifications of the cellulose have a large effect on the stoichiometry of the products.<sup>4</sup>

Although there is a considerable variation from sheet to sheet, the values for  $A''$  (hydrogen evolution at  $92^\circ\text{C.}$ ) in Figure 1 lie below the envelope of the hydrogen evolution curves at  $40^\circ\text{C.}$  It appears that at this tem-

perature more of the evolved hydrogen is consumed in the reduction of intermediate species. This inference is supported by the increase in deuterated hydrocarbons among the products.

Table IV contains the quantum yields of the hydrogen isomers from irradiation of cotton linters at the three temperatures. It is noted that there is little variation of yield of HD with temperature. The change in total hydrogen yield with temperatures is almost entirely due to changes in H<sub>2</sub> production. This constancy of HD yield demonstrates that the enhancement of quantum yield of hydrogen with temperature does not involve hydroxyl hydrogen. As the irradiation proceeds, the D/H ratio decreases as the photolysis of alcohol groups is inhibited and side reactions producing hydrogen become more important.

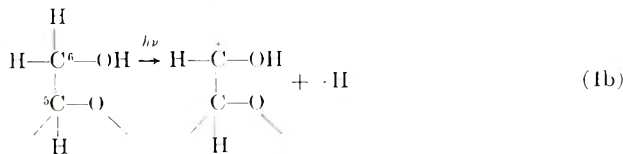
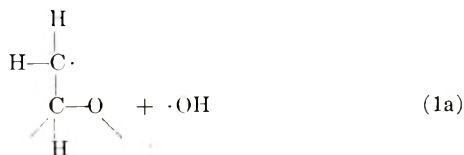
TABLE IV  
Quantum Yields of Hydrogen Isomers from the Irradiation of Cotton Linters with 2537 Å. Light at -196, +40, and +92°C.

Temp., °C.	Quantum yield, moles/Nhν			
	Total hydrogen	H <sub>2</sub>	HD	D <sub>2</sub>
-196	0.00328	0.00089	0.00236	0.00003
+40	0.00503	0.0020	0.0030	0.00005
+92	0.00419	0.00127	0.00286	0.00005

Much of the increase in the quantum yields of hydrogen for regenerated cellulose and oxycellulose can be attributed to H<sub>2</sub> rather than HD and D<sub>2</sub>.

Therefore, the dominant photolytic reaction may occur at the primary alcohol on the C<sub>6</sub> atom of the anhydroglucose unit and/or at the two secondary alcohol groups on the C<sub>2</sub> and C<sub>3</sub> carbon atoms.

If the primary alcohol is photolyzed, several dissociative reactions are possible:



In the irradiation of solid methanol at 77°K. with 2537 Å., CH<sub>3</sub> and CHO radicals are identified in the ESR spectra, and after the decay of CH<sub>3</sub>

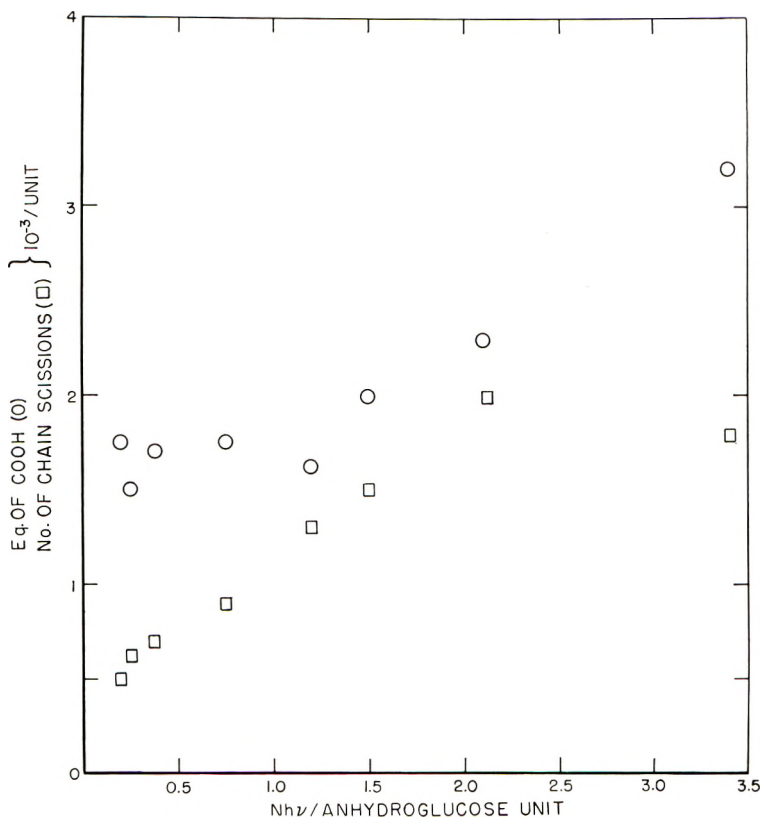


Fig. 4. Number of chain scissions and change in carboxyl group content as a function of einsteins absorbed: (O) equivalents of COOH formed; (□) number of chain scissions ( $\times 10^3$ /anhydroglucose unit).

considerable  $\text{CH}_2\text{OH}$  is found to be present.<sup>6</sup> Sullivan and Koski<sup>7</sup> suggest that CHO is produced by secondary photolysis of the  $\text{CH}_2\text{OH}$  radical. This speculation is based on the experiments of Alger et al.,<sup>8</sup> in which ESR spectra of methanol, produced by electron bombardment, were modified by ultraviolet and visible light.

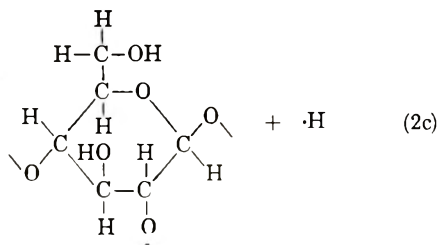
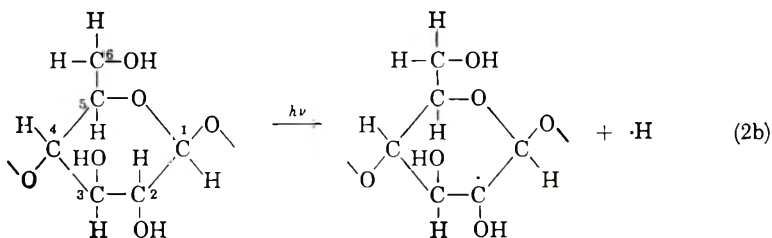
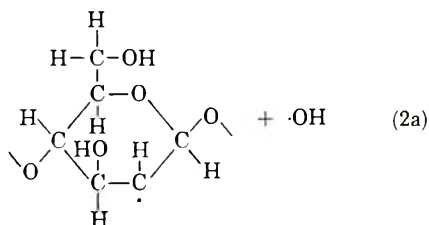
Of these three reactions, (1a) may be eliminated from consideration, as most of the deuterium would end up as HOD and  $\text{D}_2\text{O}$  rather than HD and  $\text{D}_2$ . Also, in the reducing atmosphere obviously present in these experiments, it is difficult to see how aldehyde might be formed.

The formation of an alkoxy radical (1c), is possible, although it is less favored from energetic considerations and a probable fragmentation product—formaldehyde—has not been isolated. The  $\text{CH}_3\text{O}$  radical is found only upon irradiation of methanol with 1840 Å; if it is formed by 2537 Å, light it must be immediately photolyzed to CHO.<sup>7</sup>

The radical in eq. (1b) has been identified in  $\gamma$ -irradiated sugars.<sup>9</sup> Further photolysis could conceivably result in an aldehyde group and deuterium production in the heavy-water-treated cellulose.

In a similar manner, photolysis of the secondary alcohol group on the  $\text{C}_2$  atom might result in reactions of the type shown in eqs. (2).

Equation (2a) may be eliminated for the same reasons as (1a). The radicals in eqs. (2b) and (2c) would react further to form aldehyde and, if



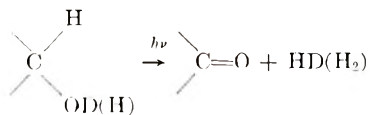
bond scission occurs between C<sub>1</sub> and C<sub>2</sub> carbon atoms, chain scission and C<sup>(1)</sup>O<sub>2</sub> evolution are possible. (Here the superscript on the carbon atom refers to the former position in the anhydroglucose ring.)

If the secondary alcohol on the number three carbon atom is photolyzed, again aldehyde formation, chain scission, and C<sup>(4)</sup>O evolution could occur.

The greater yield of CO and CO<sub>2</sub> at 92°C. could result from the thermal fragmentation of such radicals in the two and three positions. Tertiary alkoxy radicals split thermally to form ketones plus the longest chain alkyl radical.<sup>10</sup>

The absence of an appreciable temperature coefficient for hydrogen evolution vitiates possible mechanisms involving abstraction of hydrogen by hydrogen atoms. Such a process would have an activation energy of the order of 10 kcal./mole. A much more energetically favorable reaction is the formation of molecular hydrogen by disproportionation between a hydrogen atom and either the radicals formed in eqs. (1b) or (2b), or the radicals formed in eqs. (1c) or (2c), with concurrent carbonyl group formation. Although the lack of appreciable D<sub>2</sub> suggests that both (b) and (c) type radicals are not simultaneously produced, the isotopic composition of the evolved hydrogen does not allow a selection between the two types of radicals.

If the hydrogen atom disproportionates with the same radical formed by its dissociation, the net result is indistinguishable from a simple molecular mechanism, i.e.,



It is quite possible that highly absorptive radical species, rather than the carbonyl groups, are responsible for the parabolic decay in the rate of hydrogen evolution.<sup>3</sup> The alkyl radicals would be quite short-lived, except possibly at 77°K. The evolution of hydrocarbons upon heating the low temperature-irradiated cellulose may be due to reaction of these radicals. The radical species that survives at room temperature and is responsible for the post-irradiation oxidation is undoubtedly a less reactive oxygen-containing one. Unlike the complicated ESR spectra with the  $\gamma$ -irradiated cellulose, cellulose irradiated with 2537 Å. light has a simple spectrum suggesting a single radical species.<sup>11</sup>

Although direct photolysis of the glucosidic linkages is possible,<sup>12</sup> evidence indicates that much of the chain scission takes place post-irradiatively and very slowly in the presence of oxygen. Long-lived oxyradicals on the C<sub>2</sub> or C<sub>3</sub> atoms could result in this D.P. decay.

The elimination of C<sup>(1)</sup>O<sub>2</sub> and C<sup>(4)</sup>O would result in chain scission and equal amounts of arabinose (5 carbon atom) and glucose (6 carbon atom) reducing units, as found among the oligosaccharides extracted from irradiated cellulose.<sup>12</sup> The thermally activated enhancement of CO and CO<sub>2</sub> yields at 40 and 92°C. are probably due to fragmentation of radical species. The low temperature yields of these gases can be ascribed mainly to secondary photolysis of carbonyl, carboxyl and radical groups. In either case, the concurrent formation of aldehyde could occur. The gradual increase of CO yield with einsteins of absorbed radiation suggests that carbonyl groups are formed during the irradiation rather than afterward.

The amounts of chain scission and carboxyl group formation after storage in air are insensitive to both temperature (Table III) and  $Nh\nu$  (Fig. 4). The curves in Figure 4 suggest that a steady state of radicals is set up even at low doses, which is responsible for the post-irradiation chain scissions. This would be counterbalanced to some extent by a greater number of chain scissions during the irradiation. It is difficult to visualize the production of carboxyl except in the presence of oxygen.

The greater quantum yields of chain scission for deuterium-exchanged celluloses probably result from higher radical concentrations due to the lower reactivity of deuterium-containing radicals.

## References

1. Flynn, J. H., *J. Phys. Chem.*, **60**, 1332 (1956).
2. Flynn, J. H., *J. Polymer Sci.*, **27**, 83 (1958).
3. Flynn, J. H., W. K. Wilson, and W. L. Morrow, *J. Res. Natl. Bur. Std.*, **60**, 229 (1958).
4. Flynn, J. H., and W. L. Morrow, *J. Polymer Sci.*, **A2**, 81 (1964).
5. Mann, J., and H. J. Marrinan, *Trans. Faraday Soc.*, **52**, 481 (1956).
6. Sullivan, P. J., and W. S. Koski, *J. Am. Chem. Soc.*, **84**, 1 (1962); also P. J. Sullivan and W. S. Koski, paper presented at 141st Meeting, the American Chemical Society. Washington, D. C., March 1962.
7. Sullivan, P. J., private communication.
8. Alger, R. S., T. H. Anderson, and L. A. Webb, *J. Chem. Phys.*, **30**, 695 (1959).
9. Bailey, A. J., S. A. Barker, J. S. Brinacombe, and D. H. Spence, *Nature*, **190**, 259 (1961).
10. Raley, J. H., F. F. Rust, and W. E. Vaughan, *J. Am. Chem. Soc.*, **70**, 88 (1948).
11. Florin, R. E., and L. A. Wall, *J. Polymer Sci.*, **A1**, 1166 (1963).
12. Bečlik, A., and J. K. Hamilton, *Das Papier*, **13**, 77 (1959).

## Résumé

On décrit l'influence du remplacement de l'hydrogène dans des groupes hydroxylés par un deutérium sur la composition des produits et la cinétique de leur formation pendant l'irradiation de la cellulose à 2537 Å sous vide à 77, 313 et 365°K. L'hydrogène qui se dégage contient environ 50–70% de HD. Il se forme un peu de D<sub>2</sub>. Le dégagement de tout le HD ne dépend pas de la température. Manifestement la disproportionnement est le mécanisme dominant de la formation d'hydrogène, plutôt que l'abstraction ou la combinaison d'atomes. La formation de la plupart des groupes aldéhydes se fait durant la photolyse et résulte probablement directement d'une photolyse secondaire ou d'un disproportionnement des radicaux. Le dégagement de H<sub>2</sub>, CO et CO<sub>2</sub> augmente avec la température et résulte aussi bien de la photolyse des groupement fonctionnels que de la dépropagation des radicaux. La scission de la chaîne et la formation des groupes carboxylés se font pour une grande partie pendant l'oxydation après irradiation des radicaux contenant d'oxygène.

## Zusammenfassung

Der Einfluss eines Austausches des Wasserstoffes in den Hydroxylgruppen gegen Deuterium auf die Zusammensetzung der Reaktionsprodukte und die Kinetik ihrer Bildung bei der Bestrahlung von Cellulose mit einer Wellenlänge von 2537 Å im Vakuum bei 77, 313 und 365°K. wird beschrieben. Etwa 50–70% des entwickelten Wasserstoffes bestand aus HD. Es wurde nur wenig D<sub>2</sub> gebildet. Die Gesamtmenge des entwickelten HD war von der Temperatur unabhängig. Der vorherrschende Mechanismus der Wasserstoffbildung war wahrscheinlich eine Disproportionierung und nicht eine Atomabspaltung oder eine Vereinigung von Atomen. Ein Grossteil der Aldehydgruppen wird während der Photolyse gebildet und stammt wahrscheinlich aus einer Sekundärphotolyse oder Disproportionierung der Radikale. H<sub>2</sub>, CO- und CO<sub>2</sub>-Entwicklung nimmt mit steigender Temperatur zu und hat ihre Ursache in einer Photolyse funktioneller Gruppen und in einer Abspaltung aus Radikalen. Kettenspaltung und Karboxylgruppenbildung findet zu einem grossen Teil während der Oxydation langlebiger, sauerstoffhaltiger Radikale nach der Bestrahlung statt.

Received October 15, 1962

Revised December 7, 1962

## Copolymerization of Styrene. I. Copolymerization with Styrene Derivatives Containing Nitrile Groups in the Side-Chain\*

MOSHE KREISEL,† URI GARBATSKI, and DAVID H. KOHN,  
*Department of Chemistry, Technion-Israel Institute of Technology, Haifa,  
Israel*

### Synopsis

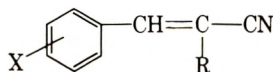
Styrene was copolymerized in bulk with cinnamitrile, benzylidenemalonitrile, ethyl benzylidenecyanoacetate, and atropitrile at 80°C. up to low conversions. The usual reaction scheme of copolymerization fitted only the pair styrene-atropitrile. The kinetic scheme of the other three pairs fitted the scheme proposed by Barb, taking into account the effect of the penultimate unit.

### INTRODUCTION

Styrene is one of the most important monomers for the production of vinyl plastics. Generally these styrene-based plastics can be divided into two groups: general-purpose homopolystyrene on one hand, and the modified polystyrenes, copolymers with various other vinyl monomers, on the other hand. The purpose of these modifications is to improve the mechanical properties of the general-purpose polystyrene, such as its low impact strength and low heat-distortion temperature.

Of the various vinyl comonomers tested, especially the copolymer of styrene with acrylonitrile has found wide use.

Consequently, the behavior of other nitriles as comonomers with styrene has been investigated. Emerson<sup>1</sup> claims, that copolymers of improved strength particularly at elevated temperatures are obtained by polymerizing styrene with a comonomer, of the general formula:



where X is a hydrogen or alkoxy group and R is a cyano or ester group.

Later, Borrows et al.<sup>2</sup> reported their study on the effect of similar comonomers with styrene.

\* Taken in part from a thesis submitted by Moshe Kreisel to the Department of Chemistry, Technion-Israel Institute of Technology, Haifa, in partial fulfillment of the degree of M.Sc.

† Present address: Chemicals and Phosphates Ltd., Haifa, Israel.



The present paper deals with a detailed investigation regarding the copolymerization of styrene with four comonomers having at least one cyano group in the side-chain.

## EXPERIMENTAL

### Materials and Preparation of Monomers

**Styrene.** Commercial Eastman product was purified by washing with aqueous sodium hydroxide, drying, and subsequently distilling at reduced pressure. The distillate was preserved at Dry Ice temperature until used.

**Cinnamionitrile.** This was prepared in 63% yield, according to Plant and Ritter<sup>3</sup> by dehydration of cinnamaldoxime with acetic anhydride (b.p. 153–157°C./37 mm.;  $n_D^{21} = 1.5970$ ). From the refractive index, it is obvious that a mixture of the isomers was obtained. The material was redistilled shortly before use.

**Benzylidenemalononitrile.** Benzylidenemalononitrile was prepared in 90% yield by the method of Corson and Stoughton<sup>4</sup> by condensing benzaldehyde with malononitrile in *tert*-amyl alcohol in the presence of piperidine as catalyst. The product melted at 83–84°C. (Corson and Stoughton reported m.p. 83.5–84°C.).

**Ethyl Benzylidenecyanoacetate.** This monomer was similarly prepared in 80% yield from equivalent quantities of benzaldehyde and ethyl cyanoacetate in a small quantity of ethanol as diluent and in the presence of piperidine as catalyst. The ester melted at 51°C. as reported by Fiquet.<sup>5</sup>

**Atroponitrile.** This was prepared by the methods of Walker<sup>6</sup> and Stewart et al.<sup>7</sup> by condensing paraformaldehyde and benzyl cyanide in methanol with sodium methylate as catalyst at 55°C. The crude product was flash-distilled without the aid of an inhibitor at b.p. 80–90°C./2 mm. and the pure product obtained in 25% yield. Because of the tendency of the product to polymerize, the distillation was carried out with maximum exclusion of light. The product was used immediately thereafter, and all the handling before polymerization carried out at below 5°C.

**Benzoyl Peroxide.** Eastman pure grade was used without further purification.

### Copolymerization

Pyrex tubes with a bulb at the lower end and a constriction near the upper end were used for polymerization.

After introduction and weighing of the monomers and the catalyst, the mixture in the bulb was frozen in a Dry Ice–acetone mixture, the tube evacuated down to 2 mm., flushed twice with nitrogen, and the tube sealed under reduced nitrogen pressure.<sup>8</sup>

Reaction mixtures consisted of 10-g. portions of monomers with catalyst (0.2% by weight) added.

The sealed reaction tubes were heated at a fixed polymerization temperature of  $80 \pm 0.5^\circ\text{C}$ .

The proper time of polymerization, i.e., the time necessary to polymerize 1–8% of the mixture, was found by trial and error.

After the polymerization, the reaction tubes were cooled to room temperature and opened. The products were repeatedly precipitated by methanol from dilute solutions of methyl ethyl ketone.

The purified products were dried in a vacuum oven at 50°C. to constant weight. The composition of the copolymers was determined by microanalysis of nitrogen content.

### Viscosity Measurements

The molecular weights were estimated from the viscosities of toluene solutions of the copolymers, measured in an Ubbelohde-type viscometer mounted in a fixed metal rack.<sup>9</sup> Precautions against the introduction of dust or any solid particles were taken as described by Streeter and Boyer.<sup>10</sup> The measurements were carried out at  $25 \pm 0.01^\circ\text{C}$ .

### Melting Ranges

The melting ranges of the various copolymers were measured under atmospheric pressure, in capillaries, with a temperature rise of about  $1^\circ\text{C}/3$  sec.

The melting ranges, as recorded, are between the temperatures when the first visible changes of the samples occurred and—as the higher limits—the temperatures when the materials became transparent, but not necessarily liquid.

## RESULTS AND DISCUSSION

The results of the various copolymerizations are summarized in Tables I–IV.

### Discussion of Results

First attempts to calculate the reactivity ratios  $r_1$  and  $r_2$  in the usual manner<sup>12</sup> gave reasonable results for the pair styrene–atropnitrile only.

Atropnitrile adds easily to itself and copolymerization proceeds at a fair rate, as with 1,1-disubstituted vinyls generally. In Figure 1,  $m_2$  is plotted against  $M_2$ , fitting a curve calculated from the simple equation:

$$\frac{m_1}{m_2} = \frac{M_1 r_1 M_1 + M_2}{M_2 r_2 M_2 + M_1} \quad (1)$$

for  $r_1 = 0.02$  and  $r_2 = 0.7$ , where styrene is  $M_1$ . These values were determined by a graphical method (Fig. 2), using the linear form of eq. (1):

$$r_2 = \frac{M_1}{M_2} \left[ \frac{m_2}{m_1} \left( 1 + \frac{M_1}{M_2} r_1 \right) - 1 \right] \quad (2)$$

The copolymerization of styrene with cinnamionitrile (I), benzylidene-malononitrile (II), or ethyl benzylidene-cyanoacetate (III), was first in-

TABLE I. Styrene ( $M_1$ ) and Cinnamionitrile ( $M_2$ )

No. of sample	$M_2$ , mole fraction of monomer 2	Time of polymerization, min.	Conversion, %	Nitrogen content of copolymer, %	$m_2$ , mole fraction in polymer	$[\eta]$	Molecular weight $\times 10^{-3}$	Melting range, °C.
Polystyrene	0.0	—	—	—	—	0.570	52.2	155-170
1/1	0.100	90	7	0.92	0.070	0.510	44.4	180-195
1/2	0.312	90	6	1.88	0.140	0.535	47.7	165-215
1/3	0.364	90	7	2.10	0.162	0.412	32.0	170-200
1/4	0.415	120	12	2.66	0.208	—	—	175-205
1/5*	0.443	300	7	2.44	0.189	0.447	36.3	190-205
1/6	0.514	90	7	2.68	0.210	0.404	41.1	175-200
1/7	0.628	120	10	3.63	0.285	0.320	21.9	200-215
1/8	0.716	120	5	4.00	0.317	0.281	17.9	185-240
1/9	0.810	120	3	4.69	0.381	0.187	9.7	195-220
1/10	0.911	300	4	5.18	0.427	0.178	8.9	195-225
1/11	0.916	300	5	5.72	0.475	0.116	4.8	195-235

\* Polymerized by ultraviolet light only.

TABLE II. Styrene ( $M_1$ ) and Benzylidenemalonitrile ( $M_2$ )

No. of sample	$M_2$ , mole fraction of monomer 2	Time of polymerization, min.	Conversion, %	Nitrogen content of copolymer, %	$m_2$ , mole fraction in polymer	$[\eta]$	Molecular weight $\times 10^{-4}$	Melting range, °C.
2/1	0.071	50	6.2	5.61	0.231	0.587	54.9	210-235
2/2	0.106	50	6.8	6.11	0.255	0.571	52.6	225-240
2/3	0.142	50	7.0	6.54	0.275	0.540	48.4	—
2/4	0.185	50	7.3	7.17	0.305	0.540	48.4	235-245
2/5	0.309	35	6.3	7.71	0.333	0.489	42.0	235-250
2/6	0.402	35	6.7	8.41	0.367	0.459	37.8	245-255
2/7	0.657	35	7.8	9.28	0.413	0.433	34.6	250-265

TABLE III  
Styrene ( $M_1$ ) and Ethyl Benzylidencyanoacetate ( $M_2$ )

No. of sample	$M_2$ , mole fraction of monomer 2	Time of polymerization, min.	Conversion, %	Nitrogen content of copolymer, %	$m_2$ , mole fraction in polymer	$[\eta]$	Molecular weight $\times 10^{-3}$	Melting range, °C.
3/1	0.100	30	2.0	2.60	0.236	0.643	63.0	205-245
3/2	0.200	30	3.2	2.82	0.261	0.632	61.4	205-250
3/3	0.300	30	4.1	3.17	0.300	0.610	58.2	225-255
3/4	0.400	30	5.1	3.46	0.338	0.593	55.8	240-260
3/5	0.500	20	4.4	3.64	0.362	0.593	55.8	260-295
3/6	0.600	20	3.2	3.90	0.397	0.565	98.8	240-285
3/7	0.700	15	2.2	4.16	0.436	0.905	106	240-290
3/8	0.870	15	1.2	4.35	0.461	—	—	245-295

TABLE IV  
Styrene ( $M_1$ ) with Acroponitrile ( $M_2$ )

No. of sample	$M_2$ , mole fraction of monomer 2	Time of polymerization, min.	Conversion, %	Nitrogen content of copolymer, %	$m_2$ , mole fraction in polymer	$[\eta]$	Molecular weight	Melting range, °C.
4/1	0.081	30	2.2	5.61	0.463	0.028	540	
4/2	0.165	30	2.2	6.26	0.523	—	—	
4/3	0.253	30	2.3	6.42	0.538	0.068	2100	~140 (dec.)
4/4	0.345	30	2.5	6.78	0.573	—	—	
4/5	0.333	30	0.4	6.83	0.578	—	—	
4/6	0.441	30	1.1	6.86	0.580	—	—	
4/7	0.543	30	0.7	7.29	0.662	—	—	

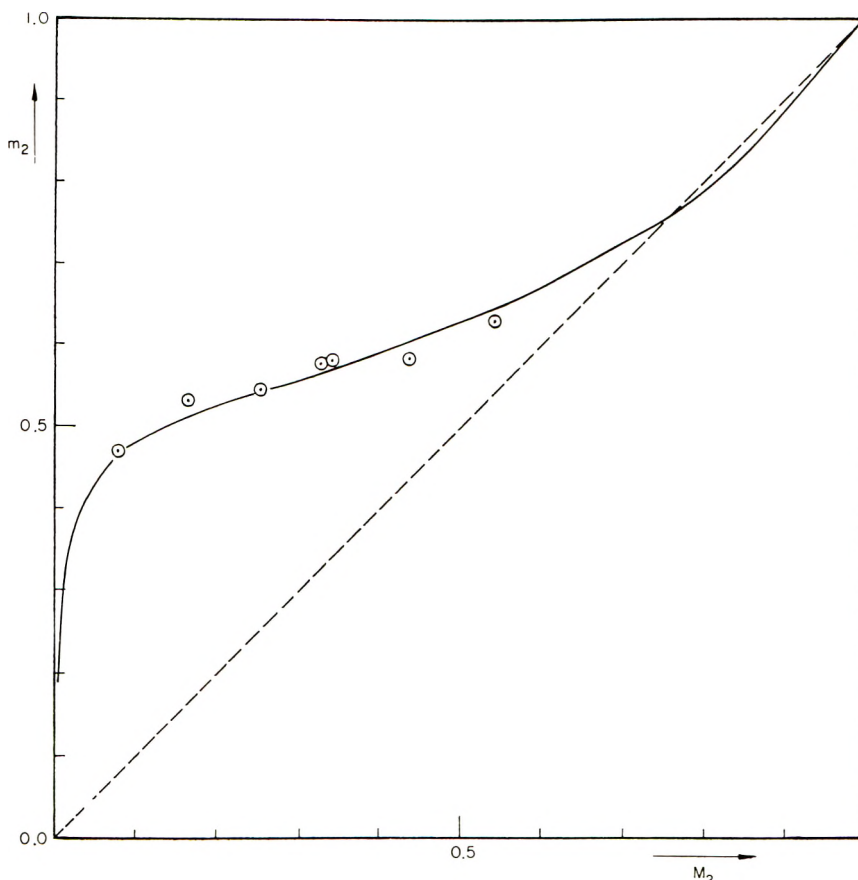


Fig. 1. Copolymerization of styrene ( $M_1$ ) with atropnitrile ( $M_2$ ). Curve calculated from eq. (1) for  $r_1 = 0.02$  and  $r_2 = 0.7$ .

vestigated by Borrows et al.<sup>2</sup> They found, that one has to assume a kinetic effect of the penultimate unit<sup>13,14</sup> for the pair styrene-benzylidenemalononitrile.

Now, a more detailed investigation shows, that this effect appears in all three pairs.

Plotting  $r_1$  against  $r_2$ , according to eq. (2), yielded widely scattered lines, centering around negative values of  $r_2$ , thus indicating the inadequacy of this simple kinetic model.

Hence it was tried to evaluate the results according to the improved scheme proposed by Merz et al.,<sup>15</sup> taking into consideration the monomer unit in the position penultimate to the active center of the growing polymer. They developed for such a case the following equation:

$$\frac{dM_1}{dM_2} = \frac{m_1}{m_2} = \frac{1 + \frac{r_1 M_1}{M_2} \left( \frac{M_2}{r_1} + M_1 \right)}{1 + \frac{r_2 M_2}{M_1} \left( \frac{r_2' M_2}{r_2} + M_1 \right)} \quad (3)$$

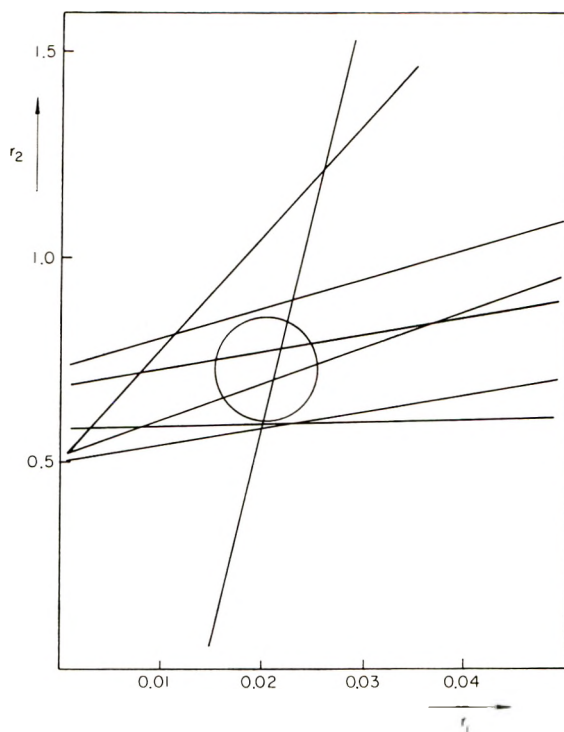


Fig. 2. Copolymerization of styrene ( $M_1$ ) with atropionitrile ( $M_2$ ). Determination of  $r_1$  and  $r_2$  by using eq. (2).  $r_1 = 0.02$ ;  $r_2 = 0.7$ .

where

$$r_1 = k_{111}/k_{112}$$

$$r_2 = k_{222}/k_{221}$$

$$r_1' = k_{211}/k_{212}$$

$$r_2' = k_{122}/k_{121}$$

where the subscripts of the  $k$  values denote (from left to right) the penultimate unit, the ultimate unit, and the newly adding monomer, respectively.

However, as none of the three comonomers investigated polymerize by themselves,  $r_2 = r_2' = 0$ , and eq. (3) reduces to:

$$\frac{m_1}{m_2} = 1 + \frac{r_1' \frac{M_1}{M_2} (r_1 M_1 + M_2)}{r_1' M_1 + M_2} \quad (4)$$

Following Barb's notation:<sup>14</sup>  $M_1/M_2 = x$  and  $m_1/m_2 = n$ , this equation can be written as:

$$n - 1 = r_1' x (1 + r_1 x) / (1 + r_1' x) \quad (5)$$

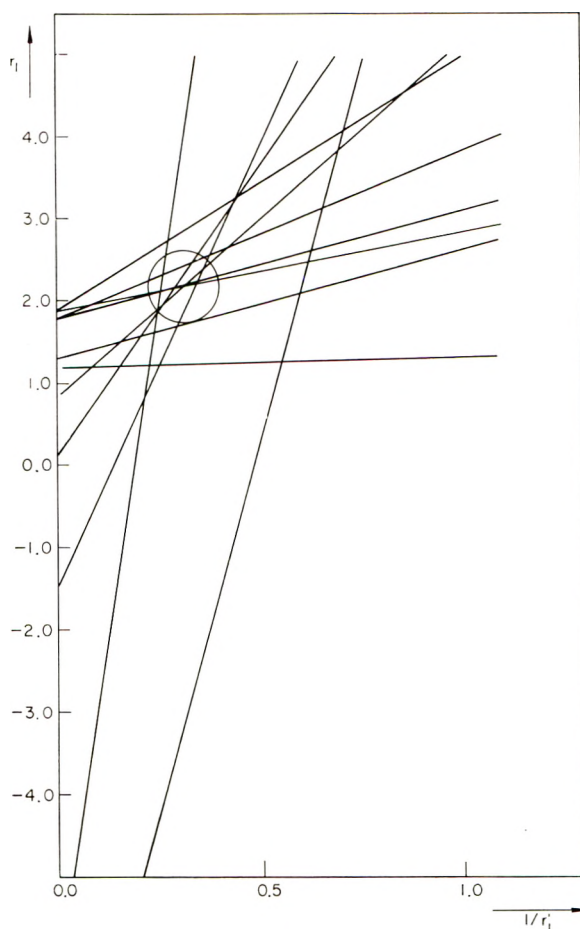


Fig. 3. Copolymerization of styrene ( $M_1$ ) with cinnamitrile ( $M_2$ ). Determination of  $r_1$  and  $r_1'$  by using eq. (6).  $r_1 = 2.2$ ;  $r_1' = 3.2$ .

or

$$r_1 = [(n - 1)/x^2](1/r_1') + (n - 2)/x \quad (6)$$

Accordingly, results were used to calculate  $r_1$  and  $r_1'$  by eq. (6) (Figs. 3, 4, and 5).

In Figures 6, 7, and 8,  $m_2$  is plotted against  $M_2$ . The curves in these figures are calculated according to eq. (4), using  $r_1$  and  $r_1'$  values as obtained in Figures 3, 4, and 5.

The  $r_1$  and  $r_1'$  values for benzylidenemalononitrile are similar to those reported by Borrows et al.,<sup>2</sup> i.e.,  $r_1 = 0.1$  and  $r_1' = 1.44$  as compared with  $r_1 = 0.125$  and  $r_1' = 1.25$  in this work.

In the case of cinnamitrile, no effect of the penultimate unit was reported by Borrows et al., whereas for ethyl benzylidenecyanoacetate no reactivity ratios are given.

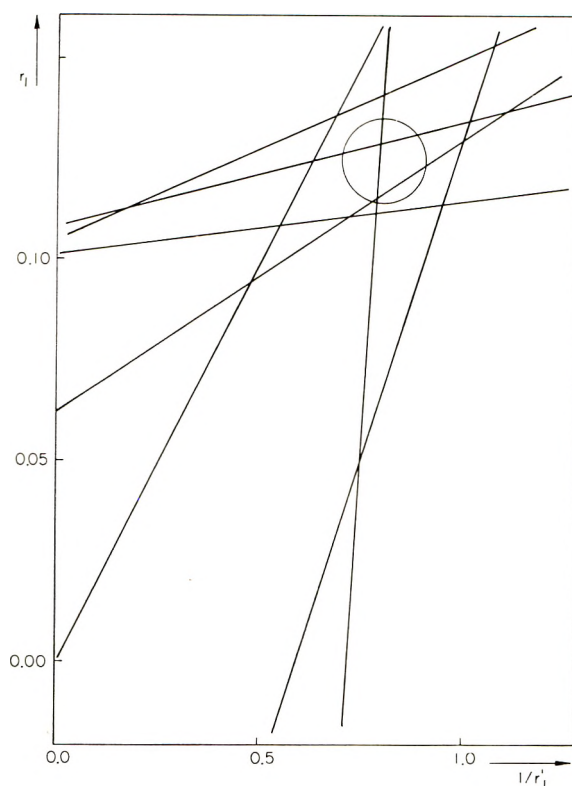


Fig. 4. Copolymerization of styrene ( $M_1$ ) with benzylidenemalononitrile ( $M_2$ ). Determination of  $r_1$  and  $r_1'$  by using eq. (6).  $r_1 = 0.125$ ;  $r_1' = 1.25$ .

A more extensive discussion on this point will be given further on.

The dependence of rates of polymerization and intrinsic viscosities on the composition of the various copolymer pairs may be summarized as follows.

(1) Styrene–cinnamonnitrile: Both intrinsic viscosity and rate of polymerization decrease with increasing comonomer content in the copolymer.

(2) Styrene–benzylidenemalononitrile: The intrinsic viscosity decreases slightly, whereas the rate of polymerization increases with rising comonomer content.

(3) Styrene–ethyl benzylidencyanoacetate: The intrinsic viscosity first decreases with increasing comonomer content, going through a minimum at  $m_2 = 0.338$ . At higher comonomer concentrations, the effect is reversed. The rate of copolymerization, on the other hand, rises at the lower comonomer concentrations, showing a maximum at approximately the composition of the above minimum. With further increase of the comonomer concentration, the rate decreases.

(4) Styrene–atropionitrile: No general picture can be drawn.

These findings are generally in accordance with those of Borrows et al.,<sup>2</sup> save for a serious discrepancy for ethyl benzylidencyanoacetate.



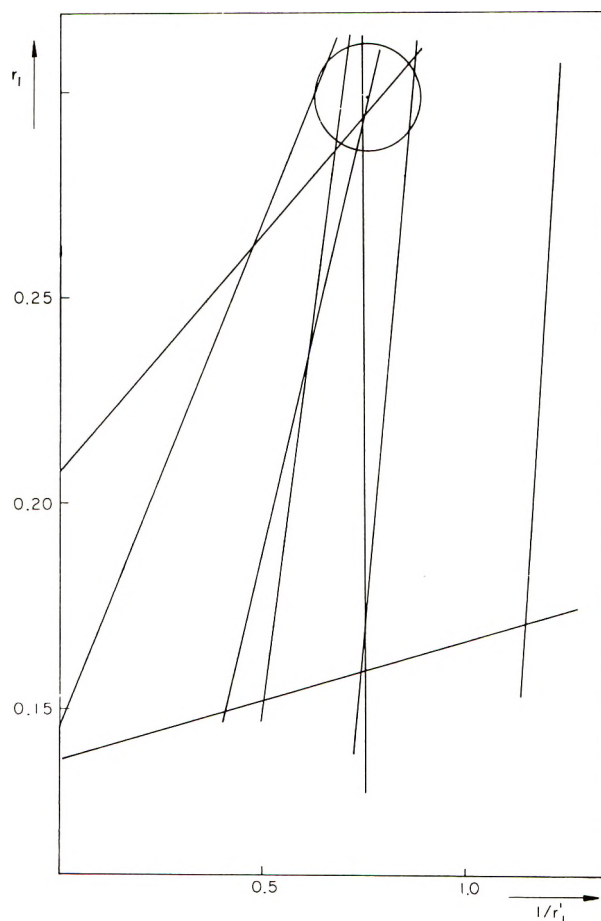


Fig. 5. Copolymerization of styrene ( $M_1$ ) with ethyl benzyldenecyanoacetate ( $M_2$ ). Determination of  $r_1$  and  $r_1'$  by using eq. (6).  $r_1 = 0.3$ ;  $r_1' = 1.3$ .

This difference may be explained by the fact that Borrows worked up to relatively high conversions (14–25%), but only up to 0.2 mole-fraction of  $M_2$  in the monomer mixture.

For the interpretation of results, it may be assumed at first, that the known relationship  $\eta$ –molecular weight for styrene:<sup>11</sup>

$$[\eta] = 4.37 \times 10^{-4} M^{0.66} \quad (7)$$

is not seriously altered on introducing chain-substituted styrene comonomers—at least when working at low proportions of  $m_2:m_1$ .

Now, molecular weight, as expressed in terms of average chain length, is in its most general form the ratio between the sums of propagation to termination rates.

The relative rate of growth is essentially a function of the sum of propagation rates, which in turn is determined<sup>12</sup> by the following two main

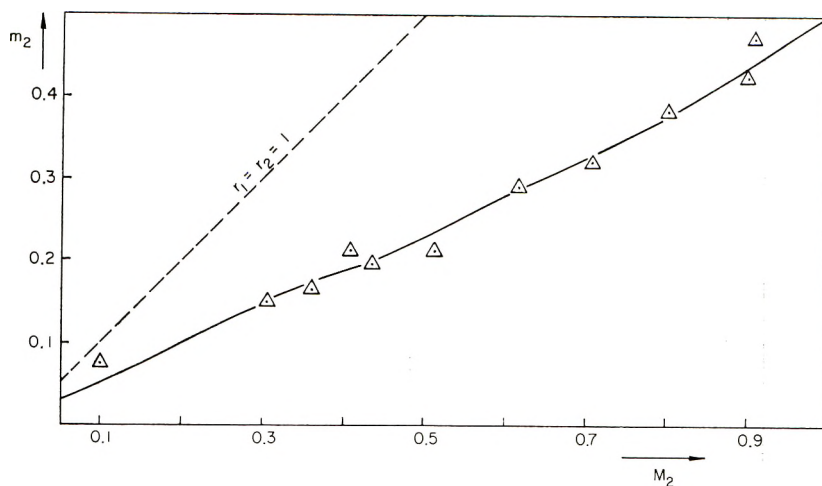


Fig. 6. Copolymerization of styrene ( $M_1$ ) with cinnamionitrile ( $M_2$ ). Curve calculated from eq. (4) for  $r_1 = 2.2$  and  $r_1' = 3.2$ .

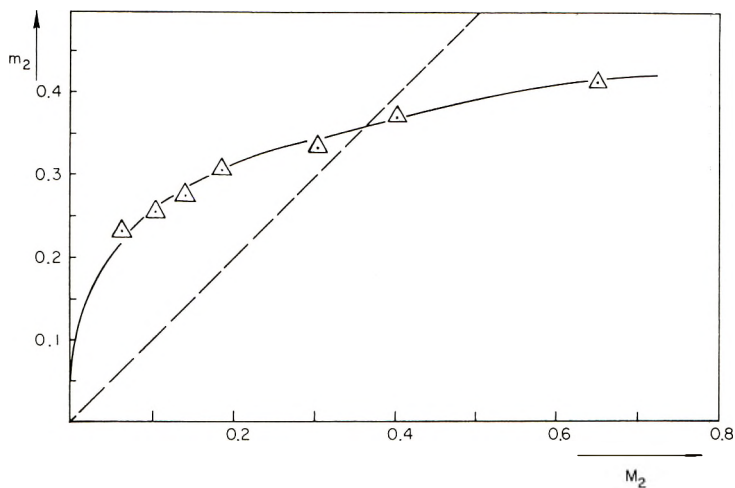


Fig. 7. Copolymerization of styrene ( $M_1$ ) with benzylidenemalononitrile ( $M_2$ ). Curve calculated from eq. (4) for  $r_1 = 0.125$  and  $r_1' = 1.25$ .

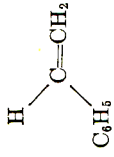
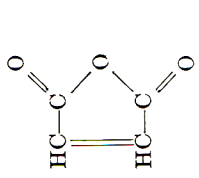
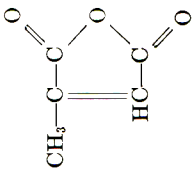
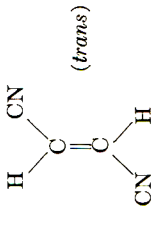
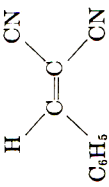
factors: (1) differences in resonance stabilization and (2) differences in polarity between the two monomers.

The first factor may be neglected, due to the structural similarity between styrene and its derivatives.

The second factor arises by the introduction of strongly negative dipoles. Accordingly, relative rates of propagation for copolymerization may be arranged as follows:

$$k_p: \quad (\text{St} + \text{I}) < (\text{St} + \text{III}) < (\text{St} + \text{II})$$

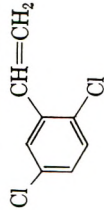
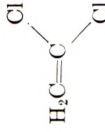
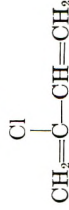
TABLE V

No.	$M_1$	$M_2$	$r_1$	$r_1'$	$r_1'/r_1$	$r_2 = r_2'$	Reference
1			0.017	0.063	3.7	0	14
2	"		0.07	0.25	3.55	0.015	14
3	"		0.07	1.0	14.3	0	14
4	"		0.1	1.44	14.4	0	2
			0.125	1.25	10.0	0	This paper

5	“	$\begin{array}{c} \text{CN} \\   \\ \text{H}-\text{C}=\text{C} \\   \quad   \\ \text{C}_6\text{H}_5 \quad \text{COOC}_2\text{H}_5 \end{array}$	0.3	1.3	4.7	0	This paper
6	“	$\begin{array}{c} \text{CN} \\   \\ \text{H}-\text{C}=\text{C} \\   \quad   \\ \text{C}_6\text{H}_5 \quad \text{H} \end{array}$	2.2	3.2	1.4	0	This paper
7	$\begin{array}{c} \text{H} \\   \\ \text{C}=\text{CH}_2 \\   \\ \text{C}_6\text{H}_5 \end{array}$	$\begin{array}{c} \text{CN} \\   \\ \text{H}_2\text{C}=\text{C} \\   \\ \text{H} \end{array}$	0.30	0.45	1.5	0.03	16
8	$\begin{array}{c} \text{CH}_3 \\   \\ \text{C}=\text{CH}_2 \\   \\ \text{C}_6\text{H}_5 \end{array}$	“	0.055	0.0903	1.7	0.06	16
9	$\begin{array}{c} \text{CH}_3\text{COO} \\   \\ \text{C}=\text{CH}_2 \\   \\ \text{C}_6\text{H}_5 \end{array}$	“	0.09	0.47	5.2	0.08	16
10	$\begin{array}{c} \text{COOCH}_3 \\   \\ \text{H}_2\text{C}=\text{C} \\   \quad   \\ \text{Cl} \quad \text{CN} \end{array}$	$\begin{array}{c} \text{CN} \\   \\ \text{H}_2\text{C}=\text{C} \\   \\ \text{CN} \end{array}$	0.245	0.40	1.6	0.91	17
11	$\begin{array}{c} \text{CH}_3 \\   \\ \text{H}_2\text{C}=\text{C} \\   \\ \text{COOCH}_3 \end{array}$	“	0.04	0.082	2.0	0.31	17

(continued)

TABLE V (continued)

No.	$M_1$	$M_2$	$r_1$	$r_1'$	$r_1'/r_1$	$r_2 = r_2'$	Reference
12			0.022	0.032	1.5	0.0092	17
13		"	0.010	0.012	1.2	0.049	17
14		"	0.000	0.057	Very large	0.0048	17

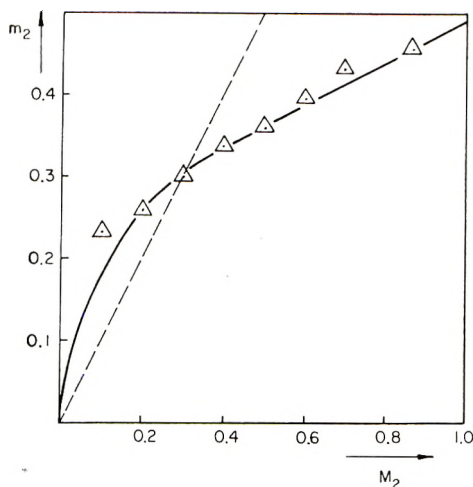


Fig. 8. Copolymerization of styrene ( $M_1$ ) with ethyl benzyldenecyanoacetate ( $M_2$ )  
Curve calculated from eq. (4) for  $r_1 = 0.3$  and  $r_1' = 1.3$ .

where St denotes styrene and I, II, and III are the afore-mentioned comonomers.

On the other hand, the rate of termination is depressed with increasing number of substituent dipole groups as well as by increasing bulkiness. As a result, relative rates of termination may be written as follows:

$$k_t: \quad (\text{St} + \text{I}) > (\text{St} + \text{II}) > (\text{St} + \text{III})$$

The empirical overall sequence for the average degree of polymerization is therefore:

$$(\text{St} + \text{I}) < (\text{St} + \text{II}) \leq (\text{St} + \text{III})$$

### Melting Ranges

The melting ranges of these three copolymers are higher than those of polystyrene, which effect can be ascribed to the presence of dipole groups as well as to the bulkiness of the substituents on the side-chain.

### Effect of the Penultimate Unit

Barb<sup>14</sup> and Ham<sup>16</sup> were the first to evaluate their experimental results by taking into account an effect of the penultimate unit in copolymerization by free radicals and to propose a general explanation for it. Now, with more practical examples available, a discussion on this subject seems to be indicated.

From the monomer pairs exhibiting such an effect it seems that a strong influence of the penultimate group exists whenever one monomer is strongly polar and the other one practically nonpolar. These monomers shall be called here P and N, respectively.

When the P type monomer does not polymerize by itself, giving  $r_2 = r_2' = 0$ , the number of parameters is reduced to two, and thus the calculations are easier to handle. In such a case, and also at low  $r_2$  values, only the ratios  $r_1$  and  $r_1'$  of the enlarged scheme are left.

Now the effect indicates a diminished activity of the monomer P toward a free radical having P as its penultimate unit. Consequently

$$r_1 = \frac{k_{NNN}}{k_{NNP}} < r_1' = \frac{k_{PNN}}{k_{PNP}}$$

Ham<sup>16</sup> proposed the use of the ratio  $r_1'/r_1$  as a measure of the relative repelling tendencies of polar monomers. One may assume that the rate of a neutral N adding to the chain should be hardly affected by the penultimate unit

$$k_{NNN} \simeq k_{PNN}$$

and thus

$$\frac{r_1'}{r_1} = \frac{k_{PNN}/k_{PNP}}{k_{NNN}/k_{NNP}} \simeq \frac{k_{NNP}}{k_{PNP}} \geq 1$$

On the basis of these assumptions, Ham's ratio  $r_1'/r_1$  may serve as a single quantitative expression for the effect of the penultimate unit.

In Table V known data are compiled, thus allowing a comparison of magnitude of this ratio for various monomer pairs. The sequence of pairs in this table enables a further comparison between monomers having various substituent groups towards a common comonomer.

Although this repulsive effect is largely due to the polarity of the molecules, no simple relationship between this effect and the polarity of the molecules as expressed by the dipole moment of the monomer could be deduced.

Extreme examples, as fumaronitrile-styrene ( $\mu = 0$ ;  $r_1'/r_1 = 14.3$ ) versus acrylonitrile-styrene ( $\mu = 3.97$ ;  $r_1'/r_1 = 1.5$ ), emphasize this fact.

Consequently, other factors have to be considered, such as the group moments of the substituents, their size, number, and place in the monomer, and the extent of orientation within the growing chain.

## References

1. Emerson, W. S., U. S. Pat. 2,498,616 (1950); *Chem. Abstr.*, **44**, 4720 (1950).
2. Borrows, E. T., R. N. Haward, J. Porges, and J. Street, *J. Appl. Chem.*, **5**, 379 (1955).
3. Plaut, H., and J. Ritter, *J. Am. Chem. Soc.*, **73**, 4076 (1951).
4. Corson, B. B., and R. W. Stoughton, *J. Am. Chem. Soc.*, **50**, 2825 (1928).
5. Fiquet, E., *Ann. Chem.*, [6], **29**, 448 (1893).
6. Walker, J. F., U. S. Pat. 2,478,990 (1949); *Chem. Abstr.*, **44**, 2009 (1950).
7. Stewart, J. M., and C. Hung Chang, *J. Org. Chem.*, **21**, 635 (1956).
8. Bartlett, P. D., *Angew. Chem.*, **67**, 45 (1955).
9. Ubbelohde, L., *Ind. Eng. Chem., Anal. Ed.*, **9**, 85 (1937).
10. Streeter, D. J., and R. F. Boyer, *J. Polymer Sci.*, **14**, 5 (1954).

11. Pepper, D. C., *J. Polymer Sci.*, **7**, 347 (1951).
12. Alfrey, T., J. J. Bohrer, and H. Mark, *Copolymerization*, Interscience, New York, 1952.
13. Mayo, F. R., and C. Walling, *Chem. Revs.*, **46**, 191 (1950).
14. Barb, W. G., *J. Polymer Sci.*, **11**, 117 (1953).
15. Merz, E., T. Alfrey, and J. Goldfinger, *J. Polymer Sci.*, **1**, 75 (1946).
16. Ham, G. E., *J. Polymer Sci.*, **14**, 87 (1954).
17. Ham, G. E., *J. Polymer Sci.*, **24**, 349 (1957).

### Résumé

Le styrène a été copolymérisé en masse avec le nitrile cinnamique (I), avec le nitrile benzylidène-malonique (II), avec le benzylidène-cyanoacétate d'éthyle (III) et avec l'atroponitrile (IV) à 80°C à faibles taux de conversion. Le schéma usuel de réaction de copolymérisation n'est vérifié que dans la paire styrène avec (IV). Le schéma cinétique des trois autres paires vérifie le schéma proposé par Barb, tenant compte de l'effet exercé par l'unité pénultième.

### Zusammenfassung

Styrol wurde in Substanz mit Cinnamonitril(I), Benzylidenmalonitril(II), Äthylbenzylidencyanoacetat(III) und Atropanitril(IV) bei 80°C zu niedrigem Umsatz copolymerisiert. Nur das Paar Styrol—(IV) entsprach dem üblichen Copolymerisationsreaktionsschema. Die anderen drei Paare entsprachen dem von Barb vorgeschlagenen Schema, das den Einfluss der vorletzten Gruppe berücksichtigt.

Received February 1, 1963



## Mean Square Length of Random Polypeptide Chains and the Length of Protein Fibers

W. G. CREWETHER, *Division of Protein Chemistry, C.S.I.R.O., Wool  
Research Laboratories, Parkville N2 (Melbourne), Victoria, Australia*

### Synopsis

Application of statistical mechanical theory gives the expression  $\bar{r}^2 = 27.9n - 20.3$  relating the mean square end-to-end length,  $\bar{r}^2$ , of a random polypeptide chain in the *trans*-form and  $n$ , the number of amino acid residues in the chain. The corresponding expressions for the *cis* and nonplanar forms are  $\bar{r}^2 = 8.6n - 0.8$  and  $\bar{r}^2 = 15.5n - 4.8$ , respectively. The first of these equations has been used to obtain an expression for the fractional decrease in length of a crosslinked, aligned  $\alpha$ -helical structure when it is converted to the random coil form. The assumptions made are that the crosslinkages undergo little lateral displacement and that the volume remains constant. The expression so obtained is  $l/l_0 = \{23.7n - 17.3 - [10\sqrt{l_0/l} - 7]^2\}^{1/2}/1.5n$  where  $l$  is the supercontracted length of the polypeptide fiber,  $l_0$  is its original length and  $n$  is the number of amino acid residues between crosslinkages.

Eyring<sup>1</sup> has used the statistical mechanical theory to obtain an expression for the mean square length of a simple hydrocarbon chain in terms of the bond length, and bond angle, and the number of bonds in each chain. Wall<sup>2</sup> has obtained an identical expression by a related procedure and extended the theory to derive expressions for the mean square lengths of polymers of isoprene in the *trans*, *cis*, and random forms.

In obtaining a similar expression for the mean square length of random polypeptide chains greater complexity is encountered because, in addition to the planarity of the peptide group with its *trans* arrangement, there are three bond lengths and bond angles to consider. Haly and Feughelman,<sup>3</sup> having shown that supercontracted wool fibers behave as elastomers, applied the Eyring expression to calculate the frequency of crosslinking from the extent of supercontraction. For this purpose they used a simple model in which each amino acid residue was represented by a single link equal in length to the distance between the  $\alpha$ -carbon atoms, with an angle of  $110^\circ$  between successive linkages, and assuming symmetrical rotation around each link.

This paper provides a more exact expression for the mean square distance between the ends of a random polypeptide chain. The expression is applicable to chains containing relatively few amino-acid residues and is considered in relation to the contraction which takes place when a highly

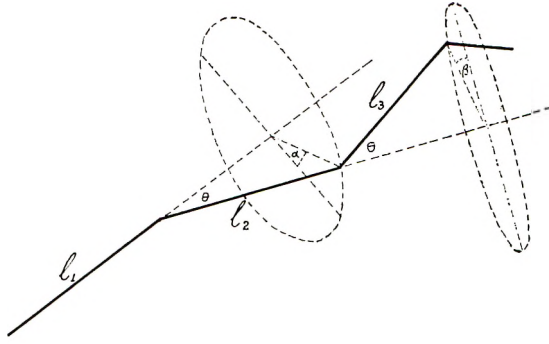


Figure 1.

crosslinked fibrous protein in the  $\alpha$ -helical conformation is converted to an elastomer.

### The Mean Square End-to-End Length of a Polypeptide Chain

Eyring<sup>1</sup> has considered the bonds comprising a paraffin chain molecule to be vectors  $\mathbf{l}_1, \mathbf{l}_2, \mathbf{l}_3$ , etc. (Fig. 1), each of which can rotate freely around the adjacent bond at a constant angle of inclination,  $\theta$ , so that the vector joining the ends of the chain,

$$\mathbf{r} = \mathbf{l}_1 + \mathbf{l}_2 + \mathbf{l}_3 + \dots + \mathbf{l}_n$$

and

$$\begin{aligned} r^2 = & \mathbf{l}_1^2 + \mathbf{l}_2^2 + \dots + 2\mathbf{l}_1\mathbf{l}_2 + 2\mathbf{l}_2\mathbf{l}_3 + \dots + 2\mathbf{l}_1\mathbf{l}_3 + 2\mathbf{l}_2\mathbf{l}_4 \\ & + \dots + 2\mathbf{l}_1\mathbf{l}_n \end{aligned}$$

Since all positions of  $\mathbf{l}_4$  at an angle  $\theta$  to  $\mathbf{l}_3$  are equally probable, the mean of  $\mathbf{l}_4$  for each position of  $\mathbf{l}_3$  is a vector of magnitude  $l \cos \theta$  in the direction of  $\mathbf{l}_3$ . The vector  $\mathbf{l}_3$ , in a similar manner, can assume with equal probability all positions at an angle  $\theta$  to  $\mathbf{l}_2$  and this also applies to the mean of vector  $\mathbf{l}_4$  with respect to  $\mathbf{l}_3$ . The mean value of  $\mathbf{l}_3$  with respect to  $\mathbf{l}_2$  is then  $l \cos \theta$  in the direction of  $\mathbf{l}_2$  and the mean value of  $\mathbf{l}_4$  with respect to  $\mathbf{l}_2$  becomes  $l \cos^2 \theta$  in the direction of  $\mathbf{l}_2$ , and so on. It follows that the mean scalar products of  $\mathbf{l}_1$  and  $\mathbf{l}_2$ ,  $\mathbf{l}_1$  and  $\mathbf{l}_3$ , and  $\mathbf{l}_1$  and  $\mathbf{l}_4$  are  $l^2 \cos \theta$ ,  $l^2 \cos^2 \theta$ , and  $l^2 \cos^3 \theta$ , respectively, and that for  $\mathbf{l}_1$  and  $\mathbf{l}_n$  is  $l^2 \cos^{(n-1)} \theta$ . Hence

$$\bar{r}^2 = nl^2 + 2(n-1)l^2 \cos \theta + 2(n-2)l^2 \cos^2 \theta + \dots + 2l^2 \cos^{(n-1)} \theta \quad (1)$$

The validity of this procedure can be demonstrated trigonometrically. Thus it can be shown that in a three-dimensional chain consisting of links  $a, b, c$ , etc. at angles  $A, B, C$  etc. to each other the distance,  $r$ , between the ends of the chain is given by

$$\begin{aligned} r^2 = & a^2 + b^2 + c^2 + d^2 + \dots + 2ab \cos A + 2bc \cos B + \dots \\ & + 2ac \cos A \cos B + 2bd \cos B \cos C + \dots + 2an \cos A \cos B \cos C \dots \\ & \cos N - (f_1 + f_2 + f_3 + \dots + f_{(n-1)}) \quad (2) \end{aligned}$$

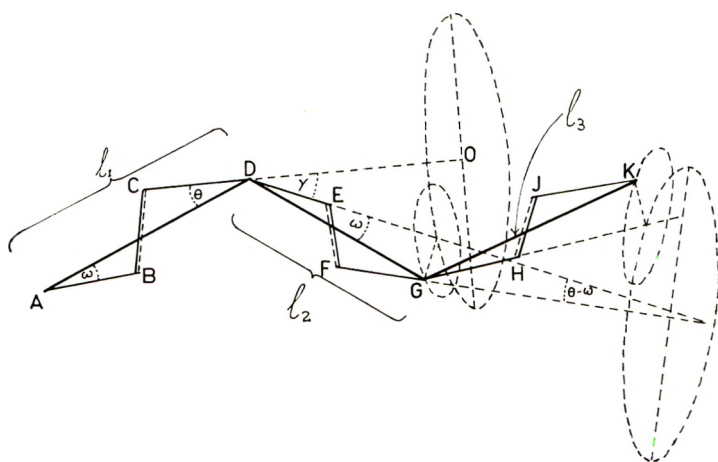


Fig. 2. Bond rotations in a *trans*-polypeptide chain.

where  $f_1, f_2$ , etc., are functions all terms of which are multiples of the sines or cosines of the angles of rotation of  $b$  around  $a$ ,  $c$  around  $b$ ,  $d$  around  $c$ , etc. These angles are indicated by  $\alpha, \beta$ , etc., in Figure 1. The mean of  $r^2$  is then equal to the sum of the invariant term of eq. (2) minus the mean values of  $f_1, f_2$ , etc. Since these means are obtained by substituting the mean values of  $\sin \alpha \cos \alpha \sin \beta \cos \beta$ , etc., in these functions and as  $\sin \alpha, \cos \alpha$ , etc., all have mean values of zero,  $\overline{f_1}, \overline{f_2}$ , etc., are also zero. For a chain with equal bond lengths and angles, therefore, we obtain the Eyring expression [eq. (1)].

We consider now a polypeptide chain ABCDE... (Fig. 2) with vectors  $\mathbf{l}_1, \mathbf{l}_2, \mathbf{l}_3$ , etc. joining adjacent  $\alpha$ -carbon atoms and making angles of  $\omega$  and  $\theta$  with the  $C_\alpha-C$  and  $N-C_\alpha$  bonds, respectively. Each of these vectors can rotate around two of their constituent bonds, AB and CD for  $\mathbf{l}_1$ , DE and FG for  $\mathbf{l}_2$ , and so on. Hence if we fix  $\mathbf{l}_1$ ,  $\mathbf{l}_2$  will lie on the surface of a cone with axis DE, and DE will in turn lie on the surface of a cone with axis CDO. Angle GDE is  $\omega$ , angle EDO is  $\gamma$ , the bond angle at the  $\alpha$ -carbon atom. Since the amide group is planar,<sup>4</sup> the bond FG is at an angle  $(\theta - \omega)$  to DE and rotates around it. For each position of  $\mathbf{l}_2$ ,  $\mathbf{l}_3$  can assume with equal probability all positions at an angle  $\omega$  to GH and GH in turn can assume with equal probability all positions at an angle  $\gamma$  to FG. Then the mean of  $\mathbf{l}_3$  for each position of  $\mathbf{l}_2$  has a magnitude  $l \cos \omega \cos \gamma$  in the direction FG and since FG is inclined to  $\mathbf{l}_2$  at a constant angle,  $\theta$ , the scalar product of  $\mathbf{l}_2$  and  $\mathbf{l}_3$  is  $l^2 \cos \omega \cos \gamma \cos \theta$ . Similarly for each position of  $\mathbf{l}_1$ , FG can assume with equal probability all positions at an angle  $(\theta - \omega)$  to DE which in turn can assume with equal probability all positions at an angle  $\gamma$  to CDO. The scalar product of  $\mathbf{l}_1$  and  $\mathbf{l}_3$  is therefore  $l^2 \cos \omega \cos^2 \gamma \cos (\theta - \omega) \cos \theta$  and by a like procedure that of  $\mathbf{l}_1$  and  $\mathbf{l}_4$  is  $l^2 \cos \omega \cos^3 \gamma \cos^2 (\theta - \omega) \cos \theta$  and so on. Hence

$$r^2 = (\mathbf{l}_1 + \mathbf{l}_2 + \dots + \mathbf{l}_n)^2$$

and

$$\begin{aligned} \bar{r}^2 &= nl^2 + 2l^2 \cos \omega \cos \gamma \cos \theta [(n-1) + (n-2) \cos \gamma \cos (\theta - \omega) \\ &+ (n-3) \cos^2 \gamma \cos^2 (\theta - \omega) + \dots + \cos^{(n-2)} \gamma \cos^{(n-2)} (\theta - \omega)] \\ &= nl^2 \left\{ 1 + \frac{2 \cos \omega \cos \gamma \cos \theta [1 - \cos^{(n-1)} \gamma \cos^{(n-1)} (\theta - \omega)]}{1 - \cos \gamma \cos (\theta - \omega)} \right\} \\ &- \frac{2l^2 \cos \omega \cos \gamma \cos \theta}{[1 - \cos \gamma \cos (\theta - \omega)]^2} \left\{ 1 - \cos^{(n-1)} \gamma \cos^{(n-1)} (\theta - \omega) \right. \\ &\quad \left. + n (\cos^n \gamma \cos^n (\theta - \omega)) \right\} \end{aligned} \quad (3)$$

The bond lengths and bond angles along the polypeptide chain vary with the amino-acid residues comprising the chain; mean values must therefore be used. Corey and Pauling<sup>4</sup> give the following mean dimensions for the planar amide group: C<sub>α</sub>-C, 1.53 Å.; C-N, 1.32 Å.; N-C, 1.47 Å.; bond angles at C<sub>α</sub>, 110°; at C, 114°; and at N, 123°. Bamford, Elliott, and Hanby<sup>5</sup> suggest that 121° may be a better value for the bond angle at N, but as this is not certain the values of Corey and Pauling have been adhered to. The corresponding values of *l*, *θ*, *γ*, and *ω* are then 3.80 Å., 22°17', 70°, and 13°17', respectively. Substituting the appropriate values in eq. (3) and neglecting terms involving high powers of *cos γ* we obtain

$$\bar{r}^2 = 27.9n - 20.3 \quad (4)$$

The approximations involved are negligible for values of *n* greater than 3. A similar expression is obtained by Wall's<sup>2</sup> procedure.

The *cis* form of the amide group can be treated in a similar manner. The general expression obtained differs from that in eq. (3) only in the substitution of (*θ* + *ω*) for (*θ* - *ω*); different numerical values for *l* (2.75 Å.), *θ* (62°33'), and *ω* (60°27') must also be used. The expression for  $\bar{r}^2$  then becomes

$$\bar{r}^2 = 8.6n - 0.8$$

If on the other hand, the planar character of the amide group were destroyed, each bond could rotate freely around adjacent bonds. The general expression would then be

$$\begin{aligned} \bar{r}^2 &= n(a^2 + b^2 + c^2) + 2n(a^2 \cos \alpha \cos \beta \cos \gamma \\ &\quad + b^2 \cos \alpha \cos \beta \cos \gamma + c^2 \cos \alpha \cos \beta \cos \gamma + ab \cos \alpha \\ &\quad + bc \cos \beta + ac \cos \gamma + ab \cos \beta \cos \gamma + bc \cos \alpha \cos \gamma \\ &\quad + ac \cos \alpha \cos \beta) / (1 - \cos \alpha \cos \beta \cos \gamma) - 2(a^2 \cos \alpha \cos \beta \cos \gamma \\ &\quad + b^2 \cos \alpha \cos \beta \cos \gamma + c^2 \cos \alpha \cos \beta \cos \gamma + ab \cos^2 \alpha \cos \beta \cos \gamma \\ &\quad + bc \cos \alpha \cos^2 \beta \cos \gamma + ac \cos^2 \alpha \cos^2 \beta \cos \gamma + ab \cos \beta \cos \gamma \\ &\quad + bc \cos \alpha \cos \gamma + ac \cos \gamma) / (1 - \cos \alpha \cos \beta \cos \gamma)^2 \end{aligned}$$

where  $a$ ,  $b$ , and  $c$  are the lengths of the three bonds constituting the amide group and  $\alpha$ ,  $\beta$ , and  $\gamma$  are the corresponding angles formed with the adjacent bonds when the bonds are produced. High powers of  $\cos \alpha$ ,  $\cos \beta$ , and  $\cos \gamma$  have been neglected in this expression. On making the appropriate substitutions we have

$$\overline{r^2} = 15.5n - 4.8$$

The *cis* and nonplanar forms of polypeptide chains in particular would be expected to behave in a nonideal fashion because many possible positions of the chains would not permit free rotation round adjacent bonds. The values of  $\theta$ ,  $\gamma$ , and  $\omega$  are such that little error is incurred by the approximation used by Haly and Feughelman<sup>3</sup> for the *trans* form. However a large error would be incurred if the *cis* form were treated in a similar manner.

#### Application to Fibrous Proteins with the $\alpha$ -Helical Conformation

If a fibrous protein consisting of aligned  $\alpha$ -helices, crosslinked at intervals, is converted to an elastomer, the root-mean-square lengths of the sections of polypeptide chain between crosslinkages are related to the number of residues between cross-linkages by eq. (4) if the chains are not restricted in other ways. Unless extensive solvation took place, the chains would cohere due to interatomic attractive forces, temporary hydrogen bonds, and the so-called "hydrophobic bonds." This would prevent randomization of the directions of the vectors joining adjacent crosslinkages along each chain, i.e., holes would not occur in large numbers.

The presence of crosslinkages imposes a further restriction on both lateral and longitudinal movement of the ends of the chain sections. Since each crosslinkage is connected to four sections of polypeptide chain any deviation of one of these chains from its mean length involves similar deviations of the other three chains from their respective mean lengths. The probability of such a deviation is the product of the probabilities for the four chains, and consequently, although the mean length of the chain sections is unaltered, the deviation from the mean would be greatly decreased by incorporation of the chain sections in a crosslinked structure. Similarly the crosslinkages tend to move at right angles to the fiber axis in all directions with equal probability. This can occur only if the random lateral movements of the atoms and random changes in length of the four sections of chain are simultaneously favorable. In general, therefore the ends of the chain sections will not deviate very greatly from their mean positions. We may therefore equate the fractional decrease in length of a polypeptide chain when it changes from the  $\alpha$ -helical conformation to a random coil with the fractional decrease in the length of the protein fiber providing suitable corrections are made for nonalignment of chain sections due to changes in the diameter of the fiber during contraction.

Flory,<sup>6</sup> in dealing with the similar problems relating to synthetic polymers, has considered the total swelling of the fiber and made suitable corrections. However, many fibrous proteins have a complex histological

structure, both cellular and subcellular. Consequently although isolated cells contract in much the same manner as the original fiber, swelling measurements on the fibers can give values which have no relation to the state of those portions of the fiber which originally occurred as aligned crystalline material. Under these circumstances the best correction that can be made is to assume that the volume of the crystalline portions of the fiber does not change during contraction and to correct for the disalignment of the ends of the sections of chain which results from the consequent increase in diameter of the fiber during contraction. Furthermore if, in the original fiber, the  $\alpha$ -helices are aligned parallel to the fiber axis the crosslinkages, though sufficiently long to connect the perimeters of the adjacent helices, will not span the distance between the centers of the helices. Consequently, when a highly crosslinked fiber becomes elastomeric, the lines joining the ends of the sections of polypeptide chain between crosslinkages will be inclined to the axis of the fiber. To permit this the contraction of the fiber must be greater than that of the individual sections of polypeptide chain.

If the  $\alpha$ -carbon atoms and an  $\alpha$ -helix are projected on a cross section at right angles to the axis of the helix, the radius of the circle inscribing these points is approximately 2.35 Å. If the  $\alpha$ -carbon atoms bearing crosslinkages are distributed around this circle in a random fashion, and the chord subtending an angle  $\theta$  at the center represents the displacement of one end of a section of polypeptide chain, the mean value of this displacement will be

$$\int_0^\pi \frac{(2 \times 2.35^2 - 2 \times 2.35^2 \cos \theta)^{1/2}}{\pi} d\theta = 3.0 \text{ Å.}$$

In addition, if the volume does not change, the diameter of the fibrillar unit in the fiber will increase by a factor  $(l_0/l)^{1/2}$ , where  $l_0$  is the original length and  $l$  the contracted length of the fiber; if the distance between the centers of adjacent helices in the original fibers is 10 Å., one end of each polypeptide will be displaced by a mean distance of  $10[(l_0/l) - 1]$  Å. because of the lateral swelling. Taking both effects into account, the mean lateral displacement of one end of each chain section will be approximately  $3 + 10 [(l_0/l)^{1/2} - 1]$  Å. The projection on the fiber axis of the line joining the ends of the chain section will then have a mean length of  $\{c^2(27.9n - 20.3) - [10(l_0/l)^{1/2} - 7]^2\}^{1/2}$  Å., where  $c = \overline{R_n}/(\overline{R_n^2})^{1/2}$ . The meridional repeat distance per amino acid residue for an  $\alpha$ -helical structure as determined by x-ray diffraction is normally close to 1.5 Å.<sup>4</sup> We may therefore write

$$l/l_0 = \{C^2(27.9n - 20.3) - [10(l_0/l)^{1/2} - 7]^2\}^{1/2}/1.5n \quad (5)$$

For a random chain in which there is no restriction on bond angle the relationship between the mean and the root mean square is:<sup>6</sup>

$$\overline{R_n} = (8\overline{R_n^2}/3\pi)^{1/2} = 0.92 (\overline{R_n^2})^{1/2}$$

Kuhn<sup>7</sup> has shown that a similar relationship holds for a chain molecule with fixed bond angles provided that the chains are sufficiently long to give a Gaussian distribution of chain lengths. For short chains  $C$  would be larger or smaller than 0.92 according as the mean deviation from the mean was greater or less than that for a Gaussian distribution. Substitution in eq. (5) gives

$$l/l_0 = \{23.7n - 17.3 - [10(l_0/l)^{1/2} - 7]^2\}^{1/2}/1.5n \quad (6)$$

The curve in Figure 3 relates  $l/l_0$  to  $n$ . It is noteworthy that when the value of  $n$  for an  $\alpha$ -helical structure falls to a value of about 9 the conversion of the aligned helical structure to an elastomer would cause practically no

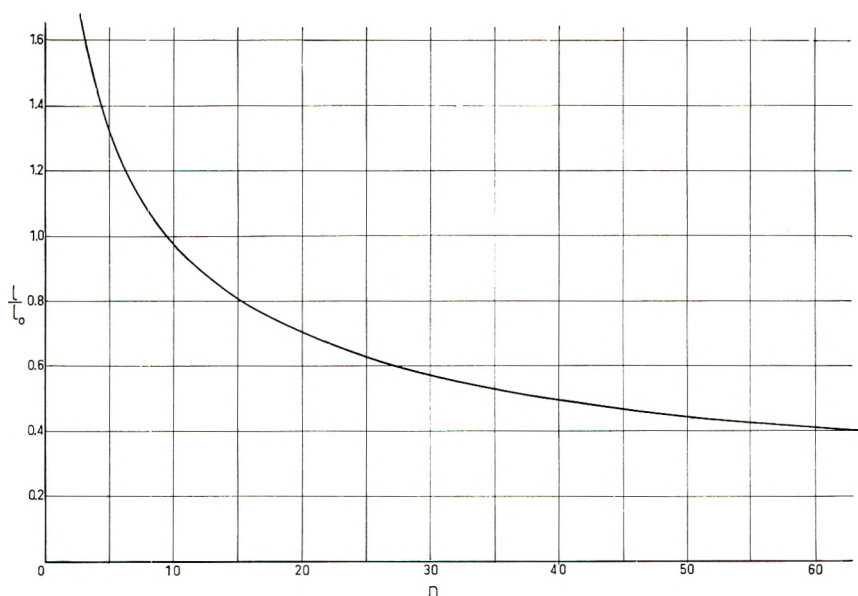


Fig. 3. Relationship between fractional length of a contracted polypeptide fiber and the number of residues between crosslinkages according to eq. (6).

change in length of the fiber. The expression in eq. (6) is only valid for structures in which the crosslinkages are evenly distributed along the chains. If the distribution were random an appropriate correction would be necessary.

The expression takes no account of residual attractive forces between the chains, of additional swelling due to solvation of the protein or of decreased contraction due to steric effects of the side-chain groups or of the main chains themselves. In due course an ideal solvent may be found in which these effects cancel each other out. Alternatively, the expression should prove useful for comparing extents of crosslinking in protein fibers. The expression has been applied to the supercontraction of keratin fibers.<sup>8</sup>

## References

1. Eyring, H., *Phys. Rev.*, **39**, 746 (1932).
2. Wall, F. T., *J. Chem. Phys.*, **11**, 67 (1943).
3. Haly, A. R., and M. Feughelman, *Textile Res. J.*, **27**, 919 (1957).
4. Corey, R. B., and L. Pauling, *Proc. Intern. Wool Textile Res. Conf. Australia*, **1955B**, 249 (1956).
5. Bamford, C. H., A. Elliott, and W. E. Hanby, *Synthetic Polypeptides*, Academic Press, New York, 1956, p. 107.
6. Flory, P., *J. Am. Chem. Soc.*, **78**, 5222 (1956).
7. Kuhn, W., *Kolloid-Z.*, **68**, 2 (1934).
8. Crewther, W. G., *J. Polymer Sci.*, **A2**, 131 (1964).

## Résumé

Une application de la théorie de mécanique statistique donne l'expression  $\bar{r}^2 = 27.9n - 20.3$  reliant  $\bar{r}^2$  le carré moyen de la distance entre extrémités d'une chaîne statistique de polypeptide dans la forme "trans" et  $n$  le nombre de groupes résiduaux amino-acides dans la chaîne. Les expressions correspondantes pour les formes "cis" et non-planaires sont respectivement  $\bar{r}^2 = 8.6n - 0.8$  et  $\bar{r}^2 = 15.5n - 4.8$ . La première de ces équations a été employée pour obtenir une expression de la diminution partielle de longueur de la structure  $\alpha$ -hélicoïdale pontée lorsqu'elle est transformée en une pelote statistique. Les hypothèses faites sont d'une part que les pontages subissent un léger déplacement latéral et d'autre part que le volume reste constant. L'expression ainsi obtenue s'exprime par:  $l/l_0 = \{23.7n - 17.3 - [10\sqrt{l_0/l} - 7]^2\}^{1/2}/1.5n$  où  $l$  est la longueur supercontractée de la fibre de polypeptide et  $l_0$  est sa longueur initiale et  $n$  est le nombre de groupes amino-acides restant entre les pontages.

## Zusammenfassung

Anwendung der statistisch-mechanischen Theorie liefert die Beziehung  $\bar{r}^2 = 27,9n - 20,3$  zwischen dem mittleren End-zu-End-Abstandsquadrat,  $\bar{r}^2$ , einer statistischen Polypeptidkette in der trans-Form und  $n$ , der Zahl der Aminosäurereste in der Kette. Die entsprechenden Ausdrücke für die cis- und nicht-ebenen Formen sind  $\bar{r}^2 = 8,6n - 0,8$  bzw.  $\bar{r}^2 = 15,5n - 4,8$ . Die erste dieser Gleichungen wurde zur Gewinnung eines Ausdruckes für die relative Längenabnahme einer vernetzten, ausgerichteten  $\alpha$ -Helixstruktur bei der Umwandlung in die Form eines statistischen Knäuels verwendet. Dabei wird die Annahme gemacht, dass die Vernetzungsstellen nur eine geringe seitliche Verschiebung erfahren und dass das Volumen konstant bleibt. Es wird der Ausdruck  $l/l_0 = \{23,7n - 17,3 - [10\sqrt{l_0/l} - 7]^2\}^{1/2}/1,5n$  erhalten, wo  $l$  die Länge der superkontrahierten Polypeptidfaser,  $l_0$  die ursprüngliche Länge und  $n$  die Anzahl der Aminosäurereste zwischen zwei Vernetzungsstellen ist.

Received October 4, 1962



## Crosslinkages in Wool Fibers and Their Relationship to the Two-Stage Supercontraction of Wool Fibers in Solutions of LiBr

W. G. CREWETHER, *Division of Protein Chemistry, C.S.I.R.O., Wool Research Laboratories, Parkville N2 (Melbourne), Victoria, Australia*

### Synopsis

Rupture of a large proportion of the disulfide bonds of wool by reduction and methylation has no effect on the extent of total supercontraction in solutions of LiBr at 98.5°C. Reduction and methylation of the disulfide bonds increases the extent of the first stage and decreases the extent of the second stage of supercontraction. No two-stage phenomenon is then observed at the normal extent of the first stage of supercontraction. The relationship between the extent of the first stage of supercontraction and the content of residual disulfide bonds is that predicted by the statistical mechanical theory for a structure containing acid-labile crosslinkages at equal intervals of about 35 residues and disulfide crosslinkages at equal intervals of about 20 residues along the  $\alpha$ -helices of the aligned structures. This is compared with the half-cystine content of the low sulfur protein fraction of the wool; approximately 1 residue in 18. Conversion of the disulfide bonds of wool into  $-\text{SCH}_2\text{CH}_2\text{S}-$  crosslinkages causes a decrease in the extent of the second stage and total supercontraction but does not affect the extent of the first stage. The relationship between the extent of total supercontraction, and the content of dithioethylene crosslinkages is almost identical with that observed for the first stage and disulfide content in *S*-methyl wool samples. The disulfide and sulfydryl contents of wool are not altered by supercontraction at pH 6. It is concluded that the first stage of supercontraction of wool fibers in solutions of LiBr is due to the conversion of aligned  $\alpha$ -helices into an elastomeric form, the extent of the first stage being restricted by disulfide and acid-labile crosslinkages. Further contraction occurs during the second stage as a result of sulfydryl-disulfide interchange reactions which eliminate the restrictive influence of the disulfide bonds. The final extent of supercontraction is limited by acid-labile crosslinkages.

### INTRODUCTION

Several model structures have been proposed to account for the two-stage supercontraction of wool fibers in solutions of LiBr, first observed by Haly and Feughelman.<sup>1</sup> This phenomenon, consisting of rapid contraction by an amount characteristic of the fiber followed by a slower second contraction process, occurs with other animal fibers<sup>2</sup> and under different contraction conditions.<sup>3</sup>

Elöd and Zahn<sup>4</sup> have shown that after supercontraction in solutions of phenol, wool has the properties of a rubber, and Haly and Feughelman<sup>1</sup> reported a similar finding for wool supercontracted in solutions of LiBr once the first stage of supercontraction was complete. On the basis of these

data they suggested that the first stage results from the rupture of weak hydrogen bonds between aligned polypeptide chains which then become elastomeric. The second stage was attributed to the rupture of stronger hydrogen bonds permitting further contraction which they believed to be finally limited by disulfide crosslinkages. Haly, Feughelman, and Griffith<sup>5</sup> later suggested that the stronger hydrogen bonds may involve tyrosine residues, but no unequivocal evidence for this could be obtained.<sup>6</sup>

The observation that Corriedale wool fibers supercontract by more than 70% in 4*M* LiBr/1*N* HCl, as compared with about 40% in solutions of LiBr at pH 6, led Crewther and Dowling<sup>3</sup> to suggest that acid-labile bonds, rather than disulfide bonds, are responsible for limiting the extent of supercontraction in neutral solutions of LiBr at 98.5°C. Crewther and Dowling<sup>3</sup> also found that the initial contraction in 6*M* LiI containing 1*N* HCl was followed by elongation of the fiber which subsequently again contracted; this was interpreted in terms of two contractile structures in the fiber. From a comparison of the elastic moduli of wool fibers which had been supercontracted to the end of the first and second stages, respectively, Feughelman and Haly<sup>7</sup> concluded that these structures consist of "zones" of two types alternating along the microfibrils. This "series-zone" model was proposed to replace their earlier model.

Crewther and Dowling<sup>8</sup> have recently reported preliminary data showing that the extent of supercontraction of wool fibers in solutions of LiBr at 98.5°C. is not limited by disulfide crosslinkages in the wool. Two hypotheses were considered to explain this fact: (1) that the contractile structures in wool are not crosslinked by disulfide bonds; (2) that disulfide bonds crosslinking polypeptide chains are broken and re-formed by a chain reaction such as sulfydryl-disulfide interchange.<sup>9,10</sup>

The first of these alternatives was accepted, largely on the basis of the effects of iodination on the supercontraction of *S*-methyl wool. A model for the contractile structures of wool was proposed in which the cystine residues, which appear to be present in all major wool proteins, were grouped in a band of noncontractile material between two contractile zones in the microfibrils having differing thermostabilities in LiBr solutions. The additional data now available regarding iodination and its effects on supercontraction<sup>11,12</sup> make it necessary to reconsider the original two alternatives and critically examine the model. The experiments described are concerned largely with the properties of wool fibers in which the disulfide bonds have been converted to *S*-methyl groups or —SCH<sub>2</sub>CH<sub>2</sub>S— crosslinkages. Some of these results have already been reported in preliminary communications.<sup>8,13</sup>

## MATERIALS AND METHODS

Two samples of Lincoln 36's wool, designated A and B, were used. Wool A was identical with that used by Lindley<sup>14</sup> in his experiments on the elastic properties of modified fibers. Wool B was from a single fleece (No. MW 114). The wool, in each case, was cleaned by extraction three times with

cold light petroleum (b.p. 55–70°C.), once with cold ethanol, and several times with cold distilled water.

LiBr and ethylene dibromide were B.D.H. laboratory reagent, methyl iodide was Merck, pure chemical, other reagents were B.D.H. Analar reagent. Thioglycollic acid was freshly distilled before use. The reduction and alkylation of the disulfide bonds of wool were carried out following the general procedure of Lindley.<sup>14</sup> In experiments with repeated reduction and methylation, 5 g. of wool was gently shaken for 24 hr. at 20°C. with 150 ml. of 0.5*M* thioglycollic acid adjusted to pH 5.0 with NaOH. The wool was washed with 150-ml. aliquots of distilled water, ethanol, and again with water, then shaken under similar conditions with 150 ml., 0.1*M* Na<sub>2</sub>HPO<sub>4</sub> containing 4 ml. of methyl iodide. This process of reduction and alkylation was repeated from one to four times. Wool A was used for these experiments.

In a similar series of experiments with wool B, 1.0-g. samples of wool were gently shaken for 18 hr. at 28°C. with 200-ml. aliquots of thioglycollate at pH 5.0 having concentrations varying from 0.005 to 1.0*M*. The wool was washed thoroughly in 200-ml. aliquots of water, ethanol, and again in water as above, then gently shaken with 1.0 ml. of methyl iodide or ethylene dibromide in 50 ml. 0.1*M* Na<sub>2</sub>HPO<sub>4</sub>. The pH of the solutions fell from about 9.0 to 8.2 during alkylation. With both treatments the wool was washed alternately with ethanol and water six times to remove excess alkylating reagent. For each washing the wool remained in the solvent for about 1 hr. Finally the wool was allowed to stand for 48 hr. in a large volume of distilled water and air-dried.

Disulfide and sulphydryl contents of the reduced and alkylated wools were determined by the methods of Leach.<sup>15</sup> The wool samples were shaken with the MeHgI reagent for 24 hr. at 20°C. in each analysis. In order to ensure that traces of residual alkylating agents were not affecting the analyses, these were repeated after the wool samples had been again washed several times in ethanol and water and redried. The results were unchanged. For a few samples the method of Shinohara<sup>16</sup> was also used for cystine analyses. Single fibers, mounted as for the normal supercontraction experiments and reduced and alkylated in aliquots of the same solutions as those used for the bulk samples, did not change in length. For convenience wool which was reduced and methylated will be referred to as *S*-methyl wool.

Unless otherwise specified, the solutions of LiBr used in supercontraction experiments were freed of Br<sub>2</sub> by the addition of traces of Na<sub>2</sub>S<sub>2</sub>O<sub>3</sub>.<sup>17</sup> The changes in length of mounted wool fibers with time of immersion in the solution of LiBr were followed by the method already described.<sup>3</sup> For the purpose of this investigation the extent of total contraction is defined as the supercontraction in unbuffered 8*M* LiBr at 98.5°C. after the contraction had remained constant for 20 min. The extent of the first stage of supercontraction is arbitrarily defined as the supercontraction after treatment for 18 hr. in unbuffered 8*M* LiBr at 20°C. The rate curves for supercontraction of untreated or reduced and methylated fibers (Fig. 5) show that after

this period the rate of supercontraction is insufficient to cause significant errors.

## RESULTS

### a. Disulfide and Sulfhydryl Contents of Modified Wool

Table I lists the (SS + SH) and SH contents of wool samples reduced in thioglycollate at pH 5 and treated with methyl iodide one to five times.

TABLE I  
Disulfide and Sulfhydryl Contents of Lincoln Wool (A) After Repeated Reduction and Methylation<sup>a</sup>

Sample no.	Number of treatments	(SS + SH), $\mu\text{mole/g.}$	(SH), $\mu\text{mole/g.}$	(SS), $\mu\text{mole/g.}$	Extent of supercontraction, %	
					First stage <sup>b</sup>	Total <sup>b</sup>
1	0	443	24	419	20.4	42.2
2	1	148	16	132	33.0	42.0
3	2	94	21	73	38.1	42.4
4	3	69	18	51	40.9	41.9
5	5	39	11	28	41.4	41.9

<sup>a</sup> Determinations by the method of Leach.<sup>15</sup>

<sup>b</sup> Mean values for six fibers.

TABLE II  
Disulfide, Sulfhydryl, and Dithioethylene Contents of Lincoln Wool (B) after Reduction and Alkylation under Various Conditions<sup>a</sup>

Sample no.	Thioglycollate concn. (pH 5), <i>M</i>	Alkylating agent	(SS + SH), $\mu\text{mole/g.}$	(SH), $\mu\text{mole/g.}$	(SS), $\mu\text{mole/g.}$	(SCH <sub>2</sub> CH <sub>2</sub> S), $\mu\text{mole/g.}^b$
7	Nil	CH <sub>3</sub> I	404	11	393	—
8	Nil	C <sub>2</sub> H <sub>5</sub> Br <sub>2</sub>	409	18	391	—
9	0.015	CH <sub>3</sub> I	397	19	378	—
10	0.05	CH <sub>3</sub> I	320	21	299	—
11	0.10	CH <sub>3</sub> I	261	18	243	—
12	0.15	CH <sub>3</sub> I	249	21	228	—
13	0.25	CH <sub>3</sub> I	168	14	154	—
14	0.50	CH <sub>3</sub> I	138	22	116	—
15	0.50	CH <sub>3</sub> I	122	13	109	—
16	0.75	CH <sub>3</sub> I	108	24	84	—
17	1.0	CH <sub>3</sub> I	96	33	63	—
18	0.015	C <sub>2</sub> H <sub>5</sub> Br <sub>2</sub>	421	21	400	0
19	0.05	C <sub>2</sub> H <sub>5</sub> Br <sub>2</sub>	390	32	358	25
20	0.15	C <sub>2</sub> H <sub>5</sub> Br <sub>2</sub>	367	45	322	55
21	0.25	C <sub>2</sub> H <sub>5</sub> Br <sub>2</sub>	307	25	285	105
22	0.50	C <sub>2</sub> H <sub>5</sub> Br <sub>2</sub>	208	45	163	214
23	0.50	C <sub>2</sub> H <sub>5</sub> Br <sub>2</sub>	232	30	202	182
24	0.75	C <sub>2</sub> H <sub>5</sub> Br <sub>2</sub>	204	32	172	211
25	1.0	C <sub>2</sub> H <sub>5</sub> Br <sub>2</sub>	192	44	148	229

<sup>a</sup> Mean values of three determinations by the method of Leach.<sup>15</sup>

<sup>b</sup> By difference.

Table II reports (SS + SH) and SH contents together with the derived values for SS contents in the series of wool samples treated with various concentrations of thioglycollate at pH 5 and subsequently reacted with methyl iodide or ethylene dibromide. With fibers alkylated with the latter reagent the content of  $-\text{SCH}_2\text{CH}_2\text{S}-$  crosslinkages was assumed to be  $[\text{SS} + \text{SH}]_0 - [\text{SS} + \text{SH}]_F + \frac{1}{2} ([\text{SH}]_F - [\text{SH}]_0)$  where the subscripts 0 and F refer to the original and final values, respectively. The elimination of air bubbles and dissolved oxygen affects the extent of reduction to a considerable extent and is probably the chief cause of variations between otherwise identical treatments in samples 14 and 15, 22 and 23.

Disulfide and sulfhydryl determinations were also carried out on samples of Corriedale 56's wool before and after supercontraction for 15 min. at 98.5°C. in 6*M* LiBr, 0.1*M* sodium succinate at pH 6.0 (Table III).

TABLE III  
Effect of Supercontraction on the Sulfhydryl and Disulfide Contents of Wool Fibers\*

Wool sample	Sulfhydryl content, μmole/g.	(SS + SH) content, μmole/g.	
		Shinohara <sup>16</sup>	Leach <sup>15</sup>
Untreated	24.4	483	483
Supercontracted	21.8	475	486

\* Corriedale 56's wool supercontracted at 98.5°C. for 14 min. in 6*M* LiBr at pH 6.0. The values are the means for two determinations.

### b. Preliminary Test of the Earlier Model

If the suggestion<sup>8</sup> that wool contains two disulfide-free contractile units were correct, the rupture of disulfide bonds should not affect greatly the relative rates and extents of the two stages of supercontraction. If, on the other hand, sulfhydryl-disulfide interchange is involved, major changes would result from this modification of the wool.

Untreated fibers (A) and *S*-methyl wool fibers (sample 2, Table I) were allowed to supercontract at 20°C. in a series of solutions of LiBr having concentrations ranging from 2.66 to 8*M*. The extent of contraction of each fiber was determined as a function of time of contraction over a total period of three days. In each solution most of the contraction occurred in the first few hours, and by the end of the three-day period the rate of contraction was negligible. Figure 1 shows that the change in slope which occurs near 20% contraction with untreated fibers is completely eliminated by reduction and methylation. With *S*-methyl wool no. 2 a similar change in slope occurs at about 32% contraction.

### c. Effect of Reduction and Methylation on the Extent of First Stage and Total Supercontraction

Table I lists the disulfide content, the extent of the first stage, and the extent of total supercontraction for fibers which had been reduced and

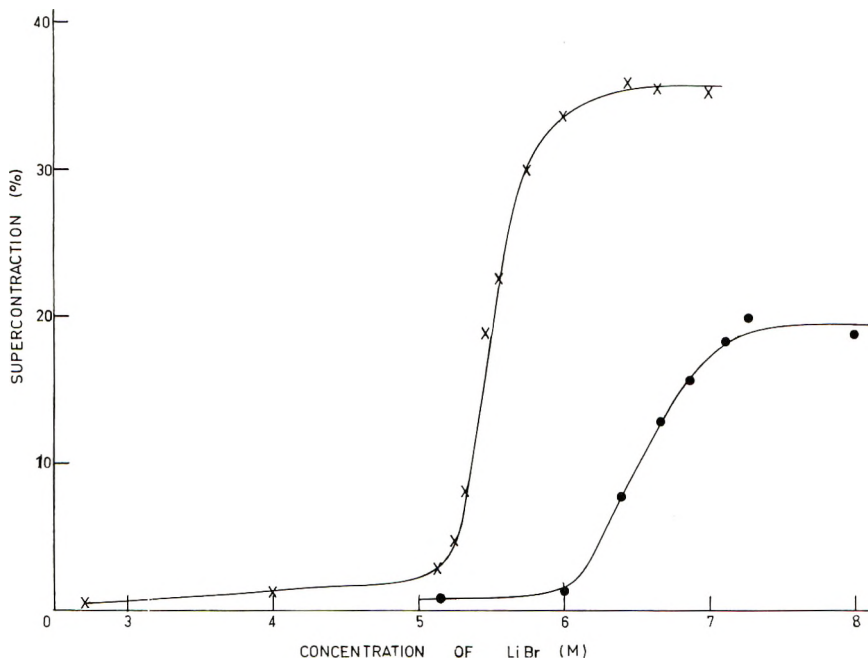


Fig. 1. Relationship between extent of supercontraction of Lincoln wool (A) after 3 days at 20°C. and concentration of LiBr: (●) untreated fibers; (×) reduced and methylated fibers (no. 2).

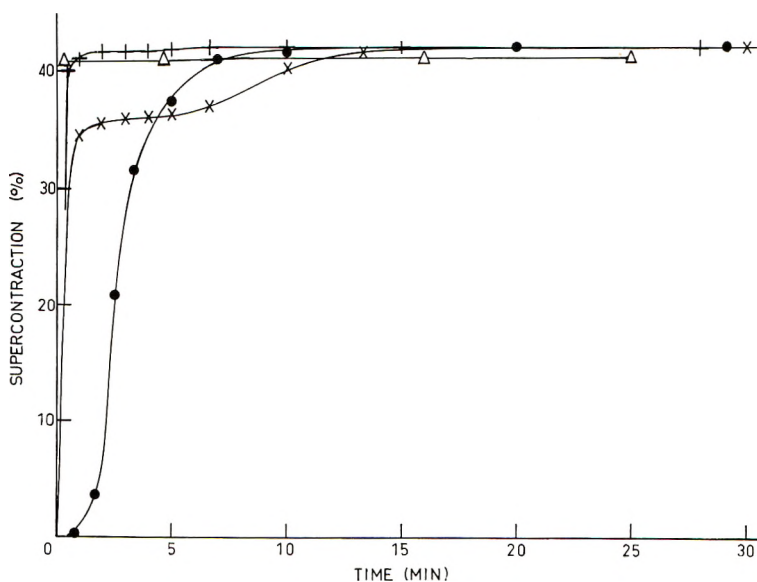


Fig. 2. Effects of repeated reduction and methylation on the extent of supercontraction of wool fibers (A) in 6M LiBr at pH 6.1, 98.5°C.: (●) untreated fibers; (×) fibers reduced and methylated once (no. 2); (+) fibers reduced and methylated three times (no. 4); (Δ) fibers reduced and methylated five times (no. 5).

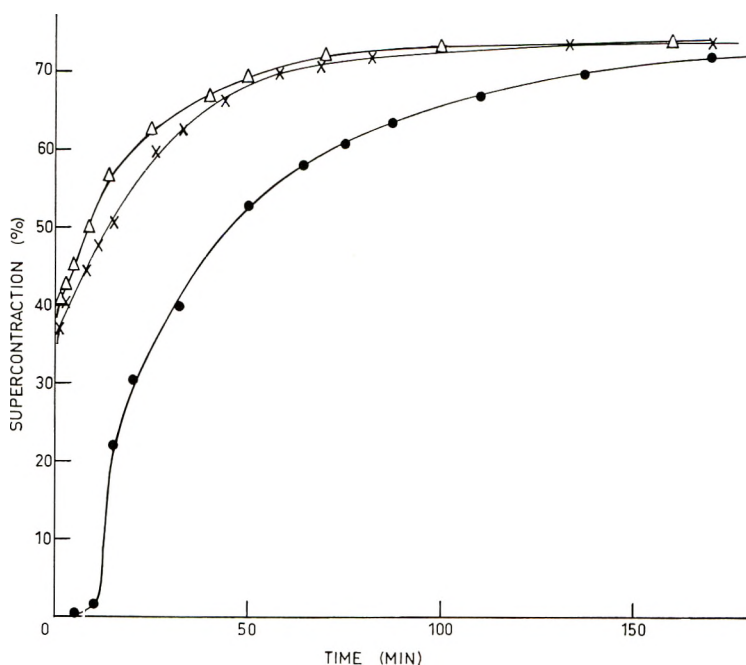


Fig. 3. Effects of repeated reduction and methylation on the extent of supercontraction of wool fibers (A) in 4M LiBr/1N HCl at 98.5°C.: (●) untreated fibers; (×) fibers reduced and methylated once (no. 2); (Δ) fibres reduced and methylated three times (no. 4).

methylated up to five times. Figures 2 and 3 show the effects of multiple reduction and methylation treatments on the rate curves for supercontraction in 6M LiBr at pH 6.1 and in 4M LiBr/1N HCl, both at 98.5°C. Although the rate of supercontraction increased progressively as disulfide bonds were converted to *S*-methyl groups (Figs. 2 and 3), there was no change in the extent of complete contraction even with 94% of the disulfide bonds broken. Once complete contraction was achieved at pH 6, the fibers remained at constant length for at least 30 min. The results were less definite in the acid solutions, as the slow contraction under these conditions made it difficult to decide whether or not contraction had ceased, but it is apparent that no large change occurred (Fig. 3). On the other hand, the extent of the first stage of supercontraction was increased by rupturing the disulfide bonds (Table I). This effect is reflected in the appearance of shelves in the rate curves for supercontraction of reduced and methylated fibers (Fig. 2) at extents of contraction much greater than is usual for untreated fibers.

Wool samples which were methylated after reduction with various concentrations of thioglycollate at pH 5 provided the data in Figure 4. This figure includes data for a wool sample having a disulfide content of 28  $\mu$  mole/g., which was reduced with 4M thioglycollate and methylated, then again reduced with 4M mercaptoethanol and again methylated. Each

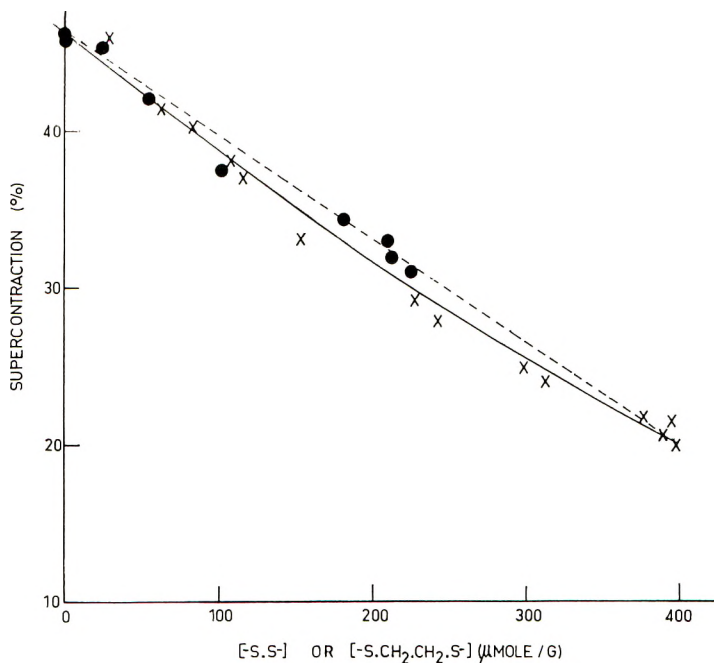


Fig. 4. Relationships between (X) extent of first stage of supercontraction and residual disulfide content of reduced and methylated wool fibers and (●) between total supercontraction and content of ( $-\text{SCH}_2\text{CH}_2\text{S}-$ ) crosslinkages. The theoretical relationship is shown by the entire line. The points refer to wool (B).

point on the curve represents mean values for three determinations of disulfide content and for 12 determinations of extent of the first stage. In order to determine the position of the extremities of the curve with considerable certainty, eight determinations of the disulfide content of untreated fibers were carried out, and 20 measurements were made of the extent of total and first stage supercontraction of untreated fibers. The broken straight line shown in Figure 4 connects the mean values representing these data. Data published in a preliminary communication<sup>10</sup> were for single disulfide determinations and six determinations of the extent of first stage for each sample.

#### d. Relationship Between Content of $-\text{SCH}_2\text{CH}_2\text{S}-$ Crosslinkages and the Extent of First Stage and Total Supercontraction

Rate curves for the supercontraction at 20°C. of fibers which had been reduced and crosslinked with ethylene dibromide (sample 22, Fig. 5) show that the extent of the first stage of supercontraction was not affected by this treatment. In addition the second stage of supercontraction at 98.5°C. was retarded and the extent of total supercontraction was decreased. This is illustrated in Figure 4. There is a striking coincidence between the curve relating first stage of supercontraction and disulfide content of *S*-methyl wool fibers and that relating  $-\text{SCH}_2\text{CH}_2\text{S}-$  con-



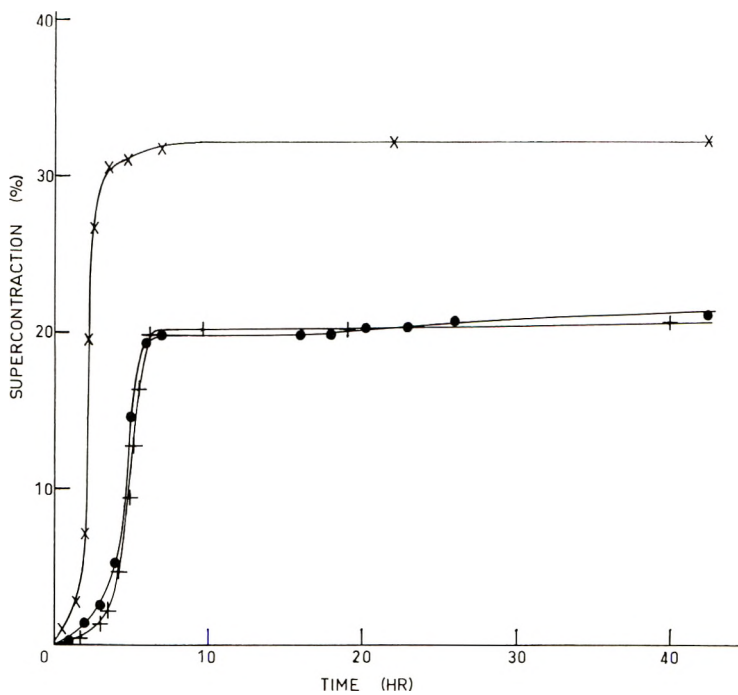


Fig. 5. Rate curves for the supercontraction in unbuffered 8M LiBr at 20°C. of (●) untreated fibers of wool (B); (×) reduced and methylated fibers, sample no. 13; and (+) reduced and crosslinked fibers, sample no. 22.

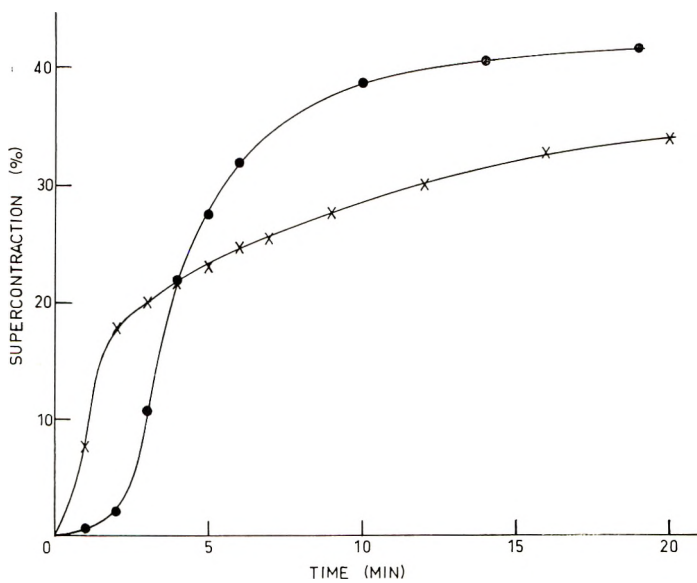


Fig. 6. Effect of treating wool fibers (B) with methyl iodide in 0.1M  $\text{Na}_2\text{HPO}_4$  on the rate of supercontraction in 6M LiBr at pH 6.4: (●) untreated; (×) treated.

tent and the extent of total contraction for the crosslinked fibers. Repeated reduction in 1.0*M* thioglycollate at pH 5 followed by treatment with ethylene dibromide did not increase the content of —SCH<sub>2</sub>CH<sub>2</sub>S— crosslinkages. As a result, no data are at present available concerning the behavior of fibers in which more than 60% of the disulfide bonds have been replaced by more stable crosslinkages.

### e. Effects of Alkylation Without Previous Reduction

Table II shows that treatment of wool fibers with methyl iodide or ethylene dibromide without previous reduction had little effect on the disulfide content but caused a small decrease in the sulfydryl content. When those fibers were allowed to supercontract in 8*M* LiBr at 98.5 or at 20°C. the extents of the first stage and complete contraction were unaltered by the alkylating treatment. However, there was some retardation of the second stage of supercontraction at 98.5°C. in 4*M* LiBr at pH 8 or in 6*M* LiBr at pH 6.4 (Fig. 6).

## DISCUSSION

### a. General Considerations

The importance of disulfide bonds in the supercontraction of keratinous fibers has already received considerable attention. Observations that hot solutions of reagents such as NaHSO<sub>3</sub>,<sup>18</sup> Na<sub>2</sub>S,<sup>19</sup> Na<sub>2</sub>S<sub>2</sub>O<sub>4</sub>,<sup>20</sup> and peracetic acid<sup>21</sup> cause extensive supercontraction gave rise to the view that disulfide bonds must be broken before supercontraction can take place. However, observations by Elöd and Zahn<sup>22,23</sup> and Alexander<sup>21</sup> that solutions of formamide, phenols, or LiBr, can bring about supercontraction of keratin fibers without change in the disulfide content led to the view that reagents which directly or indirectly rupture hydrogen bonds may cause supercontraction without rupturing disulfide bonds. This was further supported by Beaugard, Brown, and Harris,<sup>24</sup> who reported that reduction of wool and simultaneous crosslinking with ethylene dibromide did not affect the extent of supercontraction in LiBr solutions whereas supercontraction in boiling solutions of bisulfite was almost completely prevented by this treatment.

Figure 4 appears to be directly contradictory to the results reported by Beaugard, Brown, and Harris.<sup>24</sup> However, the solutions of LiBr used by the earlier workers were apparently not freed from Br<sub>2</sub>. Consequently contraction in LiBr solutions (pH about 5) ceased at the end of the first stage of supercontraction<sup>17,10</sup> when the fibers had shortened by some 13%. The first stage is unaltered in extent by reduction and crosslinking (Fig. 5), and it is not retarded by this treatment if concentrated solutions of LiBr are used. The conclusions of Beaugard, Brown, and Harris were therefore correct if applied only to the first stage of supercontraction; they do not apply to complete contraction in solutions of LiBr.

For the same reason, Alexander's<sup>21</sup> work with supercontraction in solu-

tions of LiBr, including the effect of supercontraction on the disulfide content, was confined to the first stage. Table III shows that if disulfide bonds are ruptured during complete supercontraction in solutions of LiBr they either re-form, or the number broken is an insignificant fraction of the total disulfide.

On the other hand, the observation<sup>8</sup> that reduction and methylation of a major fraction of the disulfide bonds does not affect the extent of total supercontraction (Fig. 2) demonstrates that disulfide bonds are not responsible for limiting total supercontraction;\* however, acid-labile bonds<sup>3</sup> impose such a limitation (cf. Figs. 2 and 3).

Roberts, Mandelkern, and Flory<sup>28</sup> have shown that the length of synthetic polymer fibers in the elastomeric state is approximately proportional to  $n^{1/2}$ , where  $n$  is the number of freely rotating links in the polymer chain between crosslinkages inserted while the polymer fiber is fully extended. Hence, since supercontracted wool is elastomeric,<sup>1</sup> and the disulfide bonds do not limit contraction though remaining unchanged in number, either the portions of the fiber responsible for supercontraction do not contain disulfide bonds or disulfide bonds in the contractile structures are broken and re-formed during supercontraction.<sup>8</sup>

The results of Figure 1 show that the difference in rate of contraction during the first and second stages of supercontraction is not due to differences in thermostability of two disulfide-free contractile units in the fiber. Furthermore, the increase in extent of the first stage of supercontraction with decrease in disulfide content of the fibers, and the decrease in total supercontraction when  $-\text{SCH}_2\text{CH}_2\text{S}-$  bonds replace disulfide bonds (Fig. 2 and Table IV) provide convincing evidence that disulfide bonds occur in the contractile portions of the fiber and limit the first stage of supercontraction.

On the other hand, evidence is accumulating that the rate of supercontraction, particularly in the second stage, is limited by an interchange reaction between sulfhydryl and disulfide groups. Burley<sup>9</sup> has shown that reaction of the sulfhydryl groups of wool with *N*-ethylmaleimide decreases the rate of supercontraction in solutions of phenol, and Crewther and Dowling<sup>10</sup> have made a similar observation for supercontraction in solu-

\* This general conclusion can be drawn only if two requirements are satisfied. (1) Sufficient disulfide bonds must be ruptured to ensure that disulfide bonds in the aligned structures of the fiber have been broken. In the present experiments up to 94% of the disulfide bonds of wool were broken (Table I). (2) Under conditions known to give total contraction of untreated wool fibers (SM LiBr at temperatures near 100°C.) the modified fibers must contract to a length which remains constant for a considerable period of time. No conclusion can be drawn if solution of protein within the fiber leads to elongation immediately following contraction, since the maximum extent of supercontraction is then determined by the relative rates of two opposing reactions.<sup>3,14,26</sup> The reduced and methylated fibers used in these experiments satisfy both requirements (Fig. 2). Reduced fibers,<sup>8</sup> fibers oxidized with peracetic acid,<sup>11</sup> or reduced and carboxymethylated fibers, which elongate rapidly immediately after contraction at 98.5°C., are unsuitable. This may reflect differences in the solubilities of the corresponding protein derivatives.<sup>26,27</sup>

TABLE IV  
Qualitative Effects of Reduction and Alkylation on the Supercontraction of Lincoln Wool Fibers

Treatment	Effects on extent of supercontraction		
	First stage	Complete	Second stage
Reduction and methylation	Increased	Unchanged	Decreased
Reduction and crosslinking	Unchanged	Decreased	Decreased

tions of LiBr. Retardation of the second stage of supercontraction by free Br<sub>2</sub> in the LiBr,<sup>10</sup> or by iodination,<sup>5,11</sup> nitration,<sup>29</sup> or treatment with dilute peracetic acid<sup>11</sup> find a ready explanation in terms of the interchange reaction.

In addition, the present paper shows that methylation of sulfhydryl groups of wool causes a retardation of the second stage of supercontraction (Fig. 6) and that methylation following reduction also emphasizes the two-stage effect provided there is a net decrease in sulfhydryl content as a result of the treatment (Fig. 2). The conversion of disulfide bonds to —SCH<sub>2</sub>—CH<sub>2</sub>S— linkages also retards the second stage of supercontraction<sup>30</sup> as would be expected if sulfhydryl–disulfide interchange is the rate-limiting process in this stage. There can be no reasonable doubt, therefore, that the second stage of supercontraction at pH values near neutrality is the result of an interchange reaction between sulfhydryl and disulfide groups.

Figure 4 is remarkable for the close correspondence between the results relating disulfide content and first stage for the reduced and methylated fibers and those relating dithioethylene crosslinkages and total contraction in the crosslinked fibers. It would be extraordinary if this were merely coincidence. These results would be predicted from the conclusions arrived at above only if the disulfide bonds in the aligned structures of the fibers were reduced by approximately the same fractional amount as those in the non-aligned structures. Also, it would be necessary for the ethylene dibromide to act almost quantitatively as a bifunctional reagent rather than as a monofunctional reagent. Gillespie and Springell<sup>31</sup> have, in fact, shown that the fractional reduction of disulfide bonds in the low sulfur proteins of wool approximates that in the high sulfur proteins.

### b. Model for the Aligned Structures of Wool

From the foregoing discussion it is obvious that the previous model proposed by Crewther and Dowling<sup>8</sup> for the aligned structures of wool was incorrect. The model proposed for the matrix of the fiber may still be essentially correct. It is now possible to propose a much simpler model which accounts for the available data. This model consists of polypeptide chains in the form of  $\alpha$ -helices, in parallel or near-parallel alignment, and crosslinked at intervals with disulfide and acid-labile bonds. Evidence

is presented elsewhere that these acid-labile bonds are covalent.<sup>30</sup> During the first stage of supercontraction this aligned structure is converted to an elastomer, the extent of contraction being limited by the covalent crosslinkages (disulfide and acid-labile). The second stage of supercontraction consists in further randomization of the polypeptide chains facilitated by interchange reactions between the disulfide crosslinkages and groups such as —SH, —S<sup>-</sup>, —S<sup>+</sup>, or —S<sup>·</sup>, depending on the pH and other conditions. In boiling solutions of LiBr containing HCl more extensive supercontraction occurs as a result of hydrolysis of the acid-labile crosslinkages.

The elastomeric character of the fiber,<sup>1</sup> the disappearance of the x-ray pattern,<sup>32</sup> and the accessibility of the amide hydrogen atoms for exchange with deuterium,<sup>7</sup> once the first stage of supercontraction is complete, are all necessary consequences of the model.

### c. Quantitative Aspects of the Model

Because of the elastomeric properties of supercontracted wool fibers,<sup>1,4</sup> they can be considered in terms of the theories developed for random polymers. From the expression for the mean end-to-end length of a random polypeptide chain eq. (1) is obtained:<sup>33</sup>

$$l/l_0 = \{23.7n - 17.3 - [10(l_0/l)^{1/2} - 7]^2\}^{1/2}/1.5n \quad (1)$$

where  $l_0$  is the original length of the fiber with the aligned proteins in the form of  $\alpha$ -helices,  $l$  is the length of the fiber after supercontraction, and  $n$  is the number of amino-acid residues between crosslinkages.

By substitution of the appropriate values of  $l/l_0$  for the first stage and total supercontraction in eq. (1) (0.794 and 0.530, respectively) we obtain for  $n$  the values 15 and 35, respectively. The calculated value for the number of amino-acid residues between the acid-labile crosslinkages is therefore 35, and the corresponding value for the number of residues between disulfide crosslinkages is 27.

It is not yet certain which of the soluble proteins of wool is derived from the aligned crystalline portions of the fiber, but the evidence strongly favors the low sulfur proteins. Amino-acid analysis of this protein fraction from Lincoln B, gave a value of 1 half-cystine residue in about 18 amino-acid residues,<sup>34</sup> which is in as good agreement with the calculated values as can be expected.

If values of 35 and 27 are taken to be the correct values of  $n$  for the acid-labile and disulfide crosslinkages, respectively, and if we assume that disulfides in all structures are equally reactive with reducing agents and that the crosslinkages are spaced evenly along the chains in all samples, the expected extent of the first stage of supercontraction is related to the residual disulfide content by the unbroken curve in Figure 4, which fits the data more closely than the straight line, also shown. The assumption of even spacing of crosslinkages is certainly unwarranted for the reduced and methylated fibers and probably also for the untreated fibers. For a certain mean value of  $n$ , the extent of supercontraction would be increased

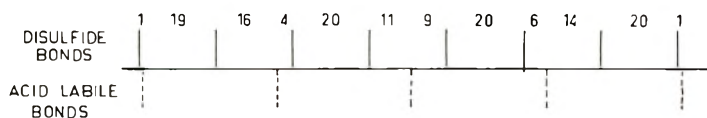


Fig. 7. Diagrammatic arrangement of disulfide and acid-labile bonds along a polypeptide chain. Disulfide bonds are at equal intervals of 20 residues, acid-labile bonds at equal intervals of 35 residues. Numerals indicate the number of residues in sections of free chain.

with increasing irregularity in the arrangement of crosslinkages along the chains. It follows that if the bonds are irregularly arranged in the untreated fiber, the value of  $n$  for the disulfide bonds will be less than 27.

If, for example, the acid-labile bonds repeat along the peptide chains at equal intervals of 35 residues and if the disulfide bonds also repeat at equal intervals, the calculated value for the first stage of supercontraction would most nearly approach the experimental value (20.6%) if there were 1 half-cystine residue in 20 residues arranged as shown in Figure 7. The calculated extent of the first stage for this model is 19.6%. The theoretical curve relating residual disulfide content and extent of the first stage of contraction (Fig. 4) would not be noticeably affected by using this model in place of one having equally spaced crosslinkages.

#### d. Other Models

Although Feughelman and Haly<sup>35</sup> have confirmed some of the data on which Crewther and Dowling<sup>13</sup> based the model discussed in this paper and consider that the model does not conflict with the available information, they prefer a model consisting of zones of two types alternating along the fiber, the "series-zone" model. Originally these zones were considered to exist in the microfibrils;<sup>7</sup> more recently,<sup>35</sup> the matrix has been considered as a possible location. The "X zones" were considered to contract during the first stage of contraction and the "Y zones" during the second stage, the lengths of the two zones being in the same ratio as the extents of contraction in the two stages.

In order to account for the disappearance of the x-ray diffraction pattern<sup>32</sup> and for the complete deuteration of the peptide imino groups<sup>7</sup> once the first stage of supercontraction is complete, Feughelman and Haly<sup>35</sup> postulate the presence of bonds which are stable to concentrated LiBr solutions but which "melt" when the temperature is raised, so giving rise to the second stage of supercontraction. They suggest that in solutions of LiBr at room temperature these bonds hold the Y zones in their original dimensions although the  $\alpha$ -helices are disrupted.

Figures 1, 4, and 5 show that the effects of these "melting bonds" disappear when the disulfide bonds are removed. Hence the most convincing model would be one in which the melting bonds are disulfide groups, the process of melting consisting of the interchange reaction. The effects of

temperature on the rate of the second stage of supercontraction are consistent with this view. With the Lincoln wool used in these experiments almost complete contraction is obtained in 48 hr. at 45°C., and even at 20°C. the rate is measurable (Fig. 5).

If the zones were situated in the microfibrils, sufficient crosslinks would be needed in the Y zones to prevent contraction during the first stage. For the random coil form of the polypeptide to have about the same length as the  $\alpha$ -helical form one crosslink would be required about every 9 residues.<sup>33</sup> A structure in which the disulfide bonds were restricted to the Y zones in which they occurred every ninth residue and with lengths of the two zones in the same ratio as the extents of the two stages of contraction<sup>7</sup> (about 1:1.3) would, in fact, give a mean cystine content consistent with the low sulfur protein fraction of wool. However the other basic requirement for this model to be satisfactory—that the elastic moduli of the X and Y zones in the contracted form are approximately equal<sup>7</sup>—would not apply for two elastomers having such a major difference in extent of crosslinking. The model is therefore untenable.

If, on the other hand the zones were considered to exist in the matrix, a similar problem arises; the Y zones having been set by the interchange reaction in a shorter form would resist extension as effectively as they resisted contraction. Hence a major difference would be expected in the elastic moduli of the two zones. In addition, the following stipulations would be necessary: that the microfibrils are firmly attached to the matrix by bonds which are stable to concentrated LiBr solutions but not disulfide in nature (or that such bonds occur in the Y zones which are then attached to the microfibrils by disulfide bonds); that the considerable cystine content of the low sulfur proteins of the fiber is restricted to noncontractile sections of the microfibrils; that rupture of disulfide bonds by reduction occurs preferentially at the extremities of the Y zones; and that although the Y zones are sufficiently rigid in the LiBr solutions to prevent contraction they are much weaker than the microfibrils when the fibers are immersed in water.<sup>36</sup>

Only the original data on which Crewther and Dowling<sup>3</sup> first postulated the existence of two contractile units appears at first sight to be more easily explained by the "series-zone" model. This observation, that Corriedale fibers heated in 6*M* LiI/1*N* HCl contract, elongate, and again contract, is evidence of two structures only if the first contraction corresponds with that of the first stage of supercontraction. Recent experiments<sup>30</sup> show that the fibers had contracted to an extent greater than the first stage of contraction before elongation intervened under these conditions. The elongation is probably due to osmotic swelling due to solution of protein and consequent imbibition of water. This explanation was proposed previously<sup>3</sup> for elongation to lengths greater than the original following contraction. Haly and Swanepoel<sup>37</sup> have made similar proposals.

It is therefore difficult to reconcile the "series-zone" model with experimental fact, whereas the model presented here is both simple and compatible with experimental data.

## References

1. Haly, A. R., and M. Feughelman, *Textile Res. J.*, **27**, 919 (1957).
2. Haly, A. R., and J. Griffith, *Textile Res. J.*, **28**, 32 (1958).
3. Crewther, W. G., and L. M. Dowling, *Textile Res. J.*, **29**, 541 (1959).
4. Elöd, E., and H. Zahn, *Melliand. Textilber.*, **30**, 17 (1949).
5. Haly, A. R., M. Feughelman, and J. C. Griffith, *Nature*, **180**, 1064 (1957).
6. Haly, A. R., and M. Feughelman, *Textile Res. J.*, **30**, 365 (1960).
7. Feughelman, M., and A. R. Haly, *Biochim. Biophys. Acta*, **32**, 596 (1959); *Kolloid Z.*, **168**, 107 (1960).
8. Crewther, W. G., and L. M. Dowling, *J. Textile Inst.*, **51**, T775 (1960).
9. Burley, R. W., *Proc. Intern. Wool Textile Res. Conf. Australia*, **1955D**, 88.
10. Crewther, W. G., and L. M. Dowling, *Textile Res. J.*, **31**, 31 (1961).
11. Crewther, W. G., and L. M. Dowling, *Textile Res. J.*, **32**, 834 (1962).
12. Crewther, W. G., and L. M. Dowling, *Australian J. Biol. Sci.*, **14**, 677 (1961).
13. Crewther, W. G., and L. M. Dowling, *Biochim. Biophys. Acta*, **46**, 605 (1961)
14. Lindley, H., *Textile Res. J.*, **27**, 690 (1957).
15. Leach, S. J., *Australian J. Chem.*, **13**, 547 (1960).
16. Shinohara, K., *J. Biol. Chem.*, **112**, 683 (1936).
17. Griffith, J., and A. E. Alexander, *Textile Res. J.*, **27**, 755 (1957).
18. Speakman, J. B., *J. Soc. Dyers Colourists*, **52**, 335 (1936).
19. Speakman, J. B., *J. Soc. Chem. Ind.*, **50T**, 1 (1931).
20. Brown, A. E., J. H. Pendergrass, and M. Harris, *Textile Res. J.*, **20**:51 (1950).
21. Alexander, P., *Ann. N. Y. Acad. Sci.*, **53**, 653 (1951).
22. Elöd, E., and H. Zahn, *Kolloid-Z.*, **108**, 94 (1944).
23. Elöd, E., and H. Zahn, *Melliand Textilber.*, **30**, 17 (1949).
24. Beauregard, L. G., A. E. Brown, and M. Harris, *Textile Res. J.*, **23**, 642 (1953).
25. Crewther, W. G., *J. Soc. Dyers Colourists*, **75**, 189 (1959).
26. O'Donnell, I. J., *Textile Res. J.*, **24**, 1058 (1954).
27. Gillespie, J. M., *Australian J. Biol. Sci.*, **13**, 81 (1960).
28. Roberts, D. E., L. Mandelkern, and P. J. Flory, *J. Am. Chem. Soc.*, **79**, 1515 (1957).
29. Crewther, W. G., and L. M. Dowling, *Textile Res. J.*, **30**, 23 (1960).
30. Crewther, W. G., *J. Polymer Sci.*, **A2**, 149 (1964).
31. Gillespie, J. M., and P. H. Springell, *Biochem. J.*, **79**, 280 (1961).
32. Haly, A. R., and J. W. Snaith, *Biochim. Biophys. Acta*, **44**, 180 (1960).
33. Crewther, W. G., *J. Polymer Sci.*, **A2**, 123 (1964).
34. Crewther, W. G., J. M. Gillespie, and A. S. Inglis, unpublished data.
35. Feughelman, M., and A. R. Haly, *Inst. Text. France: Colloque: Structure de la Laine*, Juillet, 1961, p. 159.
36. Feughelman, M., *Textile Res. J.*, **29**, 223 (1959).
37. Haly, A. R., and O. A. Swanepoel, **32**, 375 (1962).

## Résumé

La rupture d'une grande partie des liens disulfures de la laine, par réduction et méthylation n'a pas d'effet sur le degré de supercontraction totale dans des solutions de LiBr à 98.5°. La réduction et la méthylation des liens disulfures augmentent le degré de la première étape et diminuent le degré de la seconde étape de supercontraction. On n'observe pas de phénomène en deux étapes à un degré normal du premier stade de supercontraction. La relation entre le degré du premier stade de supercontraction et le taux de liens disulfures résiduels est celle prévue par la théorie de la mécanique statistique pour une structure renfermant des pontages labiles aux acides situés à des intervalles égaux d'environ 35 liens résiduels et des pontages disulfures à des intervalles égaux à environ 20 liens résiduels le long des hélices-alpha des structures alignées. Ceci est comparé aux taux en demi-cystine de la fraction protéinique faible en soufre de la laine: environ 1



lien résiduel sur 18. La conversion des liens disulfures de la laine en ramification  $-\text{SCH}_2\text{CH}_2\text{S}-$  occasionne une diminution du degré du second stade de la supercontraction totale mais n'affecte pas le degré du premier. La relation entre le degré de supercontraction totale et le taux de ramifications dithioéthylènes est à peu près identique à celle observée pour le premier stade et la teneur en disulfure dans des échantillons de laine *S*-méthylée. Le taux de disulfure et de sulphydryle de la laine n'est pas altéré par la supercontraction à pH 6. On en conclut que le premier stade de supercontraction des fibres de laine dans des solutions de LiBr est dû à la conversion des hélices- $\alpha$  alignées en une forme élastomère, le degré de ce premier stade étant limité par les pontages disulfures et les pontages labiles aux acides. La contraction ultérieure a lieu pendant la seconde étape comme étant le résultat des réactions d'échange sulphydryle-disulfure qui éliminent l'influence limitative des liens disulfures. Le degré final de supercontraction est limité par des pontages labiles aux acides.

### Zusammenfassung

Die Spaltung eines grossen Teils der Disulfidbindungen in Wolle durch Reduktion und Methylierung hat auf das Ausmass der gesamten Superkontraktion in LiBr-Lösungen bei 98,5°C keinen Einfluss. Reduktion und Methylierung der Disulfidbindungen erhöht das Ausmass der ersten Stufe der Superkontraktion und setzt das der zweiten Stufe herab. Es wird dann beim normalen Ausmass der ersten Stufe der Superkontraktion kein Zwei-Stufen-Phänomen beobachtet. Die Beziehung zwischen dem Ausmass der ersten Superkontraktionsstufe und dem Gehalt an restlichen Disulfidbindungen entspricht dem von der statistisch-mechanischen Theorie für eine Struktur mit säureempfindlichen Vernetzungen im gleichmässigen Abstand von etwa 35 Resten und mit Disulfidvernetzungen im gleichmässigen Abstand von etwa 20 Resten entlang der  $\alpha$ -Helix der ausgerichteten Struktur geforderten. Das wird mit dem Halb-Cystingehalt der schwefelarmen Proteinfraction der Wolle, etwa 1 Rest auf 18, verglichen. Umwandlung der Disulfidbindungen der Wolle in  $-\text{SCH}_2\text{CH}_2\text{S}-$  Vernetzungen verursacht eine Abnahme des Ausmasses der zweiten Stufe und der totalen Superkontraktion, lässt aber das Ausmass der ersten Stufe unbeeinflusst. Die Beziehung zwischen dem Ausmass der totalen Superkontraktion und dem Gehalt an Dithioäthylenvernetzungen ist fast mit der zwischen erster Stufe und Disulfidgehalt bei *S*-Methylwolle-Proben beobachteten identisch. Der Disulfid- und Sulphydrylgehalt von Wolle wird durch Superkontraktion bei pH 6 nicht geändert. Man kommt zu dem Schluss, dass die erste Superkontraktionsstufe von Wollfasern in LiBr-Lösungen auf die Umwandlung ausgerichteter  $\alpha$ -Helices in eine elastomere Form zurückzuführen ist; das Ausmass der ersten Stufe ist durch Disulfid und säureempfindliche Vernetzungen begrenzt. Weitere Kontraktion in der zweiten Stufe erfolgt durch Sulphydryl-Disulfid-Austauschreaktionen, welche den beschränkenden Einfluss der Disulfidbindungen eliminieren. Das Gesamtausmass der Superkontraktion ist durch säureempfindliche Vernetzungen begrenzt.

Received October 4, 1962

## Covalent Acid-Labile Crosslinkages in Wool

W. G. CREWTHER, *Division of Protein Chemistry, C.S.I.R.O., Wool Research Laboratories Parkville, N2 (Melbourne), Victoria, Australia*

### Synopsis

The extent of the first stage of supercontraction of wool fibers in 8*M* LiBr (20°C.) was unaltered by the incorporation of 1*N* HCl in the solutions, whereas the extent of total supercontraction (98.5°C.) was greatly increased by the presence of HCl in the LiBr solutions. Likewise, with reduced and methylated wool, the relationship between the extent of the first stage of supercontraction and the content of residual disulfide was not affected by the presence of HCl in the solutions. When reduced and methylated wool fibers containing few residual disulfide groups were allowed to supercontract in solutions containing 8*M* LiBr and varying concentrations of HCl, the fibers contracted rapidly until the extent of total supercontraction in neutral solutions was approached. The rate then changed suddenly and became directly proportional to the concentration of acid in the solutions. Extensive supercontraction was observed also in alkaline solutions of LiBr if carboxyl groups of the reduced and methylated fibers were first ethylated to decrease the solubility of the wool proteins. Cortical cells, which were prepared by digesting reduced and methylated wool with crude trypsin, resembled whole wool in their behavior. It was concluded that wool contains covalent crosslinkages which are hydrolyzed by acids and alkalies. Evidence is presented that these bonds are stabilized by disulfide crosslinkages. The possibility that disulfide interchange takes place during supercontraction in solutions of LiBr-HCl is discussed.

### INTRODUCTION

Crewther and Dowling<sup>1</sup> have shown that the extent of supercontraction of wool fibers in solutions of LiBr at 98.5°C. is dependent on the hydrogen ion concentration of the solutions. In near-neutral solutions of LiBr at this temperature Corriedale fibers contract by about 40%; in 4*M* LiBr containing 1*N* HCl the contraction exceeds 70%. It is significant that the only other treatment reported to give supercontraction of comparable extent<sup>2</sup> involved oxidation of the wool with ClO<sub>2</sub> followed by boiling in dilute acid solutions; the wool contracted by 62%.

Three general hypotheses can be considered to account for the greater extent of supercontraction which is observed when HCl is incorporated in the LiBr solutions.

(1) The presence of acid causes polypeptide chains containing a given number of residues to assume a shorter end-to-end length than they do in LiBr solutions containing no acid.

(2) Supercontraction in neutral solutions of LiBr is limited by histological components of the fiber other than the contractile structures, such as inter-

cellular cementing substance and the cuticle. Decomposition of these structures by the acid permits further contraction.

(3) Acid ruptures interchain crosslinkages and so increases the mean number of amino-acid residues between crosslinkages. This would result in greater contraction.<sup>3</sup> Either ionic or covalent crosslinkages could be ruptured by acid.

This paper considers the relative merits of these alternatives. Information relating to the first hypothesis was obtained by supercontracting modified fibers in alkaline solutions of LiBr and from the known configuration of simple peptides. The second alternative was investigated by contracting cortical cells in near-neutral and acid solutions of LiBr. Having obtained negative answers to hypotheses 1 and 2, the nature of possible acid-labile crosslinkages was investigated by studying the effects of the time of acid treatment and acid concentration on the supercontraction of untreated or modified wool fibers.

## MATERIALS AND METHODS

The preparation and properties of the untreated and modified Lincoln 36's wool from the two fleeces, A and B, used in these experiments have been described previously.<sup>4</sup> For convenience wool which had been reduced in thioglycollate at pH 5 and methylated is referred to as *S*-methyl wool; the system of numbering and the wool samples so designated are identical with those used and described previously.<sup>4</sup> The sample of *S*-methyl wool chiefly used, no. 17, contained 63  $\mu$ mole of disulfide/g. Disulfide and sulfhydryl contents of the wool samples were determined by using the methods of Leach.<sup>5</sup> The extent of supercontraction of single wool fibers as a function of time was measured as described previously.<sup>1</sup> The differences in rate of the first and second stages of supercontraction are greater when supercontraction occurs in highly concentrated solutions of LiBr at low temperatures. The first stage of supercontraction is therefore defined as the extent of the initial rapid contraction in 8*M* LiBr at 20°C. The total supercontraction is that finally reached in 8*M* LiBr at 98.5°C.

The LiBr and LiI used in these studies were of laboratory reagent quality. Solutions were filtered before use and free bromine or iodine was removed by addition of a trace of Na<sub>2</sub>S<sub>2</sub>O<sub>3</sub>.<sup>6</sup> When solutions of LiBr or LiI containing HCl were required to be free from Br<sub>2</sub> or I<sub>2</sub>, respectively, a more concentrated solution of the salt after addition of a trace of Na<sub>2</sub>S<sub>2</sub>O<sub>3</sub>, was diluted with a suitable concentration of HCl which had been refluxed and rapidly cooled immediately before mixing with the LiBr solution.

## RESULTS

### a. Supercontraction of Modified Wool Fibers in Alkaline Solutions of LiBr

If the disulfide bonds of wool are replaced with *S*-carboxymethyl or even *S*-methyl groups, sufficient protein dissolves in alkaline solutions of LiBr to cause the fibers to imbibe water and elongate before contraction is

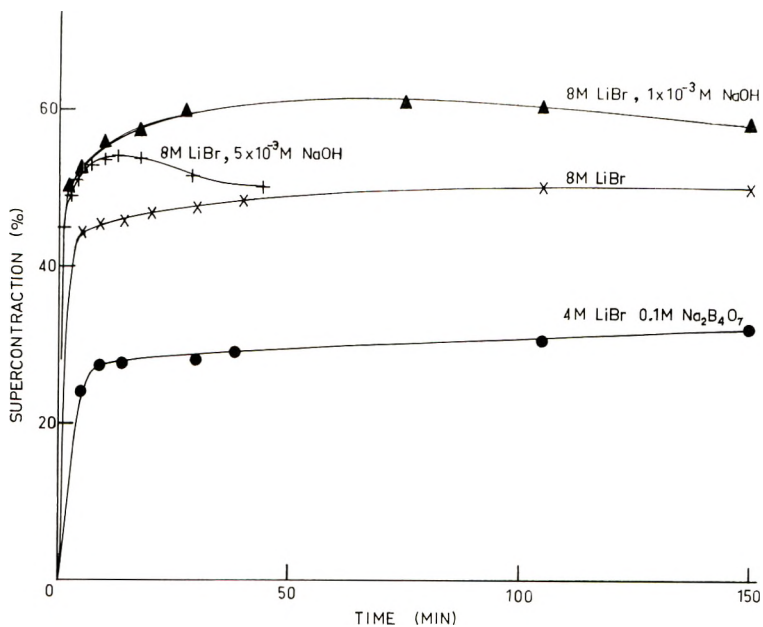


Fig. 1. Supercontraction of ethylated *S*-methyl wool fibers (B) in alkaline solutions of LiBr.

complete. Similar effects have been recorded with alkaline solutions of phenol.<sup>7</sup> As solution of the wool proteins is greatly enhanced by the increase in negative charge which results from increasing the pH,<sup>8</sup> the masking of carboxyl groups by ethylation presented a possible means of preventing solution. *S*-Methyl Lincoln wool (no. 17) was treated for 25 days at 28°C. with anhydrous ethanol containing sufficient concentrated HCl to make the solution 0.1M in HCl. After correction for the *S*-methyl content, the wool contained 655  $\mu$ equiv. ethoxyl/g. (total carboxyl content 1682  $\mu$ mole/g., Table III). With 6M LiBr at pH 6 or 4M LiBr at pH 8–8.5 this modification of the wool caused a marked decrease in the rate of supercontraction.<sup>9</sup> If as Crewther and Dowling<sup>10</sup> have suggested, the effect of LiBr solutions on fibrous proteins is due at least in part to increasing net negative charge resulting from preferential anion adsorption, this effect of ethylation could be due to the marked decrease in the number of negative charges on the proteins; consequently higher concentrations of LiBr might be expected to overcome the effect. Accordingly, the ethylated *S*-methyl wool was allowed to contract at 98.5°C. in 8M LiBr containing NaOH in concentrations ranging from  $5 \times 10^{-4}$  to  $1 \times 10^{-2}$ M. Figure 1 compares the rate curves with those obtained using 4M LiBr containing 0.1M Na<sub>2</sub>B<sub>4</sub>O<sub>7</sub> and 8M LiBr containing no added alkali. The retardation of contraction in 4M LiBr at about 30% contraction did not occur in 8M LiBr, and the extent of contraction in 8M LiBr was increased by the incorporation of alkali in the LiBr solutions.

### b. Supercontraction of Cortical Cells

A sample of *S*-methyl wool no. 17 was treated for 3 hr. at 40°C. in a 5% solution of crude trypsin (Difco 1:250) at pH 8 using a liquor ratio of 100:1. After thorough washing, the residues readily disintegrated when rubbed with a flattened rod on the bottom of a beaker containing water. The cell suspension was decanted from the larger debris and a heavy suspension of cells prepared after further washing. Aliquots of the suspension were then added to solutions of LiBr at 40°C. to give final concentrations of 7*M* LiBr and of 7*M* LiBr/1*N* HCl. Drops from the original suspension

TABLE I  
Supercontraction of Cortical Cells

Time of treatment at 40°C., min.	Extent of supercontraction, %			
	Cortical cells <sup>a</sup>		Whole fibers <sup>b</sup>	
	7 <i>M</i> LiBr	7 <i>M</i> LiBr/1 <i>N</i> HCl	7 <i>M</i> LiBr	7 <i>M</i> LiBr/1 <i>N</i> HCl
45	44.7	56.2	42.2	49.5
90	49.3	60.4	42.2	54.2
120	48.2	62.2	42.2	55.8

<sup>a</sup> Means of thirty cells.

<sup>b</sup> Means for two fibers.

and from the LiBr solutions taken at intervals of time were cooled, examined microscopically, and the length of 30 individual cells measured by means of an eye-piece scale. From the mean values the extents of supercontraction could be calculated. The results are listed in Table I. In this experiment supercontraction in the acid solution was not taken to completion.

### c. Rate Curves for Supercontraction in Salt Solutions Containing Acid

Lincoln wool fibers (A, no. 1, —SS— content 419 μmole/g.), were allowed to supercontract in 6*M* LiI/1*N* HCl at 98.5°C. and their lengths measured at intervals of time. Figure 2 shows that the fibers contracted rapidly by about 40% then, after a period during which the length remained almost constant, contraction recommenced and continued until the total contraction exceeded 70%. Curves are also provided for *S*-methyl wool samples 2 and 4, containing 132 and 51 μmole disulfide/g., respectively.<sup>4</sup> With these fibers, contraction was more rapid at all levels, but the initial rapid contraction was not greatly increased in extent. On the other hand, with untreated fibers contracting in 4*M* LiBr/1*N* HCl, there is an easily observed change in rate at about 20% contraction but no similar change in rate near 40% contraction (Fig. 2). The extent of total supercontraction of untreated Lincoln fibers from fleece A, in unacidified 8*M* LiBr, was 42%.

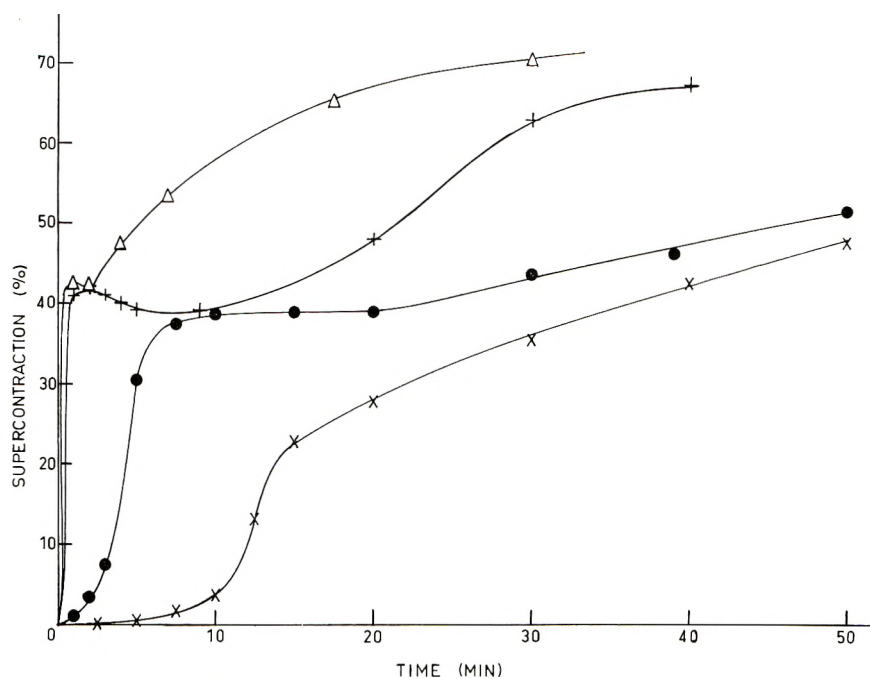


Fig. 2. Supercontraction of Lincoln wool fibers (A) and *S*-methyl wool fibers (A) at 98.5°C.: (●) untreated fibers, 6*M* LiI/1*N* HCl; (+) reduced and methylated fibers, 6*M* LiI/1*N* HCl; (Δ) fibers three times reduced and methylated, 6*M* LiI/1*N* HCl; (×) untreated fibers, 4*M* LiBr/1*N* HCl.

#### d. Rate of Supercontraction of Modified Fibers in 4*M* LiBr/1*N* HCl

Three samples of wool were modified as described by Lindley<sup>11</sup> as follows: (1) reduced 24 hr. in 0.5*M* thioglycollate at pH 5 and treated with methyl iodide in 0.1*M* Na<sub>2</sub>HPO<sub>4</sub>; (2) reduced as above and treated with ethylene dibromide in 0.1*M* Na<sub>2</sub>HPO<sub>4</sub>; (3) treated as in (2) then reduced again 24 hr. in 0.5*M* thioglycollate at pH 11 and again treated with ethylene dibromide. The disulfide contents of these fibers are listed in Table II. Figure 3 shows rate curves for the supercontraction of these fibers at 98.5°C. in 4*M* LiBr/1*N* HCl and in 4*M* LiBr at pH 8.2. The pH of the solutions

TABLE II  
Disulfide + Sulfhydryl Contents of Lincoln Wool (A) After Reduction and Alkylation<sup>a</sup>

No.	Alkylating agent	(SS + SH), μmole/g.
1	None	425
2	Methyl iodide	174
3	Ethylene dibromide	208
4	As 3, reduced pH 11, alkylated ethylene dibromide.	80

<sup>a</sup> The wool was reduced at 20°C. with 0.5*M* thioglycollate at pH 5.0 before alkylation.

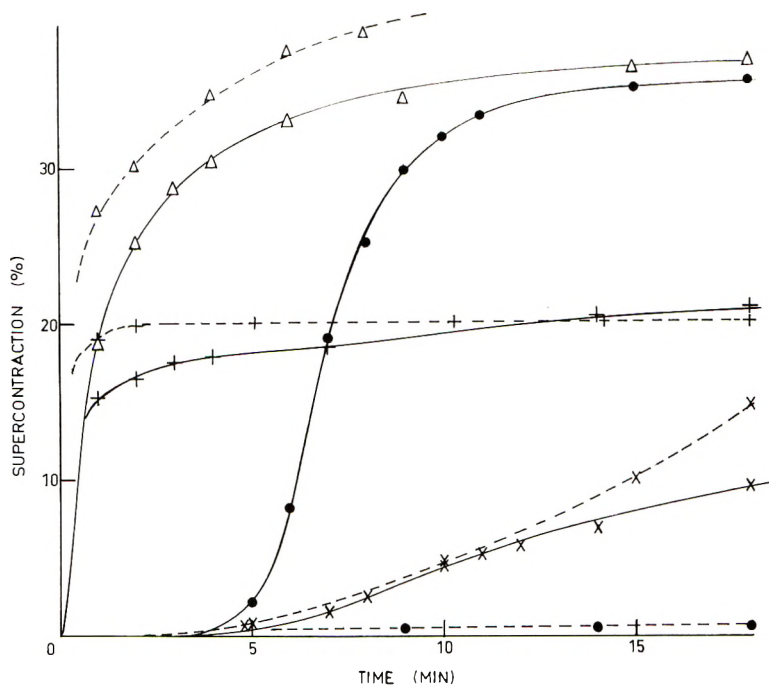


Fig. 3. Supercontraction of modified wool fibers (A) at 98.5°C. (—) in 4*M* LiBr at pH 8.2 and (- -) in 4*M* LiBr/1*N* HCl: (●) untreated fibers; (×) once reduced and crosslinked fibers; (+) twice reduced and crosslinked fibers; (Δ) reduced and methylated fiber.

had little effect on the relative initial rates of contraction of the three modified fibers (Fig. 3). However, with prolonged treatment of each type of fiber the final extent of contraction in 4*M* LiBr/1*N* HCl was much greater than in 4*M* LiBr at pH 8.2. The rates of supercontraction of the untreated fibers at pH 8.2 and in 1*N* HCl differed greatly (Fig. 3).

#### e. Extent of the First Stage of Supercontraction in Acid Solutions of LiBr

The rate curves of Figure 4 illustrate the effect of residual disulfide content on the supercontraction of *S*-methyl fibers in 8*M* LiBr/1*N* HCl at 20°C. Untreated wool fibers containing about 400 μmole disulfide/g. contracted by about 20% (mean of 8 fibers, 20.6%) over a period of a few hours, then contracted no further in the ensuing 3 days. With decreasing disulfide content the rate and extent of the first stage of supercontraction increased. Figure 5 shows that the relationship between the extent of the first stage and the disulfide content of these fibers was identical with that observed previously for supercontraction of fibers from the same wool sample in 8*M* LiBr containing no acid (pH ca. 5).<sup>4</sup>

Although the curves in Figure 4 all show a sharp transition from the first stage to a negligible or very small rate in the second stage of supercontraction, the rate of this slow process varied considerably over the range of modi-

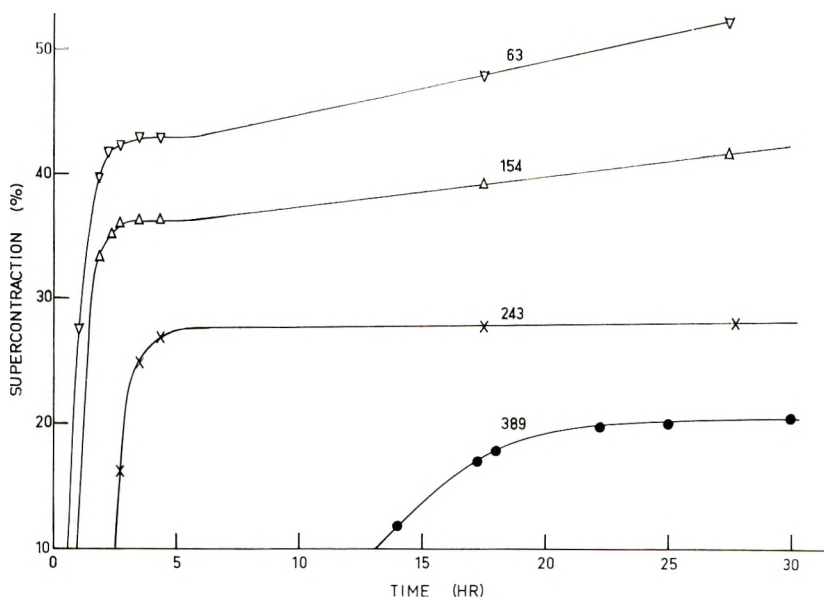


Fig. 4. Rate curves for the supercontraction of *S*-methyl wool fibers (B) at 20°C. in 8*M* LiBr/1*N* HCl. Numerals on the curves indicate residual disulphide contents in  $\mu\text{mole/g}$ .

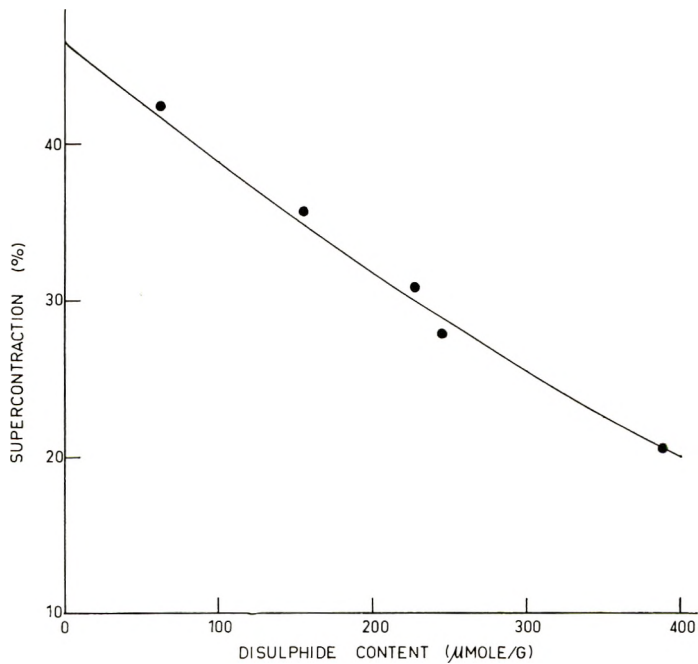


Fig. 5. Relationship between the extent of first stage supercontraction and the residual disulphide content of *S*-methyl wool fibers (B) in 8*M* LiBr/1*N* HCl. The curve indicates the corresponding relationship obtained using 8*M* LiBr containing no acid.<sup>4</sup>



fied fibers. Untreated fibers did not contract at a measurable rate at 20°C. once the first stage was complete; fibers containing only 6.3  $\mu$ mole disulfide/g. contracted during the second stage by about 0.5%/hr. for several hours, the rate then decreasing slowly as contraction proceeded.

#### f. Effect of Acid Concentration on Rate of Supercontraction

S-Methyl wool fibers from sample no. 17 were allowed to supercontract at 40°C. in solutions of 8M LiBr containing HCl varying in concentration

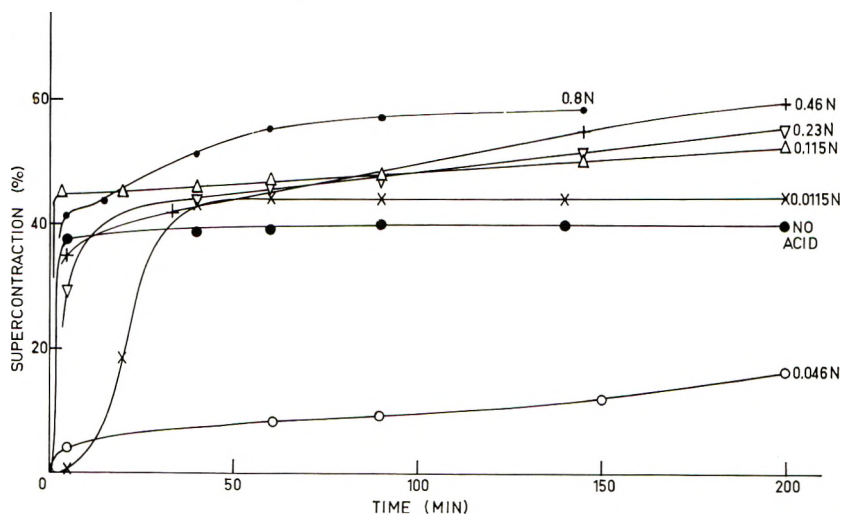


Fig. 6. Rate curves for supercontraction at 40°C. of *S*-methyl wool (no. 17) in 8M LiBr containing HCl. The acid concentrations are indicated.

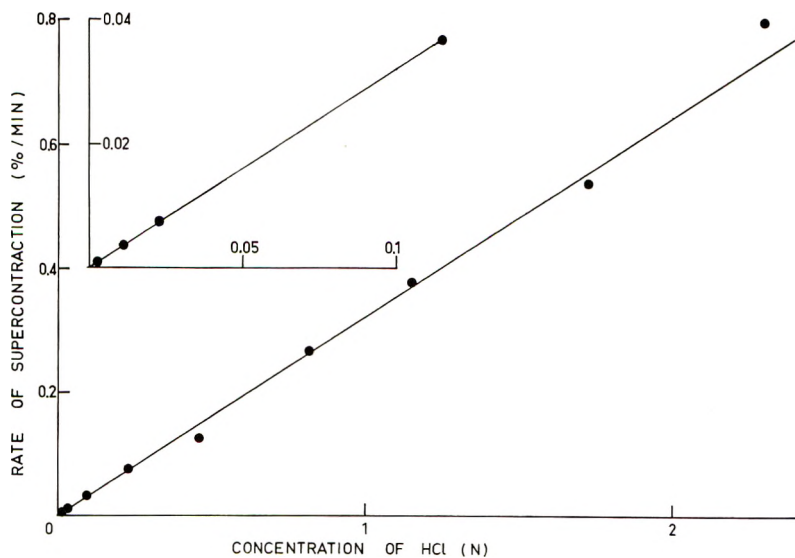


Fig. 7. Relationship between the acid concentration and rate of supercontraction of *S*-methyl wool (no. 17) in 8M LiBr/HCl at 40°C. after completion of first stage. Inset is a tenfold magnification of the curve near the origin.

from 0.0023*N* to 2.3*N*. The first stage of contraction was complete in a few minutes (Fig. 6) at about 42% contraction; a slower contraction then ensued, the rate of which depended on the concentration of acid used. Figure 7 shows that there was a good rectilinear relationship between this rate and the acid concentration over the whole range of acid concentrations. With solutions containing low concentrations of HCl the rate was constant within experimental error for several hours; with the three highest concentrations it was necessary to take the slope of a tangent to the curve at a point corresponding with completion of the first stage of contraction (42%) as a measure of rate. In addition there were marked differences in the rates of the first stage of contraction (Fig. 6), the minimum rate being observed with 0.046*N* HCl.

#### g. Effect of Residual Disulfide Bonds on Stability of the Acid-Labile Crosslinkages

Untreated fibers and *S*-methyl fibers (no. 17) were mounted in the usual manner but using a tube fitted at the base with a side-tube through which

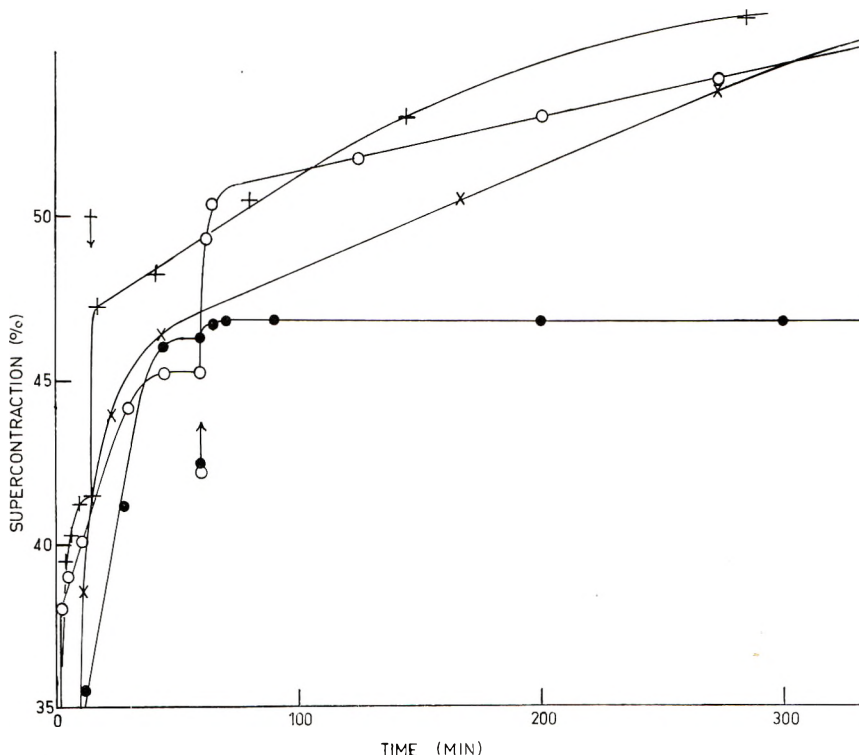


Fig. 8. Effect of residual disulfide content on the rate of supercontraction of wool fibers (B) in 8*M* LiBr/HCl. Arrows indicate the time at which 8*M* LiBr at 98.5°C. was replaced by 8*M* LiBr/HCl at 40°C.: (●) untreated fibers, 0.115*N* HCl; (○) *S*-methyl fibers (no. 17), 0.115*N* HCl; (+) *S*-methyl fibers (no. 17), 0.5*N* HCl; (×) *S*-methyl fibers (no. 17), 0.5*N* HCl, not pretreated 8*M* LiBr.

the LiBr solution could be removed by suction. The fibers were then supercontracted almost completely at 98.5°C. in 8*M* LiBr containing no acid. The LiBr solution was then sucked off, the fibers quickly rinsed at 40°C. with 8*M* LiBr containing 0.5 or 0.115*N* HCl, and the rinsing solutions immediately replaced with an aliquot of the same solution at 40°C. This temperature was chosen because the rates of contraction could be measured conveniently under these conditions. Figure 8 shows that untreated fibers contracted very slowly if at all in the LiBr/HCl solutions, whereas *S*-methyl fibers with few remaining disulfide bonds contracted at rates comparable with those recorded in Figures 6 and 7.

In other experiments at a final temperature of 98.5°C. the rates of contraction of the *S*-methyl wool fibers were correspondingly greater, whereas with untreated fibers, supercontracted by 42% before immersing the fiber in the acid solution, there was an increase to 46% contraction within 2 min. followed by elongation to 42% contraction and a subsequent very slow contraction.

## DISCUSSION

### a. Peptide Chain Configuration

In acid solution a random polypeptide chain would be expected to behave as a positively charged polyelectrolyte. As the net charge increased, the protein would tend to extend isotropically in the manner observed with synthetic polyelectrolytes<sup>12</sup> and also with the residues from extracted wool.<sup>13</sup> Hence side-chain ionization does not provide a satisfactory explanation for the increase in supercontraction when HCl is incorporated in the LiBr solutions bringing about contraction. Furthermore, this suggestion cannot explain the results in Figure 7.

However, reaction of protons with the main chains could cause a decrease in the mean end-to-end length of random peptide chains in two ways: (1) extensive protonation of the amido nitrogen atoms would eliminate the double-bond character of the adjacent C—N bond so converting a high proportion of the *trans* amide groups to the nonplanar form; (2) the formation of a few such nonplanar amide groups could catalyze the conversion of planar amide groups from the *trans* to the *cis* form.

The expression for the mean square end-to-end length of a *trans* peptide chain is  $27.9n - 20.3$ , where  $n$  is the number of residues in the chain.<sup>3</sup> The corresponding expressions for the nonplanar and *cis* forms are  $15.5n - 4.8$  and  $8.6n - 0.8$ , respectively.<sup>3</sup> Hence conversion of the *trans* form to the *cis* or nonplanar forms would result in length decreases of about 45% and 25% respectively. The observed decrease in contracted length of both Lincoln and Corriedale fibers due to the presence of acid in the LiBr solutions, about 50%, is in reasonable agreement with a *trans-cis* conversion. Apart from the lack of reasonable agreement between the calculated and observed length changes, the conversion of a large proportion of the planar amide groups to the nonplanar form can be rejected as an explana-

tion for the shortening of the polypeptide chains on the same ground as other hypotheses based on ionization of a major proportion of one type of group in the protein (see below).

The *trans-cis* transformation, on the other hand, would involve ionization of only a small fraction of the amide groups and so cannot be rejected on the basis of Figures 4, 6, and 7. However, four reasons can be listed for rejecting this suggestion. (1) Alkaline solutions of LiBr like acid solutions, cause more extensive contraction of the fibers than near-neutral solutions (Fig. 1) provided solution of the proteins is prevented. Alkaline conditions would be expected to lessen any tendency to form nonplanar amide groups and so to stabilize the *trans* form of the peptide linkage; hence extensive supercontraction in alkaline solutions would not be expected from the *trans-cis* hypothesis. (2) There is no apparent reason why disulfide crosslinkages should retard amide ionization or the resultant *trans-cis* conversion (Figs. 4 and 8). (3) X-ray diffraction, dipole, and infrared studies of several synthetic peptides have shown that the peptide linkage is planar and in the *trans* configuration. The evidence, which is reviewed by Corey and Pauling<sup>14</sup> indicates that the *trans* form is more stable than the *cis* form by some 2 kcal./mole. The only recorded exception to this appears to be poly-L-proline,<sup>15</sup> which is believed to undergo a reversible *trans-cis* transformation catalyzed by strong acids. However, in aqueous solution the *trans* form predominates, and the *cis* form is obtained only by decreasing the polarity of the solvent; it appears to be stabilized by the formation of a right-handed helix. (4) There is no evidence that peptides obtained by acid hydrolysis of proteins differ from peptides with the same sequence obtained by synthetic processes or enzymatic hydrolysis.

Attempts to obtain further direct evidence regarding this possibility by infrared spectroscopy or polarimetry proved unsuccessful. Sections of horse hair giving infrared spectra were no longer amenable after treatment with LiBr/HCl solutions while the insolubility of the various low sulfur wool protein derivatives in 8*M* LiBr containing HCl precluded polarimetric experiments.

### b. Histological Effects

There is also good reason to reject the proposal that the effect of acid in the LiBr solutions results from an attack on histological structures in the fiber other than the aligned material within the cortical cells. Table II shows that cortical cells from *S*-methyl wool contracted more extensively in 7*M* LiBr/1*N* HCl than in 7*M* LiBr, the differences being comparable with those observed with whole fibers. As cortical cells prepared in this manner are largely free from cell walls,<sup>16</sup> we may conclude that the structure modified by the acid lies within the cell. This does not prove that histological structures have no influence on the extent of supercontraction. Cortical cells usually contract further than the fibers from which they are prepared and although this is due chiefly to preferential separation of cells from the ortho-cortex there may be other effects also.

### c. Acid-Labile Bonds

The third alternative, that acid-labile crosslinkages in the contractile structures of the fiber are ruptured by the acid, provides the most reasonable explanation for the results. Some conclusions can be drawn concerning the chemical nature of these crosslinkages. The supercontraction of wool fibers in neutral solutions of LiBr takes place in two stages,<sup>17</sup> the fibers being elastomeric once the first stage is complete. Evidence has been presented elsewhere<sup>4,18</sup> that the first stage of supercontraction resulting from the conversion of an orderly array of  $\alpha$ -helices to an elastomer is limited in extent by disulfide crosslinkages. During the second stage of supercontraction sulfhydryl-disulfide interchange permits further randomization of the chains and hence, further contraction. This accounts for the observation<sup>1,4</sup> that the extent of total supercontraction is almost completely independent of the disulfide content of the fibers.

With *S*-methyl wool fibers containing very few disulfide bonds the acid-labile bonds are chiefly responsible for limiting the extent of the first stage of supercontraction in near-neutral solution whereas both disulfide and acid-labile bonds limit the extent of supercontraction in untreated fibers. Consequently the rupture of acid-labile bonds before or during the first stage of supercontraction would alter the relationship between the extent of the first stage of contraction and the disulfide content. If the contractile structures of the fiber consist of aligned polypeptide chains crosslinked by both disulfide and acid-labile crosslinkages,<sup>4,18</sup> the rupture of acid-labile crosslinkages before or during the first stage of supercontraction would cause an increase in the extent of the first stage of contraction with both untreated and *S*-methyl fibers, though quantitatively the effects would differ.

As ionic interactions would be eliminated as soon as the acid penetrated the fiber, major changes in the extent of the first stage of contraction would be expected when acid was incorporated in the LiBr solutions if the acid-labile bonds were ionic in nature. Figure 5 shows that the relationships between extent of the first stage of supercontraction and disulfide content in acid and neutral solutions of LiBr were identical. This indicates that the acid-labile bonds are covalent. The rate curves for supercontraction of reduced and crosslinked fibers (Fig. 3) and *S*-methyl fibers (Fig. 4) in LiBr/HCl solutions provide confirmatory evidence of their covalent nature. Thus the extent of the first stage of contraction for the crosslinked fiber is independent of the presence of acid in the LiBr solutions even at 98.5°C. (Fig. 3). On the other hand, *S*-methyl fibers with small disulfide contents continued to contract slowly after the first stage of supercontraction was complete (Fig. 4). This suggests that the acid is responsible for an additional time-dependent reaction in these fibers. Further evidence that the reaction with acid is dependent on time and acid concentration is provided by the effects of acid concentration on the supercontraction rate curves (Fig. 6). Figure 7 shows that the rate of the contraction caused by the incorporation of HCl in the LiBr solution is directly

proportional to the acid concentration over a wide range of concentrations. The acid therefore has a catalytic effect such as occurs in acid hydrolysis of amides, esters, etc.

Furthermore, by estimating the numbers of residual acid-labile bonds in the *S*-methyl wool at different times of contraction using the expression developed for a random polypeptide structure<sup>3,4</sup> it can be shown that the points relating time and  $\ln L$ , where  $L$  is the number of residual acid-labile bonds per unit weight of contractile material, fall near a straight line. Hence the hydrolysis as measured by extent of contraction approximates to a first-order reaction. This result, together with the rectilinear relationship between acid concentration and rate (Fig. 7), means that the effect of acid on the length of the fiber is triggered by the rupture of a single acid-labile bond.

The minimum observed for the rate of the initial contraction of *S*-methyl wool in 8*M* LiBr containing 0.045*M* HCl (Fig. 6) may well be due to preferential adsorption of anions<sup>10</sup> with consequent lowering of the isoelectric point of the wool proteins. It is apparent that the rate of the initial contraction to about 40% has no relationship with the rate of subsequent contraction.

#### d. Reactivity of Acid-Labile Covalent Crosslinkages

Figures 4 and 8 show that once the first stage of supercontraction in solutions of LiBr-HCl is complete, the rate of the ensuing contraction depends partly on the disulfide content of the fibers; the presence of large numbers of disulfide crosslinkages hinders the hydrolysis of the acid-labile crosslinkages even though the fiber is in the elastomeric state. Preliminary supercontraction of the fibers in near-neutral LiBr solutions has little effect on the rate of subsequent contraction in LiBr-HCl solutions (Fig. 8). The effect is therefore not attributable to the formation or presence of ordered structures in the fiber.

The stabilization by disulfide bonds is to be expected in terms of the explanation provided for the two stages of supercontraction of wool fibers.<sup>4,18</sup> During the second stage of supercontraction, sulfydryl-disulfide interchange permits the polypeptide chains to assume more probable forms and so contraction proceeds. At the same time the positions of the disulfide crosslinkages are changed and when contraction is complete the disulfide bonds would be arranged in the manner expected if they had been inserted in the fiber after contraction had proceeded to the limit imposed by the acid-labile bonds. If now the acid-labile crosslinkages were slowly hydrolyzed, the disulfide bonds would again begin to limit contraction. In addition they would lessen very considerably the strain on the acid-labile crosslinkages due to thermal vibration of the chains. Consequently rupture of disulfide bonds by converting them to *S*-methyl groups would be expected to accelerate hydrolysis of acid-labile crosslinkages. A similar argument applies to fibers which have undergone only the first stage of supercontraction (Fig. 4). This stabilization by disulfide bonds

suggests that the disulfide bonds and the acid-labile covalent bonds form crosslinkages in the same network.

#### e. Chemical Nature and Location of the Acid-Labile Bonds

There is at present no direct evidence regarding the chemical nature of the acid-labile bonds. The observation that almost complete conversion of the disulfide bonds of Lincoln wool to *S*-methyl groups has no significant effect on the extent of total supercontraction<sup>4,19</sup> eliminates the possibility that the large supercontraction in acid solutions is due to acid catalysis of disulfide interchange. Furthermore, random hydrolysis of peptide linkages is not responsible for the effect, since pretreatment of wool fibers with HCl solutions under widely different conditions did not increase the extent of supercontraction in LiBr solutions at pH 6 or at pH 8.2.<sup>20</sup> For this and other reasons it seems unlikely that the HCl is increasing the extent of contraction by rupturing main-chain peptide linkages. This suggests that the wool fiber contains crosslinkages, other than disulfides, which are hydrolyzed by acids or alkalies. These crosslinkages probably occur between the aligned polypeptide chains constituting the contractile structures of the fiber.

Recently it has been suggested that collagen contains both ester<sup>21</sup> and amide<sup>22</sup> crosslinkages formed by linking the side-chains of aspartic and/or glutamic acid residues with either hydroxyl groups of hydroxyproline, serine or threonine side chains or with the amino groups of lysine residues. In wool, ester crosslinkages are more probable than amide crosslinkages, since the lysine residues can be recovered almost quantitatively as the  $\epsilon$ -*N*-DNP derivative<sup>23</sup> and the basic side-chain groups can be accounted for quantitatively by the uptake of anionic dyes.<sup>24</sup> On the other hand, not all of the acidic side-chain groups of wool can be esterified by treatment with anhydrous ethanol/HCl.<sup>25</sup>

From supercontraction data it has been calculated<sup>4</sup> that Lincoln wool contains some three acid-labile crosslinkages for every four disulfide crosslinkages in the aligned structures of the fiber. If we assume that these structures are formed from the low sulfur proteins, which constitute about 60% of the fiber and contain approximately 400  $\mu$ mole half-cystine/g.,<sup>26</sup> there would be approximately 200  $\mu$ mole disulfide/g. and hence about 150  $\mu$ mole of acid-labile crosslinkages/g. of low sulfur protein. If the high sulfur proteins do not contain similar crosslinkages the content of acid-labile crosslinkages in the whole fiber would be about 90  $\mu$ mole/g.

Amino-acid analyses,<sup>27</sup> titration data,<sup>28</sup> and measurements of isoelectric points are not sufficiently accurate to disprove or suggest the presence of 90  $\mu$ mole of ester groups in a total of 1682 acidic, 1708 basic (Table III), and about 60 acetyl groups<sup>29</sup>/g. of wool. On the other hand, as esters are generally more susceptible to alkaline than to acid hydrolysis, the observation that ethylated wool supercontracts in 8*M* LiBr containing  $1 \times 10^{-3}$  *M* NaOH by more than 60% (Fig. 1) favors the view that esters are present; acid at an equal concentration in 8*M* LiBr has no comparable

TABLE III  
Basic and Acidic Amino Acid Content of Lincoln Wool (B) (24 hr. Hydrolyzate)<sup>a</sup>

Amino acid	Basic amino acids		Acidic amino acids	
	% Total N	$\mu$ mole/g.	% Total N	$\mu$ mole/g.
Lysine	$2.23 \times 2$	271		
Arginine	$5.00 \times 4$	607		
Amide	6.84	830		
Aspartic acid			5.07	615
Glutamic acid			8.79	1067
Total	14.07	1708	13.86	1682

<sup>a</sup> Amide was estimated by the method of Leach and Parkhill.<sup>39</sup> Histidine/3 content was 0.53% of total N, nitrogen content, 16.99%.

effect on the rate of supercontraction at levels of contraction exceeding 50%.

The stabilization of the acid-labile bonds by disulfide bonds (Fig. 8) suggests that disulfide and acid-labile covalent bonds occur in closely related positions within the aligned structures of the fiber. On the other hand the ready extraction of wool proteins in reagents which rupture disulfide bonds under conditions which would not be expected to rupture the acid-labile bonds<sup>26,30</sup> suggests that disulfide bonds occur in sites from which acid-labile bonds are absent. For example, in the model for the microfibril proposed by Fraser, MacRae, and Rogers,<sup>31</sup> restriction of acid-labile bonds to linkages between the two or three peptide chains forming the protofibrils would permit extraction of double or triple chain molecules once sufficient of the disulfide bonds connecting the protofibrils had been broken. If these soluble protein molecules have a molecular weight of about 60,000<sup>32</sup> and a half-cystine content of about 400  $\mu$ mole/g., we would expect some 12 disulfide and 9 acid-labile bonds per molecule. Rupture of up to eight of these acid-labile bonds could give rise to more than 500 molecular species with identical amino-acid compositions and molecular weights. This may contribute to the spectrum of protein species observed by Thompson and O'Donnell<sup>26</sup> during chromatography of the low sulfur proteins of wool on DEAE-cellulose.

#### f. Mechanisms Associated with Different Stages of Supercontraction in Solutions of LiBr Containing Acid

Since the extent of the first stage of supercontraction in LiBr/HCl solutions is equal to that obtained in near-neutral solution and is limited by disulfide bonds (Fig. 5), it is almost certainly caused by the disordering of aligned polypeptide chains.<sup>4,17</sup> There is evidence that sulfydryl-disulfide interchange, which affects the rate of the first stage<sup>19</sup> and is responsible for the second stage of supercontraction<sup>4</sup> in near-neutral solutions does not occur to an appreciable extent in acid solutions: reaction of the sulfydryl groups of the fibers with *N*-ethylmaleimide,<sup>33</sup> oxidation with peracetic acid or iodine,<sup>19,34</sup> and the presence of free bromine in the solutions



of LiBr,<sup>33</sup> which retard the second stage of contraction at pH 6, have no retarding effect on the supercontraction in acid and in some instances accelerate the contraction slightly. Figure 3 shows that fibers in which the disulfide bonds have been largely converted to *S*-methyl or —SCH<sub>2</sub>CH<sub>2</sub>S— groups contract in solutions of LiBr at a rate which is unaffected by the presence of HCl. Untreated fibers, on the other hand, contract much more slowly in the acid solutions than in neutral solutions of LiBr, presumably because sulfydryl–disulfide interchange does not proceed at an appreciable rate in solutions containing acid.<sup>35</sup> This relationship between sulfydryl–disulfide interchange and the rate, but not the extent, of the first stage of supercontraction has been explained already<sup>19</sup> in terms of a plastic matrix, parallel with the microfibrils, the viscosity of the matrix being determined in part by sulfydryl–disulfide interchange reactions.

However, Figure 2 shows that the rate curve for the supercontraction of Lincoln fibers in 6*M* LiI containing 1*N* HCl has a pronounced shelf corresponding approximately with the extent of total contraction in neutral LiBr solutions (42%). Since the helix–random coil transition occurs even more readily in solutions of LiI than in solutions of LiBr,<sup>36</sup> it seems probable that the LiI also accelerates either acid-catalyzed disulfide interchange or the hydrolysis of acid-labile bonds. In this way the change in rate which occurs at about 20% contraction in 4*M* LiBr/1*N* HCl (Fig. 2) could be obscured. The rate curves for *S*-methyl fibers in 6*M* LiI/1*N* HCl show a relatively small increase in the level of the initial rapid contraction but an acceleration of the ensuing contraction. This suggests that in solutions of LiI the initial contraction of about 40% included randomization of chains together with disulfide interchange. The observation that the extent of total supercontraction in 4*M* LiBr/1*N* HCl at 98.5°C. is not appreciably altered by converting disulfide groups to *S*-methyl groups<sup>4,19</sup> also suggests that disulfide interchange occurs in LiBr–HCl solutions. The hydrolysis of acid-labile crosslinkages would then give rise to a third stage of contraction though all three processes may take place simultaneously to some extent.

It is generally considered that disulfide interchange takes place in acid solutions only when high concentrations of acid are used.<sup>35</sup> However, if as Benesch and Benesch<sup>37</sup> suggest, this reaction takes place by interchange between disulfide groups and —S<sup>+</sup> formed by the reaction



the concentration of —S<sup>+</sup>, and hence the rate of interchange should be approximately proportional to the hydrogen ion activity. However, this may be affected by the presence of other ions,<sup>35</sup> and in addition the reactivity of disulfide groups in proteins can be greatly increased by converting the ordered structure to a random coil. This has been demonstrated for the reaction of the disulfide bonds of wool with alkali.<sup>38</sup> Hence disulfide interchange may contribute in an important manner to supercontraction in solutions of LiBr containing acid.

## CONCLUSION

The evidence suggests that wool contains covalent crosslinkages other than disulfide bonds. The process of supercontraction in solutions of LiBr containing HCl appears to consist primarily of the conversion of an ordered aligned structure to an elastomer, followed by further randomization of the polypeptide chains made possible by disulfide interchange and the hydrolysis of these covalent crosslinkages.

## References

1. Crewther, W. G., and L. M. Dowling, *Textile Res. J.*, **29**, 541 (1959).
2. Speakman, J. B., *J. Textile Inst.*, **32**, T93 (1941).
3. Crewther, W. G., *J. Polymer Sci.*, **A2**, 123 (1964).
4. Crewther, W. G., *J. Polymer Sci.*, **A2**, 131 (1964).
5. Leach, S. J., *Australian J. Chem.*, **13**, 547 (1960).
6. Griffith, J., and A. E. Alexander, *Textile Res. J.*, **27**, 755 (1957).
7. Crewther, W. G., *J. Soc. Dyers Colourists*, **75**, 189 (1959).
8. O'Donnell, I. J., *Textile Res. J.*, **24**, 1058 (1954); J. M. Gillespie, *Australian J. Biol. Sci.*, **13**, 81 (1960).
9. Crewther, W. G., and L. M. Dowling, *Textile Res. J.*, **32**, 834 (1962).
10. Crewther, W. G., and L. M. Dowling, *J. Phys. Chem.*, **62**, 678 (1958).
11. Lindley, H., *Textile Res. J.*, **27**, 690 (1957).
12. Doty, P., and J. T. Yang, *J. Am. Chem. Soc.*, **78**, 498 (1956).
13. Speakman, P. T., *J. Textile Inst.*, **51**, T256 (1960).
14. Corey, R. B., and L. Pauling, *Proc. Intern Wool Textile Res. Conf. Australia*, **1956 B**, B 249.
15. Steinberg, I. Z., W. F. Harrington, A. Berger, M. Sela, and E. Katchalski, *J. Am. Chem. Soc.*, **82**, 5263 (1960); E. Katchalski and I. Z. Steinberg, *Advan. Phys. Chem.*, **12**, 432 (1961).
16. Rogers, G. E., private communication.
17. Feughelman, M., and A. R. Haly, *Textile Res. J.*, **27**, 919 (1957); A. R. Haly and J. Griffith, *Textile Res. J.*, **28**, 32 (1958).
18. Crewther, W. G., and L. M. Dowling, *Biochim. Biophys. Acta*, **46**, 605 (1961).
19. Crewther, W. G., and L. M. Dowling, *J. Textile Inst.*, **51**, T775 (1960).
20. Crewther, W. G., and L. M. Dowling, *Textile Res. J.*, **30**, 23 (1960).
21. Gallop, P. M., S. Seifter, and E. Meilman, *Nature*, **183**, 1659 (1959); J. Bello, *Nature*, **185**, 241 (1960).
22. Veis, A., and J. Cohen, *J. Am. Chem. Soc.*, **78**, 6238 (1956); G. L. Mechanic and M. Levy, *J. Am. Chem. Soc.*, **81**, 1889 (1959).
23. Middlebrook, W. R., *Biochim. Biophys. Acta*, **7**, 547 (1951).
24. Maclaren, J. A., *Arch. Biochem. Biophys.*, **86**, 175 (1960).
25. Alexander, P., D. Carter, C. Earland, and O. E. Ford, *Biochem. J.*, **48**, 629 (1951).
26. Gillespie, J. M., I. J. O'Donnell, E. O. P. Thompson, and E. F. Woods, *J. Textile Inst.*, **51**, T703 (1960); E. O. P. Thompson, and I. J. O'Donnell, *Australian J. Biol. Sci.*, **14**, 461 (1961).
27. Thompson, E. O. P., and I. J. O'Donnell, unpublished results.
28. Steinhardt, J., C. H. Fugitt, and M. Harris, *J. Res. Natl. Bur. Std.*, **26**, 293 (1941); J. Steinhardt and E. M. Zaiser, *J. Biol. Chem.*, **183**, 789 (1950).
29. O'Donnell, I. J., E. O. P. Thompson, and A. S. Inglis, *Australian J. Biol. Sci.*, **15**, 732 (1962).
30. Lees, K., and F. F. Elsworth, *Proc. Intern. Wool Textile Res. Conf. Australia*, **1956 C**, 363 (1956).
31. Fraser, R. D. B., T. P. MacRae, and G. E. Rogers, *Nature*, **193**, 1052 (1962).

32. Harrap, B. S., unpublished results.
33. Crewther, W. G., and L. M. Dowling, *Textile Res. J.*, **31**, 31 (1961).
34. Crewther, W. G., and L. M. Dowling, in press.
35. Sanger, F., and A. P. Ryle, *Biochem. J.*, **60**, 535 (1955); F. Sanger, A. P. Ryle, L. F. Smith, and R. Kitai, *Proc. Intern. Wool Textile Res. Conf. Australia*, **1956C**, 49; Glazer, A. H., and E. J. Smith, *J. Biol. Chem.*, **236**, 416 (1961).
36. Crewther, W. G., and L. M. Dowling, *Nature*, **178**, 544 (1956).
37. Benesch, R., and R. Benesch, *J. Am. Chem. Soc.*, **80**, 1666 (1958).
38. Crewther, W. G., and L. M. Dowling, to be published.
39. Leach, S. J., and E. M. J. Parkhill, *Proc. Intern. Wool Textile Res. Conf. Australia*, **1956 C**, 92.

### Résumé

L'importance de la première étape de la supercontraction des fibres de laine dans des solutions de LiBr 8M (20°C) n'est pas altérée par l'incorporation d'HCl 1N dans ces solutions tandis que l'importance de la totalité de la supercontraction (98.5°C) est fortement accrue par la présence d'HCl dans les solutions de LiBr. De même, avec une laine réduite et méthylée, la relation entre l'importance de la première étape de supercontraction et la quantité de disulfures résiduels n'est pas affectée par la présence d'HCl dans les solutions. Quand les fibres d'une laine réduite et méthylée contenant quelques groupements disulfures résiduels sont soumises à la supercontraction dans des solutions contenant du LiBr 8M et différentes concentrations en HCl, les fibres se contractent rapidement jusqu'à atteindre à peu près l'importance de la supercontraction totale en milieu neutre. La vitesse change alors brusquement et devient directement proportionnelle à la concentration en acide dans les solutions. On a également observé une importante supercontraction dans les solutions alcalines de LiBr si les groupements carboxyles des fibres réduites et méthylées ont tout d'abord été éthylées en vue de diminuer la solubilité des protéines de la laine. Les cellules corticales qui ont été préparées en faisant digérer de la laine réduite et méthylée avec de la trypsine brute, se comportent d'une façon analogue à la laine intacte. On en conclut que la laine contient des liaisons transverses covalentes qui sont hydrolysées par les acides et les alcalis. On prouve que ces liens sont stabilisés par des ponts disulfures. On discute de la possibilité d'un échange entre les liens disulfures qui se produirait durant la supercontraction dans les solutions de LiBr-HCl.

### Zusammenfassung

Das Ausmass der ersten Superkontraktionsstufe von Wollfasern in 8M LiBr (20°C) blieb durch Einbringen von 1N HCl in die Lösungen ungeändert, während das Ausmass der gesamten Superkontraktion (98,5°C) durch Anwesenheit von HCl in der LiBr-Lösung stark hinaufgesetzt wurde. In gleicher Weise wurde bei reduzierter und methylierter Wolle die Beziehung zwischen dem Ausmass der ersten Superkontraktionsstufe und dem Gehalt an Restdisulfid durch die Anwesenheit von HCl in der Lösung nicht beeinflusst. Bei der Superkontraktion von reduziert-methylierten Wollfasern mit wenigen Restdisulfidgruppen in 8M LiBr-Lösungen mit variiertem Konzentration an HCl kontrahierten sich die Fasern rasch bis in die Nähe des Ausmasses der Gesamtsuperkontraktion in neutraler Lösung. Hier änderete sich die Geschwindigkeit schlagartig und wurde der Säurekonzentration in der Lösung proportional. Starke Superkontraktion wurde auch in alkalischer LiBr-Lösung bei vorhergehender Äthylierung der Carboxylgruppen der reduziert-methylierten Fasern zur Herabsetzung der Löslichkeit der Wollproteine beobachtet. Rindenzellen, die durch Digestion reduzierter und methylierter Wolle mit rohem Trypsin dargestellt wurden, ähnelten in ihrem Verhalten der Wolle. Man kam zu dem Schluss, dass Wolle kovalente Vernetzungen enthält, die durch Säuren und Alkalien hydrolysiert werden. Es werden Belege für die Stabilisierung dieser Bindungen durch Disulfidvernetzungen beigebracht. Die Möglichkeit eines Disulfidaustausches während der Superkontraktion in LiBr-HCl-Lösungen wird diskutiert.

Received October 4, 1962

## A Scattered-Light Study of Linear Polyethylenes

CARL J. STACY and RAYMOND L. ARNETT, *Research and Development Department, Phillips Petroleum Company, Bartlesville, Oklahoma*

### Synopsis

A scattered-light photometer particularly adapted to high temperature work has been designed and constructed. Among the desirable features are constant monitoring of the primary beam, placement of photodetectors outside the heated zone, output proportional to ratio of outputs of matched detectors, thus to Rayleigh's ratio, insensitivity of output readings to light absorption by the solution, temperature control from room temperature to 150°C. The geometrical factors affecting output readings have been analyzed and the instrument calibrated using several standards. Techniques developed for hot solution clarification and the measurement with good precision of weight-average molecular weights of ethylene polymers are described. The results for several typical unbranched Marlex polyethylenes are given covering the range 80,000-170,000. Depending on the polymer, the ratio weight-average to number-average varies from 10 to 16 for whole polymer. The  $z$ -average molecular weights estimated from the mean-square molecular radii are used to estimate  $\bar{M}_z/\bar{M}_w$  ratios.

### I. INTRODUCTION

Light-scattering techniques are now widely used in the determination of weight-average molecular weights of high polymers,<sup>1</sup> and a number of applications to polyethylenes of various types have been reported.<sup>2-15</sup> One notes that the precision for these applications usually falls short of that generally obtainable from the technique. This lack of precision is probably a result of working above room temperature both in the preparation of clarified solutions and in instrumentation.

Weight-average molecular weights of polyethylene are useful alone for a partial characterization of the polymer and, in conjunction with number-average molecular weights from other techniques, give an indication of distribution breadth. Light-scattering data, including second virial coefficients and mean square molecular radii, are valuable in polymer structure studies. The value of these parameters is sometimes limited by the precision of the data. Indeed it is often a major problem in light-scattering work even at room temperature to obtain sufficiently dust-free solutions, and to develop proper instruments for the precision desired. We felt however that that level of precision obtainable at room temperature should also be possible at polyethylene solution temperatures. The objective of this work was development of techniques to obtain such precision with polyethylene solutions.

## II. EXPERIMENTAL

### Instrumentation

The scattered-light photometer used for this work was developed in our laboratory. A block diagram of the equipment is shown in Figure 1. The various optical elements are numbered one through eighteen, and the electrical elements are labeled as to function.

The light source (1) is an air-cooled high pressure mercury lamp, BH-6, manufactured by the General Electric Company. The light assembly is mounted in an aluminum box through which air is drawn to be vented outside of the laboratory. A Fiberglas liner reduces air jet noise.

Light passes through a hole in the side of the box and thence through an interference filter (2). Wavelengths of 4050, 4358, 5460, or 5780 Å. can be isolated by interchangeable filters at this position. An achromatic lens (3) focuses an image of the source at the position of the circular limiting aperture (6). Apertures (4) and (6) together determine the total flux in the primary beam. A Polaroid disc may be placed in the beam at position (5) when desired.

An achromatic lens (8) focuses an image of aperture (6) at the center of the cell. Apertures (7), (9), (10), and (11) placed in the light path minimize stray light pickup. To avoid introduction of stray light by scattering from an aperture surface, (10) and (11) are nonlimiting. All optical elements (1) through (8) are mounted on a rigid optical bench, and are enclosed in tubing coated with flat black.

A cylindrical, light-scattering cell of the Witnauer type<sup>16</sup> is cemented with an epoxy resin to a ring with guide pins which optically align the cell on a cell table at the center of a light-tight, cylindrical chamber. The chamber serves as an electrically heated air bath with regulated heat input to maintain the cell temperature constant up to 150°C.

The primary beam, after passing through the cell and out of the cell

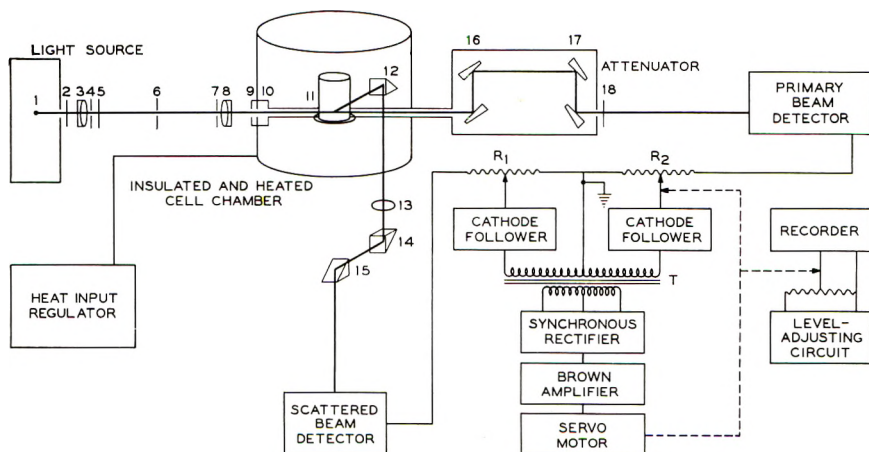


Fig. 1. Block diagram of the light-scattering instrument.

chamber, encounters an attenuator, which reduces the intensity to approximately the same level as that in the scattered beam. Similar matched light detectors can then be used.

This attenuator consists of two elements (16) and (17), each containing two optical glass wedges with a wedge angle of  $10^\circ$ . The wedges are so positioned that only the front surface reflection passes through the system; the remainder is eventually absorbed. In element (16) the two front faces are parallel and each set at the polarizing angle,  $33^\circ$ , to the optic axis. This assembly is permanently positioned around the beam axis at an angle of  $45^\circ$  from either the vertically or horizontally polarized component of the beam so that it attenuates both equally. The output beam from (16) is thus totally polarized perpendicular to the incident plane of this element. Element (17) is of similar design, but with the front wedge faces set at  $45^\circ$  to the optic axis. The incident plane of (17) is at  $90^\circ$  to that of (16) to give maximum attenuation.

The overall attenuation factor was calculated to be  $8.13 \times 10^{-7}$  for unpolarized incident light. Further attenuation, though not normally necessary, is available by use of one of three neutral filters (18). This arrangement furnishes light to the face of the primary beam photomultiplier which is always polarized in the same direction no matter what the state of polarization of the primary beam. Effects caused by photomultiplier response to polarization are thus eliminated.

Light scattered from the cell is picked up by a periscope and reflected out of the hot cell compartment. The periscope consists of prisms (12), (14), and (15), and lens (13) which collimates the light to the detector. The solution can be kept at elevated temperature while the photomultipliers are isolated from heat at all times. The periscope can be rotated about the cell axis by a motor driven gear train. The angular position of the periscope is read directly from a Veeder counter.

The electronic circuit consists of two similar light detectors, a ratio circuit, and servo loop which drives an indicator dial and recorder circuit. The detectors are end-on photomultiplier tubes, RCA type 6217, with the outputs coupled to  $R_1$  and  $R_2$  through cathode follower circuits to give a stable, low impedance output. This type photomultiplier was chosen for its relatively constant response with wavelength.

The 120-cycle modulation of the light allows use of alternating current circuits, and eliminates dark current of the photomultipliers.  $R_1$  and  $R_2$  are matched, precision potentiometer circuits calibrated to 0.01% full scale. The servo circuitry was designed to operate  $R_2$  with zero signal at T. Cathode followers are also used in coupling to T because of their stability. Provisions were made to switch  $R_1$  to accept the output voltage of the scattered-beam detector as does  $R_2$ ; a control balances the circuit so that the  $R_2$  dial comes to the same reading as the  $R_1$  dial. Thus when  $R_1$  is switched to the scattered-beam detector the ratio  $R_2/R_1$  is proportional to the ratio of scattered light to transmitted light and thus to Rayleigh's ratio.  $R_1$  is normally operated at full scale (1.0000).

This instrument not only compensates for light source fluctuations as do other instruments using ratio circuits<sup>17</sup> but also eliminates beam attenuation errors as do the Brice-type instruments using the same length light path for scattered and transmitted light.<sup>18</sup>

### Performance and Calibration

The reading of this photometer is proportional to Rayleigh's ratio but since the detector views the scattering volume through a lens composed of polymer solution the proportionality constant depends upon the refractive index of the solution. Hermans and Levinson<sup>19</sup> analyzed this dependence, which we call  $f(n)$ , and found that it depends upon whether the detector sees past the edges of the scattering volume. When it does not, they found  $f(n) = 1/n^2$ .

The detector in our photometer does see past the edges of the scattering volume and also differs in other geometrical aspects from the cases discussed by Hermans and Levinson. The mathematical approach of these authors has been applied to the case where the scattered-beam detector sees past the edges of a cylindrical primary beam; it was found that

$$f(n) = 1/n[n(d_2 - d_0) + d_0 + t(n/n_0 - 1)]$$

where  $d_2$  is the distance from the center of the scattering volume to the farther of the two aperture stops which define the field of view of the detector,  $d_0$  is the distance of the outside cell wall from the scattering volume,  $t$  is the thickness of the cell wall, and  $n_0$  is the refractive index of the cell wall. The analysis which gives the above result also reveals that, for a given angular resolution, the maximum signal is obtained when the area of the farther aperture stop (defining the scattered beam) is twice that of the nearer for the case where the scattered-beam detector sees past the edges of the primary beam; they should be the same size for the case examined by Hermans and Levinson.

The scattering volume was found to be proportional to  $1/\sin \theta$ , both by calculation and by measurements with fluorescein solutions. Angular measurements of scattering from toluene, using vertically polarized light in the primary beam, confirmed this and also indicated a low level of stray light over the angular range 30–150°; these limitations are imposed by the cell.

Calibration was made at 4358 and 5460 Å., using the Cornell standard polystyrene.\* The value of apparent turbidity for a 0.5 g./100 ml. solution was taken as  $1.36 \times 10^{-6} \text{ cm.}^{-1}$  for 5460 Å. This is an average of several published values.<sup>20</sup> The calibration constant determined by this procedure was checked by measurements of Rayleigh's ratio for both benzene and toluene (Phillips Research grade) after distillation directly into the cell using an all-glass still. The averages of literature values<sup>20</sup> used for our work are  $16.6 \times 10^{-6} \text{ cm.}^{-1}$  for benzene and  $19.8 \times 10^{-6} \text{ cm.}^{-1}$  for

\* Furnished through the courtesy of P. Debye. A summary of values of Rayleigh's ratio of the standard polystyrene is given by Carpenter and Krigbaum.<sup>20</sup>

toluene, both values for 4560 Å. Periodic checks of the calibration show satisfactory instrument stability.

### Specific Refractive Increment

An alternative to direct experimental measurement of the quantity  $\partial n/\partial c$  was found informative. Carr and Zimm<sup>21</sup> and others have approximated  $\partial n/\partial c$  by

$$\partial n/\partial c = (n' - n)/d'$$

where  $n$  is refractive index of solvent, and  $n'$  and  $d'$  are refractive index and density of polymer, respectively. We also use this relation. Measurements of  $n$  and  $d$  over a temperature range were smoothed for temperature by noting that  $(n - 1)/d$  for 1-chloronaphthalene is essentially temperature-independent, values being 0.56256 at 4358 Å. and 0.53415 at 5460 Å. For the polymer  $n'$  and  $d'$  are not directly measurable. Li et al.<sup>22</sup> describe a method of correlating these physical properties with alkyl chain length for liquid  $n$ -alkyl compounds, in which  $n_\infty$  at 5890 Å. and  $d_\infty$ , both at 25°C. were found for the limit at high chain length. Here we assume that real polyethylene chains correspond to this limit and borrow their correlation methods for use at other temperatures and wavelengths. The quantity  $d_\infty$  for liquid state has previously been correlated with temperature, by one of us (RLA) according to the expression

$$d_\infty = 0.86379 - 0.0005126t$$

where  $t$  is in degrees Centigrade.

To calculate  $n'$ , values of  $n$  at the desired wavelengths are available<sup>23-25</sup> for C<sub>7</sub>, C<sub>9</sub>, C<sub>11</sub>, C<sub>13</sub>, C<sub>14</sub>, C<sub>15</sub>, and C<sub>16</sub> at 20, 25, and 30°C. Data at higher temperatures are limited; however, measurements have been reported for C<sub>16</sub> and C<sub>36</sub> over the range 80-100°C.<sup>26</sup> Li et al.<sup>22</sup> found the equation

$$R = R_0 + a_r N$$

to correlate data for alkanes and 1-alkenes, where  $R$  is the Lorentz-Lorenz molal refraction, and  $N$  is the number of carbon atoms in the alkyl chain. As  $N$  approaches infinity, the Li relation for molal volume  $V$  approaches

$$V = V_0 + a_v N$$

and

$$(R/V)_\infty = (n_\infty^2 - 1)/(n_\infty^2 + 2) = a_r/a_v$$

For present purposes  $a_r$  was calculated at 80 and 100°C. from data for C<sub>16</sub> and C<sub>36</sub> and for 20-30°C. from data for C<sub>7</sub>-C<sub>16</sub>. The constant  $a_v$  was obtained from

$$a_v = 14.026/d_\infty$$

Values of  $n'$  calculated from  $a_r/a_v$  are listed in Table I. Alternative routes to  $n'$  are possible, for instance, extrapolation of  $n$  for  $n$ -paraffins to the desired temperatures and then to  $1/N = 0$ . Curvature was encountered



TABLE I  
Specific Refractive Increment Values for Polyethylene in 1-Chloronaphthalene

$t$ , °C.	$n'$ (4358 Å.)	$\partial n/\partial c$ (4358 Å.)	$n'$ (5460 Å.)	$\partial n/\partial c$ (5460 Å.)
20	1.48689	0.2176	1.47866	0.1874
25	1.48622	0.2162	1.47743	0.1868
30	1.48467	0.2160	1.47601	0.1865
80	1.46604	0.2170	1.45790	0.1873
100	1.45979	0.2158	1.45183	0.1861

in the latter plot, but  $n'$  values so obtained were in agreement with those given. Values of  $\partial n/\partial c$  from  $(n' - n)/d$  are given in the table for various temperatures. Though polyethylene is insoluble over most of this range, the small temperature dependence enables easy extrapolation of the results to any range desired. A plot of  $\partial n/\partial c$  versus  $t$  appears in Figure 2, along with several measurements that have been reported and recently summarized by Billmeyer.<sup>27</sup> With one exception, agreement between the present approach and the measured values above 100°C. is satisfactory. We have chosen to use the value 0.191 cc./g. (at 125°C.,  $\lambda = 5460$  Å.) to facilitate comparison with most of the molecular weight data that have appeared in the literature.

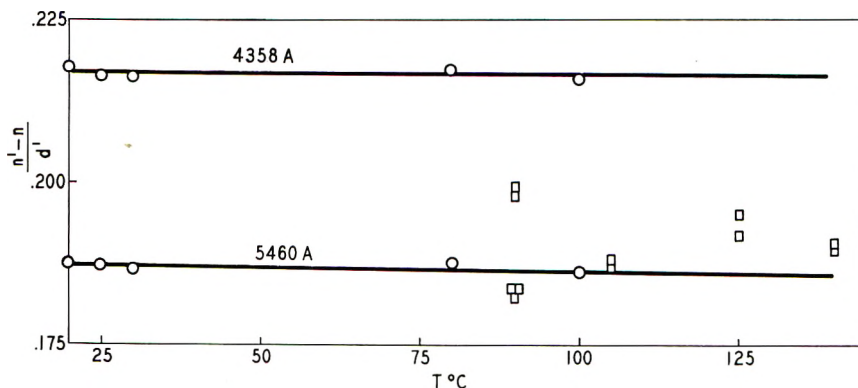


Fig. 2. Comparison of values of specific refractive increment of polyethylene in 1-chloronaphthalene: (O) calculated; (□) literature values.<sup>27</sup>

One also obtains, from the above, values of  $\partial n/\partial c$  for 4358 Å. as a function of temperature. Also, it is a means for estimating  $\partial n/\partial c$  for polyethylene for other solvents and temperatures; for instance, we calculate 0.0955 for *n*-decane at 115°C. which is in agreement with the value 0.095 experimentally measured by Billmeyer.<sup>27</sup> As expected, calculations show  $\partial n/\partial c$  to fall off rapidly with increasing chain length in the paraffins (at 100°C., 5460 Å.,  $\partial n/\partial c = 0.112$  for  $C_8$ , 0.100 for  $C_9$ , 0.092 for  $C_{10}$ , and 0.041 for  $C_{16}$ ).

**Materials**

The solvent, 1-chloronaphthalene (Eastman, white label), was purified by passage through a column of silica gel which had been activated by heating to 175°C. for several hours. This procedure removed traces of moisture which seriously interfered in preliminary attempts at clarification. In addition some colored contaminants are removed by the column. Only polyethylene samples showing no extraneous infrared bands were used and representative sampling of pelleted material was insured by reducing particle size in a Wiley mill.

**Solution Clarification**

We prefer to use filtration for clarification of linear polyethylene solutions. The commercially available type H A Millipore filters yield clean

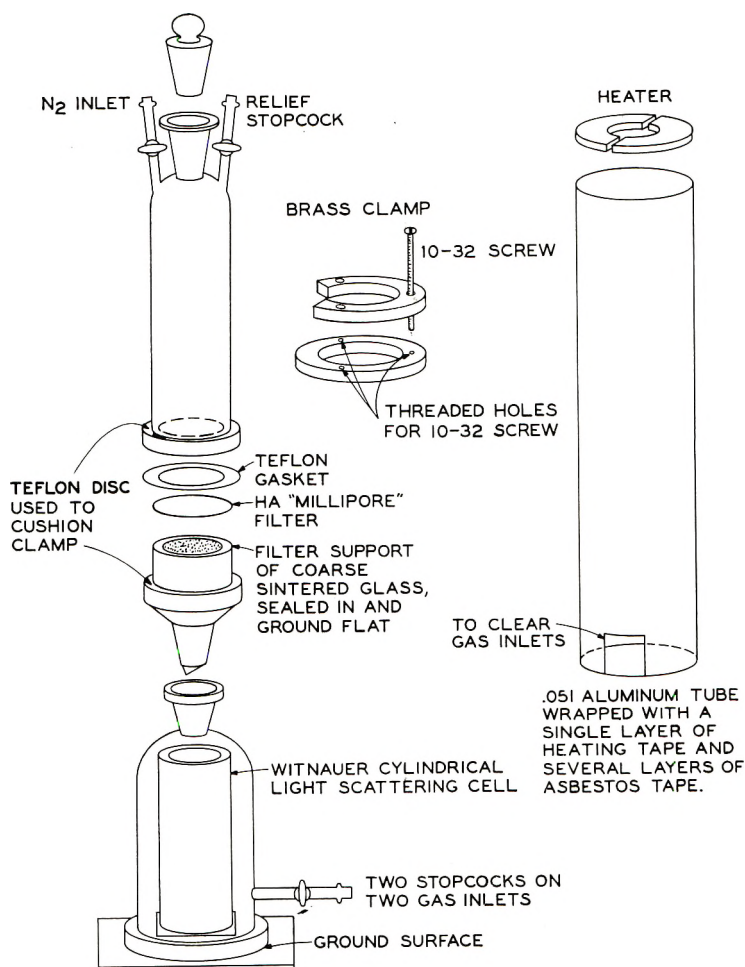


Fig. 3. Filtration apparatus for filling light-scattering cells.

solutions. A filter apparatus constructed for use of these filters at elevated temperatures is shown in Figure 3.

In a typical run about 100 ml. of 1-chloronaphthalene is recycled through the filter at room temperature until free of motes, using a filter pad that had been pre-extracted at elevated temperature. Two cells are cleaned in this manner. A 30-ml. portion is retained in one cell for measurement of solvent scattering, and the cells covered and placed in an oven at 125°C. The remaining solvent is used to prepare a solution at 125°C. of 0.01 g./ml. protected by a nitrogen atmosphere.

The heater is placed over the filter assembly, and the whole heated to 125°C. while maintaining slight nitrogen pressure in the top chamber. As soon as solution is complete, the hot pre-cleaned cell is placed under the assembly and the hot solution poured into the top chamber. By means of low nitrogen pressure, the sample is filtered directly into the clean cell. The cell is covered immediately and replaced in the oven.

The cell containing solvent is allowed to come to temperature equilibrium at 125°C. in the photometer before taking measurements. Output dial readings are made over the angular range 30–140° at ten-degree intervals, using unpolarized light.

The desired concentrations are obtained by adding increasing portions of stock solution to the solvent-containing cell. The cell and contents are quickly weighed to 0.1 g. after each addition. These measurements are repeated at each concentration, each time allowing for temperature equilibrium. From knowledge of cell weight, solvent weight, and each increment weight, concentrations may be calculated to one per cent. Checks of the last concentration by polymer recovery have shown that this procedure is satisfactory and that loss of polymer on the filter is negligibly low.

Repeat measurements on solutions held at 125°C. up to 96 hr. gave no serious changes in scattering level, showing that little degradation occurs during a run in spite of some contact with air. Infrared examination of several samples of recovered polymer revealed no significant spectral changes.

### III. RESULTS

With unpolarized light in the primary beam, the quantity  $R(\theta, c)/(1 + \cos^2\theta)$  is related to the thermodynamic and optical properties of the polymer in solution. The instrument output dial readings  $M$  are converted to Rayleigh's ratio  $R(\theta, c)$  by

$$R(\theta, c)/(1 + \cos^2\theta) = K'[f(n)]^{-1}[M(\theta, c)(\text{solution}) - M(\theta)(\text{solvent})] \sin\theta/(1 + \cos^2\theta)$$

Here  $K'$  is the calibration constant,  $c$  is the concentration of the polymer solution, and  $\theta$  is the angle the scattered beam makes with the primary beam. The quantity  $[f(n)]^{-1}$  is given very approximately by

$$[f(n)]^{-1} = n(17.2n + 2.16)$$

for the cylindrical cell in our instrument.

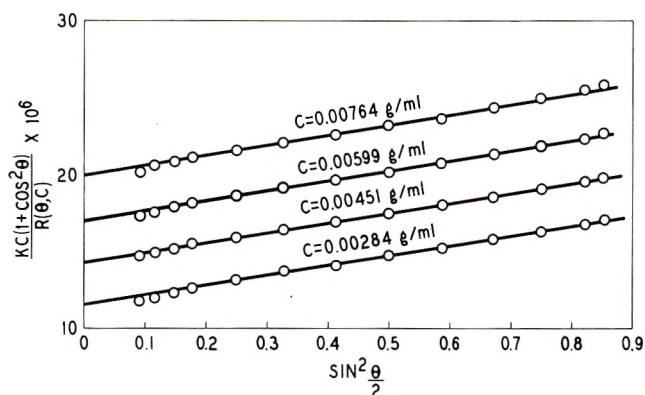


Fig. 4. Angular dependence plots for a Marlex polyethylene.

In treating our data to obtain weight-average molecular weights, the intercept in a conventional Zimm plot was found to lack precision as a result of curvature in the concentration dependence of  $Kc(1 + \cos^2\theta)/R(\theta, c)$ ;  $K = 2\pi^2 n_0^2 \lambda^{-4} N_0^{-1} (\partial n / \partial c)^2$ ,  $n_0$  being the refractive index of the solvent and  $N_0$  Avogadro's number. However, the angular dependence of  $Kc(1 + \cos^2\theta)/R(\theta, c)$  was linear; a typical plot of this quantity versus  $\sin^2(\theta/2)$  is displayed in Figure 4. An infrequent slight drop-off at low angles is attributed to trace dust contamination.

In order to account for the observed concentration dependence (for maximum polymer concentrations of about 0.02 g./ml. in early work and currently, with greater instrument sensitivity, below 0.01 g./ml.), we are obligated to use an equation of the form

$$\frac{Kc(1 + \cos^2\theta)}{R(\theta, c)} = \frac{1}{\bar{M}_w} \left[ \frac{1}{P_z(\theta)} + 2\Gamma_2 c + B(\theta)c^2 \right]$$

In this,  $P_z(\theta)$  is the  $z$ -average "particle scattering factor,"  $\Gamma_2$  (neglecting a possible slight angular dependence), is the second virial coefficient in the virial expansion of osmotic pressure  $\pi$

$$\pi/c = (RT/M)(1 + \Gamma_2 c + \Gamma_3 c^2 + \dots)$$

and  $B(\theta)$  is the coefficient of  $c^2$  given by Zimm.<sup>28</sup> Important to us here is the fact that  $B(\theta)$  approaches  $3\Gamma_3$  as a limit when  $\theta$  approaches zero;  $\Gamma_3$  is the third virial coefficient. Thus for  $\theta = 0$ , the concentration dependence should be given by

$$2Kc/R(0, c) = (1/\bar{M}_w)(1 + 2\Gamma_2 c + 3\Gamma_3 c^2)$$

It was found for linear polyethylene in 1-chloronaphthalene that the square roots of the intercepts of the curves from plots as in Figure 4 form straight lines when plotted against concentration, as in Figure 5. Such plots are often successfully applied to osmotic pressure data,<sup>29</sup> showing  $\Gamma_3 \cong \Gamma_2^2/4$ ; linearity in the present case implies that  $\Gamma_3$  is approximately equal to  $\Gamma_2^2/3$ .

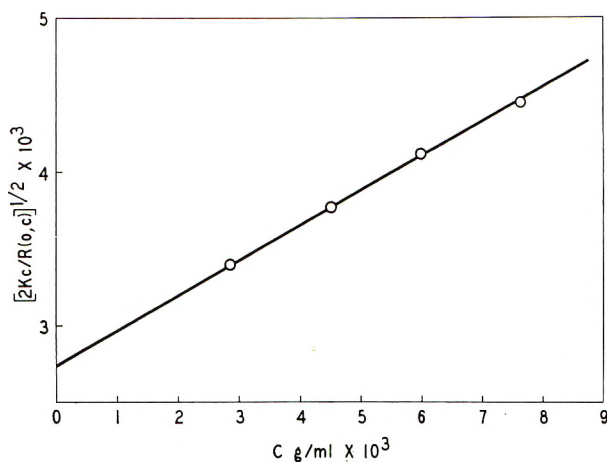


Fig. 5. Concentration dependence plot for a Marlex polyethylene.

The slopes of the angular dependence lines in Figure 4 do not vary with concentration. This slope gives the  $z$ -average of the mean-square distance of each mass unit from the center of gravity of the molecule, which is calculated by means of the usual expression

$$(\overline{r^2})_z = \frac{3\lambda^2}{16\pi^2 n^2} \left[ \frac{\text{initial slope}}{\text{intercept}} \right]$$

The square root of this quantity is hereafter designated by  $s$ .

TABLE II  
Light-Scattering Results for Several Polyethylenes

Polymer	$\overline{M}_w \times 10^{-3}$	Precision of $\overline{M}_w$ <sup>a</sup>	$s$ , A	$\overline{M}_w/\overline{M}_n$ <sup>b</sup>	$5.10s^2/\overline{M}_w$
1	92	A	400	11.4	9
2	82	A	370	10.1	9
3	101	B	390	11.4	8
4	88	A	410	10.5	10
5	104	B	330	10.7	5
6	118	A	435	10.6	8
7	122	A	400	11.6	7
8	133	A	440	11.4	7
9	165	B	460	12.4	7
10	122	B	430	15.7	8
Fractions					
A	8.3	C	200	3.0	25
B	39.0	C	245	4.3	7
C	94.0	B	375	5.7	8
D	167.0	B	450	6.4	6
E	196.0	B	510	6.0	7

<sup>a</sup> Estimated standard deviation of  $\overline{M}_w$ : (A) 3%; (B) 6%; (C) 9%.

<sup>b</sup> Number-average molecular weights from Arnett, Smith, and Buell.<sup>30</sup>

Some representative results are summarized in Table II. Precision of  $\bar{M}_w$ , estimated on an individual basis, varied considerably because of the state of development of the technique at the time each individual run was made. In the extrapolation to zero angle, the low and essentially linear angular dependence resulted in good precision, and the above treatment of the concentration dependence gave satisfactory precision in the concentration extrapolation. In the table,  $M_w$  values are classified A, B, or C, where standard deviations are estimated to be not more than 3, 6, or 9% of the value, respectively. The standard deviation of  $s$  is estimated as about 25  $\text{\AA}$  for values of  $s$  near 400  $\text{\AA}$ . These estimates were made from experience and do not imply a complete statistical analysis in each case. The results compare favorably with the better data in the literature for which the high-temperature problems of polyethylene work are absent.

#### IV. DISCUSSION

Our values of  $\bar{M}_w$  are lower than those that have been reported (values in excess of  $1 \times 10^6$  have appeared) for branched polyethylene.<sup>2-4,7,11,14</sup> A "microgel" component which has caused clarification trouble with branched polyethylenes<sup>4,14</sup> was absent in the polymers that we studied. Our  $M_w$  values are comparable with those reported by others for linear polyethylenes of similar intrinsic viscosity.<sup>5,6,8,9,16</sup> Correlations with intrinsic viscosity and with melt index were made using these data. The observation scatter is comparable to that usually found for such correlations, and values of the determined parameters are similar. Specifically, for viscosity measurements made at 130°C. on tetrahydronaphthalene solutions of whole polymer we find the constants in

$$[\eta] = 3.78 \times 10^{-4} \bar{M}_w^{0.72}$$

satisfactorily correlate all the molecular weight observations we have made, a part of which are listed in Table II.

The ratio  $\bar{M}_w/\bar{M}_n$ , where  $\bar{M}_n$  is the number-average molecular weight, is frequently given as a measure of the breadth of the molecular weight distribution of high polymers. Few instances of absolute measurements of both averages on the same linear polyethylene samples have been reported. Ebullioscopic measurements of these materials are reported elsewhere;<sup>30</sup> the values of  $M_n$  reported there are used to calculate the  $\bar{M}_w/\bar{M}_n$  ratios given in column 5 of Table II. The values of  $\bar{M}_w/\bar{M}_n$  for these polyethylenes are higher than those for other linear polymers (e.g., polystyrene). This is true even for the fractions included, though values here are much lower. Thus the suggestion of Raman and Hermans<sup>10</sup> that  $\bar{M}_w/\bar{M}_n$  is "normal," (meaning less than about three) for linear polyethylenes including Marlex polyethylenes must be rejected.

The quantity  $s$  can be used to approximate  $\bar{M}_z$  if certain assumptions are made, and  $\bar{M}_z/\bar{M}_w$  provides another index of distribution breadth. Hoeve<sup>31</sup> has most recently calculated the effect of hindrances to rotation on the conformation of linear polymethylene chains. The relationship

$$\bar{M}_z = 5.01s^2$$

is obtained from the results of his calculations for a temperature of 125°C. This would be expected to be applicable only for systems with no chain branching and no solvent effect on configuration. The former has been established for Marlex polyethylene.<sup>32</sup> Preliminary results of work now in progress in our laboratory, including both viscosity and light-scattering work in a  $\theta$ -solvent, indicate that the latter effect is not large. Relative values, at least, should be significant. Values of  $5.10s^2/M_w$  so calculated are given in column 6 in Table II.

Mr. E. C. Miller designed and constructed the mechanico-optical parts of our instrument and Mr. E. J. Marak undertook the same tasks for the electronic circuitry. Prof. P. Debye kindly supplied us with a sample of the Cornell Standard polystyrene.

### References

1. See, for instance, M. M. Fishman, *Light Scattering by Colloidal Systems: An Annotated Bibliography*, Technical Service Laboratories, River Edge, N. J., January, 1957 (also additional annual supplements).
2. Billmeyer, F. W., Jr., *J. Am. Chem. Soc.*, **75**, 6118 (1953).
3. Moore, L. D., Jr., *J. Polymer Sci.*, **20**, 137 (1956).
4. Muus, L. T., and F. W. Billmeyer, Jr., *J. Am. Chem. Soc.*, **79**, 5079 (1957).
5. Atkins, J. T., L. T. Muus, C. W. Smith, and E. T. Pieski, *J. Am. Chem. Soc.*, **79**, 5089 (1957).
6. Duch, E., and L. K uchler, *Z. Elektrochem.*, **60**, 218 (1956).
7. Nicolas, M. L., *Compt. Rend.*, **244**, 80 (1957).
8. Henry, P. M., *J. Polymer Sci.*, **36**, 3 (1959).
9. Chiang, R., *J. Polymer Sci.*, **36**, 91 (1959).
10. Raman, N. K., and J. J. Hermans, *J. Polymer Sci.*, **35**, 71 (1959).
11. Trementozzi, Q. A., *J. Polymer Sci.*, **23**, 887 (1957).
12. Kobayashi, T., A. Chitale, and H. P. Frank, *J. Polymer Sci.*, **24**, 156 (1957).
13. Trementozzi, Q. A., *J. Polymer Sci.*, **36**, 113 (1959).
14. Moore, L. D., Jr., and V. G. Peck, *J. Polymer Sci.*, **36**, 141 (1959).
15. Tung, L. H., *J. Polymer Sci.*, **36**, 287 (1959).
16. Witnauer, L. P., and H. J. Sherr, *Rev. Sci. Instr.*, **23**, 99 (1952).
17. McIntyre, D., and G. C. Doderer, *J. Res. Natl. Bur. Std.*, **62**, 153 (1959).
18. Brice, B. A., M. Halwer, and R. Speiser, *J. Opt. Soc. Am.*, **40**, 768 (1950).
19. Hermans, J. J., and S. Levinson, *J. Opt. Soc. Am.*, **41**, 460 (1951).
20. Carpenter, D. K., and W. R. Krigbaum, *J. Chem. Phys.*, **24**, 1041 (1956).
21. Carr, C. I., and B. H. Zimm, *J. Chem. Phys.*, **18**, 1616 (1950).
22. Li, K., R. L. Arnett, M. B. Epstein, R. B. Ries, L. P. Bitler, J. M. Lynch, and F. D. Rossini, *J. Phys. Chem.*, **60**, 1400 (1956).
23. Forziati, A. F., *J. Res. Nat. Bur. Std.*, **44**, 373 (1950).
24. Camin, D. L., and F. D. Rossini, *J. Phys. Chem.*, **59**, 1174 (1954).
25. Camin, D. L., A. F. Forziati, and F. D. Rossini, *J. Phys. Chem.*, **58**, 440 (1954).
26. Lauer, J. L., and R. W. King, *Anal. Chem.*, **28**, 1697 (1956).
27. Billmeyer, F. W., Jr., Paper presented at the 139th National Meeting of the American Chemical Society, St. Louis, Mo., March, 1961.
28. Zimm, B. H., *J. Chem. Phys.*, **16**, 1093 (1948).
29. Flory, P. J., *Principles of Polymer Chemistry*, Cornell Univ. Press, Ithaca, N. Y., 1953, Chapter 7.
30. Arnett, R. L., M. E. Smith, and B. O. Buell, *J. Polymer Sci.*, **A1**, 2753 (1963).
31. Hoeve, C. A. J., *J. Chem. Phys.*, **35**, 1266 (1961).
32. Smith, D. C., *Ind. Eng. Chem.*, **48**, 1161 (1956).

### Résumé

On a imaginé et construit un photomètre spécialement adapté pour mesurer la lumière diffusée lors de travaux à température élevée. Cet appareil se caractérise surtout par une focalisation constante du faisceau primaire, l'emplacement des photodétecteurs situés en dehors de la zone chauffée, le signal de sortie proportionnel au rapport des signaux des détecteurs appariés, donc au rapport de Raleigh, l'indépendance des lectures vis-à-vis de l'absorption de la lumière par la solution, le contrôle de la température à partir de la température de chambre jusque 150°C. Les facteurs géométriques pouvant affecter les lectures ont été analysés et l'instrument a été calibré au moyen de plusieurs étalons. On décrit les techniques employées pour clarifier les solutions à chaud et pour mesurer avec une bonne précision les poids moléculaires moyens en poids de polymères d'éthylène. Les résultats obtenus pour plusieurs polyéthylènes Marlex non ramifiés sont donnés pour un domaine allant de 80.000 à 170.000. Suivant le polymère, le rapport de la moyenne en poids à la moyenne en nombre varie de 10 à 16 pour le polymère entier. Les poids moléculaires moyens  $\bar{M}_z$  estimés à partir du carré moyen du rayon moléculaire ont été employés pour estimer les rapports  $\bar{M}_z/\bar{M}_w$ .

### Zusammenfassung

Ein besondere für Hochtemperaturuntersuchungen geeignetes Streulichtphotometer wurde entworfen und gebaut. Zu den erwünschten Eigenschaften gehören konstante Kontrolle des Primärstrahls, Anbringung der Photodetektoren ausserhalb der Erhitzungszone, Anzeige proportional zum Verhältnis der Anzeigeablesung abgeglicherer Detektoren, daher zum Rayleigh-Quotienten, Unempfindlichkeit der Anzeigeablesung gegen Lichtabsorption in der Lösung, Temperatureinstellung von Raumtemperatur bis 150°C. Eine Analyse der für die Anzeigenablesung wichtigen geometrischen Faktoren wird durchgeführt und das Instrument mit einigen Standards kalibriert. Verfahren zur Klärung heisser Lösungen werden entwickelt und die Bestimmung des Gewichtsmittels des Molekulargewichts von Äthylenpolymeren mit guter Genauigkeit wird beschrieben. Ergebnisse für mehrere typische unverzweigte Marlex-Polyäthylene im Bereich von 80,000 bis 170,000 werden mitgeteilt. Das Verhältnis Gewichtsmittel zu Zahlenmittel liegt für unfraktionierte Polymere zwischen 10 und 16. Das aus dem mittleren Quadrat des Molekülradius bestimmte  $Z$ -Mittel des Molekulargewichts wird zur Berechnung des Verhältnisses  $\bar{M}_z/\bar{M}_w$  verwendet.

Received April 17, 1962

Revised October 10, 1962



## Low Temperature Solution Polycondensation of Piperazine Polyamides

PAUL W. MORGAN and STEPHANIE L. KWOLEK, *Pioneering Research Division, Textile Fibers Department, E. I. du Pont de Nemours & Company, Inc., Wilmington, Delaware*

### Synopsis

A simple process is described for the preparation of condensation polymers from diamines and diacid halides, which comprises reacting equivalents of the intermediates at about room temperature in an inert solvent together with an acceptor for the by-product acid. This first paper of a series discusses the formation of polyamides from piperazines and aliphatic and aromatic diacid chlorides. Examples are poly(sebacyl piperazine) and poly(terephthaloyl dimethylpiperazine). Such variables are discussed as types of acid acceptors, solvents, reactant balance, interfering reactions, and the mechanism of the reaction. Some of the polymers are described briefly in terms of melt temperature, solubility, and molecular weight-viscosity relationships.

### INTRODUCTION

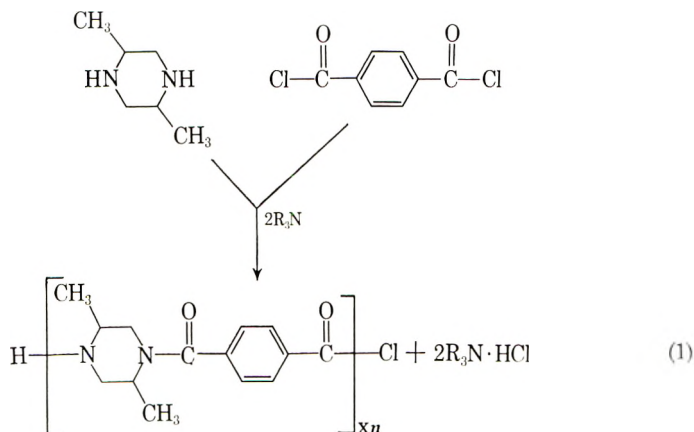
This and succeeding papers will describe a remarkably simple process for the formation of high molecular weight condensation polymers from diamines at normal temperatures in the presence of organic solvents. The method is designated broadly "solution polycondensation" although the process encompasses systems in which the reactants and polymer stay dissolved as well as systems in which the reactants are not all dissolved at the start and a great many from which the polymer precipitates.

The method comprises simply bringing together fast-reacting intermediates in an inert liquid medium and providing for the removal of acidic by-products by means of basic additives (acid acceptors). Solution polycondensation can be used to prepare many classes of polymers such as polyamides, polysulfonamides, polyureas, polyurethanes, and polyphenyl esters. Copolymers and block copolymers may be prepared by proper admixing of the reactants.

Recent papers from this laboratory<sup>1-5</sup> have described low temperature polycondensation methods which employ two immiscible liquid phases, one of which is usually water. This interfacial polycondensation method is broadly useful. However, water causes rapid hydrolysis of some acid halides and thereby interferes with slow polycondensation reactions; the use of water-insoluble diamines requires special procedures; and water-miscible solvents, such as acetone, are not useful. Solution polycondensa-

tion not only provides an additional method of making polymers from diamines, but complements the interfacial polycondensation procedure and provides a new degree of freedom in polymer making. It also sheds new light on the mechanism of low temperature polycondensations.

In this paper the method will be illustrated in detail with only one type of polymer, the polyamides formed from piperazine and diacid halides, and in particular, with the polymer from *trans*-2,5-dimethylpiperazine and terephthaloyl chloride, as in (1).



The code, 2,5-DMePip-T polyamide, is used throughout the text to designate the polymer from the *trans* isomer.

## LITERATURE

There are many references in the patent literature to the formation of polymers at temperatures below about 100°C. from diacid halides or diisocyanates and complementary reactants, such as diamines, glycols, and bisphenols in the presence of organic solvents. While most of these preparations undoubtedly formed polymers of some sort, there is often no clear evidence in the form of viscosity numbers or other data to show that high polymers were obtained.

The patents of Carothers<sup>6</sup> point out that diacid halides and diamines may be reacted in a solvent such as benzene to give a polyamide, but heat is suggested as a finishing step. Berchet<sup>7</sup> describes polysulfonamides prepared in organic solvents. Low viscosity numbers are reported. Various British, German, and French patents<sup>8-11</sup> claim polyamides, polyureas, and polysulfonamides without satisfying descriptions of the products. Wolfrom, Toy, and Chaney<sup>12</sup> prepared polyamides having low intrinsic viscosities by reaction of tetra-*O*-galactaroyl dichloride with piperazine and ethylenediamine in benzene or chloroform.

The preparation of polycarbonates from bisphenols and phosgene in pyridine or pyridine with inert diluents has recently been described by Schnell<sup>13</sup> and by Fox and Goldberg.<sup>14</sup> These are truly high polymers.

Conix<sup>15</sup> has prepared poly(phenyl esters) with high molecular weight in a similar way. Acid halide reactions with diols differ from reactions with diamines in that the glycol or bisphenol does not compete with the acid acceptor for by-product acid. Dyer and Bartels<sup>16</sup> have clearly characterized a group of polyurethanes made in bulk and in organic solvents from diisocyanates and glycols, although the polymers made in solvent systems had rather low molecular weights. Recently, Lyman<sup>17</sup> has reported procedures for obtaining high molecular weight polyurethanes from aromatic diisocyanates and ethylene glycol in a solvent. Since no by-product is evolved in the isocyanate addition reactions, they are less complex than acid halide reactions.

The literature contains reports of a variety of other polycondensation reactions carried out in solution at low temperature. Some of these are aromatic diamines with phosgene;<sup>18</sup> sodium glycolate and succinyl chloride;<sup>19</sup> glycols with aliphatic diacids;<sup>20</sup> diamines with diesters;<sup>21</sup> glycols with diacid chlorides;<sup>22</sup> glycols with dianhydrides;<sup>23</sup> bisepoxides with diamines;<sup>24</sup> a dinitrile with a diol and dry hydrogen chloride to yield a polyimino ether;<sup>25</sup> hydrochlorides of amino acid chlorides<sup>26</sup> or thiophenyl ester hydrochlorides<sup>27</sup> of peptides with a solvent and a tertiary amine.

## EXPERIMENTAL

### Materials

Piperazine and methyl-substituted piperazines may be obtained from several commercial sources. They may be purified by distillation or in some cases by crystallization from acetone or methyl ethyl ketone. Anhydrous piperazine was made by treatment of the hexahydrate with alkali followed by azeotropic distillation of remaining water with benzene. Melting points and boiling points are given in Table I.

The *cis*-2,5-dimethylpiperazine was obtained with a 98% content of *cis* isomer by fractional crystallization in bulk followed by distillation. 2,3,5,6-Tetramethylpiperazine is known to occur in five stereoisomers.<sup>28</sup> The mixture obtained from the Jefferson Chemical Co., Houston, Texas, was separated into two fractions, which were the  $\alpha$ - and  $\beta$ -isomers.

TABLE I

	M.P., °C.	B.P., °C.
Piperazine	108	145.5
2-Methylpiperazine	65-66	156.0
<i>cis</i> -2,5-Dimethylpiperazine	17-18	165.5
<i>trans</i> -2,5-Dimethylpiperazine	118	162.0
<i>cis</i> -2,6-Dimethylpiperazine	114	162.0
2,2,5,5-Tetramethylpiperazine	83-84	174-175
$\alpha$ -2,3,5,6-Tetramethylpiperazine	45	177-178
$\beta$ -2,3,5,6-Tetramethylpiperazine	<0	183.0

Most piperazines are quite hygroscopic and discolor in air and light. *trans*-2,5-Dimethylpiperazine is excellent for study because in the pure state it does not form carbonates in the air, is not especially hygroscopic, and does not discolor for long periods of time in clear bottles. Nevertheless, excessive exposure to moist air and light should be avoided to assure continued reproducibility of results.

Terephthaloyl chloride (m.p. 81.2°C.) was purchased and also prepared from the acid and thionyl chloride with dimethylformamide as the catalyst. It was purified by crystallization from hot concentrated solution in dry hexane. Incomplete solubility of the acid chloride in hexane or other solvents indicates hydrolysis to acid and a need for a repurification. The acid chloride was placed under dry nitrogen in two-ounce bottles having polyethylene-lined caps, sealed with Scotch electrical tape (Minnesota Mining and Manufacturing Co.) and stored in a desiccator or dry box.

The tertiary amines were reagent grade chemicals which were distilled through a spinning-band column or a 10-in. helices-packed column to free them from water and primary or secondary amine. They were stored in amber bottles which were flushed with dry nitrogen after use. This precaution is not always necessary, but will prolong the useful life of the sample.

Most of the solvents were subjected to simple distillation. Chloroform was A.C.S. reagent grade which was freed of alcohol stabilizer by washing three times with an equal volume of water. It was first dried with calcium chloride and then stored over a mixture of equal parts of potassium carbonate and calcium chloride in a dark bottle. Washed chloroform which was well dried in the preliminary step was stable for several weeks. Decomposing chloroform yields hydrogen chloride and phosgene. These may be detected by moist litmus paper in the vapors or by the immediate development of turbidity upon the addition of a drop of ethylenediamine.

### Polymer Preparation

The high rate of formation of 2,5-DMePip-T polyamide (from *trans*-2,5-dimethylpiperazine and terephthaloyl chloride) in solution is shown in Figure 1. Procedure A was used with magnetic stirring and temperature controlling baths. In as little time as 15 sec., which was required for mixing and addition of a precipitant, a high yield of polymer having high molecular weight was formed. Thereafter, there was a slight increase in molecular weight for several minutes. Figure 2 shows that there was an increase in both yield and molecular weight when the temperature was lowered. This effect is ascribed to a lowering of the rate of side reactions in relation to the rate of polymerization. Except for these specific experiments, the polycondensation reactions were started at 25°C. or below.

The order of mixing, that is, diamine to acid chloride or acid chloride to diamine, was not critical when mixing was fast and equivalents of reactants were used. The addition of acid chloride to diamine is preferred ordinarily because the acid chloride solution is then not exposed to humid air in the

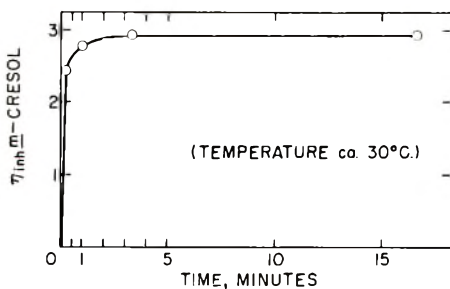


Fig. 1. Extent of polymerization vs. time for 2,5-DMePip-T polyamide prepared in chloroform.

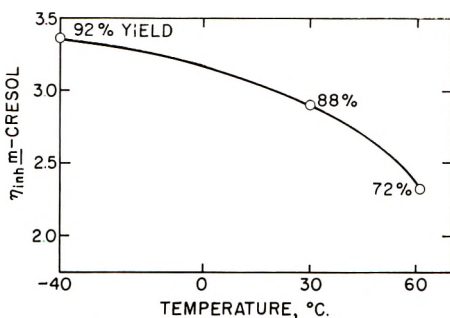


Fig. 2. Variation of extent of polymerization and yield with temperature of preparation in chloroform for 2,5-DMePip-T polyamide.

reaction vessel. Further, the system is less sensitive to excess diamine and this order of addition provides such a situation throughout the pouring step. Whenever precipitation of the polymer was expected, the reaction mixture was stirred rapidly in a blender (procedure B).

We have not found any marked sensitivity of the degree of polymerization to the reactant concentrations or the volume ratio of the solutions. The preferred concentration range is between about 1 and 8 g. of reactants/100 ml. of solvent. Lower concentrations are uneconomical and introduce larger amounts of solvent impurities. Higher concentrations may yield unstirrable masses and the heat of reaction is more difficult to control when the reactants are mixed rapidly.

The following examples are given as illustrative of variations in the technique of solution polycondensation. Other variations and some limitations will be apparent from the accompanying discussion and the tables and figures. Although all the examples employ a solvent rinse to introduce traces of the second reactant, such a step may have little or no value when the polymer precipitates rapidly from solution in a nonswollen state.

Table II presents some typical results of the preparation of several piperazine polyamides and a few properties of the polymers.

**A. 2,5-DMePip-T Polyamide in Chloroform with Triethylamine.**  
*trans*-2,5-Dimethylpiperazine (2.28 g.) and 5.6 ml. of pure triethylamine

TABLE II  
Properties of Some Piperazine Polymers Prepared by Solution Polycondensation

Polymer <sup>a</sup>	Polymerization solvent	Procedure	Yield, %	$\eta_{inh}$ ( <i>m</i> -cresol)	PMT, °C. <sup>b</sup>	Solubility		
						Formic acid	Chloroform	Dimethylformamide
Pip-6	Dichloromethane	A	75	0.90	350	+	-	+
-10	Dichloromethane	A	85	1.10	200	+	+	+
-T	Chloroform	B	85	1.35	>400	-	-	-
2-MePip-10	Dichloromethane	A <sup>e</sup>	98	1.01	120	+	+	+
-T	1,1,2-Trichloroethane	B	85	1.92	>375	-	-	-
<i>cis</i> -2,5-DMePip-T	Chloroform	E	98	0.86	335	+	+	+
<i>trans</i> -2,5-DMePip-2	Chloroform	I	76	1.55	>400	+	- <sup>e</sup>	-
-6	Chloroform	A	80	1.61	290	+	- <sup>d</sup>	-
-10	Hexane	F	99	1.60	165	+	+	+
-P	Chloroform	A	87	0.31	360	+	-	- <sup>e</sup>
-I	1,2-Dichloroethane	A	90	1.44	315	+	+	-
-T	<i>cis</i> -1,2-Dichloroethylene	B	91	2.20	>400	+	- <sup>d</sup>	-
-2C/T	Dichloromethane	A	96	0.74	>400	-	-	-

<i>cis</i> -2,6-DMePip-10	Dichloromethane	A <sup>a</sup>	84	0.43				
	Dichloromethane	E	94	1.00	+	+	+	+
	Dichloromethane	H	93	1.10	+	+	+	+
<i>cis</i> -2,6-(50/50)								
	Dichloromethane	E	98	1.09	-	-	-	-
<i>cis</i> -2,6-2,2',5,5'-TeMePip-10	Dichloromethane	E	90	0.76	+	+	+	+
	Dichloromethane	A <sup>a</sup>	99	0.89				
	Dichloromethane	E	95	0.98	-	-	-	-
	Chloroform	A	98	0.74				
$\alpha$ -2,3,5,6-TeMePip-10	Dichloromethane	E	94	0.46	+	+	+	- <sup>e</sup>
	Dichloromethane	E	90	0.33	+	+	+	-
$\beta$ -2,3,5,6-TeMePip-10	Dichloromethane	E	80	0.46	+	+	+	- <sup>e</sup>
	Dichloromethane	E	91	0.18	+	+	+	-

<sup>a</sup> Pip, MePip, DMePip, and TeMePip stand for piperazine, methylpiperazine, dimethylpiperazine, and tetramethylpiperazine with the position of the substituents designated by prefixed numbers. 2, 6, 10, P, I, and T stand for oxalyl, acetyl, sebacyl, phthaloyl, isophthaloyl, and terephthaloyl.

<sup>b</sup> Polymer melt temperature (temperature at which the polymer just leaves a molten trail on a hot bar).

<sup>c</sup> Partly soluble.

<sup>d</sup> Soluble in chloroform with methanol or formic acid added.

<sup>e</sup> Amine solution cooled in an ice bath and stirred with a magnetic stirrer. Acid chloride dripped in undiluted.

were dissolved in 100 ml. of chloroform in a 500-ml. Erlenmeyer flask. To this mixture was added a solution of 4.06 g. of terephthaloyl chloride in 80 ml. of chloroform with swirling. More chloroform (20 ml.) was used to rinse in the residues of terephthaloyl chloride at once. The mixture remained clear, but the temperature rose quickly from 25 to 42°C. and there was an increase in solution viscosity. The solution could be dry-cast on glass to produce self-supporting films, which were strong and flexible if washed free of salt with water just before they were dry.

After 5 min. the product was coagulated by pouring the solution into hexane with stirring. A fibrous precipitate was obtained as well as crystals of triethylamine hydrochloride. The precipitate was washed well with water and finally with acetone. After drying at 100°C. a 92% yield of polymer was obtained which had an inherent viscosity of 3.1 [ $\eta_{inh} = (\ln \eta_{rel})/c$  determined in *m*-cresol at 30°C.;  $c = 0.5$  g./100 ml. solution]. Viscosities were determined in *m*-cresol in all the work reported unless otherwise stated.

When the solution from the polymerization was held at room temperature for several hours, it formed a gel-like mass. The precipitated or isolated polymer was only swollen in chloroform but was readily soluble in stronger solvents.

As an alternative to the above procedure with better control of reaction conditions, the polycondensation mixture was cooled with an ice bath and stirred with a magnetic stirrer. This is applicable to systems in which no heavy precipitates form.

**B. 2,5-DMePip-T Polyamide in Benzene with Triethylamine.** A quart-size home blender was used in this experiment and for all other polymerization systems which yielded precipitates of polymer quickly. The jar and stirrer bearing were dried and the bearing sealed and lubricated with an inert substance, such as Celvacene medium vacuum grease (Distillation Products Industries). The top was covered with aluminum foil and over this was placed the plastic cap. A wide powder funnel was inserted through a  $3/4$ -in. hole in the center of the cap and foil.

The diamine and acceptor, as in procedure A, were dissolved in 100 ml. of benzene in the blender jar. The terephthaloyl chloride (4.06 g.) in 90 ml. of benzene was added rapidly through the funnel while the stirrer was simultaneously speeded up by means of a rheostat. Traces of acid chloride were rinsed in at once with 10 ml. of benzene. A precipitate formed immediately and stirring was continued at moderate speed for five minutes. The mixture was diluted with an equal volume of hexane and the precipitate collected and washed as before. Medium-pore fritted glass funnels were used for polymer collection in order to avoid contamination by paper fibers.

The white powder, obtained in 90% yield, had an inherent viscosity of 1.21.

**C. 2,5-DMePip-T Polyamide in Chloroform with Excess Diamine as the Acid Acceptor.** *trans*-2,5-Dimethylpiperazine (4.56 g.; 0.04 mole) was



TABLE III  
Endgroups and Molecular Weights of 2,5-DMePip-T Polyamide  
Prepared under Various Conditions

Pro- cedure	Ratio of diamine to acid chloride	Yield <sup>a</sup> %	$\eta_{inh}^b$	$[\eta]^b$	Endgroups $\times 10^6/g.$		Calcd. DP <sup>c</sup>	$\bar{M}_n$	
					COOH	NH		Calcd.	Found
D	4.00	85	0.26	0.27	2	780	2	240	2,560 <sup>d</sup>
	3.00	94	0.64	0.70	7	304	3	370	6,400 <sup>d</sup>
	2.50	99	1.35	1.6	8	68	5	610	26,300 <sup>d</sup>
	2.22	99	2.47	3.1	14	33	10	1,220	42,600 <sup>d</sup>
	2.10	96		3.5			21	2,560	49,000
	2.04	98		4.3			51	6,200	62,000
	2.02	97		4.9			101	12,300	71,000
	2.00	98		6.0			$\infty$	$\infty$	90,000
	2.00	97		8.5			$\infty$	$\infty$	140,000
	1.96	97		2.3			99	12,100	30,000
	1.93	90		1.55			56	6,800	19,000
	1.82	85		0.45			21	2,560	4,600 <sup>d</sup>
	1.82	100	0.30	0.32	650	0	21	2,560	3,100
	1.65	83	0.26	0.27			10.4	1,270	2,500 <sup>d</sup>
	1.64	98	0.21	0.22	1000	0	10.1	1,230	2,000 <sup>d</sup>
	1.50	80	0.22	0.23			7	850	2,100
	1.33	98	0.12	0.12	1500	0	5	610	1,350 <sup>d</sup>
	1.00	77	0.14	0.15			3	370	1,300
B <sup>e</sup>	1.00	76	1.25		104	18	$\infty$	$\infty$	16,400 <sup>d</sup>
B <sup>f</sup>	1.00	76	0.67		266	67	$\infty$	$\infty$	6,000 <sup>d</sup>
B <sup>g</sup>			6.48	9+	4	10	$\infty$	$\infty$	143,000 <sup>d</sup>
			3.30	4.5	18	13	$\infty$	$\infty$	64,500 <sup>d</sup>

<sup>a</sup> Based on the diamine for reactant ratios from 1 to 2 and on diacid chloride for ratios from 2 to 4.

<sup>b</sup> Determined in *sym*-tetrachloroethane-phenol (40:60 by weight) at 30°C.,  $c = 0.5$  g./100 ml.

<sup>c</sup> Degree of polymerization =

$$\frac{\text{moles of bifunctional reactants exclusive of any excess}}{\text{moles of endgroup}} + 1$$

In this calculation for a system employing diamine as the acid acceptor, a balanced system comprises one mole of each reactant and one mole of diamine acceptor. Diacid chloride or diamine in excess of this ratio is considered to be monofunctional endgroup. When excess acid chloride is present, one-half the diamine forms polymer and one-half is acceptor. With excess diamine over the 2:1 ratio, all of the acid chloride is assumed to react with equivalent diamine and by-product hydrogen chloride is assumed to form diamine dihydrochloride rather than monohydrochloride or react with chain-ends. One repeat unit has a DP of 2.

<sup>d</sup> Values from endgroups; the remaining values are from the viscosity-molecular weight relationship (Fig. 5).

<sup>e</sup> In methyl ethyl ketone.

<sup>f</sup> In hexane-chloroform, 80:20 by volume.

<sup>g</sup> Interfacial polycondensation in dichloromethane.<sup>22</sup>

TABLE IV  
Formation of 2,5-DMePip-T Polyamide from  
Unequal Quantities of Reactants

Diamine/diacid chloride ratio	Acceptor	Yield, %	$[\eta]^c$
95/100	Diamine <sup>a</sup>	88	1.1
100/95	Diamine	99	3.2
95/100	Triethylamine <sup>b</sup>	81	1.4
100/95	Triethylamine	87	3.1

<sup>a</sup> Procedure D.

<sup>b</sup> Procedure B in chloroform with 2 moles tertiary amine/mole diamine.

<sup>c</sup> In tetrachloroethane-phenol (40:60 by wt.) at 30°C.

dissolved in 100 ml. of chloroform in a blender. To this was added a solution of 4.06 g. (0.02 mole) of terephthaloyl chloride in 80 ml. of chloroform. More chloroform (20 ml.) was used to rinse in the last of the acid chloride. A thick gelatinous precipitate formed at once but the mixture became fluid with stirring. This precipitate was shown later to be the dimethylpiperazine dihydrochloride.

Stirring was continued 5 min., hexane (350 ml.) was added, and the precipitates were collected and washed as in A.

The granular product (92% yield) had an inherent viscosity of 2.89.

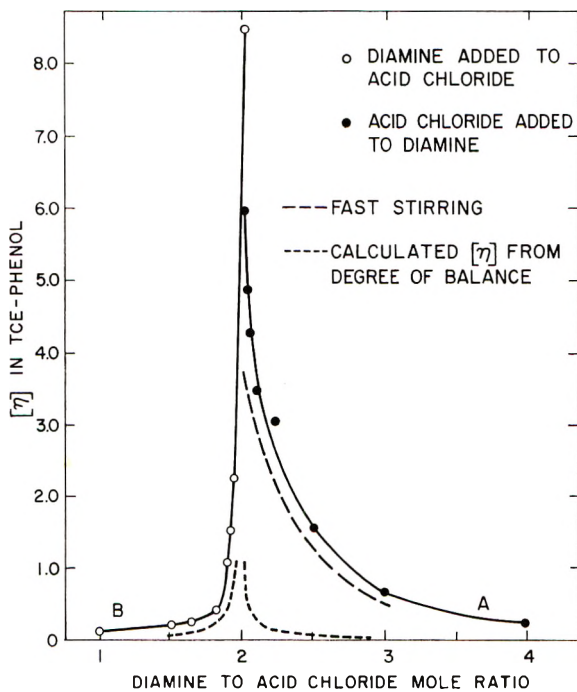


Fig. 3. Variation in extent of polymerization with reactant ratio for the preparation of 2,5-DMePip-T polyamide in chloroform.

**D. 2,5-DMePip-T Polyamide in Chloroform, Excess Diamine, Slow Addition.** Terephthaloyl chloride (4.06 g.; 0.02 mole) was dissolved in 150 ml. of chloroform in a 500 ml. flask equipped for fast stirring. A solution of *trans*-2,5-dimethylpiperazine (4.456 g.; 0.0390 mole) in 98 ml. of chloroform was added dropwise over a period of 45 min. A precipitate of diamine dihydrochloride formed as the diamine was added. Chloroform (40 ml.) was used to rinse the dropping funnel. A 75-ml. sample of the mixture was removed for a viscosity determination; the inherent viscosity was 1.61.

A solution of 0.20 g. of the dimethylpiperazine in 50 ml. of chloroform was then added over a period of 30 min. During this time the dispersion of diamine salt became very viscous. The polymer was precipitated in a fibrous form in hexane. The inherent viscosity was 5.79 and the total yield was 89%.

The experiments on molecular weight versus reactant ratio, reported in Tables III and IV and Figure 3 were carried out in this way. The initial volume of chloroform was always 150 ml. and contained either 0.02 mole of terephthaloyl chloride or 0.04 mole of 2,5-dimethylpiperazine. The volume of solution in the graduated dropping funnel was proportional to the amount of added reactant (0.20*M* in acid chloride or 0.40*M* in diamine). The temperature of the flask was kept at 25°C. When acid chloride was added to diamine, there was no precipitate until the mole ratio of diamine to diacid chloride was near to three. Thereafter the addition of diacid chloride caused a corresponding precipitation of diamine dihydrochloride.

The polymers were precipitated in hexane and washed thoroughly in water to remove salt. The samples prepared with excess acid chloride were also washed well with acetone. This caused only slight fractionation when used as a secondary wash.

**E. 2,5-DMePip-T Polyamide in Chloroform with Calcium Hydroxide.** *trans*-2,5-Dimethylpiperazine (2.28 g.) was dissolved in 100 ml. of chloroform in a blender and 5.92 g. (0.08 mole) of reagent-grade, powdered calcium hydroxide was added. To this was added over a period of 5 min. with moderate stirring, 4.06 g. of terephthaloyl chloride in 100 ml. of chloroform. Stirring was continued for 10 min. and the mixture allowed to stand for 15 min. more. At no time was there any appearance of the gelatinous diamine dihydrochloride. The soluble monohydrochloride is presumed to be a likely intermediate in the reaction. High-speed stirring and shorter reaction times can be used.

A portion of the mixture was filtered and yielded a clear solution from which very tough, transparent film was cast.

The remainder of the mixture was diluted with acetone and the precipitate was collected and washed. Washing with 2% aqueous hydrogen chloride was included to assure removal of calcium hydroxide. The overall yield was 95% and the inherent viscosity was 3.14. Viscosities up to 5.0 have been obtained.

**F. 2,5-DMePip-10 Polyamide in Hexane with Triethylamine.** Sebacyl chloride (4.28 ml.) was dissolved in 125 ml. of *n*-hexane in a blender. A

solution of 2.28 g. of *trans*-2,5-dimethylpiperazine and 5.7 ml. of triethylamine in 175 ml. of hexane was added with rapid stirring. Hexane (25 ml.) was used to rinse in the last of the diamine. Both the polymer and salt by-product precipitated at once. The mixture was stirred for 5 min. and then filtered. There was practically no dissolved solid or oil in the filtrate.

The granular product took on a chewing-gum consistency when wet with water and was, therefore, washed by kneading and working under flowing water. The dry polymer was a flexible, clear mass, which became plastic above 100°C. The yield was 95% and the inherent viscosity was 1.60.

The similar preparation in chloroform produced a stable solution of polymer which had an inherent viscosity of 1.90.

**G. 2,5-DMePip-T/2,5-DMePip-10 Ordered Copolyamide.** An unbalanced reaction mixture (mixture A) was made from 1.03 g. (0.009 mole) of *trans*-2,5-dimethylpiperazine and 2.78 ml. of triethylamine in 50 ml. of dichloromethane to which was added 2.02 g. (0.010 mole) of terephthaloyl chloride in 50 ml. of solvent plus a 10 ml. rinse. A second mixture (B) was made in a similar way containing 1.25 g. (0.011 mole) of *trans*-2,5-dimethylpiperazine 2.78 ml. of triethylamine, and 2.41 ml. (0.010 mole) of sebacyl chloride.

The two unbalanced polymerization mixtures were allowed to stand five minutes. A and B were then mixed. No precipitation occurred after 15 min. The product was precipitated with cyclohexane and washed. The yield of polymer was 71% (3.72 g.) and the inherent viscosity was 1.18. The polymer was not made gummy by water and did not melt or soften below 350°C. This type of polymerization procedure leads to the formation of a polymer with a nonstatistical distribution of monomer units.

**H. 2,6-DMePip-10/T Alternating Copolymers.** *cis*-2,6-Dimethylpiperazine is hindered sterically toward acylation at one end. That the hindrance is considerably greater toward terephthaloyl chloride than sebacyl chloride was shown by a large difference in the times required to prepare the homopolymers by procedure E.

*cis*-2,6-Dimethylpiperazine (1.14 g.; 0.01 mole) and 4.0 g. of calcium hydroxide, and 30 ml. of dichloromethane were placed in a 125 ml. Erlenmeyer flask. The suspension was stirred with a rotating magnet and cooled in ice water. Terephthaloyl chloride (1.015 g.; 0.005 mole) in 30 ml. of solvent was added and the mixture was stirred 15 min. Then sebacyl chloride (1.07 ml.) was added dropwise and the reaction continued for 30 min. The polymer was isolated by precipitation with hexane and then the gum was washed by kneading in running water. The dry polymer was dissolved in formic acid and reprecipitated with water and washed; yield, 93%; inherent viscosity 1.10.

Alternatively, the calcium hydroxide may be first neutralized with aqueous acid or formic acid.

**I. 2,5-DMePip-2 Polyamide.** *trans*-2,5-Dimethylpiperazine (8.86 g.)

was dissolved in 100 ml. of chloroform in a blender and to this was added with rapid stirring a solution of 2.55 ml. (1.493 g./ml.) of oxalyl chloride in 66 ml. of chloroform. A precipitate of diamine dihydrochloride and polymer formed at once. The stirring was continued five minutes and 150 ml. of water was added to dissolve the salt. The mixture was filtered and the polymer was washed with water and 50% aqueous acetone. The yield of white polymer was 76% and the inherent viscosity 1.55.

Clear, tough films were cast from solutions of this polymer in 1,2-dichloroethane/99% formic acid (70/30 by volume).

**J. Pip-T Polyamide; Use of a Solvent Reactive Toward Diamine.** Anhydrous piperazine (1.72 g.) and 5.6 ml. of triethylamine were dissolved in 30 ml. of chloroform in a blender. A solution of 4.06 g. terephthaloyl chloride in 150 ml. of 1,1,2,2-tetrachloroethane was added with rapid stirring. More solvent (20 ml.) was used for a rinse. A soft, but not gelatinous, precipitate formed at once. Stirring was continued 10 min., the mixture was diluted with an equal volume of hexane, and the polymer and salt were collected and washed.

The polymer was obtained in 88% yield and had an inherent viscosity of 1.11 (in concentrated  $H_2SO_4$ ).

**K. 2,5-DMePip-T Polyamide; Use of a Solvent Reactive Toward Acid Chloride.** Terephthaloyl chloride (2.03 g.) was dissolved in 50 ml. of chloroform in a blender. To this solution was added a solution of 2.28 g. *trans*-2,5-dimethylpiperazine in a mixture of 40 g. 2,6-di-*tert*-butyl-4-methylphenol and 50 ml. of chloroform. A soft precipitate of diamine salt formed. The mixture was stirred for 5 min. A small portion was set aside and there was no indication of polymer precipitation after 3 days.

The remaining solution was diluted with acetone and the product thoroughly washed. The polymer had an inherent viscosity of 1.77 and the yield was 87%.

**L. 2,5-DMePip-T Polyamide; Adding Solvents to Solid Reactants.** *trans*-2,5-Dimethylpiperazine (4.56 g.) and 4.06 g. of terephthaloyl chloride were finely ground together in a mortar without excessive pressure. The mixture was placed in a blender, the blender blades were started, and 150 ml. of chloroform was added quickly. A precipitate of diamine salt formed in a viscous polymer solution. After 5 min. the product was isolated as before. The yield was 96% and the inherent viscosity 3.60.

**M. 2,5-DMePip-T Polyamide; Starting with Diamine Salt.** *trans*-2,5-Dimethylpiperazine dihydrochloride was prepared by the addition of dry hydrogen chloride to the diamine in chloroform. The dry salt partly sublimed but did not melt up to 380°C. The solubility in chloroform was 0.008 g./100 ml. at 25°C. The salt contained 38.1% chlorine (calculated value for dihydrochloride, 37.9% Cl).

The diamine dihydrochloride (1.87 g.; 0.01 mole) and 5.6 ml. of triethylamine were placed in a flask in 50 ml. of chloroform. The salt dissolved. A solution of 2.03 g. terephthaloyl chloride in 50 ml. of chloroform was added, the mixture was allowed to stand eight minutes, and the product

was isolated as in A. The yield of polymer was 99% with an inherent viscosity of 1.32. Polymers having high molecular weight are obtained by this procedure only with strong acid acceptors and solvents which give complete solution of the starting materials.

In a second experiment 3.74 g. (0.02 mole) of *trans*-2,5-dimethylpiperazine dihydrochloride and 2.28 g. (0.02 mole) of the dimethylpiperazine were mixed in 70 ml. of chloroform in a flask. All but a small residue of the salt dissolved. The mixture was cooled to about 15°C. and 2.03 g. of terephthaloyl chloride in 30 ml. of chloroform was added with stirring in 2 min. Diamine dihydrochloride precipitated at once. Because the mixture became very viscous more chloroform (50 ml.) was added and stirring was continued 30 min. The tough, fibrous product, isolated as before, had an inherent viscosity of 5.95; yield 96%.

**N. Experiment for a Lecture or Classroom Demonstration.** Several of the preceding experiments can be adapted for use as a demonstration of fast polycondensation. The one below combines the elements of several.

*trans*-2,5-Dimethylpiperazine (2.28 g.) and triethylamine (5.5 ml.) are dissolved in 100 ml. of chloroform in a 500-ml. Erlenmeyer flask. To this is added a solution of 4.06 g. of terephthaloyl chloride in 50 ml. of chloroform. There will be evolution of heat and possibly slight foaming. The solution should remain clear and show some increase in viscosity in 1-2 min. The presence of polymer may be shown by evaporating some of the solution on a glass plate to deposit a film or by pouring some of the solution into a 100-ml. graduate or a beaker containing hexane. Long strings of polymer and powdery salt will form.

The following refinements and simplifications can be used: A few grains of an acid-base indicator, such as bromocresol green, may be added to the amine solution. The solution will be blue and will turn yellow or colorless when the diacid chloride is added. The color change will not occur if an excess of amines is present. One or both of the solid reactants may be placed in the flask and the chloroform-triethylamine mixture added. The indicator could be added to the chloroform. The amines could be dissolved in chloroform and solid acid chloride added. In the two latter methods, unwashed chloroform may be used since there is little chance for interference by the alcohol. If the solutions are cooled, polymer with higher molecular weight will be formed and the solutions may be more concentrated (not over about 8%). This will permit a clearer observation of the viscosity increase.

As a matter of safety as well as to obtain polymer with high molecular weight, all solutions should be made up just prior to their use.

## DISCUSSION

Probably the major reasons why the solution polycondensation method has not been applied broadly more successfully are (1) failure to recognize the important role of the solvent in forming high polymer, (2) the use of acid

acceptors too low in base strength, and (3) a preconceived notion that equivalence of reactants is difficult to achieve except by special methods. The recent papers on polyphenyl carbonates<sup>15</sup> and esters<sup>17</sup> have pointed out the desirability of using a polymer solvent. In the following sections, the important variables and the polymerization mechanism will be discussed and compared with those for interfacial polycondensation.

The important requirements for a successful solution polycondensation are: (1) A high-yield, moderately fast reaction; (2) an adequate solvent; (3) an adequate acid acceptor; (4) purity of solvent and reactants; (5) freedom from side reactions. Most useful systems possess these qualities in varying degrees. To some extent a lack in one respect may be overcome by high performance in another direction.

### Reaction Rate and Mixing Factors

Solution polycondensation employs the same reactions as used in interfacial polycondensation and so similar reaction rates are involved. This means that the fastest reactions have rates of the order of  $10^2$ – $10^6$  l./mole-sec. Polycondensations involving such reaction rates may be completed in a few minutes at room temperature. Acylations of piperazines with not more than one methyl substituent adjacent to each nitrogen fall in this class. While the high reaction rate provides some advantages, much slower reactions will yield polymers with high molecular weight and fast reactions may be carried out slowly (procedures D, E, and H). Piperazines with two or more methyl substituents adjacent to one or both nitrogens are acylated slowly relative to the rates for the less substituted group.<sup>29,30</sup>

Both interfacial polycondensations and solution polycondensations, in the faster rate range, show unusual insensitivity to nonequivalence of reactants in comparison with melt polycondensations. The interfacial polycondensation process is characterized by the following features, several of which contribute to this insensitivity: (1) fast reacting intermediates are used; (2) the reaction is irreversible at the reaction temperature; (3) the interface provides for the regulated flow of one reactant into an established higher concentration of the second reactant; (4) reaction takes place essentially as fast as contact of complementary reactants occurs; (5) the growing polymer is in solution or highly swollen during all or most of the polymerization reaction; (6) the aqueous phase provides for the removal of by-product acid from the polymerization zone.<sup>3,4</sup>

Fast solution polycondensations have most of the features of interfacial polycondensation. Items 1, 2, 4, and 5 are identical in both systems. Item 6 is taken care of by a precipitation of salt or by the withholding action of an acceptor. The liquid-liquid interface (item 3) performs a major role in the attainment of reactant balance in many interfacial polycondensation reactions. Yet the success of solution polycondensation shows that the interfacial boundary, while helpful as a regulating device, is not essential for the formation of polymers with high molecular weight.

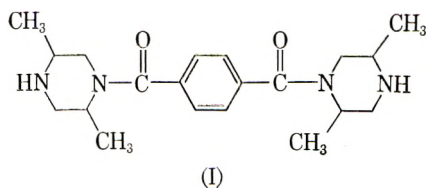
There must remain then some other factor which provides insensitivity to nonequivalence of reactants in a single-phase system.

Part of the answer is that the rate of polymerization is often faster than the rate of mixing even in the absence of an interfacial boundary. In the solution polymerization system there are presumed to be temporary interfaces or zones within which polymerization is proceeding independently of any potential effect of the ratio of the two reactants in the system as a whole. Thus, even a single drop of acid chloride solution in a large volume of diamine solution reacts rapidly with the immediately surrounding diamine before the droplet is dispersed. This leads to oligomers and polymer with higher molecular weight than would be obtained from a random reaction at the known reactant ratio. Further dropwise addition of one reactant continues this effect because each successive drop goes into a large system which consists in part of active polymer with a higher than random degree of polymerization. Eventually as the system approaches equivalence and the concentration of reactive groups is reduced, there is a greater chance of wide distribution of the increment of added reactant and the occurrence of random reaction.

The effect of this control of the polycondensation rate by mixing and diffusion is shown in Table III and Figure 3. The preparations represented by the solid lines in Figure 3 were carried out by procedure D with diamine as the acceptor. The points to the left of the peak were obtained by slow addition of diamine to acid chloride and those on the right by addition of acid chloride to diamine. The dotted lines show approximately the intrinsic viscosities which should be obtained at the various reactant ratios from a slow reaction or a reaction involving an equilibrium among the various molecular species as in the usual melt polyamidation. Calculated molecular weights for a number of reactant ratios are given in Table III and compared to some of the experimental results. The system is less sensitive to excess diamine than diacid chloride, but a lower maximum molecular weight was attained by the addition of acid chloride to diamine. The difference in sensitivity is due to the behavior of diamine as an acceptor, which is explained in a later section.

The foregoing discussion has been based on data for a procedure in which excess diamine was the acid acceptor. The following tabulation shows that similar results are obtained with a tertiary amine acceptor (see Table IV).

Another aspect of rapid local polymerization is that the direct synthesis of simple oligomers (I) cannot be carried out even in dilute solutions with rapid stirring.





Point *A* in Figure 3 represents the reactant ratio at which this compound might be obtained and point *B* would be that for the complementary derivative.

Although the 2,5-DMePip-T polyamide preparation is insensitive to an imbalance of reactants, it responds to a careful balancing of reactants when the polymer is dissolved or highly swollen and interfering side reactions are absent. The peaks in Figure 3 were obtained by slow dropwise addition of one reactant. Since the polycondensation is not reversible and the reactants are consumed essentially as fast as added, passing beyond the equivalence point to left or right does not decrease the degree of polymerization. The major portion of the reactants can be combined rapidly with little decrease in the ultimate molecular weight.

When two solutions of reactants are combined rapidly and stirred in a blender, the degree of polymerization is more sensitive to reactant ratio, as shown by the dashed line in Figure 3. As before in spite of apparent thorough mixing, the system is inhomogeneous for a short time and a local higher degree of polymerization results than calculated from the ratio of reactants.

The insensitivity of fast solution polycondensations to balance, while adequate and most useful, is not as great as for interfacial polycondensations. The latter not only perform well because of the high reaction rate, but have the introduction of the last of the aqueous reactant controlled by diffusion across the liquid interface. This is similar to the dropwise addition of one reactant which was so effective in the experiments shown in Figure 3. For comparison, the stirred solution polycondensations of 2,5-DMePip-T polyamide without dropwise addition have yielded polymers with inherent viscosities of 3-4, while interfacial polycondensation reactions with the same reagents yielded polymers with inherent viscosities of 5-10.

### Function of the Solvent

The solvent performs several functions: (1) dissolves the intermediates and provides for their mixing and contact; (2) dissolves or swells the growing polymer so that a reaction is maintained; (3) carries the acid acceptor and may affect the removal of by-product salts; (4) may affect the reaction rate, by polarity; (5) absorbs heat of reaction.

The intermediates ordinarily are dissolved in an inert solvent before the polymerization is started. A diamine may start as an insoluble salt and be caused to dissolve because of reaction with an acid acceptor (procedure M). The only conditions under which the reactants may be undissolved at the start or incompletely soluble are that solution takes place extremely rapidly or the polymer remains dissolved or swollen until all of the reactants have dissolved and been consumed (procedure L).

A primary requisite for high polymer formation in all solution polycondensations is that the solvent must dissolve or swell the polymer sufficiently to permit completion of the polymerization. This point is

enlarged upon in the section on metastable polymer solutions and in the following papers.

The selection of the organic solvent for interfacial polycondensation reactions was recognized as having a relation to the degree of polymerization.<sup>3,4</sup> For instance, in the preparation of poly(hexamethylene sebacamide) (polyamide 610) increasing molecular weights were obtained with solvents in the order cyclohexane, carbon tetrachloride, chloroform. However, all of these solvents produced polyamide 610 with an inherent viscosity number of at least one. In a solution polycondensation system only chloroform would yield polyamide 610 with a viscosity number in this range. Solution polycondensation requires a stronger polymer-solvent interaction yet the order of effectiveness for a series of solvents is the same. For polymers prepared from diamines the adequacy of the solvent may not be determined entirely by the need for polymer solubility or swelling. The combination of solvent, diamine, and acid acceptor must be such that diamine needed in the polycondensation is not precipitated as a salt with low solubility. Some of these effects are illustrated by the experiments on acid acceptors.

The range of solvents useful for solution polycondensation is extended to include many water-miscible solvents such as acetone, acetonitrile, and dioxane. Pyridine can be used for the preparation of poly(phenyl esters).<sup>15,16</sup>

Solvent polarity is known to affect the rate of reactions which produce polar products.<sup>31</sup> It affects the degree of polymerization in the preparation of polyamides from secondary diamines. Examples are given in a following paper.

### Metastable Polymer Solutions

The solution polycondensation of 2,5-DMePip-T polyamide in chloroform and certain other halogenated hydrocarbons leads to metastable or supersaturated polymer solutions. They have the normal dilute solution viscosity characteristics of a polymer dissolved in a poor solvent (Fig. 4). The intrinsic viscosity numbers are far below the values obtained by redissolving the polymer in *m*-cresol (for example, 0.87 compared to 1.35). The stability of these solutions decreases with increasing concentration and varies with the solvent.

The 2,5-DMePip-T polyamide solution for which plot *A* of Figure 4 was obtained, showed little change in viscometer flow time over a period of 5 hr. at a concentration of 3.6 g./100 ml., although some turbidity appeared earlier. The more dilute solutions made from the original preparation gelled at times inversely proportional to their concentration. The most dilute solution (0.1 g./100 ml.) required seven days for the appearance of flocs. No polymer agglomeration was observed by light scattering prior to visible precipitation.

The solution stability in several solvents decreased in the order chloroform, dichloromethane, 1,1,2-trichloroethane, 1,2-dichloroethane. In the

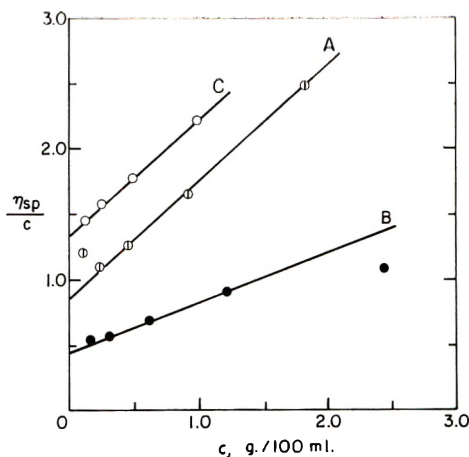


Fig. 4. Dilute solution viscosity behavior of metastable solutions of 2,5-DMePip-T polyamide prepared in chloroform: (A), (B) polymerization mixtures in chloroform at 25°C.; (C) polymer isolated from (A) and dissolved in *m*-cresol at 30°C.

last liquid, precipitation appeared to occur at once although the precipitate was translucent and pasty. It is suggested that in all solution and interfacial polycondensations a supersaturated polymer solution results, but that only in the more stable systems is observation of the effect possible. Quite stable supersaturated solutions of poly(sebacyl piperazine) have been prepared by the interfacial polymerization procedure in 1,2-dichloroethane.<sup>3,4</sup>

2,5-DMePip-T and Pip-10 polyamide precipitates formed slowly as above or rapidly by the addition of a poor solvent were not crystalline as first formed but became crystalline when washed with water. (There is the possibility of trace crystallinity not detectable in an x-ray pattern.) Similar behavior has been reported for the products of interfacial polymerization. Nevertheless, precipitation from the metastable solutions has a degree of reproducibility and responds to concentration and shearing effects in the ways expected from a crystallization process.

#### Acid Acceptors

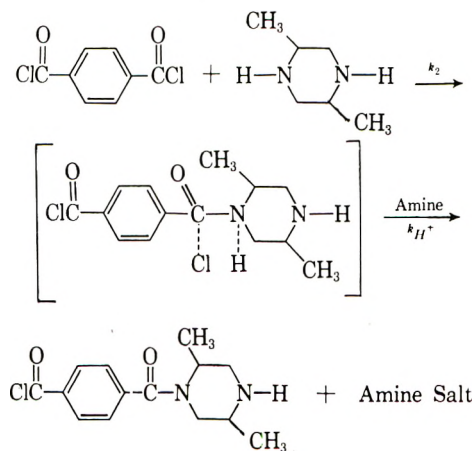
Amine acid-acceptors will be treated broadly in the following paper. The present discussion will cover only the use of excess diamine and inorganic bases.

**Excess Diamine.** Piperazine and *trans*-2,5-dimethylpiperazine are unusual, though not necessarily unique, in that solution polycondensation will proceed to high molecular weight in certain solvents in the presence of an excess of diamine as the acid acceptor. The highest molecular weight is obtained at the ratio of two moles of diamine to one of diacid chloride regardless of the order of addition of the two solutions (Fig. 3). Polymers with low molecular weight are obtained when the polymer precipitates rapidly. The peculiarities which make possible the use of the two piperazines as acid

acceptors without interference with polymer formation are the solubilities of the diamine salts and the base-strength relationships of all of the amine species.

The unusual behavior of the polycondensation reaction is most apparent when diacid chloride solution is gradually added to diamine solution (right of Fig. 3) with stirring. In chloroform, dichloromethane, and 1,1,2-trichloroethane, *trans*-2,5-dimethylpiperazine monohydrochloride is readily soluble, whereas the dihydrochloride is quite insoluble. Therefore, during the preparation of 2,5-DMePip-T polyamide by the procedure described above, precipitation of diamine dihydrochloride does not begin until a ratio of one mole of diacid chloride to three moles of diamine is reached. The polymer isolated at this point in 94% yield has a molecular weight ( $\bar{M}_n$ ) of 6400. Ninety-eight per cent of the chain ends bear amine groups.

An explanation of the behavior of the polycondensation system requires a restatement of several characteristics of the amide-forming reactions: (1) acylation rate and proton affinity of the amine groups are presumed to be proportional to their base strengths; (2) amine hydrochlorides or protonated amines are not acylated by acid chlorides; (3) the rate of reaction between acid chloride and amine is high but the rate of removal of the proton or hydrogen chloride from the protonated amide in the presence of base is still higher.



where

$$k_H > k^2 > k_{\text{reactant mixing}}$$

The strongest base present in the early period of the polycondensation procedure under discussion is free diamine. The base strength measured in water is 100 times that of the monobenzoylated diamine and over 10,000 times that of the diamine monohydrochloride (Table V). During polymerization, free diamine is the acid acceptor as long as it is available and it becomes the weakly basic soluble, monohydrochloride. Acylation takes place with free diamine and monoacylated diamine as well. If diamine

monohydrochloride should be acylated, the base forming the salt site becomes weakened and the hydrogen chloride will transfer to diamine. The effective withdrawal of two-thirds of the excess diamine from the reaction by formation of the monohydrochloride and the additional effect of a high reaction rate leads to the high degree of polymerization observed.

TABLE V  
Base Strengths of Piperazines and *N*-Alkyl Ethylenediamines

Amine	$pK_a$ in H <sub>2</sub> O at 25°C.	$E_{1/2}$ , mv. <sup>a</sup>	
		Ethyl acetate	Aceto- nitrile
Piperazine	9.81	103	65
1-Benzoylpiperazine	7.78	(275)	210
Piperazine monoion	5.57	(430)	(380)
2-Methylpiperazine <sup>b</sup>	9.90		
2-Methylpiperazine monoion	5.46		
<i>trans</i> -2,5-Dimethylpiperazine	9.69	148	85
1-Benzoyl- <i>trans</i> -2,5-dimethylpiperazine	7.5	(300)	(240)
<i>trans</i> -2,5-Dimethylpiperazine monoion	5.25	347	(400)
<i>cis</i> -2,6-Dimethylpiperazine <sup>b</sup>	9.86		
<i>cis</i> -2,6-Dimethylpiperazine monoion	5.40		
<i>N,N'</i> -Dimethylethylenediamine <sup>c</sup>	10.29		
<i>N,N'</i> -Dimethylethylenediamine monoion	7.47		
<i>N,N'</i> -Diethylethylenediamine	10.46		
<i>N,N'</i> -Diethylethylenediamine monoion	7.70		

<sup>a</sup> See Hall.<sup>33</sup> Parentheses indicate estimated values.

<sup>b</sup> Data of Keyworth.<sup>34</sup>

<sup>c</sup> Basolo et al.<sup>35</sup> present a study of this diamine and those following.

The discussion thus far has contained no formal acknowledgment of the existence of equilibria between the various amine species and the hydrogen chloride content of the system. No doubt these equilibria exist even though the balance in favor of certain products may be exceedingly high. As an example, diamine monohydrochloride must remain in equilibrium with small amounts of diamine and dissolved dihydrochloride. The latter in turn would be in a solution equilibrium with precipitated salt.

An observation relating to equilibria in the first stage of the polymerization is that momentary turbidity appears if several drops of acid chloride solution are added rapidly to the clear diamine solution. Diamine dihydrochloride precipitates because the 1:3 ratio of acid chloride to diamine is exceeded in a small region. Mixing brings more diamine into the region to form the soluble monohydrochloride.

At the 1:3 reactant ratio, when essentially all of the diamine has been either acylated at least once or has formed monohydrochloride, the strongest base would appear to be the polymer chain end. One would expect the chain ends to be protonated next and cease to react. However, only a small amount of free diamine (less than 1% of the unacylated diamine) in

equilibrium with the diamine salt need be present to more than equal the number of amine ends on the polymer. Such an equilibrium would provide a small fraction of strongly basic diamine for acylation and acceptor action throughout the remainder of the polymerization.

As more acid chloride is added to the mixture, the average molecular weight of the polymers continues to rise and polymerization is accompanied by a concurrent precipitation of diamine dihydrochloride. The dihydrochloride must be so insoluble and the system so sensitive to the least excess of hydrogen chloride over that required to form monohydrochloride from the nonacylated diamine that the dihydrochloride precipitates nearly quantitatively as the reaction proceeds. The results indicate a rapid transfer of protons or hydrogen chloride away from amide groups and monoacylated diamine, and the consequent existence of a high proportion of unprotonated amine ends on oligomers and the polymer chains. The probable participation of small equilibrium amounts of the strongly basic diamine throughout this stage of the polycondensation is postulated.

The second experiment under procedure M in which four moles of diamine monohydrochloride and one mole of diacid chloride yielded a polymer with high molecular weight confirms the suggested mode of reaction. At the start there was a small amount (about 1%) of dihydrochloride which would not dissolve. A corresponding amount of diamine then was present in solution. The experiment shows that the amine ends on the oligomers must be cleared of protons quantitatively for otherwise much more than the desired equivalent of diamine would combine with the diacid chloride and high polymer would not result. The experiment also demonstrates that polycondensation could proceed from the point of a 1:3 reactant ratio with the formation of polymer with high molecular weight without incorporation of the initially formed polymer. However, in view of the presumption of unblocked amine ends, the initial oligomers and polymer must be built upon and coupled randomly while entirely new chains are also forming.

When diamine is added slowly to excess diacid chloride (left of Fig. 3), diamine dihydrochloride appears to precipitate at once. Since the acceptor action is faster than amide formation, no more than one-half of the amine groups can be acylated. The polymerization must proceed locally by the mechanism just outlined. Even with the diminishing amount of amine to serve as the acid acceptor the oligomer ends are not blocked by protons for the final polymer chains end predominantly with carboxyl groups. The experimental curve to the left of Figure 3, rather than that on the right, represents the effect of a high reaction rate on the relation of observed molecular weights to those calculated from the reactant ratio. Other experiments in the absence of salt effects confirm this conclusion.

The use of an excess of a piperazine as the acceptor works best in those solvents from which the dihydrochloride is rapidly and completely crystallized (Table VI) and in which the monohydrochloride is soluble. Polycondensation reactions in carbon tetrachloride, benzene, acetone, dioxane

TABLE VI  
 Preparation of Polymers with Diamine as the Acid Acceptor

Polymer	Mole ratio diamine/acid chloride <sup>a</sup>	Solvent	Yield, % <sup>b</sup>	$\eta_{inh}$	Remarks
Pip-10	2	Chloroform	81	0.96	Polymer soln.; salt ppt.
Pip-T	2	Chloroform	50	0.40	Polymer and salt ppt.
2-MePip-10	2	Dichloromethane	—	—	Salt separates as oil
<i>cis</i> -2,6-DMePip-10	2	Dichloromethane	—	—	Salt separates as oil
<i>trans</i> -2,5-DMePip-10	1	Chloroform	16	0.49	Polymer soln.; salt ppt.
	2	Chloroform	100	1.90	Polymer soln.; salt ppt.
	3 <sup>c</sup>	Chloroform	80	0.53	No ppt.
	2	Dichloromethane	58	1.34	Salt ppt.
	2	Acetone	61	1.11	Polymer ppt.
	2	Benzene	67	0.23	Oil
	3	Benzene	64	0.46	Polymer in soln.
	2	Hexane	68	0.45	All materials ppt.
<i>cis</i> -2,5-DMePip-T	3	Hexane	88	0.56	All materials ppt.
	2	Chloroform	—	—	Salt was a gum
<i>trans</i> -2,5-DMePip-T	1	Chloroform	41	0.66	Some ppt.
	2	Chloroform	91	3.10	Salt ppt.
	2	Dichloromethane	89	1.93	Salt ppt.
	2	1,1,2-Trichloroethane	91	2.65	Salt ppt.
	2	Tetramethylene sulfone-chloroform (85:15 by vol.)	71	1.15	Salt ppt.
2,2,5,5-TeMePip-10	2	Dichloromethane	—	—	Salt was partly an oil
	2	Chloroform	—	—	Salt very slowly ppt'd.

<sup>a</sup> Acid chloride solution added to diamine as in procedure B.

<sup>b</sup> Yield is based on diacid chloride.

<sup>c</sup> Procedure D.

and nitrobenzene give *trans*-2,5-dimethylpiperazine salt which is a mixture of mono- and dihydrochlorides. A system from which pure diamine monohydrochloride precipitates could yield high polymer from a 1 to 3 ratio of diacid chloride to diamine. Hexane is such a solvent. A high yield of *trans*-2,5-DMePip-10 polyamide with an inherent viscosity of 0.56 was obtained in hexane upon fast addition of diacid chloride to diamine in a 1:3 ratio (Table VI). However, there was only a slight gain in molecular weight over a similar preparation in chloroform from which no precipitation occurred. The full potential of the hexane system was not attained since with triethylamine as the acceptor, a 99% yield of polymer with an inherent viscosity of 1.60 was produced.

Diamines other than piperazines which might have similar base strength and salt solubility relationships are the alkylated ethylenediamines (Table V). These have not been carefully evaluated in solution polycondensation systems, but several tests with *N,N'*-diethylethylenediamine indicated that the dihydrochloride did not precipitate completely in some solvents. Ethylenediamine does not form a monohydrochloride soluble in halogenated hydrocarbons.

**Inorganic Bases.** Inorganic bases, such as the finely divided calcium and magnesium oxides or hydroxides, may be used as acceptors if the forming polymer remains dissolved or highly swollen (Procedures E and H). Because most inorganic bases are insoluble in the organic media, these acceptors are slow to function. As much as 20 min. to several hours may be required for completion of the reaction. An excess of the base is advantageous in order to provide more surface for reaction.

Since the polycondensation reaction is usually fast, polymerization in the presence of an insoluble acceptor takes place to a large extent with the diamine acting as an intermediary acceptor. The inorganic base must then regenerate diamine from its salt. In order for this exchange to occur there must exist a slight solubility or dissociation of the diamine salts. Furthermore, the inorganic base will function best if its chloride is slightly soluble and a fresh interface of base is continually exposed. The slow introduction of diamine into the reaction by means of the interaction of a soluble diamine salt with inorganic base can be used as a route to careful balancing of the two polymer-forming reactants. This procedure was found to be the best route to polymers from the more hindered and slowly-reacting piperazines (Table II).

### Interfering Factors

Although solution polycondensations are easily and quickly performed, several causes and conditions may lead to the formation of polymer with lower molecular weight than is desired. The following discussion applies broadly to this process and not just to the few polymers reported in the present paper.

**Solvent Reactivity.** The solvent should not react rapidly with amines or acid halides. That is, it should not react during the time necessary to carry



out the polymerization. Solvents which react with amines are acids and active halides such as acetic acid or *sym*-tetrachloroethane. Solvents which react with acid halides are water, alcohols, phenols, amines, etc. What constitutes inertness will depend in part upon the reactivity of the polymer intermediates. Some solvent interference can be overcome by minimizing the contact between the reactant and the solvent.

Procedures I and J illustrate the use of a second diluent for one reactant when the principal solvent interferes in the reaction. An alternative procedure is to add a solid or liquid reactant directly to a stirred solution of the complementary reactants. Both reactants may be added to stirred solvent and, if they are solids, they may be mixed or ground together and added to solvent or the solvent may be added to them (procedure K).

**Impurities.** The fast, low temperature polycondensation reactions are surprisingly tolerant of impurities but this tolerance varies considerably with the circumstances. The purity of the reactants and solvents must be higher than for the interfacial polycondensation method. This is because in a single phase system all of the materials are in the polymerization area.

Nonreactive impurities in the solvent are harmless except insofar as they may depress the solubility of the polymer. Nonreactive impurities in the intermediates cause an incorrect measure of the reactants. The resulting imbalance is most serious as the reaction rate becomes low.

Reactive impurities in solvents are such substances as water, alcohols, acids, and phosgene. Solvents should be distilled and dry. Many A.C.S. reagent-grade solvents and some other grades are acceptable as sold. The variable importance of solvent impurities is shown by the effect of the alcohol stabilizer in chloroform on two polymerizations. 2,5-DMePip-T polyamide, prepared in unwashed chloroform, had an inherent viscosity of 2.1 whereas 2,5-DMePip-10 polyamide had an inherent viscosity of only 0.3. The sebacyl chloride reacts much faster with the alcohol than terephthaloyl chloride in a preliminary contact.

Active impurities in the intermediates are substances which react with the complementary reactant. If moisture gets into the diacid chloride, both diacid and monoacid-monochloride may form. The diacid and hydrogen chloride are not wholly inert impurities for they may take away acid acceptor or diamine as salt. The monochloride is a chain terminator. The diamine may contain carbonate, water, or monofunctional impurities from its synthesis while the acid chloride may also contain hydrogen chloride, thionyl chloride or phosphorous halides or monoacid halides from an impure acid. The seriousness of their presence will depend on the relative reaction rates of impurities and reactants. For instance, diisopropylamine can be used as an acceptor for 2,5-DMePip-T polyamide preparation, but would interfere in the reaction of terephthaloyl chloride and a bis-phenolate, which is a much slower polycondensation.

The only completely satisfactory test of purity is the formation of high polymer. Enough basic polycondensations have now been explored so that such a test is readily made.

**Amine Acid Acceptors.** Secondary and tertiary amines, used as acid acceptors, introduce several interfering reactions. These are dealt with in a following paper.

**Diacylation.** Diacylation of one amine group cannot occur with the secondary diamines, but does sometimes occur with primary diamines. This leads to branched and network polymers. This side reaction was also found in interfacial polycondensation.<sup>32</sup>

**Polymer Precipitation.** Polymer precipitation is a physical interference rather than a chemical reaction, yet it produces a limitation of molecular weight. This must be considered in analyzing the difficulties in making a polymer. The topic is covered under reactivity of polymer precipitates and choice of solvents in following papers.

### Molecular Weight Characteristics

No fractionation of polymers made by solution condensation has been carried out except for the occasional separation of a low molecular weight fraction from the main fraction of high molecular weight polymer. There has been no indication of abnormality in solution behavior or physical properties.

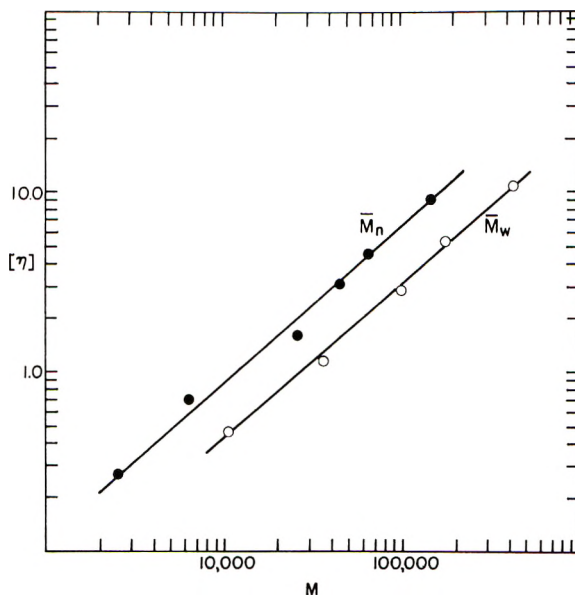


Fig. 5. Intrinsic viscosity in tetrachloroethane-phenol vs. molecular weight for 2,5-DMePip-T polyamide.

Linear plots of  $\eta_{sp}/c$  versus  $c$  over a wide range of values were obtained for dilute solutions of 2,5-DMePip-T polyamide in *sym*-tetrachloroethane-phenol (40:60 by weight) at 30°C. The plots have an average Huggins  $k'$  constant of 0.38. The number-average molecular weights ( $\bar{M}_n$  from

endgroups on whole polymers) versus intrinsic viscosity  $[\eta]$  form a linear log-log plot (Fig. 5). This plot fits the equation

$$[\eta] = 2.96 \times 10^{-4} \bar{M}_n^{0.87}$$

$\bar{M}_n$  values for polymers made in several ways and by interfacial polycondensation do not deviate greatly or in any consistent way from this line.

A limited number of values for the weight-average molecular weight ( $\bar{M}_w$ ) by light scattering yielded the equation

$$[\eta] = 1.69 \times 10^{-4} \bar{M}_w^{0.85}$$

and a ratio of  $\bar{M}_w/\bar{M}_n$  of 2.3 for polymers made by a stirred interfacial polycondensation process in dichloromethane. The ratio indicates a slightly broader than random molecular weight distribution. This is to be expected from a system in which the polymer is precipitated at an early stage of the preparation.<sup>3,4,32</sup> A single-phase system in which the polymer remains dissolved should yield a random distribution. This point has not been established experimentally with 2,5-DMePip-T polyamide. Schnell,<sup>15</sup> however, has reported that polycarbonates made in solution have a random distribution while those which precipitate yield a distribution curve with two peaks.

Exceptionally high molecular weights have been obtained for 2,5-DMePip-T polyamide ( $\bar{M}_n$  up to 400,000) by slow addition of one reactant to the other, as discussed earlier. Such a high degree of polymerization is not readily obtained with most condensation polymers nor does it appear to be necessary for the achievement of a normal range of physical properties.

Endgroup and molecular weight determinations were carried out by Vernis Good, Miss Jean Schilit, and Dr. K. Van Holde.

## References

1. Wittbecker, E. L., and P. W. Morgan, *J. Polymer Sci.*, **40**, 289 (1959).
2. Beaman, R. G., P. W. Morgan, C. R. Koller, E. L. Wittbecker, and E. E. Magat, *J. Polymer Sci.*, **40**, 329 (1959).
3. Morgan, P. W., and S. L. Kwolek, *J. Polymer Sci.*, **40**, 299 (1959).
4. Morgan, P. W., and S. L. Kwolek, *J. Polymer Sci.*, **62**, 33 (1962).
5. Morgan, P. W., *SPE J.*, **15**, 485 (1959).
6. Carothers, W. H., U. S. Pat. 2,130,523 (9/20/38), assigned to the Du Pont Company.
7. Berchet, G. J., U. S. Pat. 2,321,890 and 891 (6/15/43), assigned to the Du Pont Company.
8. Schlack, P., German Pat. 916,226 (8/5/54); French Pat. 903,983 (10/23/45), assigned to I. G. Farbenindustrie A.-G.
9. Dreyfus, H., British Pat. 615,884 (1/13/49), assigned to Celanese Corp. of America.
10. French Pat. 892,361 (4/5/44), assigned to I. G. Farbenindustrie A.-G.
11. French Pat. 1,049,443 (1953), to Farbenfabriken Bayer A.-G.
12. Wolfrom, M. L., M. S. Toy, and A. Chaney, *J. Am. Chem. Soc.*, **80**, 6328 (1958).
13. Schnell, H., *Ind. Eng. Chem.*, **51**, 157 (1959); *Angew. Chem.*, **68**, 633 (1956).

14. Fox, D. W., and E. P. Goldberg, paper presented at Polytechnic Institute of Brooklyn, Brooklyn, N. Y., March 8, 1958.
15. Conix, A., *Ind. Eng. Chem.*, **51**, 147 (1959); *Ind. Chim. Belge*, **22**, 1457 (1957).
16. Dyer, E., and G. W. Bartels, Jr., *J. Am. Chem. Soc.*, **76**, 591 (1953).
17. Lyman, D. J., *J. Polymer Sci.*, **45**, 49 (1960).
18. Michler, W., and A. Zimmermann, *Ber.*, **14**, 2177 (1881).
19. Vorländer, D., *Ann.*, **280**, 167 (1894).
20. Batzer, H., H. Holtschmidt, F. Wiloth, and B. Mohr, *Makromol. Chem.*, **7**, 82 (1951).
21. Allen, J., and J. G. N. Drewitt, U. S. Pat. 2,558,031 (6/26/51), assigned to Celanese Corp. of America.
22. Carothers, W. H., and J. A. Arvin, *J. Am. Chem. Soc.*, **51**, 2560 (1929).
23. Elwell, W. E., and D. C. McGowan, U. S. Pat. 2,585,323 (2/12/52), assigned to California Research Corp.
24. Wolfrom, M. L., J. O. Wehrmuller, E. P. Swan, and A. Chaney, *J. Org. Chem.*, **23**, 1556 (1958).
25. Coffman, D. D., and F. C. McGrew, U. S. Pat. 2,317,155 (4/20/43), assigned to the Du Pont Company.
26. Frankel, M., Y. Liwischitz, and A. Zilkha, *Experientia*, **9**, No. 5, 179 (1953); *J. Am. Chem. Soc.*, **76**, 2814 (1954).
27. Wieland, T., and H. Bernhard, *Ann.*, **582**, 218 (1953).
28. Kipping, F. B., *J. Chem. Soc.*, **1937**, 368.
29. Hall, H. K., Jr., and P. W. Morgan, *J. Org. Chem.*, **21**, 249 (1956).
30. Hall, H. K., Jr., *J. Am. Chem. Soc.*, **79**, 5439 (1957).
31. Frost, A. A., and R. G. Pearson, *Kinetics and Mechanism*, Wiley, New York, 1953, pp. 122, 260.
32. Morgan, P. W., and S. L. Kwolek, *J. Polymer Sci.*, **A1**, 1147 (1963).
33. Hall, H. K., Jr., *J. Phys. Chem.*, **60**, 63 (1956); *J. Am. Chem. Soc.*, **79**, 5444 (1957).
34. Keyworth, D. A., *J. Org. Chem.*, **24**, 1355 (1959).
35. Basolo, F., R. K. Murmann, and Y. T. Chen, *J. Am. Chem. Soc.*, **75**, 1478 (1953).

### Résumé

Un procédé simple a été décrit pour la préparation de polymères de condensation à partir de diamines et d'halogénures de diacides; il comprend la réaction d'équivalents à température de chambre environ, dans un solvant inerte, avec un accepteur pour le sous-produit acide. Cette première publication discute la formation de polyamides de pipérazines et de chlorures d'acides aliphatiques et aromatiques. Ces exemples sont les polysébacoyle-pipérazines et les polytéraphthaloyle-diméthylpipérazines. L'étude des types d'accepteurs d'acides, des solvants, de l'équilibre de la réaction, des réactions compétitives et du mécanisme de la réaction a été discutée. Quelques uns de ces polymères ont été décrits brièvement en termes de température de fusion, de solubilité et de relations entre les poids moléculaires et leurs viscosités.

### Zusammenfassung

Ein einfacher Prozess zur Darstellung von Kondensationspolymeren aus Diaminen und Halogeniden zweibasischer Säuren wird beschrieben; er besteht in der Reaktion äquivalenter Mengen der Zwischenprodukte ungefähr bei Raumtemperatur in einem inerten Lösungsmittel zusammen mit einem Acceptor für die als Nebenprodukt entstehende Säure. In der ersten Mitteilung der Reihe wird die Bildung von Polyamiden aus Piperazinen und aliphatischen und aromatischen Dicarbonsäurechloriden behandelt. Beispiele bilden Poly(sebazylpiperazin) und Poly(terephthaloyldimethylpiperazin). Im einzelnen werden verschiedene Säureacceptoren, Lösungsmittel, Mengenverhältnis der Reaktionsteilnehmer, störende Reaktionen und der Reaktionsmechanismus behandelt. Einige Polymere werden kurz in bezug auf Schmelztemperatur, Löslichkeit und Viskositäts-Molekulargewichtsbeziehung beschrieben.

Received October 10, 1962

## Amine Acid-Acceptors for the Preparation of Piperazine Polyamides by Low-Temperature Solution Polycondensation

PAUL W. MORGAN and STEPHANIE L. KWOLEK, *Pioneering  
Research Division, Textile Fibers Department, E. I. du Pont de Nemours &  
Company, Inc., Wilmington, Delaware*

### Synopsis

Polyamides from 2,5-dimethylpiperazine and terephthaloyl and sebacyl chlorides, having high molecular weight, were prepared in a single solvent system in the presence of various amine acceptors. Strongly basic, hindered secondary amines were fair acceptors, but tertiary amines were preferred. The tertiary amines performed well when the  $pK_a$  in water was equal to or greater than the  $pK_a$  of the amine group on the end of a polymer chain. The polycondensations were affected adversely by acid chloride-tertiary amine reactions, by precipitation of diamine salts, and under some conditions by precipitation of polymer.

The preceding paper<sup>1</sup> described the preparation of polyamides with high molecular weight from piperazines and aliphatic or aromatic diacid chlorides in a single liquid medium. A surprising discovery was that in some polymerization systems the acid acceptor could be a mole of excess diamine for every two moles of by-product hydrogen chloride. In this paper, we will discuss the use of tertiary amines of varying base strength as acid acceptors.

### EXPERIMENTAL

The materials, methods of purification, and polycondensation procedures were those described in the preceding paper.<sup>1</sup> For the most part, the polymers were made with high speed stirring by Procedure B, although Procedure A was also used when no precipitation of polymer was expected.

Inherent viscosities [ $\eta_{inh} = (\ln \eta_{rel})/c$ ] were determined in *m*-cresol at 30°C. with  $c = 0.5$  g./100 ml. solution.

### DISCUSSION

A requisite for polycondensation at low temperatures of a diamine and diacid halide is that the by-product acid be removed from the reaction site, for amine salts do not react. The acceptor need not be a basic substance, but must retain the by-product acid in some way while the reaction pro-

TABLE I  
Primary and Secondary Amine Acceptors for Preparation of *trans*-2,5-Dimethylpiperazine Polyamides in Chloroform

Amine acceptor	p <i>K</i> <sub>a</sub> in H <sub>2</sub> O <sup>a</sup>	<i>E</i> <sub>1/2</sub> , mv. <sup>b</sup>		Terephthalamide		Sebacamide	
		In ethyl acetate	In aceto-nitrile	$\eta_{inh}$	Yield, %	$\eta_{inh}$	Yield, %
<i>tert</i> -Butylamine	10.45 (25°C.)	130		0.14	88		
Diisobutylamine	10.50 (25°C.)	207		0.06	16		
Diisopropylamine	11.05 (25°C.)	145		2.33	92	0.86	92
<i>cis</i> -2,6-Dimethylpiperidine	10.99 (30°C.)		42	0.56	82		
2,2,6-Trimethylpiperidine	11.27 (30°C.)		64	1.72	96		
2,2,6,6-Tetramethylpiperidine	11.24 (30°C.)		56	1.23	78		

<sup>a</sup> Values from the literature or determined in this laboratory.<sup>2</sup>

<sup>b</sup> *E*<sub>1/2</sub> is the millivoltage reading at the half-titration point at 25°C. with perchloric acid as the titrant.<sup>2</sup>

ceeds. In the case of piperazine polyamides the acceptor may be a tertiary or hindered secondary amine, an inorganic base or excess diamine.

### Secondary Amine Acceptors

The use of excess piperazine as the acid acceptor is a special case and has been discussed.<sup>1</sup> Monofunctional secondary amines, such as diethylamine, piperidine, and *N*-ethylaniline, were useless because of their rapid reaction with the acid halides. In order to be useful, a secondary amine acceptor must be sterically hindered to acylation but not to protons. The results with several operable examples, such as diisopropylamine and 2,2,6,6-tetramethylpiperidine, are given in Table I. The experiments show somewhat greater interference with aliphatic than with aromatic acid chlorides.

The fact that 2,6-dimethylpiperidine is a fair acceptor for the preparation of 2,5-DMePip-T polyamide (from 2,5-*trans*-dimethylpiperazine and terephthaloyl chloride) indicates that the reaction of acid chloride with 2,6-dimethylpiperazine and 2,3,5,6-tetramethylpiperazine would be hindered. The preparation of polyamides with high molecular weight from these piperazines by solution polycondensation is difficult as has been pointed out in the preceding paper. Secondary amines are much less effective acceptors with the highly hindered piperazines.

### Tertiary Amine Acceptors

A wide range of tertiary amines are useful as acceptors in solution preparations of polyamides from sterically unhindered piperazines (Table II). There are base strength and solubility effects and side reactions which impose some limitations. We will consider first systems in which the polymer remains in solution.

**Base Strength Requirements.** The base strength of the acceptor must be above a certain range in order to obtain a polymer having high molecular weight.\* For 2,5-DMePip-T polyamide in chloroform, this was a  $pK_a$  in water  $\geq 7.0$  and for 2,5-DMePip-10 polyamide (sebacamide)  $\geq 7.4$ ; the  $pK_a$  in water is used here as a measure of basicity. The work of Hall<sup>2</sup> has shown that the relative base strengths of amines in organic solvents as determined by millivoltage readings are in the same order as  $pK_a$  values.  $E_{1/2}$  values in ethyl acetate and acetonitrile are included in the table, and either scale could be used for our purposes. The base strengths of the useful acceptors about equal or exceed the base strength of the monoacylated diamine ( $pK_a$  7.5 for monobenzoyl-2,5-dimethylpiperazine) or, in other words, the polymer chain end.

This relationship holds only when the polymer-forming reaction rate is high and the polymer does not precipitate rapidly. For example, the soluble poly(sebacyl piperazine) was prepared in dichloromethane in 93%

\* "High molecular weight" is used to indicate arbitrarily a polymer with an inherent viscosity number of at least 0.6 and a yield above 75%.

TABLE II. Tertiary Amine Acceptors for Preparation of *trans*-2,5-dimethylpiperazine Polyamides in Chloroform

Amine acceptor	$E_{1/2}$ , mv. <sup>b</sup>		Terephthalamide		Sebacamide				
	p <i>K</i> <sub>a</sub> in H <sub>2</sub> O <sup>a</sup>	In ethyl acetate	In aceto-nitrile	Polymerization	Yield,	Polymerization	Yield,		
				mixture	$\eta_{inh}$	%	mixture	$\eta_{inh}$	%
Triethylamine	10.74	197	66	Clear solution	2.97	90	Clear solution	1.60	90
Tri- <i>n</i> -propylamine	10.70	228		Clear solution	1.20 <sup>c</sup>	91			
Tri- <i>n</i> -butylamine	10.89	210		Clear solution	1.33 <sup>c</sup>	93			
<i>N</i> -Ethylpiperidine	10.45	190	84	Yellow color for short time	1.77	83			
<i>N</i> -Allylpiperidine	9.68	248		Yellow color (permanent)	1.88	87	Clear solution	1.56	85
<i>N</i> -Ethylmorpholine	7.70	290	221	Cloudy at 0.5 min. but clears	2.10	87	Clear solution	1.28	90
<i>N</i> -Methylmorpholine	7.41	298		Haze at 1 min.	1.90	86	Clear solution	1.10	70
<i>N,N</i> -Diethyl- <i>m</i> -toluidine	7.24			Orange color and precipitate	1.00	90	Yellow color and precipitate	0.73	60
<i>N,N</i> -Diethyl- <i>p</i> -toluidine	7.09			Color and precipitate	1.15	85	Precipitate	0.26	70
<i>N</i> -Allylmorpholine	7.05	354	273	Some precipitate	1.11	86	Some precipitate	0.33	84
<i>N,N</i> -Diethylamine	6.56	467	425	Orange color and precipitate	0.30	78	Precipitate at once and slight color	0.10	45
Pyridine	5.26	—	—						

<sup>a</sup> Values from the literature or determined in this laboratory at 25°C. <sup>b</sup>  $E_{1/2}$  is the millivoltage reading at the half titration point at 25.0°C. with perchloric acid as the titrant from the work of Hall.<sup>2</sup> Other organic solvents gave  $E_{1/2}$  values which have the same order. <sup>c</sup> Acceptor not purified.

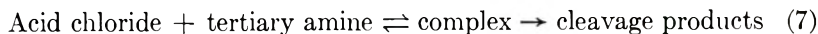
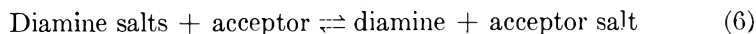
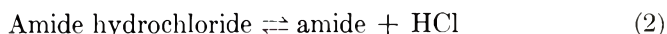
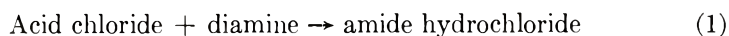
<sup>d</sup> Four moles of diethylamine (100% excess) used with each mole of diacid chloride or diamine.



yield with an inherent viscosity of 1.46 when *N,N*-dimethyl-*m*-toluidine was the acceptor. Poly(terephthaloyl piperazine), which precipitated rapidly, was obtained in very low molecular weight. Likewise preparations with *cis*-2,6-dimethylpiperazine and 2,2,5,5-tetramethylpiperazine were unsatisfactory, although the base strengths of all the piperazines do not differ greatly.

Although relative base strength is a factor in the behavior of the acceptor, it is believed that the coincidence of  $pK_a$  values of the polymer chain end and the weakest useful acceptor is fortuitous. Hall's data, for instance, indicates that if the  $pK_a$  ( $H_2O$ ) scale is to be used for the order of basicities in organic solvents, then the relative position of amines having hetero substituents near the amine function (morpholines, piperazines and related compounds) should be adjusted upward by about one  $pK_a$  unit. This only increases the difference in base strength of the polymer chain end and the weakest useful acceptor. The definition of the latter is arbitrary. For the acceptors listed in Table II the suggested adjustment of  $pK_a$  values would shift the position of *N*-ethyl- and *N*-methylmorpholines up the scale but would not transpose their position relative to the other acceptors. *N*-allyl-morpholine would be placed above the toluidines. This latter change can be justified on all points except for the low viscosity number of the 2,5-DMePip-10 polyamide.

**Reaction Equilibria.** A successful polymerization in the presence of a tertiary amine acceptor must result from the right relationship between several competing processes:



Reactions (2)–(6) are equilibria, whereas (1) and the final step of (7) are irreversible. In order for the polycondensation reaction to yield a product with high molecular weight, the second step of reaction (7) must be slow in relation to (1). If we assume for the present that the system remains homogeneous as it does for DMePip-T polyamide in chloroform, then amine ends on the polymer, diamine, and tertiary amine will all be in equilibrium with the protons at a given point. The proportion of each which is protonated presumably will be determined by their relative base strengths and concentrations. Ionization equilibria will be a secondary matter.

As acylation proceeds there will be more protons and less amine groups

and free tertiary amine molecules. In spite of the apparent increasing unfavorable condition, many reactions proceed to near completion in less than a minute. For this to occur, the rate of proton transfer must be high. As the base strength of the acceptor is decreased, presumably the equilibrium becomes less favorable for maintaining the diamine and amine ends on the polymer in an unprotonated state, which is needed for acylation. A point is reached in the scale of acceptor base strengths below which only polymers with low molecular weight are formed.

A consideration of the data shows that the decline in molecular weight is not entirely abrupt, although there is a sharp drop below an inherent viscosity of one. The break occurs at a slightly higher base strength for sebacamide than for terephthalamide. The difference is ascribed to the higher relative rate of the interfering side reactions with aliphatic acid halide compared to aromatic acid halide.

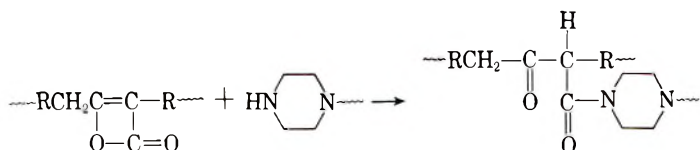
Failure of the acceptor to withhold protons from diamine or amine groups on the polymer to an extent which could have a major effect on molecular weight would not necessarily cause a large decrease in yield. The actual yields were variable. The losses up to 15–20% are mechanical and are due to incomplete polymer precipitation and adhesion to reaction vessels, loss of fine material on and through the filter, etc. The high yields at the highest molecular weights are probably due to greater toughness of the polymer precipitate. In the presence of the weaker acceptors, diamine salt precipitated. Even though the salt has a finite solubility, the equilibrium with these acceptors is so unfavorable that polycondensation proceeded poorly. Only a 45% yield of DMePip-10 polyamide was obtained with pyridine as the acceptor.

Loss of part of the diamine as a precipitate permits another interference, the interaction of acid chloride with acceptor, which is discussed in a later section. The presence of this side reaction is often shown by the formation of a yellow or orange coloration (Table II). The color may be formed only temporarily when acid chloride is added rapidly to a reaction mixture. Similarly, the addition of more than a small excess of tertiary amine acceptor reduces the molecular weight of the resulting polymer. If an unfavorable side reaction were not present, an excess of a weak acceptor could be added to extend the range of operable base strengths by the mass effect on proton equilibrium [reactions (2)–(6)]. Possibly this could be done by the use of acceptors which were hindered toward acid chloride, but not to protons.

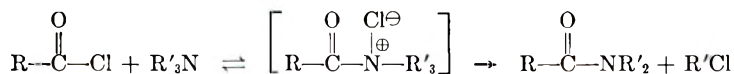
**Preparations with Precipitation of Polymer.** The foregoing discussion has considered for the most part a system in which the polymers were soluble. Precipitation of the polymer by a poor solvent in the presence of a strong acceptor restricts the molecular weight, as will be brought out in detail in following papers. The combination of a poor solvent and a weakly basic acceptor provides a situation even less favorable to polymer formation. In other words, as weaker acceptors are used, the range of useful solvents is reduced. This is illustrated in Table III.



If one adds triethylamine to a chloroform solution of sebacyl chloride (in a 2 to 1 mole ratio and following procedure A of reference 1), allows the orange-brown mixture to stand 1 min., then adds a solution of equivalent *trans*-2,5-dimethylpiperazine, an insoluble polymer results. The polyketo acids have low solubility and would no doubt reduce the solubility of polymers in which they occurred. However, the insolubility of the 2,5-DMePip-10 polyamide in strong solvents such as *m*-cresol suggests that crosslinking has occurred through reaction of the ketene dimer with diamine.



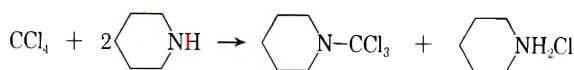
Ketene formation cannot occur with aromatic acid halides, but contact with tertiary amine is harmful and polymers with low molecular weight result. For example, when terephthaloyl chloride was substituted for sebacyl chloride in the procedure above, a polymer with an inherent viscosity of 0.30 was obtained. The literature indicates that the initial reaction between an acid halide and a tertiary amine in all cases is formation of an addition compound. If there is moisture present, an anhydride group might form. In a swollen or water-sensitive polymer, this would be a hydrolytically weak link. Another possible reaction is the formation of a monoamide group and an alkyl halide.



This reaction is known to occur in fair yield at high temperature<sup>6-8</sup> and, therefore, should take place to some extent at room temperature. In a polymerization system this would be a chain-terminating reaction. The analogous interactions of tertiary amines with chloroformates<sup>9-12</sup> and sulfonyl chlorides<sup>13</sup> are faster reactions and consequently give greater interference. The alkyl halide may react with another mole of tertiary amine to form a quaternary ammonium salt.

Fortunately, these side reactions are slow relative to the rate of polymer formation from unhindered primary and secondary diamines. Therefore, high polymers with essentially uniform structure are formed if conditions promoting the side reactions are avoided.

Tertiary amines, as well as other amines, react with many halogenated hydrocarbons, such as chloroform<sup>14,15</sup> and carbon tetrachloride.<sup>16</sup> These are not ordinarily rapid reactions and do not cause any difficulty in ordinary laboratory procedures. They could cause interference and present a hazard if solutions were stored or made up in large quantities. Copper is a catalyst for the reaction of piperidine with carbon tetrachloride.<sup>17</sup>



Bromoaliphatic hydrocarbons,<sup>15</sup> benzyl halides, and similarly reactive solvents should not be used as polymerization media.

Our thanks are expressed to Dr. H. K. Hall, Jr. for helpful discussions, data on base strengths, and samples of methyl-substituted piperidines.

### References

1. P. W. Morgan and S. L. Kwolek, *J. Polymer Sci.*, **A2**, 181 (1964).
2. Hall, H. K., Jr., *J. Phys. Chem.*, **60**, 63 (1956); *J. Am. Chem. Soc.*, **79**, 5444 (1957).
3. Hanford, W. E., and J. C. Sauer, *Organic Reactions*, Vol. III, Wiley, New York, 1946, p. 108.
4. Sonntag, N. O. V., *Chem. Revs.*, **52**, 237 (1953).
5. Frazer, A. H., and J. C. Shivers, *J. Am. Chem. Soc.*, **77**, 5595 (1955).
6. Dehn, W. M., *J. Am. Chem. Soc.*, **34**, 1406 (1912).
7. Tiffeneau, M., and K. Fuhrer, *Bull. Soc. Chim France*, **15**, 162 (1914).
8. Clarke, R. L., A. Mooradian, P. Lucas, and T. J. Slauson, *J. Am. Chem. Soc.*, **71**, 2821 (1949).
9. Hopkins, T., *J. Chem. Soc.*, **117**, 278 (1920).
10. Delaby, R., R. Damiens, and G. d'Huyteza, *Compt. Rend.*, **236**, 2076 (1953).
11. Campbell, J. A., *J. Org. Chem.*, **22**, 1259 (1957).
12. Wright, W. B., Jr., and H. J. Bradander, *J. Org. Chem.*, **26**, 4057 (1961).
13. Jones, L. W., and H. F. Whalen, *J. Am. Chem. Soc.*, **47**, 1343 (1925).
14. Foster, R., *Chem. Ind. (London)*, **78**, 1492 (1959).
15. Williams, H., *Chem. Ind. (London)*, **79**, 900 (1960).
16. Plant, D., D. S. Tarbell, and C. Whitman, *J. Am. Chem. Soc.*, **77**, 1572 (1955).
17. Cromwell, N. H., P. W. Foster, and M. M. Wheeler, *Chem. Ind. (London)*, **78**, 228 (1959).

### Résumé

Des polyamides à poids moléculaire élevé de la 2,5-diméthylpipérazine et des chlorures de téréphtaloyl et de sébacoyl ont été préparés dans un seul système de solvant en présence de divers accepteurs aminés. Les amines secondaires stériquement encombrées et fortement basiques sont de bons accepteurs, mais on leur a préféré les amines tertiaires. Les amines tertiaires conviennent si leur  $pK_a$  dans l'eau est égal ou supérieur au  $pK_a$  du groupe amine terminal de la chaîne polymérique. Les polycondensations sont limitées par des réactions entre les chlorures acides et les amines tertiaires, par la précipitation de sels de diamine et, sous certaines conditions, par la précipitation du polymère.

### Zusammenfassung

Hochmolekulare Polyamide aus 2,5-Dimethylpiperazin und Terephthaloyl- und Sebacylchlorid wurden in einem System mit einem Lösungsmittel und verschiedenen Aminacceptoren dargestellt. Starke basische, sterisch gehinderte, sekundäre Amine waren gut als Acceptoren brauchbar, es wurden aber tertiäre Amine bevorzugt. Die tertiären Amine waren gut brauchbar, wenn das  $pK_a$  in Wasser gleich oder grösser als das  $pK_a$  der Aminogruppe am Ende einer Polymerkette war. Die Polykondensation wurde durch Reaktionen zwischen Säurechlorid und tertiärem Amin, durch Ausfällung der Diaminsalze und unter gewissen Bedingungen durch Ausfällung des Polymeren ungünstig beeinflusst.

Received October 10, 1962

## Electron Spin Resonance of Irradiated Solution-Crystallized Polyethylene\*

R. SALOVEY and W. A. YAGER, *Bell Telephone Laboratories, Incorporated, Murray Hill, New Jersey*

### Synopsis

If films containing oriented lamellae of solution crystallized polyethylene are rotated in the external magnetic field, marked anisotropy in electron spin resonance is noted. When the magnetic field is perpendicular to the chains the spectrum consists of ten lines with a hyperfine component separation of 15 gauss. When the magnetic field is parallel to the chains, the spectrum is a sextet with a splitting of 34 gauss. These splittings are in fairly good agreement with the studies of McConnell et al. on irradiated malonic acid single crystals. The high resolution and stability of electron spin resonance spectra of irradiated polyethylene crystallized from solution suggest greater perfection of crystalline order than in elongated fibers. Moreover, the results on solution crystallized polyethylene indicate that the alkyl radicals are formed at random in the crystalline matrix.

### INTRODUCTION

The predominant radical formed on exposure of polyethylene to ionizing radiation is the alkyl radical produced by carbon-hydrogen bond scission:<sup>1</sup>  $-\text{CH}_2-\dot{\text{C}}\text{H}-\text{CH}_2-$ . Such radicals are relatively short-lived and probably combine rapidly to form crosslinks.<sup>2,3</sup> However, it is possible to trap the alkyl radicals at low temperatures<sup>4</sup> or in a highly crystalline matrix<sup>5</sup> and observe a characteristic six line spectrum in electron spin resonance. These spectra evidence a splitting of approximately 30 gauss and an intensity ratio corresponding to equal interaction of the magnetic moments of five protons with that of the unpaired electron.<sup>6</sup> Studying polyethylene oriented by stretching, several workers<sup>5,7</sup> have observed an anisotropy in the electron spin resonance spectrum of the irradiated polymer.

A simple model of the alkyl radical is assumed in which the proton attached to the "radical" carbon atom is at right angles to the molecular chain axis. This proton produces the anisotropic interaction with the unpaired electron.

We have noted the changes in splitting on rotating a stretched fiber (elongated about 20 times at 0.2 in./min. in air at 70°C.) of polyethylene from a position normal to one parallel to the external magnetic field.

\* Paper presented at the 142nd meeting of the American Chemical Society, Atlantic City, New Jersey, September 1962.

When the field is perpendicular to the fiber axis, we observe a ten-line spectrum; when the field is parallel, we observe a sextet. We have examined this anisotropy by studying the electron spin resonance spectra of oriented "mats" and films of solution crystallized polyethylene preparations<sup>9</sup> on rotation in the external magnetic field.

## EXPERIMENTAL

### 1. Materials

Solution-crystallized polyethylene (Marlex 6000 series, Type 50) was prepared by dissolving the polymer at a concentration of 0.4 g./l. in refluxing xylene, thermostating the resultant solution at 70°C. or at 85°C., and allowing the polymer to crystallize. The resultant suspension of crystals is either compacted to a thin film on filtration or allowed to settle to form a thick mat.

### 2. Irradiation

Two general irradiation techniques were used. In one case, samples of solution crystallized polyethylene were placed in Pyrex tubes and sealed *in vacuo*. The tubes were irradiated in a beam of 1 m.e.v. electrons from a Van de Graaff generator to about 20 Mrads. with the tube placed on powdered dry ice and an empty part of the tube shielded. Following the irradiation, the tubes were inverted into a Dewar flask of liquid nitrogen and the samples shaken into the previously shielded portion of the tube to avoid any signal from radicals trapped in the glass.

Alternately, small squares of solution crystallized polyethylene (film or mat) were placed on powdered dry ice and irradiated to about 20 Mrads. Following irradiation the samples were placed in cold Pyrex tubes and stored in liquid nitrogen in a Dewar flask. In all cases, the dose rate was about 5 Mrads./min.<sup>11</sup>

### 3. Low-Angle X-Ray Diffraction

X-ray diffraction of solution-crystallized preparations have been previously reported.<sup>11</sup> Dried films or mats were mounted in a collimated beam of x-rays and a periodicity of about 100 Å. measured. The orientation of the mass of crystals was estimated from the diffraction pattern.

### 4. Electron Spin Resonance

Electron spin resonance spectra were obtained at various temperatures between -196°C. and 25°C. for the samples in evacuated Pyrex tubes and at 25°C. for the samples in open Pyrex tubes using a Varian EPR spectrometer. We studied the spectra on varying the angle between the applied magnetic field and the surface of the mat or film of solution crystallized preparations by rotating the sample holder.

## RESULTS AND DISCUSSION

Dilute solution-crystallized preparations of polyethylene consist of large ( $\sim 10 \mu$ ) lamellae, about 100 A. thick, in which the molecular chains are normal to and fold regularly in the lamellar surfaces.<sup>9</sup> Marked anisotropy in spin resonance was noted for polyethylene crystallized at 70°C., whereas 85°C. preparations showed slight anisotropy. These results correlated well with low-angle x-ray diffraction: 70°C. preparations revealing three orders of meridional arcs corresponding to regularly oriented layers of 100 A. thick lamellae, while 85°C. preparations were not well oriented. We shall confine further discussion to such oriented preparations crystallized at 70°C.

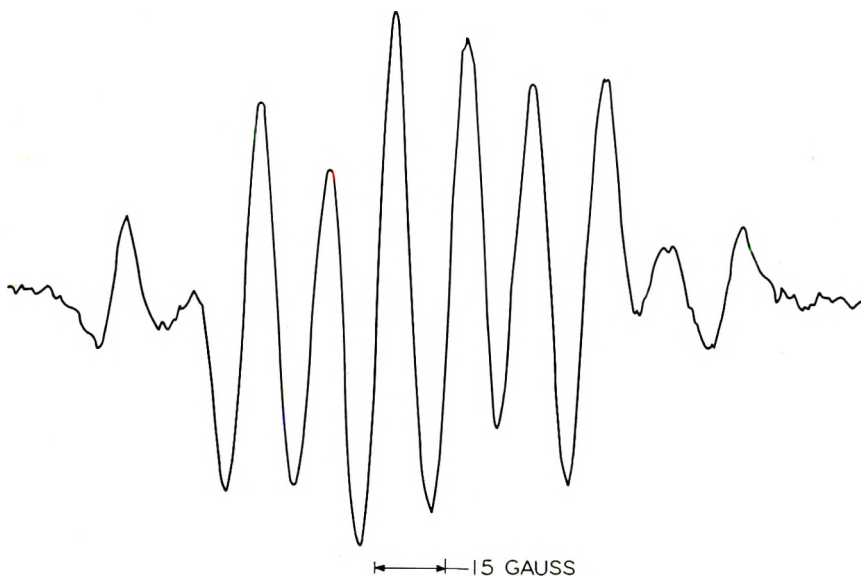


Fig. 1. Electron spin resonance spectrum of irradiated solution-crystallized polyethylene. Magnetic field normal to chains.

It will be recalled that the spectrum of the alkyl radical in unoriented polyethylene is a sextet with a splitting of about 30 gauss.<sup>6</sup> If the polymer chains are oriented by stretching before irradiation, the spin resonance spectra depends on the orientation of the molecular axis to the external applied magnetic field. If the chains are parallel to the field, the ordinary sextet is obtained. When the chain axis is perpendicular to the field, a ten-line electron spin resonance spectrum with a spacing of about 14 gauss is recorded.<sup>7</sup>

We have observed that if a mat or film of solution crystallized polyethylene is mounted so that the magnetic field is always normal to the chains, the resultant spectrum consists of ten lines (Fig. 1). However, if the single crystal preparation is rotated, the spectrum changes from ten lines when the chains are perpendicular to the magnetic field to the sextet





Fig. 2. Electron spin resonance spectrum of irradiated solution-crystallized polyethylene. Magnetic field parallel to chains.

when the chains are parallel to the field (Fig. 2). The hyperfine component separation is 15 gauss for the ten-line spectrum and 34 gauss for the sextet. These results are completely consistent with the fiber studies.<sup>5,7</sup> It is important to note that most of the polymer chain is normal to the lamellar or film surface, with segments of 80 carbon atoms between folds containing about 5 carbons.

These results are in fairly good agreement with McConnell<sup>7,8</sup> who found comparable splittings of 16 and 32.5 gauss on rotation of irradiated malonic acid single crystals in the magnetic field.

Electron spin resonance spectra of irradiated samples in evacuated tubes at  $-196^{\circ}\text{C}$ . and in air at  $25^{\circ}\text{C}$ . were almost identical in shape, although more efficient trapping occurred at the lower temperature.

From these results, we infer that the alkyl radicals reside primarily in the molecular chains normal to the lamellar surfaces or are at least randomly distributed between "straight portions" and folds (since most of the polymer is in the straight chain, the effect of radicals in the fold being negligible). It might be argued that the decay of radicals in the folds—to form crosslinks—is preferential, thereby removing and obscuring any possible preponderance of radicals formed at such sites. However, spin resonance studies using crystalline preparations in which interlamellar crosslinking is suppressed,<sup>11</sup> as well as irradiated samples kept at very low temperatures *in vacuo* (where decay is suppressed), indicate the "usual" orientation effects. Thus, it appears that radicals are not formed overwhelmingly in the folds or in disoriented defects as may have been previously implied.<sup>2</sup>

Oxygen diffusion into irradiated polyethylene may be observed by the appearance of an asymmetric single line at the center of the electron spin

resonance spectrum. This presumably indicates the peroxy radical resulting from oxygen attack on the alkyl.<sup>2</sup> We noted that the absorption intensity of the peroxy radical increased much more rapidly during measurements in air on irradiated highly elongated polyethylene fibers than on solution crystallized preparations. Apparently, oxygen penetrates more rapidly into the elongated fiber than into solution crystallized material. Also, the alkyl spectra from irradiated solution crystallized material are more sharply resolved than analogous spectra on stretched fibers. We believe that both enhanced resolution and slower oxygen penetration reflect greater perfection of packing and orientation in the solution crystallized preparations.

No evidence of radicals other than the alkyl (and peroxy) is apparent, at least until the electron spin resonance signal has decayed considerably. Therefore, radicals produced by chain scission do not appear to be important in the irradiation of these materials. This result supports the suggestion that intramolecular crosslinking rather than enhanced scission accounts for the suppression of gelation in certain irradiated single crystal preparations.<sup>11</sup>

Some comments may be in order concerning the line width which is approximately 10 gauss (full width at half maximum) in either the six- or ten-line spectrum. Calculations by one of us (W. A. Y.) have shown that if the spin density on the central carbon atom is less than unity (about 0.8), the line width is largely insensitive to orientation. That is, when the molecular chains are parallel to the magnetic field, the field is always at right angles to the C—H bond of interest. However, when the chains are normal to the field, the C—H bond direction is randomly distributed with respect to the field. Then, the observed spectrum should result from the superposition of lines corresponding to all possible directions of the C—H bond in the magnetic field and considerable line broadening should characterize the ten-line spectrum. However, if the spin density is only about 0.8 such broadening is reduced.

## CONCLUSIONS

If films containing oriented lamellae of solution crystallized polyethylene are rotated in the external magnetic field, marked anisotropy in electron spin resonance is noted. When the magnetic field is perpendicular to the chains the spectrum consists of ten lines with a hyperfine component separation of 15 gauss. When the magnetic field is parallel to the chains, the spectrum is a sextet with a splitting of 34 gauss. These splittings are in fairly good agreement with the studies of McConnell et al.<sup>8</sup> on irradiated malonic acid single crystals.

The high resolution and stability of electron spin resonance spectra of irradiated polyethylene crystallized from solution suggest greater perfection of crystalline order than in elongated fibers. Moreover, the results on solution crystallized polyethylene indicate that the alkyl radicals are formed at random in the crystalline matrix.

The experimental assistance of R. M. R. Cramer in electron spin resonance and J. V. Pascale in irradiation is gratefully acknowledged. We thank D. W. McCall and R. G. Shulman for many helpful discussions.

### References

1. Charlesby, A., D. Libby, and M. G. Ormerod, *Proc. Roy. Soc. (London)*, **A262**, 207 (1961).
2. Loy, B. R., *J. Polymer Sci.*, **44**, 341 (1960).
3. Lawton, E. J., J. S. Balwit, and R. S. Powell, *J. Chem. Phys.*, **33**, 395 (1960).
4. Smaller, B., and M. S. Matheson, *J. Chem. Phys.*, **28**, 1169 (1958).
5. Kashiwagi, M., *J. Chem. Phys.*, **36**, 575 (1962).
6. Kashiwabara, H., *J. Phys. Soc. Japan*, **16**, 2494 (1961).
7. Libby, D., and M. G. Ormerod, *J. Phys. Chem. Solids*, **18**, 316 (1961).
8. McConnell, H. M., C. Heller, T. Cole, and R. W. Fessenden, *J. Am. Chem. Soc.*, **82**, 766 (1960).
9. Keller, A., and A. O'Conner, *Discussions Faraday Soc.*, **25**, 114 (1958).
10. Salovey, R., and W. Rozenzweig, *J. Polymer Sci.*, **A1**, 2145 (1963).
11. Salovey, R., *J. Polymer Sci.*, **61**, 463 (1962).

### Résumé

Quand on laisse tourner dans un champ magnétique extérieur des films contenant des lamelles de polyéthylène cristallisé en solution, on observe une anisotropie nette de la résonance du spin électronique. Quand le champ magnétique est perpendiculaire aux chaînes polymériques, le spectre est constitué de dix lignes avec une séparation très fine de 15 gauss. Quand le champ magnétique est parallèle aux chaînes, le spectre est un sextet avec une séparation de 34 gauss. Ces séparations sont en bon accord avec les études de McConnell et collaborateurs sur des monocristaux de l'acide malonique. La haute résolution et la stabilité des spectres de résonance du spin électronique du polyéthylène irradié, cristallisé en solution, suggèrent que la orientation est plus parfaite que pour les fibres étirées. En plus, les résultats obtenus avec le polyéthylène cristallisé en solution, indiquent que les radicaux alcoyles sont formés statistiquement dans la matrice cristalline.

### Zusammenfassung

Bei der Rotation von Filmen mit orientierten Lamellen aus lösungs-kristallisiertem Polyäthylen im äusseren Magnetfeld tritt eine ausgeprägte Anisotropie der Elektronenspinresonanz auf. Im Magnetfeld senkrecht zu den Ketten besteht das Spektrum aus zehn Linien mit einem Abstand der Hyperfeinkomponenten von 15 Gauss. Im Magnetfeld parallel zu den Ketten ist das Spektrum ein Sextett mit einer Aufspaltung von 34 Gauss. Diese Aufspaltung stimmt recht gut mit den Ergebnissen von McConnell et al. an bestrahlten Malonsäureeinkristallen überein. Die hohe Auflösung und die Stabilität der Elektronenspinresonanzspektren von bestrahltem, lösungskristallisiertem Polyäthylen spricht für vollkommenere Ausbildung der kristallinen Ordnung als in gedehnten Fasern. Ausserdem zeigen die Ergebnisse an lösungskristallisiertem Polyäthylen, dass die Alkyl-radikale unregelmässig in der Kristallmatrix gebildet werden.

Received October 15, 1962

## Effect of Copper on the Autoxidation of Cellulose Suspended in Sodium Hydroxide Solution

R. I. C. MICHIE, *Textile Chemistry Department*, and S. M. NEALE,  
*Chemistry Department, The Manchester College of Science and Technology,*  
*Manchester, England*

### Synopsis

A kinetic study has been made of the depolymerization of cotton cellulose immersed in aerated solutions of sodium hydroxide and in solutions of sodium hydroxide containing dissolved copper. In absence of (added) copper the reaction rate is proportional to the thermodynamic molal activity of the sodium hydroxide over the concentration range 2-14*N*. Addition of copper causes an increase in the rate but to an extent which depends on the alkali concentration; with constant copper concentration and with increasing alkali concentration the rate now passes through a maximum at approximately 6*N* sodium hydroxide. The decrease in rate above 6*N* alkali has been ascribed to the increasing importance of oxygen solubility and of diffusion which become rate determining factors at the higher alkali concentrations. In 4*N* sodium hydroxide and at low copper concentration diffusion is taken to be unimportant; under these conditions the rate is proportional to the concentration of copper in the solution external to the cellulose but is relatively insensitive to the total amount of copper absorbed by the cellulose. However, it has previously been shown that the overall absorption of copper is probably due to contributions from two different sorbing sites in the cellulose anhydroglucose unit. The rate is found to be approximately proportional to the calculated extent of absorption by the site postulated to form the less stable complex with copper. There is some indication that copper bound in this latter position is responsible for the catalytic depolymerization.

### INTRODUCTION

The interaction of cellulose with copper under alkaline conditions is of considerable importance in the field of cellulose chemistry. Broadly, the process can be considered in two aspects, namely, chemical combination between cellulose and copper, upon which the solvent action of cuprammonium depends, and chemical degradation of cellulose, generally ascribed to autoxidation. The former has been the subject of extensive investigations of which reviews have been given by Heuser<sup>1</sup> and Reeves.<sup>2</sup> Cellulose autoxidation under the influence of alkali and copper has also aroused considerable interest, but knowledge of the reaction is somewhat unsatisfactory. Davidson,<sup>3</sup> and later Hooker, Ritter, and MacLaren<sup>4</sup> observed the autoxidation of alkali-impregnated cellulose to be catalyzed by addition of copper to the system. On the other hand, Lottermoser and Wultsch<sup>5</sup> found copper to have no catalytic action, while Sihtola and

Boström<sup>6</sup> claimed that copper actually decreased the rate of autoxidation of alkali cellulose. Huseman and Weber<sup>7,8</sup> made the interesting suggestion that the terminal aldehyde groups in the cellulose chain can be oxidized to carboxylic acid by boiling the cellulose with an alkaline copper sulfate solution and that no marked degradation was incurred as a result of the treatment. This might be taken as evidence that oxygen is essential for the degradation reaction.

The ready reaction between oxygen and cellulose dissolved in cuprammonium, observed in 1891 by Prud'homme,<sup>9</sup> has stimulated considerable interest over the last six decades, since it detracts considerably from the value of cuprammonium as a solvent for cellulose. The reaction is catalyzed by light<sup>10,11</sup> or may be largely inhibited by the addition of suitable reducing agents, such as cuprous chloride,<sup>12,13</sup> pyrogallol,<sup>14</sup> or metallic copper<sup>15</sup> or of other more easily oxidizable carbohydrates.<sup>16</sup> Kalb and von Falkenhausen<sup>17</sup> investigated the permanganate oxidation of cellulose dissolved in cuprammonium. Their results suggested a conversion of the primary alcohol groups to carboxylic acid, which also appears to be one of the main features of the aerobic oxidation of cellulose in cuprammonium.<sup>18,19</sup>

Copper salts dissolve in aqueous solutions of alkali metal hydroxides to give deep blue solutions, similar in appearance to cuprammonium. Scholder<sup>20</sup> proposed that in such alkaline conditions the copper exists as the anion  $\text{Cu}(\text{OH})_4^-$  which seems quite reasonable in view of the known tendency for copper to coordinate with four electron-donating groups.<sup>21</sup> Cellulose reacts with alkaline solutions of copper to form an insoluble complex known as sodium cupricellulose or Normann's compound, the constitution of which has been the subject of a recent investigation by Davidson and Spedding.<sup>22</sup> The insolubility of sodium cupricellulose offers the advantage of allowing direct determination of the amount of copper bound to the cellulose, which information is required to establish the kinetic dependence of the degradation reaction on copper concentration. In the present work a kinetic study has been made of the depolymerization of cotton cellulose immersed in aerated solutions of sodium hydroxide, with and without the addition of copper sulfate. The system is not strictly homogeneous, but approximates more closely to homogeneity than do the conditions obtained in earlier investigations, where the cellulose was impregnated with rather than suspended in the alkaline solution.

## EXPERIMENTAL

### Materials

The cotton was scoured, bleached Egyptian yarn, of intrinsic viscosity 8.22 dl./g. in cuprammonium hydroxide solution. To facilitate dispersion in the reaction media, the yarn was cut by hand to a staple of 1–2 mm. The sodium hydroxide solutions were made up quantitatively from reagent-grade pellets and the composition checked by titration: it was not considered necessary to remove traces of carbonate. The copper sulfate

solution was made up quantitatively from Analar pentahydrate crystals and the concentration checked by analysis. The cuprammonium solvent was supplied by James Woolley, Sons and Company Ltd. to the B.C.I.R.A. standard specification.<sup>23</sup>

### Apparatus

The reactions were carried out at  $40 \pm 0.05^\circ\text{C}$ . in tall form beakers fitted with rubber bungs. A stream of air was generated with a water pump-aspirator assembly, passed through 30% aqueous potassium hydroxide to remove  $\text{CO}_2$ , and allowed to bubble through the contents of the beakers to provide agitation and a constant supply of oxygen. The air stream left each beaker through a water cooled condenser, which was sufficient to prevent significant loss of water vapor during an experimental run.

### Procedure

The appropriate quantity of 0.1M copper sulfate solution plus water to 50 ml. was added to 250 ml. of the aerated sodium hydroxide solution. After the reattainment of thermal equilibrium, 0.300 g. of standardized cotton (dry weight 0.279 g.) was added, and the reaction allowed to proceed. At the end of the allotted period the cotton was filtered from the solution by use of a sintered glass filter of porosity No. 3: the solution was subsequently analyzed for copper content. The cotton was washed with water followed by one per cent acetic acid solution to remove the copper and finally copious amounts of water to remove the acid. Drying was effected *in vacuo* over phosphorus pentoxide.

The volume contraction on mixing the sodium hydroxide solution with water (approximately 2% at the highest concentration) was assumed to be without significant effect on the liquor-to-fiber ratio, but was taken into account in computing the final alkali concentration in each case.

### Determination of Copper

Analysis for copper was carried out by the standard procedure<sup>24</sup> of electrodeposition on a rotating platinum cathode, from acid solution, the sodium hydroxide having first been neutralized with 5N sulfuric acid. The method was found to be satisfactory in presence of up to 90 g./l. sodium sulfate, and control determinations at the various alkali concentrations gave results in good agreement with the values calculated from the amount of copper added. An attempt was also made to determine the sorption directly by extracting the copper from the alkali-free cupricellulose and titrating iodometrically: however, the results obtained by this method were less consistent and always indicated lower sorptions than those obtained by estimating the copper left in the external solution.

### Determination of Intrinsic Viscosity and Degree of Polymerization

The cuprammonium viscosities of the oxidized specimens were determined by a method similar to that suggested by Howlett and Belward,<sup>14</sup>

in which the degrading action of small amounts of oxygen is prevented by the addition of pyrogallol to the solution. The specimens were conditioned at 72°C. over a saturated aqueous solution of potassium nitrate and ammonium chloride.<sup>25</sup> An amount equivalent to 0.125 g. dry cellulose was then transferred to a 1-oz. bottle and 25 ml. cuprammonium added, followed by three drops of 50% pyrogallol solution. The bottle was closed with a rubber stopper and the whole shaken until dissolution was complete. The viscosity was determined in a B.C.I.R.A. X-type efflux viscometer<sup>23</sup> at 20°C., the solution being poured into the viscometer at the top. In the course of the investigation over thirty control measurements were made on the original cotton with a maximum variation (i.e., range) of 6%. Comparison of the pyrogallol method with the more time-consuming standard procedure<sup>23</sup> in the case of two bleached cottons gave results which differed from each other by less than 2%.

Conversion of viscosity at 0.5% solution to intrinsic viscosity  $[\eta]$  was effected using the data of Calvert and Clibbens.<sup>26</sup> The fluidity of the cuprammonium solvent was taken to be 73 poise<sup>-1</sup>. Number-average degrees of polymerization ( $\bar{P}$ ) were calculated from the relationship:<sup>27</sup>

$$[\eta] = 0.0135\bar{P}^{0.81}$$

### Calculation of Reaction Rate

The total number of bonds between repeating units in any specimen of polymer is given by  $n[1 - (1/\bar{P})]$ , where  $n$  is the total number of units and  $\bar{P}$  the number-average degree of polymerization. In a reaction involving bond scission, the decrease in the number of bonds on passing from  $\bar{P}_0$  to  $\bar{P}_t$  is given by  $n[(1/\bar{P}_t) - (1/\bar{P}_0)]$ . The ratio of this quantity to the original total number of molecules  $n/\bar{P}_0$  then gives the number of scissions per original molecule, which is here designated  $S$ . Thus  $S = (\bar{P}_0/\bar{P}_t) - 1$ .

## RESULTS

### 1. Reaction in Absence of Added Copper

The variation with time of the number scissions per original molecule  $S$  is shown in Figure 1. At each alkali concentration the rate of chain scission becomes constant after approximately 1 hr. The resulting straight lines do not extrapolate through the origin but give positive intercepts on the  $S$  axis increasing with alkali concentration, apparently to a maximum of 0.1 scissions per molecule. A similar effect was found by Schulz and Mertes<sup>28</sup> in an investigation of the action of oxygen on alkali-impregnated cellulose and was ascribed by them to the presence of weak links in the cellulose molecule. From their data it appears that the weak links occur to the extent of approximately one per 10,000 bonds while the present data indicate a figure of approximately half this value. In either case, the incidence of weak links is less than that observed in the acid hydrolysis of cellulose<sup>29</sup> and is probably of doubtful significance.

The subsequent steady rate of reaction increases continuously with in-

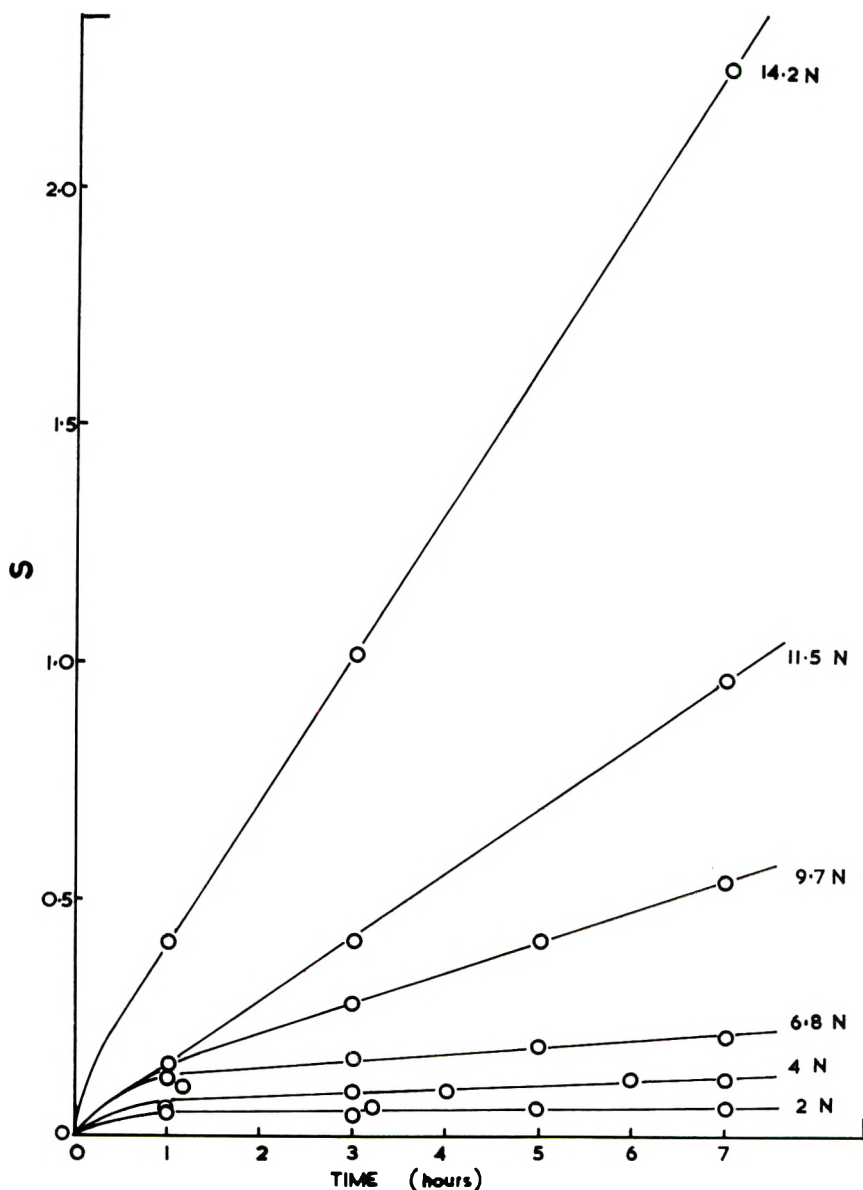


Fig. 1. Reaction in alkali alone: scissions per original molecule as a function of time and alkali concentration.

creasing alkali concentration. This contrasts with the effect observed in the case of alkali-impregnated cellulose<sup>3,30</sup> where the fiber-to-liquor ratio is very much higher than that employed here and where the rate passes through a maximum in the region of 10–12*N* sodium hydroxide. In fact, over the range studied, the rate increases roughly as the fourth power of the alkali concentration, which might be taken to indicate a fourth order reac-



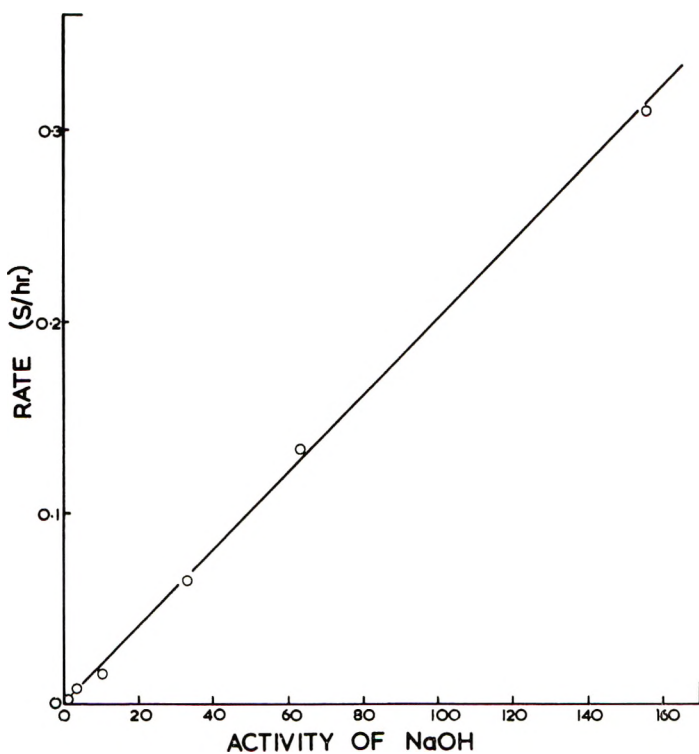


Fig. 2. Variation of reaction rate with the activity of the sodium hydroxide.

tion with respect to the sodium hydroxide. However, at such high concentration of electrolyte the activity becomes much higher than the concentration, as shown by the data<sup>31</sup> in Table I. In Figure 2 the reaction rate is plotted against the molal activity of the sodium hydroxide: the resulting plot is a straight line and indicates a direct proportionality between these two quantities, showing that the reaction is of the first order with respect to alkali activity.

Bell<sup>32</sup> has observed that the rate of oxygen uptake by alkali-impregnated jute cellulose depends on the weight of alkali present in the fiber rather than on the concentration of the solution used in the impregnation, which at

TABLE I  
Reaction Rate and Solute Activity in Sodium Hydroxide Solutions

Normality of NaOH	Molality of NaOH	Molal activity of NaOH	Reaction rate, S/hr.
1.99	2.00	1.41	0.002
3.97	4.00	3.58	0.008
6.75	6.96	10.70	0.015
9.67	10.36	33.5	0.065
11.51	12.68	63.3	0.134
14.2	16.4	156	0.310

first sight appears to conflict with the present results. The explanation for this behavior probably lies in the fact that with the solution-to-fiber ratios employed in Bell's work, the number of hydroxyls available for salt formation would be of the same order as the number of hydroxyl ions present. Thus the combination of a weak acid (cellulose) and its sodium salt would result in a buffer system so that for a given percentage of alkali in the fiber the equilibrium hydroxyl ion concentration might well be relatively insensitive to changes in the volume of water present, i.e., to the concentration of alkali used in impregnation. Such being the case, the equilibrium alkali concentration would be effectively governed by the weight of alkali present rather than by the concentration of the original solution.

### 2. Reaction in Presence of Copper

**a. Influence of Copper Concentration.** The results of varying the copper concentration at a constant alkali concentration of  $3.97N$  are shown in Figure 3 ( $S$ -time curves) and Figure 4 (absorption-time curves). As in the previous case, the rate of reaction becomes constant after a period of approximately 1 hr.; in the early stages, however, the curve is convex to the time axis, indicating an induction period rather than the presence of weak links as observed by Schulz<sup>33</sup> in the reaction between oxygen and cellulose in presence of cuprammonium hydroxide solution. Unfortunately, the present evidence regarding the absence of weak links is not entirely satisfactory, since the equilibrium copper absorption is barely attained in 1 hr.;

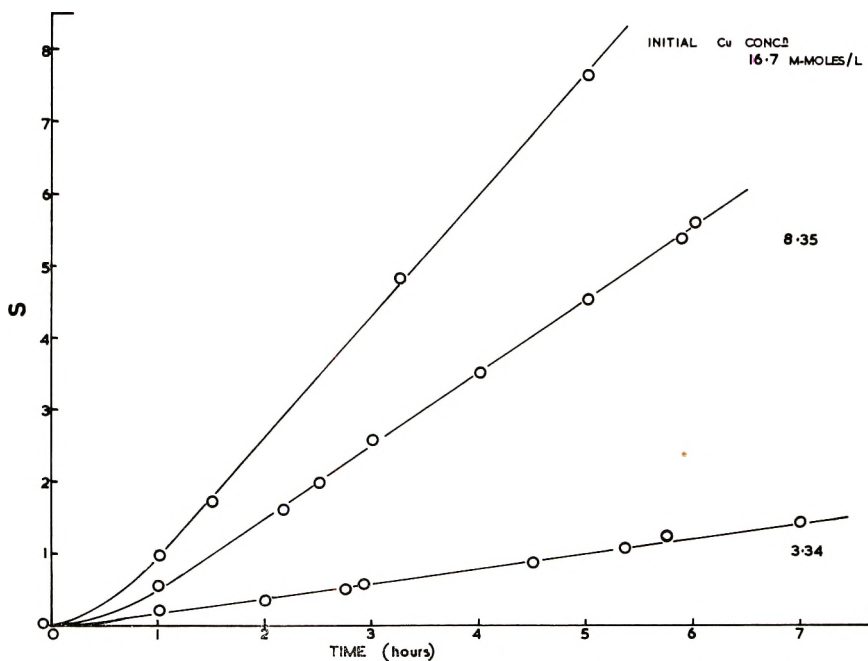


Fig. 3. Reaction in presence of  $3.97N$  alkali and copper: scissions per original molecule as a function of time and copper concentration.

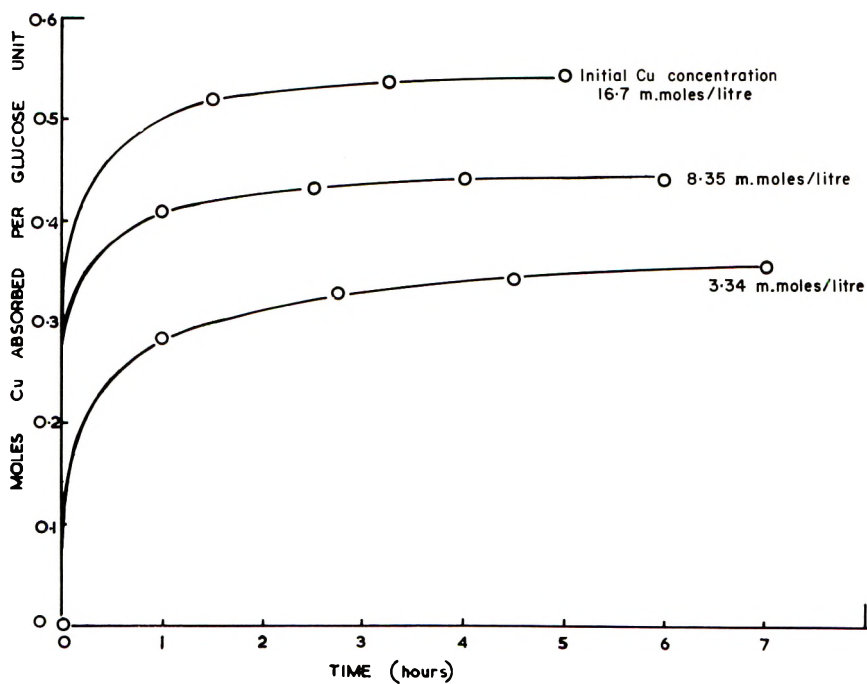


Fig. 4. Preferential absorption of copper by cellulose from 3.97N NaOH.

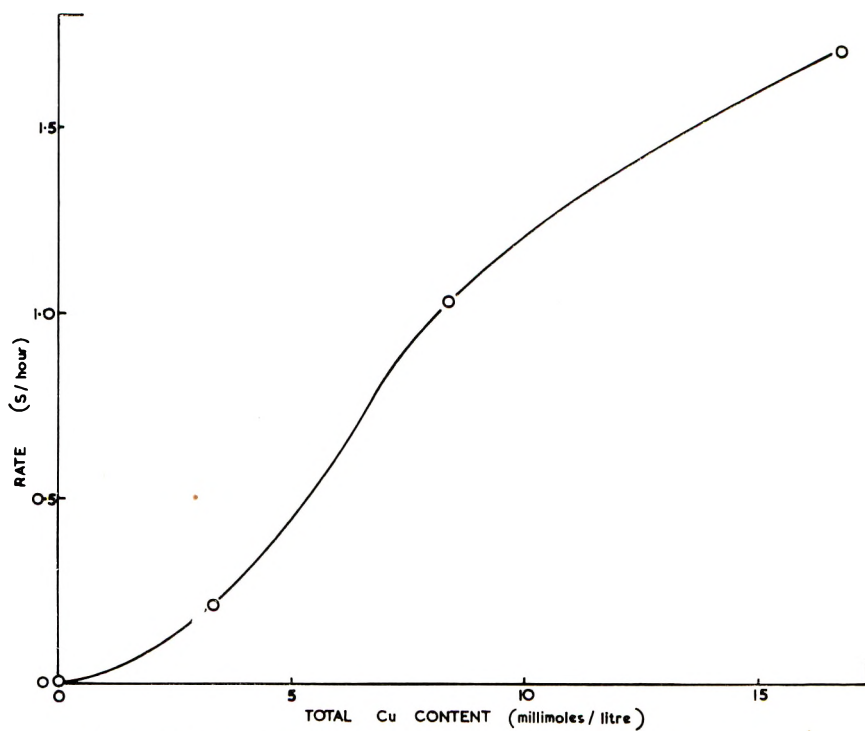


Fig. 5. Reaction rate as a function of the initial copper concentration.

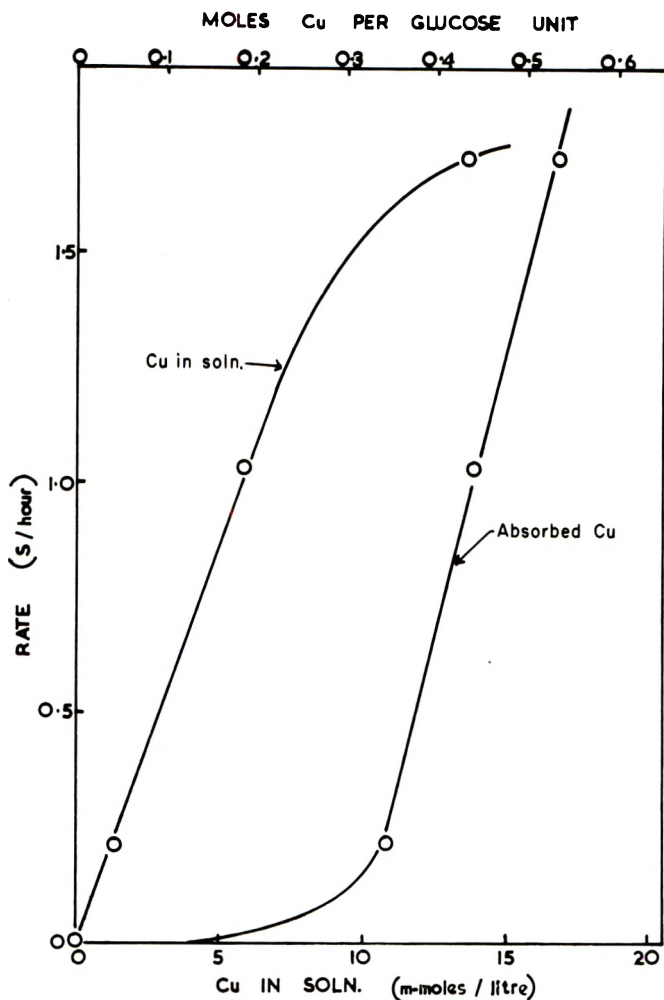


Fig. 6. Variation of reaction rate with equilibrium (external) copper concentration and with equilibrium copper uptake.

if the rate of depolymerization is connected with the extent of absorbed copper, the presence of weak links might well be masked by the relatively low copper uptake in the early stages of the process.

The relationship between reaction rate and the total copper present, shown in Figure 5, indicates an approximate proportionality between these two. However, it seems improbable that the overall copper content would determine the rate since the copper is present in at least two forms, namely, that in solution and that absorbed by the cellulose. In Figure 6 the reaction rate is related to the concentration of copper in solution and in the cellulose. From the rate-concentration curves it appears that the reaction is catalyzed by the copper in solution rather than by the absorbed copper, since at lower concentrations the rate is relatively insensitive to the extent

of absorbed copper but is proportional to the concentration in solution. However, an alternative explanation is possible, as will be shown in the discussion.

**b. Influence of Alkali Concentration.** The effect of varying the alkali concentration at constant total copper content of 16.7 millimoles/l. is shown in Figure 7 (S-time curves) and Figure 8 (absorption-time curves). Again, a brief induction period is followed by a steady reaction rate, but in presence of copper the rate does not increase continuously with alkali concentration, passing instead through a maximum at approximately 6*N*

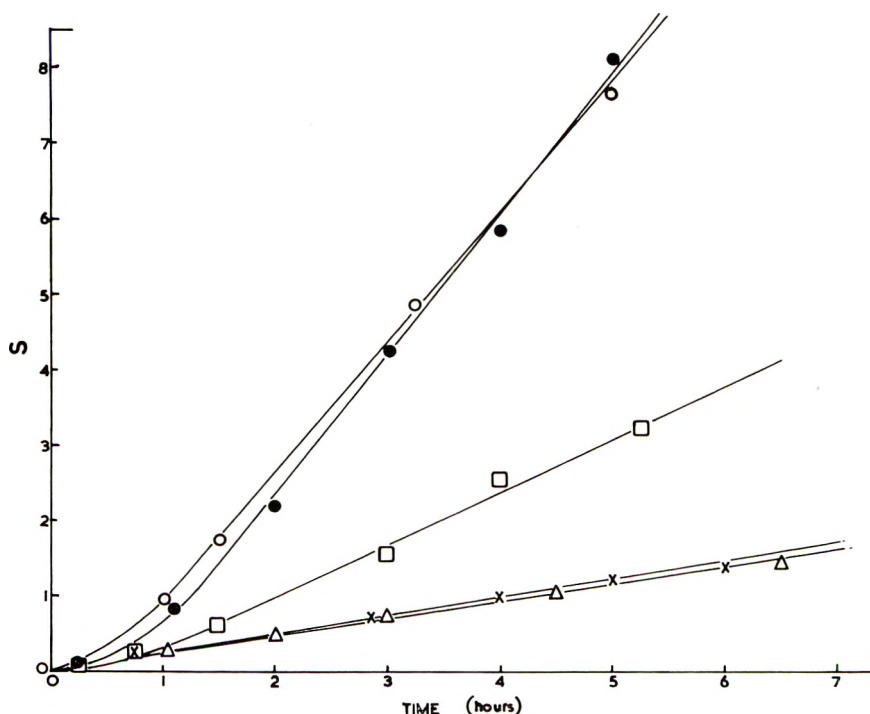


Fig. 7. Reaction in presence of alkali and 16.7 mmoles/l. copper: scissions per original molecule as a function of time and alkali concentration: (x) 1.99*N* NaOH; (O) 3.97*N* NaOH; (●) 6.75*N* NaOH; (□) 9.67*N* NaOH; (Δ) 14.16*N* NaOH.

sodium hydroxide. It seems probable that the decrease in rate above this critical concentration is due to the decreasing solubility of oxygen in the solution<sup>34-36</sup> and possibly to the incidence of diffusion effects. The reaction rates are therefore of doubtful significance *per se* but, nevertheless, have some bearing on the results obtained at lower alkali concentration: specifically, if diffusion becomes the rate-controlling factor only at alkali concentrations above 6*N* it seems reasonable to conclude that the experiments carried out in 4*N* sodium hydroxide have yielded authentic reaction rates.

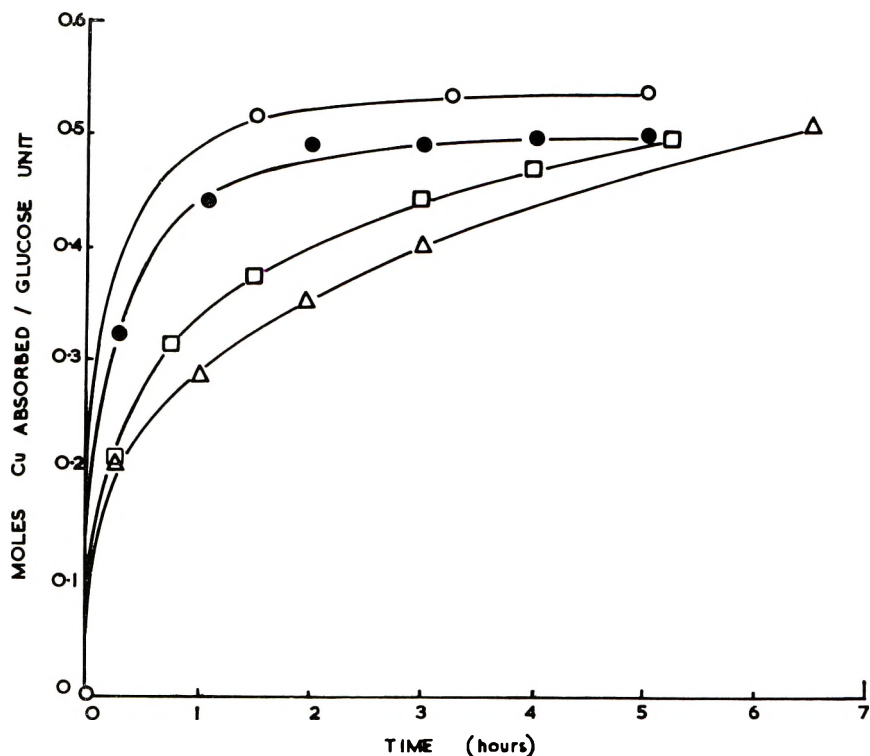


Fig. 8. Preferential absorption of copper by cellulose from NaOH solutions containing 16.7 mmoles/l. copper: (○) 3.97*N* NaOH; (●) 6.75*N* NaOH; (□) 9.67*N* NaOH; (△) 14.16*N* NaOH.

## DISCUSSION

The uptake of copper by cellulose from caustic alkaline solution has been studied in some detail by Davidson and Spedding.<sup>22</sup> Their results did not conform to the Langmuir adsorption isotherm, which might be taken to indicate that the uptake is not due to any simple combination between copper and cellulose. It has in fact been shown<sup>37</sup> that their sorption data can be accounted for quantitatively on the assumption that two different sites in the cellulose anhydroglucose unit can combine with copper, one site forming a more stable complex than the other. The foregoing data were obtained by Davidson and Spedding at a different temperature from that used in the present investigation and indicate slightly different absorptions. However, if it is assumed that for a given copper concentration the distribution of copper between the two sites is the same at both temperatures, the extent of sorption by each site can be calculated in the present system; relevant data are given in Table II. In Figure 9 the reaction rate is plotted against the calculated sorptions by site I (more stable complex) and by site II (less stable complex). It emerges that the rate is very insensitive to small sorptions by site I but is approximately proportional

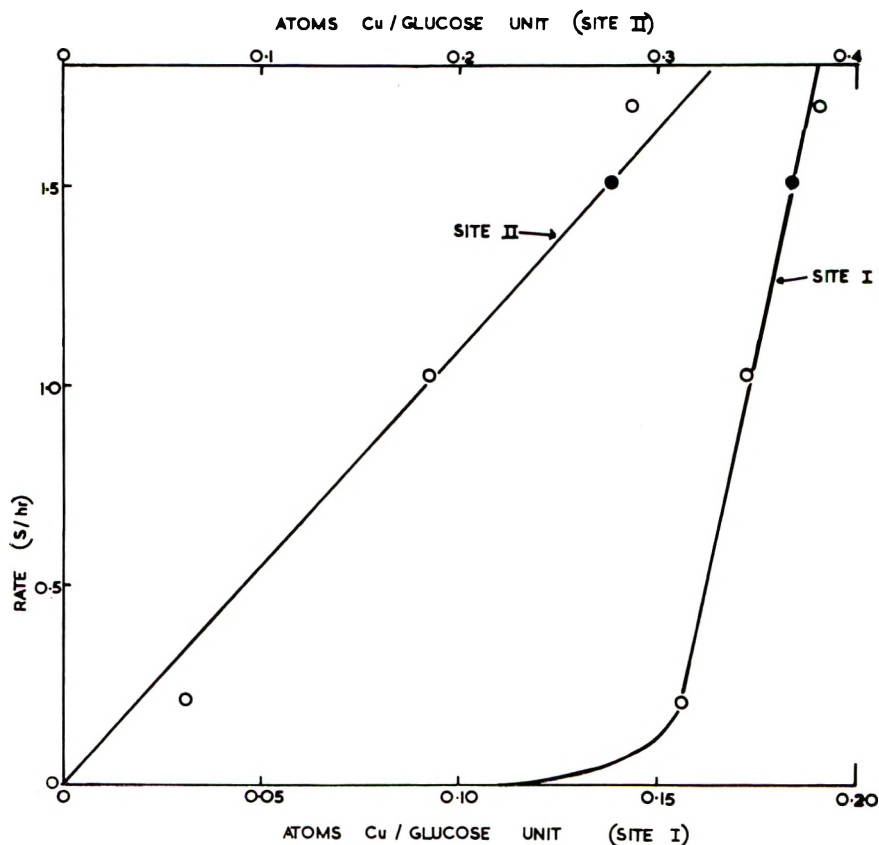


Fig. 9. Reaction rate related to the extent of sorption calculated for the two postulated sorbing sites in the cellulose anhydroglucose unit.

to the extent of uptake by site II over the whole concentration range studied.

The rate of depolymerization of cellulose suspended in sodium cuprate solution thus varies directly with the external copper concentration (cf. Fig. 6) and the extent of uptake by the (postulated) weaker sorbing site. One of these two species presumably acts as the catalyst but there is insufficient evidence to establish which one is active. It may nevertheless

TABLE II  
Copper Uptake by Cellulose from 3.97*N* Sodium Hydroxide and Reaction Rate

External Cu concn., mmoles/l.	Atoms Cu absorbed per glucose unit			Reaction rate, S/hr.
	Total	Site I	Site II	
13.5	0.524	0.381	0.143	1.70
(13.6)	0.505	0.367	0.138	1.51)
5.74	0.436	0.344	0.092	1.03
1.34	0.343	0.312	0.031	0.21

be of significance that in a preliminary experiment carried out at the highest copper content (Table II), the extent of copper uptake was, for some unexplained reason, lower than the value subsequently established; the rate of reaction was also lower, as shown by Figure 9, and this might be taken as evidence that at least part of the absorbed copper is responsible for the catalysis. In addition, the small but significant increase in rate in the first hour (Fig. 3) would be explained if the active species were absorbed, since the extent of absorption increases considerably in this period.

### References

1. Heuser, E., *The Chemistry of Cellulose*, Wiley, New York; Chapman and Hall Ltd., London, 1944, p. 149f.
2. Reeves, R. E., *Advances in Carbohydrate Chemistry*, Vol. 6, Academic Press, New York, 1951, p. 107.
3. Davidson, G. F., *J. Textile Inst.*, **23**, T95 (1932).
4. Hooker, A. H., B. H. Ritter, and S. F. M. MacLaren, U. S. Pat. 2,079,120 (1937).
5. Lottermoser, A., and F. Wulsch, *Kolloid-Z.*, **83**, 180 (1938).
6. Sihtola, H., and B. Boström, *Paperi ja Puu*, **34**, 23 (1952).
7. Huseman, E., and O. H. Weber, *J. Prakt. Chem.*, **161**, 1 (1942).
8. Huseman, E., and O. H. Weber, *Naturwissenschaften*, **30**, 280 (1942).
9. Prud'homme, M., *J. Soc. Dyers Colourists*, **7**, 148 (1891).
10. Gibson, W. H., L. Spencer, and R. McCall, *J. Chem. Soc.*, **117**, 484 (1920).
11. Staudinger, H., and I. Jurisch, *Papier Fabr.*, **35**, Tech., 459 (1937).
12. Scheller, E., *Melliand Textilber.*, **16**, 787 (1935); *Tech. Assoc. Papers*, **25**, 551 (1942).
13. Launer, H. F., and W. K. Wilson, *Anal. Chem.*, **22**, 455 (1950).
14. Howlett, F., and D. Belward, *J. Textile Inst.*, **40**, T399 (1949).
15. Doering, H., *Das Papier*, **5**, 507 (1951).
16. Melkus, K., *Kunstseide*, **10**, 446 (1928).
17. Kalb, L., and F. von Falkenhausen, *Ber.*, **60B**, 2514 (1927).
18. Ivanov, V. I., and E. D. Stakheeva-Kaverzneva, *Compt. Rend. Acad. Sci. U.R.S.S.*, **48**, 405 (1945).
19. Ivanov, V. I., and E. D. Stakheeva-Kaverzneva, *Bull. Acad. Sci. U.R.S.S. Class Sci. Chim.*, **1945**, 492.
20. Scholder, R., F. Felsenstein, and A. Apel, *Z. Anorg. Chem.*, **216**, 138 (1933).
21. Sidgwick, N. V., *The Chemical Elements and their Compounds*, Vol. I, Oxford Univ. Press, 1950, p. 156f.
22. Davidson, G. F., and H. Spedding, *J. Textile Inst.*, **49**, T621 (1958).
23. Clibbens, D. A., and A. H. Little, *J. Textile Inst.*, **27**, T285 (1936).
24. Vogel, A., *Quantitative Inorganic Analysis*, Longmans Green, London, 1943, p. 606f.
25. Edgar, G., and W. O. Swann, *J. Am. Chem. Soc.*, **44**, 570 (1922).
26. Calvert, M. A., and D. A. Clibbens, *J. Textile Inst.*, **42**, T211 (1951).
27. Michie, R. I. C., *Polymer*, **2**, 447 (1961).
28. Schulz, G. V., and F. Mertes, *Das Papier*, **13**, 469 (1959).
29. Michie, R. I. C., A. Sharples, and A. A. Walter, *J. Polymer Sci.*, **51**, 85 (1961).
30. Entwistle, D., E. H. Cole, and N. S. Wooding, *Textile Res. J.*, **19**, 527 (1949).
31. Åkerlöf, G., and G. Kegeles, *J. Am. Chem. Soc.*, **62**, 620 (1940).
32. Bell, W. A., *Nature*, **186**, 963 (1960).
33. Schulz, G. V., *Chem. Ber.*, **80**, 335 (1947).
34. Geffcken, G., *Z. Physik. Chem.*, **49**, 257 (1904).
35. Ipatieff, W. W., W. P. Teodorovitsch, and S. I. Druschina-Artemovitsch, *Z. Anorg. Chem.*, **216**, 66 (1933).



36. Levina, M. I., and N. P. Stsibarovskaya, *J. Phys. Chem. U.S.S.R.*, **12**, 653 (1939).  
37. Michie, R. I. C., *J. Textile Inst.*, **53**, T493 (1962).

### Résumé

On a fait une étude cinétique de la dépolymérisation de la cellulose de coton immergée dans des solutions aérées d'hydroxyde de sodium et dans des solutions d'hydroxyde de sodium contenant du cuivre dissous. En absence de cuivre, la vitesse de réaction est proportionnelle à l'activité thermodynamique exprimée en molalité de l'hydroxyde de sodium dans le domaine de concentrations de 2*N* à 14*N*. L'addition de cuivre provoque une augmentation de la vitesse dans une mesure qui dépend de la concentration en alcali: en présence d'une concentration constante de cuivre et une concentration croissante d'alcali, la vitesse passe par un maximum vers les 6*N* d'hydroxyde de sodium. La diminution de la vitesse au delà de 6*N* d'alcali est incriminée à l'augmentation de la solubilité de l'oxygène et de la diffusion qui deviennent des facteurs déterminant aux concentrations plus élevées en alcali. Dans l'hydroxyde de sodium 4*N* et à basse concentration de cuivre, la diffusion est sans importance: sous ces conditions la vitesse est proportionnelle à la concentration en cuivre en dehors de la cellulose, mais est en rapport avec la quantité totale de cuivre absorbée par la cellulose. Cependant, on a démontré précédemment que l'absorption totale du cuivre est probablement due à l'effet de différents endroits absorbants sur l'unité d'anhydroglucose de la cellulose. On trouve que la vitesse est approximativement proportionnelle à l'augmentation calculée de l'absorption par les endroits qui sont postulés former le complexe le moins stable avec le cuivre. Il est des indications que le cuivre fixé de cette dernière manière est responsable de la dépolymérisation catalytique.

### Zusammenfassung

Eine kinetische Untersuchung der Depolymerisation von Baumwollzellulose unter lufthältiger Natriumhydroxydlösung und Natriumhydroxydlösung mit gelöstem Kupfer wurde durchgeführt. In Abwesenheit von (zuge-setztem) Kupfer ist die Reaktionsgeschwindigkeit der thermodynamischen, molalen Aktivität von Natriumhydroxyd im Bereich von 2*N* bis 14*N* proportional. Zusatz von Kupfer verursacht eine Geschwindigkeitszunahme, deren Ausmass aber von der Alkalikonzentration abhängt: bei konstanter Kupferkonzentration geht nun die Geschwindigkeit bei steigender Alkalikonzentration bei etwa 6*N* Natriumhydroxyd durch ein Maximum. Die Geschwindigkeitsabnahme oberhalb 6*N* Alkali wurde auf die zunehmende Bedeutung der Sauerstofflöslichkeit und der Diffusion zurückgeführt, die bei den höheren Alkalikonzentrationen geschwindigkeitsbestimmend werden. In 4*N* Natriumhydroxyd und bei niedriger Kupferkonzentration scheint die Diffusion keine Bedeutung zu besitzen: unter diesen Bedingungen ist die Geschwindigkeit der Kupferkonzentration in der äusseren Lösung proportional, ist aber verhältnismässig unempfindlich gegen die von der Cellulose absorbierte Gesamtmenge an Kupfer. Es wurde jedoch früher gezeigt, dass die Gesamtabsorption von Kupfer wahrscheinlich durch Beiträge von zwei verschiedenen Sorptionsstellen im Cellulose-Anhydroglucosebaustein zustande kommt. Die Geschwindigkeit ist etwa dem für die Bildung des weniger stabilen Kupferkomplexes berechneten Absorptionsausmass proportional. Es bestehen gewisse Hinweise dafür, dass das in dieser Weise gebundene Kupfer für die katalytische Depolymerisation verantwortlich ist.

Received October 25, 1962

## Main-Chain Degradation and Thermal Stabilization of Polyoxymethylene by Ionizing Radiation

SADAO TORIKAI, *Central Research Laboratories,  
Toyo Rayon Company, Ltd., Otsu, Shiga, Japan*

### Synopsis

Polyoxymethylene dihydrate was irradiated in vacuum and in air at room temperature by  $\gamma$ -rays from  $\text{Co}^{60}$ , and the change of its thermal stability was examined. The logarithm of viscosity number decreased linearly with the logarithm of dose both in vacuum and in air. The decomposition curve of irradiated polyoxymethylene in vacuum at  $200^\circ\text{C}$ . can be divided into two components. The percentage of stable polymer of the irradiated polyoxymethylene dihydrate increased with decreasing solution viscosity, attained a value of 80–95%, and was expressed approximately as function of  $\eta/\eta_0$ . In case of irradiation in air, the stabilization was often invalidated by oxygen. The after-effects of irradiation on the stabilization could not be detected under the irradiation conditions examined in the present study. In decomposition in vacuum at  $250^\circ\text{C}$ ., the irradiated polyoxymethylene dihydrate showed a curve of three components. It seems certain that the irradiated polyoxymethylene dihydrate consists mainly of three kinds of polymer differing in their thermal stabilities. The most stable polymer comprises about one-fourth of total stable polymer. These facts might be explicable with the formation of formyloxy and methoxy endgroups by the disproportionation reaction of radicals produced primarily by main chain scissions. The inclusion of stable polymer before irradiation was noted in the case of the polyoxymethylene produced in the post-polymerization of irradiated solid formaldehyde.

### INTRODUCTION

Ionizing radiation induces various phenomena, such as ionizations or excitations of chemical bonds of polymers, which result in crosslinking, main-chain scissions, changes of side groups, trapped free radicals, and so on. In the case of polyoxymethylene, all these effects of irradiation may bring about changes in its thermal stability to some extent.

Delrin undergoes mainly degradation under irradiation, and no increase in solution viscosity or gelation is observed.<sup>1</sup> In an ideal case where there occur only main-chain scissions, radicals primarily produced by main-chain scissions might disappear mainly by the reactions of recombination and disproportionation. Then, the decrease in degree of polymerization of polyoxymethylene would be directly related to the formation of formyloxy and methoxy endgroups produced by the disproportionation reaction.

On the other hand, the thermal decomposition of polyoxymethylene in

vacuum starts from the polymer ends, and main-chain scissions hardly occur under 270°C.<sup>2</sup>

The present paper is devoted to a study of the change in thermal stability of polyoxymethylene dihydrate when subjected to  $\gamma$ -rays from a  $\text{Co}^{60}$  source. It was found that irradiated polyoxymethylene dihydrate consisted of three kinds of polymer of differing thermal stabilities. The relations between the decrease of solution viscosity and the formation of thermally stable polymer were examined.

## MATERIALS AND METHODS

### Polyoxymethylene

Polyoxymethylene dihydrate was obtained in the polymerization of formaldehyde by introducing substantially anhydrous monomer into stirred *n*-heptane containing dimethylformamide as initiator.

Another sort of polyoxymethylene of extremely high viscosity was also prepared by the post-polymerization of irradiated solid formaldehyde.<sup>3</sup>

### Irradiation

Polyoxymethylene was irradiated both in vacuum and in air at 20°C. and at a dose rate of 0.125 Mr/hr. by  $\gamma$ -rays from  $\text{Co}^{60}$ .

In vacuum irradiation, polymer was irradiated with the other vacant end of the ampoule immersed in liquid nitrogen, as shown in Figure 1 (I). This irradiation method was necessary, because the stabilization of polyoxymethylene dihydrate was often invalidated without trapping out the evolved gases, especially on long exposure to  $\gamma$ -rays.

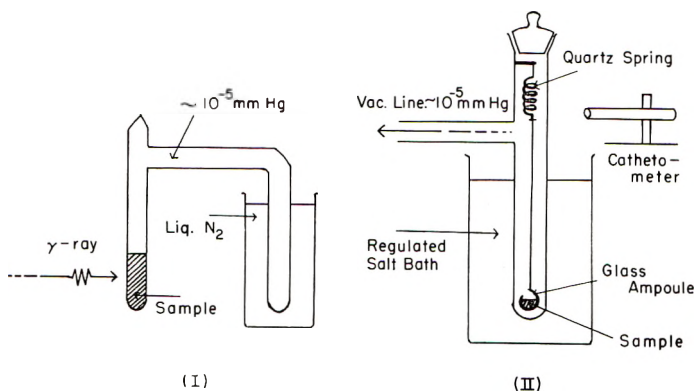


Fig. 1. Apparatus for (I) irradiation and (II) decomposition.

### Thermal Decomposition

Thermal decomposition of polyoxymethylene was carried out in vacuum ( $\sim 10^{-5}$  mm. Hg) at 200 and 250°C. The experimental apparatus is shown in Figure 1 (II). About 30 mg. of polymer was put into a glass

vessel which was connected to a quartz spring balance. After evacuation of air from the sample for 1 hr. at  $\sim 10^{-5}$  mm. Hg, heated salt was poured into the bath just before the measurement. About 6–8 min. was required for the polymer to attain a temperature of 200 or 250°C. The decrease of weight of the sample was measured by use of a quartz spring and a cathetometer.

### Solution Viscosity

The polymer was dissolved in *p*-chlorophenol containing 2%  $\alpha$ -pinene and maintained at 110°C. for 1 hr.; the viscosity number  $\eta_{sp}/c$ , was then measured at 60°C. and at a concentration of  $0.5 \pm 0.001$  g. polymer/100 cc. solvent by use of an Ostwald viscometer.

### Other Measurements

Infrared spectra, gas chromatograms, and electron spin resonance spectra were also examined. Infrared spectra were measured as films obtained by pressing polymer powder with 8–10 ton/cm.<sup>2</sup> for 16 hr.

## RESULTS

### Thermal Stabilization

Figure 2 shows plots of the decomposition of irradiated polyoxymethylene dihydrate in vacuum at 200°C. Decomposition of unirradiated polyoxymethylene dihydrate follows approximately a linear relation between logarithmic polymer residue and decomposition time. Then,

$$-d[\ln m(t)]/dt = k_1 \quad (1)$$

where  $m$  is polymer residue and  $t$  decomposition time. The coefficient  $k_1$  is estimated to be 0.18–0.22 min.<sup>-1</sup>.

On the other hand, each decomposition curve for irradiated polyoxy-

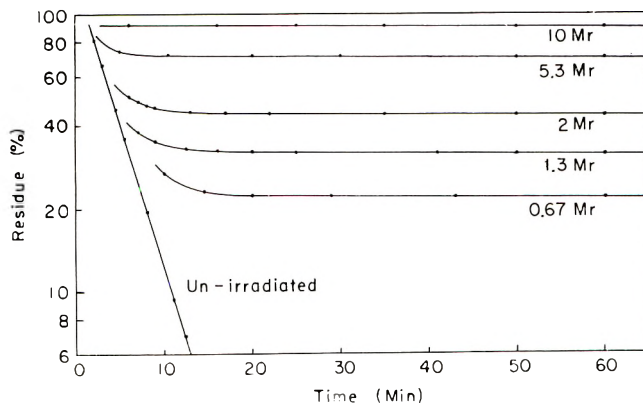


Fig. 2. Decomposition of irradiated polyoxymethylene dihydrate in vacuum at 200°C. Initial viscosity number  $\eta_0 = 2.49$ .

methylene can be divided into two components and expressed approximately as follows:

$$\begin{aligned} m &= m'_1 + m'_2 \\ -d[\ln m'_1(t)]/dt &= k'_1 \\ -d[\ln m'_2(t)]/dt &= k'_2 \end{aligned} \quad (2)$$

where  $m'_1$  is concentration of unstable polymer and  $m'_2$  of stable polymer. The concentration of stable polymer  $m'_2$  in irradiated polyoxymethylene increases with radiation dose. Although the values of  $k'_1$  from the results in Figure 2 are not so accurate, these values are approximately equal to  $k_1$ , while  $k'_2 \approx 0.0002\text{--}0.0007 \text{ min.}^{-1}$ .

### Relation between Decrease of Solution Viscosity and Formation of Stable Polymer

The logarithm of solution viscosity of polyoxymethylene decreases approximately linearly with the logarithm of dose under irradiation in vacuum at room temperature, as shown in Figure 3.<sup>1</sup>

Figure 4 shows plots of stable polymer  $m'_2$  versus radiation dose. The concentration of stable polymer  $m'_2$  attains a value of 80–95%. The initial viscosity number of the sample is higher, so the stabilization rate is larger. It is also noticeable that the polyoxymethylene polymerized from irradiated solid formaldehyde has in itself 31 or 41% of stable polymer before being subjected to irradiation.

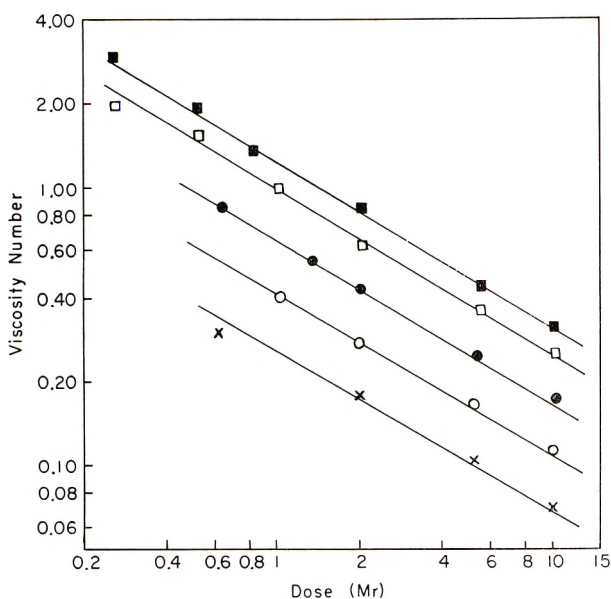


Fig. 3. Decrease of viscosity number of polyoxymethylene dihydrate by irradiation in vacuum: (●)  $\eta_0 = 2.49$ ; (○)  $\eta_0 = 0.97$ ; (×)  $\eta_0 = 0.49$ ; (■, □) polymer obtained from solid-state irradiation of formaldehyde.

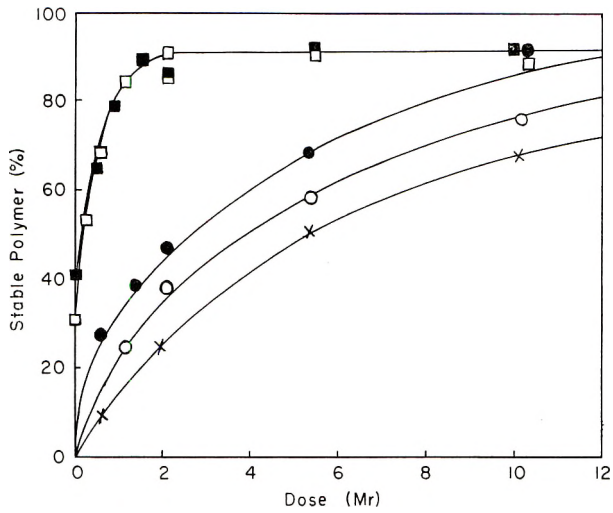


Fig. 4. Formation of stable polymer by irradiation in vacuum (decomposition in vacuum at 200°C.): (●)  $\eta_0 = 2.49$ ; (○)  $\eta_0 = 0.97$ ; (×)  $\eta_0 = 0.49$ ; (■, □) polymer obtained from solid-state irradiation of formaldehyde.

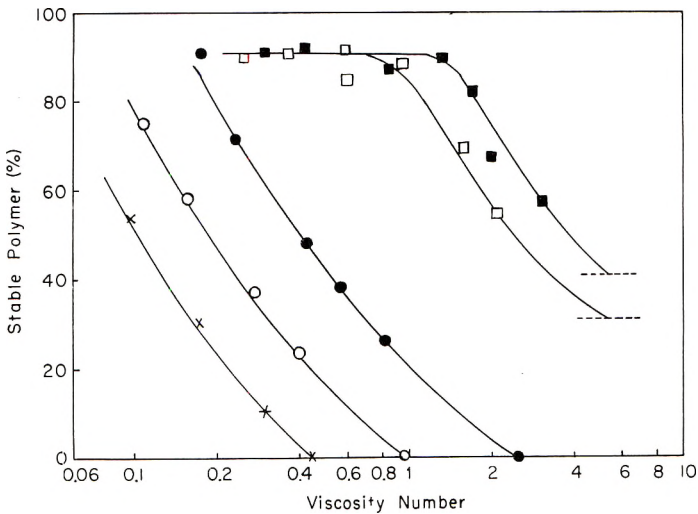


Fig. 5. Relation between decrease of viscosity number and formation of stable polymer (decomposition in vacuum at 200°C.): (●)  $\eta_0 = 2.49$ ; (○)  $\eta_0 = 0.97$ ; (×)  $\eta_0 = 0.49$ ; (■, □) polymer obtained from solid-state irradiation of formaldehyde.

From the results in Figures 3 and 4, the relation between the formation of stable polymer and the decrease of solution viscosity of polymer can be obtained. Figure 5 shows plots of stable polymer versus the logarithm of viscosity number. As the curves run parallel to each other, the stable polymer is a function of  $\eta/\eta_0$ .

$$S = f(\eta/\eta_0) = f(P/P_0) \quad (3)$$

Here we denote stable polymer as  $S(= m'_2)$ , viscosity number as  $\eta$ , and number-average degree of polymerization as  $P$ , where the relationship that  $\eta \propto P^a$  is assumed. Corrections, however, should be made for polymer which includes stable polymer before irradiation. The solution viscosity of the polyoxymethylene obtained from irradiated solid formaldehyde can be estimated by extrapolating the curves to their initial stable polymer contents, i.e., 31 and 41%, respectively. Thus, viscosity numbers of 5-6, which were correlated to values in *p*-chlorophenol solution, were obtained.

### After-Effect of Irradiation on Stabilization

The ESR spectrum of polyoxymethylene irradiated in vacuum at room temperature could not easily be assigned to the three kinds of polymer radicals. The spectrum changed into a doublet after a while both in vacuum and in air. Recently it was reported that radicals produced by main-chain scissions were detected on irradiation at low temperatures and these radicals decayed rapidly even at fairly low temperatures, while dehydrogenated radicals existed longer.<sup>4</sup>

No significant after-effect of irradiation on stabilization was observed in air or in vacuum at room temperature, as shown in Table I.

TABLE I  
After-Effect of Irradiation in Vacuum on Stabilization<sup>a</sup>

Dose, Mr	Exposure time after irradiation, hr.	Polymer stable in decomposition in vacuum at 200°C., %	
		Exposure in vacuum at room temp.	Exposure in air at room temp.
5.3	0	67	—
	24	65	67
	48	68	66
	2500	67	68
0.34	0	15	—
	24	17	16
	48	15	16
	2500	16	15

<sup>a</sup> Initial polymer  $\eta_0 = 2.45$ .

### Irradiation in Air

The stabilized polymer which had been irradiated in vacuum and contained 72% of stable polymer at 200°C. was again irradiated in air at room temperature. As Figure 6 shows, the content of stable polymer decreased with additional dose in air, though the decomposition coefficient  $k'_1$  or  $k'_2$  never changed so explicitly. Several kinds of polyoxymethylene dihydrate were irradiated directly in air; some were stabilized up to 15-30 per cent of stable polymer content, and others could not be stabilized at all. It was admitted, however, that  $k'_1$  or  $k'_2$  did not change so explicitly in air irradiation, whether stable polymer was formed or not.

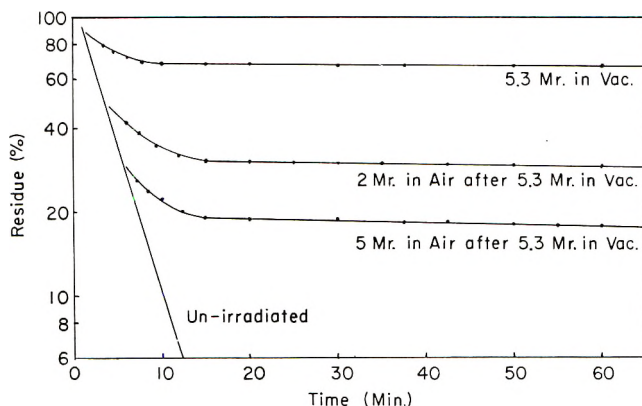


Fig. 6. Changes of thermal stability by irradiation in air at room temperature at a dose rate of 0.125 Mr/hr. (decomposition in vacuum at 200°C.).

No significant difference in the rates of viscosity decrease between vacuum and air irradiation at room temperature was observed.

#### Decomposition at 250°C.

Decomposition of the irradiated polyoxymethylene which contained about 90% of stable polymer ( $m'_2$ ) was carried out in vacuum at 250°C. As shown in Figure 7, three components appeared in the relation of the logarithm of polymer residue versus decomposition time. The decomposition of irradiated polyoxymethylene at 250°C. can be expressed approximately as follows:

$$\begin{aligned}
 m &= m''_1 + m''_2 + m''_3 \\
 -d[\ln m''_1(t)]/dt &= k''_1 \\
 -d[\ln m''_2(t)]/dt &= k''_2 \\
 -d[\ln m''_3(t)]/dt &= k''_3
 \end{aligned}
 \tag{4}$$

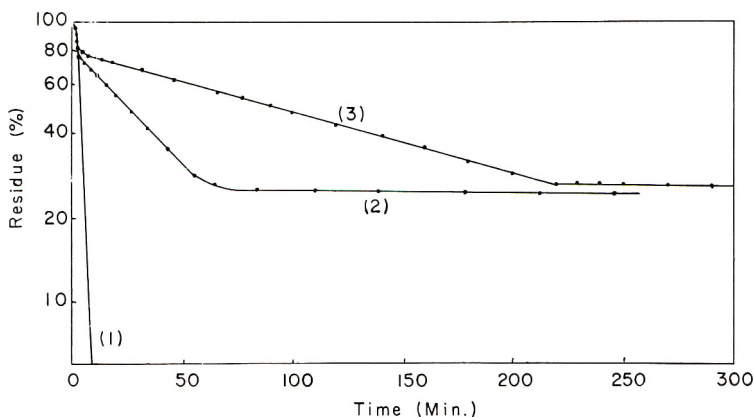


Fig. 7. Decomposition of polyoxymethylene in vacuum at 250°C.: (1) unirradiated polyoxymethylene dihydrate,  $\eta_0 \pm 2.49$ ; (2) polyoxymethylene dihydrate receiving 10 Mr irradiation, initial  $\eta_0 = 2.49$ ; (3) polymer obtained from solid-state irradiation of formaldehyde receiving 1.3 Mr irradiation.



The value  $m''_2 + m''_3$  (75–80% from Figure 7) is close to the value of  $m''_2$ , but apparent deviation is obvious between these values. However, it is interesting that the value of  $m''_3$  (25% is almost equal to one-fourth of  $m''_2$ . In Figure 7,  $k''_2 \approx 0.055\text{--}0.060 \text{ min.}^{-1}$  for the polymer polymerized by dimethylformamide as initiator and  $k''_2 \approx 0.010\text{--}0.012 \text{ min.}^{-1}$  for the polymer polymerized from irradiated solid formaldehyde, and  $k''_1 \approx 0.3\text{--}0.4 \text{ min.}^{-1}$ ,  $k''_3 \approx 0.0002\text{--}0.0005 \text{ min.}^{-1}$  for both kinds of polymer.

### Thermal Decomposition of Mixtures of Various Kinds of Polyoxymethylene

In decomposition of irradiated polyoxymethylene, intrudes a problem whether a mixture of various kinds of polyoxymethylene differing in their

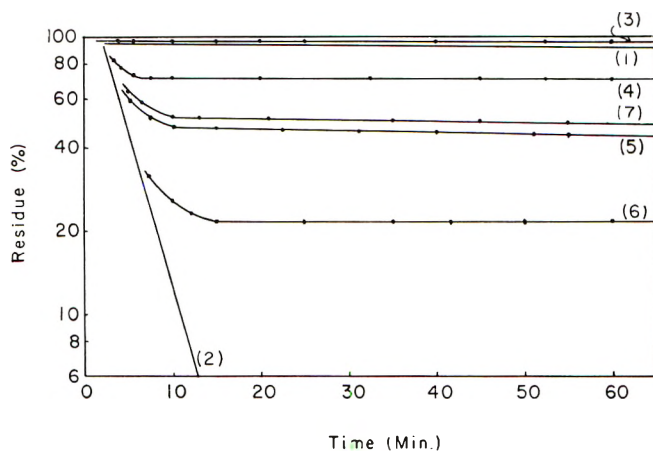


Fig. 8. Decomposition in vacuum at 200°C. of mixtures of various kinds of polyoxymethylene: (1) irradiated polyoxymethylene dihydrate; (2) polyoxymethylene dihydrate; (3) polyoxymethylene diacetate; (4) 25% dihydrate + 75% irradiated; (5) 50% dihydrate + 50% irradiated; (6) 75% dihydrate + 25% irradiated; (7) 50% dihydrate + 25% diacetate + 25% irradiated.

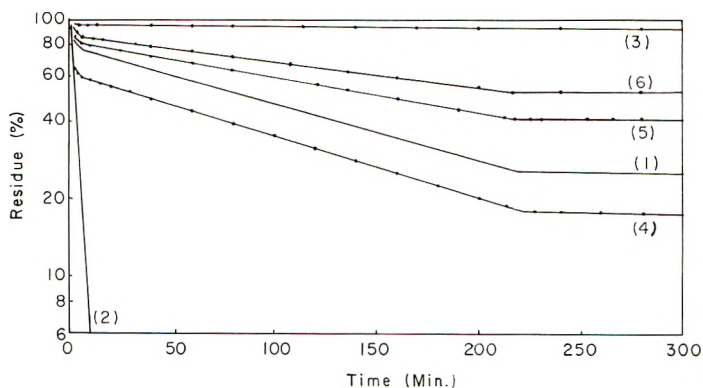


Fig. 9. Decomposition in vacuum at 250°C. of mixtures of various kinds of polyoxymethylene: (1) irradiated polyoxymethylene dihydrate; (2) polyoxymethylene dihydrate; (3) polyoxymethylene diacetate; (4) 20% dihydrate + 80% irradiated; (5) 20% diacetate + 80% irradiated; (6) 40% diacetate + 60% irradiated.

thermal stabilities shows independent decomposition of its constituents or interacted one. Mixtures of irradiated polyoxymethylene with polyoxymethylene dihydrate as unstable polymer or with polyoxymethylene diacetate as stable polymer were decomposed in vacuum at 200 and at 250°C. The percentages of stable polymer were compared with their initial mixing ratios.

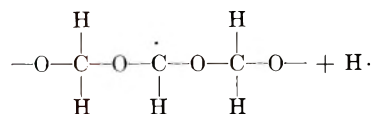
Figures 8 and 9 show the results of decomposition at 200°C. and 250°C., respectively. The stable polymer in decomposition at 200°C.,  $m'_2$  and the most stable polymer in decomposition at 250°C.,  $m''_3$  are confirmed to be almost independent of the presence of stable or unstable polymer.

## DISCUSSION

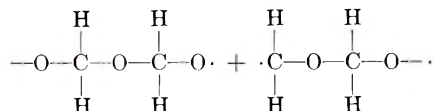
### Polymer Reactions under Vacuum Irradiation

The following four kinds of radicals should be produced primarily by vacuum irradiation of polyoxymethylene.

(A) Side-chain fracture:



(B) Main-chain fracture:



Various reactions can be derived from the combinations of radicals stated above. Considering the dehydrogenation by  $\text{H}\cdot$  in the neighborhood of the primary radicals in (A), and the difficulty of diffusion of polymer radicals in the solid state, the following reactions (C) – (I) might be considered.

(C) Recombination of radicals in (A)

(D) Combination of  $2\text{H}\cdot$

(E) Combination of  $2(-\text{O}-\overset{\cdot}{\text{C}}-\text{O}-) \rightarrow$  crosslinking

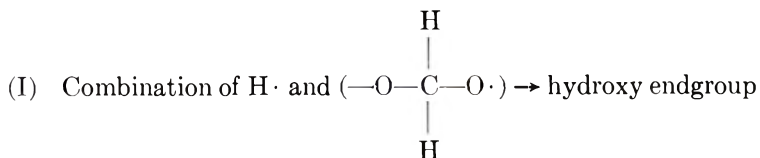
$$\begin{array}{c} \text{H} \\ | \\ -\text{O}-\text{C}-\text{O}- \\ | \\ \text{H} \end{array}$$

(F) Recombination of radicals in (B)

(G) Disproportionation of radicals in (B)  $\rightarrow$  methoxy and formyloxy endgroups

(H) Combination of  $\text{H}\cdot$  and  $(-\text{O}-\overset{\cdot}{\text{C}}-)$   $\rightarrow$  methoxy endgroup

$$\begin{array}{c} \text{H} \\ | \\ -\text{O}-\text{C}- \\ | \\ \text{H} \end{array}$$



Furthermore, reactions of one radical, such as decompositions from the radicals in (B), main-chain scissions from the polymer radical in (A) [here we also included the reactions between derived radicals from (A) or (B) and initial radicals in (A) or (B)] might be considered. Although various reactions might be conjectured also in this case, the formation of any endgroups other than hydroxy, methoxy, and formyloxy seems to be quite small.

Methoxy and formyloxy endgroups, however, could not be detected clearly in the infrared spectra of polyoxymethylene irradiated up to 200 Mr. However, gases liberated from Delrin under irradiation were reported to include various molecules having these endgroups, such as methanol, methyl formate, dimethyl ether, and dimethoxymethane, in addition to other gases such as hydrogen, carbon dioxide, carbon monoxide, formaldehyde, and methane.<sup>1</sup>

Although the definite reactions under irradiation cannot be decided at present hydroxy, formyloxy, and methoxy endgroups should be mainly produced by main-chain fractures under irradiation.

On the other hand, the crosslinking reaction (E) must be less than a half of total main-chain fractures, as long as no gelation is observed.

### Thermal Decomposition

It is well known that polyoxymethylene dimethyl ether is stable in vacuum up to 250°C. as well as polyoxymethylene diacetate. On the other hand, the thermal stability of polyoxymethylene diformate has not been reported. Qualitatively, however, polyoxymethylene diformate seems to have a thermal stability lower than that of polyoxymethylene diacetate and higher than that of polyoxymethylene dihydrate. The thermal stability of polyoxymethylene dihydrate can be shown directly in the results of the preceding section. There, the most unstable part of the three components of irradiated polyoxymethylene always exhibits the same decomposition rate as that of the initial polyoxymethylene dihydrate. This indicates that the most unstable component of irradiated polyoxymethylene is the polymer that has at least one hydroxy endgroup.

It is very difficult to consider the contribution of crosslinking to thermal stabilization. However, there may exist some contribution of crosslinks in such a case where two crosslink points in an unstable polymer chain are linked with stable polymer chains.

Assuming that the stabilization of polyoxymethylene dihydrate under irradiation is due both to main-chain fractures and crosslinkings, numerical expressions of stabilization can be deduced as follows. Here, it is assumed

that crosslinking points are equal to stable main-chain fractures, as far as the contribution to stabilization is concerned.

$$\begin{aligned}
 P &= \frac{P_0}{1 + 1/2(N - Q)P_0R} \\
 S &= \left[ \frac{\left( \sum_{\text{stable}} n_i + 2Q \right) P_0 R}{2 + (N + 2Q)P_0 R} \right]^2 \\
 &= \left[ \frac{\sum_{\text{stable}} n_i + 2Q}{(N + 2Q) - 3Q(P/P_0)} \right]^2 \left( 1 - \frac{P}{P_0} \right)^2 \quad (5)
 \end{aligned}$$

where  $P$  is the number-average degree of polymerization,  $P_0$  is the initial number-average degree of polymerization,  $S$  is the stable polymer (or stabilized polymer) content,  $R$  is the irradiation dose,  $N$  is the number of polymer ends produced per unit dose and per unit main chain,  $n_i$  is the number of  $i$ -type polymer ends produced per unit dose and per unit main chain ( $\sum_{\text{total}} n_i = N$ ), and  $Q$  is the number of branches produced per unit dose and per unit main chain. The assumptions for the above formulations are, (a) proportionality of crosslinkings and all kinds of fractures to dose and (b) random combinations of kinds of endgroups or crosslinking points, and the same distribution of degree of polymerization with respects to a combination of kinds of endgroups or crosslinking points. Assumption b is valid in case of high dose. Then, for  $P/P_0 \rightarrow 0$  ( $R \rightarrow \infty$ ),

$$S \rightarrow \left[ \left( \sum_{\text{stable}} n_i + 2Q \right) / (N + 2Q) \right]^2 \quad (6)$$

In case that the crosslinking is not produced under irradiation or is ineffective for stabilization (in case of stabilization only by main-chain scissions),

$$\begin{aligned}
 S &= \left[ \sum_{\text{stable}} n_i P_0 R / (2 + N P_0 R) \right]^2 \\
 &= \left( \sum_{\text{stable}} n_i / N \right)^2 [1 - (P/P_0)]^2 \quad (7)
 \end{aligned}$$

Particularly, for  $P/P_0 \rightarrow 0$  ( $R \rightarrow \infty$ ),

$$S \rightarrow \left( \sum_{\text{stable}} n_i / N \right)^2 \quad (8)$$

If there were no thermally stable fractures ( $\sum_{\text{stable}} n_i = 0$ ), the conversion to stable polymer by irradiation could not exceed 25%, from eq. (6), for experimentally  $N > 2Q$ .<sup>5</sup> (Any usual molecular weight distribution approaches very closely to a most probable distribution after random scissions, and the critical condition for gelation for this distribution is that  $N = 2Q$ .) This does not agree with the fact that the stable polymer reaches a level of 80–95%.

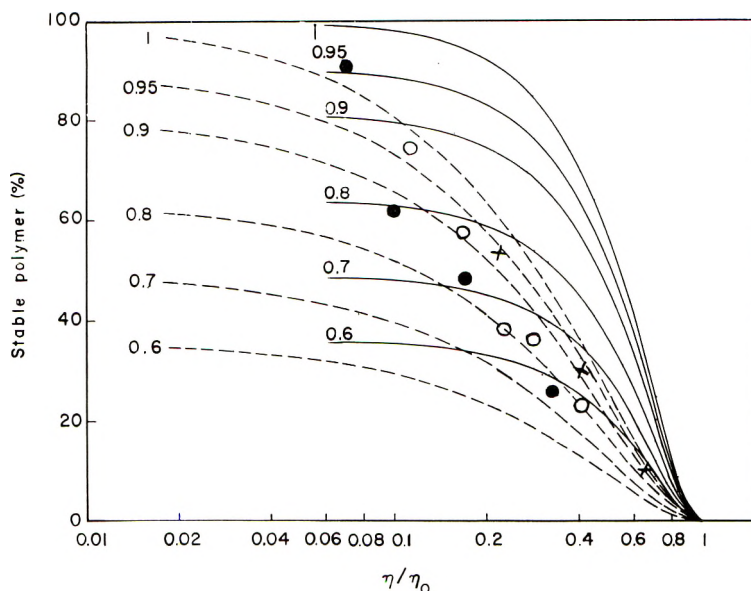


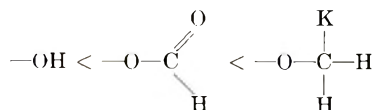
Fig. 10. Stabilization by main-chain fractures. Stable polymer formation with decrease of  $\eta/\eta_0$ : (●,○,×) experimental results (from Fig. 5), polymer stable in vacuum at 200°C.; (---) theoretical curves from eq. (6) for  $a = 1$ ; (—) theoretical curves from eq. (6) for  $a = 0.5$ . Figures on the curves show the values of stable  $n_i/N$ .

In case of stabilization only by main-chain fractures, the experimental results in Figure 5 can be compared with the calculated values from eq. (6) under the assumption that  $\eta \propto P^a$ . In Figure 10 are plotted the experimental results and the theoretical curves of various values of  $\sum_{\text{stable}} n_i/N$ . The experimental stabilization percentages with decrease of  $\eta/\eta_0$  show smaller values than those of the theoretical curves at the initial stage. This, however, seems due to the theoretical defect that the assumption  $b$  was made. Although the value of  $\sum_{\text{stable}} n_i/N$  must be estimated only from the saturation values of stabilization, the stabilization by main-chain fractures seems numerically supported.

The following assumptions seem probable.

$$N = \sum_{\text{total}} n_i = n(\text{—OH}) + n(\text{—OCOH}) + n(\text{—OCH}_3) \quad (9)$$

Thus the order of increasing thermal stabilities is



From the obtained values of  $m'_2$  and  $m''_3$  and the assumption above, the ratios of the number of  $i$ -type endgroups to the total sum of endgroups,  $n_i/N$  can be calculated by using eq. (8). In Table II are shown the values

of  $m'_2$  and  $m''_3$  for polyoxymethylene stabilized up to the saturation value and the calculated values of  $n_i/N$  from them. It is evident that the concentrations of formyloxy and methoxy endgroups formed are almost the same and take values near 50%. The difference between the fractions of formyloxy and methoxy endgroups is very small; also, the fraction of hydroxy endgroups is equally small.

TABLE II  
Constituents of the Polyoxymethylene Stabilized up to Saturation Value

	I, % <sup>a</sup>	II, % <sup>b</sup>
Experimental Results		
Stable part (polymer stable on decomposition at 200°C.)	90	93
Most stable part (polymer most stable on decomposition at 250°C.)	26	27
Calculation of kinds of endgroups		
Hydroxy	5	4
Formyloxy	44	44
Methoxy	51	52

<sup>a</sup> 10 Mr-irradiated polyoxymethylene dihydrate, initial viscosity 2.49.

<sup>b</sup> 1.3 Mr-irradiated polyoxymethylene polymerized from irradiated solid formaldehyde.

It seems that the disproportionation reaction, (*G*), in the case of the two-radical mechanism, mainly constitutes the stabilization and the degradation of polyoxymethylene under ionizing radiation in vacuum.

From the discussion above, other kinds of acetal resins might also be stabilized by irradiation in vacuum by the same principle.

And we hope that the results obtained in this paper will provide some experimental controls in the study of the changes of thermal stability of polyoxymethylene by block-graft copolymerization or by scavenging polymer radicals, under or after irradiation.

The author is greatly indebted to Dr. H. Kobayashi and Dr. E. Mukoyama for their interest and suggestions for this study. He is also indebted to Mr. M. Higuchi, Mr. T. Ichimura, and Mr. S. Saito for the collaborations in the experiments.

## References

1. Sobajima, S., S. Onishi, and I. Nitta, *Ann. Rept. Japanese Assoc. Radiation Res. Polymers*, **1**, 209 (1960).
2. Kern, W., and H. Cherdon, *Makromol. Chem.*, **40**, 101 (1960); W. Kern, H. Cherdon, and V. Jaacks, *Angew. Chem.*, **73**, 177 (1961).
3. Chachaty, C., M. Magat, and L. Ter Minassian, *J. Polymer Sci.*, **48**, 139 (1960); M. Magat, *ibid.*, **48**, 379 (1960); Y. Tsuda, *ibid.*, **49**, 369 (1961).
4. Onishi, S., Y. Nakajima, and I. Nitta, paper presented at the Annual Meeting of the Japan Chemical Society, 1962.
5. Charlesby, A., *Atomic Radiation and Polymers*, Pergamon Press, New York, 1960.

### Résumé

On a étudié le changement de stabilité thermique du polyoxyméthylène—dihydraté irradié, sous vide et à l'air, à température de chambre, à l'aide de rayons-gamma du  $\text{Co}^{60}$ . Le logarithme de l'indice viscosimétrique diminue linéairement en fonction du logarithme de l'intensité et ce tant sous vide qu'à l'air. La courbe de décomposition du polyoxyméthylène irradié sous vide à  $200^\circ\text{C}$ , peut être subdivisée en deux composantes. Le pourcentage de polymère stable de polyoxyméthylène dihydraté irradié augmente lorsque la viscosité de la solution diminue, il peut atteindre de 80 à 95% et s'exprime approximativement comme fonction de  $\eta/\eta_0$ . Lors de l'irradiation à l'air, la stabilisation est cependant souvent diminuée par l'oxygène. Les effets ultérieurs de l'irradiation sur la stabilisation ne peuvent être mis en évidence dans les conditions d'irradiation que nous étudions dans cette communication. Lors de la décomposition sous vide à  $250^\circ\text{C}$ , le polyoxyméthylène-dihydraté présente une courbe à 3 composantes. Il semble certain que le polyoxyméthylène-dihydraté irradié soit composé dès le départ de 3 sortes de polymères qui diffèrent par leur stabilité thermique. Le polymère le plus stable forme à peu près le quart du pourcentage total en polymère stable. Ces phénomènes peuvent trouver une explication dans la formation de groupes terminaux formyloxy et méthoxy lors de la réaction de disproportionnement des radicaux produits par les scissions de la chaîne primaire. On a observé qu'il y avait du polymère stable avant l'irradiation lorsque le polyoxyméthylène dihydraté était produit par post-polymérisation du formaldéhyde irradié à l'état solide.

### Zusammenfassung

Polyoxymethylen-dihydrat wurde im Vakuum und unter Luft bei Raumtemperatur mit  $\gamma$ -Strahlen von  $\text{Co-60}$  bestrahlt und die Veränderung seiner thermischen Stabilität untersucht.  $\log$  (Viskositätszahl) nahm mit  $\log$  (Dosis) sowohl in Vakuum als auch unter Luft linear ab. Die Zersetzungskurve von bestrahltem Polyoxymethylen im Vakuum bei  $200^\circ\text{C}$  kann in zwei Komponenten zerlegt werden. Der Prozentgehalt des bestrahlten Polyoxymethylen-dihydrates an stabilen Polymeren nahm mit fallender Lösungsviskosität zu, erreichte bis zu 80–95% und liess sich annähert als Funktion von  $\eta/\eta_0$  darstellen. Im Falle der Bestrahlung unter Luft wurde die Stabilisierung oft durch Sauerstoff beeinträchtigt. Bestrahlungs-Nacheffekte für die Stabilisierung konnten unter den hier angewendeten Bestrahlungsbedingungen nicht nachgewiesen werden. Bei der Zersetzung im Vakuum bei  $250^\circ\text{C}$  zeigte das bestrahlte Polyoxymethylen-dihydrat eine Kurve für drei Komponenten. Es scheint sicher zu sein, dass das bestrahlte Polyoxymethylen in der Hauptsache aus drei Polymerarten von verschiedener thermischer Stabilität besteht. Der Prozentgehalt an hochgradig stabilem Polymeren beträgt etwa ein Viertel des totalen Prozentgehaltes an stabilem Polymeren. Diese Tatsachen können durch die Bildung von Formyloxy- und Methoxyendgruppen durch Disproportionierung der bei der Hauptkettenspaltung entstandenen Primär-radikale erklärt werden. Die Inklusion von stabilem Polymeren vor der Bestrahlung wurde im Falle des bei der Nachpolymerisation von im festen Zustand bestrahlten Formaldehyd gebildeten Polyoxymethylens festgestellt.

Received November 13, 1962

## Studies on Structure and Properties of Aromatic Polyamides. II. Structural Elucidation of Poly(*m*-xylylene Adipamide)\*

NAOYA YODA† and IKUO MATSUBARA,‡ *Basic Research Laboratory, Toyo Rayon Company, Ltd., Tebiro, Kamakura, Japan*

### Synopsis

X-ray diffraction and infrared spectra of poly(*m*-xylylene adipamide) were investigated. On the basis of x-ray diffraction studies, the twisted form of molecular model for the polymer structure of poly(*m*-xylylene adipamide) was proposed which shows the calculated value of 15.2 Å. to be an identity period consistent with the observed value from x-ray diffraction. The assignment of infrared absorption bands were made with the aid of polarization measurements combined with the techniques of deuteration and iodine treatment of the polymer. It was established on the experimental evidences that the band at  $725\text{ cm.}^{-1}$  is assigned to the amide V vibration. The intense bands at 1639, 1545, and  $1266\text{ cm.}^{-1}$  are ascribed to the amide I, II, and III vibrations, respectively. A tentative assignment of the amide VI and VII was also made. The infrared spectra show that the observed dichroism of the amide characteristic bands of the highly oriented specimen is much lower than that of aliphatic polyamides. This is also consistent with the proposed twisted model for the polymer structure of poly(*m*-xylylene adipamide).

### INTRODUCTION

The infrared spectra of polyamides reported to date have been limited to aliphatic polyamides.<sup>1-7</sup> Various features of the vibrational assignment of aromatic polyamides, especially in the lower frequency region, remain to be solved. Kinoshita<sup>8</sup> has studied the crystal structures of a series of aliphatic polyamides by x-ray methods. As to the crystal structures of aromatic polyamides, however, only the x-ray diffraction studies on molecular packing of polyamide made from *p*-xylylenediamine and sebacic acid were recently reported by Vogelsong,<sup>9</sup> who proposed a crystal structure possessing a preferred orientation of about  $5^\circ$  off the fiber axis.

In this paper we wish to report in detail the structural elucidation of poly(*m*-xylylene adipamide) by x-ray diffraction and infrared spectroscopic

\* Presented in part at the 12th Annual Meeting of the Chemical Society of Japan, Kyoto University, April 3 (1959).

† Present address: Department of Chemistry, University of Arizona, Tucson, Arizona.

‡ Present address, Central Research Laboratories, Toyo Rayon Co., Ltd., Ishiyama, Otsu, Japan.



studies. On the basis of the x-ray crystallographic evidence, we postulate a sterically twisted form of molecular model for the structure of poly(*m*-xylylene adipamide) which shows a calculated value of 15.2 Å. as an identity period as being consistent with observed value of x-ray diffraction.

Deuteration of the polyamide by treatment with heavy water proved to be useful for the assignment of the amide characteristic vibrations.<sup>10</sup> Iodine is known to interact with polyamides by forming a charge-transfer type complex with the amide C=O groups,<sup>7,11</sup> thereby causing a considerable change in the absorption bands of amide characteristic vibrations.<sup>7</sup> These two techniques have been successfully applied to poly(*m*-xylylene adipamide) as an aid in interpreting the infrared spectrum of this polymer.

## EXPERIMENTAL

### Samples

Poly(*m*-xylylene adipamide) was obtained by the polycondensation of purified *m*-xylylene diamine and adipic acid as described in the previous paper.<sup>12</sup>

Thin films of the polymer were prepared directly from the molten sample. Films cast from formic acid solution were also investigated. They were quenched, elongated, and then annealed at a temperature ca. 20°C. below the melting point.

Deuteration of the polymer films was carried out under vacuum at 80°C./10<sup>-4</sup> mm. Hg in the presence of heavy water vapor by using the similar apparatus described by Tadokoro et al.<sup>13</sup> After repeated processes of deuterium exchange reaction with heavy water vapor, the films were deuterated to a considerable extent. Almost completely deuterated films have been prepared by contact with heavy water vapor for 1 hr. at a temperature just below the melting point of the polymer. Iodine treatment of the polymer was carried out by immersing the film into a 20% aqueous solution of potassium iodide containing 5% of iodine for 5–20 hr.

### X-Ray Diffraction

X-ray diffraction patterns of the filaments were obtained using nickel-filtered copper *K* $\alpha$  radiation. For qualitative studies, flat-plate cameras were used. A cylindrical camera (radius, 30.0 mm.) was used to obtain as many of the diffraction spots as possible for the determination of both the fiber identity period and the unit cell.

### Infrared Absorption Measurement

The infrared spectra in the region 4000–300 cm.<sup>-1</sup> were recorded with a Perkin-Elmer Model 21 spectrophotometer (with sodium chloride optics) and a Japan Spectroscopic Model DS-402G spectrophotometer (with grating optics). Polarization measurements on oriented specimens were made in the 4000–600 cm.<sup>-1</sup> region by using a silver chloride polarizer.

## RESULTS AND DISCUSSION

**X-Ray Diffraction Measurement and Structural Elucidation of poly(*m*-Xylylene Adipamide)**

The x-ray diffraction patterns of undrawn and drawn filaments are shown in Figures 1 and 2, respectively. It can be seen from the crystalline pattern that the crystallization occurs immediately after melt-spinning. It is reasonably presumed that aromatic nuclei along the polymer chain effects the easy crystallization of polyamide in the ordinary melt-spinning condition.

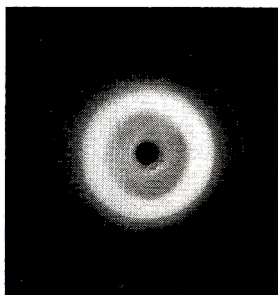


Fig. 1. X-ray diffraction pattern of undrawn filament of poly(*m*-xylylene adipamide).

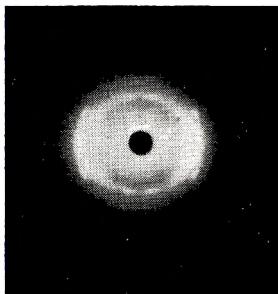


Fig. 2. X-ray diffraction pattern of elongated filament of poly(*m*-xylylene adipamide) drawn along the fiber axis.

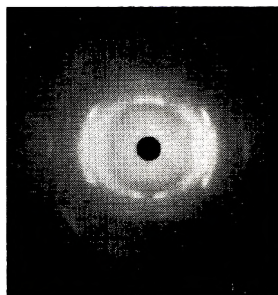


Fig. 3. X-ray diffraction pattern of annealed filament of poly(*m*-xylylene adipamide) drawn along the fiber axis.

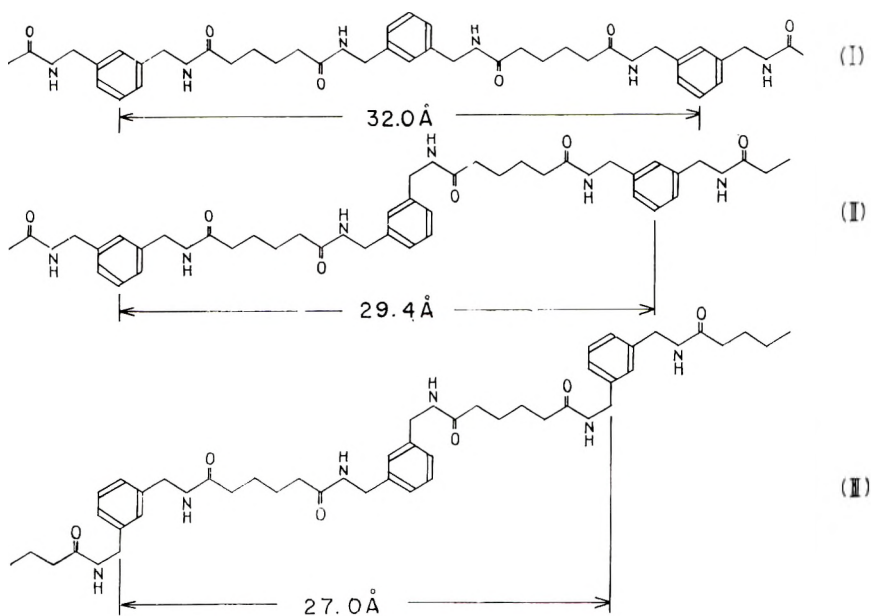


Fig. 4. The planar molecular configurations of poly(*m*-xylylene adipamide).

The drawn fibers were further crystallized by annealing under nitrogen at about 187°C./10 min. Figure 3 shows the x-ray diffraction pattern of heat-treated filament obtained with a cylindrical camera.

Qualitative estimation of layer line spacings for poly(*m*-xylylene adipamide) indicated that one chemical unit is involved in the crystallographic repeat along the fiber axis. The observed fiber identity period was found to be 15.2 Å., and the following triclinic unit cell has been found by reciprocal lattice methods to account for the diffraction spots: (projected unit cell base)

$$a' = 5.10 \text{ \AA.}$$

$$b' = 4.70 \text{ \AA.}$$

$$\gamma' = 69^{\circ}36'$$

The density calculated for this unit cell, assuming one chain molecule passes through it, is 1.20 g./cc., while the measured density of the drawn fibers is 1.22 g./cc. This is not entirely satisfactory in view of the fact that measured densities of crystalline polymers are usually lower than the calculated ones. At present, however, we can only ascribe it to a kind of density anomaly such as that found in some of the synthetic polypeptides.<sup>14</sup>

As to the planar molecular configuration of poly(*m*-xylylene adipamide), the types of possible structures (I), (II), and (III) in Figure 4 can be taken into consideration. Thus the fiber identity period is calculated on the basis of normally accepted bond length and bond angle values<sup>15,16</sup> for each structure to afford the results of 32.0 Å. (I), 29.4 Å. (II), and 27.0 Å. (III).

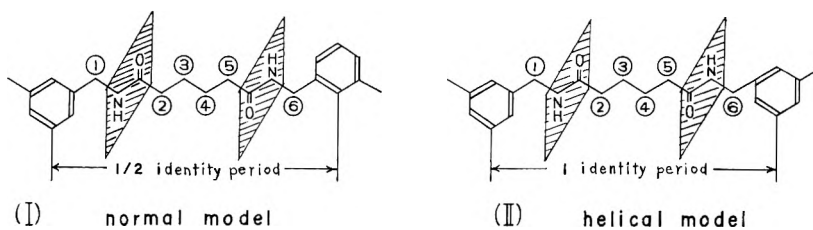


Fig. 5. The molecular conformations of poly(*m*-xylylene adipamide).

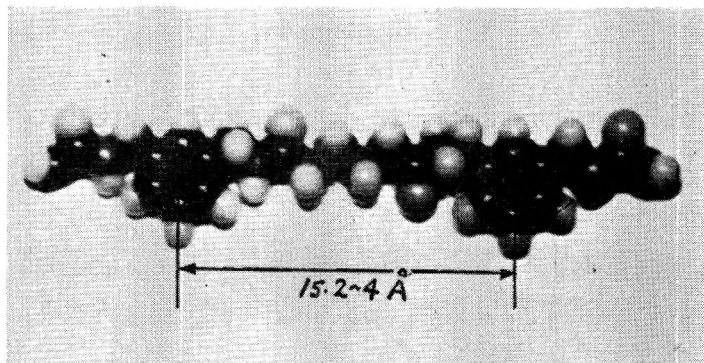


Fig. 6. The twisted molecular model of poly(*m*-xylylene adipamide).

respectively, as shown in Figure 4. Since these values do not agree with the observed fiber identity period, another molecular model should be introduced.

It should be noted that all the calculated values are about twice the observed one, and these molecular models have planar structures. A structure is therefore proposed for poly(*m*-xylylene adipamide) in which the molecule is twisted from the planar structure by an internal rotation angle of about  $30^\circ$  at each of the six carbon atoms, so that, contrary to the case of the planar models, only one chemical unit is required to complete the fiber identity period as shown in Figure 5. Figure 6 shows the twisted model, for which the fiber identity period is calculated to be 15.2-4 Å. The proposed molecular model is in full accord with the features of the x-ray diffraction patterns. Although no attempt has been made to locate atoms in the unit cell by consideration of the relative intensities of the reflections, it seems very likely that the molecules are linked by complete hydrogen bonds to form sheets, which are packed together with reasonable van der Waals distances between them.

### Infrared Absorption Spectrum

The infrared spectra of poly(*m*-xylylene adipamide) films prepared directly from the molten polymer which were quenched and annealed are shown in Figure 7. The film cast from formic acid solution gave the spectrum essentially identical with that of the annealed film. One of the char-

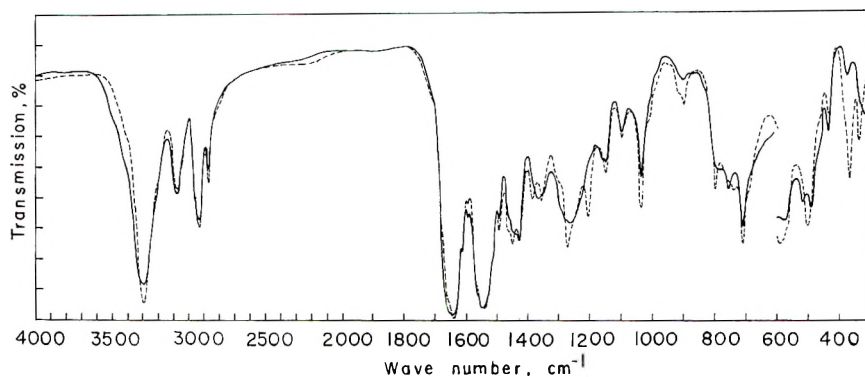


Fig. 7. Infrared spectra of unoriented poly(*m*-xylylene adipamide): (—) quenched film; (--) annealed film.

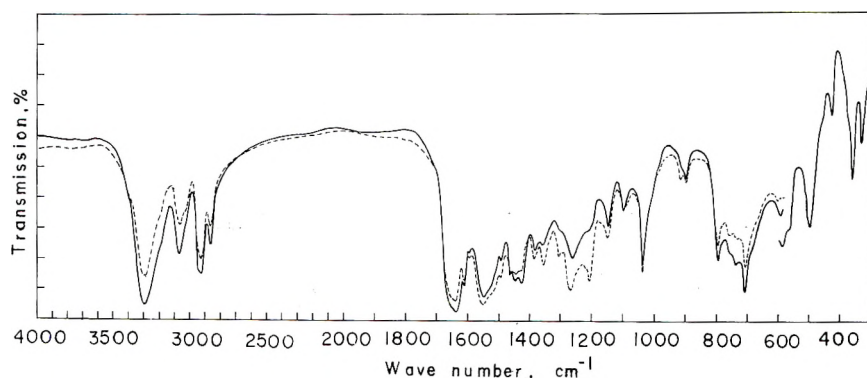


Fig. 8. Infrared spectrum of stretched and annealed poly(*m*-xylylene adipamide): (—) electric vector perpendicular to stretching direction; (--) electric vector parallel to stretching direction.

Characteristic features of the spectrum of this polymer is that the number of bands whose intensity varies with the crystallinity of the specimen is quite large as compared with ordinary aliphatic polyamides. This would indicate that not only rotational isomerism occurs at the polymethylene chain, but rotations involving bonds near the benzene ring may not be negligible. There must be some intermolecular interactions in the crystalline regions, because the bands at ca. 790 cm.<sup>-1</sup> and 900 cm.<sup>-1</sup> are sensitive to the change in the crystallinity of specimen, and they are assigned with confidence to the C—H out-of-plane deformation modes of *meta*-substituted benzene ring.<sup>17</sup>

Poly(*m*-xylylene adipamide) exhibits several prominent bands which are known from the detailed analyses of the spectra of simple monosubstituted amides<sup>18,19</sup> to be characteristic of the *trans*—CONH— group. The intense band at 1639 cm.<sup>-1</sup> is assigned to the amide I vibration which mainly involves the C=O stretching mode, and the bands at 1545 cm.<sup>-1</sup> and 1266 cm.<sup>-1</sup>, respectively, are assigned to the amide II and III vibrations which

correspond to the coupled N—H in-plane deformation and C—N stretching modes. The band at  $3297\text{ cm.}^{-1}$  is assigned to the N—H stretching mode and the weak band at  $3074\text{ cm.}^{-1}$  to the first overtone of the amide II vibration.<sup>1</sup> Although in the case of simple monosubstituted amides the

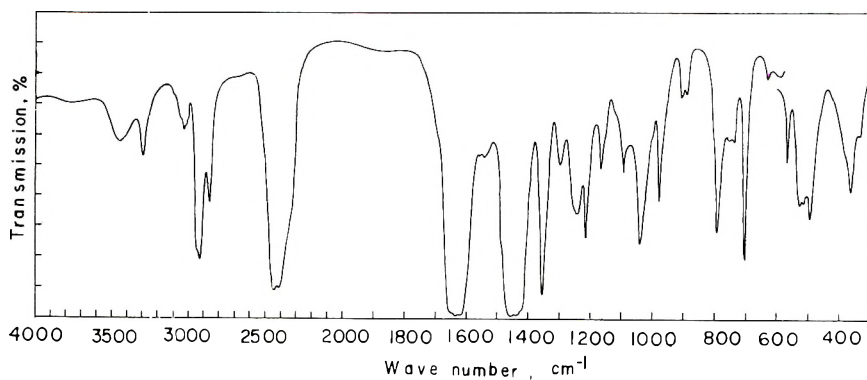


Fig. 9. Infrared spectrum of highly deuterated poly(*m*-xylylene adipamide).

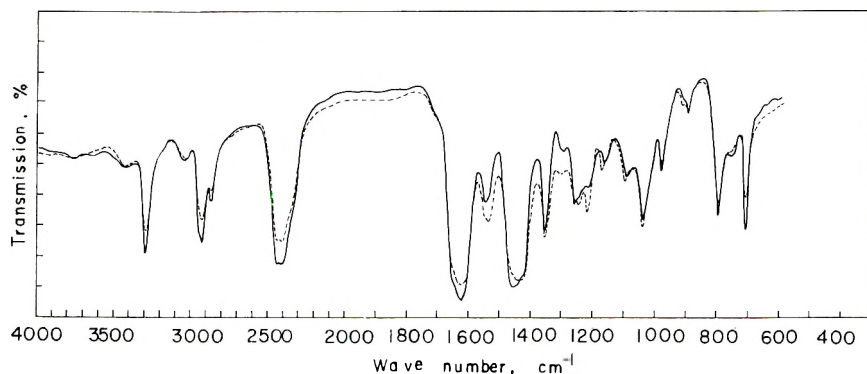


Fig. 10. Infrared spectrum of oriented and deuterated poly(*m*-xylylene adipamide): (—) electric vector perpendicular to stretching direction; (--) electric vector parallel to stretching direction.

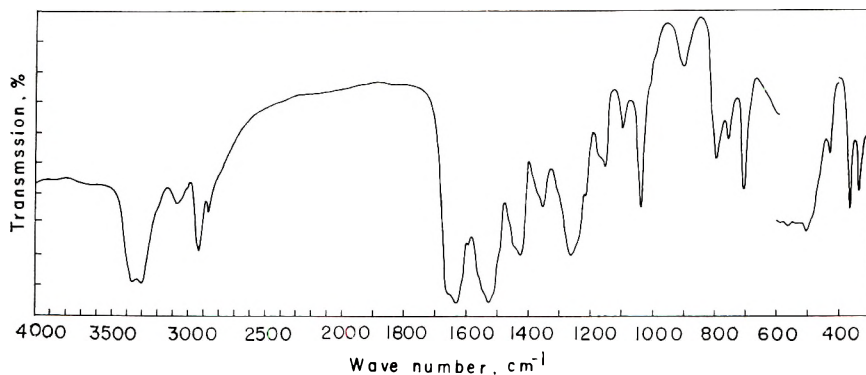


Fig. 11. Infrared spectrum of iodine-treated poly(*m*-xylylene adipamide).

TABLE I  
 Infrared Absorption Bands of Poly(*m*-xylylene adipamide)<sup>a</sup>

Wave number, cm. <sup>-1</sup>	Intensity <sup>b</sup>	Dichroism <sup>c</sup>	Phase <sup>d</sup>	Assignment
3297	<i>vs</i>	$\sigma$		N—H stretch.
3074	<i>m</i>	$\sigma$		2 × Amide II
3032	<i>w sh</i>	$\sigma$		C—H stretch. (aromatic)
3022	<i>vw sh</i>	?		
3005	<i>vw sh</i>	?		
2944	<i>m sh</i>	$\sigma$		
2925	<i>s</i>	$\sigma$		
2865	<i>m</i>	$\sigma$		CH <sub>2</sub> antisym. stretch.
1639	<i>vs</i>	$\sigma$		CH <sub>2</sub> sym. stretch.
1611	<i>m</i>	$\sigma$		Amide I: C=O stretch.
1593	<i>w</i>	$\sigma$		Ring stretch
1545	<i>vs</i>	$\pi$		Amide II: N—H in-plane bend. + C—N stretch.
1493	<i>w</i>	$\pi$		Ring in-plane deform.
1460	<i>m sh</i>	$\sigma$		CH <sub>2</sub> bend.
1447	<i>s</i>	$\sigma$		
1423	<i>s</i>	$\sigma$		
1382	<i>m</i>	$\pi$	C	CH <sub>2</sub> twist. and wag.
1378	<i>vw sh</i>	$\pi$		
1360	<i>vw sh</i>	$\pi$	A	
1351	<i>m</i>	$\pi$	C	
1335	<i>vw sh</i>	$\pi$		
1310	<i>vw sh</i>	$\pi$		
1300	<i>w</i>	$\pi$		
1292	<i>vw sh</i>	$\pi$		
1277	<i>s</i>	$\pi$		Amide III: N—H in-plane bend. + C—N stretch.
1266	<i>s</i>	$\pi$	C	
1260	<i>s</i>	$\pi$	A	
1240	<i>m sh</i>	$\pi$		
1215	<i>vw sh</i>	$\pi$		C—H in-plane deform. (aromatic)
1206	<i>m</i>	$\pi$	C	
1156	<i>w</i>	$\pi$	A	C—H in-plane deform. (aromatic)
1147	<i>w</i>	$\pi$	C	

(continued)

bands at about 3300 cm.<sup>-1</sup> and 3100 cm.<sup>-1</sup> are considered to be due to the Fermi resonance between the fundamental N—H stretching and the first overtone of the amide II vibration,<sup>20</sup> it is not yet certain whether the spectrum of the complex polymer might be explained in the same way. The polarized infrared spectrum of stretched and oriented crystalline specimen is shown in Figure 8. Although the specimen is highly oriented, the observed dichroism of the amide characteristic bands are much lower than those of aliphatic polyamides. This may indicate that the transition moments of these vibrations are inclined to the orthogonal directions of the chain axis to a considerable extent because of the twisted configuration of the molecule.

TABLE I (continued)

Wave number, cm. <sup>-1</sup>	Intensity <sup>b</sup>	Dichroism <sup>c</sup>	Phase <sup>d</sup>	Assignment
1091	<i>w</i>	$\sigma$		Skeletal stretch.
1083	<i>vw sh</i>	$\sigma$		
1062	<i>vw sh</i>	$\sigma$		
1033	<i>m</i>	$\pi$	C	
1002	<i>vw sh</i>	$\sigma$		
993	<i>vw sh</i>	$\sigma$		C—H out-of-plane deform. ( <i>m</i> -substitution)
908	<i>w</i>	?	C	
894	<i>w</i>	$\sigma$	C	
794	<i>m</i>	$\sigma$	C	
787	<i>m</i>	$\sigma$	A	C—H out-of-plane deform. ( <i>m</i> -substitution)
765	<i>m sh</i>	$\sigma$		CH <sub>2</sub> rock.
752	<i>m</i>	$\sigma$	A	
738	<i>m</i>	$\sigma$	C	
725	<i>m sh</i>	$\sigma$	C	Amide V: N—H out-of-plane bend.
705	<i>s</i>	$\sigma$	C	Ring out-of-plane deform.
684	<i>w sh</i>	$\sigma$	C	
600	<i>w</i>	$\pi$		Amide VI: C=O out-of-plane bend.
590	<i>w</i>	$\sigma$	C	
581	<i>w</i>	—		Ring in-plane deform.
573	<i>w</i>	—	A	
566	<i>w</i>	—	C	
500	<i>w</i>	—	C	
490	<i>w</i>	—	A	Ring in-plane deform.
430	<i>vw</i>	—		Ring out-of-plane deform.
365	<i>w</i>	—	C	Amide VII: CO—NH torsion
336	<i>vw</i>	—	C	
310	<i>w</i>	—	A	

<sup>a</sup> Other unassigned bands: 3405 cm.<sup>-1</sup>, *vw sh*,  $\sigma$ ; 3215 cm.<sup>-1</sup>, *vw sh*,  $\sigma$ ; 1655 cm.<sup>-1</sup>, *s sh*,  $\sigma$ ; 1563 cm.<sup>-1</sup>, *s sh*,  $\pi$ ; 1528 cm.<sup>-1</sup>, *s sh*,  $\pi$ ; 1508 cm.<sup>-1</sup>, *w sh*,  $\pi$ ; 1194 cm.<sup>-1</sup>, *vw sh*,  $\pi$ ; 1172 cm.<sup>-1</sup>, *vw sh*,  $\pi$ ; 1131 cm.<sup>-1</sup>, *vw sh*, ?; 1122 cm.<sup>-1</sup>, *vw, sh*,  $\sigma$ ; 984 cm.<sup>-1</sup>, *vw, sh*, ?; 938 cm.<sup>-1</sup>, *vw*,  $\sigma$ ; 912 cm.<sup>-1</sup>, *w*,  $\pi$ ; 870 cm.<sup>-1</sup>, *vw*, ?; 828 cm.<sup>-1</sup>, *vw sh*, ?; 674 cm.<sup>-1</sup>, *vw sh*, ?; 516 cm.<sup>-1</sup>, *vw sh*, —; 462 cm.<sup>-1</sup>, *vw sh*, —.

<sup>b</sup> *s* = strong, *m* = medium, *w* = weak, *sh* = shoulder, *v* = very.

<sup>c</sup>  $\pi$  = parallel,  $\sigma$  = perpendicular.

<sup>d</sup> C = crystalline, A = amorphous.

The amide V mode which is primarily due to the N—H out-of-plane deformation vibration is the most sensitive to the crystalline form and the crystallinity of the specimen among all the amide characteristic vibrations. In the case of aliphatic polyamides it has been established that the amide V band appears at around 690 cm.<sup>-1</sup> for the  $\alpha$  crystalline form and at around 720 cm.<sup>-1</sup> for the  $\gamma$  crystalline form.<sup>6</sup> The intensity of amide V band of poly( $\epsilon$ -capramide), (nylon 6) has been found to vary with the crystallinity of the specimen.<sup>21</sup>

In the spectrum of poly(*m*-xylylene adipamide), many strong bands cluster around the region where amide V is expected to appear. By the



TABLE II. Infrared Absorption Bands of Deuterated Poly(*m*-xylylene adipamide)<sup>a</sup>

Wave number, cm. <sup>-1</sup>	Intensity <sup>b</sup>	Dichroism <sup>b</sup>	Assignment
3300	<i>w</i>	$\sigma$	(N—H stretch.)
3100	<i>vw sh</i>	?	C—H stretch. (aromatic)
3055	<i>vw sh</i>	$\sigma$	
3031	<i>w</i>	$\sigma$	
3022	<i>vw sh</i>	$\pi$	
3005	<i>vw sh</i>	?	
2944	<i>m sh</i>	$\sigma$	
2925	<i>s</i>	$\sigma$	CH <sub>2</sub> antisym. stretch.
2865	<i>m</i>	$\sigma$	CH <sub>2</sub> sym. stretch.
2440	<i>vs</i>	$\sigma$	N—D stretch.
2410	<i>vs</i>	$\sigma$	Amide II' + Amide III'
1624	<i>vs</i>	$\sigma$	Amide I: C=O stretch.
1611	<i>w sh</i>	$\sigma$	Ring stretch.
1590	<i>vw sh</i>	$\pi$	
1540	<i>w</i>	$\pi$	
1530	<i>w</i>	$\pi$	(Amide II)
1450	<i>vs</i>	$\sigma$	Amide II': C—N stretch.
1430	<i>vs</i>	$\pi$	CH <sub>2</sub> bend.
1420	<i>s sh</i>	$\pi$	
1380	<i>vw sh</i>	$\pi$	
1350	<i>s</i>	?	CH <sub>2</sub> twist. and wag.
1295	<i>w</i>	$\pi$	
1285	<i>w</i>	$\pi$	
1251	<i>m</i>	$\sigma$	
1237	<i>m</i>	$\pi$	
1212	<i>m</i>	$\pi$	
1166	<i>w</i>	$\pi$	C—H in-plane deform. (aromatic)
1160	<i>w</i>	$\pi$	C—H in-plane deform. (aromatic)
1148	<i>vw sh</i>	$\pi$	
1089	<i>w</i>	$\pi$	
1052	<i>vw sh</i>	$\pi$	
1037	<i>s</i>	$\pi$	
1016	<i>vw sh</i>	$\pi$	
1000	<i>vw sh</i>	?	Skeletal stretch.
977	<i>m</i>	$\sigma$	Amide III': N—D in-plane bend.
907	<i>w</i>	$\pi$	
896	<i>vw sh</i>	?	C—H out-of-plane deform. ( <i>m</i> -substitution)
887	<i>w</i>	$\sigma$	
787	<i>s</i>	$\sigma$	C—H out-of-plane deform. ( <i>m</i> -substitution)
752	<i>w</i>	$\sigma$	
737	<i>w sh</i>	$\sigma$	CH <sub>2</sub> rock.
703	<i>s</i>	$\sigma$	Ring out-of-plane deform.
566	<i>w</i>	—	Ring in-plane deform.
526	<i>m</i>	—	Amide V': N—D out-of-plane bend.
517	<i>m</i>	—	
494	<i>m</i>	—	Ring in-plane deform.
377	<i>vw sh</i>	—	Amide VII: CO—NH torsion
363	<i>m</i>	—	
334	<i>w</i>	—	

<sup>a</sup> Other unassigned bands: 1557 cm.<sup>-1</sup>, *vw sh*,  $\pi$ ; 1505 cm.<sup>-1</sup>, *vw*,  $\pi$ ; 1485 cm.<sup>-1</sup>, *vw sh*,  $\pi$ ; 953 cm.<sup>-1</sup>, *vw sh*,  $\sigma$ ; 912 cm.<sup>-1</sup>, *vw sh*, ?; 860 cm.<sup>-1</sup>, *vw sh*,  $\sigma$ ; 630 cm.<sup>-1</sup>, *vw*,  $\pi$ ; 428 cm.<sup>-1</sup>, *vw sh*, —.

<sup>b</sup> See the footnotes in Table I.

deuteration of the specimen, however, much of the difficulty in the assignment of this vibration would be eliminated. The infrared spectrum of a highly deuterated poly(*m*-xylylene adipamide) is shown in Figure 9, and the polarized spectrum of an oriented specimen of the deuterated polymer is illustrated in Figure 10. In these spectra the weak band originally observed at  $725\text{ cm.}^{-1}$  has completely disappeared, and therefore this band is to be assigned to the amide V vibration. The bands with peaks at  $526\text{ cm.}^{-1}$  and  $517\text{ cm.}^{-1}$  which failed to occur in the original spectrum should correspond to the amide V' band. This is primarily due to the N—D out-of-plane deformation vibration. The amide II' and III' bands which correspond respectively to the C—N stretching and the N—D in-plane deformation modes appear at  $1450\text{ cm.}^{-1}$  and at  $977\text{ cm.}^{-1}$ . Contrary to the case of aliphatic polyamides, the amide III' band shows a slight perpendicular dichroism. This would be another indication of a twisted configuration of the poly(*m*-xylylene adipamide) molecule. The new intense bands at  $2440\text{ cm.}^{-1}$  and at  $2410\text{ cm.}^{-1}$  are considered to be due to the Fermi resonance between the N—D stretching vibration and combination amide II' + amide III'.

The assignment of the amide V vibration was further confirmed by the iodine treatment of the polymer. When iodine is absorbed by a polyamide, it is considered to form a charge-transfer type complex with the amide C=O groups, thus rendering a considerable portion of the N—H groups free from hydrogen bonding.<sup>7</sup> Indeed, the effect of the iodine treatment on the infrared spectrum of typical aliphatic polyamides turns out to be the increase of the N—H stretching frequency by ca.  $60\text{ cm.}^{-1}$  and the disappearance of amide V band.<sup>7</sup> Moreover the new intense band appears at around  $570\text{ cm.}^{-1}$  which may correspond to the out-of-plane deformation vibration of free N—H group.<sup>21</sup> By the iodine treatment of poly(*m*-xylylene adipamide), the band at  $725\text{ cm.}^{-1}$  which was assigned from deuteration studies to the amide V band disappears. Furthermore, the similar spectral changes to those of aliphatic polyamides were observed in other amide characteristic bands as illustrated in Figure 11. Those facts indicate the correctness of our assignment of the amide V vibration.

By analogy with the case of poly( $\epsilon$ -capramide)<sup>7</sup> and other aliphatic polyamides,<sup>21</sup> the weak band at  $590\text{ cm.}^{-1}$  may be assigned to amide VI, which corresponds to the C=O out-of-plane deformation vibration.<sup>18,19</sup> The amide VII band, which is expected to appear in the  $400 \sim 200\text{ cm.}^{-1}$  region, involves the torsional mode around the CO—NH bond and its frequency is quite sensitive to the conformation of polyamide chains.<sup>22</sup> In the case of aliphatic polyamides, the comparatively strong band appearing in the  $350\text{--}300\text{ cm.}^{-1}$  region is most reasonably assigned to the amide VII, because its frequency has been found to change systematically with the crystalline form and consequently with the chain conformation of the polymer.<sup>21</sup> Poly (*m*-xylylene adipamide) shows two "crystalline" bands at  $365\text{ cm.}^{-1}$  and at  $336\text{ cm.}^{-1}$  and an "amorphous" band at  $310\text{ cm.}^{-1}$ . Although it is hard to give complete assignment of these bands

owing to their complicated nature, we may at least relate them to the amide VII mode. As to the amide IV band, which corresponds to the O=C—N bending vibration,<sup>18,19</sup> no definite assignment can yet be made. Other absorption bands were tentatively assigned to the vibrations of the methylene chain or of the benzene ring. More detailed studies of skeletal deformation modes would be required before the spectrum in the lower frequency region can be satisfactorily interpreted.

The vibrational frequencies observed in the spectra of poly(*m*-xylylene adipamide) and the deuterated poly(*m*-xylylene adipamide) are summarized in Tables I and II, respectively, together with the assignment.

The infrared experimental results suggest that this polymer molecule takes a sterically twisted conformation along the fiber axis which is also supported by x-ray diffraction analysis.

The author takes pleasure in acknowledging the support and interest of Dr. H. Kobayashi, the Director of Research Department and Dr. M. Watanabe. Sincere thanks are also due to Dr. Y. Kinoshita and Dr. A. Miyake for their stimulating discussions.

### References

1. Cannon, C. G., *Spectrochim. Acta*, **16**, 302 (1960).
2. Tobin, M. C., and M. J. Carrano, *J. Chem. Phys.*, **25**, 1044 (1956).
3. Starkweather, H. W., Jr. and R. E. Moynihan, *J. Polymer Sci.*, **22**, 363 (1956).
4. Sandeman, I., and A. Keller, *J. Polymer Sci.*, **19**, 401 (1956).
5. Koshimo, A., *Kobunshi Kagaku*, **17**, 545, 679 (1960).
6. Miyake, A., *J. Polymer Sci.*, **44**, 223 (1960).
7. Arimoto, H., *Kobunshi Kagaku*, **19**, 101, 205, 456 (1962).
8. Kinoshita, Y., *Makromol. Chem.*, **33**, 1 (1959).
9. Vogelsong, D. C., *J. Polymer Sci.*, **57**, 985 (1962).
10. Cannon, C. G., in *Physical Methods of Investigating Textiles*, by R. Meredith and J. W. S. Hearle, Eds, Interscience, New York-London, 1958, Chap. 2.
11. Tranter, T. C., and R. C. Collins, *J. Textile Inst.*, **52**, T88 (1961).
12. Yoda, N., *Bull. Chem. Soc. Japan*, **35**, 1349 (1962).
13. Tadokoro, H., S. Seki, and I. Nitta, *Nippon Kagaku Zasshi*, **78**, 1060 (1957).
14. Bamford, C. H., A. Elliott and W. E. Hanby, *Synthetic Polypeptides*, Academic Press, New York, 1956, Chap. VII and VIII.
15. Bailey, M., *Acta Cryst.*, **2**, 120 (1949).
16. Pauling, L., and R. B. Corey, *Proc. Natl. Acad. Sci., U.S.*, **39**, 253 (1953).
17. Shimanouchi, T., Y. Kakiuchi, and I. Gamo, *J. Chem. Phys.*, **25**, 1245 (1956).
18. Miyazawa, T., T. Shimanouchi, and S. Mizushima, *J. Chem. Phys.*, **24**, 408 (1956).
19. Miyazawa, T., T. Shimanouchi, and S. Mizushima, *J. Chem. Phys.*, **29**, 611 (1958).
20. Miyazawa, T., *J. Mol. Spectr.*, **4**, 168 (1960).
21. Matsubara, I., unpublished results.
22. Miyazawa, T., *Bull. Chem. Soc. Japan*, **34**, 691 (1961).

### Résumé

On a étudié la diffraction aux rayons-X et le spectre infrarouge du polyadipamide de *m*-xylylène. Se basant sur des études de diffraction aux rayons-X, on a proposé la forme torsionnée modèle moléculaire pour la structure polymérique du polyadipamide

de *m*-xylylène; la valeur calculée de 15.2 Å. pour la période d'identité est compatible avec la valeur observée par diffraction-X. L'attribution des bandes d'absorption infrarouge a été faite à l'aide de mesures de polarisation combinées à des techniques de deutération et un traitement du polymère à l'iode. Les résultats expérimentaux démontrent clairement que la bande à  $725\text{ cm}^{-1}$  doit être attribuée à la vibration V de l'amide. Les bandes intenses à 1639, 1545 et  $1266\text{ cm}^{-1}$  sont attribuées respectivement aux vibrations I, II et III de l'amide. On a essayé également une attribution de l'amide VI et VII. Les spectres infra-rouges montrent que le dichroïsme observé des bandes caractéristiques de l'amide de substances fortement orientées est beaucoup plus faible que celui des polyamides aliphatiques. Ceci est aussi en concordance avec le modèle torsionné proposé pour la structure polymérique du polyadipamide de *m*-xylylène.

### Zusammenfassung

Das Röntgendiagramm und Infrarotspektrum von Poly-*m*-xylylenadipamid wurden untersucht. Auf Grund von Röntgenbeugungsmessungen wurde die verdrehte Form des Molekülmodells für die Polymerstruktur von Poly-*m*-xylylenadipamid vorgeschlagen, die einen berechneten Wert von 15,2 Å. als Identitätsperiode in Übereinstimmung mit dem beobachteten Röntgenbeugungswert ergibt. Die Zuordnung der Infrarotabsorptionsbanden wurde mit Hilfe von Polarisationsmessungen in Kombination mit Deuterierung und Jodbehandlung des Polymeren, durchgeführt. Die experimentellen Befunde lassen eine Zuordnung der Bande bei  $725\text{ cm}^{-1}$  zur Amid-V-schwingung als gesichert erscheinen. Die starken Banden bei 1639, 1545 und  $1266\text{ cm}^{-1}$  werden den Amid-I-II- bzw. -III-schwingungen zugeschrieben. Eine vorläufige Zuordnung von Amid-VI- und -VII wurde ebenfalls durchgeführt. Die Infrarotspektren zeigen, dass der beobachtete Dichroismus der charakteristischen Amidbanden der hochorientierten Probe viel geringer als der der aliphatischen Polyamide ist. Das steht auch mit dem vorgeschlagenen, verdrehten Modell für die Polymerstruktur von Poly-*m*-xylylenadipamid in Übereinstimmung.

Received May 7, 1962

Revised October 18, 1962

## Polymers Containing the 2,5-Diphenylthiazolo[5,4-d]thiazole Moiety\*†

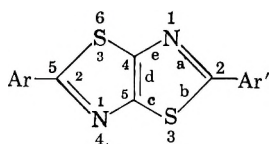
CHARLES J. FOX, *Research Laboratories, Eastman Kodak  
Company, Rochester, New York*

### Synopsis

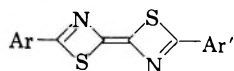
Polycarbonates, alternating copolycarbonates, and polyesters were prepared from bisphenols containing the 2,5-diphenylthiazolo[5,4-d]thiazole moiety. The bisphenols used were 2,5-bis(4-hydroxyphenyl)thiazolo[5,4-d]thiazole, 2,5-bis-(3-hydroxyphenyl)-thiazolo[5,4-d]thiazole, and 2,5-bis(4-hydroxy-3-methoxyphenyl)thiazolo[5,4-d]thiazole. The relative degrees of crystallinity for these polymers were determined and are discussed in relation to some of the physical properties. The degree of crystallinity observed for the polycarbonates varied from low to high, depending on the position of substitution in the phenyl rings. The alternating copolycarbonates with neopentyl glycol were all of a low degree of crystallinity and increased solubility. The polyadipates and polysebacates prepared were of a relatively high degree of crystallinity in spite of the flexibility permitted by the aliphatic diacid linkage. The solubilities of these polyesters were appreciable, even though the crystallinity was high.

### INTRODUCTION

A recent study of the reaction of dithiooxamide with aromatic aldehydes<sup>1</sup> has clarified the structure of the main product as 2,5-diarylthiazolo[5,4-d]thiazole:\*



The structure of this product was previously interpreted by Ephraim<sup>2</sup> as

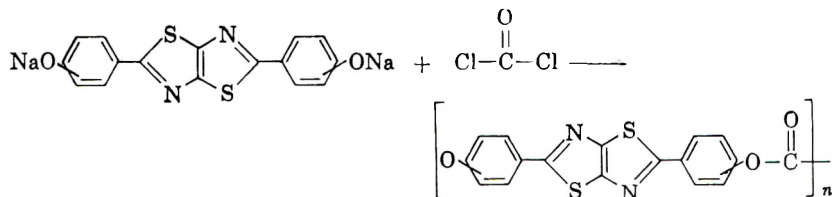


In this paper the [5,4-d]notation will be omitted for brevity. The availability of the 2,5-bishydroxyphenylthiazolothiazoles offers a means of obtaining polymers containing this moiety by the well-established pro-

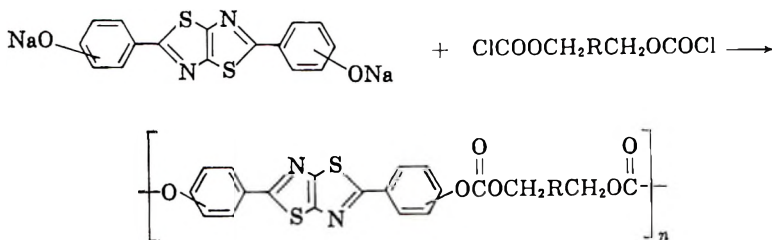
\* Alternate nomenclature: 2,5-diaryl-1,4-dithia-3,6-diaza-1,4-dihydropentalene.

† Communication No. 2306 from the Kodak Research Laboratories.

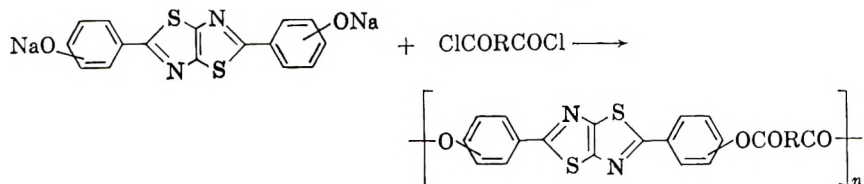
cedure of interfacial polymerization.<sup>3</sup> This technique permits the preparation of polycarbonates by employing phosgene:



Alternating copolycarbonates are prepared by employing bischloroformates of alkyl glycols:



Polyesters are obtained by employing diacid chlorides:



The polycarbonates<sup>5</sup> and polyesters<sup>1</sup> of bisphenols previously described have been those in which the two phenylene groups in the bisphenol were separated by an alkyl group. An exception to this was the polyadipate of 4,4'-dihydroxybiphenyl.<sup>5</sup> The polymers described in the present paper were prepared from bisphenols in which the phenyl groups are separated by two fused five-membered rings. This grouping imparts rigidity and linearity to the polymer chain at this point. This also introduces entirely different requirements for crystallization than were previously encountered for bisphenol polymers. Some of the physical properties were examined for polymers in which the 2,5-diphenylthiazolothiazole unit was maintained constant while the position of the polymer linkage on the phenyl rings and the structure of the diacid component employed were varied.

## EXPERIMENTAL

### I. Bisphenols

A general procedure for the preparation of substituted 2,5-diphenylthiazolothiazoles has been described in the literature.<sup>1</sup> This procedure was

used in the present work to prepare the previously described 2,5-bis(4-hydroxyphenyl)thiazolothiazole and the 2,5-bis(3-hydroxyphenyl)thiazolothiazole. The observed melting point for the 3-hydroxyphenyl derivative was 344–346°C. (lit. value<sup>1</sup> 328–332°C.). Difficulty was encountered in obtaining an appreciable quantity of the 2,5-bis(2-hydroxyphenyl)thiazolothiazole. No attempts were made to prepare polymers of this derivative.

A new compound, 2,5-bis(4-hydroxy-3-methoxyphenyl)thiazolothiazole, was prepared by this procedure as follows: A mixture of 20 g. (0.166 mole) of dithiooxamide, 100 g. (0.66 mole) of vanillin (4-hydroxy-3-methoxybenzaldehyde), and 30 g. of phenol was heated to 220°C. The mixture was stirred as soon as it was sufficiently molten. Heating was continued for 30 min. after solution was completed and water began to distill. The mixture was allowed to cool, but not to solidify, and was diluted with 200 ml. of ethanol. The solid product which separated was recrystallized from cyclohexanone. The yield was 12 g. (19% of the theoretical), m.p. 264–265°C.

ANAL. Calcd. for  $C_{18}H_{14}O_4N_2S_2$ : C, 56.0%; H, 3.6%; N, 7.2%; S, 16.6%. Found: C, 56.5%; H, 3.7%; N, 7.2%; S, 15.9%.

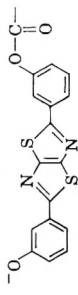
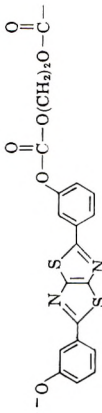
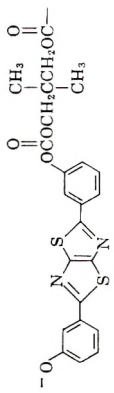
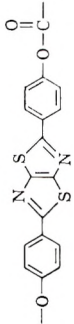
## II. Bischloroformates

The bischloroformates of ethylene glycol and neopentyl glycol were prepared by dissolving the glycol in an excess of liquid phosgene and permitting the excess of phosgene to distill slowly from the mixture.<sup>6</sup> Remaining traces of phosgene were removed by bubbling dry nitrogen through the solution and finally evacuating the vessel containing the bischloroformate residue.

## III. Polycarbonates

The polycarbonates or alternating copolycarbonates were prepared by the interfacial polycondensation technique.<sup>3,6</sup> The alternating copolycarbonate of 2,5-bis(4-hydroxy-3-methoxyphenyl)thiazolothiazole and neopentyl glycol was prepared by first dissolving 1.93 g. (0.005 mole) of 2,5-bis(4-hydroxy-3-methoxyphenyl)thiazolothiazole in a solution of 0.45 g. (0.011 mole) of sodium hydroxide in 50 ml. of water. Five drops of tri-*n*-butylamine and 25 ml. of 1,1,2,2-tetrachloroethane were added, and the resulting two-phase mixture was stirred vigorously at room temperature. A solution of 1.15 g. (0.005 mole) of neopentyl glycol bischloroformate in 50 ml. of tetrachloroethane was added in one portion to the stirred mixture and stirring was continued for 30 min. The resulting emulsion was broken by acidification with acetic acid. The tetrachloroethane layer was separated, washed with water, and dried over calcium chloride. The light-yellow, fibrous product was obtained quantitatively by precipitation from tetrachloroethane solution into ethyl alcohol.

TABLE I  
Polymers Containing the 2,5-Diarylthiazolo [5,4-d]thiazole Moiety

Formula	Repeating unit	Melting point, °C.	Relative degree of crystallinity	Logarithmic viscosity number	Solvent	Description
I		350-360	Low (acetone-treated)	—	Hexamethylphosphoramide	Fibrous
II		267-275	High	—	Tetra-chloro-ethane	Powder
III		149-156	Low-medium (acetone-treated)	0.30	Methylene chloride	Fibrous
IV		317-332	High	—	None	Powder



V		182-213	Low (acetone-treated)	1.07	Tetra-chloro-ethane	Fibrous
VI		287-295	Medium	—	Hexa-methyl-phosphor-amide	Fibrous
VII		180-226	Low (acetone-treated)	0.81	Tetra-chloro-ethane	Fibrous
VIII		335-340	Low-medium (acetone-treated)	—	50% Phenol-chloro-benzene	Fibrous
IX		285-293	High (acetone-treated)	0.16	Tetra-chloro-ethane	Powder
X		197-220	High	0.23	Tetra-chloro-ethane	Powder

On small-scale runs (0.005 mole), methylene chloride was also a suitable solvent for the preparation of this polymer. On a larger scale (0.05 mole), the polymer separated from solution in the methylene chloride during the polymerization.

When the polycarbonate of 2,5-bis(4-hydroxy-3-methoxyphenyl)thiazolothiazole was prepared by this procedure, the polymer separated quantitatively from the mixture during the polymerization. The solid was separated by filtration, washed, and dried.

All of the polymers were prepared by this procedure and are described in Tables I and II.

TABLE II  
Elemental Analyses of Polymers Described in Table I

Formula	Calcd., %				Found, %			
	C	H	N	S	C	H	N	S
I	58.0	2.3	8.0	18.1	58.5	2.4	7.6	14.0
II	55.2	3.5	6.1	14.0	53.8	2.9	6.1	13.3
III	57.2	3.7	5.8	13.3	55.7	4.3	5.3	9.9
IV	58.0	2.3	8.0	18.1	55.6	2.8	7.8	16.7
V	57.3	3.7	5.8	13.3	55.1	4.4	4.7	10.1
VI	55.2	2.9	6.8	15.5	55.2	3.2	6.9	15.1
VII	55.3	4.1	5.2	11.8	55.1	4.0	5.3	10.8
VIII	58.8	2.9	6.9	15.7	55.5	3.6	5.5	12.8
IX	60.6	3.7	6.4	14.7	59.5	4.2	5.3	12.5
X	61.2	5.1	5.1	11.5	60.6	5.0	4.4	9.9

#### IV. Physical Data

The melting points of the polymers were determined by microscopic examination of a sample on a hot stage.

The relative degree of crystallinity for each of the polymers was determined by a visual examination of the x-ray diffraction pattern. When a polymer showed little or no crystallinity, attempts were made to cause it to crystallize by soaking it in acetone. This is noted in Table I in the column describing the relative degree of crystallinity.

The solubility of each of the polymers was determined in a series of solvents with decreasing solvent power in the order 50% phenol-chlorobenzene > hexamethylphosphoramide > tetrachloroethane > methylene chloride. The polymers were insoluble in the solvents in the series lower than the one listed in Table I.

The logarithmic viscosity number<sup>7</sup> ( $\ln \eta_{rel}/C$ ) was determined for a 0.25% solution of each of the soluble polymers in the designated solvent. These results are recorded in Table I.

#### RESULTS AND DISCUSSION

The physical and analytical data for the polycarbonates, alternating copolycarbonates, and polyesters which were prepared are presented in

Tables I and II. In carrying out the polymerizations, no effort was made to study the degree of polymerization in relation to the experimental conditions. The limited solubility of some of the polymeric products in the organic solvent may have prevented their building up to high molecular weight polymers. This was possibly true for polymer IV, which was not fibrous and was too insoluble to permit a viscosity measurement. However, this was not necessarily a limiting factor, since polymers I, VI, and VIII precipitated from the mixture during polymerization and were undoubtedly of high molecular weight, as evidenced by the tough, fibrous appearance of the product. These polymers were also too insoluble to permit a viscosity measurement. The viscosity measurements for the soluble polymers showed them to be of appreciable molecular weight.

The variables responsible for crystallinity or noncrystallinity in polymers were discussed in relation to the packing efficiency of the polymer chain by Bunn.<sup>8</sup> The occasion to compare the crystallinity of polymers containing bisphenols with variations in structure does not often occur because of the low degree of crystallinity and high solubility generally encountered with bisphenol polycarbonates and polyesters.<sup>4,5</sup> A discussion of the properties of polymers containing the 2,5-diphenylthiazolothiazole moiety requires consideration of the steric requirements. The thiazolothiazole moiety is planar and, together with the phenyl groups in the 2,5-position, forms a linear, nonflexible molecule. Efficient packing of polymer chains containing this moiety would be expected as a consequence of this rigidity and linearity.

### Polycarbonates

It was not surprising to find that the polycarbonate (IV) of 2,5-bis(4-hydroxyphenyl)thiazolothiazole was highly crystalline and insoluble, owing to the effective packing imposed by the 2,5-diphenylthiazolothiazole moiety and maintained by the polycarbonate linkage in the *para* position. This is analogous to the crystalline polycarbonate of 4,4'-dihydroxydiphenylmethane,<sup>4</sup> which would be expected to have much less rigidity than this example.

It would be reasonable to expect the packing efficiency and hence the crystallinity of the polymer chain to be diminished by changing the steric requirements of the molecule. This could be readily accomplished by either changing the position of substitution on the phenyl ring (i.e., from *para* to *meta*) or by changing the structure of the diacid component joining the bisphenols to an irregular or bulky group. Thus, the high crystallinity of the insoluble polymer IV was reduced (*A*) by introducing a methoxy group in the *meta* positions while maintaining the carbonate linkages in the *para* positions so that the resulting polymer VI was found to have intermediate crystallinity and solubility in hot hexamethylphosphoramide; and (*B*) was reduced even further by changing the carbonate linkages from the *para* position to the *meta* position so that polymer I was found to

have low crystallinity even after acetone treatment, although solubility was still limited to hot hexamethylphosphoramide.

### Alternating Copolycarbonates

The relationship of the structure of the diacid component to solubility and crystallinity was also investigated. Several examples of alternating copolycarbonates were obtained by allowing the bischloroformate of a glycol to react with one of the bishydroxyphenylthiazolothiazole compounds. This approach ensured regular alternation of the glycol and the bisphenol, since the acid chloride was entirely restricted to the glycol segment.

High crystallinity was observed for polymer II, obtained from ethylene glycol bischloroformate and 2,5-bis(3-hydroxyphenyl)thiazolothiazole, even though the carbonate linkages are in the *meta* positions. This polymer was initially soluble in tetrachloroethane, but gradually became insoluble in the solid form. In contrast to this result, low crystallinity was observed when the bischloroformate of the bulky neopentyl glycol replaced ethylene glycol as in each of polymers III, V, and VII, even when the carbonate linkage was in *para* positions (polymer V). The solubility was increased so that in each of these examples methylene chloride was a suitable solvent.

### Polyesters

Polyesters of dicarboxylic acids and bisphenols may also be highly crystalline, depending on the structures of both the bisphenol and the diacid. Whereas the polyterephthalates described by Levine and Temins were crystalline, the polyesters of aliphatic diacids were noncrystalline.<sup>5</sup> Exceptions to this have involved bisphenols with either no central carbon atom or with only a methylene group between the phenyl rings. Thus, a relatively high degree of crystallinity was observed for the polyadipates of 4,4'-dihydroxybiphenyl and 4,4'-dihydroxydiphenylmethane.

The polyadipate (IX) of 2,5-bis(4-hydroxy-3-methoxyphenyl)thiazolothiazole was also found to be highly crystalline after treatment with acetone. This is in contrast to the corresponding polysuccinate (VIII), which remained at a low to medium degree of crystallinity even after treatment with acetone. Surprisingly, a high degree of crystallinity was observed for the corresponding sebacate (X). It is interesting that the methoxy group in the *meta* position was not effective in appreciably reducing the crystallinity of the adipate and the sebacate. This is in contrast to the polycarbonate (VI) which had an intermediate degree of crystallinity. Polymers IX and X were soluble in spite of their high crystallinity, and this may result from the influence of the methoxy groups in the *meta* positions.

The author wishes to express his appreciation to Mr. L. E. Contois for determining the relative crystallinity of the polymers by means of the x-ray diffraction patterns, and to Mr. J. J. Saturno for determining the melting points.

### References

1. Johnson, J. R., and R. Ketcham, *J. Am. Chem. Soc.*, **82**, 2719 (1960).
2. Ephraim, J., *Ber.*, **24**, 1026 (1891).
3. Morgan, P. W., *SPE J.*, **15**, 485 (1959).
4. Schnell, H., *Ind. Eng. Chem.*, **51**, 157 (1959).
5. Levine, M., and S. C. Temin, *J. Polymer Sci.*, **28**, 179 (1958).
6. Merrill, S. H., *J. Polymer Sci.*, **55**, 343 (1961).
7. International Union of Pure and Applied Chemistry, Report on Nomenclature in the Field of Macromolecules, *J. Polymer Sci.*, **8**, 257 (1952).
8. Bunn, C. W., in *Fibres From Synthetic Polymers*, R. Hill, Ed., Elsevier, New York, 1953, p. 235.

### Résumé

On a préparé des polycarbonates, des copolycarbonates alternants et des polyesters à partir de bisphénols contenant le groupe 2,5-diphénylthiazolo-[5,4-d]-thiazolique. Les bisphénols employés étaient le 2,5-bis(4-hydroxyphényl)thiazolo[5,4-d]thiazol, 2,5-bis(3-hydroxyphényl)thiazolo[5,4-d]thiazol, 2,5-bis(4-hydroxy-3-méthoxyphényl)thiazolo[5,4-d]thiazol. Les degrés de cristallinité de ces polymères ont été déterminés et sont discutés en relation avec quelques propriétés physiques. Les degrés de cristallinité observés pour le polycarbonates varient depuis des valeurs très basses jusqu'à des valeurs élevées, en fonction de la position des substituants dans le noyau phényle. Les copolycarbonates alternants avec le glycol néopentylque étaient tous peu cristallins et de solubilité plus élevée. Les polyadipates et polysébacates obtenus avaient une cristallinité relativement élevée en dépit de la flexibilité due au lien aliphatique diacide. Les solubilités de ces polyesters étaient appréciables malgré le taux de cristallinité élevée.

### Zusammenfassung

Polykarbonate, alternierende Copolykarbonate und Polyester wurden aus Bisphenolen mit dem Diphenylthiazolo-[5,4-d]-thiazolrest dargestellt. Die verwendeten Bisphenole waren 2,5-Bis-(4-hydroxyphenyl)-thiazolo-[5,4-d]-thiazol, 2,5-Bis-(3-hydroxyphenyl)-thiazolo-[5,4-d]-thiazol und 2,5-Bis-(4-hydroxy-3-methoxyphenyl)-thiazolo-[5,4-d]-thiazol. Der relative Kristallinitätsgrad dieser Polymeren wurde bestimmt und in seinen Beziehungen zu einigen physikalischen Eigenschaften diskutiert. Der Kristallinitätsgrad der Polykarbonate stieg in Abhängigkeit von der Stellung der Substituenten in den Phenylringen von niedrigen zu hohen Werten an. Die alternierenden Copolykarbonate mit Neopentylglykol besaßen alle einen niedrigen Kristallinitätsgrad und erhöhte Löslichkeit. Die dargestellten Polyadipate und Polysebacate lagen trotz der durch die aliphatische Dicarbonsäure ermöglichten Biegsamkeit bezüglich des Kristallinitätsgrades relativ hoch. Die Löslichkeit dieser Polyester war ungeachtet der hohen Kristallinität beträchtlich.

Received July 30, 1962

Revised October 29, 1962

## Chain Entanglements and Elastic Behavior of Polybutadiene Networks

GERARD KRAUS and G. A. MOCZVIGEMBA, *Phillips Petroleum Company, Bartlesville, Oklahoma*

### Synopsis

The role of chain entanglements in determining the stress-strain properties of polybutadiene networks has been investigated. The number of entanglements was varied by changing the primary molecular weight and chemical crosslink concentration. Networks essentially free of entanglements were prepared by endgroup coupling of carboxy-terminated polybutadiene of 5500 molecular weight. Conventional sulfur or peroxide vulcanizates obeyed the Mooney-Rivlin stress-strain relation, the constant  $C_2$  which represents the deviation from simple kinetic theory diminishing with the time allowed for approaching elastic equilibrium. The constant  $C_2$  was found to increase with both the total physical crosslinking and the entanglement contribution to this quantity. The endgroup vulcanizates obeyed the simple kinetic theory of rubber elasticity and approached elastic equilibrium much more rapidly than sulfur or peroxide vulcanizates. The evidence presented suggests that the apparent deviation of elastomeric vulcanizates from the kinetic theory of rubber elasticity resulting in the appearance of the Mooney-Rivlin  $C_2$  term in the stress-strain relation arises from a slow relaxation process involving the entanglement crosslinks.

### I. INTRODUCTION

It is well established that, in addition to chemical crosslinks, physical chain entanglements contribute to the building of such polymeric networks as vulcanized rubber. The latter are not only of importance in questions of vulcanization stoichiometry, where they must be carefully distinguished from true chemical crosslinks, but undoubtedly contribute also to the physical properties of the vulcanizate. While the effect of entanglements on the rheological properties of linear polymers has received considerable attention in the literature, very little has been said regarding their influence on the physical properties of vulcanized rubbers, despite the fact that the effects of various types of chemical crosslinks have been studied in considerable detail. In the present paper we examine the effects of entanglements on the stress-strain relation of amorphous polybutadienes.

### II. THEORETICAL BACKGROUND

The kinetic theory of rubber elasticity leads to the well-known equilibrium stress-strain relationship<sup>1</sup>

$$F/A = \nu RT(\alpha - \alpha^{-2}), \quad (1)$$

where  $F$  is the equilibrium force of retraction at extension ratio  $\alpha$ ,  $A$  is the original, undeformed cross section,  $\nu$  is the number of elastically effective network chains per unit volume of rubber, and  $R$  and  $T$  have their usual meaning. This equation has been shown to hold for rubbers swollen in solvents (with inclusion of a factor  $v_r^{1/3}$  in the right-hand side,  $v_r$  being the volume fraction of rubber in the sample), but usually does not appear to hold for dry rubbers. For the latter, better agreement with experiment is obtained with a relation of the form

$$F/A = C_1(\alpha - \alpha^{-2}) + C_2(\alpha - \alpha^{-2})/\alpha \quad (2)$$

originally proposed by Mooney<sup>2</sup> and Rivlin.<sup>3</sup> The parameter  $C_1$  has been identified with  $\nu RT$ , but the physical significance of  $C_2$  remains uncertain.<sup>4</sup> Ciferri and Flory have concluded it to arise from difficulty of attaining elastic equilibrium.<sup>5</sup>

The number of elastically effective network chains depends on the number of chemical crosslinks introduced, the primary molecular weight of the polymer (which determines the number of inactive chain ends), and the number of physical chain entanglements which have become trapped between crosslinks to assume the function of additional crosslinks. Thus, generally the total number of network chains (physical) is equal to the number of chains contributed by crosslinks (chemical) less the number of chain ends plus the number of chains contributed by entanglements. Empirical relationships of the form

$$\nu = \nu^* - (b/M) + a[1 - (b/M\nu^*)] \quad (3)$$

have enjoyed some notable success in polysiloxane,<sup>6</sup> natural rubber,<sup>7</sup> and polybutadiene<sup>8</sup> networks. Here  $\nu^*/2$  is the number of chemical crosslinks,  $M$  the primary molecular weight of the rubber,  $b$  a parameter approximately equal to twice the density, and  $a/2$  the total number of entanglements in a polymer of infinite molecular weight. In polydisperse rubbers the molecular weight  $M$  is presumably to be taken as the number-average, since the free chain end correction term  $b/M$  is obviously related to the number of chains from which the network is built up.

The determination of an equilibrium modulus in a dry rubber is complicated by the fact that the approach to equilibrium in most networks is extremely slow. Usually, in applying eq. (2) to arrive at a value of  $C_1$  no attempt is made to insure attainment of a true equilibrium.<sup>4</sup> Stress relaxation studies on gum vulcanizates of noncrystallizing rubbers show that the fractional stress decay is smaller at high extension than at low ones.<sup>9</sup> The constant  $C_2$ , therefore, should decrease and might possibly vanish altogether as true equilibrium is approached.<sup>5</sup> One possible explanation might be that the relaxation involves slippage of the entanglement crosslinks. This hypothesis furnishes the basis of the present investigation.

The number of entanglement crosslinks introduced in a random crosslinking process as distinguished from chemical crosslinkages is subject to some control by the primary molecular weight, as shown by eq. (3). However, we shall not make quantitative use of this equation in the present study, since we do not wish to make the conclusions dependent on the particular entanglement function chosen. Instead we note that for primary molecular weights of the order of  $10^5$  the free chain end term must be of the order of  $10^{-5}$  moles/cc. If we are able to prepare a series of vulcanizates, all with  $\nu \approx 10^{-4}$  moles/cc. for widely different combinations of sulfur and primary molecular weights, we can be confident of achieving different ratios of entanglements to crosslinks, as the chemical crosslink concentration will be at least approximately proportional to the sulfur added.<sup>8</sup> Another highly effective way to greatly reduce the entanglement crosslinking is to build up the network from low molecular weight polymers with reactive endgroups. If a polymer whose molecular weight is less than the critical entanglement spacing molecular weight ( $M_e$ ) is vulcanized through the endgroups, the resulting network should be relatively free of entanglements. In the present work we have examined polybutadiene networks of both types. We shall show that the reduction in the amount of entanglement crosslinking in a network indeed leads to greatly diminished values of  $C_2$  and to more rapid attainment of elastic equilibrium.

### III. EXPERIMENTAL

#### A. Polymers

The polybutadienes used for preparation of randomly crosslinked networks were prepared by initiation with *n*-butyllithium. Their weight-average molecular weights were determined from their intrinsic viscosities in toluene at 25°C., a calibration against light-scattering molecular weights developed by Stacy and Gregg<sup>10</sup> being used:

$$[\eta] = 1.56 \times 10^{-4} \bar{M}_w^{0.78}$$

Number-average molecular weights were estimated from initiator levels after correction for initiator destroyed by impurities in the polymerization system. In all cases close agreement resulted between  $\bar{M}_n$  and  $\bar{M}_w$ , illustrating the extreme narrowness of the molecular weight distribution. The microstructure of these polymers is approximately: *cis* 40%, *trans* 50%, vinyl 10%.

Carboxy-terminated polybutadiene used in the preparation of end-linked vulcanizates was a semicommercial product of Phillips Petroleum Company sold under the trade name Butarez CTL. This polymer has a molecular weight of approximately 5500 and a carboxy content of 1.66%. The double bond configuration of this rubber is *cis* 31%, *trans* 43%,



and vinyl 26%. This polymer has been described in earlier publications from these laboratories.<sup>11, 12</sup>

### B. Preparation of Vulcanizates

Conventional crosslinked networks were prepared by sulfur vulcanization, the following recipe being used: polymer, 100 parts; zinc oxide, 3 phr; stearic acid, 2 phr; Resin 731 (disproportionated rosin acid), 3 phr; Flexamine [mixture of diarylamine-ketone reaction product (65%) and *N,N'*-diphenyl-*p*-phenylenediamine (35%)], 1 phr; Santocure (*N*-cyclohexylbenzothiazole sulfenamide), 1.2 phr; sulfur, variable. All batches were mixed on a cool two-roll mill to avoid degradation. Slabs were cured for 45 min. at 153°C., this time having been established as sufficient for the attainment of level cure.

Limited data were obtained on peroxide vulcanizates. Di-Cup 40 C (40% dicumyl peroxide on an inert support) was used as the crosslinking agent at the 0.4 and 0.8% levels. The polymer used for the peroxide vulcanizates had a primary molecular weight of  $\bar{M}_w = 210,000$ .

Endlinked networks were prepared by incorporating the coupling agent, hexa[1-(2-methyl)azirdinyl]triphosphaterazine (Interchemical Corporation), on a roll mill and curing for various lengths of time at 122°C. between aluminum foil. These vulcanizates continue to post-cure at room temperature for several days. Accordingly, measurements were taken on these vulcanizates after 1, 3, and 4 weeks, respectively. Little difference was noted between the 3- and 4-week samples.

### C. Stress-Extension Measurements

All measurements were taken at 25°C. on a table model Instron tester. Two procedures were used to arrive at the "equilibrium" stress-strain curve. In the first, a 15-min. period as allowed for relaxation at each elongation, and points were taken in increasing order of extension ratio. In the second procedure, the samples were stretched to the desired extension ratio on a rack and allowed to relax in the dark under vacuum for 10 hr., after which they were transferred to the preset jaws of the Instron for determination of the stress. Special clamps were used which allowed the transfer to be made in 2-3 sec. No disturbance of the elastic equilibrium could be detected due to the transfer. This technique was used not only to save instrument time, but principally to guard against degradation during the prolonged relaxation periods. In the discussions following, results obtained by the two procedures are referred to as 15-min. and 10-hr. data, respectively.

### D. Swelling Determinations

Equilibrium swelling measurements were conducted in *n*-heptane as described previously.<sup>8, 13</sup>

## IV. RESULTS AND DISCUSSION

## A. Sulfur Vulcanizates

An attempt was made to prepare vulcanizates of equal network chain density from rubbers of widely different molecular weights by controlling the number of chemical crosslinks, i.e., by adjustment of the sulfur in the formulation. In this manner we hoped to obtain two sets of networks of different proportion of chemical to entanglement crosslinkages at two levels of total physical crosslinking. As may be seen from the data of Table I and Figures 1 and 2 ( $C_1$  and  $v_r$  are both measures of physical crosslinking), this was accomplished only to a fair degree. In general, the adjustment in sulfur concentration was not drastic enough to overcome the large effect of the primary molecular weight differences. Nevertheless, in view of the discussion in Section II of this report, it is clear that a significant spread in crosslink-to-entanglement ratio must have been achieved.

Figure 1 shows the stress-strain curves obtained by allowing only 15 min. to attain elastic equilibrium, a procedure similar to those frequently used in the literature.<sup>4</sup> Figure 2 shows the result of allowing 10 hr. for attainment of equilibrium. Both sets of data follow eq. (2); however, both  $C_1$  and particularly  $C_2$  are seen to change (Table I). The value of  $C_2$  decreases consistently with the additional time allowed for attainment of equilibrium. Since the physical relaxation of stress in vulcanized rubbers is approximately linear with the logarithm of time,<sup>9</sup> it would be impractical to prolong the measurement in an attempt to eliminate  $C_2$  altogether (see also Fig. 6). We merely note at this point that the relaxation processes at hand lead to a reduction in the value of the parameter  $C_2$ .

We next inquire into the possible relationship between  $C_2$  and entanglement crosslinks. In each set of data, A to D and E to H, the entangle-

TABLE I  
Results on Sulfur Vulcanizates

Vulcanizate	$\bar{M}_n \times 10^{-3}$	$\bar{M}_w \times 10^{-3}$	[S], phr	$v_r$	15-min. values		10 hr. values	
					$C_1$	$C_2$	$C_1$	$C_2$
					$\times 10^{-6}$ , dynes/ cm. <sup>2</sup>	$\times 10^{-6}$ , dynes/ cm. <sup>2</sup>	$\times 10^{-6}$ , dynes/ cm. <sup>2</sup>	$\times 10^{-6}$ , dynes/ cm. <sup>2</sup>
A	70	83	2.72	0.364	2.7	4.85	3.0	3.4
B	125	138	2.25	0.388	3.25	6.4	3.3	5.3
C	196	205	1.98	0.392	3.45	6.8	4.1	4.5
D	288	290	1.75	0.397	3.6	6.95	3.8	5.4
E	70	83	1.35	0.248	1.35	2.75	1.5	1.8
F	125	138	0.92	0.264	1.35	5.1	1.6	3.0
G	196	205	0.68	0.243	1.75	4.8	1.4	4.2
H	288	290	0.50	0.292	2.05	5.9	1.8	5.3

ment crosslinking should increase as we proceed downward in the table. The value of  $C_2$  likewise increases (with two slight irregularities). Comparison at equal primary molecular weight (A-E, B-F, etc.) leads to the same result. At the higher sulfur levels more entanglements become isolated between crosslinks to become elastically active so that both chemical

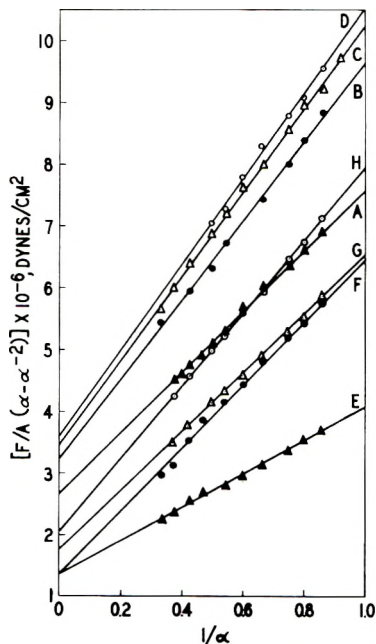


Fig. 1. Stress-strain data for sulfur vulcanizates (15-min. data).

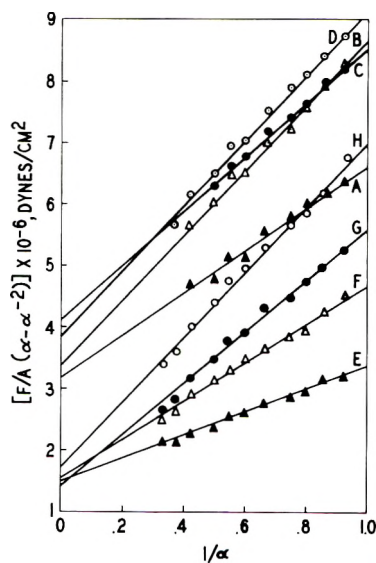


Fig. 2. Stress-strain data for sulfur vulcanizates (10-hr. data).

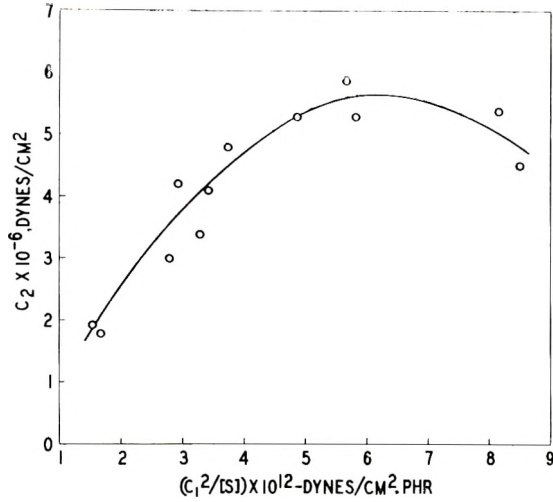


Fig. 3. Dependence of  $C_2$  on crosslinking and entanglements.

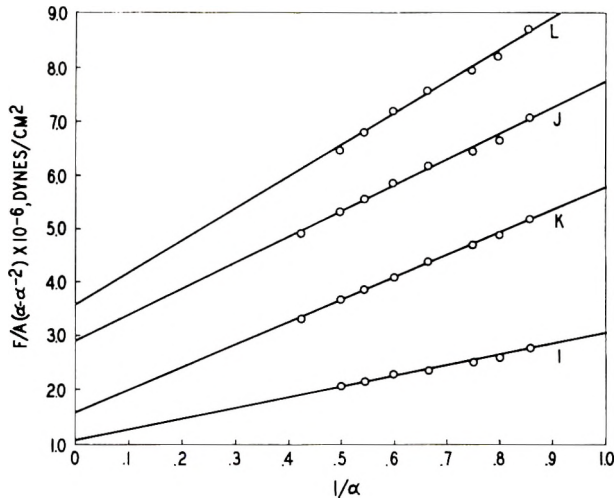


Fig. 4. Stress-strain data for vulcanizates from blends of high and low molecular weight polymers (10-hr. data).

and entanglement crosslinking increase. Indeed,  $C_2$  is found to increase also. However,  $C_2$  is evidently not a simple function of the entanglement-to-crosslink ratio, but appears to increase with total crosslinking as well. The latter effect is well known in natural rubber vulcanizates where frequently  $C_2 \approx C_1$ . A plot of  $C_2$  against  $C_1^2/[S]$ , a variable which gives recognition to both total and entanglement crosslinking, yields a reasonably good correlation (Fig. 3). The 10-hr. data were used in the construction of this figure; a similar relation is obtained with the 15-min. data.

Included in Figure 3 are data on networks from two blends designed to test the effect of polydispersity in molecular weight. Over the relatively narrow range of molecular weight distribution encountered here there appears to be no complication from this variable. The stress-strain curves for these blends are shown in Figure 4, numerical data are presented in Table II.

TABLE II  
Sulfur Vulcanizates from Blends

Vul- canizate	$\bar{M}_n$ $\times 10^{-3}$	$\bar{M}_w$ $\times 10^{-3}$	[S], phr	$v_r$	$C_1 \times 10^{-6}$ , dynes/cm. <sup>2</sup>	$C_2 \times 10^{-6}$ , dynes/cm. <sup>2</sup>
I	125 <sup>a</sup>	218	0.75	0.204	1.1 <sup>c</sup>	1.9 <sup>c</sup>
J	125 <sup>a</sup>	218	2.25	0.375	2.9	4.8
K	125 <sup>b</sup>	161	0.75	0.260	1.6	4.1
L	125 <sup>b</sup>	161	2.25	0.395	3.55	5.9

<sup>a</sup> Blend data:  $w_1 = 0.44$ ,  $\bar{M}_{n_1} = 70,000$ ,  $\bar{M}_{w_1} = 83,000$ ;  $w_2 = 0.56$ ,  $\bar{M}_{n_2} = 325,000$ ,  $\bar{M}_{w_2} = 325,000$ .

<sup>b</sup> Blend data:  $w_1 = 0.82$ ,  $\bar{M}_{n_1} = 110,000$ ,  $\bar{M}_{w_1} = 125,000$ ;  $w_2 = 0.18$ ,  $\bar{M}_{n_2} = 325,000$ ,  $\bar{M}_{w_2} = 325,000$ .

<sup>c</sup> Data throughout are 10-hr. values.

### B. Endgroup Vulcanizates

The entanglement spacing molecular weight for *n*-butyllithium polymerized polybutadiene has been estimated at 6000.<sup>8</sup> This result has been confirmed by the location of the break in the bulk viscosity-molecular weight relation.<sup>14</sup> It would not be expected that the slight difference in the microstructure of Butarez CTL (see Experimental Section) would cause this value to be greatly different. With a molecular weight of 5500 for this polymer, networks built up by endgroup coupling should, therefore, be relatively free from chain entanglements. The networks are unique in other respects. They will possess network chains of relatively uniform length and, if an attempt is made to obtain different "states of cure," the network can differ only in the amounts of sol and free chain ends, while the network chain length will be confined to integral multiples of the primary molecular weight. Also, with a hexafunctional coupling agent, such as used in the present study, crosslinks of different functionality will coexist in the network. Because of polymerization reactions of the aziridinyl groups,<sup>15,16</sup> functionalities in excess of 6 will be possible. These side reactions also explain why the tightest networks are obtained at substantial excess quantities of coupling agent.

Figure 5 shows typical equilibrium stress-strain curves for these vulcanizates; a summary of all the data is given in Table III. It is conspicuous that these networks obey the simple kinetic theory eq. (1); even 15-min. determinations give only a small  $C_2$  term. Attainment of elastic equilibrium in these networks is quite rapid. A comparison of stress relaxation in typical sulfur and aziridinyl/carboxy endgroup vulcanizates

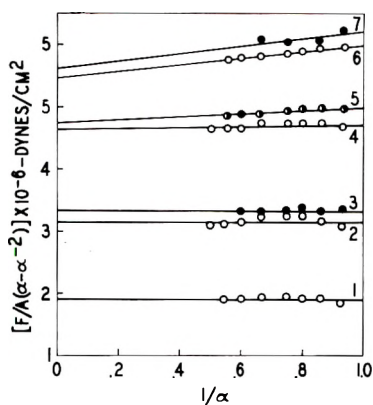


Fig. 5. Stress-strain behavior of endgroup vulcanizates (15-min. data). Plots 6 and 7 are displaced upward by one unit.

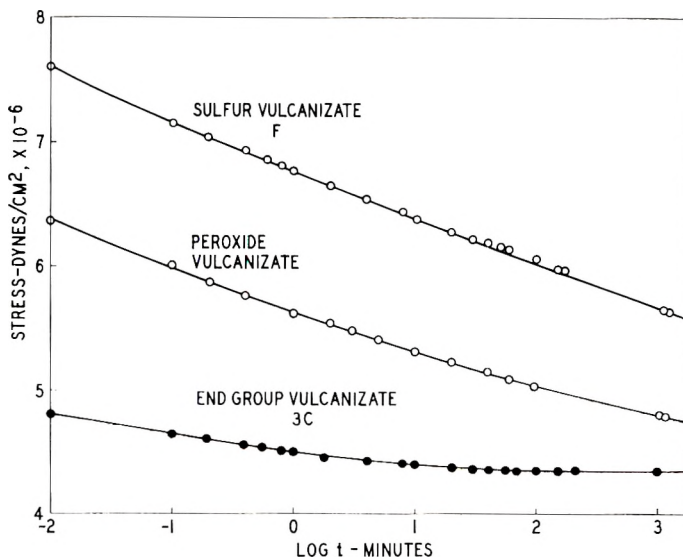


Fig. 6. Stress relaxation of typical random and endgroup vulcanizates at 25°C.,  $\alpha = 1.667$ .

is shown in Figure 6. To demonstrate that the slow relaxation of sulfur vulcanizates is not a consequence of crosslink scission, a peroxide vulcanizate has been included for comparison. It is seen that the latter network, in which the chemical crosslinks are carbon-carbon bonds, behaves exactly as the sulfur vulcanizate. For this particular vulcanizate, which was prepared with 0.8% Di-Cup 40 C,  $C_1 = 2.7 \times 10^6$  dynes/cm.<sup>2</sup> and  $C_2 = 4.0 \times 10^6$  dynes/cm.<sup>2</sup>. Similar results were obtained with the less highly crosslinked peroxide vulcanizate.

The endgroup vulcanizates contain very little sol and appear to approach a limit of  $C_1 = 4.8 \times 10^6$  dynes/cm.<sup>2</sup>, corresponding to  $\nu = 1.9 \times$

TABLE III  
 Results on Endgroup Vulcanizates

Vulcanizate	Mole ratio aziridinyl: carboxyl	Cure time at 122°C., min.	Post- cure time at 25°C., weeks	$v_r$	Sol frac- tion	$C_1$	$C_2$
						$\times 10^{-6}$ , dynes/ cm. <sup>2</sup>	$\times 10^{-6}$ , dynes/ cm. <sup>2</sup>
1a	1.1	30	1	0.251	—	1.40	0
1b	1.1	30	2	0.271	—	1.75	0
1c	1.1	30	4	0.276	0.112	1.90 <sup>a</sup>	0 <sup>a</sup>
2a	1.1	60	1	0.298	—	2.85	0
2b	1.1	60	2	0.312	—	3.07	0
2c	1.1	60	4	0.309	0.056	3.13 <sup>a</sup>	0 <sup>a</sup>
3a	1.1	120	1	0.305	—	2.85	0
3b	1.1	120	2	0.315	—	3.05	0
3c	1.1	120	4	0.311	0.066	3.33 <sup>a</sup>	0 <sup>a</sup>
4a	1.5	30	1	0.328	—	3.75	0
4b	1.5	30	2	0.351	—	4.80	0
4c	1.5	30	4	0.348	0.032	4.65 <sup>a</sup>	0.08 <sup>a</sup>
5a	1.5	60	1	0.331	—	3.90	0
5b	1.5	60	2	0.350	—	4.65	0
5c	1.5	60	4	0.348	0.032	4.75 <sup>a</sup>	0.25 <sup>a</sup>
6a	2	30	1	0.331	—	4.10	0
6b	2	30	2	0.348	—	4.45	0
6c	2	30	4	0.349	0.037	4.45 <sup>a</sup>	0.55 <sup>a</sup>
7a	2	60	1	0.339	—	4.0	0
7b	2	60	2	0.347	—	4.5	0
7c	2	60	4	0.344	0.041	4.6 <sup>a</sup>	0.60 <sup>a</sup>

<sup>a</sup> 15-min. values; all others are 10-hr. values.

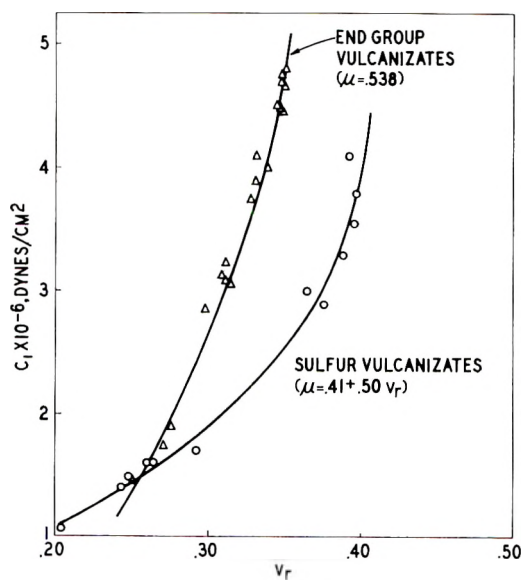


Fig. 7. Elastic behavior vs. swelling equilibrium in *n*-heptane. Solid lines represent fits to Flory-Rehner equation.

$10^{-4}$  moles/cc. or  $M_e = 4700$ , in satisfactory agreement with the molecular weight of the parent polymer. The elastic constant  $C_1$  shows the expected good correlation with the equilibrium inverse swelling ratio  $v_r$  (Fig. 7). The solid line is drawn according to the Flory-Rehner theory of swelling<sup>17</sup> with a constant value of the solvent interaction parameter ( $\mu = 0.538$ ):

$$C_1 = \nu RT = -RT[\ln(1 - v_r) + v_r + \mu v_r^2]/V_s [v_r^{1/3} - (2v_r/f)] \quad (4)$$

The average functionality of the crosslinks ( $f$ ) has been rather arbitrarily chosen at 4. The calculation, however, is not sensitive to small variations in  $f$ . The sulfur vulcanizates require choice of a concentration-dependent  $\mu$ , a condition not uncommon in elastomeric networks.<sup>13</sup> The concentration dependence is not caused by sulfuration of butadiene units, as the sulfur concentration does not increase regularly with  $v_r$  in the present series (see Tables I and II). While the differences in  $\mu$  for the two types of networks is undoubtedly due in part to the different microstructure of the polymer chains, the reason for the constancy of  $\mu$  in the endgroup vulcanizates as contrasted to its concentration dependence in random networks is not clear.

### References

1. Flory, P. J., *Principles of Polymer Chemistry*, Cornell Univ. Press, Ithaca, N. Y., 1953, Chap. 11.
2. Mooney, M., *J. Appl. Phys.*, **19**, 434 (1948).
3. Rivlin, R. S., *Proc. Roy. Soc. (London)*, **A240**, 459, 491, 509 (1948).
4. Gumbrell, S. M., L. Mullins, and R. S. Rivlin, *Trans. Faraday Soc.*, **49**, 1495 (1953).
5. Ciferri, A., and P. J. Flory, *J. Appl. Phys.*, **30**, 1498 (1959).
6. Bueche, A. M., *J. Polymer Sci.*, **19**, 297 (1956).
7. Mullins, L., *J. Appl. Polymer Sci.*, **2**, 1 (1959).
8. Kraus, G., *J. Appl. Polymer Sci.*, in press.
9. Gent, A. N., *Proc. Rubber Technol. Conf., 4th Conf., London*, **1962**.
10. Stacy, C. J., and R. Q. Gregg, Phillips Petroleum Company, unpublished results.
11. Uraneck, C. A., H. L. Hsieh, and O. G. Buck, *J. Polymer Sci.*, **46**, 535 (1960).
12. Crouch, W. W., and J. N. Short, *Rubber Plastics Age*, **42**, 276 (1961).
13. Kraus, G., *Rubber World*, **135**, 67, 254 (1956).
14. Kraus, G., and J. T. Gruver, *J. Polymer Sci.*, in press.
15. Brit. Pats. 837,709 and 837,710, to Albright and Wilson, Ltd.
16. Barb, W. G., *J. Chem. Soc.*, **1955**, 2564; *ibid.*, **1955**, 2577.
17. Flory, P. J., and J. Rehner, Jr., *J. Chem. Phys.*, **11**, 512 (1943); P. J. Flory, *ibid.*, **18**, 108 (1950).

### Résumé

On a étudié le rôle de l'enchevêtrement des chaînes dans la détermination des propriétés à la traction de réseaux de polybutadiène. On a varié le taux d'enchevêtrement en changeant le poids moléculaire primaire et la concentration en points chimiques. On a préparé des réseaux essentiellement exempts en enchevêtrement en couplant les groupes terminaux de polybutadiène de poids moléculaire de 5.500 terminés par des groupes carboxyles. Des vulcanisats conventionnellement formés par sulfuration ou peroxydation, obéissaient à la relation de la force de tension de Mooney-Rivlin, la constante  $C_2$



qui représente la déviation par rapport à la théorie cinétique simple, diminuent avec le temps pour se rapprocher de l'équilibre élastique. Il a été trouvé que la constante  $C_2$  augmente à la fois avec le pontage physique total et la contribution d'enchevêtrement à cette quantité. Les groupes terminaux des vulcanisats obéissaient à la théorie cinétique simple de l'élasticité du caoutchouc et approchaient plus rapidement de l'équilibre élastique que les vulcanisats sulfurés ou peroxydés. L'évidence présentée suggère que les déviations apparentes des vulcanisats élastomériques par rapport à la théorie cinétique de l'élasticité du caoutchouc, qui se traduisent par l'apparition du terme  $C_2$  de Mooney-Rivlin dans la relation de force de tension, résultent d'un processus de relaxation lente incluant les ponts d'enchevêtrement.

### Zusammenfassung

Die Rolle von Kettenverschlingungen bei der Bestimmung der Spannungs-Dehnungs-Eigenschaften von Polybutadiennetzwerken wurde untersucht. Die Zahl der Verschlingungen wurde durch Änderung des Primärmolekulargewichts und der chemischen Vernetzungskonzentration variiert. Praktisch verschlingungsfreie Netzwerke wurden durch Kupplung von Polybutadienen mit Karboxy-Endgruppen vom Molekulargewicht 5500 dargestellt. Konventionelle Schwefel- oder Peroxydvulkanisate befolgten die Mooney-Rivlin-Spannungs-Dehnungsbeziehung, wobei die für die Abweichung von der einfachen kinetischen Theorie charakteristische Konstante  $C_2$  mit der zur Einstellung des elastischen Gleichgewichts zur Verfügung stehenden Zeit abnahm. Die Konstante  $C_2$  stieg sowohl mit der gesamten physikalischen Vernetzung, als auch mit dem Verschlingungsbeitrag zu dieser Grösse an. Die Endgruppenvulkanisate gehorchten der einfachen kinetischen Theorie der Kautschukelastizität und erreichten den elastischen Gleichgewichtszustand viel rascher als Schwefel- oder Peroxydvulkanisate. Die angeführten Ergebnisse sprechen dafür, dass die Abweichungen elastomerer Vulkanisate von der kinetischen Theorie der Kautschukelastizität, die zum Auftreten des Mooney-Rivlin-Terms  $C_2$  in der Spannungs-Dehnungsbeziehung führen, durch einen langsamen, auf den Verschlingungsvernetzungen beruhenden Relaxationsprozess bedingt sind.

Received November 1, 1962

## Monte-Carlo Calculations of the Dimensions of Coiling Type Polymers in Solutions of Finite Concentration

SYDNEY BLUESTONE and MARJORIE J. VOLD, *Department of Chemistry, University of Southern California, Los Angeles, California*

### Synopsis

The mean end-to-end distances for linear polymers of 101 segments has been computed for nonintersecting random walks on a five-choice cubic lattice on which a second chain is also present, as a function of the distance between the two chains (i.e., polymer concentration). The polymer dimensions appear to decrease with concentration, linearly at first and then more slowly. The results compare favorably with experiment and with some of the approximate analytic theories and poorly with others.

This paper presents the results of Monte-Carlo calculations of the mean end-to-end distance of flexible linear polymers of 101 segments "generated" by taking nonintersecting random walks on a five-choice simple cubic lattice starting at varying distances from a similar preformed chain of the same length, thus simulating the effect of concentration. This general procedure for studying the coiling of flexible linear polymers was developed extensively by Wall and colleagues.<sup>1</sup> Recently some of the results have been validated by a totally independent computer simulation procedure by Verdier and Stockmayer.<sup>2</sup> However, it has not previously been applied to solutions of finite concentration.

The effect of concentration has been investigated analytically by several workers<sup>3-5</sup> using a technique developed by Zimm.<sup>6</sup> The work leads to an expression of the form:

$$A_2 = (N_0\beta n^2/2M^2)h(Z) \quad (1)$$

$$Z = (3/2\pi\langle R_0^2 \rangle)^{3/2}\beta n^2 \quad (2)$$

where  $A_2$  is the osmotic second virial coefficient,  $N_0$  is Avogadro's number,  $\beta$  is the binary cluster integral and, for the particular lattice model used in this work has the value unity,  $n$  the number of segments in the polymer molecule,  $M$  its molecular weight,  $\langle R_0^2 \rangle$  the mean square end-to-end distance in the random walk approximation to chain statistics and  $h(Z)$  is a function, known only for small  $Z$ , which is unity at  $Z = 0$  and decreases as  $Z$  increases. Good reviews of this and related work are given by Stockmayer<sup>3</sup> and by Casassa.<sup>7</sup> Additional analytical theoretical work has been done by Yamakawa,<sup>8</sup> Fixman,<sup>9-11</sup> and by Grimley.<sup>12</sup> Fixman's work has been

fairly successful in predicting the osmotic behavior of moderately concentrated solutions. Grimley developed the mean radius of gyration as a power series in the concentration and calculated the coefficient of the linear term explicitly, enabling direct comparison with our work at low concentration.

Intuitively one would expect the occupancy of lattice sites by the first chain to restrict the growth of the second even when no segment-segment interaction energy at finite separation is postulated. It is this purely geometric effect which has been calculated although the increase in the number of segment-segment nearest neighbors was also counted to facilitate subsequent use of the data.

Notable progress has also been made by Debye and colleagues<sup>13</sup> in the use of light scattering near the critical solution temperature as a measure of the radius of gyration. Simha and Zakin<sup>14</sup> have used the viscosity of solutions of moderate concentration to estimate the mean separation at which polymer coils begin to overlap. A theoretical treatment of molecular sizes at finite concentration has likewise been given by Krigbaum in an appendix to a paper by Kawai and Saito.<sup>15</sup> The latter attribute the increase  $\eta_{sp}/c$  at low concentrations to expansion of the coil but the measurements at such concentrations are very difficult and the results correspondingly uncertain. The work of Krigbaum leads to a stronger dependence of  $\alpha$  on concentration than does that of Kawai and Saito.

$$\alpha^2 = \langle R^2 \rangle / \langle R_0^2 \rangle \quad (3)$$

$\langle R^2 \rangle$  is the mean square displacement length (end-to-end distance) and  $\langle R_0^2 \rangle$  its value for random walk statistics neglecting any excluded volume effects. Some comparisons with our work can be effected and are generally encouraging although hampered by the low chain lengths to which our work is presently restricted.

## COMPUTATIONS

A procedure was devised based on that of Wall and Erpenbeck<sup>16</sup> and tested for validity on a group of 250 isolated chains (zero concentration) by comparison with the works of Wall and Erpenbeck<sup>16</sup> and Wall and Mazur.<sup>1</sup> The general procedure is to select at random the coordinates of the  $(n + 1)$ th segment from among the five available when the segments are located on a simple cubic lattice. (The backward sixth step would make the  $(n + 1)$ th and  $(n - 1)$ th segment coincide and is hence forbidden. Using a five-choice lattice makes four segment-segment bond angles  $90^\circ$  and one  $180^\circ$  which is physically unreal. However, Wall and colleagues and also Verdier and Stockmayer<sup>2</sup> have shown that the results are insensitive to the type of three-dimensional lattice used.)

A given "walk" (partially grown chain) is abandoned as soon as the  $(n + 1)$ th step coincides with any of the previous  $n$ . To overcome the serious inefficiency (attrition) resulting from this necessity, Wall and Erpenbeck,<sup>16</sup>

noting that most attrition resulted from small closed loops, generated many  $s$  step chains ( $s$  varied in the range 15–40) and used several of these a fixed number of times ( $p$ ) to generate long chains. A given chain was discarded entirely when overlap occurred. We used 17-step nonintersecting blocks but discarded only the current block when overlap occurred. New 17-step blocks, except the first in some cases, were used for each chain. This procedure is faster than that of Wall and Erpenbeck but does lead to a bias in that tightly coiled blocks are preferentially retained. We assume that this bias cancels out in calculating the ratios of mean dimensions at different concentrations.

The choice of step among the six possibilities was made by changing the  $x$ ,  $y$ , or  $z$  coordinate by  $\pm 1$  according to the value of a pseudo-random integer between one and six generated by means of a recursion formula described by Rotenberg<sup>17</sup> and adapted to the word length of our H800 computer and tested for randomness by the chi-square test on several series of numbers generated. Whenever the backward step was chosen it was ignored and an alternative choice made.

Initially the chain was begun at the origin and the test sequence for intersections consisted in direct comparison of the coordinates tentatively selected for the  $(n + 1)$ th segment with those of each of the  $n$  previous segments. Later a much faster technique was developed. A  $50 \times 52$  two-dimensional matrix was set up representing the probable limits of the  $x$  and  $y$  coordinates with a single bit telling the  $z$  coordinate by its location in the 48 bit H800 word (54 bits but 56 are used for internal checking). Then when a given point was tentatively selected as the  $(n + 1)$ th it could be examined for prior occurrence in a single short sequence of operations. If the point is unoccupied, the memory cell of the computer corresponding to its  $x$  and  $y$  coordinates will have a zero in the corresponding  $z$  bit. This situation can be readily tested by means of the Boolean AND operation by use of a suitably constructed test word. A very similar procedure tests each of the four nonbonded nearest neighbors of each point after the whole chain has grown. This convenient programming device limits the length of chain that can be grown (although a series of matrices could be set up) first by the number of bits available per word and then by the size of the computer's memory.

### Results for Isolated Chains

Figure 1 shows average values of  $R^2/n$  weighted according to the procedure of Wall and Mazur.<sup>1</sup>

$$\langle R^2 \rangle / n = \sum_{i=0}^j N_i \langle R^2 \rangle_i n^{-1} \exp \{ -i\epsilon/kT \} / \sum_{i=0}^j N_i \exp \{ -i\epsilon/kT \} \quad (4)$$

$R$  is the end-to-end distance for  $n$  steps ( $n + 1$  lattice points),  $N_i$  is the number of chains having a mean square end-to-end distance  $\langle R^2 \rangle_i$  and a total of  $i$  nearest nonbonded neighbors ranging from zero to a maximum of  $j$ . The effective segment–segment interaction energy is  $\epsilon/kT$  in multiples

of  $kT$  ranging from  $-0.25$  to  $+0.25$ . The run consisted of 225 chains, all of which reached 101 links or 102 lattice points in 6 blocks of 17 steps.

Despite the fluctuations to be expected for such a small sample it is apparent that the results are in qualitative accord with those of Wall and Mazur.<sup>1</sup> They found that segment-segment attraction just balanced the excluded volume effect to give a theta point at  $\epsilon/kT = -0.50$  for the four-choice cubic lattice, we find the identical effect at  $\epsilon/kT = -0.25$  for the five-choice cubic lattice. At  $\epsilon/kT = 0$  our results give a linear log-log plot for  $n > 33$  whose slope is 1.24. Wall and Erpenbeck<sup>16</sup> report 1.18

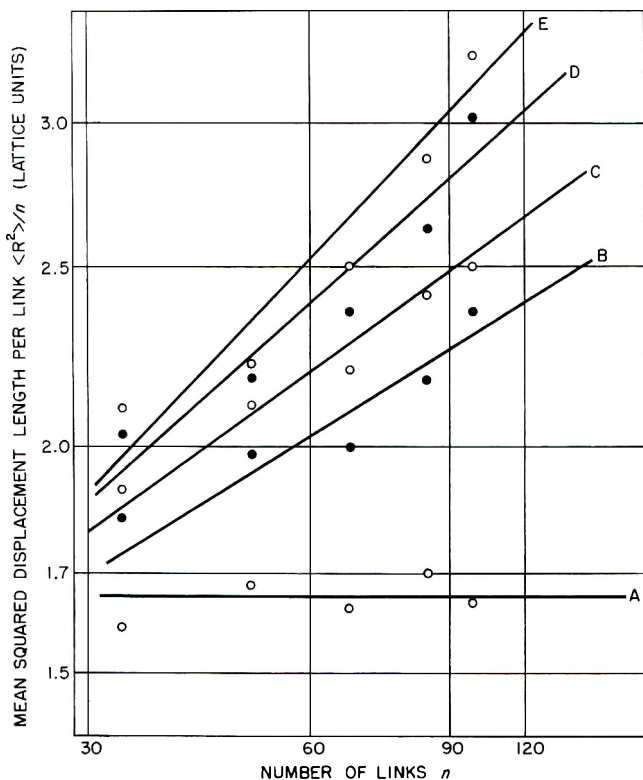


Fig. 1. Mean chain dimensions as a function of chain length and segment-segment interaction energy ( $\epsilon$ ). Values of  $\epsilon/kT$ : (A)  $-0.25$ ; (B)  $-0.10$ ; (C)  $0.0$ ; (D)  $+0.10$ ; (E)  $0.25$ .

for three-dimensional lattices, but Stockmayer<sup>3</sup> finds 1.20 fits their data equally well. However our entire curves are ca. 10% low in the absolute value of  $\langle R^2 \rangle$ . For example, we find  $\langle R^2 \rangle / n = 2.11$  at  $n = 50$  and  $\epsilon/kT = 0$ , while the value (read from a figure) given by Wall, Hiller, and Atchison<sup>18</sup> is 2.3. Our statistical bias does not, of course, affect the first 17-segment block, and  $\langle R^2 \rangle / n$  for this  $n$  does not lie on the curves of Figure 1, but instead agrees exactly with the results of Wall et al.<sup>18</sup> We consider that these results validate our computer technique.

### Procedure for the Two-Chain Problem

The general procedure employed was to store the coordinates of all occupied lattice points of some one previously generated isolated chain in the computer's memory. A second chain of the same length (102 lattice points) was then generated in 6 blocks of 17 points each with the first point located a given distance away from the center of mass of chain 1. In all 1545 successful chains were generated. When a growing chain intersected itself all steps of the current block were discarded as before but when the second chain intersected the first it was discarded entirely.

The attrition rate for this latter process depends on the initial separation between the center of mass of chain 1 and the initial lattice point of chain 2. It averaged 44% at 4.4 lattice unit lengths, 35% at a distance of 8.4–9.5 and 10% at 13.5 lattice units. The root-mean-square gyration radius of 50 isolated chains was 6.4 lattice units. Most (>70%) of the initial separations were in the range 8.4–9.5.

Several different means of selecting chain 1 were used as well as several initial separations. Since no systematic differences were detected all runs were combined. In some cases a single chain 1 having nearly average properties was used to generate about 100 chains 2 at various starting distances. In one run 450 chains 1 were generated and each used to generate one chain 2. The computer output comprised the values of  $R^2/n$  for the second chain, its total number of nonbonded nearest neighbors (from either chain), and the separation  $\delta$  of the centers of mass for the two chains.

In general the separation of the mean centers of mass showed a dispersion of values with a pronounced tendency for the second chain to drift away from the first as it grew. As the separation of the centers of mass increases one would expect to find the mean dimensions of chain 2 approach those for isolated chains. Instead they began to exceed those for isolated chains as soon as the separation became of the order of 2.5 times the radius of gyration of an isolated chain. We believe that this anomaly arises from the fact that all of the chains 2 showing it arose from chains that began close together and subsequently grew mostly in the direction away from chain 1. At smaller separations the distances between centers of mass and between initial lattice points of chain 2 and the centers of mass of chain 1 were comparable.

### Results for the Two-Chain Problem

Values obtained for  $\langle R^2 \rangle/n$  and  $\bar{\delta}$  are summarized in Table I. Values of  $R^2/n$  for all  $\delta$  given by the indicated  $\delta \pm 0.5$  have been averaged. The number of chains in each interval varied from 19 to 133 and is given in the table. Also given are the expansion factors  $\alpha$  and  $\gamma$ .

$$\gamma^2 = \langle R^2 \rangle / \langle R^2 \rangle_{\rho=0} \quad (5)$$

The value of  $\langle R^2 \rangle_{\rho=0}$  is taken from our own work on isolated chains. The value of  $\langle R_0^2 \rangle$  needed to compute  $\alpha$  is taken from that at our theta point

TABLE I  
Mean Chain Dimensions as a Function of Chain Separation

Separation of centers of mass $\delta$ (lattice units) <sup>a</sup>	No. of points	Expansion and compression ratios <sup>b</sup>		Mean square displacement length/segment $\langle R^2 \rangle/n$
		$\alpha$	$\gamma$	
5.5	19	0.966	0.790	1.560
6.5	33	1.027	0.839	1.761
7.5	57	1.070	0.872	1.902
8.5	66	1.040	0.850	1.809
9.5	97	1.053	0.860	1.851
10.5	111	1.062	0.874	1.886
11.5	130	1.105	0.903	2.041
12.5	125	1.145	0.936	2.190
13.5	133	1.130	0.926	2.143
14.5	103			2.787
15.5	105	1.170	0.948	2.246
16.5	81	1.200	0.982	2.413
17.5	75			2.870
18.5	59			2.891
19.5	33			2.869
20.5	43			3.706
$\infty$	275	1.225	1.000	2.500

<sup>a</sup>  $\bar{\delta}$  is the mean separation of the centers of mass for all  $\delta \pm 0.5$  lattice unit regardless of the location of the center of mass of the preformed chain or the starting point of the second.

<sup>b</sup>  $\alpha^2 = \langle R^2 \rangle / \langle R_0^2 \rangle$  where  $R_0^2$  is the mean displacement length at the theta point. All points are for  $n = 101$  links.  $\gamma^2 = \langle R^2 \rangle / \langle R^2 \rangle_{\delta=\infty}$ . Values are calculated from  $\langle R^2 \rangle/n$  but values of  $\alpha > 1.225$  or  $\gamma > 1.000$  have been disregarded. See text.

( $\epsilon/kT = -0.25$ ) in the effort to cancel out the statistical bias previously noted.

## DISCUSSION

### Segment Distribution for Isolated Chain Molecules

Debye and Bueche<sup>20</sup> have presented a distribution of segments about the center of mass which can be well approximated by the Gaussian form:

$$\rho = (3/2\pi R_g^2)^{3/2} n \exp \{ (3/2R_g^2)r^2 \} \quad (6)$$

where  $\rho$  is the segment density (number per unit volume) at a distance  $r$  from the center of mass.  $R_g$  is the radius of gyration of the polymer molecule. It is easy to calculate from eq. (6) the fraction of total segments expected in a given interval of  $r^2$ . The results were compared with the segment distribution of some 5000+ segments for a short run of 5G isolated chains whose mean radius of gyration was 6.4 lattice units. The experimental density is lower than that calculated at small  $r$  and much larger, percentagewise, at larger  $r$ . In order to exhibit the effect clearly the results have been plotted on a semilogarithmic scale in Figure 2. The

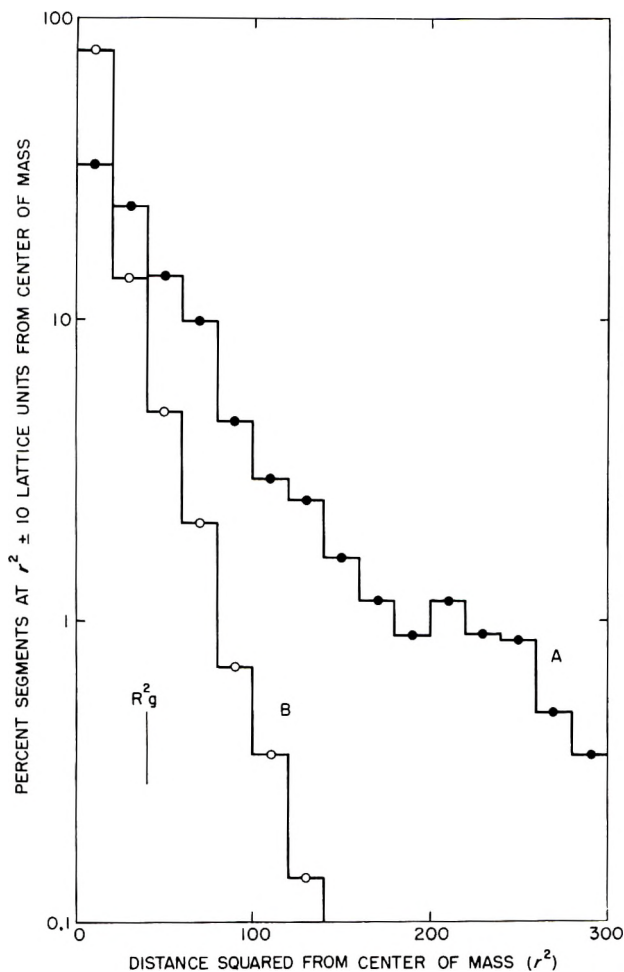


Fig. 2. Distribution of chain segments with respect to the center of mass of isolated chains.  $R_g^2$  is the mean squared radius of gyration of the 50 chains of 101 links each. (A) Monte-Carlo calculation; (B) Gaussian distribution.

physical meaning of the result is that polymer molecules will begin to interact with each other at lower concentrations than the Gaussian distribution would predict. The compression as calculated in this paper is one result of such interaction.

### Concentration Dependence of the Compression

Before the raw data of Table I can be transformed into graphs of the expansion factor  $\alpha$  or the compression factor  $\gamma$  as functions of polymer concentration it is necessary to establish a correspondence between the mean distances between centers of mass of the molecular pairs of the Table I and the effective concentration. The simplest (and most naive) way of accomplishing this end is to assign a volume of  $1/\delta^3$  to each polymer mole-



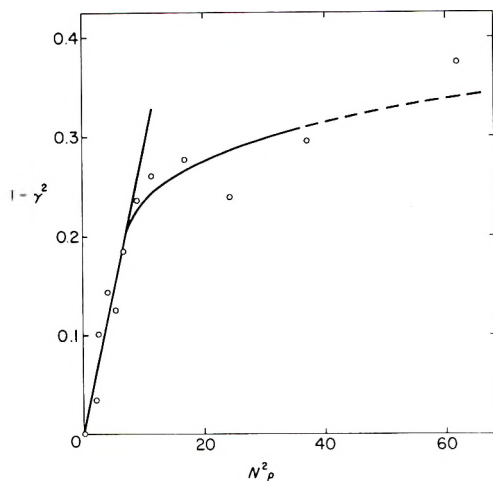


Fig. 3. The effect of polymer concentration on mean chain dimension.  $\langle R^2 \rangle / \langle R^2 \rangle_{\rho=0}$  for 101 link chains.  $R^2$  is the mean square end-to-end distance.

cule. Alternatively, for each preassigned concentration  $\rho$ , each value of the separation of the centers of mass has a calculable frequency of occurrence, and the mean compression ( $\bar{\gamma}$ ) or expansion factor ( $\bar{\alpha}$ ) can be found as a function of the concentration from the data of Table I by using the relation adapted from the treatment of Chandrasekar:<sup>19</sup>

$$\bar{\alpha}(\rho) = \frac{\int_0^{\infty} \alpha(\bar{\delta}) 4\pi\rho\bar{\delta}^2 \exp \left\{ -4/3\pi\rho\bar{\delta}^3 \right\} d\bar{\delta}}{\int_0^{\infty} 4\pi\rho\bar{\delta}^2 \exp \left\{ -4/3\pi\rho\bar{\delta}^3 \right\} d\bar{\delta}} \quad (7)$$

where all symbols have been previously defined. The integrations can be carried out graphically (since the integrands fall to virtually zero at not too great  $\bar{\delta}$ ) or analytically (by representing  $\alpha(\bar{\delta})$  or  $\gamma(\bar{\delta})$  by an empirical formula).

The values of  $\alpha$  and  $\gamma$  listed in Table I apply strictly to one member of a pair, the other member of which still retains the configuration of an isolated chain. Presumably, if the fixed chain had been allowed to "wobble" after the manner employed by Verdier and Stockmayer<sup>2</sup> the observed effects on the mean dimensions would have been divided equally between the two members of each pair and one should employ the relations:

$$\alpha(\bar{\delta}) = (\alpha_0 + \alpha_{\text{calc}})/2 \quad (8a)$$

$$\gamma(\bar{\delta}) = (1 + \gamma_{\text{calc}})/2 \quad (8b)$$

where  $\alpha(\bar{\delta})$  and  $\gamma(\bar{\delta})$  are those to be used in eq. (7) and its analogy for  $\gamma(\rho)$  and  $\alpha_{\text{calc}}$  and  $\gamma_{\text{calc}}$  are the values occurring in Table I. The alternative, since neither procedure is fully justifiable, is to use the unmodified values from Table I directly. None of the qualitative features of the results are altered whichever the choice. Quantitative agreement with the approximate analytical treatment of others is slightly improved by the

more elaborate calculation. The most striking difference in the two procedures is in the numerical values of the concentration. Because of the coincidence that the polymer chains contain 101 links the concentration unit of Figure 3 ( $n^2\rho$ , where  $n$  is the number of links and  $\rho$  the number of polymer molecules per unit volume) is nearly equal to the volume per cent polymer. For the smallest values of  $\delta$  this reaches values which seem inordinately high. In comparing results with previous analytical treatments we have used both procedures, giving the results of the simpler one in the figures but including the salient numerical comparisons for both in the text.

Grimley<sup>12</sup> gives a calculation for the mean square radius of gyration as a power series in the polymer concentration. If the radius of gyration and end-to-end distance remain proportional to each other this result, including only the linear term, can be written

$$1 - \gamma^2 = Kn^2\rho \quad (9)$$

where  $\gamma$  is the compression factor,  $(\langle R^2 \rangle / \langle R^2 \rangle_{\rho=0})^{1/2}$ ,  $n$  is the number of links,  $\rho$  is the number of polymer molecules per unit volume (one unit cube of the lattice), and  $K$  is a constant having the value

$$K = (2/3\pi)^{1/2} M^2 (\partial A_2 / \partial M) \quad (10)$$

$M$  is the molecular weight of the polymer, and  $A_2$  the osmotic second virial coefficient expressed in suitable units.  $A_2$  cannot be calculated from eq. (1) for this case, since the function  $h(Z)$  is known only for small  $Z$  ( $\leq \sim 0.15$ ) whereas  $Z = 1.57$  according to the defining eq. (2) and 0.72 according to the approximate relation (11).

$$\alpha^5 - \alpha^3 = 1.28Z \quad (11)$$

However, by making use of the empirical relation

$$A_2 = c'M^{-\lambda} \quad (12)$$

where  $c'$  and  $\lambda$  are constants and of eq. (1) remembering that  $\rho = N_0c/M$  where  $c$  is concentration in grams/unit volume one finds

$$1 - \gamma^2 = 0.23\lambda h(Z)n^2\rho \quad (9a)$$

Figure 3 is plot of  $n^2\rho$  versus the compression factor ( $1 - \gamma^2$ ) for values of  $\gamma$  taken directly from Table I. The curve is linear up to a value of  $n^2\rho \sim 6$  with a slope corresponding to  $\lambda h(Z) = 0.13$ . The more sophisticated calculation described above is qualitatively similar but assigns a value of  $n^2\rho$  of 1.5 to the region where departure from linearity becomes conspicuous and gives a value of  $\lambda h(Z) = 0.33$ . The value of  $h(Z)$  is unknown for this model system, but it is probably somewhat less than unity. The corresponding  $\lambda$  values in the range of those observed experimentally, for example by Flory and Krigbaum,<sup>21</sup>

The compression effect has been determined directly for two well fractionated samples of polystyrene in cyclohexane with aggregation numbers

of  $9.6 \times 10^3$  and  $2.7 \times 10^4$  by Debye, Chu, Coil, and Woermann<sup>13</sup> from the concentration dependence of the dissymmetry of light scattering. They found that the radius of gyration decreased rapidly at first and then more slowly with increasing concentration with overall decreases of factors of 2.6 and 3.2 near the critical solution temperature. Since  $\alpha$  is known to vary exponentially with aggregation number, at least for lattice models, it seems at least interesting to assume the same type of variation for  $\gamma$ , again with a proportionality of end-to-end distance and radius of gyration, and make the long extrapolation to find a limiting  $\gamma$  of 0.95 for an aggregation number of 102 for polystyrene in cyclohexane. This is rather higher than the largest value from Table I (0.79) or the limiting value (0.87) at high concentrations calculated from eq. (7) written for  $\bar{\gamma}(\rho)$ . However, the value for a given polymer-solvent pair depends on the intermolecular potential, whereas we have taken only geometrical effects into account. Considering this factor as well as the length of the extrapolation, the comparison seems fairly close.

Fixman's calculation<sup>10</sup> of the effect of concentration on polymer dimensions uses an interaction potential of the form

$$V(R) = kT(4/\sqrt{\pi})A_0 \exp \{-BR^2\} \quad (13)$$

where  $R$  is the separation of centers of mass of two polymer molecules and  $A_0$  and  $B$  are constants. The expansion factor  $\alpha$  is calculated as a function of  $A_0$  by using a dimensionless concentration variable  $\nu'$  defined by

$$\begin{aligned} \nu' &= \pi^{3/2} \beta'^{-3/2} \rho \\ \beta' &= 9.61 / \langle R_0 \rangle^2 \end{aligned} \quad (14)$$

For our system with  $\langle R_0 \rangle^2 = 166.5$  in lattice units squared  $\nu' = 404\rho$ . The problem in comparing our results with Fixman's is in selecting an appropriate  $A_0$ . He finds

$$A_0 = 7.18\alpha_0^{-3}Z \quad (15)$$

which is equivalent to

$$A_0 = 5.63(\alpha_0^2 - 1) \quad (16)$$

if equation (11) holds, which, however, appears not to be the case as previously discussed. With this uncertainty  $A_0$  may be taken anywhere between 6.4 and 2.8. Neither affords a perfect comparison, since the intermolecular potential corresponding to our purely geometric segment-segment interaction will not be represented exactly by eq. (13). We prefer to use the lower value since this choice brings the two sets of results into coincidence at infinite dilution.

As can be seen in Figure 4, the Monte-Carlo calculations for  $\alpha$  show it decreasing more rapidly with increasing concentration than does the Fixman calculation. The Monte-Carlo values then begin to level off while the calculated values of Fixman are still decreasing almost linearly. That

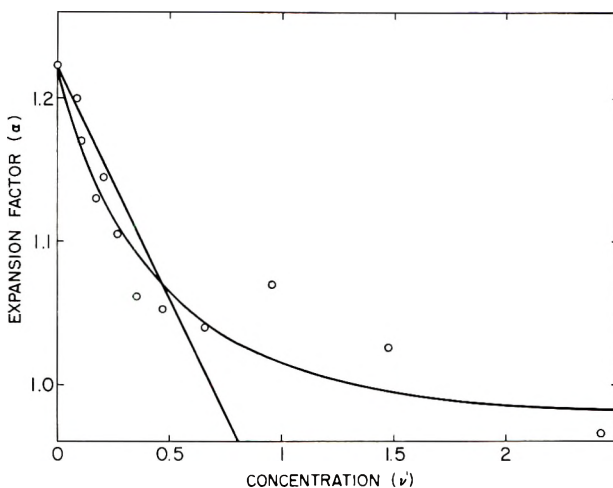


Fig. 4. The effect of polymer concentration on the chain expansion factor  $\alpha$ . The unit of concentration is given by  $0.189 \langle R_0^2 \rangle^3 / 2\rho$ , where  $\rho$  is the number of molecules/unit volume and  $\langle R_0^2 \rangle$  is the mean squared end-to-end distance at infinite dilution. (A) Monte-Carlo calculations; (B) results of Fixman for intermolecular potential parameter,  $A = 2.8$ .

leveling off should occur at high concentrations has been predicted by Fixman<sup>10</sup> and also by Krigbaum.<sup>15</sup> That the concentration at which the effect is observed should be smaller for short chains than for long ones is reasonable since the high segment density limits the decrease in  $\alpha$ . If a sufficiently economical Monte-Carlo procedure can be devised, it would be interesting to see whether the marked divergence between numerical and analytical results, which is only insignificantly changed by use of eqs. (7) and (8a), would decrease for longer chains.

### Segment-Segment Interactions

For isolated chains the mean number of nearest neighbor interactions per segment is given in Table II. After an initial increase this number remains nearly constant. We would expect a further decrease with increasing chain length corresponding to the diminishing segment density for any coil whose linear dimensions are proportional to more than the  $1/3$  power of the number of segments. Only about 20% of the 101 link chains pick up one or more additional nearest neighbors when grown in the vicinity of a preformed chain. This suggests that little mutual penetration occurs. The compressed chains are those that succeed in coiling themselves quite efficiently in the space allotted to them averaged together with those that happen to grow in a direction away from the preformed chain and are but little affected by it. That the compression which occurs for polymer molecules in good solvents does not involve much actual chain entanglement has been demonstrated for polystyrene in benzene at 25°C. by Gill and Toggenburger<sup>22</sup> using a method based on strain birefringence.

They find only 2-3 actual "junctions" per molecule at concentrations of 11-14 g./100 cc. for polystyrene with a viscosity-average molecular weight near  $10^6$  or an aggregation number near  $10^4$ . Although our result, ca. 0.2 junctions/molecule, is based on too few data for real validity, it differs from that of Gill and Toggenburger in the expected direction of less mutual penetration for shorter chains of higher segment density.

TABLE II  
Segment-Segment Interactions for Isolated Chains

Number of links	Nearest neighbors per link
33	0.173
50	0.187
67	0.191
84	0.199
101	0.197

The authors are grateful to the National Science Foundation for a grant, G19507, in support of this and other work. We acknowledge also the help of the Computer Sciences Laboratory of the University of Southern California with its H800 computer furnished by the Minneapolis-Honeywell Co., and its able programmer, Mr. Laszlo Engelman.

### References

1. Wall, F. T., and J. Mazur, *Ann. N. Y. Acad. Sci.*, **89**, 608 (1961). References to earlier work are given.
2. Verdier, P. H., and W. H. Stockmayer, *J. Chem. Phys.*, **36**, 227 (1962).
3. Stockmayer, W. H., *Makromol. Chem.*, **35**, 54 (1960).
4. Kurata, M., and H. Yamakawa, *J. Chem. Phys.*, **29**, 311 (1958).
5. Albrecht, H. C., *J. Chem. Phys.*, **27**, 1002 (1957).
6. Zimm, B. H., *J. Chem. Phys.*, **14**, 164 (1946).
7. Casassa, E. F., *Ann. Revs. Phys. Chem.*, **11**, 477 (1960).
8. Yamakawa, H., *J. Chem. Phys.*, **34**, 1360 (1960).
9. Fixman, M., *J. Chem. Phys.*, **33**, 370 (1960).
10. Fixman, M., *Ann. N. Y. Acad. Sci.*, **89**, 657 (1961).
11. Fixman, M., *J. Polymer Sci.*, **47**, 91 (1960).
12. Grimley, T. B., *Trans. Faraday Soc.*, **57**, 1974 (1961).
13. Debye, P., B. Chu, and D. Woermann, *J. Chem. Phys.*, **36**, 1803 (1962); P. Debye, H. Coil, and D. Woermann, *ibid.*, **33**, 1746 (1960).
14. Simha, R., and J. L. Zakin, *J. Chem. Phys.*, **33**, 1791 (1960).
15. Kawai, T., and K. Saito (with appendix by W. R. Krigbaum), *J. Polymer Sci.*, **26**, 213 (1957).
16. Wall, F. T., and J. J. Erpenbeck, *J. Chem. Phys.*, **30**, 634 (1959).
17. Rotenberg, A., *J. Assoc. Comp. Mach.*, **7**, 75 (1960).
18. Wall, F. T., L. H. Hiller, and W. F. Atchison, *J. Assoc. Comp. Mach.*, **23**, 913, 2314 (1955).
19. Chandrasekar, S., *Rev. Mod. Phys.*, **15**, 86 (1943).
20. Debye, P., and F. Bueche, *J. Chem. Phys.*, **20**, 1337 (1952).
21. Krigbaum, W. R., and P. J. Flory, *J. Am. Chem. Soc.*, **75**, 1775 (1953).
22. Gill, S. G., and R. Toggenburger, *J. Polymer Sci.*, **60**, S69 (1962).

### Résumé

On a calculé les distances moyennes terminales de polymères à 101 segments, subissant des mouvements statistiques, sans s'entrecroiser, dans un réseau cubique à cinq degrés de liberté, dans lequel se trouve une seconde chaîne en fonction de la distance entre les deux chaînes (c.à.d. concentration en polymères). Les dimensions du polymère décroissent en fonction de la concentration, linéairement d'abord, plus lentement ensuite. Les résultats concordent avec l'expérience et avec certaines théories analytiques approchées mais médiocrement avec les autres.

### Zusammenfassung

Die mittleren End-zu-End-Abstände für lineare Polymere aus 101 Segmenten wurde für nicht kreuzenden Irrflug in einem kubischen Gitter mit fünf Auswahlmöglichkeiten, in den auch eine zweite Kette vorhanden ist, als Funktion des Abstandes zwischen den beiden Ketten (d.h. der Polymerkonzentration) berechnet. Die Polymerdimensionen scheinen mit der Konzentration zuerst linear und dann langsamer abzunehmen. Die Ergebnisse zeigen gute Übereinstimmung mit dem Experiment und mit einigen analytischen theoretischen Näherungsausdrücken, mit anderen jedoch eine recht schlechte.

Received November 2, 1962

## Calibration of Light-Scattering Instruments. II. The Volume Correction\*

MILTON KERKER, JOSIP P. KRATOHVIL, and EGON MATIJEVIĆ,  
*Department of Chemistry, Clarkson College of Technology, Potsdam,  
New York*

### Synopsis

The physical nature of the volume correction,  $C_v$ , used in the determination of turbidity by light-scattering measurements at  $90^\circ$  is reviewed, and errors and limitations in earlier formulations are pointed out. Formulations are given for three cases; viz., (I) when the height of the incident beam is within the central scattering volume,  $V_c$ ; (II) when the field of view of the detector is completely within the beam; (III) the intermediate case when the vertical edges of the beam are in the excess volume,  $V_e$ . The volume correction is calculated for several geometries.

A number of correction factors must be considered in the determination of the absolute intensity of light scattering from pure liquids and solutions. Among these, the volume correction,  $C_v$ , arises because of the variation in the total volume of liquid that is seen by the detector as the refractive index of the liquid changes, and because not all of the elements of volume which are seen scatter through cones of equal solid angle. Several workers<sup>1-8</sup> have formulated this correction, each giving different formulas and geometrical constructions. Errors or unnecessary limitations appear in all of these formulations. We will attempt here to clarify this situation by outlining the physical problem, reviewing the errors and limitations in the earlier work, deriving formulations applicable under various conditions, and applying the newly derived formulations to the geometries corresponding to several instruments. These considerations apply to scattering at  $90^\circ$  and for rectangular or semioctagonal cells.

### A. The Physical Problem

The geometry, considerably exaggerated in order to clarify the various relations, is shown in Figure 1, where the symbolism of Carpenter and Krigbaum<sup>6,7</sup> has been retained as much as possible. This is the view of the perpendicular plane along the  $90^\circ$  axis. The parallel incident beam of the height  $h'$  and width  $w$  enters the cell of half-width  $l_1$  in the direction perpendicular to the plane of the drawing. The dimensions of the rectangular

\* This work has been supported by the U.S. Atomic Energy Commission, Contract No. AT(30-1)-1801.

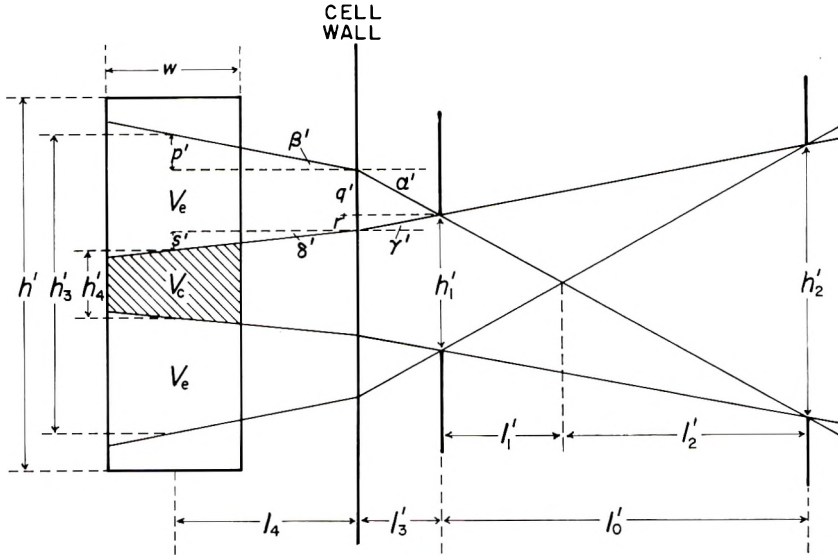


Fig. 1. Side view of the scattered beam. Incident beam height  $h'$  and width  $w$ , half-width of cell  $l$ , apertures heights  $h_1'$  and  $h_2'$  and widths  $h_1$  and  $h_2$ . Case II (see text) applies to this geometry.

apertures in front of the detector are  $h_1$  and  $h_1'$  and  $h_2$  and  $h_2'$ . The non-primed quantities throughout this paper correspond to the dimensions in the scattering plane, and prime quantities to those perpendicular to the scattering plane, the latter being shown in Figure 1. In the central region,  $V_l$ , all elements of volume subtend essentially the same solid angle,  $\Omega$ , through an aperture of dimensions  $h_2 \times h_2'$ . However, as one moves out of this region, the solid angle subtended decreases until the edge of the field of view is reached. It is assumed that the scattered intensity per unit volume in each of the two regions of excess volume,  $V_e$ , is, on the average, half that in the central region. The volume correction,  $C_v$ , corrects the signal actually received to that which would be obtained by scattering through solid angle,  $\Omega$ , from the region of volume  $V = h_1 \times h_1' \times w$ . This region,  $V$ , is somewhat more extensive than  $V_c$  (compare Fig. 1). Accordingly, if both  $V_c$  and  $V_e$  are completely illuminated,

$$C_v = V/(V_c + V_e) \quad (1)$$

Several comments are now in order regarding the geometry. Both Carr and Zimm<sup>1,2</sup> and Carpenter and Krigbaum<sup>6,7</sup> place aperture  $h_1 \times h_1'$  directly on the cell wall. However, the geometry depicted in Figure 1 is more general, and the relations to be derived will reduce properly whenever aperture  $h_1 \times h_1'$  is at the cell wall, i.e., when  $l_3 = 0$ .

Some of the workers<sup>1,2,5-7</sup> have treated only the case where the height of the incident beam, as determined by  $h'$ , is completely within the central region,  $V_c$ , and for which the vertical dimension to be considered is simply  $h'$ . For this case, the planar geometry in the horizontal scattering plane



(perpendicular to that shown in Fig. 1) is sufficient to describe the problem.  $C_v$  is then usually defined so that it corrects to the volume  $V = h_1 \times h' \times w$ . However, it is possible (a) for the detector's field of view to be completely within the height of the incident beam, or (b) for the edge of the incident beam to be in the region of excess volume,  $V_e$ . In such cases the volume correction must be treated accordingly.

Earlier workers,<sup>1-3,5,8</sup> neglecting refraction at the cell boundary, considered that  $V_e$  was determined by aperture  $h_1 \times h'_1$  and was therefore equal to  $V$ . Carpenter and Krigbaum<sup>6,7</sup> have correctly designated the central region,  $V_e$ , as shown in Figure 1 by the trapezoidal cross-hatched area.

**B. Earlier Formulations**

Deželić<sup>9</sup> has pointed out that the formula given by Carr and Zimm<sup>1,2</sup> which is used most frequently is incorrect and should be

$$C_v = 1 - [l_4(h_1 + h_2)/l_0] / [2nh_1 + l_4(h_1 + h_2)/l_0] \tag{2}$$

by the notation of Figure 1. The error arises on page 33 of Carr's thesis,<sup>1</sup> where the formulation of the fractional correction is given as  $V_e/(V + 2V_e)$  instead of  $V_e/(V + V_e)$ . Sedlaček<sup>4</sup> has also given eq. (2) but without

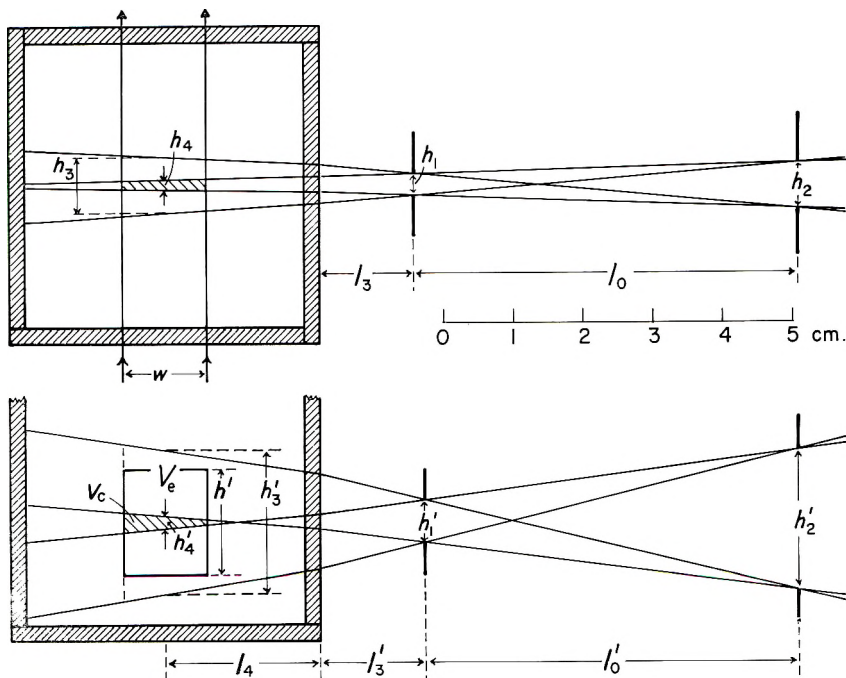


Fig. 2. The top (upper) and side views of the scattered beam of a standard model Brice-Phoenix light-scattering photometer with standard apertures and cell of inside dimensions  $40 \times 40$  mm. The drawing is to scale for refractive index of the medium in the cell  $n = 1.52$ . Symbols correspond to the same quantities as in Fig. 1. Case III applies.

comment. It should be pointed out that this equation was originally derived only for the case where the aperture  $h_1 \times h'_1$  is at the cell wall, and cannot be applied when this is not the case. In addition to the above error, Carr and Zimm's treatment uses  $V = h_1 \times h' \times w$  for the central region rather than  $V_c$ . Also, it is limited to the case where the height of the beam is completely within the central region,  $V_c$ . Furthermore, the unnecessary assumption is made that the angle  $\alpha$  in Figure 1 is sufficiently small so that  $\tan \alpha = \alpha$ . A similar assumption is made regarding the angle  $\beta$ .

Maron and Lou's<sup>5</sup> equation for  $C_v$  is incorrect because they neglected the factor of one-half in the region of the excess volume, as already pointed out by Carpenter and Krigbaum.<sup>6,7</sup> They also limited their treatment to the case where the height of the beam is within the central region. In their geometry the two apertures  $h_1 \times h'_1$  and  $h_2 \times h'_2$  are of equal dimensions, so that for this case the region  $V_c = h_1 \times h'_1 \times w$  and the region  $V = h_1 \times h' \times w$ , assuming that  $h' < h'_4$ .

Kerker, Lee, and Chou<sup>8</sup> consider the case where the view of the detector is completely within the beam. They do take the factor of one-half into consideration. However, they too use  $V$ , rather than  $V_c$ , for the central region and also make the small angle approximation for  $\tan \alpha$  and  $\tan \beta$ .

Carpenter and Krigbaum<sup>6,7</sup> use the same geometry as Carr and Zimm, i.e., their treatment is limited to the case where the aperture  $h_1 \times h'_1$  is at the cell wall. Also, in their case, the vertical dimension of the beam is completely within the central region. Within these limitations their formulas are correct. However, in Figure 2 of their paper,<sup>7</sup>  $h_3$  and  $h_4$  are drawn incorrectly. We point this out since this can cause confusion if one tries to verify the formulas directly from their drawing. This error also appears in Carpenter's thesis.<sup>6</sup>

### C. The New Formulations of $C_v$

**Case I:**  $h' \leq h'_4$ . In this case the height of the incident beam,  $h'$ , is completely within the central region,  $V_c$ , and eq. (3) applies:

$$C_v = [2h_1/(h_3 + h_4)](h'_1/h') \quad (3)$$

where

$$h_3 = h_1 + (h_2 + h_1)l_3/l_0 + 2l_4/(n^2\{1 + [2l_0/(h_2 + h_1)]^2\} - 1)^{1/2} \quad (4)$$

and

$$h_4 = h_1 - (h_2 - h_1)l_3/l_0 - 2l_4/(n^2\{1 + [2l_0/(h_2 - h_1)]^2\} - 1)^{1/2} \quad (5)$$

(see Appendix for derivation of  $h_3$  and  $h_4$ ).  $n$  is the refractive index of the medium in the cell. The second term in eqs. (4) and (5) goes to zero whenever the first aperture is at the cell wall ( $l_3 = 0$ ) and eqs. (4) and (5) then reduce to the corresponding ones given by Carpenter and Krigbaum. The corrected volume,  $V$ , is  $h_1 \times w \times h'_1$ . If the corrected volume,  $V = h_1 \times$

$h' \times w$ , as defined by Carpenter and Krigbaum, then one obtains their formula

$$C_v = 2h_1/(h_3 + h_4) \tag{3a}$$

**Case II:**  $h' \geq h'_3$ . In this case the field of view of the detector is completely within the beam, and the geometry of Figure 1 applies directly. Accordingly,

$$\begin{aligned} C_v &= [h_1/.5(h_3 + h_4)][h'_1/.5(h'_3 + h'_4)] \\ &= 4h_1h'_1/(h_3 + h_4)(h'_3 + h'_4) \end{aligned} \tag{6}$$

where  $h_3$  and  $h_4$  or  $h'_3$  and  $h'_4$  are given by eqs. (4) and (5) (corresponding primed quantities being used for  $h'_3$  and  $h'_4$ ). The corrected volume is again  $h_1 \times w \times h'_1$ .

**Case III:**  $h'_3 \geq h' \geq h'_4$ . In this case radiation reaches the detector from only part of the excess region (Fig. 2). Accordingly, the dimension  $0.5(h'_3 + h'_4)$  must be replaced by the smaller dimension  $h'_4 + (h' - h'_4)f$ . In this case, the term  $(h' - h'_4)$  is multiplied by a factor  $f$ , which has a value between  $1/2$  and 1 rather than a value of  $1/2$  as in case II. This is the factor which corrects for the reduced solid angle subtended through aperture  $h_2 \times h'_2$  in the excess volume,  $V_e$ . Accordingly,

$$C_v = [2h_1/(h_3 + h_4)]\{h'_1/[h'_4 + (h' - h'_4)f]\} \tag{7}$$

Then, when  $h' = h'_4$ ,  $f = 1$  and when  $h' = h'_3$ ,  $f = 1/2$ , reducing eq. (7) to eqs. (3) and (6), respectively (cases I and II). For intermediate values of  $h'$ , corresponding to case III,

$$C_v = [2h_1/(h_3 + h_4)]h'_1/\{h'_4 + 0.5(h' - h'_4)[1 + (h'_3 - h')/(h'_3 - h'_4)]\} \tag{8}$$

where  $h_3$ ,  $h'_3$ ,  $h_4$ , and  $h'_4$  are calculated by means of eqs. (4) and (5). Here it is assumed that the scattering intensity per unit volume decreases linearly as one moves through region  $V_e$ . The corrected volume is now  $h_1 \times w \times h'_1$ .

A few words of comment are in order regarding the geometry depicted in Figure 2 as an illustration for case III. This geometry corresponds to that of a standard model of the Brice-Phoenix light-scattering photometer<sup>3</sup> (Phoenix Precision Instrument Company, Philadelphia, Pa.) with standard apertures and square or semioctagonal cells of inside dimensions  $40 \times 40$  mm. The picture is drawn to scale for refractive index of the medium in the cell  $n = 1.52$  (benzene). The limiting rays in the vertical plane, defining the central region  $V_c$ , cross over before reaching the illuminated volume in the cell. This leads, algebraically, to a negative value for  $h'_4$  [from eq. (5)] and the question arises whether the equations developed for case III are applicable to this geometry. Simple geometrical considerations show that the equations for case III apply when the absolute value of  $h'_4$  is used.

### D. Applications

We have been able to obtain sufficiently detailed information to calculate  $C_v$  for only three instruments, viz., two commercial photometers: Brice-Phoenix<sup>3</sup> and Oster-Aminco<sup>10</sup> (American Instrument Company, Silver Spring, Md.), and the instrument described by Carr and Zimm.<sup>1,2</sup> Brice's method<sup>3</sup> for obtaining absolute intensities with the Brice-Phoenix instrument eliminates the necessity for the volume correction [compare eqs. (13), (18), and (19) in Brice's paper<sup>3</sup>]. This is true regardless of the fact that Brice's formulation for the volume correction [eq. (6) in reference 3] is not correct (compare case III above). However, when the Brice-Phoenix instrument is calibrated by comparison of the scattering of the medium under investigation with that of a medium of different refractive index but of known turbidity, the relative volume correction,  $C'_v$  (the ratio of  $C_v$  for two media of different refractive indices) is significant and should not

TABLE I  
Dimensions of Several Light-Scattering Instruments and the Corresponding Volume Corrections

Dimensions, cm.	Brice-Phoenix photometer		Oster- Aminco photometer	Carr-Zimm <sup>a</sup>	
	Standard apertures	Reduced apertures		Horn cell	Square cell
$w$	1.20		0.40	0.8	0.8
$h'$	1.50		0.75	0.8	0.8
$h_1$	0.30	0.30	0.15	0.949	0.817
$h'_1$	0.60	0.30	0.28		
$h_2$	0.65	0.30	0.15	0.8	0.8
$h'_2$	2.00	0.30	0.28		
$l_0$	5.50		1.50	5.62	7.56
$l'_0$	5.35		1.50		
$l_3$	1.35		0.55	0	0
$l'_3$	1.50		0.55		
$l_4$	2.22		1.45	2.8	0.86
Case applicable	III	II	III	I <sup>b</sup>	I <sup>b</sup>
$C_v$ , benzene	0.387 (0.771) <sup>c</sup>	0.438	0.500	0.783 (0.811) <sup>e</sup>	
$C_v$ , water	0.362 (0.756) <sup>c</sup>	0.418	0.479	0.762 (0.791) <sup>c</sup>	
$C'_v$ (benzene/water)	1.070 (1.021) <sup>c</sup>	1.048	1.043 (1.105) <sup>d</sup>	1.027 (1.025) <sup>e</sup>	
$C_v$ , butanone					0.925 (0.930) <sup>e</sup>
$C'_v$ (benzene-horn cell/butanone- square cell)				0.846 (0.873) <sup>e</sup>	

<sup>a</sup> Carr's thesis<sup>1</sup> (p. 41, Tables 8 and 9).

<sup>b</sup> Calculated from eq. (3a).

<sup>c</sup> Calculated by means of the "uncorrected" Carr-Zimm equation.

<sup>d</sup> Given by Deželić.<sup>9</sup>

be neglected. This is illustrated in Table I for refractive indices corresponding to water and benzene. Even when the geometry of Brice-Phoenix instrument is changed in such a way that case II applies (i.e., by reducing both apertures  $h_1 \times h'_1$  and  $h_2 \times h'_2$  to the size of  $3 \times 3$  mm.)  $C'_v$  amounts still to about 5% for the benzene-water combination (Table I).

Furthermore, the value of  $C_v$  and  $C'_v$  depends upon the formulation used. Using the Carr and Zimm equation as originally presented<sup>1,2</sup> we obtain  $C'_v = 1.02$  for benzene-water when the standard Brice-Phoenix dimensions are used. The "corrected" Carr-Zimm equation [eq. (2) of this paper] leads to  $C'_v = 1.04$  for the same case whereas the correct expression, eq. (8), gives  $C'_v = 1.07$ . Similar results are obtained for the Oster-Aminco instrument; e.g., Deželić<sup>9</sup> reported a value of  $C'_v = 1.105$  for benzene-water using the equation given by Kerker et. al.<sup>8</sup> which compares with our newly calculated value of 1.04 [eq. (8)]. It is worthwhile mentioning that, contrary to some claims in the literature,<sup>9,11</sup> the field of view of the detector in the Oster-Aminco photometer does not appear to be completely within the height of the incident beam. This is true for any receiving nosepiece normally supplied by the manufacturer.

Case I applies, at least, to some of the instrumental arrangements described by Carr and Zimm.<sup>1,2</sup> In Carr's thesis,<sup>1</sup> sufficiently detailed information is given for consideration of the possible influence of the form of the volume correction on the value of the Rayleigh ratio,  $R_{90}$ , of pure liquids. He determined  $R_{90}$  of several liquids, using a cell equipped with Rayleigh horns at the exit and back faces, by comparison with a standard polystyrene-butanone solution contained in a square cell.  $R_{90}$  of this latter solution was, in turn, determined by use of a reflecting diffusor. When eq. (3) of our paper is applied to the relevant geometries and refractive indices, the value of the correction,  $C'_v$ , corresponding to the case of benzene in the horn cell relative to butanone in the square cell, becomes lower by about 3% than the value calculated from the "uncorrected" Carr and Zimm equation, i.e., 0.846 instead of 0.873 (reference 1, page 41). This leads to a correspondingly lower value of  $R_{90}$  of benzene. Moreover, there is a computational error (page 41, Table 8; for polystyrene-butanone solution in the horn cell;  $C_v = 0.799$  rather than 0.835) which could lead to an even smaller  $R_{90}$  value for the polystyrene-butanone solution which served as a secondary standard. All this indicates that the Carr and Zimm values for  $R_{90}$  of benzene are too high bringing their results more into line with those that we have recently suggested<sup>12</sup> as more likely. Deželić's results for  $R_{90}$  of benzene and toluene and turbidity of standard polystyrenes in toluene (reference 9, Table III and IV) should also be lower by about 6%, in accordance with the calculations of  $C'_v$  for Oster-Aminco photometer discussed above.

Finally, we would like to make a comment on the results of Carpenter and Krigbaum<sup>6,7</sup> for  $R_{90}$  of benzene and toluene and for the turbidity of Cornell polystyrene in toluene. The values they obtained for a wavelength of 436 m $\mu$  are the highest among all reported values (compare Tables V,

VI, and IX of the previous report<sup>12</sup>). On the other hand, their values for 546  $\mu$ , with the exception of  $R_{90}$  of toluene, occupy a considerably lower position among the results of other workers. We suggest that this is due to the experimental method used. According to Carpenter's thesis<sup>6</sup> (p. 67-68), the absolute measurements were performed with unpolarized incident light, and a polaroid analyzer was used in front of the photomultiplier tube. The total amount of light scattered was determined by adding the horizontal and vertical components. Since polaroid sheets never achieve a 100% polarization, particularly in the blue region of the spectrum,<sup>13</sup> the total amount of light received by the detector in Carpenter's experiments is certainly larger than the sum of the horizontal and vertical components, and the discrepancy should be greater for 436  $\mu$  than for 546  $\mu$ . Consideration of this effect would place their  $R_{90}$  values closer to those we have suggested.<sup>12</sup>

### Appendix

Equations (4) and (5) are obtained from a construction identical to that of Figure 1, except that the corresponding (unprimed) quantities in the horizontal scattering plane are used (primed quantities being used for  $h'_3$  and  $h'_4$ ).

$$h_3 = h_1 + 2p + 2q \quad (9)$$

where

$$q = \frac{1}{2}(h_2 + h_1)(l_3/l_0) \quad (10)$$

$$\begin{aligned} p &= l_4 \tan \beta \\ &= l_4 / [(1/\sin^2 \beta) - 1]^{1/2} \\ &= l_4 / [(n^2/\sin^2 \alpha) - 1]^{1/2} \end{aligned} \quad (11)$$

and

$$\sin \alpha = \frac{1}{2}(h_2 + h_1) / [l_0^2 + \frac{1}{4}(h_2 + h_1)^2]^{1/2} \quad (12)$$

Similarly,

$$h_4 = h_1 - 2r - 2s \quad (13)$$

where

$$\begin{aligned} r &= \frac{1}{2}(h_2 - h_1)(l_3/l_0) \\ s &= l_4 \tan \delta \\ &= l_4 / [(1/\sin^2 \delta) - 1]^{1/2} \\ &= l_4 / [(n^2/\sin^2 \gamma) - 1]^{1/2} \end{aligned} \quad (14)$$

$$(15)$$

and

$$\sin \gamma = \frac{1}{2}(h_2 - h_1) / [l_0^2 + \frac{1}{4}(h_2 - h_1)^2]^{1/2} \quad (16)$$

### References

1. Carr, C. I., Thesis, University of California, Berkeley, Calif., 1949.
2. Carr, C. I., and B. H. Zimm, *J. Chem. Phys.*, **18**, 1616 (1950).
3. Brice, B. A., M. Halwer, and R. Speiser, *J. Opt. Soc. Am.*, **40**, 768 (1950).
4. Sedlaček, B., *Chem. Listy*, **47**, 1113 (1953).
5. Maron, S. H., and R. L. H. Lou, *J. Polymer Sci.*, **14**, 273 (1954).
6. Carpenter, D. K., Thesis, Duke University, Durham, N.C., 1955.
7. Carpenter, D. K., and W. R. Krigbaum, *J. Chem. Phys.*, **24**, 1041 (1956).
8. Kerker, M., D. Lee, and A. Chou, *J. Am. Chem. Soc.*, **80**, 1539 (1958).
9. Deželić, Gj., *Croat. Chem. Acta*, **33**, 99 (1961).
10. Oster, G., *Anal. Chem.*, **25**, 1165 (1953).
11. Hermans, J. J., and S. Levinson, *J. Opt. Soc. Am.*, **41**, 460 (1951).
12. Kratochvil, J. P., Gj. Deželić, M. Kerker, and E. Matijević, *J. Polymer Sci.*, **57**, 59 (1962).
13. See, e.g., W. Heller, in A. Weissberger, Ed., *Physical Methods of Organic Chemistry*, 3rd Ed., Part III, Interscience, New York, 1960, p. 2201.

### Résumé

La nature physique de la correction de volume  $C_v$ , utilisée lors de la détermination de la turbidité par des mesures de diffusion lumineuse à  $90^\circ$ , a été revue et on a pu relever certaines erreurs et restrictions dans les formules utilisées antérieurement. On donne des formules pour les trois cas suivants: (I) lorsque la hauteur du rayon incident se situe au centre du volume diffusant  $V_e$ ; (II) lorsque le champ de vue du détecteur est situé entièrement à l'intérieur du faisceau; (III) ce cas intermédiaire où les bords verticaux du rayon sont dans le volume excédent  $V_e$ . On a calculé la correction de volume pour différentes géométries.

### Zusammenfassung

Ein Überblick über die physikalische Natur der bei der Trübighkeitsbestimmung durch Lichtstreuungsmessungen bei  $90^\circ$  benützten Volumskorrektur,  $C_v$ , wird gegeben und Irrtümer sowie die Grenzen früherer Formulierungen werden aufgezeigt. Formeln werden für drei Fälle angegeben, nämlich (I) die Höhe des einfallenden Strahles liegt innerhalb des zentralen Streuvolumens,  $V_e$ , (II) das Gesichtsfeld des Detektors liegt vollständig innerhalb des Strahles und (III) der dazwischenliegende Fall, dass sich die vertikalen Kanten des Strahls im Überschussvolumen,  $V_e$ , befinden. Die Volumskorrektur wird für verschiedene geometrische Bedingungen berechnet.

Received November 5, 1962

## Effect of Molecular Weight and Its Distribution on Stretching of Polyacrylonitrile Gel

HIDEHIKO KOBAYASHI, KIICHIRO SASAGURI, and YOSHISATO FUJISAKI, *Research Laboratory, Cashmilon Plant, Asahi Chemical Industry Company, Fuji, Japan*, and TOSHIHIKO AMANO, *Textile Research Laboratory, Asahi Chemical Industry Company, Takatsuki, Japan*

### Synopsis

The present studies were designed to secure information about the effect of molecular weight and its distribution on the hot-stretchability (defined as maximum hot draw ratio possible without breakage under given condition) of the coagulated gel obtained by extruding a concentrated solution of polyacrylonitrile dissolved in 70% nitric acid into dilute nitric acid solution. After washing, the coagulated threads thus obtained were stretched at 100–140°C. In the case of fractionated polyacrylonitrile, the results obtained under the above conditions showed a maximum hot-stretchability at  $M = 80,000$ . Below this point, hot-stretchability was lowered with decrease of molecular weight. For polymers having a molecular weight larger than this value, it was also depressed as molecular weight increased and approached a certain value. For whole polymers, hot-stretchability distribution curves obtained from molecular weight distribution curves by substituting molecular weight with corresponding hot-stretchability were studied. It was found that the maximum stretchability of a whole polymer was the weight average value of those of its constituent polymer species. The effect of molecular weight of the polymer on the mechanical properties of fibers and their fine structure was investigated by means of tensile and x-ray measurement.

### INTRODUCTION

Many investigations have been made of the effect of molecular weight and its distribution on the physical properties of polymers in solid state and in solution. On the other hand, despite the industrial importance, relatively little has been published about the effect of molecular weight and molecular weight distribution on the maximum draw ratio of polymer gel. For polyacrylonitrile, only qualitative results were reported by Ham<sup>1</sup> and Hunyer.<sup>2</sup>

In a study of the mechanical properties of fibers, analysis of the spinning process (coagulation of spinning solution and hot-stretching of coagulated thread) is of great importance, especially hot-stretchability (defined as maximum hot draw ratio possible without filament breakage under specified conditions) of coagulated gel is very important because it directly influences the mechanical properties of fibers. Ideally, perhaps, interpretation of a given property of a fiber should proceed from consideration of the contribution of each molecular species to that property, the final result being obtained by summing the contributions from all species present.



All the wet spinning processes have in common the extrusion of a concentrated polymer solution through a spinneret orifice into a solution capable of coagulating the polymer. According to our unpublished results, the molecular weight of a polymer has little effect on the coagulation behavior, provided the temperature of coagulation bath is low and the viscosity of the polymer solution is constant. On the other hand, hot-stretchability of the coagulated thread is greatly affected by molecular weight and its distribution.

## EXPERIMENTAL

### 1. Materials

Acrylonitrile monomer was obtained from Monsanto Chemical Co. and distilled at atmospheric pressure. Polymerization was carried out in water suspension with  $\alpha, \alpha'$ -azobisisobutyronitrile (AIBN).  $\beta$ -Mercaptoethanol ( $\beta$ -EtSH) was used for the control of molecular weight. Polyacrylonitrile polymerized with organic catalyst by suspension polymerization is known to have a fairly narrow molecular weight distribution compared with that obtained in aqueous phase with redox catalysts.<sup>3</sup>

Polymerization conditions are listed in Table I, along with molecular weights and distribution indexes,  $\bar{M}_w/\bar{M}_n$ . Viscosity-average molecular weights were obtained from viscosity measurements of dilute polymer solutions in dimethylformamide at 35°C.; the calculations were based on eq. (1):<sup>4</sup>

$$[\eta] = 2.78 \times 10^{-4} M^{0.76} \quad (1)$$

Weight-average and number-average molecular weights of the polymer samples were calculated from their molecular weight distribution curves. Accordingly, the reliability of these values will depend on the accuracy of the molecular weight distribution curves. To confirm the reliability of this method, light-scattering and diffusion-intrinsic viscosity methods were used to obtain two different average molecular weights for sample A-5. According to the results of these measurements, the weight-average molecular weight was 168,000, and the average molecular weight obtained from diffusion-intrinsic viscosity method<sup>4</sup> was 50,000. It is known that the average of molecular weights obtained by the measurements of diffusion and intrinsic viscosity approximates the number-average molecular weight.<sup>4</sup> According to these results, the weight-average molecular weight of 142,000 and the number-average molecular weight of 46,300 calculated from the molecular weight distribution curves are considered reasonable.

Dimethylformamide used for the determinations of intrinsic viscosities was obtained from Nitto Chemical Co. and distilled at a pressure of 10 mm. Hg. The middle fraction, ( $d_4^{25}$  0.9443–0.9444), was used: the refractive index and viscosity of this fraction agreed with values quoted by du Pont<sup>5</sup> for pure dimethylformamide. Dimethyl sulfoxide, used for fractionation,

TABLE I  
Preparations of Polymers

Sam- ple no.	Acrylo- nitrile, g.	AIBN, g.	$\beta$ -EtSH, g.	H <sub>2</sub> O, g.	Temp., °C.	Time, hr.	pH (by H <sub>2</sub> SO <sub>4</sub> )	Conver- sion, %	$\bar{M}_v$	$\bar{M}_w$	$\bar{M}_n$	$\bar{M}_w/\bar{M}_n$
A-1	100	0.25	1.0	300	60	4	2.1	68.9	30,500	31,500	16,400	1.92
A-2	100	0.3	0.33	300	60	4	2.1	64.9	82,000	83,000	28,700	2.90
A-3	100	0.3	0.35	300	60	4	2.1	65.9	86,000	86,100	30,900	2.79
A-4	100	0.3	0.28	300	60	4	2.1	66.7	92,200	94,300	36,500	2.57
A-5	100	0.3	0.16	300	60	4	2.1	66.0	141,000	142,000	46,300	3.10
A-6	100	0.25	0.75	300	60	4	2.1	63.0	45,000	49,300	26,200	1.89
A-7	100	0.25	0.2	300	60	4	2.1	—	150,000	153,000	49,000	3.12
A-8	100	0.25	0.16	300	60	4	2.1	36.7	239,000	239,000	81,400	3.30

was obtained from Stephan Chemical Co. It was distilled at a pressure of 10 mm. Hg. The middle fraction was used.

## 2. Determination of Molecular Weight Distribution

Various methods have been proposed for the fractionation of polyacrylonitrile.<sup>6-11</sup> In the case of a polymer which may crystallize, it is desirable to adopt fractionation conditions which allow the precipitate to separate as a totally amorphous liquid. We have recently found that, by using a suit-

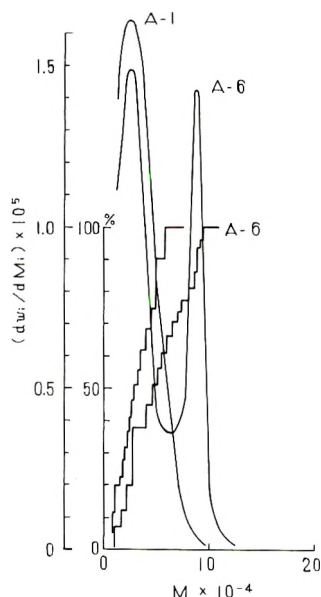


Fig. 1. Molecular weight distribution curves of polyacrylonitrile samples A-1 and A-6.

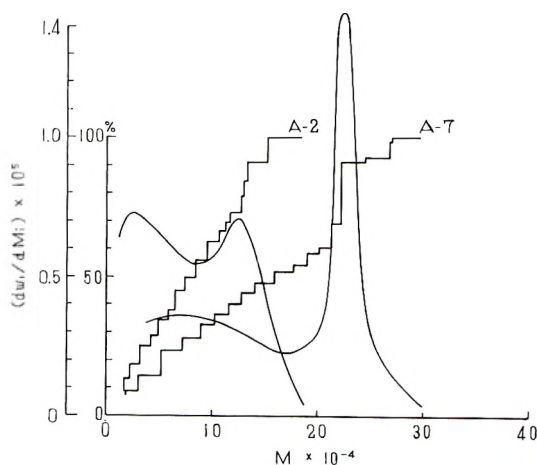


Fig. 2. Molecular weight distribution curves of polyacrylonitrile samples A-2 and A-7.

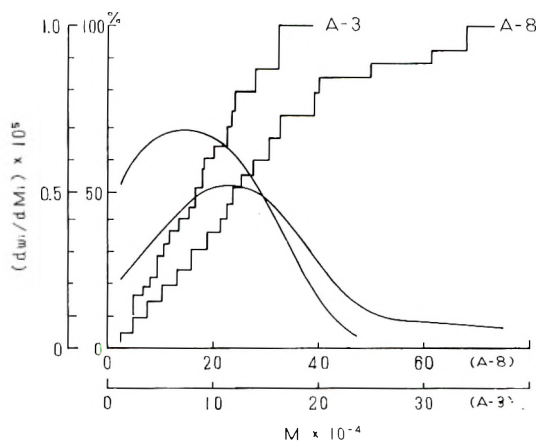


Fig. 3. Molecular weight distribution curves of polyacrylonitrile samples A-3 and A-8.

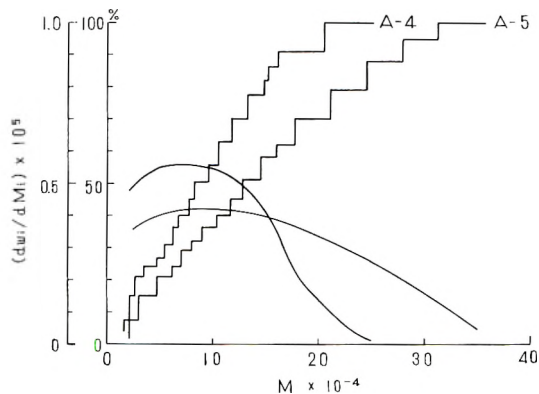


Fig. 4. Molecular weight distribution curves of polyacrylonitrile samples A-4 and A-5.

able initial polymer concentration, dimethyl sulfoxide-toluene, a solvent-precipitant system, is superior to other systems.<sup>11</sup> Samples were separated into 17-22 primary fractions. Fractionation was carried out at 35°C. Toluene was added through a capillary tube to the well stirred solution of polymer in dimethyl sulfoxide until the mixture became cloudy. The precipitate (gel) was dissolved by raising the temperature of the bath by a few degrees, and then allowed to reprecipitate by lowering the bath temperature to 35°C. The precipitate was separated by decantation or centrifugation, dissolved in dimethylformamide, and isolated in water. The fractions separated by the above method were washed several times with ethyl alcohol and then dried under vacuum at 50°C. to constant weight. The procedure was repeated for the isolation of the remaining polymer. In the case of the samples with high average molecular weights, especially samples A-5, A-7, and A-8, the high molecular weight fractions were obtained by refractionation method. Molecular weight distribution curves obtained

by the above method are given in Figures 1-4. As shown in these figures, the molecular weight distribution curves of samples A-2, A-6, and A-7 show two peaks in distribution. Especially the peak appearing in the high molecular weight region is pretty sharp, which cannot be explained by the general kinetic theory of polymerization. As pointed out previously,<sup>10</sup> however, these peaks are based on the nature of the polymer samples, and not on the peculiarities of the fractionation method. This fact may indicate some special phenomena occurred in suspension polymerization in water.

### 3. Spinning Experiments

The spinning solutions were prepared with 70% nitric acid which contains less than 0.0003% of nitrous acid.

Polyacrylonitrile was dissolved to give a viscosity of 1000 poises at 0°C. unless otherwise specified. The spinning apparatus used in this experiment is shown schematically in Figure 5. After deaeration and filtration, the

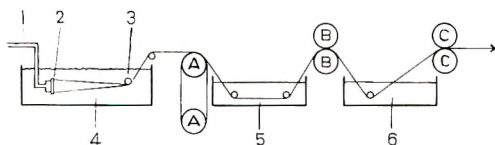


Fig. 5. Wet spinning process of polyacrylonitrile.

solution was passed through a conduit (1) and was extruded into the cold coagulating bath through a spinneret (2) to form a multifilamentary coagulated thread. The temperature of the spinning solution, the coagulant liquid, and dilute aqueous nitric acid solution as between  $-2^{\circ}\text{C}$ . and  $0^{\circ}\text{C}$ . In this coagulation process, the thread was allowed to shrink 20-33%. The coagulated thread was wound around a guide roller (3) which was positioned in the coagulating bath (4). The coagulated thread in gel state was then wound around a guide roller, (A) and led to a washing bath, (5). The washing bath was at room temperature. During passage through the bath, the thread was washed until it was substantially free of nitric acid. These water-swollen filaments, after leaving the washing bath, were led into a stretching bath (6) and were stretched between two rollers, (B) and (C). Generally hot water at  $100^{\circ}\text{C}$ . was used in the stretch bath, but in some cases, saturated steam at  $100-140^{\circ}\text{C}$ . was used instead of hot water. Linear velocity of extrusion of the spinning solution through the nozzle was at 6.3 or 7.5 m./min. Roller A was driven at a constant surface speed of 5 m./min.

### 4. X-Ray Diffraction Measurements

X-ray scattering intensities were measured with a Shimadzu diffractometer by use of a Geiger counter and  $\text{CuK}\alpha$  radiation. Monochromatization is achieved by means of balanced filters (Ni and Co films). The

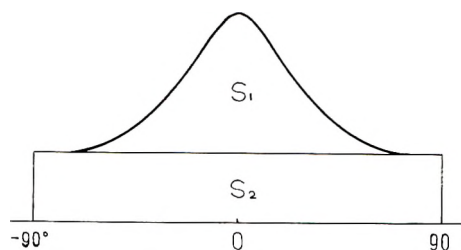


Fig. 6. Schematic azimuthal intensity curve. Amorphous and background scatterings are not shown.

orientation factor  $O$  was obtained from an azimuthal intensity curve along the 5.27 Å. arc according to eq. (2):

$$O = [(180 - \varphi_{in})/180] [A_1/(A_1 + A_2)] \times 100 \quad (2)$$

where  $\varphi_{in}$  is the integral breadth of the part,  $S_1$ ,  $A_1$  is the area of this part, and  $A_2$  is that of  $S_2$ , as shown in Figure 6. An estimation of crystallite size  $D$  was made from an integral breadth  $\beta$  of the 5.27 Å. reflection by the use of eq. (3)

$$D = \lambda/(\beta \cos \theta) \quad (3)$$

Where  $\lambda$  is the wavelength and  $\theta$  is the Bragg angle for the 5.27 Å. reflection. Per cent crystallinity was calculated on the practically unoriented state from the ratio of integrated intensities of the 5.27 Å. reflection to total scattering of the sample over a range of  $2\theta$  from  $13^\circ$  to  $23^\circ$ .

## RESULTS AND DISCUSSION

According to the results in Table II, the hot-stretchability of the coagulated thread (water-swollen filaments) changes with the concentration of aqueous nitric acid solution in the coagulation bath, shrinkage of the thread in the coagulation process, and the molecular weight of the polymer. As a matter of course, the nitric acid concentration in the solvent, the temperatures of the coagulation bath and the stretching bath, and the viscosity of the spinning solution are also important for hot-stretchability, and they were arranged to be constant in present experiments. Hot-stretchabilities at  $100^\circ\text{C}$ . of gelled threads coagulated in 30% and 36% nitric acid were plotted against the viscosity-average molecular weight in Figure 7. This shows a maximum at  $\bar{M}_v = 80,000$ .

A similar experiment was carried out on fractionated polyacrylonitrile. As is clear from Figure 8, the results were similar to those from unfractionated polymers, but there is a sharper peak at  $M = 80,000$ , and above and below this critical value, hot-stretchability decreases rapidly. Here, effects of other factors on hot-stretchability should be apparent, but it seems that the characteristic dependency of hot-stretchability on molecular weight might not be affected even if other factors (coagulation temperature, nitric

TABLE II  
 The Effects of Spinning Conditions on Hot-Stretchability<sup>a</sup>

Linear velocity of extrusion, m./min.	Coagulating bath concn. (HNO <sub>3</sub> ), %	Hot-stretchability							
		A-1	A-2	A-3	A-4	A-5	A-6	A-7	A-8
7.5 <sup>b</sup>	37.5	4.0	12.0	11.4	11.8	—	8.8	9.6	—
"	36.0	—	11.8	10.8	11.3	10.2	8.4	9.3	7.8
"	34.5	—	11.4	10.6	10.7	9.8	7.8	9.0	7.4
"	33.0	—	11.0	10.6	10.2	9.3	7.4	8.8	7.0
"	31.5	—	10.7	9.7	10.0	9.0	7.2	8.6	6.7
"	30.0	—	10.6	9.7	9.6	8.5	6.8	8.2	6.4
"	28.5	—	—	—	—	8.2	—	—	—
6.3 <sup>c</sup>	37.5	—	11.4	11.2	11.4	—	—	—	—
"	36.0	—	10.9	10.4	10.8	9.6	—	—	—
"	34.5	—	10.9	10.2	10.2	9.0	—	—	—
"	33.0	—	10.5	9.8	10.0	9.4	—	—	—
"	31.5	—	10.3	9.4	8.8	8.2	—	—	—
"	30.0	—	9.3	9.3	8.8	8.4	—	—	—

<sup>a</sup> Spinning conditions: viscosity of spinning solution, 1000 poises at 0°C.; temperature of coagulating bath, 0°C.; speed of the first roller (roller A in Fig. 5), 5 m./min.

<sup>b</sup> Shrinkage of gel in coagulating process was 33.3%.

<sup>c</sup> Shrinkage of gel in coagulating process was 20.6%.

acid concentration in coagulation bath, and viscosity of spinning solution) were changed.

It is presumed that the hot-stretchability of the coagulated thread of an unfractionated polymer would be describable by a certain average value of its constituent polymer species. In order to clarify such a presumed effect of molecular weight on stretching of gel, several polymers (samples A-1,

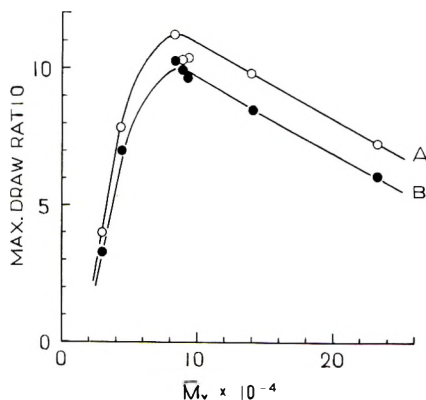


Fig. 7. Effect of molecular weight on maximum draw ratio at 100°C.: (A) 36 wt.-% nitric acid was used as the coagulant; (B) 30 wt.-% nitric acid was used as the coagulant. Spinning conditions: viscosity of spinning solution, 1000 poises at 0°C.; linear velocity of extrusion of spinning solution through the nozzle, 7.5 m./min.; temperature of coagulating bath, 0°C.; temperature of hot-stretching bath, 100°C.

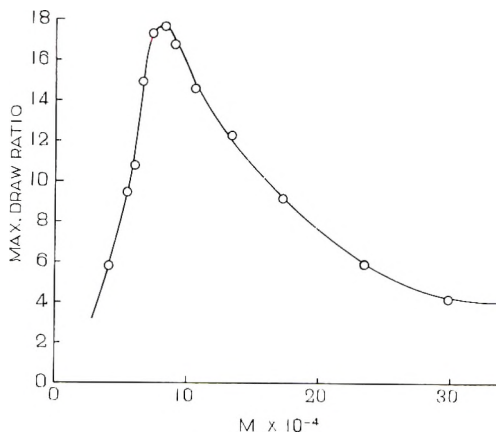


Fig. 8. Relationship between maximum draw ratio and molecular weight of polyacrylonitrile fractions. Spinning conditions: viscosity of spinning solution, 1000 poises at 0°C.; linear velocity of extrusion of spinning solution through the nozzle, 7.5 m./min.; Nitric acid concentration in coagulating bath, 33, wt.-%; temperature of coagulating bath, 0°C.; temperature of hot-stretching bath, 100°C.

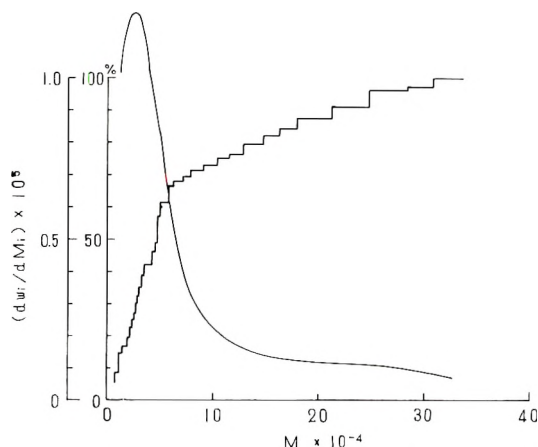


Fig. 9. Molecular weight distribution curves obtained for polyacrylonitrile sample M-1.

A-4, A-5, A-6, and A-7) used above were mixed to give a certain average molecular weight and molecular weight distribution. Their molecular weight distribution curves are shown in Figures 9-15 and their average molecular weight and other characteristic values in Table III. These mixed polymers were spun under the stated conditions. The results obtained are indicated in Table IV. It seemed that hot-stretchability of coagulated thread of a polymer decreases with broadening of molecular weight distribution. From polymer series M-1 to M-4, which have approximately the same weight-average molecular weight but different distribution indices ( $\bar{M}_w/\bar{M}_n$ ) over the range from 2.88 to 3.85, we can observe the effect of molecular weight distribution on hot-stretchability. For polymer series



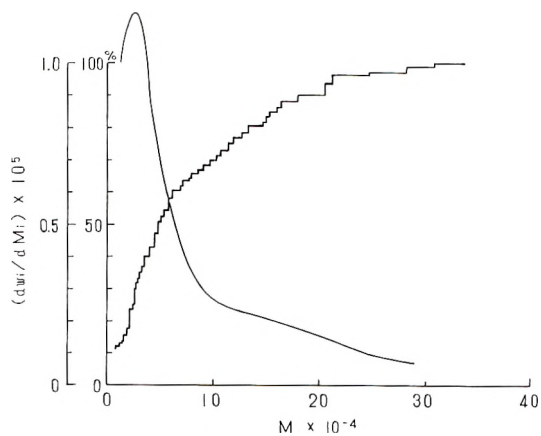


Fig. 13. Molecular weight distribution curves obtained for polyacrylonitrile sample M-2.

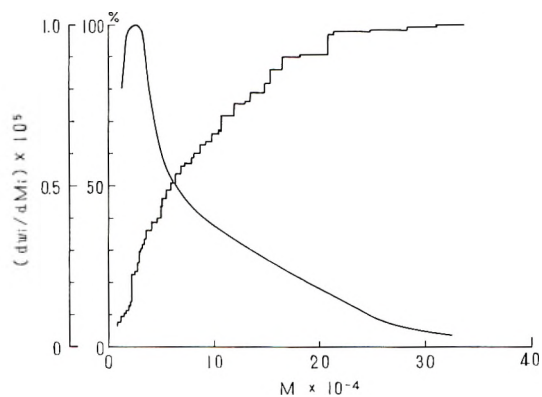


Fig. 11. Molecular weight distribution curves obtained for polyacrylonitrile sample M-3.

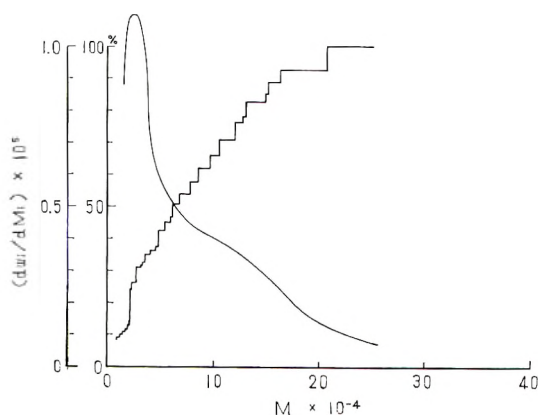


Fig. 12. Molecular weight distribution curves obtained for polyacrylonitrile sample M-4.

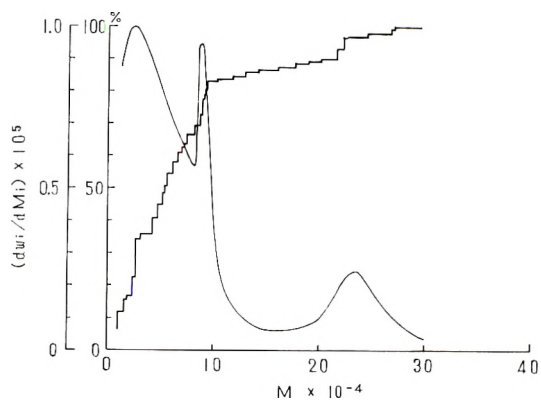


Fig. 13. Molecular weight distribution curves obtained for polyacrylonitrile sample M-5.

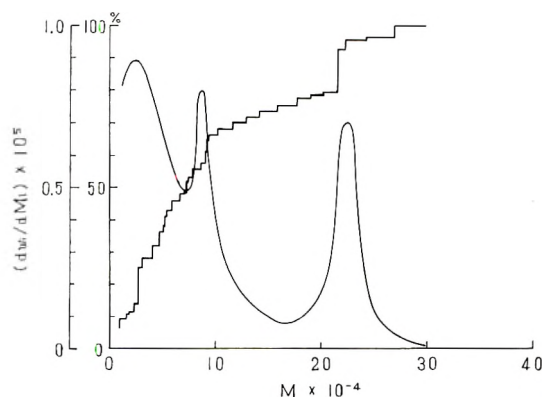


Fig. 14. Molecular weight distribution curves obtained for polyacrylonitrile sample M-6.

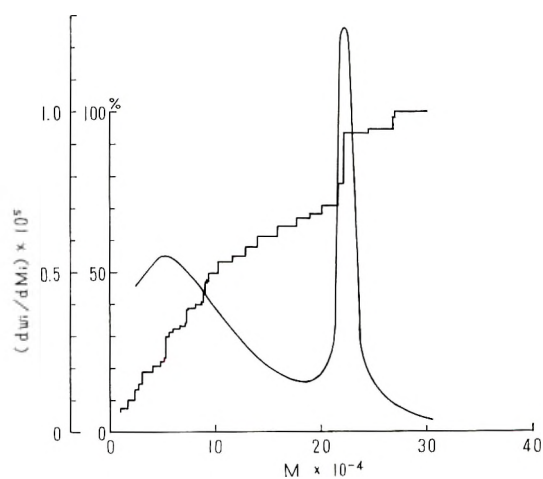


Fig. 15. Molecular weight distribution curves obtained for polyacrylonitrile sample M-7.

TABLE III  
 Preparation of Mixed Polymers

	Mixed samples						
	M-1	M-2	M-3	M-4	M-5	M-6	M-7
Mixing ratio, wt.-%							
A-1	58	40	27	16	—	—	—
A-4	—	36	62	84	—	—	—
A-5	42	24	11	—	—	—	—
A-6	—	—	—	—	75	50	25
A-7	—	—	—	—	25	50	75
$\bar{M}_v$	86,000	84,400	83,900	81,500	—	—	—
$\bar{M}_w^{(calc.)^a}$	86,200	85,000	85,800	88,400	71,700	97,600	124,000
$\bar{M}_n^{(calc.)^a}$	21,400	25,000	29,100	30,700	23,700	26,900	42,300
$\bar{M}_w/\bar{M}_n$	3.85	3.33	2.95	2.88	3.03	3.62	2.92

<sup>a</sup> Weight-average and number-average molecular weights were calculated from molecular weight distribution curves.

 TABLE IV  
 The Effects of Spinning Conditions on Hot-Stretchability of Mixed Polymers<sup>a</sup>

Linear velocity of extrusion m./min.	Coagulating bath concn. (HNO <sub>3</sub> ), %	Hot-stretchability						
		M-1	M-2	M-3	M-4	M-5	M-6	M-7
7.5 <sup>b</sup>	37.5	—	—	10.6	—	9.2	9.2	9.5
"	36.0	—	9.2	10.0	10.6	8.7	9.0	9.3
"	34.5	7.5	8.3	9.0	9.2	8.2	8.7	9.2
"	33.0	6.7	7.8	8.8	9.0	7.8	8.2	8.8
"	31.5	5.9	7.2	8.6	8.9	7.4	7.6	8.4
"	30.0	5.0	6.4	8.5	8.8	7.0	7.0	8.2
"	28.5	—	6.2	—	8.3	—	—	—
6.3 <sup>c</sup>	37.5	—	—	10.1	—	—	—	—
"	36.0	—	8.6	9.6	10.0	—	—	—
"	34.5	5.8	8.3	9.0	8.9	—	—	—
"	33.0	5.4	7.4	8.5	8.8	—	—	—
"	31.5	4.9	6.8	7.9	8.4	—	—	—
"	30.0	4.5	6.4	7.2	8.0	—	—	—
"	28.5	—	5.6	—	7.2	—	—	—

<sup>a</sup> Spinning conditions: viscosity of spinning solution, 1000 poises at 0°C.; temperature of coagulating bath, 0°C.; Speed of first roller (roller A in Fig. 5), 5 m./min.

<sup>b</sup> Shrinkage of gel in coagulation process was 33.3%.

<sup>c</sup> Shrinkage of gel in coagulating process was 20.6%.

M-5 to M-7, which have different average molecular weights and different molecular weight distributions, it is difficult to estimate the effect of molecular weight and molecular weight distribution separately.

We tried to generalize the effect of these two factors, molecular weight and its distribution. The relationship between molecular weight  $M$  and

hot-stretchability  $S$  of coagulated thread is shown in Figure 8; hot-stretchability of coagulated thread can be described as a function of molecular weight having a maximum at  $M = 80,000$ .

$$S = f(M) \quad (4)$$

In the molecular weight distribution curve of a given polymer sample, the amount  $W$  of a polymer species of molecular weight  $M$ , is predicted by eq. (5):

$$W = g(M) \quad (5)$$

Using the two equations (4) and (5), we can write,

$$W = F(S) \quad (6)$$

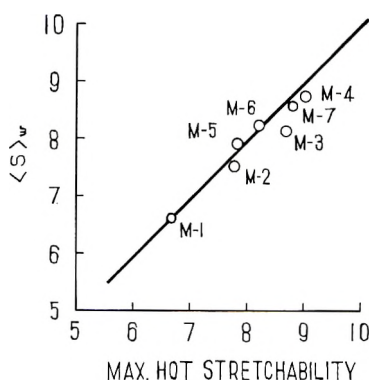


Fig. 16. Relationship between maximum hot-stretchabilities and  $\langle s \rangle_w$  for various unfractionated polyacrylonitrile samples.

Accordingly, molecular weight  $M_i$  in the molecular weight distribution curve is replaced by corresponding hot-stretchability,  $S_i$ , obtained in Figure 8, thus changing the plots to the distribution curve of hot-stretchability. We tried to calculate the weight-average value of hot-stretchability of a polymer sample from the distribution curve of hot-stretchability obtained above.

$$\langle S \rangle_w = \frac{\sum S_i W_i}{\sum W_i} \quad (7)$$

where  $W_i$  is the weight of a polymer species having hot-stretchability of  $S_i$ . According to this general theory, hot-stretchabilities of mixed polymer series M-1 to M-7 were calculated and compared with the maximum hot-stretchabilities observed for the same polymer samples. As shown in Figure 16, there is a remarkable agreement of the results calculated by the proposed procedure with those observed.

We will discuss the results qualitatively. Hot-stretching acts on the polymer chains to be orientated with intermolecular friction force. Many weaker junctions in the gel structure would be broken with less energy giving some resisting force to stretching operation, thus causing the orienta-

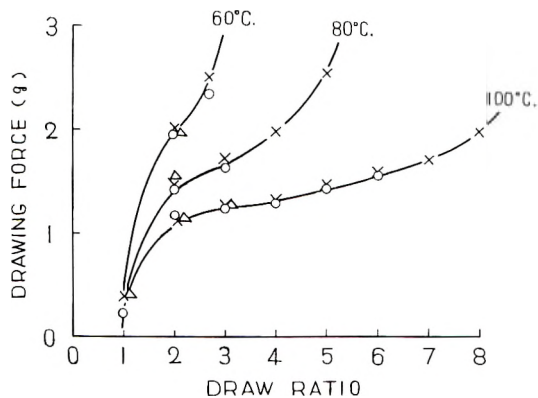


Fig. 17. Relationship between drawing force and draw ratio of coagulated thread at 60, 80, and 100°C. Molecular weights of samples: (○) 239,000; (×) 82,000; (△) 30,500.

tion of the polymer chains. The density of the polymer chain in gel is much higher than that in ordinary solution, and the chains are entangled with each other, many of them being bonded with secondary force. The bondings between polymer chains will develop to such an extent that we can hardly distinguish individual polymer chains, and this structure plays an important role in hot-stretching of the coagulated thread. Therefore, it is expected that the force necessary for the deformation of the network structure in stretching process is almost independent on the molecular weight of the polymer. This conclusion may be sustained by the results as shown in Figure 17. That is, the stretching force did not depend upon molecular weight.

The shorter polymer chains, however, could be stretched better than longer ones because the ratio of end-to-end distance of a fully stretched polymer chain to that of an unstretched polymer chain becomes smaller with the decrease in molecular weight, and the decrease in molecular weight causes the lowering of the maximum hot stretchability. On the other hand, the longer the polymer chain is, the more probable that it passes through two or more strong junctions which cannot be broken by hot-stretching at the temperature stated above. As it is difficult to stretch beyond the shortest chain length among many polymer chains connecting two strong junctions, hot-stretchability of coagulated threads may decrease with the increase in molecular weight.

Furthermore, we investigated the stretching behavior of coagulated thread at higher temperatures. Results are summarized in Table V. In Figure 18, the maximum hot-stretchabilities of coagulated threads are plotted against stretching temperatures and molecular weight of polymers. Some interesting results are pointed out. For polyacrylonitrile of lower molecular weight, hot-stretchability of the coagulated thread is not improved by increasing the stretching temperature or decreasing the viscosity

TABLE V  
The Effect of Temperature on Hot-Stretchability<sup>a</sup>

Sam- ple no.	$\bar{M}_w$	Polymer con- centration in spinning solution, g./100 cc.	Vis- cos- ity, at 0°C., poises	Hot-stretchability				
				for various stretching temperatures				
				100°C.	110°C.	120°C.	130°C.	140°C.
A-9	40,000	27	170	5.6	5.6	5.0	2.8	—
		34	400	5.8	5.6	4.8	3.2	—
		38	1050	5.1	5.3	4.5	4.1	3.4
		40	2200	4.8	3.6	3.4		
A-10	126,000	10	54	11.4	13.5	17.0	—	—
		16	440	10.4	11.4	13.4	16.8	21.0
		19	990	9.0	10.3	11.2	15.0	18.8
		23	1850	8.6	9.8	10.8	11.0	15.0
A-11	218,000	12	1020	7.8	8.4	9.0	10.4	12.4
A-12	264,000	6	130	8.6	10.6	12.6	14.4	16.2
		8	510	7.0	8.6	9.4	10.6	12.2
		10	930	6.8	7.6	8.4	9.2	10.6
		11	2200	4.6	5.8	7.2	8.0	9.0

<sup>a</sup> Spinning conditions: linear velocity of extrusion of spinning solution through the nozzle, 6.3 m./min.;  $\text{HNO}_3$  in coagulating bath, 32 wt.-%; temperature of coagulating bath, 0°C.; Speed of first roller (roller A in Fig. 5): 5 m./min. Shrinkage of gel in coagulating process was 20.6%.

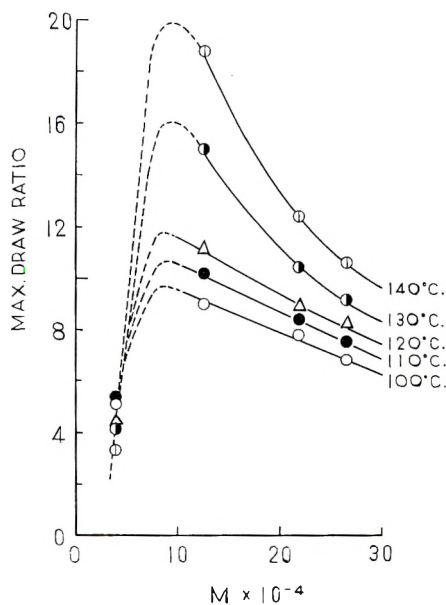


Fig. 18. Effect of molecular weight on hot-stretchability at high temperature. Spinning solutions of viscosity of about 1000 poises were used (see Table V).

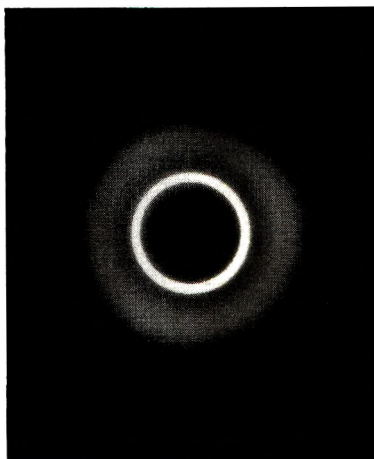


Fig. 19. X-ray diffraction pattern of gelled fiber with  $\text{CuK}\alpha$  radiation monochromatized by LiF crystal.

(by decreasing polymer concentration) of the spinning solution. It may be concluded that we cannot expect high hot-stretchability for polymers of low molecular weight. For the other polymers, hot-stretchability was increased with rising temperature or with lowering viscosity (decreasing polymer concentration) of spinning solution. It should be noted that hot-stretchability at high temperatures also depended markedly upon molecular weight. Also, hot-stretchability shows a maximum value at a certain molecular weight. This molecular weight may not differ appreciably from 80,000, which was noted above to be the maximum stretchability in the case of  $100^\circ\text{C}$ .-stretching, although this is not very sure because we have insufficient data. From this fact, it is assumed that the junctions are very strong even at high temperature. Increase in hot-stretchability with temperature is due to flow of polymer chains.

It was concluded before that in coagulated threads, there are many strong junctions which cannot be broken by stretching at  $140^\circ\text{C}$ . Polyacrylonitrile solution in 70% nitric acid was extruded into dilute nitric acid at  $0^\circ\text{C}$ . and washed completely with water. Swollen threads thus obtained were investigated by x-ray diffraction. As shown in Figure 19, the coagulated thread was crystallized to some extent, even in the gelled state. No crystallite orientation was observed for these gelled threads. The fact that spherulites arise in film prepared from polyacrylonitrile solution has been reported,<sup>12</sup> and it is believed that in the spherulite, polymer chains are folded. It would be interesting to study the polymer chain configuration in the crystallite in the gelled state; however, the answer cannot be derived from this experiment. In our case, whether or not polymer chains are folded at first in the gelled state cannot be determined, because folded polymer chains are probably stretched in the early stages of drawing.

Crystallinity, crystallite orientation, and size of the stretched fibers were measured by x-ray diffraction. The three kinds of polymers listed in Table I were spun under the stated conditions and then dried. The data are listed

in Table VI, which shows values of hot draw ratio, molecular weight, and tensile strength. A few interesting phenomena can be found. Crystallinity does not depend upon hot draw ratio and crystallite size was only slightly changed, whereas both are independent of the molecular weight. This means that in polyacrylonitrile, the strong secondary bondings between functional groups are so much dominant in crystallization process that other factors, molecular weight or stretching of polymer chains and so on, are not so concerned. Also, crystallites grown in gelled state are too small to be broken up more by drawing. It has been observed, however, in polyacrylonitrile that well grown crystallites, if heat-treated, are destroyed with elongation as is the case for other polymers.

The relationship between draw ratio and crystallite orientation was obtained in connection with molecular weight. Sample A-1, which has a weight-average molecular weight of 30,000, is easily oriented, even on stretching only  $\times 2$ , to a high degree of crystallite orientation of 57%. On the other hand, sample A-8, which has a high weight average molecular weight of 239,000, only shows a degree of crystallite orientation of 47.6% after 600% elongation. It was stated before that the maximum hot-stretchability became smaller with decrease in molecular weight. The fact

TABLE VI  
The Effect of Molecular Weight on the Fine Structure of Fibers

Sam- ple no.	$\bar{M}_w$	Hot-draw ratio <sup>a</sup>	Orien- tation, %	Crystal size, A.	Crys- tallinity, %	Tensile strength (dry), g./den.
A-1	30,500	1	17.3	45.7	45.2	0.51
		2	57.6	43.5	46.8	1.35
		3	56.5	38.8	43.9	—
		4	52.5	39.8	46.7	—
A-3	86,000	1	15.4	42.1	47.3	0.70
		2	33.2	39.7	44.8	1.44
		3	41.6	40.4	43.7	1.93
		4	50.2	38.8	45.5	2.80
		5	59.2	39.1	45.3	3.08
		6	67.0	37.5	45.3	4.10
		7	66.5	38.3	46.8	4.55
A-8	239,000	8	67.3	37.5	48.8	5.02
		1	6.9	43.1	46.5	0.37
		2	17.1	42.9	42.0	1.37
		3	19.6	37.8	45.6	1.86
		4	27.2	38.8	43.2	2.44
		5	37.7	39.8	43.2	2.51
		6	39.2	37.5	46.6	3.22
7	47.6	39.7	44.2	—		

<sup>a</sup> Spinning conditions: viscosity of spinning solution, 1000 poises at 0°C.; linear velocity of extrusion of spinning solution through the nozzle, 7.5 m./min. (shrinkage of gel in coagulating process was 33.3%; nitric acid concentration in coagulating bath, 32. wt.-%; temperature of coagulating bath, 0°C.; temperature of hot-stretching bath, 100°C.



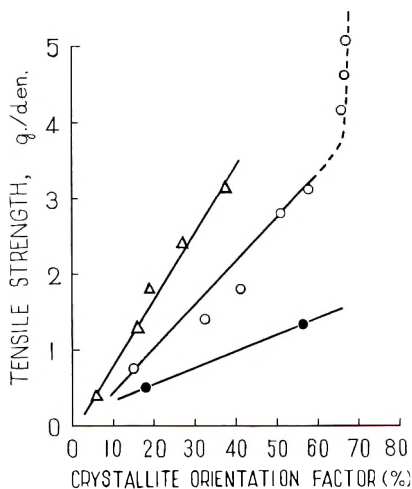


Fig. 20. Relationship between dry tensile strength and crystallite orientation factor for various samples: (●) A-1; (○) A-3; (△) A-8.

was mainly derived from the chain length of polymer molecules, and it is probable that the shorter the molecular chain, the smaller the ratio of end-to-end distance of stretched polymer chain to that of a coiled polymer chain will become. Now supposing that maximum hot draw ratio depends on the chain length of the polymer molecules, then orientation of the polymer chain at constant draw ratio must be increased in inverse proportion to the length of the molecular chain. This conclusion is supported by the results in Table VI. Tensile strengths are plotted in Figure 20 at different crystallite orientation factors, measured by x-ray, on the polymers with molecular weights of 30,000, 86,000, and 239,000. A fiber of higher molecular weight has a higher tensile strength than a fiber of lower molecular weight having the same degree of crystallite orientation. This result suggests the possibility of getting a fiber of higher strength by improving the molecular orientation or increasing the molecular weight of the polymer.

A noteworthy phenomenon here is this: the tensile strength of sample A-3 increased despite the unchanged degree of orientation of crystallites when the stretch ratio was greater than six, which is shown in Figure 20. Then, it is supposed that tensile strength is not only affected by crystallite orientation but by molecular orientation in the amorphous portion. When we take the information about orientation of polymer chains in the amorphous region (obtained from dichroism measurements) into consideration, it is easily understood that the degree of molecular orientation in the amorphous region becomes larger as crystallite orientation does in crystalline region. However, it was observed at the same time that hot-stretching beyond a certain ratio increased the degree of orientation of polymer chains in amorphous regions but not the orientation of crystallites. These results are to be discussed in another report, but it was confirmed that the results stated above on sample A-3 in Figure 20 is due to the fact that the degree of

orientation of polymer chains in the amorphous region increases even after the orientation of crystallites stopped increasing.

The authors wish to thank the Directors of Asahi Chemical Industry Company for their permission to publish this paper, and Mr. K. Ishii and Mr. H. Kawakami for assistance in the experimental work. The authors are also greatly indebted to Dr. C. Nakayama and Dr. K. Katayama for encouraging help and advice, and to Dr. S. Rosenbaum and Mr. S. Mori for their help in the preparation of the manuscript.

### References

1. Ham, G. E., *Textile Res. J.*, **24**, 597 (1954).
2. Hunyar, A., *Faserforsch.*, **6**, 300 (1955).
3. Krigbaum, W. R., and A. M. Kalliar, *J. Polymer Sci.*, **32**, 323 (1958).
4. Kobayashi, H., *J. Polymer Sci.*, **39**, 369 (1959).
5. E. I. du Pont de Nemours, Product Information Bulletin, D.M.F. (1954).
6. Houtz, R. C., *Textile Res. J.*, **20**, 786 (1950).
7. Herrent, P., *J. Polymer Sci.*, **8**, 346 (1952).
8. Kobayashi, H., *Kobunshi Kagaku*, **13**, 18 (1956).
9. Kobayashi, H., *J. Polymer Sci.*, **26**, 230 (1957).
10. Fujisaki, Y., and H. Kobayashi, *Kobunshi Kagaku*, **18**, 305, 312 (1961).
11. Kobayashi, H., and Y. Fujisaki, *J. Polymer Sci.*, **B1**, 15 (1963).
12. Holland, V. F., *J. Polymer Sci.*, **43**, 572 (1960).

### Résumé

Le but de cette étude a été d'obtenir des informations sur l'effet des poids moléculaires et leur distribution sur l'étirement (taux d'étirage maximum) des gels obtenus par extrusion de solutions concentrées de polyacrylonitrile dans l'acide nitrique à 70% et coagulation par une solution diluée d'acide nitrique. Les fils coagulés ont été lavés et étirés dans l'eau chaude (ou vapeur saturante). Avec le polyacrylonitrile fractionné on a montré un maximum d'étirement à  $M = 80.000$ . Au-dessous de cette valeur, l'étirement décroît avec une diminution de poids moléculaire; au-dessus, elle diminue avec une augmentation de poids moléculaire et tend vers une certaine valeur. Avec des polymères polydispersés, des courbes de distribution d'étirement obtenus en remplaçant le poids moléculaire par l'étirement correspondant, ont été examinées. On a trouvé que l'étirement maximum d'un polymère polydispersé représente la moyenne en poids de celles des espèces des polymères constituant. L'effet du poids moléculaire sur les propriétés mécaniques des fibres et leur structure fine a été étudié à l'aide de rayons-X.

### Zusammenfassung

Das Ziel dieser Untersuchung war die Bestimmung des Einflusses des Molekulargewichts und seiner Verteilung auf die Berstreckbarkeit von Gelen, die durch Auspressen einer konzentrierten Lösung von Polyacrylnitril in 70%-ger Salpetersäure in ein Fällbad von verdünnter Salpetersäure erhalten wurden. Die koagulierten Fäden wurden gewaschen und dann in heissem Wasser (oder Nassdampf) verstreckt. Bei fraktioniertem Polyacrylnitril wurde unter diesen Bedingungen ein Maximum in der Verstreckbarkeit bei  $M = 80.000$  gefunden. Unterhalb dieses Wertes wurde die Verstreckbarkeit mit abnehmendem Molekulargewicht kleiner; oberhalb desselben strebte sie mit steigendem Molekulargewicht einem bestimmten Werte zu. An polydispersen Polymeren wurden Verstreckbarkeitsverteilungskurven, die aus den Molekulargewichtsverteilungskurven durch Ersatz des Molekulargewichts durch die entsprechende Verstreckbarkeit erhalten wurden, studiert. Es wurde festgestellt, dass die maximale Verstreckbarkeit durch den Gewichtsmittelwert der Komponenten gegeben ist. Der Einfluss des Molekulargewichtes auf die mechanischen Eigenschaften der Fasern und ihre Feinstruktur wurde röntgenographisch untersucht.

Received November 5, 1962

# Diffusion and Sorption of Vapors in Ethylene-Propylene Copolymers. I. Equilibrium Sorption\*

H. K. FRENSDORFF, *Elastomer Chemicals Department, E. I. du Pont  
de Nemours & Co., Inc., Wilmington, Delaware*

## Synopsis

Equilibrium sorption of cyclohexane, *n*-hexane, carbon tetrachloride, *n*-pentane, benzene, trichlorotrifluoroethane, and methylene chloride in ethylene-propylene copolymers at 10°, 23°, and 40°C. has been measured. These penetrants range from most soluble to least, in the order given. The propylene content of the copolymer has very little effect on equilibrium sorption, and the heats of dilution are small. The concentration dependence of the results is discussed in terms of the Flory-Huggins equation. Correlation between sorption and solubility parameter is considered.

## Introduction

Investigations of the equilibria between organic vapors and rubbery polymers have been confined to a limited number of systems. Among the more comprehensive studies of this kind are those of Prager et al.<sup>1</sup> on the sorption of aliphatic hydrocarbons in polyisobutylene, those of Gee et al.<sup>2</sup> on the benzene-natural rubber equilibrium, and those of Tager and co-workers<sup>3</sup> on the equilibrium between benzene and butadiene-styrene as well as butadiene-acrylonitrile copolymers. The recent development of ethylene-propylene copolymers has made available a new series of non-crystalline rubbery polymers whose sorption properties are of interest. The present paper is concerned with equilibrium sorption measurements of these copolymers, while the second paper of this series will treat of their diffusion properties.

The equilibrium between polymer and solvent vapor is customarily expressed in terms of the Flory-Huggins equation:<sup>4</sup>

$$\ln a_1/v_1 = v_2 + \chi_1 v_2^2 \quad (1)$$

where  $a_1$  is the activity of the solvent vapor,  $v_1$  the volume fraction of solvent,  $v_2 = 1 - v_1$  the volume fraction of polymer, and  $\chi_1$  the polymer-solvent interaction parameter, which is related to the heat of mixing for the system. For some systems the parameter  $\chi_1$  is essentially constant over the entire composition range, e.g. rubber-benzene<sup>2</sup> and polyisobutylene-

\* Contribution No. 120 from the Elastomer Chemicals Department.

aliphatic hydrocarbons;<sup>1</sup> for others it may rise or fall with increasing solvent content.<sup>4</sup> For low solvent concentrations eq. 1 can be approximated by neglecting the  $v_1^2$  term:

$$\ln a_1/v_1 = C_1 - C_2v_1 \quad (2)$$

$$\text{if } C_1 = 1 + \chi_1 \text{ and } C_2 = 1 + 2\chi_1 \quad (3)$$

The parameter  $\chi_1$  is low, usually below 0.5, for liquids in which the polymer is soluble, and high for liquids which do not dissolve the polymer.<sup>4</sup> A quantitative relation has been given by Scott and Magat:<sup>5</sup>

$$\chi_1 = \chi_1^s + K[V_1(\delta_1 - \delta_2)^2]/RT \quad (4)$$

where  $\chi_1^s$ , the reciprocal of the coordination number, is usually taken to be about 0.25,  $V_1$  is the molar volume of the liquid solvent,  $\delta_1$  and  $\delta_2$  are the solubility parameters<sup>6</sup> of the solvent and the polymer respectively,  $R$  and  $T$  have their usual significance, and  $K$  is an empirical constant relating to the polarity of the components.

The interaction parameter  $\chi_1$  can also be determined from swelling measurements on crosslinked elastomers, the results being in fair agreement with those on vapor sorption.<sup>4</sup> Such measurements have been reported, for instance) by Scott and Magat,<sup>5</sup> who applied eq. (4) to their results and found the constant  $K$  to be unity for natural rubber and polychloroprene, and between 2 and 3 for the more polar Buna N. Shvarts,<sup>7</sup> in a very extensive study of the swelling of crosslinked rubbers, employed a graphical method of determining  $K$  and  $\delta_2$ . He found it necessary to employ several values of  $K$  for each elastomer examined, each value applying to a different group of solvents. For example, the results observed with natural rubber and 115 different solvents required five separate values of  $K$ . Obviously, the predictive capacity of eq. (4) is considerably impaired by these findings.

### Experimental

The gravimetric sorption-diffusion apparatus was based on that of Prager and Long.<sup>8</sup> It employed a quartz helix balance, the extension of which was read with a Gaertner microscope-slide cathetometer. The entire apparatus was kept in a constant-temperature room ( $\pm 1^\circ\text{C}$ .), while the part of the sorption tube containing the polymer sample was surrounded by a water bath controlled to better than  $0.05^\circ\text{C}$ . Pressures were measured by means of a Wallace and Tiernan Model FA-135 precision mercurial manometer. A Welch Duo-Seal pump, Model 1402 VE, which reduced the pressure of inert gas in the system to below  $10^{-3}$  mm. Hg, was used.

The ethylene-propylene copolymer samples were prepared in perchloroethylene with a vanadium oxychloride-triisobutyl aluminum catalyst. They were essentially noncrystalline, high molecular weight (viscosity-average MW above 100,000), rubbery polymers. An infrared method based on the  $8.7 \mu$  absorption band was used for determining the propylene content of the samples. It was calibrated by means of samples made with

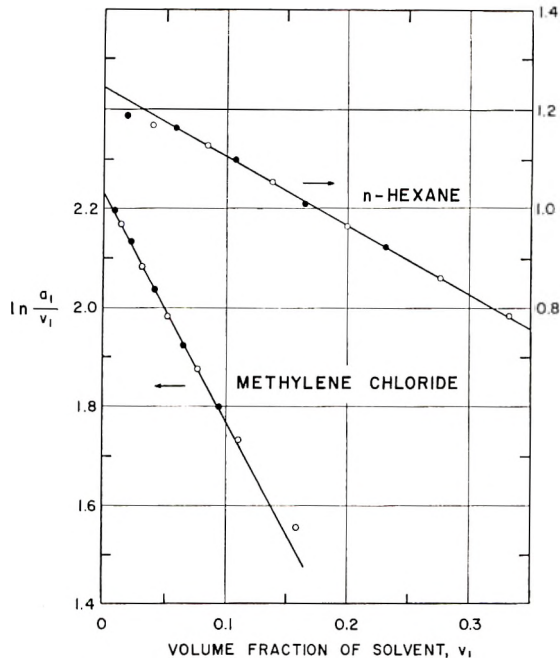


Fig. 1. Typical sorption results plotted according to eq. (2): (O) ascending pressure; (●) descending pressure.

ethylene- $C^{14}$ , of which the ethylene content had been determined by radio assay. The propylene content was in every instance expressed in mole per cent. The films for sorption measurements were hot-pressed between aluminum plates to a thickness of 0.07–0.12 mm. A typical sample size was 15 by 30 mm., which corresponds to a weight of 30–40 mg. The samples were suspended from the quartz springs by means of 40-gauge copper wire.

The solvents used were of the best grade available, usually analytical reagent grade. Except for benzene, which was purified twice by partial freezing, they were used as received but stored over a desiccant. The measured vapor pressures of the solvents were within 1% of the literature values.

The sorption measurements were carried out by incremental addition and subtraction of solvent vapor from a small bulb in which the carefully degassed liquid was stored. Equilibrium was assumed to have been attained when the sample weight changed by less than 0.003 mg. in 10 min. This required from 15 min. to more than 1 hr., depending on sample thickness, temperature, vapor pressure, and solvent.

The volume fraction of solvent at equilibrium was calculated on the assumption that sorption is accompanied by negligible change in total volume. This is the commonly accepted procedure, and Gee<sup>2</sup> has shown by direct measurements that the volume change on mixing for natural

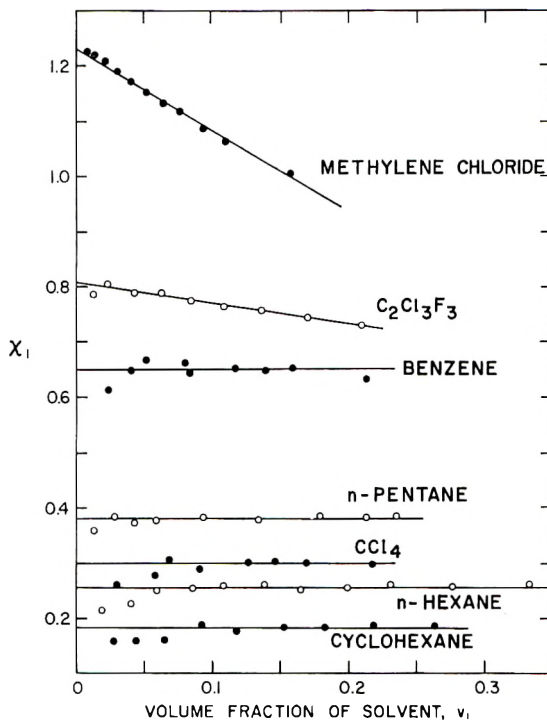


Fig. 2. Interaction parameter  $\chi_1$  for sorption of vapors in 51 mole-% propylene copolymer at 23°C.

rubber-benzene is indeed negligible. The vapor activity  $a_1$  was taken to be the ratio of the measured pressure to the vapor pressure of the pure solvent at the temperature of the measurement, since nonideality corrections are very small for the low pressures employed. Because of the very high sensitivity of the quartz helix balance, the uncertainty of the volume fraction of solvent was very small (0.1% or less). Consequently, the pressure measurement constituted the major source of error. This was particularly so at the lowest pressures, where the uncertainty in the measured pressure (estimated at 0.1–0.2 mm. Hg) represented as much as 1–3% of the total, corresponding to an error of 0.01–0.03 in  $\ln a_1$ . No doubt this accounts for the scatter seen in Figures 1 and 2 at the lowest volume fractions of solvent.

### Results and Discussion

Plots of the sorption results according to eq. (2) were quite close to linear for the range of vapor pressures covered, namely up to  $a_1 = 0.75$  at 10 and 23°C. and up to  $a_1 = 0.45$  at 40°C. Two typical plots are shown in Figure 1. Accordingly, the results in Table I are given in terms of the constants  $C_1$  and  $C_2$  of eq. (2). This equation may be regarded as an empirical one when the conditions represented by eq. (3) are not met.

TABLE I  
Sorption in 51-Mole-% Propylene Copolymer  
[Expressed in terms of the constants in eq. (2)]

	10°C.		23°C.		40°C.	
	$C_1$	$C_2$	$C_1$	$C_2$	$C_1$	$C_2$
Cyclohexane			1.17	1.3		
<i>n</i> -Hexane	1.25	1.5	1.25	1.4	1.27	2.0
Carbon tetrachloride	1.29	1.4	1.29	1.5	1.27	1.8
<i>n</i> -Pentane			1.36	1.6		
Benzene	1.68	2.1	1.66	2.3	1.60	2.6
1,1,2-Trichloro-1,2,2-trifluoro-ethane	1.83	2.7	1.79	2.7	1.73	3.0
Methylene chloride	2.30	4.8	2.23	4.6	2.12	5.1

The interaction parameter  $\chi_1$  of the Flory-Huggins equation can be derived either from the original data or from the constants in Table I by means of the equation

$$\chi_1 = [C_1 - v_1(C_2 + 1)]/(1 - 2v_1) - 1 \quad (5)$$

where, as in eq. (2), the  $v_1^2$  term has been neglected. The dependence of  $\chi_1$  on  $v_1$  at 23°C. is illustrated by the plots of Figure 2. It falls with increasing  $v_1$  for the poorer solvents but is independent of concentration for the better ones. Table I summarizes all the measurements. The value of  $\chi_1$  is independent of  $v_1$  if  $(C_2 - 1)$  is approximately equal to  $2(C_1 - 1)$ , when, according to eq. (5),  $\chi_1$  reduces to  $C_1 - 1$ . Thus the better solvents have a constant value of  $\chi_1$  at 10 and 23°C., but even for these  $\chi_1$  decreases somewhat with rising solvent content at 40°C., where

$$C_2 - 1 > 2(C_1 - 1) \quad (6)$$

As mentioned in the Introduction, cases of both constant and varying  $\chi_1$  have been reported previously.<sup>1,4</sup> The instances of nonconstant  $\chi_1$  indicate that the assumptions made in the derivation of the Flory-Huggins equation are not completely adequate for these cases.

The constants in Table I show comparatively little change with temperature for the interval covered. This is a consequence of the low heat of dilution commonly observed in systems of this type.<sup>2,4</sup> The heat of dilution, defined as the change in heat content on transferring one mole of solvent from the pure liquid to an infinite quantity of polymer-solvent mixture of the specified composition, is given by<sup>4</sup>

$$\Delta\bar{H}_1 = -RT^2(\delta \ln a_1/\delta T)_{P, v_2} \quad (7)$$

which, on combination with eq. (2), gives

$$\Delta\bar{H}_1 = -RT^2[\delta C_1/\delta T - v_1(\delta C_2/\delta T)] \quad (8)$$

Because of the small temperature effect, the heats of dilution cannot be determined with very great accuracy, but approximate values, determined

from the ratio of the 10 to the 40°C. constants in Table I, are given in Table II. As expected, they are higher for the poor solvents, but even for those they are quite small compared with the heats of vaporization, which are of the order of 8 kcal./mole. The heat of sorption, i.e., the enthalpy change on transference of one mole of solvent from the vapor phase to an infinite quantity of polymer-solvent mixture, is equal to the heat of dilution minus the heat of vaporization. Accordingly, the low heats of dilution indicate that the sorption process is quite similar to condensation of the vapor in its own liquid phase, as far as heat content is concerned.

TABLE II  
Heats of Dilution at  $v_1 = 0$

	$\Delta H_1$ , kcal./mole
<i>n</i> -Hexane	0.1
Carbon tetrachloride	0.1
Benzene	0.4
1,1,2-Trichloro-1,2,2-trifluoroethane	0.6
Methylene chloride	1.0

Because of the chemical similarity of the ethylene and propylene units the effect of copolymer composition on equilibrium sorption is expected to be slight. An indication of this similarity can be obtained by the effect of composition on the solubility parameters of the copolymers. The latter, estimated by Small's method<sup>9</sup> of group contributions and shown in the last column of Table III, do not vary over a very wide range. As expected from the above considerations, equilibrium sorption of methylene chloride was indeed observed to vary comparatively little with copolymer composition (see Table III).

TABLE III  
Effect of Copolymer Composition on Methylene Chloride Sorption at 23°C.

Propylene in copolymer, mole-%	$C_1$	$C_2$	$\delta^a$
29	2.33	4.9	7.89
51	2.23	4.6	7.78
78	2.22	4.5	7.67

<sup>a</sup> Estimated by the method of Small.<sup>9</sup>

The relationship between  $\chi_1$  and the nature of the solvent can be examined by the method of Shvarts.<sup>7</sup> This consists of plotting the data according to the linear form of eq. (4):

$$\delta_1 = \delta_2 \pm [RT/(\chi_1 - \chi_1^s)/KV_1]^{1/2} \quad (9)$$

as is done in Figure 3. The values of  $\delta_1$  and  $V_1$  were taken from the compilation of Bristow and Watson,<sup>10</sup> except those of trichlorotrifluoroethane



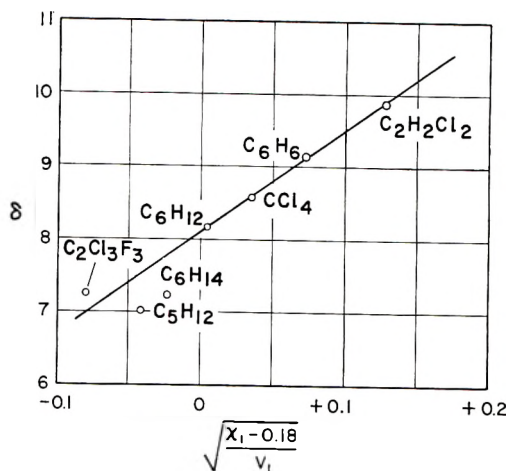


Fig. 3. Correlation between interaction parameter and solubility parameter plotted according to eq. (9).

which were calculated from its published properties.<sup>11</sup> The values of  $\chi_1$  were those of Figure 2, while  $\chi_1^s$  was taken to be 0.18 rather than the more usual value of 0.2–0.25, in order to accommodate the low  $\chi_1$  observed for cyclohexane (0.18).

Four of the seven points in Figure 3 lie on a pretty good straight line. Not enough different solvents were examined to decide whether it was possible to represent all the data by means of several straight lines with the same intercept, the rather arbitrary procedure used by Shvarts. All that can be said is that there is qualitative agreement with eq. (4), i.e., that in general, solvents with solubility parameters closer to that of the polymer are sorbed more strongly, which is really the only conclusion which can be drawn from the extensive data of Shvarts. The intercept of the line in Figure 3 indicates that the solubility parameter of the 51 mole-% copolymer is 8.1, in reasonable agreement with the estimate of 7.8 (Table III). The slope, on the other hand, corresponds to a value of  $K = 2.7$ , to be compared, for instance, with values of 2.1–2.7 used by Scott and Magat<sup>5</sup> for Buna N and 0.4–4.1 derived from the data of Shvarts<sup>7</sup> for natural rubber.

### References

1. Prager, S., E. Bagley, and F. A. Long, *J. Am. Chem. Soc.*, **75**, 2742 (1953).
2. Gee, G., and L. R. G. Treloar, *Trans. Faraday Soc.*, **38**, 147 (1942); G. Gee, and W. T. C. Orr, *Trans. Faraday Soc.*, **42**, 507 (1946).
3. Tager, A. A., L. K. Kosova, D. Yu. Karlinskaya, and I. A. Yurina, *Colloid J. (U.S.S.R.)*, **17**, 299 (1955); A. A. Tager, and L. K. Kosova, *Colloid J. (U.S.S.R.)*, **17**, 373 (1955).
4. Flory, P. J., *Principles of Polymer Chemistry*, Cornell Univ. Press, 1953, pp. 511–518, 542–546, 576–584.
5. Scott, R. L., and M. Magat, *J. Chem. Phys.*, **13**, 172 (1945); *J. Chem. Phys.*, **13**, 178 (1945); *J. Polymer Sci.*, **4**, 555 (1949).

6. Hildebrand, J. H., and R. L. Scott, *Solubility of Nonelectrolytes*, 3rd ed., Reinhold, New York, 1950.
7. Shvarts, A. G., *Colloid J. (U.S.S.R.)*, **19**, 375 (1957).
8. Prager, S., and F. A. Long, *J. Am. Chem. Soc.*, **73**, 4072 (1951).
9. Small, P. A., *J. Appl. Chem. (London)*, **3**, 71 (1953).
10. Bristow, G. M., and W. F. Watson, *Trans. Faraday Soc.*, **54**, 1731 (1958).
11. Benning, A. F., and R. C. McHarness, *Thermodynamic Properties of "Freon-113" Trichlorotrifluoroethane*, E. I. du Pont de Nemours & Co., 1938.

### Résumé

On a mesuré l'équilibre d'absorption du cyclohexane, de l'hexane-*n*, du benzène, du trichlorotrifluoroéthane et du chlorure de méthylène dans des copolymères éthylène-propylène à 10°, 23° et 40°C. Ces agents de pénétration deviennent, suivant l'ordre établi ci-dessus, de moins en moins solubles dans le copolymère. La quantité de propylène dans le copolymère a un très petit effet sur l'équilibre d'absorption et les chaleurs de dilution sont faibles. La dépendance de la concentration sur les résultats est discutée en se basant sur l'équation de Flory-Huggins. On a aussi considéré la corrélation entre l'absorption et le paramètre de solubilité.

### Zusammenfassung

Die Gleichgewichtssorption von Cyclohexan, *n*-Hexan, Tetrachlorkohlenstoff, *n*-Pentan, Benzol, Trichlorotrifluoräthan und Methylenchlorid in Äthylen-Propylenkopolymeren wurde bei 10°, 23° und 40°C gemessen. Diese Stoffe werden in der angegebenen Reihenfolge in zunehmendem Mass weniger im Copolymeren löslich. Der Propylengehalt des Copolymeren hat auf die Gleichgewichtssorption wenig Einfluss und die Verdünnungswärmen sind klein. Die Ergebnisse werden in bezug auf die Konzentrationsabhängigkeit auf Grundlage der Flory-Huggins-Gleichung diskutiert. Eine Korrelation zwischen Sorptions- und Löslichkeitsparametern wird erörtert.

Received September 10, 1962

## Diffusion and Sorption of Vapors in Ethylene-Propylene Copolymers. II. Diffusion\*

H. K. FRENSDORFF, *Elastomer Chemicals Department, E. I. du Pont de Nemours & Co., Inc., Wilmington, Delaware*

### Synopsis

The diffusion rates of methylene chloride, benzene, *n*-pentane, *n*-hexane, and cyclohexane in a copolymer of 51 mole-% propylene and 49% ethylene at 23°C. and penetrant concentrations of up to 10 vol.-% have been measured, as have the rates of benzene diffusion in copolymers containing 31-100% propylene units at 10, 23, and 40°C. Integral diffusion coefficients were calculated from the initial diffusion rates; differential diffusion coefficients from the final rates. Comparison of the two types of diffusion coefficients leads to the conclusion that their concentration dependence flattens out at the very lowest penetrant concentrations. The diffusion coefficients fall and the activation energies rise as the propylene content of the copolymers increases. Diffusion in low-propylene copolymers occurs at rates comparable to those in natural rubber, while the rates in atactic polypropylene are slower by about an order of 1 magnitude. Even so, the latter are about 10 times faster than in polyisobutylene.

### Introduction

The previous paper of this series<sup>1</sup> dealt with the sorption of vapors in ethylene-propylene copolymers, while the present one is concerned with their diffusion properties. Diffusion of gases and vapors in polymers has been studied extensively, a comprehensive review having been made by Barrer.<sup>2</sup> Whereas the diffusion coefficients for permanent gases in polymers are essentially concentration-independent, largely because of the low solubility of gases, those for vapors and liquids have been found to vary strongly with concentration. Moreover, diffusion coefficients for vapors in polymers below their glass-transition temperatures are often time-dependent as well as concentration-dependent.<sup>2</sup> Consequently, the results of diffusion measurements on polymers above their glass-transition temperature, which do not ordinarily show this non-Fickian behavior, provide more easily interpreted information.

Of the polymers which are elastomeric, i.e., above their glass-transition temperature, at room temperature, only natural rubber and polyisobutylene have been subjected to extensive vapor diffusion measurements, the former by Hayes and Park,<sup>3</sup> Aitken and Barrer,<sup>4</sup> and Barrer and Ferguson,<sup>5</sup> the latter by Prager and Long,<sup>6</sup> Blyholder and Prager,<sup>7</sup> and Pollard.<sup>8</sup> Thus, the present study of another room-temperature elastomer appeared

\* Contribution No. 122 from the Elastomer Chemicals Department.

worthwhile. Among the diffusion studies of polymers which become rubbery somewhat above room temperature are those made by Kokes et al.<sup>9</sup> on polyvinyl acetate, Barrer et al.<sup>10</sup> and Vanderkooi et al.<sup>11</sup> on ethyl cellulose, and Zhurkov and Ryskin<sup>12</sup> on various vinyl polymers.

There are two basic methods of measuring diffusion coefficients: the time-lag method, in which steady-state diffusion is measured manometrically, and the sorption-desorption method, which is based on gravimetric measurements of the rate of approach to equilibrium. The former is particularly suitable for measurements of the diffusion of permanent gases, as in the extensive measurements of van Amerongen,<sup>13</sup> but has also been used with the vapors of low-boiling liquids by Barrer and co-workers.<sup>4,5,10</sup> The following discussion is confined to the sorption-desorption method, which is especially appropriate to measurements of vapor diffusion.

The mathematics of diffusion and the methods of treating diffusion data have been thoroughly discussed by Crank.<sup>14</sup> For systems in which the diffusion coefficient is a function of penetrant concentration, this involves the solution of Fick's equation

$$\delta C/\delta t = \delta/\delta x [D(C)\delta(C/\delta x)] \quad (1)$$

for the appropriate boundary conditions and concentration dependence. In eq. (1),  $C$  represents penetrant concentration,  $t$  time,  $x$  distance along the direction of diffusion, and  $D(C)$  the differential diffusion coefficient. In some cases the concentration dependence of the diffusion coefficient has been reported to be linear,<sup>3</sup>

$$D(C) = D(0)(1 + AC) \quad (2)$$

and in others it was observed to have an exponential form,<sup>6,8</sup>

$$D(C) = D(0) \exp \{BC\} \quad (3)$$

Analysis of diffusion results is not straightforward because eq. (1) in combination with either eq. (2) or (3) cannot be solved explicitly for the boundary conditions involved in the usual gravimetric diffusion experiment, which consists of measuring the weight gain or loss with time of a thin polymer film, initially at uniform penetrant concentration, after a sudden change of solvent vapor pressure.

The two methods which have been used to analyze the data for systems with variable diffusion coefficients circumvent the intractability of the above equations by focussing attention on either the early stages or the final stages of the diffusion process, where limiting conditions make mathematical analysis simpler.

During the early stages of a diffusion experiment the concentration at the center of the film is nearly constant with time and distance. This situation approximates the case of initial diffusion into a semi-infinite medium, where the quantity of penetrant taken up is given by<sup>14</sup>

$$M_t/M_\infty = 4(\bar{D}t/a^2\pi)^{1/2} \quad (4)$$

Here  $M_t$  is the total quantity of penetrant which has entered (or left) the film in time  $t$ ,  $M_\infty$  is the corresponding quantity after infinite time,  $a$  is the film thickness, and  $\bar{D}$  the *integral* diffusion coefficient, which represents some kind of average diffusion coefficient for the penetrant concentration range involved. Accordingly, the first method of analyzing diffusion data consists of plotting  $M_t$  against the square root of time and deriving the integral diffusion coefficient from the slope of the initial linear portion of the plot according to eq. (4).

Crank<sup>14</sup> has discussed in detail the relationship between the differential and integral diffusion coefficients. For sorption runs (initial penetrant concentration zero) or desorption runs (final concentration zero) he gives the approximate relation

$$\bar{D} \approx 1/C_0 \int_0^{C_0} D(C) dC, \quad (5)$$

where  $C_0$  is the equilibrium penetrant concentration. This equation is a better approximation, as Crank has shown, if  $\bar{D}$  is taken to be the mean of the integral diffusion coefficient obtained from a sorption run ( $\bar{D}_s$ ) and a desorption run ( $\bar{D}_d$ ) at the same equilibrium pressures. This is the procedure commonly adopted by the workers using this first method.<sup>3,6,8,9</sup>

The second method of analyzing gravimetric diffusion data is based on the fact that the penetrant concentration, and hence the diffusion coefficient, is nearly uniform throughout the film during the late stages of the diffusion experiment, when equilibrium has almost been reached. For this condition, i.e., constant diffusion coefficient, eq. (1) can be solved explicitly,<sup>14</sup> the relevant equation for long times being

$$[d \ln (M_\infty - M_t)]/dt = \pi^2 D(C)/a^2 \quad (6)$$

Accordingly, the second method of analyzing the data, which has been used by Zhurkov and Ryskin,<sup>12</sup> consists of plotting  $\ln (M_\infty - M_t)$  against time and computing the differential diffusion coefficient from the slope of the final linear portion of the plot according to eq. (6). During a sorption run the final uniform penetrant concentration approaches  $C_0$ ; during a desorption run it approaches zero. Hence this treatment applied to sorption runs gives  $D(C_0)$ , while desorption runs yield  $D(0)$ .

The advantage of the first method over the second is that the former employs the early measurements, which are known with greater precision than the late ones. Its disadvantage is that integral rather than differential diffusion coefficients are obtained and that  $D(0)$  must be obtained by extrapolation. Since the usual experimental measurements provide the data for application of either method and their results complement each other, it was decided to apply both of them in the present work.

During the diffusion process the polymer swells. This change in dimensions is equivalent to the occurrence of mass flow in addition to molecular diffusion. Diffusion coefficients which have been corrected for mass flow are termed intrinsic diffusion coefficients and are given by<sup>3</sup>

$$\mathfrak{D} = D/(1 - v_1)^3$$

where  $v_1$  is the volume fraction of penetrant. Since the penetrant concentrations were small in the present work, this correction would not affect the conclusions drawn and, consequently, has not been made.

### Experimental

The gravimetric sorption-diffusion apparatus, like that of Prager and Long<sup>6</sup> based on a quartz helix balance, is described in the first paper of this series.<sup>1</sup> The ethylene-propylene copolymer samples were prepared and analyzed as described previously.<sup>1</sup> The sample of "atactic" polypropylene was prepared by extracting with boiling *n*-heptane a sample of polypropylene made with a titanium trichloride-triisobutyl aluminum catalyst, and then drying and re-extracting the soluble fraction (53%) with boiling ethyl ether. The ether-soluble fraction, about 27% of the initial material, was used for the diffusion measurements. It showed a slight amount of crystallinity, estimated to be of the order of 10% by its density and its infrared absorption at 10.0  $\mu$ .

Films for diffusion runs were prepared by solvent-casting on mercury. It was found that they shrank considerably on initial exposure to solvent vapors, their area decreasing by about 15%, owing apparently to the relief of strains introduced during casting. Consequently, the films were pre-exposed for several hours to a vapor pressure well above that to be used for the diffusion runs. After this, the area was remeasured, and the thickness was calculated from the area and the density of the polymer. A single film was used for a number of runs, but its thickness, redetermined occasionally, increased only little after the initial conditioning. Film thicknesses of 0.1–0.4 mm. and sample weights of 60–150 mg. were used. The quartz helix had a sensitivity of about 0.75 mg./mm., and its length was read to within 0.002 mm.

Sorption runs were started by sudden admission of the desired vapor pressure from the main manifold to the sample space, which had previously been pumped out thoroughly. Then time versus spring length measurements were taken until equilibrium was reached, which was assumed to have occurred when the rate of weight change had decreased to 0.002 mg./10 min. or less. The sample thickness was chosen such that equilibrium was attained in 40–120 min. Like that of Prager and Long,<sup>6</sup> the present apparatus included a large buffer volume (5 l.) so that the pressure of the vapor in the manifold would not change appreciably as sorption in the sample took place.

A desorption run was started, immediately after sorption equilibrium had been reached, by shutting the stopcock between the main manifold and the sample space, condensing the vapor in the former by means of a liquid-nitrogen trap, quickly reopening the stopcock, and then recommencing time versus spring length readings. Attainment of desorption equilibrium usually took one and one-half to two times as long as establishment of sorption equilibrium.

Data from a typical run, plotted according to eqs. (4) and (6) are shown

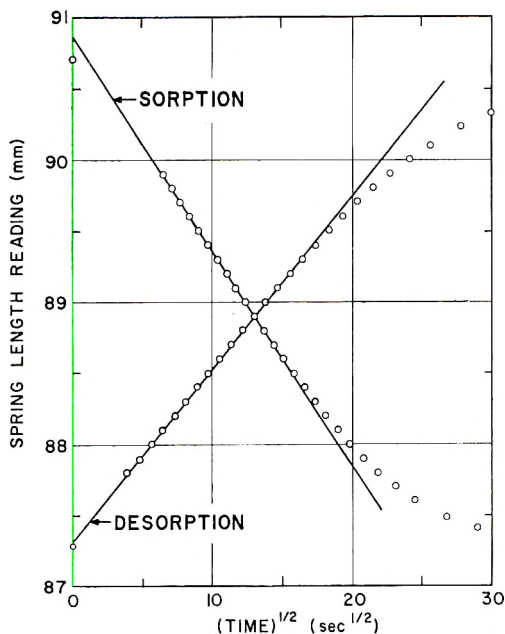


Fig. 1. Typical plot according to eq. (4): *n*-pentane (equilibrium volume fraction 0.0411) in 51% propylene copolymer at 23°C. Sample: volume 94.85 mm.<sup>3</sup>, thickness 0.163 mm., penetrant sorbed at equilibrium 4.061 mm.<sup>3</sup>, pressure 71.5 mm. Hg, spring sensitivity 0.7384 mg./mm. Sorption: slope 0.150 mm./sec.<sup>1/2</sup>,  $\bar{D}_s$   $10.0 \times 10^{-8}$  cm.<sup>2</sup>/sec. Desorption: slope 0.123 mm./sec.<sup>1/2</sup>,  $\bar{D}_d$   $6.7 \times 10^{-8}$  cm.<sup>2</sup>/sec.

in Figures 1 and 2, respectively. The failure of the sorption line in Figure 1 to go through the zero-time reading, which was observed in most runs, is probably caused partly by timing error and partly by a slight delay in establishing the equilibrium solvent concentration at the surfaces of the sample. Since this delay was small, amounting to 1 or 2 sec. for sorption and even less for desorption, its effect on the results was considered negligible. As Figures 1 and 2 show, the precision of the data is quite adequate. In some cases there was a little more scatter at the long-time end of the semilog plots like Figure 2, owing to the greater relative error of the points near equilibrium. However, adequate lines could always be drawn by focussing attention on the points for intermediate times.

The diffusion coefficients obtained from the two types of runs by the two methods of analysis are defined as follows. Integral diffusion coefficients for sorption and desorption, respectively, designated  $\bar{D}_s$  and  $\bar{D}_d$ , were obtained by application of eq. (4) to the initial slopes of plots like Figure 1. The mean integral diffusion coefficient is defined as

$$\bar{D} = \frac{1}{2}(\bar{D}_d + \bar{D}_s) \quad (7)$$

The differential diffusion coefficients obtained by application of eq. (6) to the final slopes of semilog plots like Figure 2 are designated  $D(C_0)$  for sorption runs and  $D(0)$  for desorption runs. The various diffusion coefficients

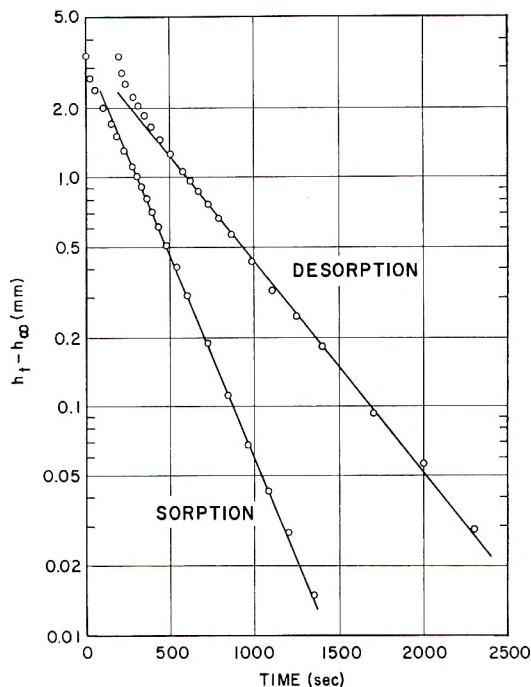


Fig. 2. Typical plot according to eq. (6): data from same run as Figure 1;  $h_t =$  cathetometer reading at time  $t$ ;  $h_0 - h_{\infty} = 3.42$  mm. Desorption plot offset 200 sec. to right. Sorption: slope  $4.05 \times 10^{-3}$  sec. $^{-1}$ ,  $D(C_0)$   $10.9 \times 10^{-8}$  cm. $^2$ /sec. Desorption: slope  $2.11 \times 10^{-3}$  sec. $^{-1}$ ,  $D(0)$   $5.7 \times 10^{-8}$  cm. $^2$ /sec.

divided by the mean observed  $D(0)$  are designated relative diffusion coefficients.

Diffusion coefficients obtained with sample films of different thicknesses agreed satisfactorily. This is illustrated by the results for *n*-pentane in Figure 4, which shows the points obtained in four runs with a film 0.0307 cm. thick and in six runs with another of 0.0169 cm. thickness. This agreement is taken as evidence that diffusion in these systems is Fickian.

## Results and Discussion

### *Concentration Dependence of the Diffusion Coefficients*

Figures 3, 4, and 5 illustrate the concentration dependence of the diffusion coefficients for the five penetrants studied. In order to make them comparable, all the diffusion coefficients are expressed in terms of the diffusion coefficient for zero penetrant concentration,  $D(0)$ .

All five different diffusion coefficients, obtained as discussed above, are shown for methylene chloride in Figure 3. Qualitatively, the relations are as expected:  $D(0)$  is independent of concentration while  $\bar{D}_d$ ,  $\bar{D}$ ,  $\bar{D}_s$ , and  $D(C_0)$  are increasingly concentration-dependent. The points all lie on fairly straight lines, suggesting the linear concentration dependence of eq. (2)



as observed, for instance, by Hayes and Park<sup>3</sup> or Aitken and Barrer.<sup>4</sup> However, as the latter authors have pointed out, eqs. (2) and (3) become equivalent for very low concentrations, and indeed the data in Figure 3, as those in Figures 4 and 5, give fairly straight lines when plotted semilogarithmi-

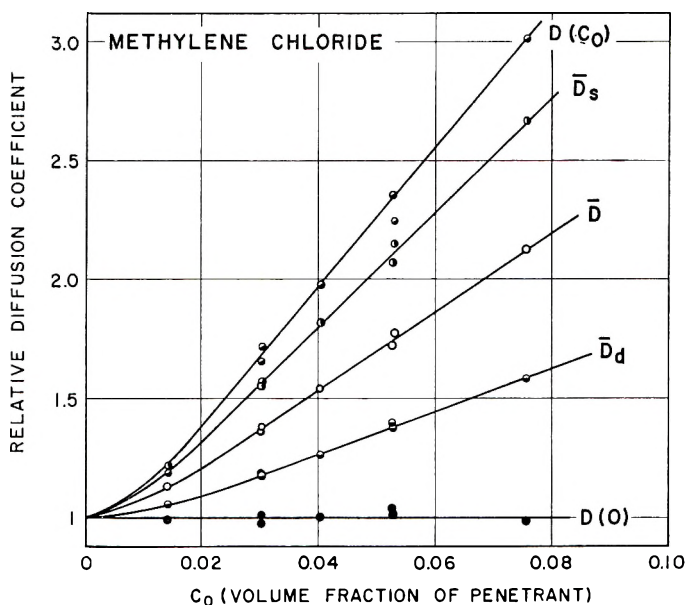


Fig. 3. Concentration dependence of diffusion coefficients for methylene chloride in 51% propylene copolymer at 23°C.

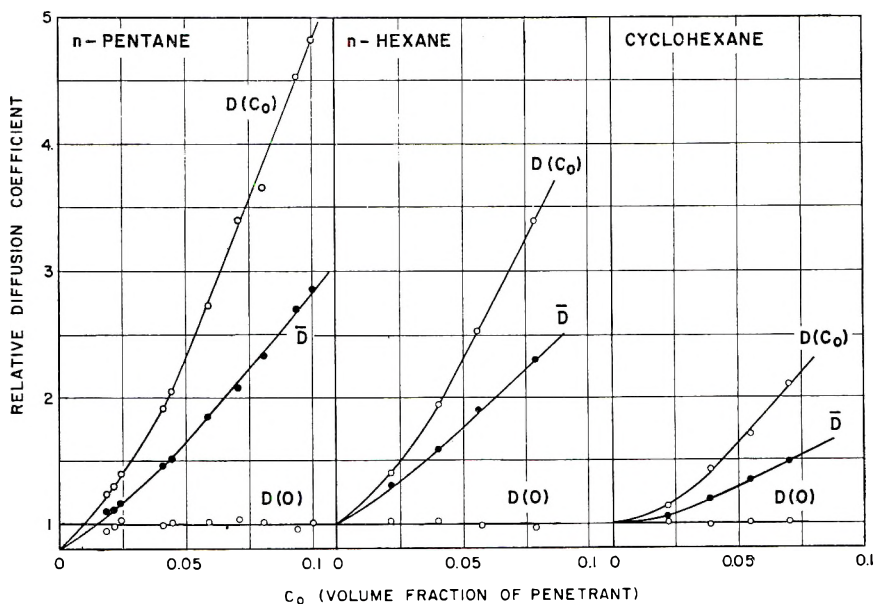


Fig. 4. Concentration dependence of diffusion coefficients for *n*-pentane, *n*-hexane, and cyclohexane in 51% propylene copolymer at 23°C.

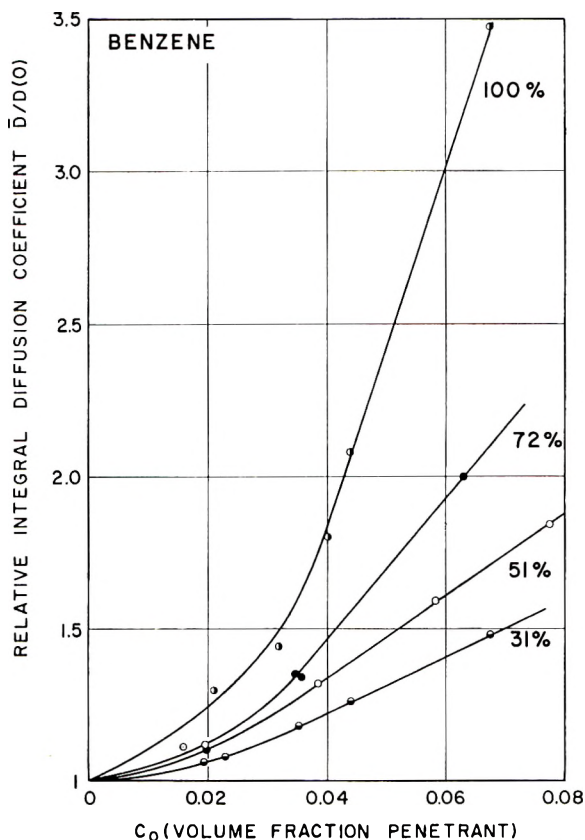


Fig. 5. Concentration dependence of integral diffusion coefficients  $\bar{D}$  for benzene in various copolymers at 23°C. Numbers on curves are propylene contents of copolymers in mole per cent.

cally, although the fit is not quite as good as on a linear scale. Hence, there is no real disagreement with the exponential concentration dependence of eq. (3) as reported, for instance, by Prager and Long<sup>6</sup> as well as by Pollard.<sup>8</sup>

Regardless of the functional form of the concentration dependence, all the diffusion coefficients must become identical; i.e., the relative diffusion coefficients must approach unity, at zero penetrant concentration. As is apparent from the data in Figures 3-5, linear or semilogarithmic extrapolation to zero concentration of the integral diffusion coefficients and of  $D(C_0)$  leads to values lower than  $D(0)$ . Moreover, the four diffusion coefficients generally extrapolate to different values at zero concentration.

This discrepancy can be resolved by assuming that the linear concentration dependence of the diffusion coefficients does not persist to the very lowest concentrations but that it flattens out, and the plots have been drawn accordingly. A similar observation has been made by Zhurkov and Ryskin,<sup>12</sup> who noted a flattening out of  $D(C_0)$  for the diffusion of methanol in polyvinyl acetate at a concentration of about 0.5%. However, most

other workers<sup>2-10</sup> have assumed the linear, or exponential, relationship between  $\bar{D}$  and concentration to hold down to zero concentration and, indeed, have used it for obtaining  $D(0)$  by extrapolation. In the present work  $D(0)$  is obtained directly by the use of the final desorption rate, as discussed in the Introduction. The validity of this method needs to be demonstrated in order to show that the nonlinearity at the lowest concentrations is real.

Support for the present method is furnished by the fact that the measured values of  $D(0)$  were always concentration-independent, as demonstrated by the data in Figures 3 and 4. Further supporting evidence can be adduced by calculating the expected desorption curves from eq. 1 in combination with an appropriate concentration dependence, as is done in the Appendix, where it is shown that semilogarithmic plots of the final desorption rates are linear over a wide enough range and that their slopes indeed correspond to  $D(0)$ .

Accordingly, it is concluded that the directly measured  $D(0)$  values are valid, that the concentration dependence of the diffusion coefficients does flatten out at the lowest concentrations, and that linear or exponential extrapolation of  $\bar{D}$  gives values of  $D(0)$  which are too low, by 10% or more, for ethylene-propylene copolymers. The published data do not exclude the possibility that a similar situation exists for the other rubbery polymers, because the curvature comes in at very low penetrant concentrations, say below 0.02 volume fraction, where measurements of the integral diffusion coefficient are difficult, imprecise, and hence rarely attempted.

The slopes of plots of  $D(C_0)$  versus concentration should be twice those for  $\bar{D}$ , to the approximation of eq. (5). This was found to be approximately so, as illustrated in Figures 3 and 4.

Various theories have been suggested to explain the concentration dependence of the diffusion coefficients. Prager and Long<sup>6</sup> mention both the "loosening" of the polymer structure by the penetrant molecules and the greater ease of hole formation because the polymer-penetrant interactions are weaker than those between polymer and polymer. Aitken and Barrer<sup>4</sup> invoke the zone theory of diffusion. However, as Barrer<sup>2</sup> has pointed out, there is at present no satisfactory quantitative theory for this concentration dependence.

#### *Effect of Penetrant Size and Shape*

It is implicit in the hole theory of diffusion<sup>15</sup> that the activation energy for diffusion should rise and the diffusion coefficient should fall as the size of the penetrant molecule increases. This prediction has been borne out by the measurements of diffusion in polymers. While quantitative relations can be best established in studies which embrace a fairly wide range of penetrant molecular sizes as, for instance, in the studies of gas diffusion by van Amerongen,<sup>13</sup> Prager and Long<sup>6</sup> have discussed the effects of chain length and branching in  $C_3$  to  $C_6$  hydrocarbons. The penetrants used in the present study represent only a relatively narrow range of penetrant molecular size. Hence only qualitative correlation is possible.

TABLE I  
 Diffusion in 51% Propylene Copolymer at 23°C.

Penetrant	Approximate molecular:		$D(0) \times 10^8$ , cm. <sup>2</sup> /sec.	Slope of $D/D(0)$ vs. $C_0$ , (volume fraction) <sup>-1</sup>
	Dimens., A.	Vol., A. <sup>3</sup>		
Methylene chloride	3.6; 4.5; 6.4	104	12.9	16
Benzene	3.6; 6.3; 7.0	159	6.1	12
<i>n</i> -Pentane	3.9; 4.4; 8.4	144	5.9	23
<i>n</i> -Hexane	3.9; 4.4; 9.8	168	4.1	18
Cyclohexane	4.7; 6.3; 7.0	195	2.1	9

 TABLE II  
 Diffusion of Benzene in Ethylene-Propylene Copolymers

Propylene in copolymer, mole-%	$T_g$ , °C.	$D(0) \times 10^8$ , cm. <sup>2</sup> /sec., at:				$E_a$ , kcal./mole
		10°C.	14°C.	23°C.	40°C.	
31	-64	4.4		10.5	27	10.6
51	-49	2.0		6.1	18.8	13.1
72	-35	0.67		2.3	8.9	15.2
100	-19		0.27	0.64	4.3	19.8

The molecular dimensions given in Table I were estimated by measuring Courtauld molecular models of the respective penetrants in three mutually perpendicular directions, the volume being that of the rectangular parallelepiped corresponding to the three dimensions. Crude though this method may be, it ought to give a fair relative ranking of the molecular sizes in question. The results in Table I show the molecular volumes to fall into three groups: methylene chloride has the smallest and cyclohexane the largest volume, while the three others are intermediate. The diffusion coefficients fall into about the same groupings. The comparison between pentane and hexane shows that not only molecular cross section matters, which is the same for these two species, but that the length also affects the diffusion rate.

The concentration dependence, as indicated in the last column of Table I, is based on the slopes of the linear portions of the curves in Figures 3, 4, and 5. It is of the same order as that reported by Prager and Long<sup>6</sup> for aliphatic hydrocarbons in polyisobutylene (14–26 in weight units). It is worthy of note that the slope is considerably lower for the two cyclic compounds than for the three noncyclic ones.

#### *Effect of Copolymer Composition*

The existence of ethylene-propylene copolymers, which have become available only in recent years, permits a study of the effect of methyl groups, more or less randomly distributed along an essentially linear carbon

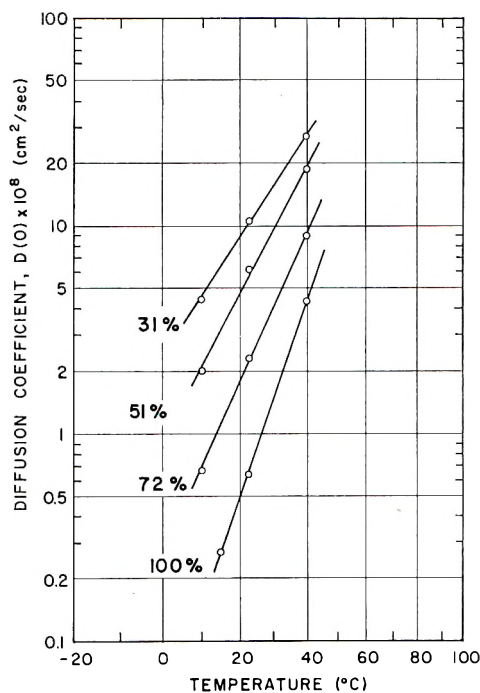


Fig. 6. Temperature dependence of diffusion coefficient for benzene in various copolymers. Numbers on curves are propylene contents of copolymers in mole per cent.

backbone, on diffusion properties and, hence, on the mobility of the polymer chains.

Results for four different copolymers at three different temperatures are summarized in Table II and illustrated in Figures 5 and 6. Measurements on copolymers of very low propylene content, which are usually crystalline and hence not directly comparable to the others, were omitted. The results show how rapidly the diffusion coefficients for benzene, and presumably also for other vapors, decrease as the propylene content goes up. The temperature dependence of the diffusion coefficient and, accordingly, the apparent activation energy  $E_a$  rise as the coefficients themselves fall, in accordance with the standard picture of activated diffusion.<sup>15</sup> The points of Figure 6 are on almost straight lines, although there is some indication of downward curvature indicative of decreasing activation energy with rising temperature, which has been reported by a number of workers.<sup>2,3,13</sup> The temperature range of the present work is not wide enough to permit a definite conclusion in this regard.

Both the decrease in diffusion coefficient and the increase in activation energy imply that methyl side groups reduce the flexibility of the polymer chains, i.e., their ability to get out of the way of the diffusing species. This decrease in chain flexibility is in accordance with the rise of the glass-transition temperatures with increasing propylene content, as shown by the softening temperatures  $T_s$  in Table II, which were determined by Garrett<sup>16</sup> on

the samples actually used for the diffusion measurements. They are the temperatures where the very rapid drop in modulus takes place and they approximate dilatometrically measured glass-transition temperatures. Agreement between the  $T_g$  values in Table II and dilatometric glass-transition temperatures of ethylene-propylene copolymers reported by Manaresi and Gianella<sup>17</sup> is very satisfactory.

As is apparent from the plots in Figure 5, the concentration dependence of the diffusion coefficients for benzene becomes markedly stronger as the propylene content of the copolymer rises. This is perhaps to be expected, because of the increase in activation energy with propylene content.

#### *Comparison with Other Polymers*

It is of interest to compare the present results with those on other polymers. According to the data of Hayes and Park<sup>3</sup> for diffusion of benzene in natural rubber,  $D(0)$  is about  $14 \times 10^{-8}$  cm.<sup>2</sup>/sec. at 25°C. and  $E_a$  is about 11 kcal./mole at that temperature, although the latter decreases appreciably as the temperature is raised. It is apparent, therefore, that diffusion in the low-propylene copolymer is at just about the same rate as in natural rubber.

Comparisons with polyisobutylene are provided by the results of Pollard,<sup>8</sup> who gives a  $D(0)$  of  $0.47 \times 10^{-8}$  for benzene in polyisobutylene at 40°C., and Prager and Long,<sup>6</sup> who obtained  $0.26 \times 10^{-8}$  for *n*-pentane in the same polymer at 35°C. Thus diffusion in polyisobutylene is one order of magnitude slower than in atactic polypropylene, and two orders lower than in low-propylene copolymer.

It appears from these comparisons that the mobility of a polyethylene chain with not too many pendent methyl groups on it—say, one for every six main-chain carbons or less—is comparable to that of the natural rubber chain. While the latter has more methyl groups (one for every four main-chain carbons), its over-all mobility is enhanced by the presence of the double bonds. Polyisobutylene, on the other hand, has two pendent methyls on every second carbon, which apparently reduce the ease of rotation about the main-chain axis to a much greater extent than the single methyl groups on every second carbon in polypropylene. It might be interesting to make comparable measurements on a hydrocarbon polymer with a methyl group attached to every chain carbon, e.g., polyethylidene, if such a material were available and were noncrystalline.

#### **Appendix**

It has been shown in the Introduction that diffusion with concentration-dependent diffusion coefficient will approximate the case of concentration-independent diffusion coefficient as equilibrium is approached; i.e., the final portion of a plot of  $\ln(M_\infty - M_t)$  versus time will be linear. It is the purpose of this Appendix to demonstrate that this linear portion is long enough to be used in practice and that its slope for desorption does correspond to  $D(0)$ .

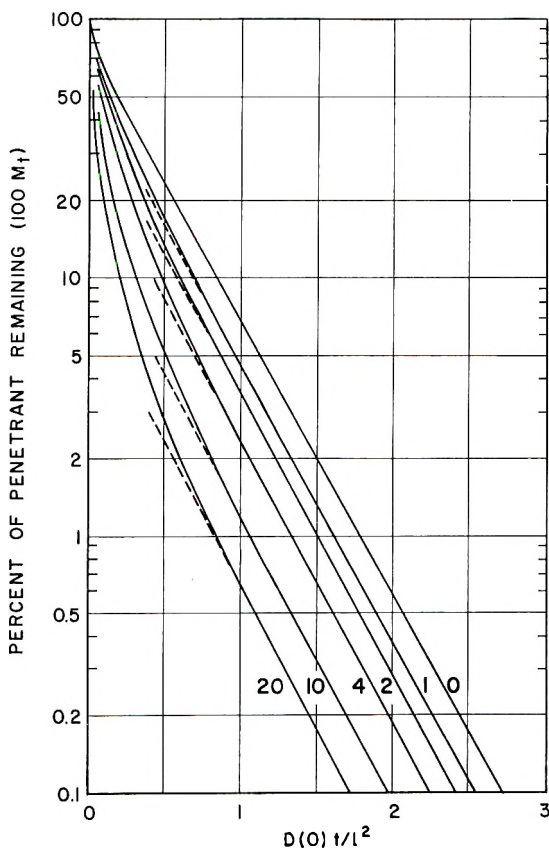


Fig. 7. Calculated desorption curves for concentration-dependent diffusion coefficient. Numbers on curves are  $A'$  in eq. (A2).

Crank<sup>14</sup> gives a very comprehensive discussion of numerical methods for solving the diffusion equation for variable diffusion coefficient and also shows the results of a number of such calculations. However, the examples given by him are not detailed enough in the long-time region to demonstrate our point. Accordingly, it was decided to calculate some appropriate cases. For the present purpose, the linear dependence of  $D(C)$  on  $C$  was chosen, but the results would be similar for exponential dependence as long as  $D(C_0)$  were not too high a multiple of  $D(0)$ .

The diffusion equation in its nondimensional form<sup>14</sup> is

$$\delta C' / \delta T = \delta / \delta X D [(\delta C' / \delta X)] \quad (\text{A1})$$

where concentration  $C'$  is in units of equilibrium concentration  $C_0$ , the distance  $X$  in units of half-thickness  $a/2$ , the time  $T$  in units of  $4D(0)/a^2$ , and the diffusion coefficient  $D'$  in units of the zero-concentration diffusion coefficient  $D(0)$ . In these units the linear concentration dependence of the diffusion coefficient becomes

$$D' = D(C)/D(0) = 1 + A'C' \quad (\text{A2})$$

Numerical solution of eq. (A1) for various values of the parameter  $A'$  was accomplished by means of Lees's Implicit Difference Method<sup>18</sup> on an IBM 7070 computer. The boundary conditions were those for desorption:

$$C' = 1 \text{ at } T = 0 \quad \text{for } -1 \leq X \leq 1$$

and  $C' = 0 \text{ at } T > 0 \quad \text{for } X = \pm 1$  (A3)

The fraction of penetrant  $M_t$  remaining in the sheet at  $T$  was computed by

$$M_t = \int_0^1 C' dX \quad (\text{A4})$$

The results of this calculation are given in Figure 7. It can be seen that the slopes of the linear portions are all identical with that of the concentration-independent curve ( $A' = 0$ ) and correspond to the theoretical value according to eq. (6), i.e.,  $-\pi^2/4$ . For our measurements  $D(C_0)$  was always below  $5D(0)$ , corresponding to  $A' = 4$ , and generally below  $3D(0)$ , corresponding to  $A' = 2$  (see Figs. 3-5). As is apparent from the curves of Figure 7, for these values of  $A'$  the curves are linear up to 10% of the initial quantity of penetrant in the sheet. Thus, the linear portion is more than adequate for obtaining a slope from measured data. This is illustrated by Figure 2 for an actual case in which  $D(C_0)/D(0)$  is about 2, corresponding to  $A' = 1$ . Here the linear portion starts at about 25% of the initial solvent content, in reasonable agreement with the calculated curve for Figure 7.

It is concluded, in the light of these calculated results, that correct values of  $D(0)$  and  $D(C_0)$  are obtained from the semilogarithmic plots of the raw diffusion data. The method may not be usable with systems of extremely strong concentration dependence, and it requires rather precise data for the final approach to diffusion equilibrium.

The numerical calculations were undertaken by Mr. John A. Beutler, Jr., and Miss Noelle Allison of the du Pont Engineering Research Laboratory. Their assistance is hereby gratefully acknowledged.

### References

1. Frensdorff, H. K., *J. Polymer Sci.*, **A2**, 333 (1964).
2. Barrer, R. M., *J. Phys. Chem.*, **61**, 178 (1957).
3. Hayes, M. J., and G. S. Park, *Trans. Faraday Soc.*, **51**, 1134 (1955); *ibid.*, **52**, 949 (1956).
4. Aitken, A., and R. M. Barrer, *Trans. Faraday Soc.*, **51**, 116 (1955).
5. Barrer, R. M., and R. R. Fergusson, *Trans. Faraday Soc.*, **54**, 989 (1958).
6. Prager, S., and F. A. Long, *J. Am. Chem. Soc.*, **73**, 4072 (1951).
7. Blyholder, G., and S. Prager, *J. Phys. Chem.*, **64**, 702 (1960).
8. Pollard, E. G., Thesis, Cornell University, 1956.
9. Kokes, R. J., F. A. Long, and J. L. Hoard, *J. Chem. Phys.*, **20**, 1711 (1952).
10. Barrer, R. M., J. A. Barrie, and J. Slater, *J. Polymer Sci.*, **27**, 177 (1958).
11. Vanderkooi, W. N., M. W. Long, and R. A. Mock, *J. Polymer Sci.*, **56**, 57 (1962).
12. Zhurkov, S. N., and G. Ya. Ryskin, *Zh. Tekhn. Fiz.*, **24**, 797 (1954); Ryskin, G. Ya., *Zh. Tekhn. Fiz.*, **25**, 458 (1955).



13. van Amerongen, G. J., *J. Appl. Phys.*, **17**, 972 (1946); *J. Polymer Sci.*, **5**, 307 (1950).
14. Crank, J., *The Mathematics of Diffusion*, Oxford Univ., 1956.
15. Glasstone, S., K. J. Laidler, and H. Eyring, *The Theory of Rate Processes*, McGraw-Hill, New York, 1941.
16. Garrett, R. R., in preparation.
17. Manaresi, P., and V. Gianella, *J. Appl. Polymer Sci.*, **4**, 251 (1960).
18. Lees, M., *J. Soc. Ind. Appl. Math.*, **7**, 167 (1959).

### Résumé

On a mesuré les vitesses de diffusion du chlorure de méthyle, du benzène, du *n*-pentane, du *n*-hexane et du cyclohexane dans un copolymère de 51% en moles de propylène et 49% d'éthylène à 23° et les concentrations de diffusant allant jusque 10% (volume). De même les vitesses de diffusion du benzène dans des copolymères contenant 31 à 100% de propylène ont été mesurées à 10°, 23° et à 40°C. On a calculé les coefficients intégraux de diffusion à partir des vitesses de diffusion initiales, et les coefficients différentiels de diffusion à partir des vitesses finales. La comparaison des deux types de coefficients de diffusion mène à la conclusion que leur dépendance de la concentration se résorbe aux plus faibles concentrations. Les coefficients de diffusion diminuent et les énergies d'activation augmentent quand le taux de propylène augmente dans le copolymère. La diffusion dans les copolymères, contenant peu de propylène, se fait à une vitesse comparable à celle dans le caoutchouc naturel; par contre, la vitesse dans le polypropylène atactique est plus lente d'environ un ordre de grandeur. Néanmoins elle est environ dix fois plus rapide que dans le polyisobutylène.

### Zusammenfassung

Die Diffusionsgeschwindigkeit von Methylenchlorid, Benzol, *n*-Pentan, *n*-Hexan und Cyclohexan in einem Propylen (51 Mol%)–Äthylen (49 Mol%)–Copolymeren wurde bei 23°C und bei Konzentrationen des diffundierenden Stoffes bis hinauf zu 10 Volum% ebenso wie die Geschwindigkeit der Benzol-diffusion in Copolymeren mit 31 bis 100% Propylenbausteinen bei 10°, 23° und 40°C gemessen. Aus der Anfangsdiffusionsgeschwindigkeit wurden integrale Diffusionskoeffizienten berechnet, aus der Endgeschwindigkeit differentielle Diffusionskoeffizienten. Ein Vergleich der beiden Typen von Diffusionskoeffizienten führt zu dem Schluss, dass ihre Konzentrationsabhängigkeit bei den allerniedrigsten Konzentrationen abflacht. Mit zunehmendem Propylengehalt des Copolymeren fallen die Diffusionskoeffizienten ab und die Aktivierungsenergie nimmt zu. Die Geschwindigkeit der Diffusion in Copolymeren mit niedrigem Propylengehalt ist derjenigen in Naturkautschuk vergleichbar, während die Geschwindigkeit in ataktischem Polypropylen um etwa eine Größenordnung niedriger ist. Die letztere ist aber immer noch 10mal rascher als in Polyisobutylen.

Received September 10, 1962

## Emulsion Polymerization of Vinyl Monomers by Transition Metal Compounds

RICHARD S. BERGER and E. A. YOUNGMAN, *Shell Development Company, Emeryville Research Center, Emeryville, California*

### Synopsis

A number of transition metal ions and complexes of the type which effect the stereospecific polymerization of butadiene in aqueous emulsion catalyze the polymerization of other vinyl monomers as well. In contrast to experience with butadiene, the structure of all products was typical of free-radical propagation reactions. The catalysis was somewhat selective, a given transition metal compound being active for some monomers but not for others. A mechanism involving coordinate complex formation between catalyst and monomer, generation of a free-radical initiator by redox reaction within the complex, and noncoordinated free-radical propagation is postulated. Copolymerization studies support such a mechanism; copolymer compositions were always typical of free-radical catalysis, even when the catalyst was active in homopolymerization of only one member of the monomer pair. Butadiene polymerizations using many of the same catalysts clearly proceed by different, little understood mechanisms. Attempted copolymerizations with butadiene gave only polybutadiene; the comonomers had no effect on polymer microstructure but generally reduced polymerization rate.

### INTRODUCTION

Important additions to the vast array of stereospecific polymerization systems have been made rather recently with the discoveries that good control over the steric course of certain poly additions could be obtained in water or other highly polar media. In simultaneous but independent communications Luttinger<sup>1</sup> and Wilkinson et al.<sup>2</sup> reported the stereospecific *trans*-polymerization of acetylene by various Group VIII compounds combined with hydridic reducing agents. Luttinger used alcohol, water, or other polar solvents, while the Wilkinson group employed tetrahydrofuran. Reinhart et al.<sup>3</sup> effected the highly specific *trans*-1,4-polymerization of butadiene in water using rhodium salts. The great potential value of relatively simple Group VIII compounds in stereospecific polymerizations carried out in water was most forcefully demonstrated by the work in these laboratories by Canale et al.<sup>4</sup> Polybutadienes of high *cis*-1,4-, *trans*-1,4- or 1,2 microstructure, depending upon the transition metal compound employed as catalyst, were obtained in aqueous emulsion.

It was of obvious interest to determine if the new catalysts could effect the stereospecific polymerization of typical vinyl monomers other than butadiene and to gather evidence bearing on the polymerization mechanism.

There have been no reports in the scientific literature of studies along these lines. However, in the first report of their brilliant discovery and development of processes for the catalytic conversion of olefins to carbonyl compounds by means of platinum metal compounds in water, Smidt et al.<sup>5</sup> mention but do not elaborate upon the formation of resins from olefins and especially from vinyl and allyl compounds when glacial acetic acid is the solvent at higher temperatures and long reaction times. Also, since the completion of our work, two patents of interest appeared. In the first of these a number of monomers were oligomerized in alcohol using Group VIII metal chlorides as catalyst.<sup>6</sup> In the second, the polymerization of acrylonitrile by  $\text{VOCl}_3$  combined with an alkali metal borohydride at a pH below 2 in water was described.<sup>7</sup> None of these cases provides any indication of stereospecificity in the addition reaction.

As in the superficially analogous Ziegler systems, stereoregulating catalysts all appear to have the capacity to form coordination complexes with monomer. A logical starting point for this study was therefore the use of an effective butadiene catalyst known to form a coordinate complex with a monomer of interest. Kharasch<sup>8</sup> first prepared and isolated a palladium chloride-styrene complex  $(\text{C}_8\text{H}_8\text{PdCl}_2)_2$ , by displacing benzonitrile from  $(\text{C}_6\text{H}_5\text{CN})_2\text{PdCl}_2$ . His analyses gave values for palladium which were somewhat low. He attributed the low palladium content to the presence of polystyrene. Palladium chloride did indeed polymerize styrene readily in aqueous emulsion. Many other transition metal compounds and some other monomers were then tested. Finally, copolymerization was employed to elucidate the nature of propagation.

## EXPERIMENTAL

### Materials

Monomers were commercial materials, fractionally distilled to remove impurities and inhibitors. The purified monomers were stored under nitrogen in a refrigerator. Transition metal halides were generally commercial samples used as received. Distilled water was deoxygenated by refluxing while passing a stream of oxygen-free nitrogen through the liquid. Polymerizations were carried out in 250-cc. brown hydrogen peroxide bottles with rubber serum caps over which metal screw caps were fitted. The bottles were flushed with nitrogen; solid catalysts were added followed by additional flushing. Five flushing and evacuating cycles were usually employed. Water (40 ml.), a solution of the emulsifier (usually 1.5 g. sodium hexadecylbenzene sulfonate, Nacconol NRSF, Allied Chemical and Dye Corp., National Aniline Division) in 10 ml. water and monomer or monomers were then injected by syringe through a hole in the metal cap and through the serum cap. Bottles in metal cages were tumbled end over end in a thermostated bath. Polymers were recovered by pouring the reaction mixtures into methanol. Polymers were characterized by intrinsic viscosity determinations, infrared and/or ultraviolet

spectra and, in some cases, by solubility in appropriate solvents, and elemental analyses. Usually an attempt was made to induce crystallization by heating the polymer in the presence of poor solvents.

## RESULTS

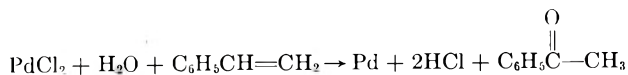
### Styrene

A selected few of the many metal ion-ligand combinations tested for polymerization of styrene are shown in Table I. Control experiments

TABLE I  
Transition Metal Complex Catalysts for Polymerization of Styrene

Catalyst	Amt. catalyst, mmole	Styrene/ catalyst mole ratio	Time, hr.	Temp., °C.	Yield, %
PdCl <sub>2</sub> ·2H <sub>2</sub> O	0.25	400	17	50	24
PdCl <sub>2</sub> ·2H <sub>2</sub> O	0.10	1,000	16	70	79
PdCl <sub>2</sub> ·2H <sub>2</sub> O	0.25	400	17	50	1
<i>p</i> -Benzoquinone	0.25				
Pd(pyridine) <sub>2</sub> Cl <sub>2</sub>	0.10	1,000	41	50	92
PdCl <sub>2</sub> ·2H <sub>2</sub> O	0.10	1,000	17	50	95
<i>o</i> -Phenylenediamine	0.10				
PdCl <sub>2</sub> ·2H <sub>2</sub> O	0.10	1,000	64	50	4
<i>o</i> -Phenylenediamine	0.10				
Benzoquinone	0.10				
PdCl <sub>2</sub> ·2H <sub>2</sub> O	0.10	1,000	41	50	56
KCN	0.10				
PdCl <sub>2</sub> ·2C <sub>6</sub> H <sub>5</sub> CN	0.26	400	16	50	51
Na <sub>2</sub> PdCl <sub>4</sub>	0.10	1,000	41	50	31
(NH <sub>4</sub> ) <sub>2</sub> PdCl <sub>4</sub>	0.10	1,000	41	50	46
PdCl <sub>2</sub> ·2H <sub>2</sub> O	0.10	1,000	41	50	34
(C <sub>6</sub> H <sub>5</sub> ) <sub>3</sub> P	0.20	500			
H <sub>2</sub> PtCl <sub>6</sub> ·6H <sub>2</sub> O	0.06	8,350	17	50	82
H <sub>2</sub> PtCl <sub>6</sub> ·6H <sub>2</sub> O	0.08	1,250	88	25	82
PtCl <sub>2</sub>	0.74	135	65	50	20
PtCl <sub>2</sub> ·2(C <sub>6</sub> H <sub>5</sub> ) <sub>3</sub> P	0.50	200	64	50	61
TiCl <sub>3</sub>	1.6	62	89	50	33
RhCl <sub>3</sub> ·3H <sub>2</sub> O	1.0	100	89	50	trace
RhCl <sub>3</sub> ·3H <sub>2</sub> O	1.0	100	64	50	5
(C <sub>6</sub> H <sub>5</sub> ) <sub>3</sub> P	4.0	400			

involving water, emulsifier, and styrene gave no polymer. Polymer molecular weights were quite high (intrinsic viscosities of 3–5 dl./g.) suggesting few propagating species. In the case of palladium catalysts the polymers were grey, presumably due to palladium metal. Reduction to metal is expected on the basis of work by Smidt et al.<sup>5</sup>



Small quantities of acetophenone could be detected in these polymerizations. It is not certain that metallic palladium results exclusively from this side reaction or whether it also forms as a step in polymerization (e.g., termination).

When cyanide ion was present in the reaction mixture along with  $\text{PdCl}_2$  an enhancement in activity was noted when the  $\text{CN/Pd}$  ratio was less than 4. In these cases there was less reduction to metallic Pd (as judged by color of the polymer; at  $\text{CN/Pd} = 4$ , the polymer was white rather than grey).

Polymerizations were inhibited by *p*-benzoquinone and by small quantities of oxygen. Other compounds tested but found to be inactive include  $\text{RhCl}_3 \cdot 3\text{H}_2\text{O}$ ,  $\text{CeCl}_3$ ,  $\text{CrCl}_3$ ,  $\text{IrCl}_3$ ,  $\text{MnCl}_2$ ,  $\text{Ni}(\text{CN})_2$  and  $\text{RuCl}_3$ . Addition of hydridic reducing agents converted  $\text{RhCl}_3 \cdot 3\text{H}_2\text{O}$  and  $\text{RuCl}_3$  to moderately active catalysts.

### Methyl Methacrylate

Some similarities and some notable differences in reactivity of styrene and methyl methacrylate toward particular catalysts were observed (Table II). In general, methyl methacrylate was less reactive than styrene.  $\text{RhCl}_3 \cdot 3\text{H}_2\text{O}$ , however, showed moderate activity for methyl methacrylate but was inactive for styrene polymerization. With  $\text{TiCl}_3$  the situation was reversed, styrene being polymerized but methacrylate not. Pyridine did not enhance the reactivity of  $\text{PdCl}_2$  toward this monomer (in contrast to styrene) but cyanide ion did.

TABLE II  
Transition Metal Complex Catalysts for Polymerization of Methyl Methacrylate at 50°C.

Catalyst	Amt. catalyst, mmole	Monomer/catalyst mole ratio	Time, hr.	Yield, %
$\text{PdCl}_2 \cdot 2\text{H}_2\text{O}$	1.0	90	53	29
$\text{PdCl}_2 \cdot 2\text{H}_2\text{O}$	1.0	90	53	31
Pyridine	2.0	45		
$\text{PdCl}_2 \cdot 2\text{H}_2\text{O}$	0.5	180	42	87
<i>o</i> -Phenylenediamine	0.5			
$\text{PdCl}_2 \cdot 2\text{H}_2\text{O}$	1.0	90	41	76
KCN	2.0	45		
$\text{PdCl}_2 \cdot 2\text{C}_6\text{H}_5\text{CN}$	0.5	180	41	44
$\text{H}_2\text{PtCl}_6 \cdot 6\text{H}_2\text{O}$	0.24	360	40	43
$\text{RhCl}_3 \cdot 3\text{H}_2\text{O}$	1.0	90	89	25

In the few experiments made, isopropyl methacrylate behaved about the same as the methyl ester.

The intrinsic viscosities of the methyl methacrylate polymers ranged from about 0.3 to 4.0 dl./g. with most samples having  $[\eta] > 1.0$ . The infrared spectra were identical to that of atactic poly-(methyl methacrylate).

TABLE III  
Copolymerizations with Butadiene (BD) at 50°C.

Catalyst	Amt. catalyst, mmole	BD, g.	Vinyl comonomer	Amt. comonomers, g.	Time, hr.	Yield, %	Polymer composition
RhCl <sub>3</sub> ·3H <sub>2</sub> O	1	10.5	—	—	44	98	99% <i>trans</i> -1,4 PBD
RhCl <sub>3</sub> ·3H <sub>2</sub> O	1	—	Methyl methacrylate	9.6	89	25	—
RhCl <sub>3</sub> ·3H <sub>2</sub> O	1	11.0	Methyl methacrylate	9.6	44	35 <sup>a</sup>	99% <i>trans</i> -1,4 PBD
RhCl <sub>3</sub> ·3H <sub>2</sub> O	1	—	Styrene	10.0	89	Trace	—
RhCl <sub>3</sub> ·3H <sub>2</sub> O	1	10.9	Styrene	10.0	42	76 <sup>a</sup>	99% <i>trans</i> -1,4 PBD
PdCl <sub>2</sub> ·2H <sub>2</sub> O	8	8.7	—	—	88	21	73% 1,2; 27% <i>trans</i> -1,4 PBD
PdCl <sub>2</sub> ·2H <sub>2</sub> O	0.10	—	Styrene	10.0	40	41	—
PdCl <sub>2</sub> ·2H <sub>2</sub> O	8	10.0	Styrene	10.0	88	10 <sup>a</sup>	77% 1,2; 23% <i>trans</i> -1,4 PBD
RhCl <sub>3</sub> ·3H <sub>2</sub> O	—	—	Acrolein	8.4	41	0	—
RhCl <sub>3</sub> ·3H <sub>2</sub> O	1	10.5	Acrolein	8.4	24	43 <sup>a</sup>	99% <i>trans</i> -1,4 PBD slight
RhCl <sub>3</sub> ·3H <sub>2</sub> O	1	10.0	Acrolein	8.4	64	61 <sup>a</sup>	carbonyl in IR
RhCl <sub>3</sub> ·3H <sub>2</sub> O	1	—	Acrylonitrile	8.0	64	0	—
RhCl <sub>3</sub> ·3H <sub>2</sub> O	1	10.0	Acrylonitrile	8.0	64	4 <sup>a</sup>	99% <i>trans</i> -1,4 PBD, small CN peak in IR

<sup>a</sup> Based on butadiene charged.

### Other Monomers

A brief survey of the applicability of several transition metal catalysts to other vinyl monomers was made. None of the experiments was very successful in terms of catalyst efficiency.

Acrylonitrile failed to polymerize under conditions successful for styrene and methyl methacrylate with  $\text{RhCl}_3 \cdot 3\text{H}_2\text{O}$  or  $\text{PdCl}_2 \cdot 2\text{H}_2\text{O}$  with added *o*-phenylenediamine. Only  $\text{H}_2\text{PtCl}_6 \cdot 6\text{H}_2\text{O}$  showed a slight activity.

Acrolein, although a very reactive monomer, was not polymerized by  $\text{RhCl}_3 \cdot 3\text{H}_2\text{O}$ . This catalyst is very effective for the stereospecific polymerization of butadiene.

A number of catalysts were tested with vinyl acetate and vinyl chloride; none yielded solid polymer, although monomer was not recoverable from the tests employing  $\text{RhCl}_3$  or  $\text{H}_2\text{PtCl}_6$  and vinyl chloride. The nature of the low molecular weight products (not precipitated by methanol) was not determined.

### Copolymerizations with Butadiene

In an attempt to relate the established stereospecific butadiene polymerizations to the present studies, copolymerizations were carried out. Copolymerizations of butadiene with methyl methacrylate, styrene, acrolein, and acrylonitrile were attempted employing  $\text{RhCl}_3$  and/or  $\text{PdCl}_2$ . Both of these catalysts are effective and quite selective in polymerization of butadiene, the former yielding a very high *trans*-1,4 structure while the latter gives a product high in the 1,2 form. Copolymerization did not take place. The comonomers had no effect upon the microstructure of the polybutadienes produced, although their presence in the reaction mixture reduced the rate of butadiene homopolymerization (Table III).

TABLE IV  
Copolymerizations of Styrene and Methyl Methacrylate at 50°C.

Catalyst	Monomer charge, S/MMA by wt. Conversion, %		Polymer analyses	
			Styrene, wt.-% <sup>a</sup>	MMA, wt.-% <sup>b</sup>
$(\text{C}_6\text{H}_5\text{COO})_2$	50/50	28	47	53
$\text{PdCl}_2 \cdot 2\text{H}_2\text{O}$	50/50	25	N.A. <sup>c</sup>	52
$\text{PdCl}_2 \cdot 2\text{H}_2\text{O}$	50/50	14	58	48
$\text{PdCl}_2 \cdot 2\text{H}_2\text{O}$	60/31	23	64	38
$\text{PdCl}_2 \cdot 2\text{H}_2\text{O}$	29/71	22	37	68
$\text{H}_2\text{PtCl}_6 \cdot 6\text{H}_2\text{O}$	50/50	26	46	53
$\text{RhCl}_3 \cdot 3\text{H}_2\text{O}$	50/50	3	N.A.	50
$\text{RhCl}_3 \cdot 3\text{H}_2\text{O}$	50/50	1	N.A.	51
$\text{PdCl}_2 \cdot 2\text{C}_6\text{H}_5\text{CN}$	50/50	19	N.A.	51
$\text{Pd}(\text{py})_2\text{Cl}_2$	50/50	5	N.A.	46
$\text{TiCl}_3$	50/50	8	N.A.	50

<sup>a</sup> From ultraviolet spectra, intensity at 270 m $\mu$ .

<sup>b</sup> From infrared spectra, intensity at 5.75  $\mu$ .

<sup>c</sup> N.A. = not analyzed.

### Other Copolymerizations

Other copolymerizations were carried out in search of evidence bearing on the mechanism of propagation. The styrene–methyl methacrylate pair was studied most, but acrylonitrile–styrene and acrylonitrile–methyl methacrylate were also examined briefly. For the styrene–methyl methacrylate pair, catalysts active in the homopolymerization of both monomers ( $\text{PdCl}_2$ ,  $\text{H}_2\text{PtCl}_6$ ), active only for styrene ( $\text{TiCl}_3$ ), or active only for methyl methacrylate ( $\text{RhCl}_3$ ) were tested. In the other cases, the catalyst ( $\text{H}_2\text{PtCl}_6$ ) was weakly active for acrylonitrile and quite active for the comonomers styrene and methyl methacrylate. Results are presented in Tables IV and V.

TABLE V  
Copolymerizations Involving Acrylonitrile

Monomers	Wt. monomers, g.	Catalyst	Amt. catalyst, mmole	Time, hr.	Temp., °C.	Result <sup>a</sup>
Acrylonitrile Styrene	8.0 10.0	$\text{H}_2\text{PtCl}_6 \cdot 6\text{H}_2\text{O}$	1.2	88	50	4.4 g. polymer, 28.2% acrylonitrile units found. Calc. for free radical copolymer, 29.2%.
Acrylonitrile Methyl methacrylate	8.0 9.6					

<sup>a</sup> Copolymer composition calculated from nitrogen analyses.

### DISCUSSION

A number of transition metal ions and complexes were found to catalyze the polymerization of styrene, methyl methacrylate and other vinyl monomers in aqueous emulsion. These catalysts, principally involving Pd, Pt, Rh, Ru, or Ti, were somewhat specific in their ability to promote polymerization of the various monomers. Sensitivity to oxygen and typical free-radical inhibitors and lack of detectable stereoregularity in the products suggested that polymerization was occurring by a free-radical mechanism. A free-radical propagation mechanism is clearly established by the copolymerizations of styrene–methyl methacrylate, acrylonitrile–styrene, and acrylonitrile–methyl methacrylate. In all of the cases studied the composition of the products agreed well with that expected for classical free-radical polymerizations.

The copolymerizations of styrene with methyl methacrylate employing  $\text{TiCl}_3$  and  $\text{RhCl}_3 \cdot 3\text{H}_2\text{O}$  are particularly enlightening.  $\text{TiCl}_3$  initiated the homopolymerization of styrene but not methyl methacrylate while



$\text{RhCl}_3 \cdot 3\text{H}_2\text{O}$  polymerized methyl methacrylate but not styrene. Each was effective in copolymerization of this monomer pair, giving copolymers of identical composition.

The selectivity of certain catalysts for certain monomers, the sensitivity to oxygen and other radical inhibitors (in the instance where this was studied) and results of the copolymerization experiments may be accommodated by postulating that polymerization takes place when: (1) complex forms between monomer and transition metal species, and (2) redox reaction takes place within the complex to generate a free-radical species which escapes to propagate polymerization.

Complex formation appears to be a necessary but insufficient requisite for polymerization activity. Thus  $\text{PdCl}_2$  is known to form complexes with both styrene and acrylonitrile, yet only styrene is homopolymerized by this catalyst. Apparently the required generation of radicals occurs only within the styrene- $\text{PdCl}_2$  complex.

$\text{H}_2\text{PtCl}_6$  is extremely active for styrene polymerization but only weakly active for acrylonitrile. The copolymerization rate for this pair is between the rates for homopolymerization. This finding may be rationalized within the framework of our postulated mechanism by assuming that acrylonitrile complexes most readily and strongly while the styrene  $\text{H}_2\text{PtCl}_6$  complex most efficiently produces radicals. The presence of acrylonitrile thus reduces the rate of initiation; once initiated, the two monomers enter the growing chain as expected in a free-radical copolymerization.

Stereospecific polymerization of butadiene by many of these same transition metal catalysts clearly proceeds by a different, little understood mechanism (or mechanisms). Attempted copolymerizations of butadiene with other vinyl monomers gave no copolymer even when the transition metal compound catalyzed homopolymerization of each monomer. Indeed, only polybutadiene was obtained. The polybutadienes had the microstructure that would have been obtained in the absence of the comonomer; in most cases the polymerization rate was reduced, however. These studies cast little new light upon the unique polymerizability of butadiene by transition metal catalysts in aqueous emulsion. We can only echo what has already been stated in or can be inferred from the published reports, namely, that the butadiene polymerizations have no conventional free-radical character and that a coordinated propagation takes place. In sharp contrast, the vinyl monomers studied in this work undergo free-radical polymerization initiated by a redox reaction which apparently occurs within a monomer-catalyst complex. The comonomer appears to compete effectively with butadiene in coordinate complex formation as evidenced by its ability to reduce the rate of polybutadiene formation; yet the comonomer is not polymerized. Elucidation of these and other features of the polymerizations awaits further study.

We wish to express our thanks to Dr. A. J. Canale for his early interest in exploring this area of polymerization catalysis and for many stimulating discussions.

### References

1. Luttinger, L. B., *Chem. Ind. (London)*, **1960**, 1135; *J. Org. Chem.*, **27**, 1591 (1962).
2. Green, M. L. H., M. Nehmé, and G. Wilkinson, *Chem. Ind. (London)*, **1960**, 1136.
3. Reinhart, R. E., H. P. Smith, H. S. Witt, and H. Romeyn, Jr., *J. Am. Chem. Soc.*, **83**, 4864 (1961).
4. Canale, A. J., W. A. Hewett, T. M. Shryne, and E. A. Youngman, *Chem. Ind. (London)*, **1962**, 1054.
5. Smidt, J., et al., *Angew. Chem.*, **71**, 176 (1959).
6. Anderson, T. (to the du Pont Company), French Pat. 1,229,702.
7. Linn, W. J. (to the du Pont Company), U. S. Pat. 2,961,433.
8. Kharasch, M. S., R. C. Seyler, and F. R. Mayo, *J. Am. Chem. Soc.*, **60**, 882 (1938).

### Résumé

Un certain nombre de complexes et ions de métaux de transition qui polymérise stéréospécifiquement le butadiène en émulsion dans l'eau, catalyse également la polymérisation d'autres monomères vinyliques. Contrastant avec les résultats obtenus dans le cas du butadiène, la structure de tous les produits répondent typiquement à une réaction de propagation par radicaux libres. La catalyse s'avère assez sélective, un composé métallique de transition donné étant actif pour certains monomères mais pas pour d'autres. On imagine un mécanisme comportant la formation d'un complexe de coordination entre le catalyseur et le monomère ainsi que la formation d'un initiateur radicalaire par réaction d'oxydo-réduction entre le complexe et le radical libre non coordonné. Les études de copolymérisation corroborent un tel mécanisme; la composition des copolymères est toujours caractéristique d'une catalyse radicalaire, même lorsque le catalyseur n'est actif en homopolymérisation que pour l'un des deux monomères. La polymérisation du butadiène par plusieurs de ces catalyseurs s'effectue incontestablement par divers mécanismes peu expliqués à ce jour. Les essais de copolymérisation du butadiène donnent seulement du polybutadiène; les comonomères n'ont pas d'effet sur la microstructure mais généralement réduisent la vitesse de polymérisation.

### Zusammenfassung

Eine Anzahl von Übergangsmetallionen und -komplexen vom gleichen Typ, wie sie die stereospezifische Polymerisation von Butadien in wässriger Emulsion bewirken, katalysieren auch die Polymerisation anderer Vinylmonomere. Im Gegensatz zu den Erfahrungen an Butadien war die Struktur aller Produkte typisch für eine radikalische Wachstumsreaktion. Die Katalyse war selektiv in dem Sinne, dass eine gegebene Übergangsmetallverbindung für gewisse Monomere wirksam, für andere aber unwirksam war. Ein Mechanismus mit Bildung eines koordinativen Komplexes zwischen Katalysator und Monomerem, Erzeugung eines Radikalstarters durch Redoxreaktion innerhalb des Komplexes und nichtkoordinativem radikalischen Wachstum wird aufgestellt. Copolymerisationsversuche bestätigen diesen Mechanismus; die Copolymerzusammensetzung entsprach immer einem Radikalmechanismus, auch wenn der Katalysator nur bei der Homopolymerisation eines der beiden Monomeren wirksam war. Bei Verwendung vieler dieser Katalysatoren verläuft die Butadienpolymerisation offenbar nach anderen, noch nicht aufgeklärten Mechanismen. Bei Copolymerisationsversuchen mit Butadien wurde lediglich Polybutadien erhalten; die Comonomeren hatten keinen Einfluss auf die Mikrostruktur der Polymeren, setzten aber im allgemeinen die Polymerisationsgeschwindigkeit herab.

Received October 22, 1962

Revised January 22, 1963

# Cationic Polymerization of 3-Methylbutene-1.

## I. Polymerizations at Moderately Low Temperatures

J. P. KENNEDY, L. S. MINCKLER, JR., and R. M. THOMAS,  
*Chemicals Research Division, Esso Research and Engineering Company,  
Linden, New Jersey*

### Synopsis

The cationic polymerization of 3-methylbutene-1 was investigated with the use of aluminum chloride and aluminum bromide initiators in the temperature range of  $-62$  to  $-102^{\circ}\text{C}$ . Polymerizations are homogeneous in the presence of pentane, and above  $-50^{\circ}\text{C}$ . in methyl chloride. However, the polymer tends to precipitate below  $-50^{\circ}\text{C}$ . in methyl chloride. The molecular weight of poly-3-methylbutene-1 increases with decreasing temperatures at the same conversion level. Significantly, the molecular weights increase with conversion and seem to reach their maximum at high conversions. Higher molecular weights were obtained in *n*-pentane-alkyl chloride mixtures than in methyl chloride solution alone. The molecular weights are independent of catalyst concentrations in the range investigated ( $31.8$ - $7.97 \times 10^{-4}$  mole/l.  $\text{AlBr}_3$  and  $57.6$ - $28.8 \times 10^{-4}$  mole/l.  $\text{AlCl}_3$ ). The rate of homogeneous polymerization with aluminum bromide in propane solvent was studied. The rate is first order in monomer concentration and catalyst concentration and the rate constant is  $0.610$  l./mole sec. The apparent activation energy calculated from the Arrhenius plot is  $6.57$  kcal./mole. In methyl bromide the rate of polymerization increases significantly (effect of the dielectric constant). In toluene the molecular weight as well as the rate is strongly depressed indicating the preponderance of a chain breaking mechanism involving this solvent.

### INTRODUCTION

3-Methylbutene-1 (or isopropylethylene or isoamylene) has been little studied as a monomer in cationic polymerizations. In 1927 Norris and Joubert<sup>1</sup> found that 3-methylbutene-1 polymerized to form dimers in the presence of 70%  $\text{H}_2\text{SO}_4$  after 25 days at room temperature. Lower concentrations of acid failed to produce polymer. Higher acid concentrations gave trimers and high oligomers after 6 days. In 1934 Dutch workers<sup>2</sup> reported that 3-methylbutene-1 reacts slowly at  $-80^{\circ}\text{C}$ . with aluminum chloride to give a viscous substance. Also, 3-methylbutene-1 was used as a raw material for making a polymer gasoline (hydrogenated dimers) with solid phosphoric acid.<sup>3</sup> Webb<sup>4</sup> mentioned the polymerizability of 3-methylbutene-1 with boron trifluoride. Poly-3-methylbutene-1 was disclosed in a patent by Thomas and Reynolds in 1945.<sup>5</sup> These authors polymerized 3-methylbutene-1 with a solution of aluminum chloride in

ethyl chloride at  $-78^{\circ}\text{C}$ . The product they obtained was a colorless, amorphous, tough, semi-solid material with rather low molecular weight.

In the course of our fundamental studies on cationic polymerizations, a systematic investigation of the Lewis acid-initiated polymerization of 3-methylbutene-1 was undertaken. This resulted in the synthesis of a crystalline modification of poly-3-methyl-butene-1 at low temperature levels which has already been reported.<sup>6</sup>

In this paper we report kinetic results obtained with the 3-methylbutene-1-Lewis acid system in various solvents at temperatures of  $-102^{\circ}\text{C}$ . and above. Particularly, we investigated  $\text{AlBr}_3$  and  $\text{AlCl}_3$  as electrophilic catalysts in propane, carbon disulfide, and methyl chloride diluents. Investigations at still lower temperatures (to  $-150^{\circ}\text{C}$ .) have also been carried out and will be reported.

## EXPERIMENTAL

### 1. Materials Used

Aluminum chloride, anhydrous sublimed, Fisher certified reagent was used without further purification.

Aluminum bromide was anhydrous Fisher certified reagent. The chemical is shipped in sealed vials and it is almost completely colorless; a faint yellow tinge is caused by bromine which is formed by decomposition in the presence of traces of moisture. No iron impurities (e.g.,  $\text{FeBr}_3$ ) could be detected. In some cases the material was redistilled before use, but reproducible results were obtained without this purification.

3-Methylbutene-1 gas (C.P. grade, The Matheson Company) was scrubbed with barium oxide before condensing in the dry box. Gas chromatographic analysis on a 2,5-hexadiene column indicated the following composition: 3-methylbutene-1 99.78 wt.-%, propane 0.18 wt.-%, butene 0.01 wt.-%, higher than  $\text{C}_6$  hydrocarbons 0.02 wt.-%. Figure 1 shows the density of liquid 3-methylbutene-1 at various temperatures. The monomer which was used in larger-scale experiments was a Phillips pure grade. It was passed through towers filled with anhydrous calcium chloride and barium oxide. Vapor-phase chromatography showed the following composition: 3-methylbutene-1 99.97 wt.-%, isoprene 0.019 wt.-%, 2-methylbutene-2 0.007 wt.-%, pentene-1 0.001 wt.-%.

Carbon disulfide (reagent grade, Matheson, Coleman & Bell Company) was stored over molecular sieves. Before use the material was filtered and chilled to Dry Ice temperature and cold-filtered to freeze out adventitious foreign sulfides or dissolved sulfur. Gas chromatographic analysis showed the presence of two unidentified trace impurities.

Propane (instrument grade, The Matheson Company) was used without further purification. It was led into the dry box and condensed at  $-78^{\circ}\text{C}$ . Gas chromatography with a 50-ft. 2,5-hexadiene column at  $0^{\circ}\text{C}$ . indicated 99.9 wt.-% propane and traces of ethane, isobutane, and *n*-butane.

*n*-Pentane (Phillips Company, 99+%) was kept over molecular sieves (5A) and distilled before use. Gas chromatographic analysis indicated the following composition: *n*-pentane 97.9 wt.-%, isopentane 1.2 wt.-%, 2,2-dimethylbutane 0.7 wt.-%, 2-methylpentane 0.1 wt.-%, 3-methylpentane 0.1 wt.-%, and traces of isobutane, *n*-butane, unsaturated C<sub>5</sub>, and *n*-hexane.

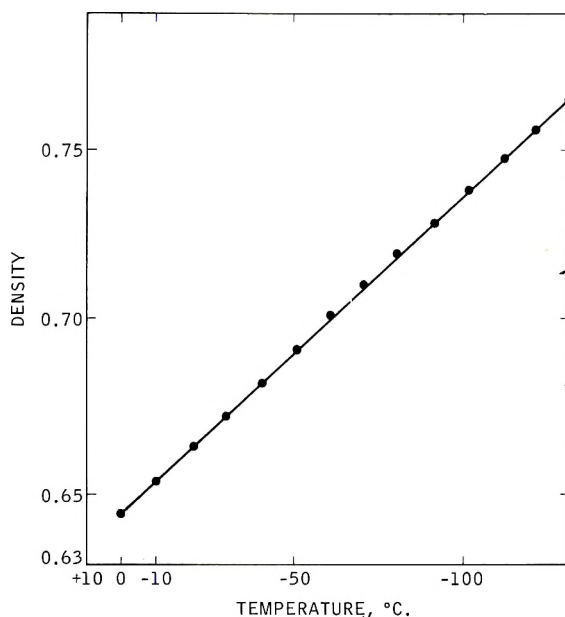


Fig. 1. Density of liquid 3-methylbutene-1.

Methyl chloride (The Matheson Company) was passed through scrubbers containing anhydrous calcium chloride, 96–98% sulfuric acid, and sodium hydroxide flakes in larger-scale experiments, while it was scrubbed with molecular sieves and barium oxide for small-scale runs in the dry box.

Methyl bromide (The Matheson Company, 99.5% purity) was used without further purification. The chemical was distilled into the dry box. Gas chromatographic analysis indicated the presence of 0.5 wt.-% methyl chloride and traces of CO<sub>2</sub>.

## 2. Procedures

**Catalyst Preparation.** Aluminum chloride solutions were prepared by adding the salt to methyl chloride, refluxing for 15 min., and filtering. The concentration of the solution was determined by titration.<sup>7</sup> Aluminum bromide catalyst solutions were prepared by crushing a submerged sealed vial of 100 g. aluminum bromide under 200 ml. of carbon disulfide. This catalyst stock solution was diluted with desired amounts of carbon disulfide just before each experiment.

**Experimental Technique.** All manipulations and experiments with  $\text{AlBr}_3$  and some with  $\text{AlCl}_3$  were carried out in a dry box under nitrogen atmosphere. General equipment was described earlier.<sup>8</sup> The average moisture content in the atmosphere was about 50 ppm. A typical polymerization experiment was carried out as follows. The reactor was submerged in the cooling bath filled with a hydrocarbon heat exchange fluid. The precooled solvent (usually propane) and monomer were introduced into the flask and thermoequilibrated for about 20–30 min. The total volume of monomer and diluent was usually 300 ml., and monomer concentration was 1 mole/l. At zero time, 10 ml. of precooled catalyst solution of suitable concentration was introduced into the vigorously stirred mixture. Polymerization started immediately. At suitable time intervals 10-ml. aliquots were withdrawn from the homogeneous reaction mixture with a precooled pipet and the sample quenched in cold methanol. The withdrawing of samples started as soon as it was possible after catalyst introduction. Temperature fluctuations were less than  $\pm 1.0^\circ\text{C}$ . during the experiment. The samples were precipitated with methanol and dried at  $60^\circ\text{C}$ . *in vacuo*. Larger-scale experiments with aluminum chloride catalyst were carried out in a stirred three-liter brass reactor (to insure better heat transfer) with a glass cover under nitrogen atmosphere. The reactor was submerged in liquid ethylene at its boiling point ( $-102^\circ\text{C}$ .). Sampling was accomplished by application of nitrogen pressure on the system and collecting an aliquot from the sampling tube. A typical charge was as follows: 155 ml. 3-methylbutene-1, 2303 ml. *n*-pentane, and 1022 ml. aluminum chloride catalyst solution (0.0198 moles/l. methyl chloride). This reaction was homogeneous. When the pentane was replaced by methyl chloride the reaction was homogeneous above  $-50^\circ\text{C}$ ., while at lower temperatures the polymer precipitated from the solution. The catalyst was added last, at zero time. Where it was desirable to use various catalyst concentrations suitable adjustments were made to maintain the same solvent system. For rate studies, 200-ml. samples were taken in a chilled graduate at specified time intervals and quenched immediately in an excess of isopropanol. The polymer was washed with fresh isopropanol and dried under vacuum. The poly-3-methylbutene-1 obtained through cationic polymerization is a colorless, amorphous, somewhat rubbery material. It is soluble in hydrocarbons, carbon disulfide, carbon tetrachloride, and ethers, but is insoluble in alcohol and acetone. Its second-order transition point is in the range  $-25$  to  $-15^\circ\text{C}$ .

**Molecular Weights.** Inherent viscosities of unfractionated polymer samples in diisobutylene solution (1 mg./1 ml.) at  $20^\circ\text{C}$ .<sup>9</sup> were determined. End-group unsaturation was established by the iodine-mercuric acetate method.<sup>10,11</sup> Independent vapor-phase osmometer determinations and end-group analyses as well as solution viscosity studies (for approximate weight-average molecular weights) were carried out on selected samples. These results indicated that the range of inherent viscosities (0.2–0.6) obtained in these studies corresponds to 5,000–70,000 number-average and 20,000–

120,000 weight-average molecular weights. Since the molecular weights are given in units of inherent viscosities, only qualitative molecular weight conclusions (trends) can be made.

## RESULTS

### 1. Molecular Weight Studies

**Effect of Temperature.** The effect of temperature on the molecular weights of poly-3-methylbutene-1 is shown in Figure 2. In this series of experiments 10 ml. of 0.0329 mole/l.  $\text{AlBr}_3$  in  $\text{CS}_2$  was added to 300 ml. of 1.0 mole/l. 3-methylbutene-1 in propane at  $-62$ ,  $-69$ ,  $-78$ ,  $-85$ , and  $-90^\circ\text{C}$ . Final catalyst concentration was  $10.6 \times 10^{-4}$  mole/l. At various time intervals appropriate samples were withdrawn and the conversion and the viscosities determined.

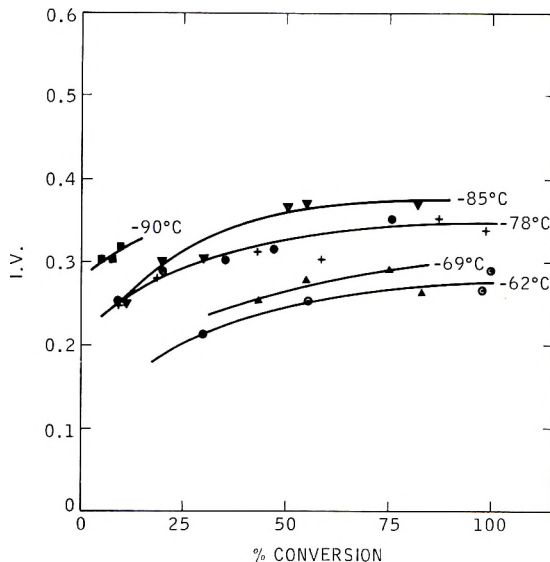


Fig. 2. The effect of temperature on the molecular weight of poly-3-methylbutene-1 obtained with  $\text{AlBr}_3$  catalyst.

The results of a similar larger-scale series of runs (see experimental part) in which  $\text{AlCl}_3$  was used as catalyst are shown in Figure 3. Detailed experimental conditions are shown in the legend to Figure 3.

Apparently the molecular weights increase with decreasing temperature at identical conversion levels in every system investigated. The fact that molecular weights increase as temperatures decrease is well established in most cationic and anionic systems. Apparently, the activation energy of chain breaking or terminating is higher than that for propagation, so that they can be "frozen out" at lower temperatures. Polymerization was quite

slow with  $\text{AlBr}_3$  at  $-90^\circ\text{C}$ . so that only a few data points were collected and these at low conversions.

The fact that the molecular weights increase with conversion and seem to reach their maximum at high conversions is significant. Slowly increasing molecular weights are quite unusual in vinyl type polymerizations. Both in free radical or ionic mechanisms the final molecular weights are reached within very short periods of time. When aliquots of reaction mixtures are analyzed as a function of time one usually finds unreacted monomers and high polymers. Intermediate species (oligomers) are absent, except in "living" polymers<sup>12</sup> with carbanion propagating centers. Our system, however, cannot be a true "living" polymer because the  $[\text{M}]/[\text{C}]$  ratio does not seem to affect product molecular weight in the expected fashion.

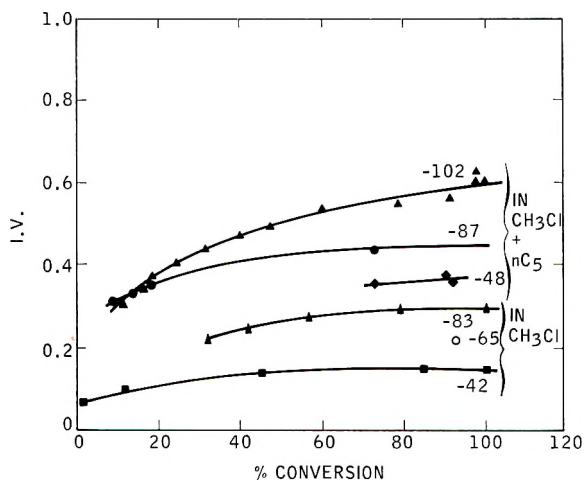
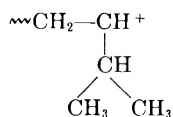


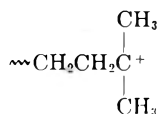
Fig. 3. The effect of temperature on the molecular weight of poly-3-methylbutene-1 obtained with  $\text{AlCl}_3$  catalyst. At temperatures of  $-102$ ,  $-87$ , and  $-48^\circ\text{C}$ .: catalyst concentration was  $28.8 \times 10^{-4}$  moles/l., monomer concentration 0.416 moles/l., composition of the diluent: 70 vol.-% *n*-pentane + 30 vol.-% methyl chloride. At  $-83^\circ\text{C}$ ., catalyst concentration was  $138 \times 10^{-4}$  moles/l., monomer concentration 1.8 moles/l., At  $-65^\circ\text{C}$ ., catalyst concentration was  $29 \times 10^{-4}$  moles/l., monomer concentration 1.94 moles/l. At  $-42^\circ\text{C}$ ., catalyst concentration was  $31 \times 10^{-4}$  moles/l., monomer concentration, 0.91 moles/l. The diluent was pure methyl chloride in the runs at  $-83$ ,  $-65$ , and  $-42^\circ\text{C}$ .

Perhaps the increase in molecular weight with conversion can be explained as follows: As the concentration of monomer decreases throughout a run, the lifetime of the carbonium ions





will increase and hence the rearrangement to the more stable ion



will be favored. If the latter ion tends to undergo chain transfer with monomer less readily than the former, the molecular weight will increase as observed.

The effect of pentane in the  $\text{AlCl}_3$  runs is noteworthy. Increased molecular weights were obtained from polymerizations in the presence of this hydrocarbon as compared to results from runs conducted in the absence of this solvent. This effect becomes even more significant considering that the monomer concentrations in the runs with pentane were 2–5 times lower than those without pentane. Differences in catalyst concentrations cannot be invoked to explain the phenomenon because it has been shown (see below) that differences in catalyst concentration do not affect the molecular weight. It should be pointed out that in runs with pure methyl chloride the polymer tends to precipitate out of solution (“quasiheterogeneous” polymerization) below about  $-50^\circ\text{C}$ . Nonetheless, limited propagation in the precipitated or swollen phase is not believed to account for decreased molecular weights. It is shown in Figure 3 through comparison of runs at  $-42$  and  $-48^\circ\text{C}$ . that *n*-pentane greatly increases molecular weight even though precipitation of polymer is not involved. One possible explanation for increased molecular weights in the presence of pentane could be the suppression of solvent transfer involving methyl chloride.

**Effect of Catalyst Concentration.** The influence of catalyst concentration on molecular weight was investigated with the use of  $\text{AlBr}_3$  and  $\text{AlCl}_3$  catalysts.  $\text{AlBr}_3$  (10 ml.) in carbon disulfide solutions of varying strength was introduced into 300 ml. of 1.0 mole/l. 3-methylbutene-1 mixtures with propane at  $-78^\circ\text{C}$ . Sampling technique was similar to that used previously. Figures 4 and 5 show the findings for  $\text{AlBr}_3$  and  $\text{AlCl}_3$  systems, respectively. Experimental details used with the  $\text{AlCl}_3$  catalyst are given in the legend of Figure 5.

Apparently in these systems the molecular weights are independent of catalyst concentration. Unchanged molecular weights obtained with various catalyst concentrations indicate unimolecular termination. The molecular weight-increasing effect of pentane is apparent when  $\text{AlCl}_3$  is used in this representation (Fig. 5). Also as pointed out before, molecular weights increase with conversion. The molecular weight curve obtained with  $\text{AlBr}_3$  in propane and that with  $\text{AlCl}_3$  in methyl chloride are parallel to each other (from about 10% conversion) and show a vertical displacement in favor of the  $\text{AlCl}_3$  system. Increased molecular weights could be due to differences in the catalyst ( $\text{AlCl}_3$  vs.  $\text{AlBr}_3$ ), the solvent ( $\text{CH}_3\text{Cl}$  vs.  $\text{C}_3\text{H}_8$ ), or monomer concentrations (1 vs. 1.67 mole/l.). Increased

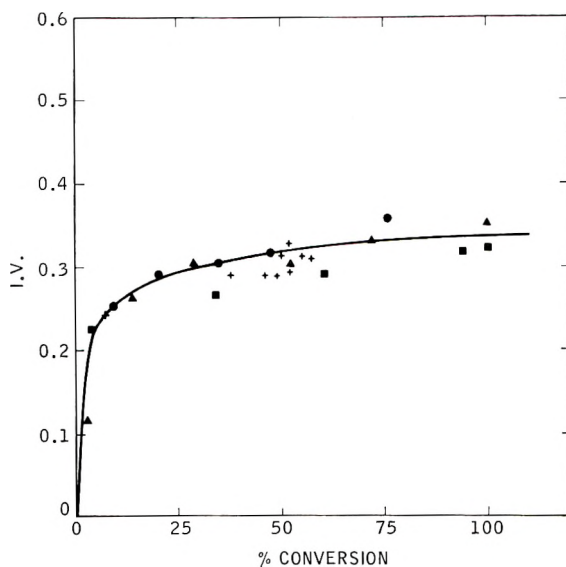


Fig. 4. The effect of  $\text{AlBr}_3$  concentration on the molecular weight of poly-3-methylbutene-1 at  $-78^\circ\text{C}$ .: ( $\blacksquare$ )  $31.8 \times 10^{-4}$  mole/l.; ( $\blacktriangle$ )  $15.8 \times 10^{-4}$  mole/l.; ( $\bullet$ )  $10.6 \times 10^{-4}$  mole/l.; (+)  $7.97 \times 10^{-4}$  mole/l.

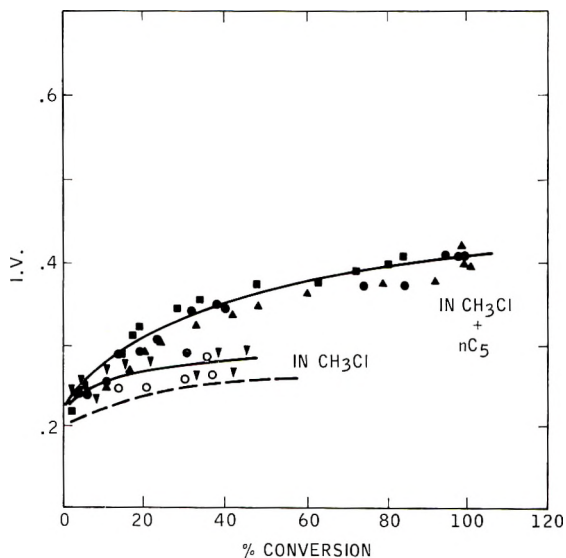


Fig. 5. The effect of  $\text{AlCl}_3$  concentration on the molecular weight of poly-3-methylbutene-1 at  $-102^\circ\text{C}$ . in methyl chloride + *n*-pentane, monomer concentration 0.416 moles/l., diluent composed of 70 vol.-% *n*-pentane + 30 vol.-% methyl chloride: cat. ( $\blacktriangle$ )  $28.8 \times 10^{-4}$  mole/l.; ( $\bullet$ )  $43.3 \times 10^{-4}$  mole/l.; ( $\blacksquare$ )  $57.6 \times 10^{-4}$  mole/l.; in methyl chloride: monomer concentration 1.67 mole/l.; ( $\circ$ )  $290 \times 10^{-4}$  mole/l., ( $\blacktriangledown$ )  $230 \times 10^{-4}$  mole/l., ( $\circ$ )  $160 \times 10^{-4}$  mole/l. The broken line is the  $\text{AlBr}_3$  curve of Fig. 4.

monomer concentrations are expected to increase molecular weight. Whether or not the catalyst and/or the solvent have additional influence cannot be confidently decided from available information.

The shape of the molecular weight curves deserves comment. None of these curves (Figs. 2-5) can be smoothly extrapolated back to zero, and there always appears to be a distinct break at low conversion levels. It would appear that such a distinct break indicates a change in mechanism, e.g., after a short upsurge in the molecular weight a lesser rate of growth takes over. One way of explaining this situation would be to assume the creation of a molecular weight "poison" which after a certain amount of growth would interfere with propagation. However, rate data (see below) do not corroborate this hypothesis. The rates are reproducible straight

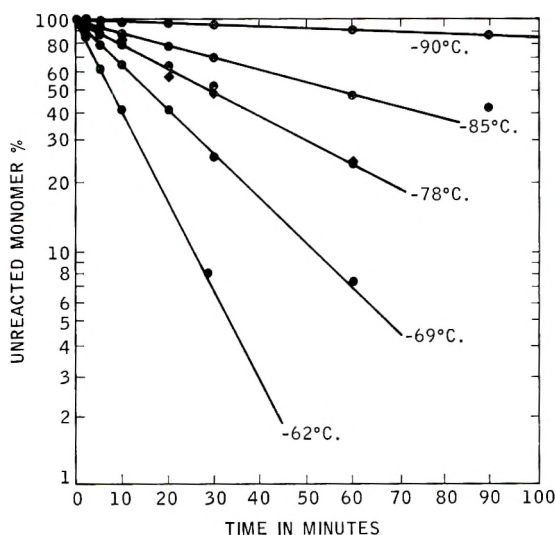


Fig. 6. Rate of polymerization at various temperatures.

lines (Fig. 6) and do not indicate any retardation (concavity toward the ordinate) which would be expected to occur in the presence of a poison.

The phenomenon can be easily explained by assuming changes in the molecular weight distribution. The viscosity-average molecular weights ( $\bar{M}_v$ ) which we are measuring are, just as the weight-average molecular weights ( $\bar{M}_w$ ), strongly sensitive to long chains. At the first instance of the polymerization some statistical amount of the catalyst initiates a certain number of chains and the carbonium ion grows to a certain length. The molecular weight distribution is fairly sharp at this point. As polymerization progresses, the chains grow, terminate, and initiate new chains. Thus the  $\bar{M}_v$  will increase somewhat, but the main change is the broadening of the  $\bar{M}_v$  distribution. From rate measurements we know that propagation proceeds smoothly until high conversion levels are reached.

## 2. Rate Studies

The rate of the homogeneous polymerization of 3-methylbutene-1 with  $\text{AlBr}_3$  catalyst in propane solvent was studied in detail. The catalyst was dissolved in carbon disulfide vehicle. Precooled catalyst solutions were introduced into stirred monomer-solvent mixtures under various experimental conditions, and the rate of polymerization was determined by weight measurements on samples withdrawn from the reaction mixture.

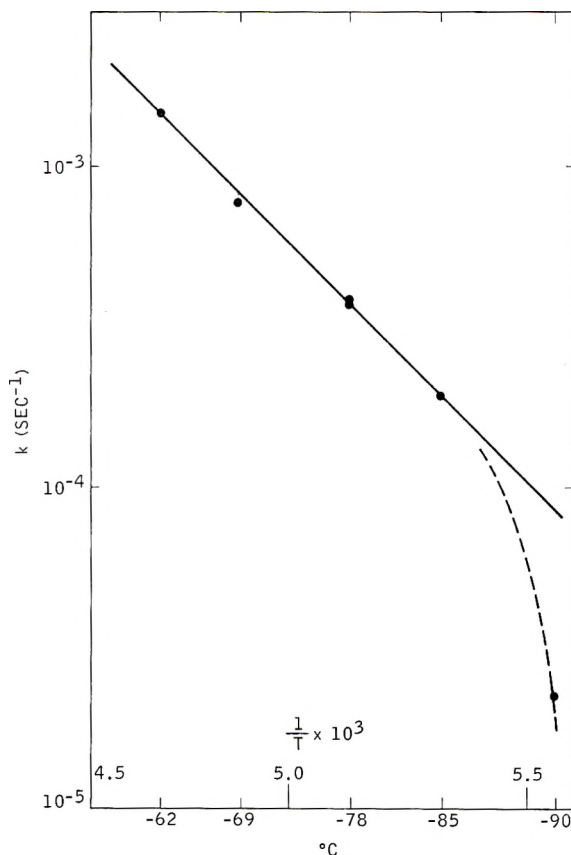


Fig. 7. Arrhenius plot of the 3-methylbutene-1-propane- $\text{AlBr}_3$ -carbon disulfide system.

First it was established that the rate was first-order in monomer. Subsequently, the influence of temperature on the rate was investigated. Thus, in a series of experiments, 10 ml. of 0.0329 mole/l.  $\text{AlBr}_3$  in  $\text{CS}_2$  was added to 300 ml. of 1.0 mole/l. monomer solution at various temperatures. Figure 6 shows the rate data obtained in this system. Above  $-60^{\circ}\text{C}$ . the reaction was too fast to be followed, whereas at  $-90^{\circ}\text{C}$ . and below the rate became too slow. The first-order (or apparent) rate constants were calculated, and an Arrhenius-type plot was constructed (Fig. 7). The apparent

activation energy calculated from this plot is 6.57 kcal./mole. The value obtained at  $-90^{\circ}\text{C}$ . greatly deviates from the linear portion of the plot. It is possible that some undetermined physical factor (complication due to insolubility at low temperatures, or freezing out of  $\text{CS}_2$ ) is responsible for this deviation, rather than a true change in the mechanism. A second possibility is that the activation energy of initiation is high enough so that this process becomes rate-determining at low temperatures.

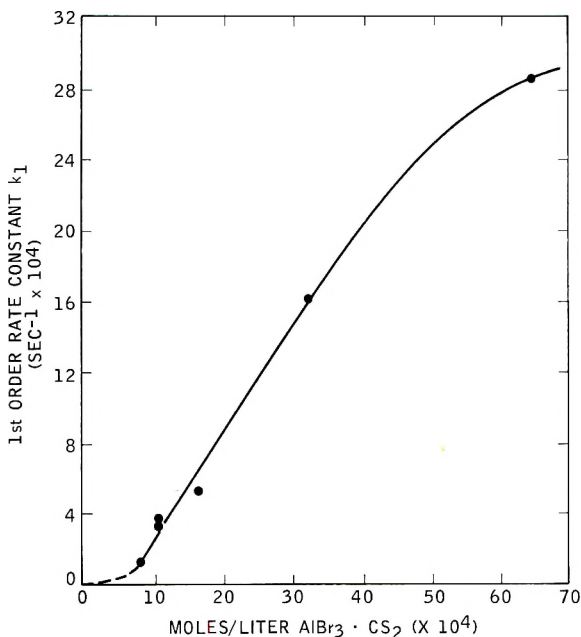


Fig. 8. Influence of catalyst concentration on polymerization of 3-methylbutene-1 in propane at  $-78^{\circ}\text{C}$ .

In another series of experiments, the influence of catalyst concentration on the rate of polymerization has been investigated.  $\text{AlBr}_3$  catalyst solutions (10 ml.) of various concentrations were added to 300 ml. of 1.0 mole/l. 3-methylbutene-1 in propane diluent at  $-78^{\circ}\text{C}$ . In Figure 8 the first-order rate constant  $k_1$  for monomer disappearance is plotted against catalyst concentration.

From these experiments the true, overall rate constant  $k_0$  can be obtained in the following manner.

Assuming that

$$-d[\text{M}]/dt = k_0 [\text{M}] [\text{C}]$$

i.e., the reaction is first order in monomer and in catalyst and that  $[\text{C}]$  is constant during an experiment under steady-state conditions, we can write

$$-d \ln [\text{M}]/dt = k_0 [\text{C}]$$

By integration we obtain

$$\ln [M] = -k_0[C]t + \text{Const.}$$

at  $t = 0$ ,  $\text{Const.} = \ln [M_0]$ .

Thus  $\ln [M]/[M_0] = -k_0 [C] t$ .

and since

$$\ln [M]/[M_0] = -k_1 t$$

Therefore

$$k_1 = k_0[C]$$

Thus, the plot of  $k_1$  versus  $[C]$  should be a straight line whose slope is  $k_0$ . That this is indeed the case was found experimentally over a wide catalyst concentration range ( $5\text{--}40 \times 10^4$  mole/l.) (Figure 8). On this basis the true overall rate constant of the system was calculated as 0.610 l./mole-sec.

The fact that the curve deviates from linearity at higher catalyst concentrations can be explained by local monomer depletion. At high  $\text{AlBr}_3$  concentrations the monomer is apparently consumed faster than it is replenished, which decreases the rate of polymerization. Another possible explanation could be that at high catalyst concentrations the cocatalyst (probably traces of water) concentration becomes rate-determining, i.e. the effective catalyst concentration is less than the  $\text{AlBr}_3$  actually introduced because of lack of cocatalyst. It should be pointed out that the curve does not go through the origin. This deviation could be used as a measure of the level of impurities present. Thus, the concentration of catalyst-consuming "poisons" in this system is equivalent to  $5 \times 10^{-4}$  moles/l.  $\text{AlBr}_3$ .

### 3. Influence of Dielectric Constant

The influence of solvents with higher dielectric constants on the rate of polymerization was investigated. Significantly, it was found that when  $\text{AlBr}_3$  was dissolved in methyl bromide whose dielectric constant is 14.86 at  $-78^\circ\text{C}$ ., the rates became too fast to follow in the same catalyst concentration range as those studied in propane, i.e., above  $10.3 \times 10^{-4}$  mole/l. the rate was too fast to follow, whereas below  $1.98 \times 10^{-4}$  mole/l.  $\text{AlBr}_3$  it was too slow for convenient investigation.

The rate-increasing role of methyl bromide was independently confirmed. In one experiment, 135 ml. precooled methyl bromide was introduced into a 3-methylbutene-1/carbon disulfide system (1 mole/l. monomer in 310 ml. total volume) in which polymerization progressed at a measurable rate at  $-100^\circ\text{C}$ . (catalyst concentration was 0.051 moles/l. in 310 ml.). Immediately after the addition of this chemical the temperature rose rapidly to  $-90^\circ\text{C}$ ., and a distinct yellow color developed indicating an abundance of carbonium ions. Four minutes later, 100% conversion was reached and the reactor was filled with jellylike polymer.

Experiments in toluene as basic diluent showed that both rate of polymerization and molecular weights were depressed as compared with those

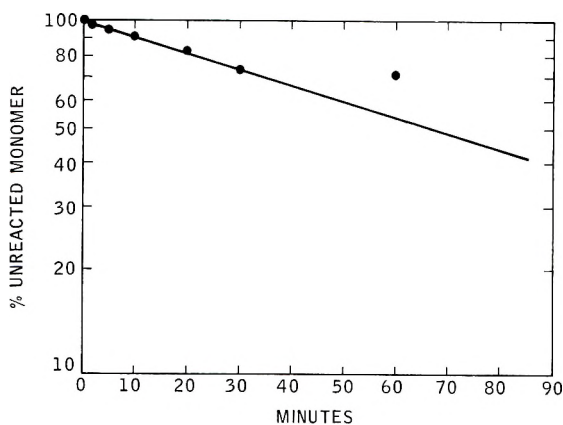


Fig. 9. Rate of polymerization of 3-methylbutene-1 with  $\text{AlBr}_3$  in toluene at  $-78^\circ\text{C}$ .

obtained in propane under similar experimental conditions. The isolated polymers were heavy oils, whereas in propane tough masses were obtained (monomer concentration 1.0 mole/l. of toluene, final catalyst concentration  $4.84 \times 10^{-2}$  mole/l.  $\text{AlBr}_3$  in  $\text{CS}_2$ , temperature  $-78^\circ\text{C}$ .) On the basis of Figure 9, the first-order rate constant is  $1.725 \times 10^{-4}$  sec. $^{-1}$ . The last point in Figure 9 falls off the first-order plot, indicating that the rate could have slowed down. Unfortunately, no more experimental points are available in this range. In calculating the first-order rate constant we disregarded this value.

These results are not surprising, since it is known that toluene is an effective chain transfer agent in electrophilic polymerizations.<sup>13-16</sup> Apparently, chain breaking (probably by solvent transfer) not only depresses the chain length but also retards the rate. Such low molecular weights indicate that the basicity of the monomer is only little higher than that of toluene. If toluene were more basic toward  $\text{AlBr}_3$  than the monomer, no polymerization could have taken place. Isobutene, on the other hand, polymerizes readily to high molecular weight products in the same solvent, indicating that there is a large difference between the basicities of these monomers.

The authors are indebted to Dr. F. P. Baldwin for helpful criticism and to Dr. I. H. Billick for stimulating discussions in the course of this work. Mr. J. Hrabinski's skillful assistance is gratefully acknowledged.

### References

1. Norris, R. G. W., and J. P. Joubert, *J. Am. Chem. Soc.*, **49**, 873 (1927).
2. Leendertse, J. J., A. J. Tulleners, and H. L. Waterman, *Rec. Trav. Chim.*, **53**, 715 (1934).
3. Schaad, R. E., in *The Chemistry of Petroleum Hydrocarbons*, Reinhold, New York, 1955, p. 236.
4. Webb, W. L., U. S. Pat. 2,099,090 to Standard Oil of Indiana, 1937.
5. Thomas, R. M., and H. C. Reynolds, U. S. Pat. 2,387,784 to Standard Oil (N. J.), 1945.
6. Kennedy, J. P., and R. M. Thomas, *Makromol. Chem.*, **53**, 28 (1962).
7. Kennedy, J. P., and R. M. Thomas, *J. Polymer Sci.*, **46**, 481 (1960).

8. Kennedy, J. P., and R. M. Thomas, in *Advances in Chemistry*, No. 43, American Chemical Society, 1962, p. 111.
9. Flory, P. J., *Principles of Polymer Chemistry*, Cornell Univ. Press, Ithaca, N. Y., 1953, p. 309.
10. Gallo, S. G., H. K. Wiese, and J. F. Nelson, *Ind. Eng. Chem.*, **40**, 1277 (1948).
11. McNall, L. R., and L. T. Eby, *Anal. Chem.*, **29**, 951 (1957).
12. Szwarc, M., *Nature*, **178**, 1168 (1956).
13. Overberger, C. C., and F. G. Endres, *J. Am. Chem. Soc.*, **75**, 5349 (1953).
14. Plesch, P. H., *J. Chem. Soc.*, **1953**, 1653.
15. Plesch, P. H., *J. Chem. Soc.*, **1953**, 1659.
16. Plesch, P. H., *J. Chem. Soc.*, **1953**, 1662.

### Résumé

On a étudié entre  $-62^{\circ}$  et  $-102^{\circ}\text{C}$  la polymérisation cationique du 3 méthyl-butène-1, en employant comme initiateurs le chlorure d'aluminium et le bromure d'aluminium. Les polymérisations sont homogènes en présence de pentane et également au-dessus de  $-50^{\circ}\text{C}$  en présence du chlorure de méthyle. Par contre le polymère a tendance de précipiter en-dessous de  $50^{\circ}\text{C}$  dans le chlorure de méthyle. Pour le même degré de conversion le poids moléculaire du poly(3-méthyl-butène-1) augmente quand la température diminue. Il est significatif que les poids moléculaires augmentent avec le degré de conversion et ils semblent atteindre leur maximum aux conversions élevées. On a obtenu des poids moléculaires plus hauts dans des mélanges de chlorure d'alcoyle et *n*-pentane qu'en solution dans le chlorure de méthyle seul. Les poids moléculaires sont indépendants des concentrations du catalyseur dans le domaine étudié ( $31,8$  à  $7,97 \times 10^{-4}$  mole/l.  $\text{AlBr}_3$  et  $57,6$  à  $28,8 \times 10^{-4}$  mole/l.  $\text{AlCl}_3$ ). On a étudié la vitesse de polymérisation homogène en présence du bromure d'aluminium en solution dans le propane. La vitesse est de  $0,610$  l. mole $^{-1}$  sec $^{-1}$ . L'énergie d'activation apparente, calculée à partir de l'équation d'Arrhénius est  $6,57$  kcal/mole. La vitesse de polymérisation augmente d'une manière significative dans le bromure de méthyle (effet de la constante diélectrique). Dans le toluène le poids moléculaire aussi bien que la vitesse sont fortement diminués. Ceci indique la prépondérance du mécanisme de rupture de chaîne impliquant ce solvant.

### Zusammenfassung

Die kationische Polymerisation von 3-Methylbuten-1 mit Aluminium-chlorid und Aluminiumbromid wurde im Bereich von  $-62$  bis  $-102^{\circ}\text{C}$  untersucht. Die Polymerisation verläuft in Gegenwart von Pentan und oberhalb  $-50^{\circ}\text{C}$  in Methylchlorid homogen. Unterhalb  $-50^{\circ}$  neigt das Polymere in Methylchlorid zum Ausfallen. Das Molekulargewicht von Poly-3-methylbuten-1 nimmt bei gleichem Umsatz mit fallender Temperatur zu. Das Molekulargewicht zeigt eine charakteristische Zunahme mit dem Umsatz und scheint bei hohem Umsatz ein Maximum zu erreichen. In *n*-Pentan-Alkylchlorid-Gemischen wurden höhere Molekulargewichte erhalten als in Methylchloridlösung allein. Die Molekulargewichte sind im untersuchten Bereich ( $31,8$  bis  $7,97 \times 10^{-4}$  Mol/l  $\text{AlBr}_3$  und  $57,6$  bis  $28,8 \times 10^{-4}$  Mol/l  $\text{AlCl}_3$ ) von der Katalysatorkonzentration unabhängig. Die Geschwindigkeit der homogenen Polymerisation mit Aluminiumbromid in Propan als Lösungsmittel wurde untersucht. Die Geschwindigkeit ist von erster Ordnung in bezug auf Monomer- und Katalysatorkonzentration und die Geschwindigkeitskonstante beträgt  $0,601$  l Mol $^{-1}$  sek $^{-1}$ . Aus dem Arrheniusdiagramm berechnet sich die scheinbare Aktivierungsenergie zu  $6,57$  kcal/Mol. In Methylbromid nimmt die Polymerisationsgeschwindigkeit in charakteristischer Weise zu (Einfluss der Dielektrizitätskonstanten). In Toluol werden Molekulargewicht und Geschwindigkeit stark herabgesetzt, was auf das Vorherrschen eines Kettenabbruchmechanismus bei diesem Lösungsmittel hinweist.

Received September 21, 1962

Revised October 22, 1962



## Cationic Polymerizations of 3-Methylbutene-1. II. Polymerizations at Extremely Low Temperatures

J. P. KENNEDY, *Chemicals Research Division, Esso Research and Engineering Company, Linden, New Jersey*

### Synopsis

The cationic polymerization of 3-methylbutene-1 has been studied at extremely low temperatures e.g.,  $-130^{\circ}\text{C}$ . and below. Practically no polymerization occurs, even at high catalyst concentrations, and the system lies "dormant" at  $-150^{\circ}\text{C}$ . The molecular weight-conversion curve obtained with  $\text{AlCl}_3$  is a straight line which can be extrapolated through the origin. The slope of this line is determined by monomer concentrations. Higher molecular weights are obtained at the same conversion with higher monomer concentrations. With boron trifluoride catalyst, the linear part of the curve does not extrapolate back through the origin. Product molecular weights were higher in ethyl chloride than in pentene with  $\text{BF}_3$  at the same conversion level at  $-130^{\circ}\text{C}$ .

### Introduction

In the first paper of this series we discussed the kinetics of the cationic polymerization of 3-methylbutene-1 at temperatures ranging from  $-50$  to  $-100^{\circ}\text{C}$ .,<sup>1</sup> where rubbery and amorphous polymers are obtained. At  $-130^{\circ}\text{C}$ . or lower, crystalline products are formed.<sup>2</sup> In a further publication we described the x-ray characterization of two crystalline modifications ( $\alpha$  and  $\beta$  forms) of cationically obtained poly-3-methylbutene-1.<sup>3</sup> At this time we present kinetic experiments on crystalline poly-3-methylbutene-1 in the temperature range from  $-100$  to  $-150^{\circ}\text{C}$ .

### Experimental

The origin and purity of most of the materials used in this study has been described.<sup>1,3</sup> General experimental and polymerization techniques were identical to those used earlier.<sup>1</sup> The preparation of aluminum chloride catalyst was reported.<sup>3</sup> Boron trifluoride catalyst solutions were prepared by saturating ethyl chloride or *n*-pentane with the gas at  $-78^{\circ}\text{C}$ . and pre-cooling to experimental temperatures (usually  $-130^{\circ}\text{C}$ .).

No complications were encountered when boron trifluoride-ethyl chloride solutions were cooled down to  $-130^{\circ}\text{C}$ ., but phase separation occurred in pentane at about  $-120^{\circ}\text{C}$ . When solid boron trifluoride was added to pentane (at  $-140^{\circ}\text{C}$ .), a snow-white, heavy suspension was obtained. When this slurry warmed up, the boron trifluoride melted (m.p.  $-127^{\circ}\text{C}$ .), and collected in a separate heavy liquid phase below the hydrocarbon. On heating, this lower phase started to boil under the surface of the quies-

cent pentane layer and on continued heating it boiled off until completely disappeared. Similarly, when a pentane solution of boron trifluoride, which was saturated at  $-78^{\circ}\text{C}$ ., was cooled down it became milky at around  $-127^{\circ}\text{C}$ .. Below  $-130^{\circ}\text{C}$ .. the boron trifluoride froze out and became a continuous solid phase which clung to the walls of the container. In order to maintain our prechosen temperature level of  $-130^{\circ}\text{C}$ .. we added the heterogeneous  $\text{BF}_3$  catalyst suspension ( $-125$  to  $-127^{\circ}\text{C}$ .) to the reaction mixture stirred at  $-130^{\circ}\text{C}$ .. Because of the volatility of boron trifluoride, its concentrations are ill defined and are not specified.

### Results and Discussion

The effect of temperature on conversions and molecular weights of crystalline poly-3-methylbutene-1 has been investigated. In a typical experiment, precooled  $\text{AlCl}_3$  catalyst in ethyl chloride solvent was added to 3-methylbutene-1 stirred at  $-130^{\circ}\text{C}$ .. The withdrawing of aliquots was started as soon as feasible. After samples indicated that the reaction was progressing smoothly (55 min. after catalyst introduction) the temperature was suddenly dropped to  $-150^{\circ}\text{C}$ .. by introducing liquid nitrogen into the reactor and lowering the thermocontrol. The temperature was maintained at this level for the next 145 min., and sampling was continued periodically. After a total of 200 min. the temperature was quickly raised to  $-130^{\circ}\text{C}$ ., where it was maintained for another 95 min. Finally, the temperature

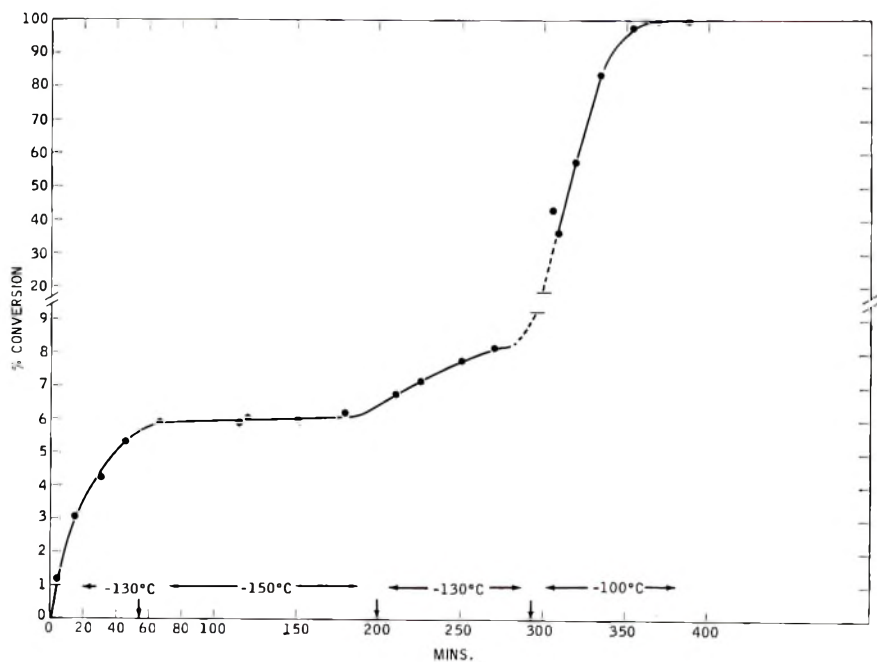


Fig. 1. Conversion vs. time of 3-methylbutene-1 polymerization at extremely low temperatures.

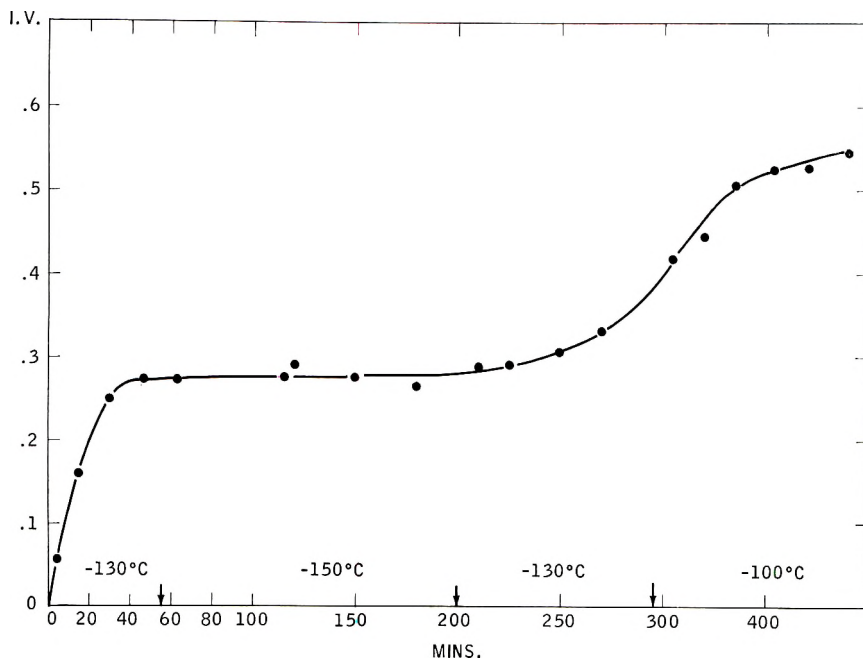


Fig. 2. Molecular weights vs. time of 3-methylbutene-1 polymerization at extremely low temperatures.

was raised to  $-100^{\circ}\text{C}.$ , and after 100 min. more of stirring at this level, the experiment was terminated.

Figures 1 and 2 show the changes of molecular weights and conversions as a function of time. Conversions start to increase exponentially at  $-130^{\circ}\text{C}.$  until the temperature is dropped to  $-150^{\circ}\text{C}.$  Remarkably, polymerization is slowed down tremendously within this  $20^{\circ}\text{C}.$  interval. Conversions increase only from 5.9% to about 6.2% over a period of 145 min. at  $-150^{\circ}\text{C}.$  As soon as the temperature is raised back to  $-130^{\circ}\text{C}.$  the rate picks up exactly where it was interrupted by dropping the temperature. If the (almost) horizontal section at  $-150^{\circ}\text{C}.$  is cut out from Figure 1, the curve continues exponentially (except for the 0.3% conversion increase) as if there was not a quiescent period. Crystalline polymer is formed during this part of the experiment. When the temperature is raised to  $-100^{\circ}\text{C}.$ , the polymerization suddenly "takes off" and rapidly reaches 100% conversion. Again, it is remarkable that a relatively small temperature increase (from  $-130$  to  $-100^{\circ}\text{C}.$ ) can induce such a large rate effect. Rubbery, amorphous products were obtained at this temperature level. Conversions were always relatively low at  $-130^{\circ}\text{C}.$ , and even the highest catalyst concentrations brought the reaction to a maximum of 25% completion. At these catalyst concentrations and at higher temperatures, e.g., at  $-100^{\circ}\text{C}.$ , 100% conversions were obtained.

The molecular weight pattern essentially follows that of conversion (Fig. 2). Initially, molecular weight rises exponentially at  $-130^{\circ}\text{C}.$ , but

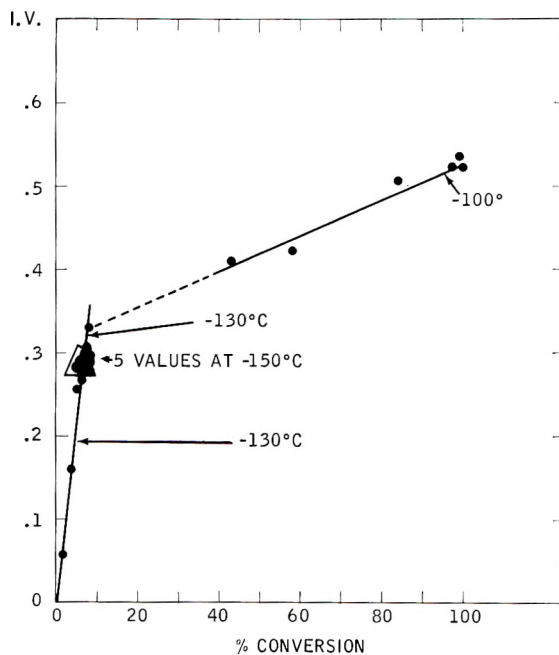


Fig. 3. Molecular weight vs. conversion (combination of Figs. 1 and 2) of 3-methylbutene-1 polymerization at extremely low temperatures.

levels off and remains unchanged when the temperature is dropped to  $-150^{\circ}\text{C}$ . Practically no polymerization takes place at this very low temperature. However, the propagating ability of the chains is not destroyed, they only lie dormant; when the temperature is raised to  $-130^{\circ}\text{C}$ , growth picks up again. No sudden increase in molecular weights occurs when the temperature is increased to  $-100^{\circ}\text{C}$ . The fact that conversions rise quickly from 9 to  $\sim 90\%$  without a simultaneous rise in molecular weights indicates that new initiation occurred and dormant catalyst or catalyst-monomer complexes suddenly start to grow. We have no evidence of branching which would also account for these facts.

The molecular weight and conversion curves are combined in Figure 3, where we plotted changes in molecular weights as a function of conversion at various temperatures. The first straight line describes the situation until the point when the temperature was raised to  $-100^{\circ}\text{C}$ . The  $-150^{\circ}\text{C}$ . interval appears as a single point on the curve indicating that the reaction "froze" at this temperature. The resumption of polymerization is indicated by four experimental values obtained in the second  $-130^{\circ}\text{C}$ . range. The slope decreases significantly when the temperature is raised to  $-100^{\circ}\text{C}$ ., but the curve remains linear. The two parts of the curve are connected with a broken line which corresponds with the broken line in Figure 1 indicating a warming up range of  $-130$  to  $-100^{\circ}\text{C}$ .

It is important that crystalline polymer ( $\alpha$  modification) was formed during the relatively slow polymerization period at  $-130^{\circ}\text{C}$ ., whereas

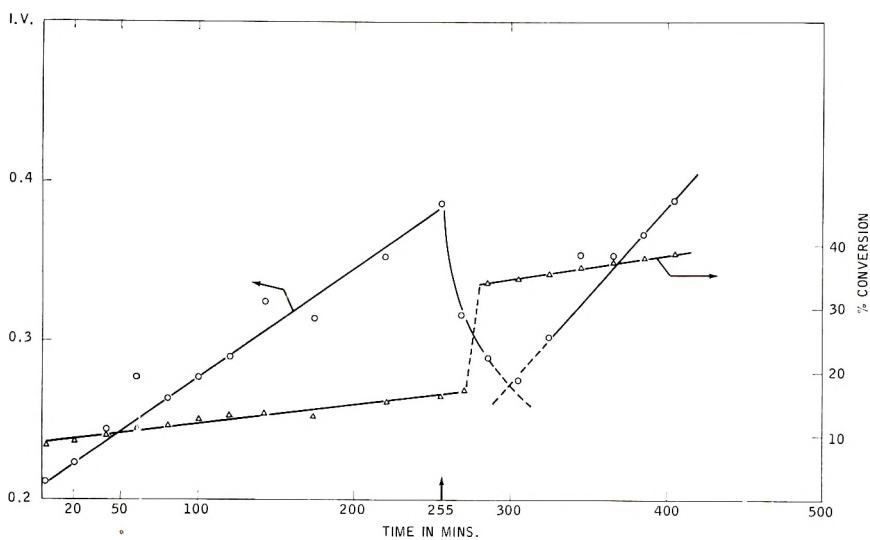


Fig. 4. Plots of conversions and molecular weights vs. time in the 3-methylbutene-1-aluminum chloride-ethyl chloride system at  $-130^{\circ}\text{C}$ .

amorphous material was obtained when the rate increased many fold at  $-100^{\circ}\text{C}$ .

In another series of experiment, fresh catalyst solution was introduced into a smoothly progressing polymerization at  $-130^{\circ}\text{C}$ . and concurrent changes in conversion and molecular weight were determined. Figure 4 shows the findings. The fresh catalyst was added after 255 min. of stirring at  $-130^{\circ}\text{C}$ . Conversions, which until this point progressed steadily to 17%, jumped to 34%. The molecular weights, which also increased almost linearly, however, rapidly decreased until a minimum was reached. After this sudden dip, the molecular weights started to rise again. The second increase was essentially parallel to that experienced before fresh catalyst solution was introduced.

This situation can be explained by the fact that fresh catalyst introduction means fresh initiation. Newly formed short chains temporarily depress average molecular weight until these units grow sufficiently to compensate for the average reducing effect of short chains. As soon as the new chains reach a certain length the molecular weight curve turns upward again. Significantly, the first part of the molecular weight as well as the conversion curves (prior to fresh catalyst introduction) are essentially parallel to the second part of the respective curves.

Figure 5 shows the combined molecular weight-conversion curves (combination of the curves in Figure 4). The point of fresh catalyst introduction is indicated by the arrow. Again, the first and the second parts of the experimental curves are essentially parallel indicating identical reaction mechanisms for both introductions of catalyst. Significantly, the extrapolated line goes through the origin.

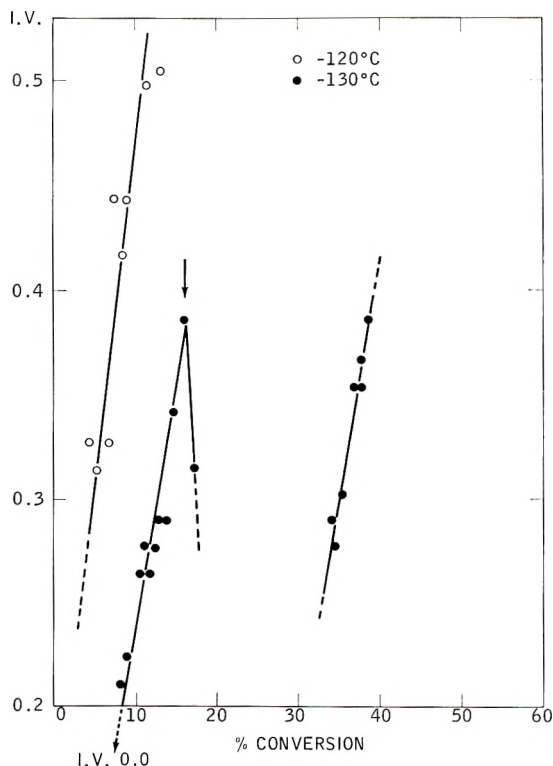


Fig. 5. Molecular weights vs. conversion in the 3-methylbutene-1-aluminum chloride-ethyl chloride system at  $-120$  and  $-130^{\circ}\text{C}$ .

Figure 5 also shows a molecular weight-conversion plot of an experiment carried out at  $-120^{\circ}\text{C}$ . The overall pattern is visibly identical to that of the experiment at  $-130^{\circ}\text{C}$ . A significant difference lies in the fact that this straight line does not go through the origin on extrapolation (it crosses the ordinate at about an inherent viscosity of  $\text{I.V.} = 0.1$ ). Earlier molecular weight-conversion curves obtained with a similar system at  $-78^{\circ}\text{C}$ .<sup>1</sup> indicate somewhat curved lines which extrapolate to the ordinate at even higher inherent viscosity values (about 0.2-0.3). This indicates the influence of temperature on the molecular weight distribution. The common features of these experiments at  $-130^{\circ}\text{C}$ . are straight molecular weight-conversion curves which on extrapolation go through the origin (Figs. 3, 5, and 6). It appears significant that these curves indicate immediate initiation after catalyst introduction followed by steady, uninterrupted propagation. Chain transfer and termination steps are apparently negligible (at least at low conversion levels). These findings seem to indicate a "living" polymer where (at given monomer and catalyst concentrations) growth is a function of time or conversion (and temperature). A forthcoming publication will discuss this aspect of the polymerization and the effect of monomer concentration on the rate.

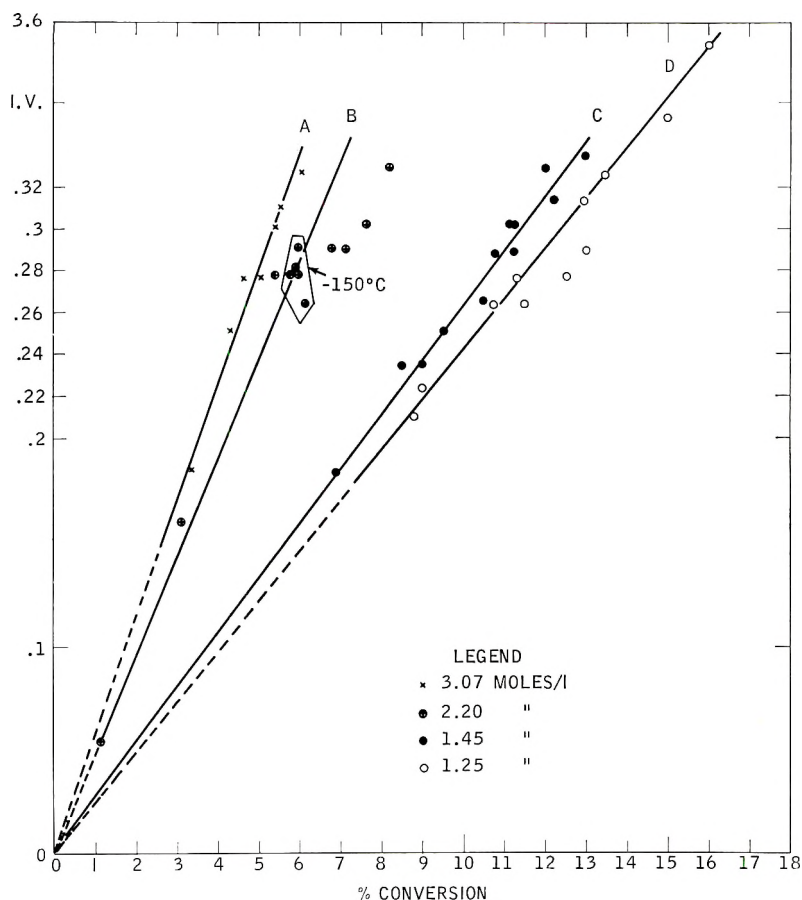
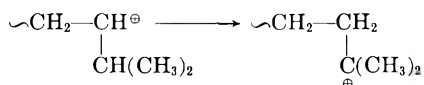


Fig. 6. Molecular weight vs. % conversion of various monomer concentrations at  $-130^{\circ}\text{C}$ .

Apparently this is a system with relatively slow propagation and one in which chain breaking and termination reactions are negligible. Lack of chain breaking and termination could be due to the stable tertiary carbonium ion which is the actual propagating species. The original secondary carbonium ion rearranges itself to the more stable tertiary one before propagation can take place,<sup>2</sup> e.g.,



Probably this hydride shift is extremely rapid and not rate-determining.

It should be emphasized that at higher conversions the molecular weight-conversion curve deviates from that of a straight line and converges to a maximum. This has been shown already at higher temperatures.<sup>1</sup> Thus, the straight molecular weight-conversion lines represent only the initial

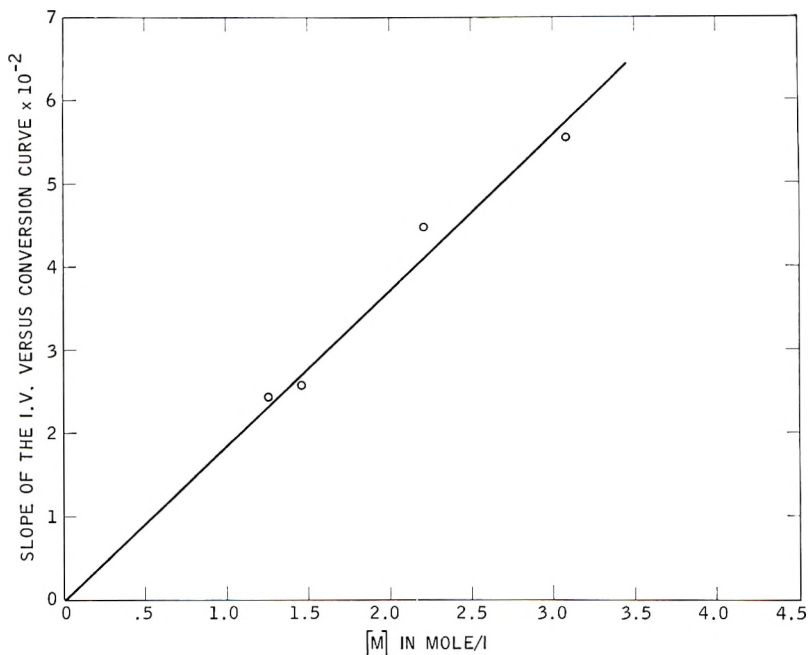


Fig. 7. Slopes of inherent viscosity-conversion curves vs. monomer concentration.

part of an otherwise first-order curve. Apparently, the lowering of temperature to  $-130^{\circ}\text{C}$ . decreases the rate of propagation to such an extent that this straight initial portion of the total overall curve can be studied.

The effect of monomer concentration on molecular weight-conversion curves has been investigated. In a series of experiments, solutions of  $\text{AlCl}_3$  in ethyl chloride were added to mixtures containing various concentrations of 3-methylbutene-1 and ethyl chloride at  $-130^{\circ}\text{C}$ . Molecular weights and conversions were determined simultaneously in samples withdrawn over a period of 100–300 minutes after catalyst introduction. Figure 6 shows the results. All experiments with  $\text{AlCl}_3$  in ethyl chloride solvent at  $-130^{\circ}\text{C}$ . resulted in straight molecular weight-conversion lines which on extrapolation crossed the origin. The slopes of these lines, however, were different and apparently depended on monomer concentration. The monomer concentrations (in mole/liter) employed are indicated in Figure 6. Line *B* in Figure 6 is identical to that shown in Figure 3; the five values obtained at  $-150^{\circ}\text{C}$ . are encircled. Indeed, the slope of the plot gave a straight line which also could be extrapolated through the origin. This is shown in Figure 7.

The exact physical meaning of this plot has not yet been derived. However, qualitatively it indicates that the higher the monomer concentration the faster the build up of molecular weights at the same conversion level.

In another series of experiments, 3-methylbutene-1 polymerizations were carried out in liquid vinyl chloride diluent with aluminum chloride-



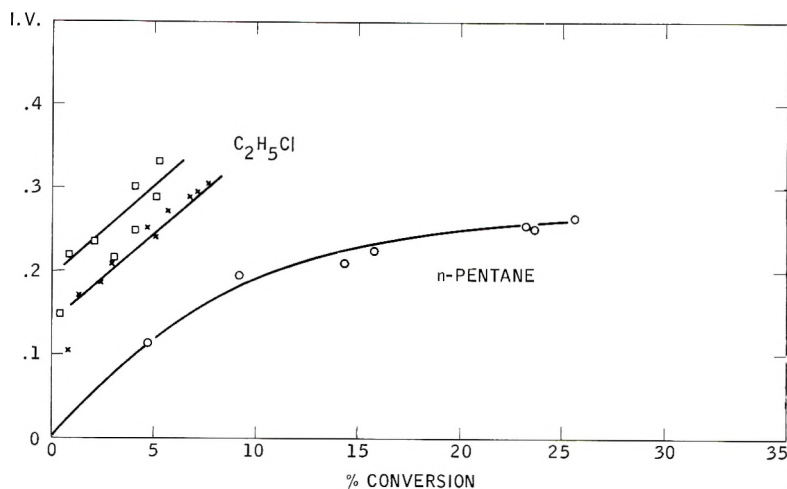


Fig. 8. Dependence of molecular weight on conversion of the 3-methylbutene-1-BF<sub>3</sub> system in various solvents at  $-130^{\circ}\text{C}$ .

ethyl chloride catalyst at  $-130^{\circ}\text{C}$ . Polymerizations under these conditions were generally retarded, e.g., the conversions remained below 5% after 300 min. and the inherent viscosities never exceeded 0.4. This finding is unusual, since the cationic polymerization of isobutene proceeds readily in vinyl chloride diluent,<sup>4</sup> even at  $-185^{\circ}\text{C}$ .<sup>5</sup> Apparently the  $\text{CH}_2=\text{CHCl}\cdot\text{AlCl}_3$  complex is weak enough against the strong base isobutene, but is too stable to polymerize easily the weaker base 3-methylbutene-1.

Similar experiments were conducted with BF<sub>3</sub> catalyst in ethyl chloride and *n*-pentane solvents. Catalyst solutions were prepared by saturating the respective solvent. Some of the results are summarized in Figure 8 by plotting molecular weights against conversion obtained at  $-130^{\circ}\text{C}$ . Reproducibility of the runs is satisfactory as indicated by the two runs in ethyl chloride. It should be pointed out that the higher of the two ethyl chloride curves was obtained in an experiment which was started and maintained at  $-150^{\circ}\text{C}$ . for 180 min. During this time interval at this temperature level there was practically no polymerization. When the temperature was raised rapidly to  $-130^{\circ}\text{C}$ . polymerization started and was followed by continuous sampling. The curved line in Figure 8 shows the results of an experiment in pentane. No polymerization occurred for 80 min. at  $-130^{\circ}\text{C}$ . using as catalyst 100 ml. of *n*-pentane saturated with BF<sub>3</sub> at  $-78^{\circ}\text{C}$ . When an additional 5 ml. of liquid (pure) BF<sub>3</sub> was added to the reaction mixture, polymerization started. Differences in viscosities obtained in ethyl chloride and in pentane solvents at  $-130^{\circ}\text{C}$ . are significant, since catalyst concentrations (which were ill defined in these experiments) do not affect molecular weights.<sup>1</sup> Apparently higher molecular weight product is obtained in the solvent with the higher dielectric constant.

The rate of polymerization is greatly increased when ethyl chloride is

added to a quiescent monomer-BF<sub>3</sub>-pentane mixture at -125°C. Similar results have already been reported for the monomer-AlBr<sub>3</sub>-carbon disulfide system at -100°C. to which methyl bromide was added.<sup>1</sup>

It is also significant that the linear part of the viscosity-conversion curve does not extrapolate to the origin. Apparently, the first phase of the polymerization involves a short but vigorous build-up in molecular weights (around 0.15 inherent viscosity at -130°C.). This situation is very similar to that observed with AlCl<sub>3</sub> and AlBr<sub>3</sub> catalysts at higher temperatures.<sup>1</sup> The fact that the linear part of the molecular weight-conversion line cannot be extrapolated back to zero origin, as is the case with aluminum chloride-initiated polymerizations under similar experimental conditions, indicates the possible effect of the nature of the catalysts on molecular weight distribution.

I am deeply grateful to R. M. Thomas for constructive criticism during the course of this work.

### References

1. Kennedy, J. P., L. S. Minckler, Jr., and R. M. Thomas, *J. Polymer Sci.*, **A2**, 367 (1964).
2. Kennedy, J. P., and R. M. Thomas, *Makromol. Chem.*, **53**, 28 (1962).
3. Kennedy, J. P., and R. M. Thomas, *Makromol. Chem.*, **64**, 1 (1963).
4. Kennedy, J. P., and R. M. Thomas, *J. Polymer Sci.*, **49**, 189 (1961).
5. Kennedy, J. P., and R. M. Thomas, *Polymerization and Polycondensation Processes*, Advances in Chemistry Series 34, American Chemical Society, Washington, D. C., 1962, Chap. 7.

### Résumé

On a étudié la polymérisation du 3-méthylbutène-1 à des températures extrêmement basses, c'est à dire, -130°C et plus bas. On ne constate pratiquement pas de polymérisation, même pas à des concentrations élevées en catalyseur et le système est "dormant" à -150°C. Dans le cas du AlCl<sub>3</sub> le graphique poids moléculaire-conversion donne une droite qui peut être extrapolée par l'origine. La pente de ces droites est déterminée par la concentration en monomère. Avec des concentrations en monomère plus élevées, on obtient à la même conversion des produits dont le poids moléculaire est plus élevé. Avec le BF<sub>3</sub> comme catalyseur, la partie linéaire de la courbe ne passe pas par l'origine en extrapolant. Avec ce même catalyseur, à -130°C et à la même conversion, les poids moléculaires étaient plus élevés dans le chlorure d'éthyle que dans le pentène.

### Zusammenfassung

Die kationische Polymerisation von 3-Methylbuten-1 wurde bei extrem niedriger Temperatur, z.B. -130°C und darunter untersucht. Auch bei hoher Katalysatorkonzentration findet praktisch keine Polymerisation statt und das System befindet sich bei -150°C in einem Ruhezustand. Die mit AlCl<sub>3</sub> erhaltene Molekulargewichts-Umsatzkurve bildet eine Gerade, die zum Ursprung extrapoliert werden kann. Bei gleichem Geraden, die zum Ursprung extrapoliert werden kann. Bei gleichem höherer Monomerkonzentration höhere Molekulargewichte erhalten. Mit Bortrifluorid als Katalysator lässt sich der lineare Teil der Kurve nicht zum Ursprung zurückextrapolieren. Das Molekulargewicht des Polymeren war beim gleichen Umsatz bei -130°C in Äthylchlorid höher als in Penten.

Received January 3, 1963

Revised January 18, 1963

## The Molecular Structure of Perfluorocarbon Polymers. II. Pyrolysis of Polytetrafluoroethylene\*

J. C. SIEGLE, L. T. MUUS,† TUNG-PO LIN,‡ and H. A. LARSEN,  
*Plastics Department, E. I. du Pont de Nemours & Company, Inc., Du Pont  
Experimental Station, Wilmington, Delaware*

### Synopsis

Vacuum pyrolysis of thin samples of polytetrafluoroethylene follows first-order kinetics with monomer as the only important decomposition product in the temperature range 360–510°C. The rate constant for vacuum pyrolysis is independent of both the melt viscosity and the type of polymer and is characterized by an activation enthalpy of 83.0 kcal./mole and a frequency factor of  $3 \times 10^{19}$  sec.<sup>-1</sup>. The molecular weight is found to decrease during pyrolysis. A plausible reaction mechanism consistent with these facts involves random chain cleavage, depropagation with short kinetic chain length, and termination by disproportionation. For thick samples the rate of vacuum pyrolysis is controlled by diffusion of monomer. The course of pyrolysis is changed by the presence of monomer or gaseous pyrolysis products. Accumulation of monomer reduces the rate of pyrolysis as measured by the weight loss and results in formation of a waxy product consisting of low molecular weight fluorocarbons.

### INTRODUCTION

High thermal stability combined with extreme chemical inertness and solvent resistance is a characteristic property of polytetrafluoroethylene. The high thermal stability is reflected by a rate of pyrolysis that is small compared to that of other organic polymers. The pyrolytic decomposition in vacuum of polytetrafluoroethylene above 450°C. has been the subject of several papers.<sup>1-3</sup> Monomer is the major pyrolysis product implying that depropagation is an important step in the reaction mechanism whereas chain transfer does not occur to an appreciable extent. Several reaction mechanisms were suggested.<sup>1-3</sup> However, an unequivocal assignment of mechanism is complicated by the fact that conventional methods for molecular weight determination are inapplicable to polytetrafluoroethylene.

\* Presented in part at the 130th National Meeting of the American Chemical Society, Atlantic City, N. J., Sept. 17, 1956. For the first paper in this series, see reference 6.

† Present Address: Physical Chemistry Department, Aarhus University, Aarhus, Denmark.

‡ Present Address: Mathematics Department, San Fernando State College, Northridge, California.

This paper presents further experimental data, outlines the thermodynamics of the pyrolysis, and suggests a plausible reaction mechanism.

## EXPERIMENTAL

### Manometric Method

The pressure of the gaseous pyrolysis products from thin polymer films was measured as a function of time at constant temperature in an apparatus similar to that used by Madorsky and co-workers.<sup>1-3</sup> A multiplying manometer was used to determine the pressure generated by the gaseous pyrolysis products in a calibrated volume. Weight loss data free from the complicating effect of diffusion were obtained by this method which requires only small (30-100 mg.) and thin (50-100  $\mu$ ) polymer samples.

TABLE I  
Mass Spectrographic Analysis of the Gaseous Products from Vacuum Pyrolysis of  
50-100  $\mu$  Polytetrafluoroethylene Films at 510°C.

Conversion, %	Mole fraction					
	CF <sub>1</sub>	C <sub>2</sub> F <sub>4</sub>	C <sub>2</sub> F <sub>6</sub>	C <sub>3</sub> F <sub>6</sub>	C <sub>3</sub> F <sub>8</sub>	SiF <sub>4</sub>
0-20	0.001	0.972	None	0.0265	None	None
50-60	0.0023	0.9695	None	0.0257	None	0.0023
85-90	0.0086	0.9397	None	0.0255	0.0073	0.017

The high monomer content of the gaseous degradation products (Table I) facilitates the conversion of manometric readings into weight loss. An insignificant error is introduced by assuming that tetrafluoroethylene is the only pyrolysis product in vacuum.

### Weighing Method

The weight reduction during pyrolysis was determined with a sensitive tungsten wire spring balance (1 mm. extension = ca. 8 mg.) enclosed in a vacuum system. The position of the lower end of the spring was observed with a cathetometer read to 0.01 mm. with a filar micrometer eye piece. The sample was placed in the pyrolysis zone where it was contained in an aluminum cup suspended from the spring balance. Constant temperature in the pyrolysis zone was maintained by a closely fitted aluminum block heated electrically to 310-510°C.

The weighing method required a larger sample (500-700 mg., 50-100  $\mu$ ) than the manometric method. Excellent agreement was obtained between the data from the two methods when sample size in the weighing method was kept at a minimum. It was observed, however, that the use of a larger sample of thin film in the weighing experiment occasionally resulted in a reaction mechanism that was controlled by diffusion. This change was probably caused by flow of thin film into thicker layers.

### Molecular Weight Measurements

Measurements of standard specific gravity<sup>4,5</sup> by an infrared technique<sup>6</sup> were made to indicate changes of molecular weight caused by vacuum pyrolysis at 480°C. The relationship between standard specific gravity and molecular weight is shown in Figure 2 of reference 5. Changes of molecular weight can be followed by this technique until the molecular weight has decreased to about  $8 \times 10^5$  (standard specific gravity of 2.27). For samples of lower molecular weight, the standard specific gravity approaches the crystalline density<sup>6</sup> of 2.30, and this method breaks down.

### Samples

Weight loss experiments were made on 50–100  $\mu$  films of polytetrafluoroethylene (samples I–V) with melt viscosities at 380°C. in the range of  $10^9$ – $10^{11}$  poises and standard specific gravities of 2.17–2.29 (Table II). (This is the thickness range used also for the thermal degradation of polymethyl methacrylate.<sup>7</sup> Melt viscosities were measured with a capillary rheometer similar to that described in ASTM D-1238-52T. The ratio of the length of the capillary to its diameter was unity. Shear stress was in the range  $1$ – $4 \times 10^6$  dynes/cm.<sup>2</sup>.) Molecular weights by standard specific gravity were between  $3 \times 10^5$  and  $4 \times 10^7$ . Changes of molecular weight were measured on a 30  $\mu$  film of polytetrafluoroethylene (sample VI) which had a standard specific gravity of 2.21 and a molecular weight by standard specific gravity of  $9 \times 10^6$ .

## RESULTS

### Pyrolysis in Vacuum

Table I shows the composition of the gaseous degradation products from vacuum pyrolysis of thin films of polytetrafluoroethylene. The monomer, tetrafluoroethylene, is by far the major component (94–97 mole-%). The composition is the same at all conversions. Table I is in good agreement with previous analyses.<sup>1,8</sup>

Typical curves for the vacuum pyrolysis are shown in Figure 1 for sample I pyrolyzed at three different temperatures. The data at 450 and 510°C. were obtained by the manometric method, those at 480°C. both by the manometric and the weighing method. All weight loss data for vacuum pyrolysis are listed in Table II. The first-order experimental rate constant ( $k_{\text{exptl}}$ ) may be expressed with high precision by

$$k_{\text{exptl}} = 3 \times 10^{19} \exp\{-83000/RT\} \text{ sec.}^{-1} \quad (1)$$

in close agreement with the equation of Madorsky and co-workers<sup>1</sup>

$$k_{\text{exptl}} = 4.7 \times 10^{18} \exp\{-80500/RT\} \text{ sec.}^{-1} \quad (2)$$

TABLE II  
Rate Constant for Vacuum Pyrolysis of Thin Polytetrafluoroethylene Films

Sample	Melt viscosity (380°C.), poises	Molecular weight by standard specific gravity	Rate constant $k_{\text{expt}}$ , sec. <sup>-1</sup>				
			360°C.	380°C.	450°C.	480°C.	510°C.
I	$10^{10}$ - $10^{11}$	$1 \times 10^7$ - $4 \times 10^7$	$5.5 \times 10^{-10}$	$8.65 \times 10^{-9}$	$2.15 \times 10^{-6}$	$2.48 \times 10^{-5}$	$2.12 \times 10^{-4}$
II	$10^{10}$ - $10^{11}$	$1 \times 10^6$ - $1 \times 10^7$	—	—	$2.75 \times 10^{-6}$	$2.49 \times 10^{-5}$	—
III	$10^9$ - $10^{10}$	$3 \times 10^3$ - $1 \times 10^6$	—	—	$2.48 \times 10^{-6}$	$2.48 \times 10^{-5}$	$2.12 \times 10^{-4}$
IV	—	$1 \times 10^6$ - $1 \times 10^7$	—	—	—	$2.52 \times 10^{-5}$	$2.15 \times 10^{-4}$
V	—	$8 \times 10^{6a}$	—	—	—	$2.48 \times 10^{-5}$	—
VI	—	$9 \times 10^6$	—	—	—	$2.61 \times 10^{-5}$	—

<sup>a</sup> Molecular weight by counting radioactive sulfonic acid endgroups.

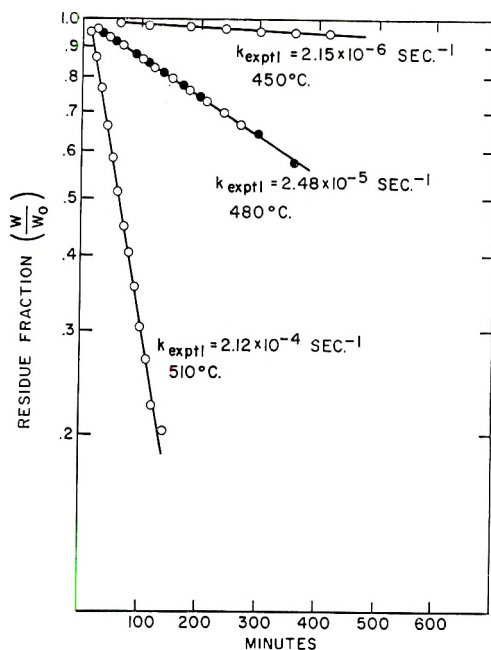


Fig. 1. Vacuum pyrolysis of 50–100  $\mu$  film of sample I: (O) manometric method (sample weight 30–100 mg.); (●) weighing method (sample weight 500–700 mg.).

### Effect of Sample Thickness

Figure 2 demonstrates the effect of sample thickness on the rate curve for vacuum pyrolysis. The uppermost curve for a 1.5 mm. sheet shows less reduction in weight with time than the straight line for a 50–100  $\mu$  film of the same polymer (sample I, 480°C.). The initial concavity toward the time axis of the curve for the 1.5 mm. sheet is indicative of diffusion-controlled release of gaseous pyrolysis products. A steady state is reached in about 100 min. After this time, the 1.5 mm. sample curve becomes linear and parallel to that for the 50–100  $\mu$  sample pyrolyzed at the same temperature, since diffusion no longer is rate-controlling.

A similar effect of diffusion is displayed by the sigmoidal curve for the 50–100  $\mu$  film from sample III which has a very low initial melt viscosity (Table II). The first part of the pyrolysis curve follows one of the linear curves for a thin film. After about 180 min., sample III flowed into a compact mass with the effect of making the release of gaseous pyrolysis products controlled by diffusion. A steady state subsequently is reached in about 500 min. with the result that the pyrolysis curve returns to linearity with a slope identical to that for a thin film.

### Pyrolysis in Presence of Monomer and Gaseous Pyrolysis Products

Figure 3 compares the results from experiments on 50–100  $\mu$  films at 480°C. carried out (a) in vacuum, (b) under autogenous pressure restricted

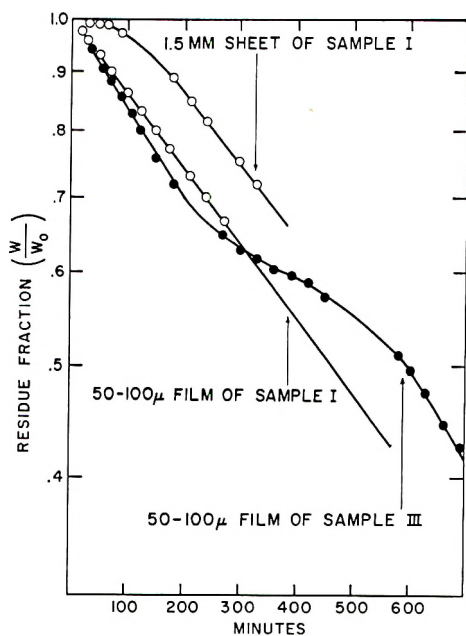


Fig. 2. Vacuum pyrolysis at 480°C. of 1.5 mm. sheet of sample I, 50-100  $\mu$  film of sample I, and 50-100  $\mu$  film of sample III.

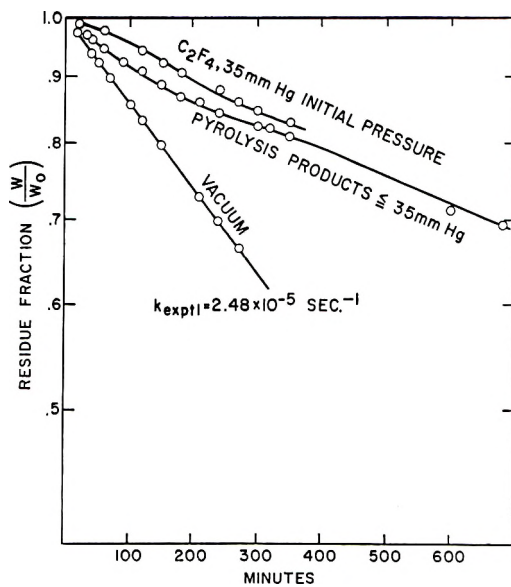


Fig. 3. Pyrolysis at 480°C. of 50-100  $\mu$  film of sample I in vacuum, under autogenous pressure, and under an initial monomer pressure.



to 35 mm. Hg by a manostat, and (c) under an initial monomer pressure of 35 mm. Hg with subsequent limitation of the pressure to 35 mm. Hg. As expected, the weight loss is less for these experiments than for the vacuum experiment. The gaseous pyrolysis products in experiments under autogenous pressure have a composition (at 85% conversion, in mole fractions:  $\text{CF}_4$  0.009;  $\text{C}_2\text{F}_4$  0.157;  $\text{C}_3\text{F}_6$  0.125;  $\text{C}_3\text{F}_8$  0.264; higher fluorocarbons 0.029;  $\text{SiF}_4$  0.106;  $\text{CO}_2$  0.141;  $\text{N}_2$  0.155) which differs from that consisting predominantly of monomer in vacuum pyrolysis. A white product was formed when polytetrafluoroethylene was pyrolyzed in the presence of its gaseous decomposition products. In accord with earlier observations,<sup>9</sup> this product is a white waxy mixture of fluorocarbons which melts at about 250°C. and sublims in the temperature range 300–500°C. under atmospheric pressure. The melting point suggests a chain length between forty and sixty carbon atoms.

### Molecular Weight Changes

Pyrolysis in vacuum at 480°C. caused a substantial reduction in molecular weight, as shown in Figure 4.

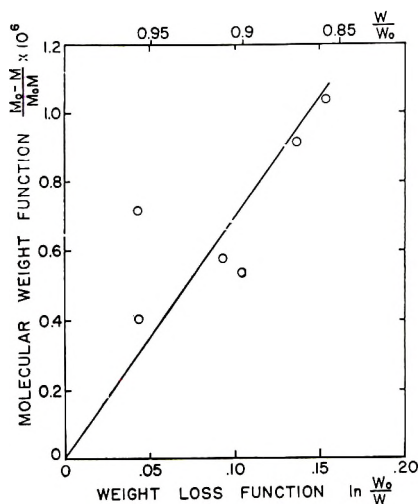


Fig. 4. Change of molecular weight during vacuum pyrolysis at 480°C. of sample VI.

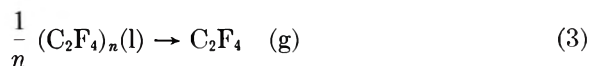
### Polymerization

A pyrolysis experiment was carried out at 380°C. on a 50–100  $\mu$  film of sample I under a monomer pressure of 80 mm. Hg. The pressure was kept constant by adding tetrafluoroethylene. After 700 hr. the samples gained 4% in weight.

## DISCUSSION

## Thermodynamics

The thermodynamics of the depolymerization reaction:



may be calculated with the use of the following available data.

The enthalpy, entropy, and heat-capacity of tetrafluoroethylene in the ideal gaseous state at 1 atm. pressure have been tabulated in the temperature range 50–5000°K.<sup>10</sup>

The molar heat capacity of the amorphous (liquid) polytetrafluoroethylene is not available, but that of the crystalline polymer has been determined for the temperature range 40–120°C.,<sup>11</sup> and is given by the equation:

$$C_p(\text{s}) = 15.44 + 0.0250 T \text{ cal./mole-deg.} \quad (4)$$

where  $T$  is the absolute temperature and mole refers to  $\text{C}_2\text{F}_4$ . It seems reasonable to assume that the differences in specific heats between the amorphous and crystalline states of polytetrafluoroethylene and of polytrifluorochloroethylene are approximately the same. Data for the latter polymer are available<sup>12</sup> and were combined with eq. (4) to derive the following expression for the molar heat capacity of amorphous polytetrafluoroethylene in the temperature range 40–120°C.:

$$C_p(\text{l}) = 15.39 + 0.0336 T \text{ cal./mole-deg.} \quad (5)$$

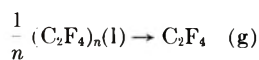
Use of this equation over the wider temperature range 25–500°C. is of sufficient accuracy for the purpose of the present discussion, because the free energy of depolymerization ( $\Delta F_d^\circ$ ) of polytetrafluoroethylene is not sensitive to the manner of extrapolation.

The enthalpy of depolymerization of crystalline polytetrafluoroethylene into gaseous monomer at 1 atm. pressure is calculated to be 41.12 kcal./mole at 25°C. on the basis of recent thermochemical data.<sup>13–18</sup> This value, in contrast to those suggested elsewhere,<sup>19,20</sup> is based on reactions with completely defined end products. Published values for the heat of melting of the polymer are in the range 840–2030 cal./mole.<sup>19,21</sup> The best value is probably 1370 cal./mole at the melting point (327°C.).<sup>22</sup> This value, together with eqs. (4) and (5), leads to a heat of melting of 218 cal./mole at 25°C. The enthalpy ( $\Delta H_d^\circ$ ) of depolymerization (reaction 3) of amorphous polymer is therefore 20.90 kcal./mole at 25°C. The entropy of crystalline polytetrafluoroethylene at 40°C. is reported to be 27.37 e.u.<sup>23</sup> The entropy of amorphous polymer at 25°C. is therefore 25.96 e.u.

The above data form the basis for calculating the thermodynamic data listed in Table III.

The ceiling temperature<sup>24</sup> of polytetrafluoroethylene is 712°C., as shown in Table III.

TABLE III  
Thermodynamics of Depolymerization



Temperature, °C.	Enthalpy $\Delta H_d^\circ$ , kcal./mole	Entropy $\Delta S_d^\circ$ , cal./mole-deg.	Free energy $\Delta F_d^\circ$ , kcal./mole	Equilibrium $\text{C}_2\text{F}_4$ pressure, mm. Hg
25	40.90	45.72	27.27	—
327	38.59	40.51	14.28	0.0048
360	38.25	39.95	12.96	0.0255
390	37.91	39.45	11.77	0.100
420	37.57	38.92	10.59	0.35
450	37.19	38.39	9.43	1.07
480	36.80	37.88	8.29	2.9
510	36.39	37.33	7.16	7.6
712	32.96	33.46	0	760

### Kinetics

The following experimental observations serve to characterize the reaction mechanism for pyrolysis in vacuum: (1) the pyrolysis product is essentially monomer; (2) the rate of pyrolysis is independent of initial molecular weight as measured by standard specific gravity or by melt viscosity; (3) the pyrolysis follows first-order kinetics over the entire conversion range. In addition, the available experimental evidence indicates that the molecular weight decreases during vacuum pyrolysis, and that in the temperature range 450–510°C. endgroups have no apparent effect on the rate of pyrolysis. (The rate of pyrolysis of an experimental polymer which supposedly had trifluoromethyl endgroups was recently shown also to follow eq. (1) by Boyd.<sup>25</sup>)

A plausible reaction mechanism therefore appears to be random initiation followed by depropagation for short kinetic chain length and termination by second-order disproportionation. (A similar point of view was expressed by Friedman.<sup>26</sup>)

The rate constant for this mechanism may be written (see Appendix)

$$k_{\text{exptl}} = (2m_0/d_0)^{1/2} k_d (k_i/k_t)^{1/2} \quad (6)$$

where  $m_0$  is the molecular weight of monomer;  $k_d$ ,  $k_i$ , and  $k_t$  are the rate constants for depropagation, initiation, and termination, respectively, and  $d_0$  is the density of polymer. At 480°C. the polymer density is  $1.34 \times 10^3$  g./l.,<sup>27</sup> and eq. (6) becomes

$$k_{\text{exptl}} = 0.39 k_d (k_i/k_t)^{1/2} \quad (7)$$

### Activation Enthalpies

The suggested reaction mechanism is compatible with the available experimental evidence on activation energies. The enthalpy of depropaga-

tion at 480°C. is 36.8 kcal./mole according to Table III. The activation enthalpy for propagation is probably 5–9 kcal./mole.<sup>23</sup> The activation enthalpy for depropagation is therefore close to 43.8 kcal./mole.

The initiation step for random cleavage is rupture of a C—C bond. The enthalpy of reaction for such a dissociation is calculated from free radical thermodynamics<sup>29</sup> to be 81.6 kcal./mole. The activation enthalpy for recombination of radicals is usually close to zero,<sup>30</sup> hence the activation enthalpy for initiation is 81.6 kcal./mole. Since the experimental activation enthalpy [eq. (1)] is 83.0 kcal./mole, the activation enthalpy for termination may be evaluated according to eq. (7) as follows:

$$\Delta H_t^\ddagger = 2(43.8-83.0) + 81.6 = 3.2 \text{ kcal./mole}$$

This value for  $\Delta H_t^\ddagger$  is reasonable since the termination step (disproportionation) is a three-center reaction in the exothermic direction ( $\Delta H_t^\circ \approx -57$  kcal./mole).<sup>29</sup> The action enthalpy for this type of reaction is usually small.<sup>31</sup>

### Frequency Factors

Derivation of acceptable values for the kinetic chain length (see below) makes it necessary to assume that the frequency factor for the initiation step  $A_i$  lies above the range ( $10^{12}$ – $10^{14}$  sec.<sup>-1</sup>) usually expected for unimolecular reactions. This is a reasonable assumption, since many scission reactions involving free radicals have frequency factors above this range.<sup>32</sup> It is assumed here that  $A_i$  is the same as the frequency factor for the decomposition of ethane into methyl radicals ( $10^{17.3}$ ).<sup>32</sup>

The depropagation reaction, on the other hand, is assumed to be a normal unimolecular reaction with the frequency factor  $A_d = 10^{13}$  as verified for the depropagation step in the photodegradation of polymethyl methacrylate.<sup>33</sup>

Since  $\log A_{\text{exptl}} = 19.5$ , eq. (7) leads to:

$$\log A_i = 17.3 + 2(13-19.5) + 2 \log 0.39 = 3.5 \quad (8)$$

This value for  $A_i$  gives  $k_t = 2.5 \times 10^2$  l./mole-sec. of 360°C. and  $k_t = 4.0 \times 10^2$  l./mole-sec. at 510°C. These rates of termination are closely similar to those for polymethyl methacrylate.<sup>33</sup>

### Kinetic Chain Length

The kinetic chain length  $l$  for depropagation is related to weight loss and change of molecular weight. Equations (18), (20), and (23) of the Appendix lead to

$$(M_0 - M)/MM_0 = (1/2m_0l)\ln(W_0/W) \quad (9)$$

The data of Figure 4 fit this functionality reasonably well. The slope of the line in Figure 4 indicates a kinetic chain length of 720. This value is considerably smaller than the initial degree of polymerization, which ranges from  $3 \times 10^3$  to  $4 \times 10^5$  for the samples used in this study.

The kinetic chain length can also be expressed in terms of individual reaction rate constants as given by the expression (see Appendix)

$$\log l = \log k_d^{-1/2} \log k_t^{-1/2} \log k_i + 1/2 \log(m_0/2d_0) \quad (10)$$

Substitution of the above discussed values of activation enthalpies and frequency factors for each step gives the following numerical expression for  $l$ :

$$\begin{aligned} \log l &= 13.0^{-1/2}(3.5 + 17.3) - [43.8^{-1/2}(3.2 + 81.6)]10^3/4.576T + \log 0.195 \\ &= 1.9 - 306/T \end{aligned} \quad (10a)$$

Thus,  $l$  is 25 at 360°C. and 32 at 510°C. It should be noted that this method of estimating kinetic chain length is very sensitive to small changes in the parameters entering into eq. (10) and therefore to the details of the assumptions regarding activation enthalpies and frequency factors. For the calculated value of kinetic chain length to equal the experimental value of 720 at 480°C. it is necessary to assume a value of 15.94 for  $\log A_i$  if other values remain unchanged. In this instance  $\log A_t$  would equal 2.14 and eq. (10) would become:

$$\log l = 3.26 - 306/T \quad (10b)$$

### Steady-State Assumption

In the proposed mechanism, the steady-state assumption is valid only when  $k_d/k_t \ll 1$ . The activation enthalpies and frequency factors derived above give  $k_d/k_t$  values of  $10^{-4.4}$  at 360°C. and  $10^{-1.8}$  at 510°C., thus justifying the steady-state approximation.

The authors wish to acknowledge the many helpful suggestions by Mr. W. M. D. Bryant and Drs. C. A. Sperati and H. W. Starkweather, Jr. during the course of this work.

### APPENDIX

For the proposed reaction mechanism, the rate of weight loss,  $-dW/dt$ , is proportional to the rate of monomer evolution which in turn is the product of the rate constant,  $k_d$ , for depropagation and the total number of free radicals,  $R$  (in moles),

$$-dW/dt = m_0 k_d R \quad (11)$$

where  $m_0$  is the molecular weight of monomer.

The total number of polymer molecules,  $N$  (in moles), is changed during pyrolysis by the process of initiation (by random cleavage) and termination (by disproportionation) according to the following rate equation:

$$dN/dt = -k_i W/m_0 + d_0 k_t R^2/W \quad (12)$$

where  $k_i$  and  $k_t$  are the rate constants for initiation and termination, respectively;  $d_0$  is the density of the sample. The quantity  $(W/m_0)$  is the total number of monomer units in the sample and therefore is approxi-

mately the number of links which might be broken during pyrolysis. This definition of  $k_t$  considers the radicals of different chain length as separate entities. However, in other definitions of  $k_t$ , radicals might be treated as a single entity and the last terms in both eqs. (12) and (16) would have an additional factor of 2. Since the number-average molecular weight (for convenience written here as  $M$ ) is equal to  $W/N$ , it follows that

$$(1/M) dM/dt = (1/W)dW/dt - (M/W)dN/dt \quad (13)$$

and

$$dM/dt = -m_c k_a MR/W + k_i M^2/m_0 - d_0 k_t M^2 R^2/W^2 = k_i M^2/m_0 - d_0 k_t M(M + m_0 l) R^2/W^2 \quad (14)$$

where

$$l = k_a R / (d_0 k_t R^2 / W) = k_a W / (d_0 k_t R) \quad (15)$$

is the average kinetic chain length. The total number of free radicals,  $R$ , is determined by introducing the assumption of steady state, i.e.,  $dR/dt = 0$ . Since

$$dR/dt = 2k_i W/m_0 - d_0 k_t R^2/W \quad (16)$$

and therefore

$$R = [2k_i / (m_0 d_0 k_t)]^{1/2} W \quad (17)$$

eqs. (11), (14), and (15) may be rewritten as

$$-dW/dt = k_a [2m_0 k_i / (d_0 k_t)]^{1/2} W \quad (18)$$

$$-dM/dt = k_i M(M/m_0 + 2l) \quad (19)$$

$$l = (2m_c/d_0)^{1/2} k_a / (4k_t k_i)^{1/2} \quad (20)$$

The kinetic chain length consequently is independent of time, and the weight loss follows a first-order expression with

$$k_{\text{exptl}} = (2m_0/d_0)^{1/2} k_a (k_i/k_t)^{1/2} \quad (21)$$

Equations (20) and (21) can be combined to give

$$l = k_{\text{exptl}} / 2k_i \quad (22)$$

This treatment is invalid if  $l$  is too large, since the assumption of a steady state will not hold. On the other hand, for  $l \ll M/m_0$ , eq. (19) may be integrated to give the well-known equation

$$(1/M) - (1/M_0) = m_0^{-1} k_i t$$

where  $M_0$  is the initial number-average molecular weight.

The derivation given above is valid regardless of the type of initial molecular weight distribution. For the special case of the "most probable"

distribution, eqs. (18), (19), and (20) may be derived also from the publication by Boyd,<sup>34</sup> which includes additional kinetic schemes of general interest.

### References

1. Madorsky, S. L., V. E. Hart, S. Strauss, and V. A. Sedlak, *J. Res. Natl. Bur. Std.*, **51**, 327 (1953).
2. Florin, R. E., L. A. Wall, D. W. Brown, L. A. Hymo, and J. D. Michaelsen, *J. Res. Natl. Bur. Std.*, **53**, 121 (1954).
3. Wall, L. A., and J. D. Michaelsen, *J. Res. Natl. Bur. Std.*, **56**, 27 (1956).
4. Doban, R. C., A. C. Knight, J. H. Peterson, and C. A. Sperati, paper presented at the 130th National Meeting of the American Chemical Society, Atlantic City, N. J., September 18, 1956; cf. also ASTM D1457-56T.
5. Sperati, C. A., and H. W. Starkweather, Jr., *Advan. Polymer Sci.*, **2**, 465 (1961).
6. Moynihan, R. E., *J. Am. Chem. Soc.*, **81**, 1045 (1959).
7. Grassie, N., and H. W. Melville, *Proc. Roy. Soc. (London)*, **A199**, 1 (1949).
8. Lewis, E. E., and M. A. Naylor, *J. Am. Chem. Soc.*, **69**, 1968 (1947).
9. Miller, W. T., Jr., in *Preparation, Properties and Technology of Fluorine and Organic Fluoro Compounds*, C. Slesser and S. R. Schram, Eds., McGraw-Hill, New York, 1951, Chapter 32.
10. Mann, D. E., N. Acquista, and E. K. Plyler, *J. Res. Natl. Bur. Std.*, **52**, 67 (1954).
11. Marx, P., and M. Dole, *J. Am. Chem. Soc.*, **77**, 4771 (1955).
12. Hoffman, J. D., *J. Am. Chem. Soc.*, **74**, 1696 (1952).
13. Scott, D. W., W. D. Good, and G. Waddington, *J. Am. Chem. Soc.*, **77**, 245 (1955).
14. Rossini, F. D., D. D. Wagman, W. H. Evans, S. Levine, and I. Jaffe, *Natl. Bur. Std. Circ.*, No. 500; Washington, D. C., 1952.
15. Neugebauer, C. A., and J. L. Margrave, *J. Phys. Chem.*, **60**, 1318 (1956).
16. Neugebauer, C. A., Thesis, Univ. Wisconsin (1957).
17. Kirkbride, F. W., and F. G. Davidson, *Nature*, **174**, 79 (1954).
18. Jessup, R. S., R. E. McCoskey, and R. A. Nelson, *J. Am. Chem. Soc.*, **77**, 244 (1955).
19. Duus, H. C., *Ind. Eng. Chem.*, **47**, 1445 (1955).
20. Patrick, C. R., *Nature*, **181**, 698 (1958).
21. McGeer, P. L., and H. C. Duus, *J. Chem. Phys.*, **20**, 1813 (1952).
22. Starkweather, H. W., Jr., and R. H. Boyd, *J. Phys. Chem.*, **64**, 410 (1960).
23. Furukawa, G. T., R. E. McCoskey, and G. J. King, *J. Res. Natl. Bur. Std.*, **49**, 273 (1952).
24. Dainton, F. S., and K. J. Ivin, *Trans. Faraday Soc.*, **46**, 331 (1950); *Nature*, **162**, 705 (1948).
25. Boyd, D. R. J., private communication.
26. Friedman, H. L., U.S. Dept. Comm., Office Tech. Serv. PB Rept. 145182, 1959.
27. Lupton, J. M., paper presented at the 134th National Meeting of the American Chemical Society, Chicago, Ill., September 12, 1958.
28. Walling, C., *Free Radicals in Solution*, Wiley, New York, 1957, p. 95.
29. Bryant, W. M. D., *J. Polymer Sci.*, **56**, 277 (1962).
30. Hougen, A. O., and K. M. Watson, *Chemical Process Principles*, Wiley, New York, 1947, p. 893.
31. Glasstone, S., K. J. Laidler, and H. Eyring, *The Theory of Rate Processes*, McGraw-Hill, New York, 1941, p. 151.
32. Benson, S. W., *The Foundations of Chemical Kinetics*, McGraw-Hill, New York, 1960, p. 262.
33. Cowley, P. R. E. J., and H. W. Melville, *Proc. Roy. Soc. (London)*, **A211**, 320 (1952).
34. Boyd, R., *J. Chem. Phys.*, **31**, 321 (1959). This paper also lists further references.

### Résumé

La pyrolyse sous vide de minces échantillons de polyéthylène tétrafluoré suit une cinétique de premier ordre avec production de monomère comme seul produit important de décomposition dans le domaine de 360 à 510°C. La constante de vitesse de la pyrolyse sous vide est indépendante et de la viscosité à l'état fondu et du type de polymère. Elle est caractérisée par une enthalpie d'activation de 83.0 kcal/mole et un facteur de fréquence de  $3 \times 10^{19} \text{ sec}^{-1}$ . On a trouvé que le poids moléculaire diminue durant la pyrolyse. Un mécanisme de réaction plausible compatible avec ces faits suppose une scission de chaîne statistique, une dépropagation avec de courtes longueurs de chaînes cinétiques et une terminaison par disproportionnement. Pour des échantillons épais, la vitesse de pyrolyse sous vide est contrôlée par la diffusion du monomère. Le cours de la pyrolyse est modifié par la présence de monomère ou de produits gazeux de pyrolyse. L'accumulation de monomère diminue la vitesse de pyrolyse. Elle a été mesurée par la perte de poids et résulte de la formation de produit plastique fluorocarboné de bas poids moléculaire.

### Zusammenfassung

Die Vakuumpyrolyse dünner Polytetrafluoräthylenproben folgt einer Kinetik erster Ordnung, wobei im Temperaturbereich von 360 bis 510° das Monomere das einzige wichtige Zersetzungsprodukt bildet. Die Geschwindigkeitskonstante der Vakuumpyrolyse ist von Schmelzviskosität und Polymertypus unabhängig und durch eine Aktivierungsenthalpie von 83,0 kcal/Mol und einen Frequenzfaktor von  $3 \times 10^{19} \text{ sek}^{-1}$  charakterisiert. Das Molekulargewicht nimmt während der Pyrolyse ab. Ein mit diesen Tatsachen in Übereinstimmung stehender plausibler Reaktionsmechanismus besteht aus statistischer Kettenspaltung, Monomerabspaltung mit kurzer kinetischer Kettenlänge und Kettenabbruch durch Disproportionierung. Bei dicken Proben wird die Geschwindigkeit der Vakuumpyrolyse durch die Diffusion des Monomeren bestimmt. Der Pyrolyseverlauf wird durch Anwesenheit von Monomerem oder gasförmigen Pyrolyseprodukten verändert. Ansammlung von Monomerem setzt die durch den Gewichtsverlust gemessene Pyrolysegeschwindigkeit herab und führt zur Bildung eines wachstumsartigen, aus niedermolekularen Fluorkohlenstoffen bestehenden Produktes.

Received November 8, 1962





hexane (I) and 1,2,4,5-diepoxy-pentane (II) could be expected to afford the tetrahydropyran (III) and tetrahydrofuran (IV) recurring units, respectively.

The known polymerization of oxiranes by certain cationic and anionic catalysts to very high molecular weight polyethers furnishes a wide range of conditions under which these diepoxides can be polymerized. The catalysts phosphorus pentafluoride,<sup>4,5</sup> aluminum isopropoxide-zinc chloride,<sup>6</sup> aluminum alkyls with cocatalysts,<sup>7-10</sup> and zinc alkyls on supports or with cocatalysts<sup>11-13</sup> are particularly effective for the conversion of oxiranes to high molecular weight polymers. These catalysts provide systems for both heterogeneous and homogeneous polymerization of the diepoxides.

## EXPERIMENTAL

### Monomers

The two diepoxide monomers, 1,2,5,6-diepoxyhexane (I) and 1,2,4,5-diepoxy-pentane (II) were prepared by epoxidation of the respective dienes, 1,5-hexadiene and 1,4-pentadiene,<sup>14</sup> with perbenzoic acid in cold chloroform. The monomer, 3,4-epoxytetrahydrofuran, was prepared by treating 2,5-dihydrofuran with hypochlorous acid and then reacting the resulting chlorohydrin, 3-chloro-4-hydroxytetrahydrofuran, with aqueous sodium hydroxide to obtain the monoepoxide.<sup>15</sup> After initial distillation under reduced pressure, the three monomers were dried over anhydrous calcium sulfate and freshly distilled under nitrogen through a spinning band column at atmospheric pressure before each polymerization run. The infrared spectra (liquid film) of the two diepoxide monomers exhibited absorption bands at 1258 and 835  $\text{cm}^{-1}$ , characteristic of the epoxide moiety.<sup>16</sup> The infrared spectrum (liquid film) of 3,4-epoxytetrahydrofuran exhibited absorption bands at 1076, 890, 853, and 815  $\text{cm}^{-1}$  which are attributed to cyclic ether groups.<sup>16</sup>

### Catalysts and Solvents

The catalysts aluminum isopropoxide<sup>17</sup> and diethylzinc<sup>18</sup> were stored in tightly sealed glass containers under nitrogen. The triisobutyl aluminum purchased from the Hercules Powder Company contained on analysis 13.2% aluminum (calculated 13.6%). Mallinckrodt AR grade zinc chloride (anhydrous) was ground as finely as possible in an agate mortar in a nitrogen-filled dry box before being used in the polymerization studies. Phosphorus pentafluoride was obtained from the thermal decomposition (150-160°C.) of benzenediazonium hexafluorophosphate (Ozark-Mahoning Co.), and swept with dry purified nitrogen into the reaction systems. Stannic chloride (J. T. Baker, AR grade) was refluxed over phosphorus pentoxide, distilled under reduced pressure, and stored in a glass-stoppered bottle under nitrogen. Commercial grade acetylacetone was dried over calcium sulfate and distilled.

Purified *n*-heptane was refluxed over sodium, distilled, and stored over sodium ribbon. After purification, the nitrobenzene was dried over magnesium sulfate and distilled under reduced pressure before being used in the polymerization studies. The halide solvents, methylene dichloride and ethylene dichloride, were stored over phosphorus pentoxide and distilled therefrom just before use.

### Polymerization of 1,2,5,6-Diepoxyhexane

**Aluminum Isopropoxide-Zinc Chloride.** In trial 1 (Table I), the monomer and catalyst were weighed into a sealed, nitrogen-filled polymerization tube. In trial 2, the monomer, solvent, and catalyst were sealed in a 100-ml. serum bottle with a serum-type rubber stopper. Both systems were agitated in thermostatted baths for the duration of the polymerization.

The polymers were isolated by dissolving the reaction products in benzene, washing the benzene solutions with water, drying over anhydrous sodium sulfate, filtering, and pouring the concentrated benzene solutions into pentane to precipitate the polymers. The polymers were dried under reduced pressure.

**Diethylzinc and Triisobutyl aluminum.** In a nitrogen-filled dry box, the solvent, catalysts, water or chelating agent, and alumina were added

TABLE I  
Polymerization of 1,2,5,6-Diepoxyhexane

Trial	Catalyst <sup>a</sup>	Temp., °C.	Time, hr.	$[\eta]$ <sup>b</sup>	Con- ver- sion, %	Solubility <sup>c</sup>
1	AIP-ZnCl <sub>2</sub> <sup>d</sup>	150	48	0.13	50	Viscous oil
2	AIP-ZnCl <sub>2</sub> <sup>d</sup>	80	480	—	—	Insoluble
3	ZnEt <sub>2</sub> -Al <sub>2</sub> O <sub>3</sub> <sup>e</sup>	25	48	—	—	Insoluble
4	ZnEt <sub>2</sub> -H <sub>2</sub> O (1:1)	25	3	0.45	87	5% soluble
5	ZnEt <sub>2</sub> -H <sub>2</sub> O (1:1)	0	1	—	88	8% soluble
6	ZnEt <sub>2</sub> -AA (1:1)	25	168	—	—	Viscous oil
7	ZnEt <sub>2</sub> -AA-H <sub>2</sub> O (1:0.5:0.5)	25	144	—	—	Viscous oil
8	Al( <i>i</i> -Bu) <sub>3</sub>	0	3	0.26	50	5% soluble
9	Al( <i>i</i> -Bu) <sub>3</sub> -H <sub>2</sub> O (1:1)	25	48	0.22	39	3% soluble
10	Al( <i>i</i> -Bu) <sub>3</sub> -AA (1:1)	25	168	—	—	Viscous oil

<sup>a</sup> No solvent was used in trial 1; 20 ml. of heptane was employed for 2-10. With the exception of trials 1 and 2, 5.7 g. (0.05 mole) of monomer and 0.0025 mole of catalyst and cocatalyst were employed.

<sup>b</sup> Inherent viscosities were determined in a mixture of phenol and *sym*-tetrachloroethane (100:66 by weight) at concentration of 0.11-0.17 g./100 ml.

<sup>c</sup> Solubilities were determined in the same solvent as used for measuring  $[\eta]$ . The polymers were insoluble in chloroform.

<sup>d</sup> Aluminum isopropoxide, 0.066 g.; ZnCl<sub>2</sub>, 0.036 g.; monomer, 5.0 g.

<sup>e</sup> Alumina, 2.0 g. (8-14 mesh) was activated at 600°C. for 20 hr.

to 100-ml. serum bottles. The bottles were capped with serum-type rubber stoppers and liquid reagents were transferred to the polymerization bottles with calibrated hypodermic syringes. The diethylzinc-alumina catalyst (trial 3, Table I), was first heated at 80°C. for 1 hr. and allowed to come to room temperature before addition of monomer. After allowing the bottles and contents to come to the desired polymerization temperatures (ice bath or room temperature), the monomer was measured out and added to the systems by injection through the rubber stoppers with a calibrated hypodermic syringe.

Polymer recovery was achieved by decomposition of the catalyst with methanol and removal of the solvent and unpolymerized monomer under reduced pressure. The solid polymeric residues were washed with dilute sulfuric acid, water, and dried under reduced pressure. The yields, solubilities, and inherent viscosities were determined on the resulting polymers.

**Phosphorus Pentafluoride.** The polymerizations with  $\text{PF}_5$  (Table II), were run under nitrogen in side-armed flasks fitted with ebullator tubes. The catalyst was swept with dry purified nitrogen into the reaction systems. In all systems studied, the solvent, monomer, and water were added before the desired amount of catalyst was bubbled in below the surface of the solutions. Polymerization was achieved in thermostatted baths without agitation. With the exception of water, liquid reagents were added to the systems with standard calibrated hypodermic syringes. Water was transferred to the systems by use of precision calibrated Hamilton microliter syringes. In all cases studied, except trials 1-3, it was assumed that decomposition of a given molar amount of benzenediazonium hexafluorophos-

TABLE II  
Polymerization of 1,2,5,6-Diepoxyhexane with  $\text{PF}_5^a$

Trial	Catalyst	Temp., °C.	Time, hr.	$[\eta]^b$	Conver- sion, %	Solubility <sup>c</sup>
1	$\text{PF}_5$	-30	8	0.18	90	50%
2	$\text{PF}_5$	25	12	—	95	Dark, insoluble
3	$\text{PF}_5$	-75	3	—	Low	—
4	$\text{PF}_5$	-30	24	0.14	95	62%
5	$\text{PF}_5$	6	24	0.10	90	Dark, 100%
6	$\text{PF}_5\text{-H}_2\text{O}$ (1:1)	-30	24	0.18	98	100%
7	$\text{PF}_5\text{-H}_2\text{O}$ (1:1)	-10	24	0.19	90	100%
8	$\text{PF}_5\text{-THF}$ (1:1)	-30	24	—	98	100%

<sup>a</sup> With the exception of trial 5, where 20 ml. of nitrobenzene was used as a solvent, 20 ml. of 1,2-dichloroethane was employed. Trials 1-3 contained 5.0 g. of monomer and the catalyst was fed into the system until foam appeared on the surface or a yellow color was detected in the solution. Trials 4-8 contained 5.7 g. (0.05 mole) of monomer, 0.315 g. (0.0025 mole) of  $\text{PF}_5$  based on the benzene diazonium hexafluorophosphate decomposed.

<sup>b</sup> Inherent viscosities were determined in chloroform at concentrations of 0.2-0.45 g./100 ml.

<sup>c</sup> In chloroform.

phate salt would furnish the same molar amount of phosphorus pentafluoride to the reaction systems.

The polymerization reactions were terminated by addition of methanol to decompose the catalyst, and the solvent was evaporated under reduced pressure. The resulting white polymeric residues were dissolved in chloroform at room temperature. After filtering, the volume of the solutions were reduced and poured into stirred pentane to precipitate the polymers. The resulting polymers were dried under reduced pressure.

The effects of water on the phosphorus pentafluoride catalyst were investigated by varying the water content in seven polymerization systems (Table III) while holding the other reaction variables constant. After 8 hr., 10-ml. aliquots were withdrawn from the systems which had not gelled prior to that time and pipetted into 5 ml. of methanol to stop the reaction. The polymers were isolated to determine the yields and inherent viscosities. Polymers that appeared to gel before 8 hr. were worked up at the time of gelation.

The effect of  $\text{PF}_5$  concentration was also studied (Table IV).

TABLE III  
Effects of Water on the Polymerization of 1,2,5,6-Diepoxyhexane with Phosphorus Pentafluoride<sup>a</sup>

Trial	$\text{PF}_5:\text{H}_2\text{O}$ (mole ratio)	Conversion (8 hr.), % <sup>b</sup>	$[\eta]$ (8 hr.) <sup>c</sup>	Gel time, hr.
1	1:0	43	0.100	24
2	1:0.25	59	0.168	20
3	1:0.5	83	0.179	11
4	1:1	94	0.184	8
5	1:1.5	100	0.286	5
6	1:2	98	0.112	6
7	1:4	94	0.097	No gel

<sup>a</sup> Solvent, methylene dichloride (25 ml.); temperature,  $-10^\circ\text{C}$ .; monomer, 5.7 g. (0.005 mole);  $\text{PF}_5$ , 0.315 g. (0.0025 mole).

<sup>b</sup> Calculated on basis of total amount of monomer added.

<sup>c</sup> Inherent viscosities determined in a mixture of phenol and tetrachloroethane (100:66 by weight) at concentrations of 0.25 g./100 ml.

TABLE IV  
Effects of Phosphorus Pentafluoride Concentration on the Polymerization of 1,2,5,6-Diepoxyhexane<sup>a</sup>

Trial	Monomer: $\text{PF}_5:\text{H}_2\text{O}$ (mole ratio)	Time, hr.	Conversion, %	$[\eta]$ <sup>b</sup>
1	200:1:1	48	24	0.142
2	200:1:1.5	48	16	0.157
3	100:1:1	24	24	0.206
4	200:1:0	168	26	0.370

<sup>a</sup> Solvent, methylene chloride (25 ml.); temperature,  $-10^\circ\text{C}$ .; monomer, 5.7 g. (0.05 mole).

<sup>b</sup> Inherent viscosities determined in a mixture of phenol and tetrachloroethane (100:66 by weight) at concentrations of 0.25 g./100 ml.

### Polymerization of 1,2,4,5-Diepoxy pentane and 3,4-Epoxytetrahydrofuran

Polymerization of these monomers (Tables V and VI) was accomplished as described for the polymerization of 1,2,5,6-diepoxyhexane where the same catalysts were employed. The polymerizations with stannic chloride were carried out in serum bottles under nitrogen at  $-78^{\circ}\text{C}$ .

TABLE V  
Polymerization of 1,2,4,5-Diepoxy pentane

Trial	Catalyst <sup>a</sup>	Temp., $^{\circ}\text{C}$ .	Time, hr.	Solvent	Con- version, % <sup>b</sup>
1	$\text{PF}_5 \cdot \text{H}_2\text{O}$ (1:1)	-10	4	1,2-Dichloroethane	45
2	$\text{PF}_5 \cdot \text{H}_2\text{O}$ (1:1)	-78	24	Methylene chloride	26
3	$\text{Al}(i\text{-Bu})_3 \cdot \text{H}_2\text{O}$ (1:1)	0	1	Heptane	72
4	$\text{ZnEt}_2 \cdot \text{H}_2\text{O}$ (1:1)	25	3	Heptane	66
5	$\text{SnCl}_4$	-78	1	Methylene chloride	84

<sup>a</sup> Polymerizations were run in 25 ml. of solvent with 5.0 g. (0.05 mole) of monomer. Trials 1-4 contained 0.0025 mole of catalyst; trial 5 contained 1.38 g. (0.005 mole).

<sup>b</sup> All polymers were white, insoluble, amorphous solids.

TABLE VI  
Polymerization of 3,4-Epoxytetrahydrofuran

Trial	Catalyst <sup>a</sup>	Temp., $^{\circ}\text{C}$ .	Time, hr.	Solvent	Con- version, % <sup>b</sup>
1	$\text{PF}_5 \cdot \text{H}_2\text{O}$ (1:1)	25	2	Methylene chloride	98
2	$\text{Al}(i\text{-Bu})_3 \cdot \text{H}_2\text{O}$ (1:1)	25	3	Heptane	71
3	$\text{ZnEt}_2 \cdot \text{H}_2\text{O}$ (1:1)	25	3	Heptane	93
4	$\text{SnCl}_4$	-78	0.5	Methylene chloride	81

<sup>a</sup> Polymerizations were run in 25 ml. of solvent with 4.3 g. (0.05 mole) of monomer. Trials 1-3 contained 0.0025 mole of catalyst; trial 4 contained 1.38 g. (0.005 mole).

<sup>b</sup> All polymers were white, insoluble, amorphous solids.

### Molecular Weight Determination

A number-average molecular weight, 3800, of a sample of poly-1,2,5,6-diepoxyhexane (Table II, trial 6,  $[\eta]_i = 0.18$ ) was obtained on a Mechrolab 301A vapor pressure osmometer. All inherent viscosities were calculated by use of a concentration scale in grams of solute per 100 ml. solvent at  $25^{\circ}\text{C}$ .

### Differential Thermal Analysis and X-Ray Diffraction

Differential thermal analyses<sup>19</sup> were obtained on finely ground polymer samples packed into the thermocouple well. Alumina was employed as a reference material, and the analyses were run under dry nitrogen at a heating rate of  $6^{\circ}\text{C}/\text{min}$ .

Powder patterns on finely ground polymer samples were obtained by use of copper  $K\alpha$  radiation.

### Infrared Spectra

Infrared spectra for the poly-1,2,5,6-diepoxyhexane polymers prepared with both cationic and anionic catalysts were obtained as chloroform solutions, films, and potassium bromide pellets. The spectra showed an absorption maximum at  $1094\text{ cm.}^{-1}$  (unstrained ether). In a few polymer samples, very weak maxima were observed at  $3500$  (hydroxyl) and  $1258\text{ cm.}^{-1}$  (oxirane).

The infrared spectra for the model compounds tetrahydropyran, tetrahydrofuran, and diethyl cellosolve were obtained as liquid films. The ether absorption maxima occurred in these compounds at  $1095$ ,  $1075$ , and  $1105\text{ cm.}^{-1}$ , respectively.

The infrared spectra for the poly-1,2,4,5-diepoxy-pentane and poly-3,4-epoxytetrahydrofuran polymers (Nujol and potassium bromide pellets) showed a strong, broad ether absorption maxima at  $1105\text{ cm.}^{-1}$ .

## RESULTS AND DISCUSSION

### Polymerization

The metal alkyl-water and phosphorus pentafluoride-water catalysts are both effective for the conversion of the diepoxides to polymer. In the case of 1,2,5,6-diepoxyhexane, the diethyl-zinc water system affords the highest molecular weight polymer (Table I). The polymer produced by this system is largely insoluble, but is not necessarily crosslinked. The limit of solubility of poly-1,2,5,6-diepoxyhexane in chloroform seems to occur at about an inherent viscosity of 0.15; above this a better solvent must be employed. The difficult solubility of this polymer can be attributed to its somewhat rigid structure. The phosphorus pentafluoride-water catalyst system at the same catalyst concentration afforded completely chloroform-soluble polymer in most of the trials (Table II), but the viscosity of the resulting polymers was always below 0.18.

Water is apparently necessary to the phosphorus pentafluoride system (Table III). An induction period was noticed when no water was intentionally added to the system. Further, the yields, molecular weights (inherent viscosities), and the rates of the polymerizations are affected by the amount of water. The optimum ratio of phosphorus pentafluoride to water appears to be 1:1.5, although this assumes the decomposition of benzene-diazonium hexafluorophosphate to be quantitative.

The mole ratio of monomer to phosphorus pentafluoride was changed from 20:1 (Table II and III) to 200:1 and 100:1 (Table IV) in order to determine the effects on yield, molecular weight, and polymerization rates. In general, the lower catalyst ratio affords higher molecular weight polymer, but lower yields and a slower rate. It appears that other factors such

as impurity concentrations and extraneous water show a large effect at this low concentration, since the results are somewhat inconsistent within this set.

The polymerization of 1,2,4,5-diepoxy-pentane and 3,4-epoxytetrahydrofuran yielded insoluble polymers with all catalyst systems tried. The monomer 3,4-epoxytetrahydrofuran was polymerized in an effort to obtain a polymer which would be formed by the selective opening of the epoxide ring, leaving the furan ring untouched. Such a polymer would serve as a model for poly-1,2,4,5-diepoxy-pentane (IV) formed by cyclopolymerization, since it also contains the furan ring.

It is very probable that both these polymers are cross linked and not just difficultly soluble because of their rigid structures and high linear molecular weight. This is evidenced by the facts that: (1) every catalyst system, even those which gave soluble, relatively low molecular weight poly-1,2,5,6-diepoxyhexane (III), afforded insoluble poly-1,2,4,5-diepoxy-pentane (IV) and poly-3,4-epoxytetrahydrofuran and (2) the infrared spectra of these polymers showed broad absorption maxima at  $1105\text{ cm.}^{-1}$  (open chain ether). The model compounds tetrahydrofuran, tetrahydropyran, and diethyl cellosolve show maxima at 1075, 1095, and  $1105\text{ cm.}^{-1}$ , respectively.

Since it has been demonstrated that tetrahydrofuran will form copolymers with propylene oxide<sup>20</sup> and that alkylene oxides are cocatalysts in the Lewis acid polymerization of tetrahydrofuran,<sup>21</sup> it is not surprising that 3,4-epoxytetrahydrofuran would polymerize to afford crosslinked polymers.

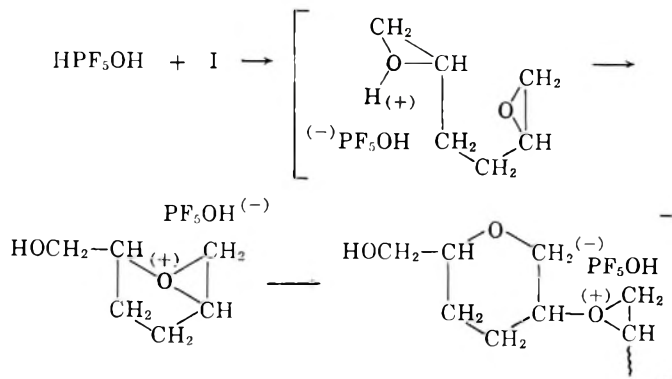
Structure III, containing the tetrahydropyran unit resulting from a cyclopolymerization, is assigned to poly-1,2,5,6-diepoxyhexane on the basis of the following observations: (1) soluble polymers could be obtained from 1,2,5,6-diepoxyhexane (I); (2) the polymers contained no residual epoxide moieties; and (3) the infrared spectra of the polymer samples showed maxima (C—O—C stretching) characteristic of the strainless model compounds tetrahydropyran and diethyl cellosolve.

Since, according to the infrared spectra of tetrahydrofuran and tetrahydropyran, the five-membered cyclic ether shows greater ring strain, it is not unexpected that 1,2,4,5-diepoxy-pentane (II) does not produce a soluble polymer. Although little difference apparently exists between the kinetics of intra-intermolecular and inter-intermolecular propagation,<sup>22</sup> the difference in the frequency factor for the intramolecular and intermolecular steps would be expected to be relatively large in the formation of the somewhat strained furan ring.

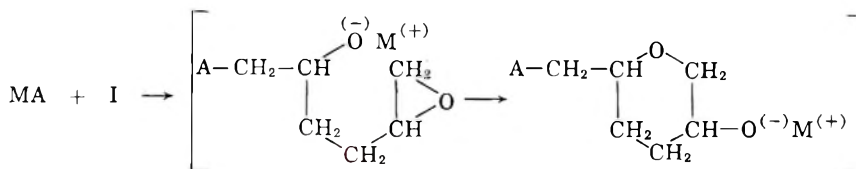
Structure III for poly-1,2,5,6-diepoxyhexane can be accommodated by either an anionic or cationic cyclopolymerization mechanism. The phosphorus pentafluoride-water catalyst undoubtedly acts analogously to the boron trifluoride-water system. The acceptor properties of phosphorus pentafluoride are much greater than phosphorous trifluoride, but slightly less than boron trifluoride.<sup>23</sup>



Cationic:



Anionic:



### Physical Properties of Poly-1,2,5,6-diepoxyhexane

A reprecipitated sample of poly 1,2,5,6-diepoxyhexane with an inherent viscosity of 0.18 (Table II, trial 6) had a number-average molecular weight of 3800. This molecular weight-viscosity relationship is consistent with a rigid polymer chain.<sup>24</sup> This molecular weight obtained after a precipitation which would remove low molecular weight fractions, is also consistent with the molecular weight, 2280 (20 recurring units) which could be expected from a monomer to catalyst ratio of 20:1.

Differential thermal analyses were obtained for polymer samples obtained with phosphorus pentafluoride-water (Table II, trial 6) and diethylzinc-water (Table I, trial 4) catalysts. The polymer prepared with diethylzinc exhibited a sharp exotherm at 120°C. and no endotherm up to 200°C., while the polymer prepared with phosphorus pentafluoride showed a broad exotherm at 115°C. and a shallow endotherm near 200°C. Both polymers started to decompose near 200°C. The exotherms at 115 and 120°C. may be attributed to exothermic crystallization or annealing in which rotation and orientation of chain segments into crystallites below the crystalline transition temperatures is taking place.

This explanation is supported by two other observations. First, when the polymer samples are heated at 125°C. for 1 hr., allowed to cool, and then subjected to differential thermal analysis, no exotherms were observed. Second, the x-ray diffraction patterns of powder samples of annealed polymer prepared with the diethylzinc catalyst showed a higher degree of crystallinity than that obtained for the untreated sample.

Poly-1,2,5,6-diepoxyhexane prepared with diethylzinc has a higher degree of crystallinity than that prepared with phosphorus pentafluoride. Since the polymer obtained from phosphorus pentafluoride has a transition temperature at 200°C. and the polymers begin to decompose above this temperature, the corresponding transition temperature for the polymer obtained from diethylzinc is probably above 200°C. This is compatible with the shapes of the exotherm peaks observed for the two polymer samples.

This research was supported in part by a grant from the Petroleum Research Fund, administered by the American Chemical Society. Grateful acknowledgment is hereby made to the donors of this fund. We also wish to thank Dr. R. T. Woodhams and Dr. T. Dudley of the Dunlop Research Centre, Toronto, Canada, for a differential thermal analysis check on one of our polymer samples and for their helpful discussion concerning the interpretation of the results. We are grateful to Dr. H. Haight, University of Iowa, for his assistance in obtaining the x-ray patterns. A generous gift of 2,5-dihydrofuran was obtained from General Aniline and Film Corp.

### References

1. Stille, J. K., *Introduction to Polymer Chemistry*, Wiley, New York-London, 1962, p. 222.
2. Stille, J. K., and D. A. Frey, *J. Am. Chem. Soc.*, **83**, 1697 (1961).
3. Miller, W. L., and W. B. Black, *Preprints of papers, Division of Polymer Chemistry, American Chemical Society*, **3**, No. 2, 345 (1962).
4. Muetterties, E. L., U. S. Pat. 2,856,370 (Oct. 14, 1958).
5. Wittbecker, E. L., H. K. Hall, Jr. and T. W. Campbell, *J. Am. Chem. Soc.*, **82**, 1218 (1960).
6. Miller, R. A., and C. C. Price, *J. Polymer Sci.*, **34**, 161 (1959).
7. Kambara, S., and M. Hatano, *J. Polymer Sci.*, **27**, 584 (1958).
8. Ebert, P. E., and C. C. Price, *J. Polymer Sci.*, **34**, 157 (1959).
9. Colclough, R. O., G. Gee, and A. H. Jagger, *J. Polymer Sci.*, **48**, 273 (1960).
10. Vandenberg, E. J., *J. Polymer Sci.*, **47**, 486, 489 (1960).
11. Furukawa, J., T. Tsuruta, R. Sakata, T. Saegusa, and A. Kawasaki, *Makromol. Chem.*, **32**, 90 (1959).
12. Furukawa, J., T. Saegusa, T. Tsuruta, and G. Kakogawa, *Makromol. Chem.*, **36**, 25 (1959).
13. Sakata, R., T. Tsuruta, T. Saegusa, and J. Furukawa, *Makromol. Chem.*, **40**, 67 (1960).
14. Everett, J. L., and G. A. R. Kon, *J. Chem. Soc.*, **1950**, 3131.
15. Hawkins, E. G. E., *J. Chem. Soc.*, **1959**, 248.
16. Bellamy, L. J., *The Infrared Spectra of Complex Molecules*, Wiley, New York, 1958, p. 118.
17. Young, W. C., W. H. Hartung, and F. S. Crosley, *J. Am. Chem. Soc.*, **58**, 101 (1936).
18. Noller, C. R., *Organic Synthesis*, Vol. II, Wiley, New York, 1955, p. 184.
19. Ke, B., *Organic Analysis*, Vol. IV, Interscience, New York, 1960, p. 361.
20. Dickinson, L. A., *J. Polymer Sci.*, **58**, 857 (1962).
21. Saegusa, T., H. Imai, and J. Furukawa, *Makromol. Chem.*, **54**, 218 (1962).
22. Gibbs, W. E., and J. T. Murry, *J. Polymer Sci.*, **58**, 1211 (1962).
23. Muetterties, E. L., *J. Inorg. Nuclear Chem.*, **16**, 52 (1960).
24. Flory, P. J., *Principles of Polymer Chemistry*, Cornell Univ. Press, Ithaca, N. Y., 1953, p. 611.

### Résumé

Il est possible de polymériser le 1,2,5,6-diépoxyhexane à l'aide de divers catalyseurs pour obtenir un polymère possédant des unités tétrahydropyrane résultantes d'un mécanisme de cyclopolymérisation. Un système catalytique pentafluorure de phosphore-eau donne un polymère soluble possédant une viscosité intrinsèque de 0.37. Les vitesses de polymérisation, les degrés de conversion, les poids moléculaires sont fonction du rapport catalyseur-monomère et de la quantité d'eau présente. Un système diéthyl zinc-eau donne un poids moléculaire plus élevé de solubilité très limitée, la fraction soluble possédant une viscosité intrinsèque de 0.45. Par contre, le 1,2,4,5-diépoxy-pentane polymérise en un polymère complètement insoluble pour les systèmes catalytiques envisagés. Les films de rayons-X et les analyses thermiques différentielles prouvent que les échantillons de poly-1,2,5,6-diépoxyhexane, préparés par le système diéthyl zinc-eau, possèdent un plus haut degré de cristallinité que les polymères préparés à l'aide du système pentafluorure de phosphore-eau, ainsi qu'il a été prouvé par analyse aux rayons-X et par analyse thermique différentielle.

### Zusammenfassung

Das monomere 1,2,5,6-Diepoxyhexan kann mit einer Vielfalt von Katalysatoren zu einem Polymeren mit Tetrahydropyranbausteinen als Ergebnis eines Cyclopolymerisationsmechanismus polymerisiert werden. Ein Phosphorpentafluorid-Wasser-Katalysatorsystem liefert lösliche Polymere mit Viskositätszahlen bis hinauf zu 0,37. Polymerisationsgeschwindigkeit, Umsatz und Molekulargewicht der Polymeren werden sowohl durch das Verhältnis von Katalysator zu Monomerem als auch durch die Menge des vorhandenen Wassers beeinflusst. Ein Diäthylzink-Wasser-Katalysatorsystem liefert ein höhermolekulares Polymeres mit sehr beschränkter Löslichkeit, dessen löslicher Anteil eine Viskositätszahl von 0,45 besitzt. Im Gegensatz dazu polymerisiert 1,2,4,5-Diepoxy-pentan mit allen verwendeten Katalysatorsystemen zu einem völlig unlöslichen Polymeren. Mit dem Diäthylzink-Wasser-Katalysator hergestellte Poly-1,2,5,6-diepoxyhexanproben zeigen röntgenographisch und differentialthermoanalytisch einen höheren Kristallinitätsgrad als mit dem Phosphorpentafluorid-Wasser-Katalysator gewonnene Proben.

Received November 5, 1962

## Anionic Block Polymerization. II. Preparation and Properties of Block Copolymers

M. BAER, *Monsanto Chemical Company, Plastics Division, Springfield, Massachusetts*

### Synopsis

Block copolymers were prepared by anionic polymerization and their dynamic mechanical properties and thermal stability were compared with those of random copolymers and mechanical blends of similar composition. The block copolymers were prepared by means of Na-naphthalene as the initiator, under conditions leading in most cases to almost complete absence of contaminating homopolymers. The composition, structure, and molecular weight of the block copolymers were determined by (a) molecular weight determinations of the polymers before and after addition of the second monomer to the preformed polymeric anions, and (b) by fractionation and chemical analysis of the resulting fractions. The block copolymers prepared were of the type: poly( $\alpha$ -methylstyrene) - polystyrene - poly( $\alpha$ -methylstyrene), polystyrene - poly( $\alpha$ -methylstyrene)-polystyrene, poly(methyl methacrylate)-polystyrene-poly(methyl methacrylate), and poly(ethylene oxide)-polystyrene-poly(ethylene oxide). The various block copolymer systems showed considerable differences in dynamic mechanical properties among themselves; they also had properties differing from those of copolymers and blends.

### INTRODUCTION

The purpose of this work was to prepare block copolymers of known composition, architecture, and molecular weight in order to compare the properties of block copolymers with those of copolymers and mechanical blends of similar composition. For this purpose it was necessary that the block copolymers be well defined and essentially free from contaminating homopolymers.

While properties of block copolymers prepared by condensation reactions have been described in the literature, little can be found concerning properties of block copolymers prepared by addition reactions. Preparation of addition block copolymers has been described before,<sup>1-6</sup> but judging from the sizeable amount of homopolymers contaminating many of these, it is doubtful that the block copolymers could have been of good uniformity. Mechanical properties were not reported.

The softening points of acrylonitrile-acrylamide block copolymers have been compared by Miller<sup>7</sup> with those of a random copolymer. However, polymer crystallinity would be expected in this case, to play a role as important as polymer architecture and block size, since copolymerization will tend to destroy crystallinity, while a block structure will preserve it.

The glass transition temperatures of random acrylonitrile–methyl methacrylate copolymers have been compared by Beevers and White<sup>8</sup> with those of block copolymers, and significant differences were found. Also in this case copolymerization affects the degree of crystallinity of polyacrylonitrile<sup>9</sup> and complicates the interpretation of the real effect of block structure.

## EXPERIMENTAL

### Materials

Methyl methacrylate (Rohm and Haas Co.), washed with a dilute caustic solution, followed by repeated water washings, was dried by passing through a long column packed with a molecular sieve. The monomer after storing over calcium hydride was distilled under nitrogen at reduced pressure, and the middle fraction was collected over calcium hydride. A clean Na ribbon was added, and the monomer was allowed to stand at room temperature until a considerable amount of polymer had coated the metal. The monomer was distilled *in vacuo* as described for styrene,<sup>10</sup> with the exception that the first distillate was collected over calcium hydride rather than on a Na mirror, which would cause immediate polymerization. The same techniques described for styrene<sup>10</sup> were used throughout, including dilution of the monomer with an equal volume of 1,2-dimethoxyethane.

Ethylene oxide (Mathieson Co.) was condensed in a receiver under nitrogen, stored over 85% KOH pellets for four days, refluxed over KOH pellets for 1½ hr., and distilled in an efficient column. The middle fraction was collected under nitrogen, stored for two days over calcium hydride, degassed several times at liquid nitrogen temperature, and distilled twice under vacuum at  $-45$  to  $-50^{\circ}\text{C}$ . (each time leaving behind some liquid which could contain the ethylene oxide hydrate, reported to be stable at these temperatures). The ethylene oxide was collected directly into graduated ampules and diluted by distilling in an equal volume of dimethoxyethane.

The purification of styrene,  $\alpha$ -methylstyrene, dimethoxyethane, nitrogen, and the method for Na-naphthalene preparation were previously described.<sup>10</sup>

### Polymerization

The equipment used for polymerization was described before.<sup>10</sup> The techniques used for charging the reactor with monomers and solvent, for titrating the solvent before polymerization, and for sampling the polymer solutions at each polymerization stage have also been described.<sup>10</sup> A typical batch would consist of about 500 g. of dimethoxyethane, about 50 g. of total monomers, and 8–15 ml. of a 0.078M solution of Na-naphthalene in dimethoxyethane as initiator. The monomers used were always diluted with an about equal volume of solvent (dimethoxyethane) and the agitator speed was set at about 1500 rpm during monomer addition.

TABLE I  
Anionic Block Copolymers of Styrene: Polymerization Conditions

Run no. <sup>a</sup>	[M]/[I] <sup>b</sup>	Monomer charged	Temperature, °C.	Polymerization time, min.	Conversion, %
8-A	220	Styrene	-70	10	101
8-B		MMA	-72	10	100
9-A	236	Styrene	-65	10	100
9-B		MMA	-65	10	100
28-A	421	Styrene	-70	30	101
28-B		$\alpha$ MS	-30 to -60	150	99.5
30-A	362	$\alpha$ MS	+20 to -65	360	82.5
30-B		Styrene	-65	10	98 <sup>c</sup>
31-A	ca. 350 <sup>d</sup>	$\alpha$ MS	+22 to -65	210	74
31-B		Styrene	-50	10	97 <sup>c</sup>
36-A	406	Styrene	-40	30	92? <sup>c</sup>
36-B		EO	+70	6 days	49

<sup>a</sup> A = polymer formed in the first addition of monomer to the initiator; B = block copolymer formed by block copolymerization on preformed polymer A.

<sup>b</sup> Mole ratio of monomer to initiator in the first polymerization step.

<sup>c</sup> Overall conversion; it includes any monomer not polymerized in the first step.

<sup>d</sup> Some loss of initiator on charging.

TABLE II  
Anionic Block Copolymers of Styrene

Run no.	Monomer charged	$\bar{M}_{nk}$ $\times 10^{-4}$	$\bar{M}_r$ $\times 10^{-4}$	$\bar{M}_n$ $\times 10^{-4}$	$W_{(B)}/W_{(A)}$ <sup>a</sup>	$\bar{M}_{n(B)}/\bar{M}_{n(A)}$ <sup>b/</sup>	$\bar{M}_{r(B)}/\bar{M}_{r(A)}$ <sup>c/</sup>
8-A	Styrene	4.75	6.6	5.9			
8-B	MMA	9.95	13.1 <sup>d</sup>	—	2.18		1.98
9-A	Styrene	4.89	7.6	6.5			
9-B	MMA	10.7	13.1 <sup>d</sup>		2.19		1.73
28-A	Styrene	8.7	11.0	8.1			
28-B	$\alpha$ MS	17.9	17.0 <sup>d</sup>	13.2	2.04	1.62	1.55
30-A	$\alpha$ MS	7.03 <sup>e</sup>	8.6				
30-B	Styrene	16.2	38.3 <sup>d</sup>		2.30		4.45
31-A	$\alpha$ MS		8.1	7.2			
31-B	Styrene		20.0	18.0	2.54	2.50	2.47
36-A	Styrene	8.45		9.9			
36-B	EO	10.48		12.0 <sup>f</sup>	1.20 <sup>g</sup>	1.22	

<sup>a</sup> Ratio of the weight of block copolymer B over the weight of preformed polymer A.

<sup>b</sup> Ratio of osmotic  $\bar{M}_n$  of block copolymer B over the osmotic  $\bar{M}_n$  of preformed polymer A.

<sup>c</sup> Ratio of  $\bar{M}_r$  of block copolymer B over  $\bar{M}_r$  of preformed polymer A.

<sup>d</sup> Calculated from intrinsic viscosity of block copolymer B.

<sup>e</sup> Value calculated from the actual degree of monomer conversion.

<sup>f</sup>  $\bar{M}_n$  of block copolymer after purification.

<sup>g</sup> This represents the weight of block copolymer, after purification, over the weight of preformed polystyrene.

*Block Copolymers of Styrene and Methyl Methacrylate (S-MMA)*

Runs 8 and 9 were prepared by adding styrene monomer at  $-65$  to  $-70^{\circ}\text{C}$ . to the violently agitated solution of Na-naphthalene in dimethoxyethane. In run 9 it was noticed that some solvent had crystallized, trapping some red polystyrene anions which were thus prevented from reacting in the following MMA addition. The deep red color of polystyrene anions discharged immediately on addition of MMA in batch 8, but in run 9 the complete disappearance of red color occurred only after the crystals of solvent, occluding the polystyrene, had completely melted. Details on the two runs are found in Tables I and II.

The polymer solutions were precipitated into a large excess of methanol and dried to constant weight.

*Block Copolymers of Styrene and  $\alpha$ -Methylstyrene (S- $\alpha$ MS)*

**$\alpha$ MS-S- $\alpha$ MS Block Copolymer.** This type of block copolymer (run 28) was obtained by first preparing the polystyrene dianion at  $-70^{\circ}\text{C}$ . and by later adding  $\alpha$ MS at  $-60^{\circ}\text{C}$ . with good agitation. The ruby-red batch was maintained at  $-30^{\circ}\text{C}$ . for one hour, at  $-40$  to  $-50^{\circ}\text{C}$ . for another hour, and finally at  $-60^{\circ}\text{C}$ . for an additional hour. The color was destroyed, as usual, by addition of methanol followed by glacial acetic acid.

**S- $\alpha$ MS-S Block Copolymers.** Dimethoxyethane was titrated at  $20^{\circ}\text{C}$ . with Na-naphthalene until a faint green color persisted;  $\alpha$ MS was charged and the solution titrated again at  $20^{\circ}\text{C}$ . to give a very faint pink color (the titration consumed less than 0.1 ml. of a  $0.08M$  Na-naphthalene solution).

In run 30, the desired charge of Na-naphthalene was added, with good agitation, with resulting formation of a deep ruby-red color. The  $\alpha$ MS was allowed to polymerize at  $20^{\circ}\text{C}$ . for 70 min.; the batch was cooled to  $-55^{\circ}\text{C}$ . and allowed to polymerize for  $4\frac{1}{2}$  hr. while slowly cooling to a final temperature of  $-65^{\circ}\text{C}$ . At the end of this time, the color had faded to a less intense red color. The styrene solution was added at  $-65^{\circ}\text{C}$ . with good agitation.

For run 31, the batch containing 27.3 g. of  $\alpha$ MS was maintained at  $23^{\circ}\text{C}$ . for 2 hr.; during this time the continuously fading pink color was reformed by occasional titration with small amounts of Na-naphthalene solution (about 2 ml. of a  $0.075M$  solution was consumed). The desired charge of initiator solution was added to the batch at  $0^{\circ}\text{C}$ . and the color turned ruby red; the batch was kept at this temperature for 15 min., cooled rapidly to  $-50^{\circ}\text{C}$ ., and maintained at  $-50$  to  $-65^{\circ}\text{C}$ . for  $2\frac{1}{2}$  hr. At the end of this time, the styrene solution was charged.

The solutions of S- $\alpha$ MS block copolymers were precipitated into methanol, washed with methanol, and dried to constant weight. A summary of the pertinent data of the above batches is found in Tables I and II.

*Block Copolymers of Styrene and Ethylene Oxide (S-EO)*

A solution of live polystyrene, prepared by usual procedures, was syphoned from the reactor by means of nitrogen pressure into a carefully dried

and nitrogen purged pressure bottle, while maintaining a nitrogen atmosphere on the bottle throughout. The ethylene oxide solution was added with a syringe to the polymer solution (cooled to  $-10^{\circ}\text{C}.$ ) with resulting large increase of polymer solution viscosity and immediate color disappearance. The bottle was sealed and placed in an oil bath at  $70^{\circ}\text{C}.$  for six days. At the end of this time the polymer solution was neutralized with acetic acid and the degree of conversion was determined by sampling the batch and determining the solids by vacuum drying at  $55^{\circ}\text{C}.$

### Purification and Fractionation of Block Copolymers

Fractionations were conducted by conventional procedures by using a 1% solution of polymer in a separatory funnel. The desired range of precipitant was first established by fractionation of pure homopolymers in the same solvent-precipitant system. These homopolymers were of about the same molecular weight range of the block copolymers.

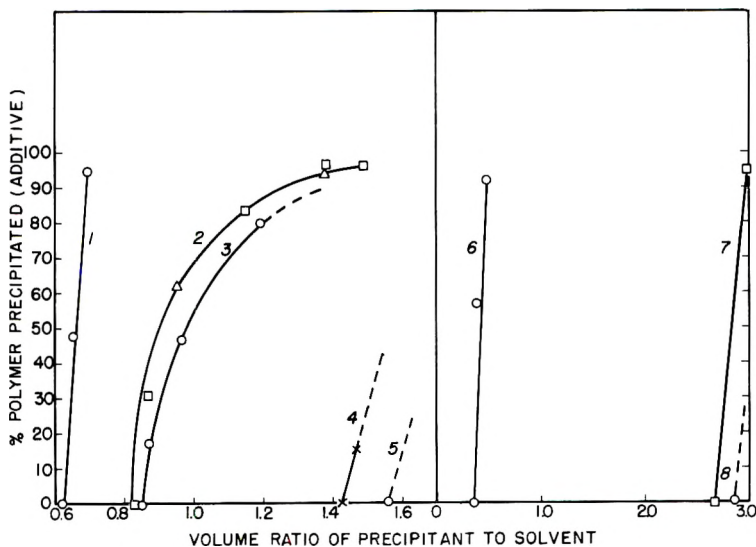


Fig. 1. Fractional separation of S-MMA block copolymers and comparison with precipitation values of the homopolymers. (*Left*): Solvent, benzene-acetone (1:1 volume ratio); precipitant, hexane: (1) poly-MMA ( $\bar{M}_v = 193,000$ ); (2) block copolymer 9-B; (3) block copolymer 8-B; (4) polystyrene-1 ( $\bar{M}_v = 250,000$ ); (5) polystyrene-2 ( $\bar{M}_v = 80,000$ ). (*Right*): Solvent, benzene-monochlorobenzene (1:1 volume ratio), precipitant, methanol (0.01%  $\text{CaCl}_2$ ): (6) polystyrene-2; (7) block copolymer 9-B; (8) poly-MMA ( $\bar{M}_v = 193,000$ ).

The fractions withdrawn from the separatory funnel were centrifuged; the clear supernatant layer was placed back in the separatory funnel, while the bottom gel was diluted with solvent and precipitated. The polymers obtained were normally further purified by reprecipitation.

The homopolymers used for precipitation studies are: polystyrene-1 polymerized by free radical polymerization and purified by precipitation



in methanol,  $\bar{M}_v = 250,000$ ; polystyrene-2 prepared by anionic polymerization,  $\bar{M}_v = 80,000$ ; poly(methyl methacrylate) prepared by anionic polymerization,  $\bar{M}_v = 193,000$ ; poly( $\alpha$ -methylstyrene) prepared by anionic polymerization,  $\bar{M}_v = 160,000$ .

**S-MMA Block Copolymers.** The fractionation procedures used are the ones given by Ceresa<sup>11</sup> and were designed to give a wide spread between the precipitation values of polystyrene and poly-MMA. Two solvent-precipitant systems were used: (1) a 1/1 benzene-monochlorobenzene solvent with methanol as a precipitant, and (2) a 1/1 benzene-acetone solvent with hexane as a precipitant. The former precipitates polystyrene first and poly-MMA last, while the order is reversed in the latter system. The fractionation data is described graphically in Figure 1, while the fractionation values are given in Table III.

TABLE III  
Fractionation of S-MMA Block Copolymers 8-B and 9-B  
(Solvent: 1/1 Benzene-Acetone; Precipitant: Hexane)

Block copolymer	Fraction	Vol. precipitant/ vol. solvent	Weight % of fraction	Cumulative weight, %	MMA in fraction, % <sup>a</sup>	MMA total, % <sup>b</sup>
9-B <sup>c</sup>	I	0.87	30.8	30.8	71	
9-B	II	1.38	64.6	95.4	53	
9-B	III	>1.50	5.1	100.5	17	57 (56.2)
9-B <sup>c</sup>	a	0.90	61.5	61.5		
9-B	b	1.15	22	83.5		
9-B	c	1.38	9	92.5		
8-B <sup>d</sup>	I	0.87	17.2	17.2	69	
8-B	II	0.97	29.3	46.5	58	
8-B	III	1.20	32.9	79.4	51	
8-B	IV	>1.20	17.8	97.2	31	51.2 (55.6)

<sup>a</sup> Determined by infrared.

<sup>b</sup> Calculated as  $\Sigma$  (weight fraction  $\times$  % MMA of fraction). Value in parentheses is value calculated from monomers' charge and conversion, corrected for composition of polymer extracted with cyclohexane.

<sup>c</sup> This polymer had previously been extracted with cyclohexane; the weight loss was 3.19% of essentially pure polystyrene.

<sup>d</sup> This polymer had previously been extracted with cyclohexane; the weight loss was 4.25% of soluble material of 5% MMA content.

Prior to fractionation the block polymers were extracted at 35–45°C. with cyclohexane (a theta solvent for polystyrene at 34°C.) until no polymer could be detected in the cyclohexane solution. The results are tabulated in Table IV.

The polymers purified by cyclohexane extraction could not be extracted with acetonitrile (a selective solvent for poly-MMA) since the polymers would immediately peptize in it and form an extremely fine dispersion.

TABLE IV  
Extraction of S-MMA Block Copolymers with Cyclohexane

Block copolymer	Polymer extracted in cyclohexane, %	MMA in extracted polymer, %
8-B	4.25	5.35
9-B	2.52	0

**S- $\alpha$ MS Block Copolymers.** The fractionation results are described graphically in Figure 2, tabulated in Table V, and summarized in Table VI.

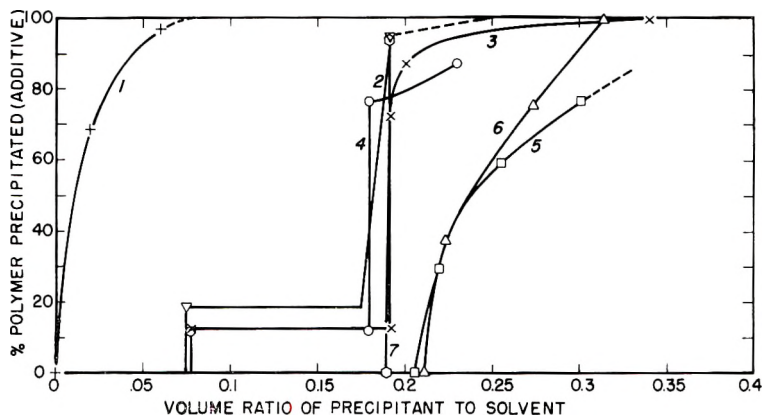


Fig. 2. Fractional separation of S- $\alpha$ MS block copolymers and comparison with precipitation values of the homopolymers: (1) poly- $\alpha$ MS ( $\bar{M}_v = 160,000$ ); (2) block copolymer 30-B; (3) block copolymer 28-B-R; (4) block copolymer 28-B; (5) polystyrene-1 ( $\bar{M}_v = 250,000$ ); (6) polystyrene-2 ( $\bar{M}_v = 80,000$ ); (7) block copolymer 31-B. Solvent, methyl ethyl ketone-benzene (6:1 volume ratio); precipitant, methanol (0.01%  $\text{CaCl}_2$ ).

**Styrene-Ethylene Oxide Block Copolymer (S-EO).** An aliquot of the S-EO block copolymer (run 36), as obtained in the original dimethoxyethane solvent, was precipitated by adding the solution dropwise to well stirred water heated at  $90^\circ\text{C}$ . The fine precipitate was separated from the cloudy aqueous solution, washed with water, dried, dissolved in 5% concentration in chloroform, and reprecipitated as a very fine powder by adding dropwise to boiling water. The precipitate was washed repeatedly with water, dried, and submitted to a second reprecipitation from chloroform solution into water. The dried polymer (36-B-I) weighed 18.45 g.

The aqueous solutions obtained above were combined and taken to dryness *in vacuo* at  $45^\circ\text{C}$ . The residue was dissolved in chloroform and precipitated in boiling water, to give 1.38 g. of a water-insoluble precipitate (36-B-II). The clear aqueous filtrate was taken to dryness to give 0.88 g. of a rather hard, waxy material (36-B-III) which had an infrared spectrum identical to that of polyethylene oxide.

Fraction 36-B-I was extracted with cyclohexane at 38–45°C. until no polymer could be detected in the extracts. The cyclohexane solution was concentrated and precipitated into methanol to give 2.06 g. of polymer (36-B-I-b) which contains essentially pure polystyrene. The residue from

TABLE V  
Fractionation of S- $\alpha$ MS Block Copolymers  
(Solvent: 6/1 Methyl Ethyl Ketone–Benzene; Precipitant: Methanol with 0.01% CaCl<sub>2</sub>)

Block copolymer	Fraction	Vol. precipitant/ vol. solvent	Weight% of fraction	Cumulative weight, %	$\alpha$ MS, % <sup>a</sup>
28-B	I	0.190	76.2	76.2	—
28-B	II	0.230	11.0	87.2	64.5
28-B	III	>0.30	11.0	98.2	<5
28-B	R-I	0.192	72.7	72.7	60.5
28-B	R-II	0.200	14.7	87.4	62.5
28-B	R-III	>0.30	14.3	102	<5
28-B* <sup>b</sup>	A	0.078	16.5	16.5	77
28-B*	B	0.192	79.7	96.2	56
28-B*	C	>0.21	3.3	99.5	—
30-B	I	0.075	18.8	18.8	95
30-B	II	0.192	76.1	94.9	34
30-B	III	>0.24	5.1	100.0	—
31-B	I	0.192	93.6	93.6	51
31-B	II	0.200	4.6	98.2	47
31-B	III	>0.30	1.8	100.0	—

<sup>a</sup> Determined by infrared.

<sup>b</sup> Polymer 28-B\* is a composite of fractions 28-B-I and 28-B-R-I.

TABLE VI  
Summary of Fractionation Data of S- $\alpha$ MS Block Copolymers

Block copolymer	Weight % of material	Composition of fractions		Overall composition, $\alpha$ MS, %	
		$\alpha$ MS, %	S, % <sup>a</sup>	From fractions	Calculated
28-B	~12	77	23	~52	51
	~76	56	44		
	~12	trace	~100		
30-B	18.8	95	5		
	76.1	33.8	66.2		
	5.1	Not determined <sup>b</sup>			
31-B	93.6	51	49		
	4.6	47	53		
	1.8	Not determined <sup>b</sup>			
				49.8+ <sup>c</sup>	50.6

<sup>a</sup> Obtained by difference.

<sup>b</sup> Could not be determined because of contamination by silicone grease.

<sup>c</sup> The value should be increased by the amount of  $\alpha$ MS (probably low) contained in the last fraction, not analyzed.

TABLE VII  
Fractionation of S-EO Block Copolymer

Fraction	Weight of fraction, g.	Weight, %	Infrared observations
36-B-I-a	16.39	79.3	Large amounts of S and EO; no carbonyl or hydroxyl bands
36-B-I-b	2.06	9.9	Essentially pure polystyrene
36-B-II	1.38	6.6	Large amounts of S and EO
36-B-III	0.88	4.2	Essentially pure poly-EO

extraction (36-B-I-a) is the pure S-EO block copolymer. The results are tabulated in Table VII.

From the amounts of styrene and EO charged and polymerized in run 36, and from the fractionation data of Table VII, the fate of the monomers and the composition of the block copolymer can be computed: (a) the purified block copolymer contains 21.1% EO and 78.9% S; (b) 82.5% of the EO polymerized formed a block copolymer; (c) 17.5% of the EO polymerized formed poly-EO; (d) 49% of the EO charged did polymerize; (e) 13.5% of the polystyrene formed initially did not react with EO.

Pure block 36-B-I-a is soluble in methyl ethyl ketone and chloroform; these solutions when added to a large excess of methanol do not give a precipitate, but only a faint bluish colloidal opalescence.<sup>12</sup> The polymer is not soluble nor dispersible in water.

### Properties of Block Copolymers

#### *Dynamic Mechanical Properties*

The mechanical properties investigated were the shear modulus and damping. The measurements were made with a recording torsion pendulum at a frequency of about 1 cycle/sec. The instrument has been described by Nielsen.<sup>13</sup>

Test specimens ( $4 \times \frac{3}{8} \times 0.025$  in.) were compression-molded between polished plates with a 0.025-in. spacer at temperatures varying between 170 and 200°C., depending on the glass temperature of the samples.

In this work, the temperature corresponding to a damping maximum is called the glass temperature,  $T_g$ . In reality the temperature of maximum damping does not coincide with the true  $T_g$ , but it is normally located about 10°C. above it.

The dynamic mechanical properties of the various polymers are found in Figures 3-8.

#### *Decomposition Temperature*

The heat stability of the various block copolymers, homopolymers, and uniform copolymers was compared by means of thermogravimetric analysis.

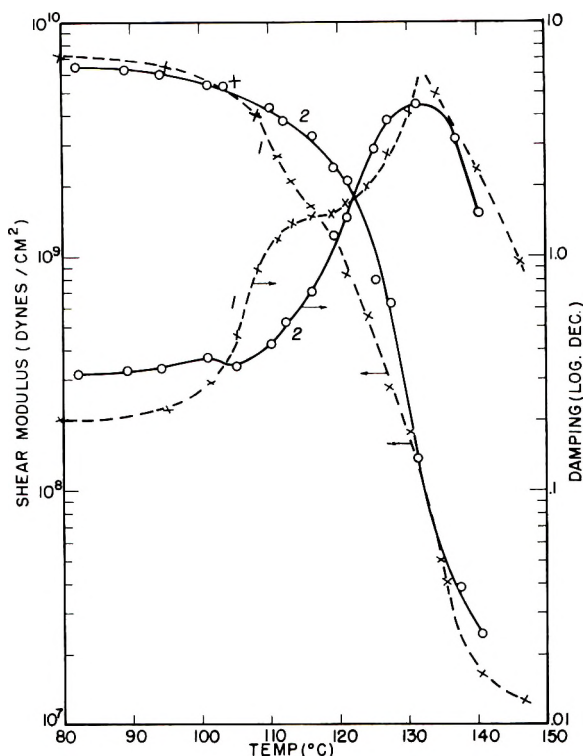


Fig. 3. Dynamic mechanical properties: (1) S-MMA block copolymer 8-B-II (58% MMA); (2) poly-MMA (by anionic polymerization).

The instrument used was an Aminco Thermo-Grav. A vacuum of 2 mm. Hg and heating rate of 6°C./min. were used. The decomposition curves were found to be reproducible within  $\pm 5^\circ\text{C}$ . and not be dependent on small variations in vacuum.

The decomposition temperature was taken to be the temperature at which the weight loss of the sample reached a maximum. It was determined by taking the tangent to the curve at the point of maximum inflection. The results are tabulated in Table VIII, while some of the decomposition curves are shown in Figure 9.

In Table VIII are given the decomposition temperature maxima for poly- $\alpha$ MS ( $T_1$ ) and polystyrene ( $T_2$ ) for the various polymers, and the weight per cent lost at the end of the first decomposition.

#### *Infrared Examination of Block Copolymers*

**S- $\alpha$ MS Block Copolymers.** Quantitative determinations of block copolymer composition were made by using a ratio of the infrared absorption bands at  $8.11\mu$  to  $11.08\mu$  due, respectively, to poly- $\alpha$ MS and polystyrene. A calibration curve was obtained by plotting known compositions

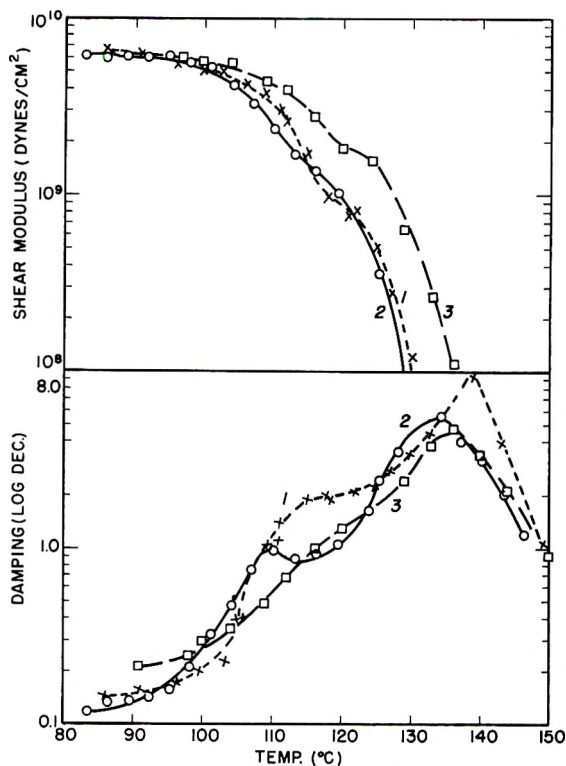


Fig. 4. Dynamic mechanical properties: (1) S-MMA block copolymer 9-B, fraction II (53% MMA); (2) S-MMA block copolymer 9-B, not fractionated (56% MMA); (3) S-MMA block copolymer 9-B, fraction I (71% MMA).

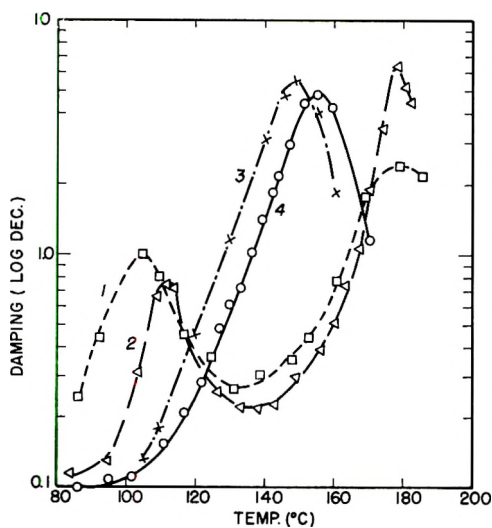


Fig. 5. Dynamic mechanical properties, damping vs. temperature: (1) blend of polystyrene and poly- $\alpha$ MS (coprecipitated into methanol from benzene solution); (2) blend of polystyrene and poly- $\alpha$ MS (freeze-dried from benzene); (3) S- $\alpha$ MS block copolymer 28-B (51%  $\alpha$ MS); (4) S- $\alpha$ MS block copolymer 28-B, fraction B (56%  $\alpha$ MS).

TABLE VIII  
Thermogravimetric Analysis  
(Heating Rate: 6°C./min.; Vacuum: 2.0 mm. Hg)

Polymer	$\alpha$ MS in polymer, %	$T_1$ , °C.	Weight lost at the end of $T_1$ , %	$T_2$ , °C.
Polystyrene-2 (anionic polymerization)				395-405
Polystyrene-1 (free radical polymerization)				400
Poly- $\alpha$ MS (anionic polymerization)	100	305-320		
$\alpha$ MS-S- $\alpha$ MS block (28-B), not fractionated	51	318	51	397
$\alpha$ MS-S- $\alpha$ MS block, fraction 28-B-II	60-62	300-310	58	390
S- $\alpha$ MS-S block, fraction 30-B-II	34	320	36	398
S- $\alpha$ MS-S block, fraction 31-B-I	51	310	52	395
S- $\alpha$ MS random copolymer	~45	365		
Styrene-EO block, fraction 36-B-I-a				385
Poly-MMA (anionic polymerization)				357
S-MMA random copolymer				390
MMA-S-MMA block (9-B), not fractionated				375

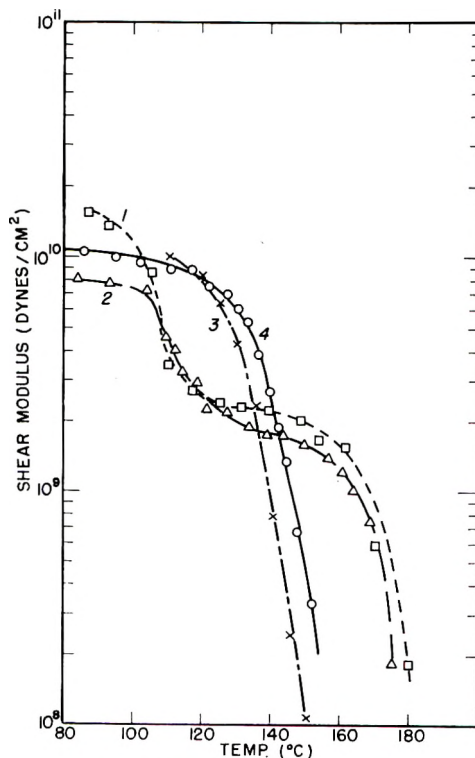


Fig. 6. Dynamic mechanical properties, modulus vs. temperature: (1) blend of polystyrene and poly- $\alpha$ MS (coprecipitated into methanol from benzene solution); (2) blend of polystyrene and poly- $\alpha$ MS (freeze-dried from benzene); (3) S- $\alpha$ MS block copolymer 28-B (51%  $\alpha$ MS); (4) S- $\alpha$ MS block copolymer 28-B, fraction B (56%  $\alpha$ MS).

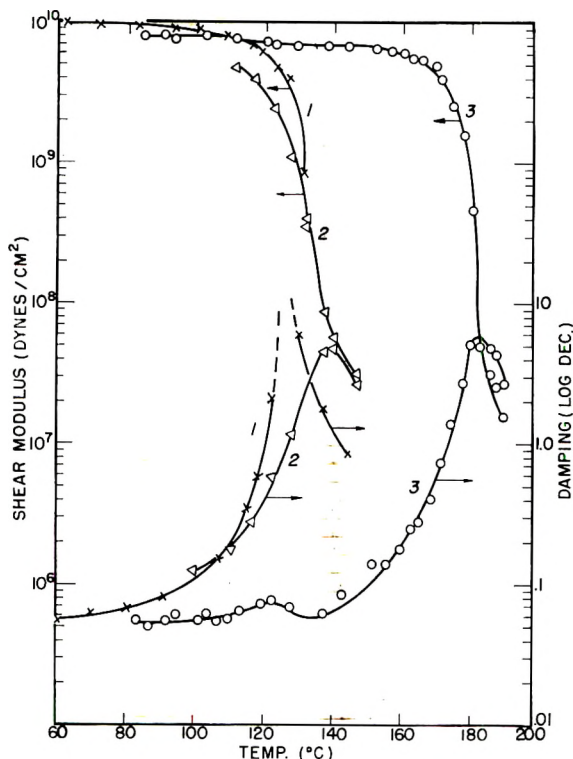


Fig. 7. Dynamic mechanical properties: (1) random S- $\alpha$ MS copolymer (45%  $\alpha$ MS); (2) S- $\alpha$ MS block copolymer 31-B, not fractionated (50%  $\alpha$ MS); (3) poly- $\alpha$ MS (by anionic polymerization).

of mixtures of poly- $\alpha$ MS and polystyrene, versus the ratio  $\text{Abs}_{.8.11}/\text{Abs}_{.11.08}$  of these absorptions.

**S-MMA Block Copolymers.** Infrared absorption bands at  $5.75\mu$  and  $14.3\mu$  due, respectively, to poly-MMA and polystyrene were used for the determination of block copolymer composition. Chloroform and carbon disulfide were used as the individual solvents in the determinations of the respective amounts of poly-MMA and polystyrene in the block copolymer. Calibration curves were obtained by determining the absorption of known blends of polystyrene and poly-MMA in the two individual solvents.

#### *Intrinsic Viscosity- $\bar{M}_v$ Relationship*

The following relationships were used: for polystyrene,  $[\eta] = 5.74 \times 10^{-5}M^{0.78}$  in toluene at  $25^\circ\text{C}$ .;<sup>14</sup> for poly( $\alpha$ -methylstyrene),  $[\eta] = 1.16 \times 10^{-4}M^{0.714}$  in toluene at  $25^\circ\text{C}$ .;<sup>15</sup> for poly(methyl methacrylate),  $[\eta] = 0.57 \times 10^{-4}M^{0.76}$  in benzene at  $25^\circ\text{C}$ .<sup>16</sup>

For a block copolymer AB the  $\bar{M}_v$  of the block copolymer was computed from the observed  $[\eta]_{AB}$  as follows:

$$M^*_{AB} = w_1M^*_A + w_2M^*_B \quad (1)$$



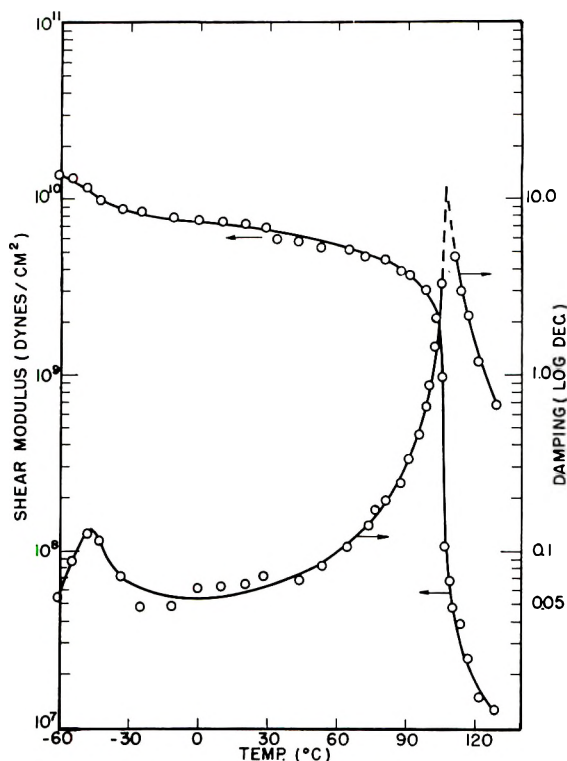


Fig. 8. Dynamic mechanical properties of S-EO Block Copolymer: S-EO block copolymer 36-B, fraction I-a (21% EO).

where (neglecting possible interactions)  $M^*_A$  is the computed  $\bar{M}_v$  for A, assuming the entire block copolymer of intrinsic viscosity  $[\eta]_{AB}$ , to be pure A,  $M^*_B$  is the computed  $\bar{M}_v$  for B, assuming the entire block copolymer of intrinsic viscosity  $[\eta]_{AB}$ , to be pure B,  $M^*_{AB}$  is the computed average  $\bar{M}_v$  for block copolymer AB, and  $w_1$  and  $w_2$  are, respectively, the weight fractions of polymers A and B in the block copolymer.

## DISCUSSION

The polymerization conditions used for the preparation of block copolymers were the ones found to lead to best purity in the study of block polymerization of styrene upon polystyrene.<sup>10</sup> The agitation and the molar ratios of monomer to initiator  $[M]/[I]$  chosen were designed to insure that essentially no residual initiator would be present at the end of the first monomer polymerization. A summary of the polymerization conditions used in the preparation of the various block copolymers is found in Table I. In Table II are given the kinetic number-average molecular weights ( $\bar{M}_{nk}$ ) for the polymer formed at the end of the polymerization of the first monomer (defined as A in the Table) and for the block polymer, formed at the end of the second monomer polymerization (defined as B). The

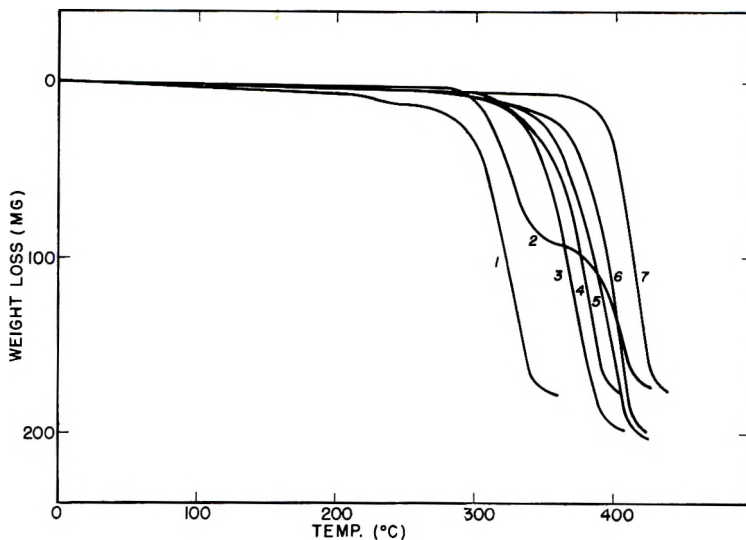


Fig. 9. Thermogravimetric analysis of various block copolymers, random copolymers, and homopolymers: (1) poly- $\alpha$ MS (polymerized anionically); (2) S- $\alpha$ MS block copolymer 31-B, fraction I (51%  $\alpha$ MS); (3) poly-MMA (polymerized anionically); (4) S- $\alpha$ MS random copolymer (45%  $\alpha$ MS); (5) S-MMA block copolymer 9-B (56% MMA); (6) S-MMA random copolymer (50% MMA); (7) polystyrene. Sample weight = 192–198 mg., temp. rise = 6°C./min., vacuum 2 mm. Hg.

$\bar{M}_v/\bar{M}_n$  ratios for the prepolymers A range around 1.2; the resulting polymers, therefore, are not monodisperse.

As discussed before,<sup>10</sup> one can gain a good understanding of the completeness of initiator consumption and the course of block polymerization by comparing the weight ratio of block polymer over the initial polymer ( $W_{(B)}/W_{(A)}$ ) with the molecular weight ratios  $\bar{M}_{n(B)}/\bar{M}_{n(A)}$  and/or  $\bar{M}_{v(B)}/\bar{M}_{v(A)}$ .

The reliability of  $\bar{M}_v$  of the block copolymer, computed according to eq. (1) (experimental section) is not known. Miller<sup>7</sup> used the same approach and found good agreement between observed and computed values. Good agreement is also obtained if one uses the intrinsic viscosity and compositional data obtained by Woodward and Smets<sup>2</sup> for their S-MMA block copolymers. The  $\bar{M}_n$  obtained by them is in good agreement with the  $\bar{M}_v$  computed by using eq. (1) and the  $[\eta]-\bar{M}_v$  relationships chosen in our work for polystyrene<sup>14</sup> and poly(methyl methacrylate).<sup>16</sup>

### Styrene-Methyl Methacrylate Block Copolymers

The block polymers prepared were of the type MMA-S-MMA. As proven by Graham et al.<sup>3,17</sup> (and confirmed in the course of our work), MMA anions are not sufficiently nucleophilic to initiate styrene polymerization; block copolymers of the S-MMA-S type cannot, therefore, be prepared by anionic polymerization.

The block copolymers, as prepared, are not contaminated by poly-MMA (Table III and Figure 1). A small amount of polymer low in MMA content is contained in polymer 8-B, while polymer 9-B contains 2.5% of polystyrene which, as previously described, is the result of mechanical occlusion of polystyrene anions in frozen solvent crystals (Table IV).

Fractionation data show that for both block copolymers, the bulk of the material is of uniform composition. This is also confirmed by the fair correlation between the weight ratios ( $W$ ) and the  $\bar{M}_w$  ratios in Table II.

**Dynamic Mechanical Properties.** Unfractionated S-MMA block polymer 9-B shows (Fig. 4) two damping maxima which correspond to the glass transition temperature  $T_g$  of polystyrene (110°C.) and poly-MMA (133°C.) Figure 3. This would suggest the presence of two phases even though the moldings are optically clear and only show a slight Tyndall effect when exposed to a light beam. If two phases were present they would be expected to be considerably smaller than the wavelength of light in order to explain clarity despite the large refractive index difference between polystyrene and poly-MMA. Annealing at a temperature above 140°C. for 17 hr. results in slightly greater peak sharpness, which could be interpreted as increased phase separation. The random S-MMA copolymer (1:1/weight ratio), which must be a single-phase system, yields a single damping peak at about 105°C.

In Figure 4 are compared the dynamic mechanical properties of the unfractionated S-MMA block copolymer 9B and its fractions (all molded specimens are optically clear). While the unfractionated block shows two distinct transition temperatures, the block fractions show the  $T_g$  of poly-MMA and only a shoulder where the  $T_g$  of polystyrene is normally located. The same dynamic properties are observed with a different S-MMA block copolymer (Fig. 3). The pure S-MMA block copolymers, therefore, differ in mechanical properties from a polyblend (two distinct damping maxima) and a random copolymer (single damping maximum).

### Styrene- $\alpha$ -Methylstyrene Block Copolymers

Block copolymers of the type  $\alpha$ MS-S- $\alpha$ MS and S- $\alpha$ MS-S were prepared by reversing the order of monomer addition. This is in contradistinction with the styrene-MMA system where only polymers of the MMA-S-MMA type can be made.

Considerable difficulty was encountered in the preparation of pure block copolymers because of the slow propagation rate of  $\alpha$ MS at the low temperatures needed<sup>18,19</sup> to bring polymerization to essential completion. Long reaction times increased the chance of destruction of some of the live anions. Uniform block copolymers of the S- $\alpha$ MS-S type were prepared by titrating  $\alpha$ MS at room temperature with Na-naphthalene and by avoiding polymerization temperatures above 0°C. When polymerization was initiated and conducted at 20°C. for some time, some fading of the ruby-red color of the  $\alpha$ MS anion was always observed. This may be the result of attack on the solvent by the strongly basic polymeric anion,

or to its chain transfer with the methyl group of  $\alpha$ MS, or to slow reacting impurities contained in the monomer, as suggested by Wenger.<sup>20</sup>

In the preparation of the  $\alpha$ MS-S- $\alpha$ MS block copolymer (run 28) some termination of the polystyrene anions took place, as shown by the fractionation data (Tables V, and VI and Fig. 2). Formation of new chains on addition of  $\alpha$ MS to polystyrene is suggested by a  $W$  ratio higher than the  $\bar{M}_n$  ratio in Table II; fractionation data, however, do not reveal a large  $\alpha$ MS-rich fraction which could be expected to contain some poly- $\alpha$ MS.

In the case of block copolymers of the S- $\alpha$ MS-S type, molecular weight and fractionation data clearly show that very pure and uniform block copolymers were obtained by polymerizing  $\alpha$ MS at low temperatures (run 31), while rather heterogeneous polymers were obtained by polymerizing  $\alpha$ MS for a long time at room temperature.

**Dynamic Mechanical Properties.** In Figures 5 and 6 are compared the properties of a  $\alpha$ MS-S- $\alpha$ MS block copolymer, a pure fraction of it, and mechanical blends of polystyrene and poly- $\alpha$ -MS. In Figure 7 are compared the properties of a S- $\alpha$ MS-S block copolymer with those of poly- $\alpha$ MS (prepared by anionic polymerization) and a 55/45 S- $\alpha$ MS random copolymer (prepared by low conversion, free-radical polymerization).

Intimate blends of polystyrene and poly- $\alpha$ MS were prepared by (a) precipitation in methanol of a common benzene solution of the two polymers, or (b) by rapid freezing of the above solution, followed by vacuum freeze-drying. The moldings of both mechanical blends were cloudy. The incompatibility of the two homopolymers was also confirmed by the presence of two distinct damping maxima.

The block copolymers have unusual mechanical properties in that they show a single  $T_g$  value intermediate between the glass transitions of 115°C. (polystyrene) and 183°C. (poly- $\alpha$ MS). While the block copolymers are similar to a random copolymer in that they have a single damping maximum, they have  $T_g$  values, ranging from 140 to 155°C., which are higher than that of a copolymer of similar composition; the copolymer displays a narrower and sharper damping curve than the block copolymers.

The single  $T_g$  of the block copolymers suggests that they are a one-phase system or that if two phases are present they must be extremely small. A single phase could also result from two compatible polymers or from a three-component system comprised by two mutually incompatible polymers which are rendered compatible by a mutual solvent, in this case the block copolymer. In the latter case, however, one would expect a broadening of the damping curve which was not observed. In order to encourage phase separation, in the event that two phases were actually present, a block copolymer was annealed at 190°C., which is above the glass transition of both components. No change was observed in the damping curve, and there was no indication of phase separation.

It is important to note that while the molded unfractionated block copolymers were transparent, all the molded block copolymer fractions were cloudy to opaque, but still displayed a single damping maximum. We are

unable to explain why an opaque (two-phase) system does not show two damping maxima, unless the opacity is the result of crystallinity rather than compositional heterogeneity. Poly- $\alpha$ MS and a S- $\alpha$ MS block fraction were examined (before and after prolonged heating in octane at 155°C. in sealed bottles) under x-rays and found to have regions of definite order but only a very slight degree of crystallinity. We are doubtful that such moderate degree of crystallinity could fully explain the opacity of the molded samples.

In connection with the opacity of the molded fractions, in contrast with the clarity of the molded unfractionated block copolymers, the following observations were made. (1) Opaque moldings were obtained if the polymers were exposed for a long time, while in solution, to the same solvent-nonsolvent mixture present during fractionation. The polymer recovered was opaque whether it was collected in fractions or in its entirety; it remained opaque even if dissolved in benzene and then reprecipitated in methanol or if heated for some time above its glass transition. (2) Clear moldings were obtained if the original block copolymers were dissolved in benzene and precipitated in methanol or if dissolved in the solvent-nonsolvent mixture present during fractionation and immediately precipitated in methanol.

The above observations strongly suggest that the individual blocks of the block copolymers, when exposed for a long time to a poor solvent, aggregate each with its own kind, to form separate phases or perhaps some paracrystalline regions.

### Styrene-Ethylene Oxide Block Copolymers

Block copolymers of the EO-S-EO type were prepared by adding EO to polystyrene anions. The polymerization procedure used was the same as the one described by Richards and Szwarc.<sup>12</sup> Block polymers of the S-EO-S type cannot be made by reversing the order of monomer addition since alkoxide anions are not sufficiently basic to polymerize styrene.

Formation of poly(ethylene oxide) during block polymerization suggests a sizeable amount of chain transfer of the ethoxide anion with ethylene oxide on prolonged heating at 70°C. The composition of the pure block checks well with the increase in molecular weight observed on adding EO to polystyrene (Table II). Infrared examination of the pure block shows the presence of EO and S with practically no carbonyl or hydroxyl bands.

The block copolymer gave a clear and colorless molding which showed (Fig. 8) two distinct glass transitions, one corresponding to the  $T_g$  of polystyrene and one corresponding to the  $T_g$  of amorphous poly-EO (about -49°C.). Intimate blends of polystyrene and 20% poly(ethylene oxide) of  $M_w$ -20,000 (Carbowax 20M) did not give clear moldings.

### Decomposition Temperatures of Block Copolymers

The heat stabilities of various block copolymers, homopolymers, and uniform copolymers were compared by means of thermogravimetric analysis (Table VIII and Figure 9). The following conclusions can be drawn.

1. Polystyrene samples have the same decomposition temperature independent of the type of polymerization used (free radical or anionic). This throws considerable doubt on the theory of "weak links" in polystyrene (prepared by free radical polymerization) being responsible for its instability. Anionic polystyrene should be completely devoid of internal or terminal unsaturation and would not be expected to have the same type of weak links.

2. A uniform S- $\alpha$ MS copolymer is more stable than poly- $\alpha$ MS or any of the S- $\alpha$ MS block copolymers. While the copolymer shows only one decomposition temperature, the block copolymers show two decomposition maxima. The weight loss at the end of the first decomposition is about equal to the  $\alpha$ MS content of the block copolymer and does not appear to depend on the distribution of the blocks, that is, on whether the terminal blocks are polystyrene or poly- $\alpha$ MS.

3. The S-EO block copolymers display only one decomposition temperature.

4. The S-MMA block copolymers show only one decomposition temperature which is lower than that of the S-MMA copolymer and intermediate between the decomposition temperatures of polystyrene and poly-MMA.

The writer is particularly indebted to Mr. R. A. Isaksen who helped in collecting and interpreting a good number of the dynamic mechanical data. Ideas concerning the effect of heat history on possible phase changes originated with him. The writer is also indebted to Mr. P. Shapras for infrared analyses, to Dr. M. Ezrin for osmotic measurements, to Dr. R. L. Miller for x-ray determinations, and to Mr. R. Durepo for his assistance in the experimental work. Discussions and consultations with Mr. Q. A. Trementozzi, Dr. J. D. Cotman, and Dr. L. E. Nielsen were helpful and are gratefully acknowledged.

### References

1. Szwarc, M., and A. Rembaum, *J. Polymer Sci.*, **22**, 189 (1956).
2. Woodward, A. E., and G. Smets, *J. Polymer Sci.*, **17**, 51 (1955).
3. Graham, R. K., D. L. Dunkelberger, and E. S. Cohn, *J. Polymer Sci.*, **42**, 501 (1960).
4. Graham, R. K., J. R. Panchack, and M. J. Kampf, *J. Polymer Sci.*, **44**, 411 (1960).
5. Champetier, G., M. Fontanille, and P. Sigwalt, *Compt. Rend.*, **250**, 3653 (1960).
6. Leng, M., and P. Rempp, *Compt. Rend.*, **250**, 2720 (1960).
7. Miller, M. L., *Can. J. Chem.*, **36**, 309 (1958).
8. Beevers, R. B., and E. F. T. White, *Trans. Faraday Soc.*, **56**, 1529 (1960).
9. Beevers, R. B., E. F. T. White, and L. Brown, *Trans. Faraday Soc.*, **56**, 1535 (1960).
10. Baer, M., *J. Polymer Sci.*, **A1**, 2171 (1963).
11. Ceresa, R. J., in *Techniques of Polymer Characterization*, P. W. Allen, Ed., Academic Press, New York, 1959, p. 239.
12. Richards, D. H., and M. Szwarc, *Trans. Faraday Soc.*, **55**, 1644 (1959).
13. Nielsen, L. E., *Rev. Sci. Instr.*, **22**, 690 (1951).
14. Trementozzi, Q. A., *J. Phys. Colloid Chem.*, **54**, 1227 (1950).
15. Worsfold, D. J. and S. Bywater, *Can. J. Chem.*, **36**, 1141 (1958).
16. Flory, P. J., *Principles of Polymer Chemistry*, Cornell Univ. Press, Ithaca, N. Y., 1953, p. 312.

17. Graham, R. K., D. L. Dunkelberger, and W. E. Goode, *J. Am. Chem. Soc.*, **82**, 400 (1960).
18. McCormick, H. W., *J. Polymer Sci.*, **25**, 488 (1957).
19. Worsfold, D. J., and S. Bywater, *J. Polymer Sci.*, **26**, 299 (1957).
20. Wenger, F., *J. Am. Chem. Soc.*, **82**, 4281 (1960).

### Résumé

On a préparé des copolymères séquencés par polymérisation anionique et on a comparé leur propriétés dynamiques mécaniques et leur stabilité thermique avec celles des copolymères conventionnels et des mélanges mécaniques de composition analogue. On a employé du sodium-naphtalène comme initiateur dans des conditions menant la plupart du temps à une absence presque complète d'homopolymères contaminants. La composition, la structure et le poids moléculaire des copolymères séquencés ont été déterminés par (a) des déterminations du poids moléculaire des polymères avant et après l'addition du second monomère aux anions polymériques formés auparavant et (b) par fractionnement et analyse chimique des fractions obtenues. Les copolymères séquencés préparés étaient du type: poly( $\alpha$ -méthylstyrène)-polystyrène-poly( $\alpha$ -méthylstyrène), polystyrène-poly( $\alpha$ -méthylstyrène)-polystyrène, poly(méthacrylate de méthyle)-polystyrène-poly(méthacrylate de méthyle) et poly(oxyde d'éthylène)-polystyrène-poly(oxyde d'éthylène). Les différents systèmes des copolymères séquencés diffèrent considérablement entr'eux quant à leurs propriétés dynamiques et mécaniques; ils ont aussi des propriétés différentes de celles des copolymères et des mélanges de polymères.

### Zusammenfassung

Blockcopolymeren wurden durch anionische Polymerisation dargestellt und ihre dynamisch-mechanischen Eigenschaften und thermische Stabilität mit denjenigen von statistischen Copolymeren und von mechanischen Gemischen ähnlicher Zusammensetzung verglichen. Die Blockcopolymeren wurden mit Na-Naphthalin als Starter unter Bedingungen dargestellt, die in den meisten Fällen zu fast völligem Fehlen von Homopolymeren als Verunreinigung führten. Zusammensetzung, Struktur und Molekulargewicht der Blockcopolymeren wurde (a) durch Molekulargewichtsbestimmung an den Polymeren vor und nach Zusatz des zweiten Monomeren zu den vorgebildeten polymeren Anionen und (b) durch Fraktionierung und chemische Analyse der erhaltenen Fraktionen bestimmt. Die dargestellten Blockcopolymeren waren von folgendem Typ: Poly- $\alpha$ -methylstyrol-Polystyrol-Poly- $\alpha$ -methylstyrol, Polystyrol-Poly- $\alpha$ -methylstyrol-Polystyrol, Polymethylmethacrylat-Polystyrol-Polymethylmethacrylat und Polyäthylenoxyd-Polystyrol-Polyäthylenoxyd. Die verschiedenen Blockcopolymerensysteme zeigten untereinander beträchtliche Unterschiede in den dynamisch-mechanischen Eigenschaften: ihre Eigenschaften unterschieden sich auch von denjenigen der Copolymeren und Gemische.

Received March 17, 1962

Revised November 6, 1962

## Linear Condensation Polymers from Phenolphthalein and Related Compounds

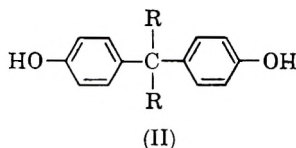
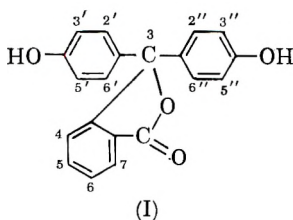
P. W. MORGAN, *Pioneering Research Division, Textile Fibers Department, E. I. du Pont de Nemours & Company, Inc., Wilmington, Delaware*

### Synopsis

Phenolphthalein, phenolphthalimidine, phenolisatin, and similar compounds were found to react as bisphenols with aliphatic and aromatic diacid chlorides, bischloroformates, and phosgene to form linear, high molecular weight products. Interfacial and low and high temperature solution polycondensation procedures were used. The polymers were colorless and readily formed films or fibers from a wide variety of solvents. Several peculiarities in solubility behavior were encountered. The glass transition and melting temperatures of all of the polymers were much higher than values for similar polymers derived from bisphenol A. Water absorption was relatively high, and stability to discoloration by ultraviolet light was good. The majority of the products did not crystallize readily.

### INTRODUCTION

Phenolphthalein (I) was first synthesized in 1871 by Baeyer<sup>1</sup> from phenol and phthalic anhydride. Phenolphthalein and related structures are familiar to most chemists as acid-base indicators, dyes, and drugs. As a result, it is common to associate a high degree of color with them and to overlook their formal structure as bisphenols based on bis(hydroxyphenyl)-methane (II).

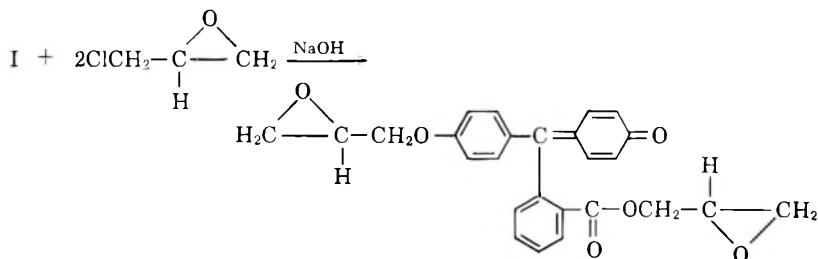


There have been many studies of the use of bisphenols of type II in polymers for application in coatings, photographic film, and plastics.<sup>2-5</sup> One of the recent large-scale developments in the field of condensation polymers is the polycarbonate from bisphenol A (formula II where R is methyl<sup>3,6</sup>). Of the many variations in the structure of aromatic polyesters which have been described, the majority have contained hydrocarbon or halogen substituents and very few have employed polar substituents. If the bis(hydroxy-



phenyl)phthaleins, sulfonephthaleins, phthalimidines, oxindoles, and similar structures would act as bisphenols in condensation polymerizations, then a wide range of new chemical compositions would be available. Such changes should produce unusual effects on melting point, solubility, chemical stability, and other properties of interest, as well as provide the possibility of post reactions on the finished polymer.

A search of the literature showed that nearly seventy years ago Bistrzycki and Nencki<sup>7</sup> and Meyer and Meyer<sup>8</sup> combined phenolphthalein and fluorescein with benzoyl chloride and alkali to form colorless dibenzoates. This is a significant portent of the polymer-forming ability of these compounds. A Swiss patent<sup>9</sup> and a report by Bafna and Shah<sup>10</sup> describe resins from phenolphthalein and formaldehyde. Lo<sup>11</sup> made epoxy resins by first combining phenolphthalein with epichlorohydrin and alkali. This reaction yielded primarily a monoether-monoester, which retained a yellow color because of its quinomethine structure.



The present paper describes the preparation and properties of about fifty aromatic and aliphatic polyesters based on phenolphthalein and related compounds. For the most part, low temperature polycondensation procedures were used, but examples of a high temperature method are given.

Since this work was completed Korshak, Vinogradova, and Salazkin<sup>12</sup> have reported the preparation of the adipate, sebacate, isophthalate, and terephthalate of phenolphthalein and a variety of copolymers by a high temperature solution process. Several patents have also been issued to Howe<sup>13</sup> which claim the polycarbonates from various phenolphthaleins, fluoresceins, and phenolsulfonephthaleins. No specific properties are given except for several polymers from phenolphthalein.

## EXPERIMENTAL

### Intermediates

A variety of phthaleins and fluoresceins may be purchased. Phenolphthalein is very pure as sold in reagent grade and forms high polymers without any treatment. Other materials were purified or synthesized as follows.

**Dibenzoyl Phenolphthalein.** Phenolphthalein (31.8 g., 0.1 mole) and 28 ml. of triethylamine (0.2 mole) were dispersed in 300 ml. of 1,1,2-

trichloroethane and the mixture was cooled in ice water. Benzoyl chloride (23 ml., 0.2 mole) was added slowly with swirling and cooling. The mixture was evaporated to dryness and the product was washed with water to remove salt. After the ester had been crystallized three times from 95% ethanol, its melting point was 173–174°C. Bistrzycki and Nencki<sup>7</sup> obtained a melting point of 169°C.

ANAL. Calcd. for  $C_{31}H_{22}O_6$ : C, 77.52%; H, 4.25%. Found: C, 77.66, 77.50%; H, 4.36, 4.44%.

**Diacetyl Phenolphthalein.** Phenolphthalein was acetylated by warming 5 g. of it in 50 ml. of acetic anhydride with 0.2 g. potassium acetate for 2 hr. The product was recrystallized from aqueous alcohol. The melting point was 146°C. Baeyer<sup>1</sup> reported a melting point of 143°C.

**Phenolphthalein Dimethyl Ether.** Phenolphthalein was methylated by refluxing for 18 hr. in methyl iodide in the presence of concentrated aqueous sodium hydroxide.<sup>14</sup> The product was dissolved in ether and extracted with dilute alkali to remove unchanged material. It was then chromatographed as a benzene solution on an alumina column (Woehlm neutral; activity grade 1). Elution was with benzene-petroleum ether. The adsorbed material was colored red to orange, but the dimethyl ether was eluted as a colorless viscous oil which could not be crystallized. There is a report of a crystalline form of this compound melting at 100°C.<sup>14</sup>

ANAL. Calcd. for  $C_{22}H_{18}O_4$ : C, 76.26%; H, 5.27%. Found: C, 76.0%; H, 5.3%.

**3',3'',5',5''-Tetraiodophenolphthalein.** This compound was purchased and recrystallized three times from acetone-alcohol mixtures. On a hot bar<sup>15</sup> it had a melting point at about 325°C. and at a slightly higher temperature decomposed with the evolution of iodine;<sup>16</sup> the literature value is 270–272°C. (dec.).

**3',3'',5',5''-Tetrachlorophenolphthalein.** Phenolphthalein was chlorinated in glacial acetic acid by slowly introducing the calculated amount of chlorine gas with stirring at 25°C. The product crystallized from benzene. The melting point was 230°C. (hot bar); the literature value is 215°C.<sup>17,18</sup>

**4,5,6,7-Tetrachlorophenolphthalein.** Tetrachlorophthalic anhydride (80 g.), 160 g. of melted anhydrous phenol, and 80 g. of fuming sulfuric acid (20%  $SO_3$ ) were stirred and heated at 150°C. for 12 hr. in a round-bottomed flask. The dark red mixture was allowed to stand another 16 hr. and was then poured into cold water. The red-brown solid was collected and washed. It was dissolved in aqueous alkali and filtered to remove the insoluble fluoran. The phthalein was precipitated with hydrochloric acid and recrystallized from aqueous alcohol. The purest fraction (12 g.) melted at 325°C. (hot bar). The reported melting point is 316–317°C. (dec.).<sup>19</sup>

***o*-Cresolphthalein.** Phthalic anhydride (15 g.), 25 g. of *o*-cresol, and 25 g. of anhydrous zinc chloride were mixed and heated at 125°C. for 8 hr. The dark red tar was extracted repeatedly with boiling water (2 l.). The

residue was extracted with three 500-ml. portions of 50% aqueous sodium hydroxide. The alkaline filtrate was neutralized with dilute hydrochloric acid and the tan product was crystallized from aqueous alcohol; yield 19 g. (54%) melting at 222–223°C. (capillary tube). The reported melting point is 216°C.<sup>20</sup>

**3,3-Bis(4-hydroxyphenyl)phthalimidine.** Phenolphthalein (100 g.) was dissolved in 1000 ml. of 28% aqueous ammonia and allowed to stand at room temperature for 11 days.<sup>21</sup> The color changed to a dull claret. The solution was poured into a mixture of ice and concentrated hydrochloric acid and the product was collected and washed with water. The amide was dissolved in hot alcohol and, after treatment with charcoal, water was added to start recrystallization. The yield was 90 g., m.p. 282°C. (hot bar).

**3,3-Bis(4-hydroxyphenyl)-*N*-methylphthalimidine.** This preparation was carried out as above with 40% aqueous methylamine. The reaction was much faster, and the solution was colorless within 20 hr. Recovery and crystallization were as above; yield, 98%; m.p. 273°C. (hot bar).

ANAL. Calcd. for  $C_{21}H_{17}O_3N$ : C, 76.11%; H, 5.17%; N, 4.23%. Found: C, 75.5%; H, 5.2%; N, 4.2%.

**3,3-Bis(4-hydroxyphenyl)oxindole.** This compound was purchased. Because some of the polymers prepared from it were insoluble, purification and analyses were carried out. The compound was recrystallized from ethanol and melted then at 267–268°C. (dec. in capillary).<sup>22</sup>

ANAL. Calcd. for  $C_{20}H_{15}O_3N$ : N, 4.43%; O, 15.13%. Found: N, 4.38, 4.35%; O, 15.2, 14.9%.

**3,3-Bis(4-hydroxyphenyl)-5,7-dichlorooxindole.** 5,7-Dichloroisatin (20 g.) was added to 80 g. of phenol at 30°C. with stirring. Some undissolved material was removed by filtration. Concentrated sulfuric acid (10 ml.) was then added dropwise to the cooled solution. The initial deep red color faded quickly to orange, and after 20 min. the mixture was added to 1500 ml. of ice water. The mass was washed with water, dissolved in ethanol, decolorized, and crystallized in the form of colorless plates by addition of water to the hot solution. The product melted at 246°C. (hot bar). The reported melting point is 276–277°C.<sup>23</sup>

ANAL. Calcd. for  $C_{20}H_{13}O_3Cl_2N$ : C, 62.19%; H, 3.39%; Cl, 18.36%. Found: C, 61.5%; H, 3.7%; Cl, 18.6%.

**Fluorescein.** Fluorescein is normally sold as the water-soluble disodio derivative. This was dissolved in water to form a neutral solution. The free phenol was precipitated by the addition of hydrochloric acid and washed and dried. The crude product was subjected to vacuum sublimation as described in the literature.<sup>24</sup> The sublimed product was somewhat improved in quality.

The highest purity was obtained by crystallization of the acid-precipitated material from acetone-alcohol. This step yielded fine red needles.

**Acid Chlorides.** The acid chlorides were purified by methods described in previous publications from this labora<sup>t</sup>ory.<sup>25</sup>

### Polymer Preparation

Examples are given of the several techniques employed.

**Interfacial Polycondensation.** Phenolphthalein (3.18 g.) and 0.80 g. of sodium hydroxide were dissolved in 100 ml. of water in a blender jar. While the mixture was rapidly stirred, a solution of 2.03 g. of isophthaloyl chloride in 30 ml. of 1,2-dichloroethane was added all at once. The blood-red color was quickly reduced to a light pink. Stirring was continued for 5 min. Hexane (300 ml.) was added to precipitate the polymer, which was filtered and washed with water; yield 4.22 g.;  $\eta_{inh}$  0.93. (All inherent viscosities, except as otherwise indicated, were determined in *sym*-tetrachloroethane/phenol (40/60 by weight) at 0.5 g./100 ml. and at 30°C.)

**Interfacial Polycondensation with Phosgene Gas.** Phenolphthalein (3.98 g., 0.0125 mole), 1.0 g. of sodium hydroxide and 1.0 g. of tetraethylammonium chloride were dissolved in 120 ml. of water in a blender jar. 1,2-Dichloroethane (30 ml.) was added. While the mixture was stirred vigorously, phosgene gas was passed in until the color faded. Stirring was continued for 2 min. Acetone was added to precipitate the colorless product, which was collected, washed, and dried; yield 53%;  $\eta_{inh}$  0.51.

A second experiment was started as above but, after the first loss of color, the color was returned by adding several drops of a 20% solution of sodium hydroxide and phosgene was passed in again. This was repeated two more times. The total time was about 20 min. The polymer, isolated as before, was obtained in 93% yield with an  $\eta_{inh}$  of 2.20.

Similar experiments with 2,2-bis(4-hydroxyphenyl)propane, in which the pH was alternated from about 12 to 7 for each phosgene addition, yielded polycarbonates with  $\eta_{inh}$  0.57 (80% yield) and 5.46 (93% yield), respectively.

**Low Temperature Solution Polycondensation.** Phenolphthalein (3.18 g.) and 2.8 ml. of triethylamine were added to 50 ml. of 1,2-dichloroethane. Not all of the bisphenol dissolved. There was no color. The mixture was cooled to 10°C., 2.03 g. of solid isophthaloyl chloride was added, and the reaction mixture was swirled. Triethylamine hydrochloride precipitated in a gelatinous form while the finely powdered bisphenol dissolved. The solution slowly became more viscous and at 90 min. it was poured into acetone in a blender. The washed and dried granular product weighed 4.04 g. (90%) and had an inherent viscosity of 0.67.

**High Temperature Solution Polycondensation.** In a round-bottomed flask equipped with a stirrer, nitrogen inlet tube, HCL outlet tube, and condenser was placed 3.98 g. of phenolphthalein, 0.20 g. of triethylamine hydrochloride and 25 ml. of *o*-dichlorobenzene. This mixture was heated to 210°C. under nitrogen flow and a solution of 2.564 g. of isophthaloyl chloride in 25 ml. of *o*-dichlorobenzene was added dropwise through a funnel. The mixture was heated until the evolution of hydrogen chloride

ceased, a period of about 4 hr. Some solvent vapor was carried out with the nitrogen and thus assisted in flushing out the hydrogen chloride. The polymer remained dissolved in the hot solvent, but would gel if allowed to cool. The polymer was precipitated in hexane and washed with alcohol, 50/50 alcohol-water and water; yield 5.19 g.;  $\eta_{inh}$  0.97.

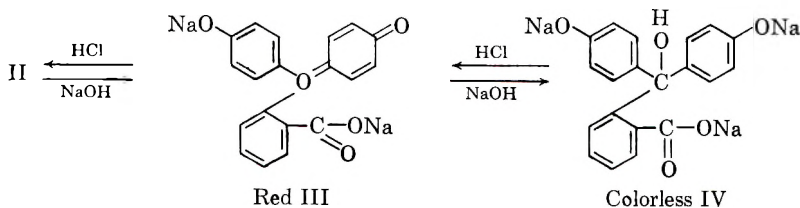
The polymer retained a pale yellow tint, which was not present in the products of low temperature methods. The color was discharged when the polymer was swollen in tetrahydrofuran or dissolved in amide solvents.

**Fluorescein and Sulfonephthalein Polymers.** Poly(fluorescein isophthalate) was prepared with an inherent viscosity of 0.3. Its properties are given in Tables I and VI.

A number of other commercially available fluoresceins were reacted with isophthaloyl chloride and yielded highly colored, high melting products which had inherent viscosities of about 0.05. Among these were Erythrosin B, tetraiodofluorescein, tetraiodotetrachlorofluorescein (Rose Bengal, Color Index No. 779), and disodio-3'-hydroxymercuri-5',5''-dibromofluorescein (Mercurochrome, trademark of Hynson, Westcott and Dunning, Inc.). Phenolsulfonephthalein (phenol red) did not yield a polymer with isophthaloyl chloride by the interfacial polycondensation method.

## DISCUSSION

In view of the high degree of coloration of the hydroxyphenyl phthaleins in aqueous alkali, it is not obvious that they would be suitable for the preparation of condensation polymers, especially by routes such as the interfacial polycondensation method. The color-forming reaction has been much studied and is believed to result from an equilibrium in which the colored form has a quinomethine structure (III).<sup>25</sup>

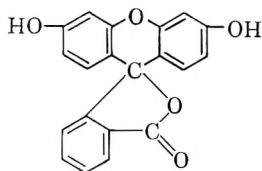


In very concentrated alkali a third form is obtained which is a colorless trisodium salt (IV). The reactions are rapidly reversible with acid. Although the color is very intense, only part of the phenolphthalein is in the quinone form in aqueous solution.

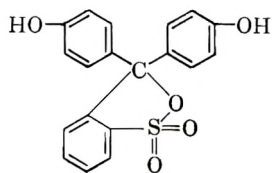
Despite the unusual condition of the phthaleins in alkaline solution, they are very readily acylated with acid chlorides and polymers are easily prepared when two equivalents of alkali are used. Three equivalents of alkali inhibit polymerization.

Besides the many bisphenols of the phthalein type, there are the closely related fluoresceins (V) and sulfonephthaleins (VI) as well as a variety of

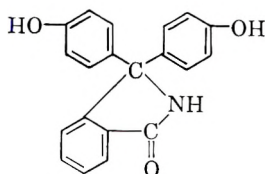
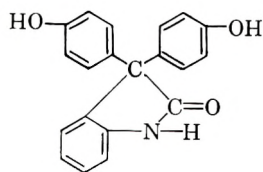
bisphenols with other heterocyclic ring structures, such as the phthalimides (VII) and isatins (VIII).



Fluorescein V



Phenolsulfonephthalein VI

Phenolphthalimidine;  
3,3-Bis(4-hydroxyphenyl)  
isooxindole VIIPhenolisatin;  
3,3-Bis(4-hydroxyphenyl)  
oxindole VIII

Pure VII and VIII are not transformed into highly colored quinomethine structures by alkali and their use in polymer-making is straightforward except for some reactivity of the amide hydrogen.

Fluorescein forms a colorless dibenzoate<sup>8,27</sup> and poly(fluorescein isophthalate) with an  $\eta_{inh}$  of 0.3 was prepared which was slightly colored. However, the highest inherent viscosity for any polymer from a fluorescein derivative was 0.08. All of these products retained the high color of the parent fluorescein. Fluorescein and its ring-substitution products are highly colored even as the free phenols and may, therefore, exist to a considerable extent as the quinomethine structure in the absence of alkali. They are also difficult to purify because of low solubility in organic solvents and poor crystallizability. The general difficulty in forming polymers from this group of compounds, as well as phenolsulfonephthalein, may be laid to a combination of low purity, high solubility in alkaline solution, and incomplete reversal from the quinomethine to bisphenol structure.

Tables I through V list several groups of polyesters and some of their properties.

### Interfacial Polycondensation Variables

Interfacial polycondensation of polyesters is best performed with a solvent for the polymer<sup>4</sup> and a concentrated organic solvent phase. Chlorinated hydrocarbons with an active hydrogen atom were especially effective and the best of these was 1,2-dichloroethane. An equally concentrated aqueous phase would probably be advantageous, but this is often not possible because of the low solubility of many bisphenoxides.

TABLE I  
Aromatic Polyesters from Phenolphthaleins by Interfacial Polycondensation

Substituents in phenolphthalein	Diacid	$\eta_{inh}$	Yield, %	PMT, °C. <sup>a</sup>	Solubility <sup>b</sup>
None	Isophthalic	1.78	98	355	1-4p-8h-10s, 11
	5-Chloroisophthalic	2.05	75	390 (dec.)	1-7, 11-12
	5-tert-Butylisophthalic	0.67	97	343 (softens gradually)	1-8o-10o, 11
	Terephthalic	0.63	94	340 (fairly sharp)	1-10o, 11p
		1.12	94	>400	
	2,5-Dichloroterephthalic	0.72	93	316 (fairly sharp)	1-10g, 11g
	Tetrachloroterephthalic	0.37	92	>400	1-4o-8g, 10g, 11o
	Phthalic	0.19	93	268 (sharp)	1-11g
	Isophthalic	0.37	79	300 (sharp)	1-11g
	Isophthalic	0.54	99	326 (sharp)	1-7, 9, 11s
	Isophthalic	0.40	91	>400 (dec. at 380°)	1-8
4,5,6,7-Tetrachloro	Isophthalic	0.31	99	360 (sharp)	1-8o, 10s, 11g
3',3"-Dimethyl	Isophthalic	0.49	92	295	1-10g, 11g
Fluorescein <sup>c</sup>	Isophthalic	0.31	93	335	1-10, 12p

<sup>a</sup> The polymer melt temperature (PMT) was taken as the lowest point at which the polymer melted or left a trail under light pressure on a chromepated temperature gradient bar.<sup>15</sup>

<sup>b</sup> Solubility was tested at 1-3% solids in the following solvents: (1) 1,2-dichloroethane-trifluoroacetic acid (70/30 by weight), (2) tetrachloroethane-phenol (40/60 by weight), (3) *m*-cresol, (4) piperidine, (5) chloroform, (6) tetrahydrofuran, (7) dimethylacetamide, (8) dimethyl sulfoxide, (9) cyclohexanone, (10) methyl ethyl ketone, (11) benzene, (12) formic acid (98-100%). Whenever the polymers were insoluble at room temperature, the mixtures were heated to boiling or a maximum of 80°C. Hyphens indicate solubility in all intervening solvents in the series. Small letters indicate restricted solubility effects as listed: (s) swollen without agglomeration, (p) noticeably partly soluble, (g) forms plastic gum, (o) forms oily phase, (h) soluble only hot, (w) soluble with small amount of water. For example, 1-4o-8g, 10g, 11o means the polymer is soluble in solvents 1, 2, 3, 5, 6, and 7; forms oils in 4 and 11; forms gums in 8 and 10; and is insoluble in 9 and 12.

<sup>c</sup> Polymer retained a pale yellow coloration.

TABLE II  
Polyesters from Bis(4-hydroxyphenyl)phthalimides and Oxindoles

Bisphenol	Diacid	$\eta_{inh}$	Yield, %	PMT, °C.	Solubility <sup>a</sup>
Phenolphthalimide	Isophthalic	0.76	94	>400 (dec.)	1-6w-9, 12s
	5-Chloroisophthalic	0.41	93	>400 (dec.)	1-9, 12s
	5- <i>tert</i> -Butylisophthalic	0.43	88	380	1-5o-10s
	Terephthalic	0.56	94	>400	1-6w-9
	2,5-Dichloroterephthalic	0.57	97	>400	1-6w-9
	Tetrachloroterephthalic	0.12	58	>400	1-5g-8g, 9
	Sebacic	0.30	66	187	1-10o, 11o, 12
Phenol <i>N</i> -methylphthalimide	Carbonic	0.38	85	>400 (dec.)	1-6w-9, 12o
	Isophthalic	0.99	97	395 (dec.)	1-4s, 9s
	Terephthalic	0.43	98	>400	1-4p
	Sebacic	0.46	53	170	1-12
	Isophthalic	0.38	100	320	1-10g
3,3-Bis(4-hydroxyphenyl)-oxindole <sup>b</sup>	5-Chloroisophthalic	0.26	97	265 (dec.)	1-10g
	5- <i>tert</i> -Butylisophthalic	0.31	79	340	1-11s
	Sebacic	Insol.	100	120 (softens)	1s, 4
	Isophthalic	0.63	87	>400	1h-7p-11s
Sebacic	Insol.	91	307	1s, 4	

<sup>a</sup> See notes to Table I for explanation.

<sup>b</sup> The polyesters tabulated were made by low temperature solution polycondensation.



TABLE III  
Comparison of Aliphatic Polyesters from Phenolphthalein and 2,2-bis(4-hydroxyphenyl)propane

Diacid <sup>a</sup>	Phenolphthalein ester			2,2-Bis(4-hydroxyphenyl)propane ester				
	$\eta_{inh}$	Yield, %	PMT, °C.	Solubility <sup>b</sup>	$\eta_{inh}$	Yield, %	PMT, °C.	Solubility <sup>b</sup>
10	0.60	90	190	1-11o, 12g	0.56	94	<50	1-12s
9	0.38	90	160	1-11o, 12g	0.28	96	<50	1-11o, 12s
8	0.59	95	210	1-10g, 11g, 12s	0.37	91	<50	1-12s
6	0.45	94	225	1-10o, 11g, 12s	0.31	80	85	1-12s
5	0.53	86	210	1-10o, 11g, 12s	0.49	93	110	1-12s
4	0.60	99	240	1-10g, 11g, 12s	0.54	97	145	1-11o, 12s
2	0.10	46	—	—	0.08	79	—	—
1	0.86	87	350 (dec.) <sup>c</sup>	1-10g, 11g	0.86	90	230 <sup>d</sup>	1-9, 11
SI <sup>e</sup>	0.94	96	330 (dec.)	1-9	0.73	100	270 (dec.)	1, 4, 5p, 6s, 11s

<sup>a</sup> Numbers indicate the number of carbon atoms in the diacid.

<sup>b</sup> See notes to Table I for explanation.

<sup>c</sup> PMT of 270°C, reported by Howe.<sup>12</sup>

<sup>d</sup> Samples with higher viscosity stick and melt at temperatures as high as 375°C.

<sup>e</sup> Thiocarbonate.

TABLE IV  
 Copolymers of Phenolphthalein

Diol with phenolphthalein <sup>a</sup>	Diacid	$\eta_{inh}$	Yield, %	PMT, °C.	Solubility <sup>b</sup>
None	Isophthalic/ terephthalic (50/50)	0.88	84	345 <sup>c</sup>	
Ethylene glycol <sup>d</sup>	Carbonic	0.23	90	190	1-10o, 11g, 12
2,2-Bis(4-hydroxyphenyl)- propane <sup>e</sup>	Carbonic	0.67	100	312 <sup>a</sup>	1-10g, 11g
2,2-Bis(4-hydroxy-3,5-dichloro- phenyl)propane <sup>d</sup>	Carbonic	1.43	100	335	1-10g, 11g
2,2-Bis(4-hydroxyphenyl)propane	Isophthalic	0.85	91	300	
Phenolphthalein	Isophthalic	0.43	81	330	
3',3',5',5'-Tetraiodophenol- phthalein	Isophthalic	0.38	87	345	

<sup>a</sup> In amount to form a 50/50 copolymer.

<sup>b</sup> See notes to Table I for explanation.

<sup>c</sup> PMT (capillary tube) of 310°C. reported by Korshak, Vinogradova, and Salazkin.<sup>12</sup>

<sup>d</sup> Introduced as the bischloroformate to yield an alternating copolymer.

<sup>e</sup> PMT of 250°C. reported by Howe.<sup>13</sup>

TABLE V  
Polysulfonates from Phenolphthalein

Disulfonyl chloride	$\eta_{inh}$	Yield, %	PMT, °C.	Solubility <sup>a</sup>
<i>m</i> -Benzene	0.26	100	220	1-4p-11g, 12s
4,4'-Biphenyl	0.41	97	316	1-3,5-11g

<sup>a</sup> See notes to Table I for explanation.

Poly(phenolphthalein isophthalate) and similar polyesters having high molecular weights were prepared without the catalysts<sup>4</sup> or detergents<sup>5</sup> which are needed in the preparation of polyesters from bisphenol A. However, quaternary ammonium salts did accelerate the reactions and led to increases in molecular weights. Detergents did not help unless the polymer had solubility characteristics such that it precipitated rapidly or collected as a viscous mass on the blender walls in the absence of detergents.

The rapid loss of the deep red and blue colors of the phenolphthaleins upon polycondensation (5-30 sec.) emphasized the high speed of this process and showed clearly any inhomogeneities in the mixing. Complete color loss was found not to mean necessarily that the phthalein was used up but that the pH had dropped below the point for the color change. Even in systems which had produced high molecular weight polymer, a faint pink often remained or it could be obtained by the addition of a small amount of alkali. The amount of phenolphthalein needed to yield color is, of course, very small. With readily hydrolyzed acid chlorides and with alkali equivalent to the phenol, the color was quickly lost and polymers with low molecular weight were obtained. This led to a simple modification of the polymerization method which then yielded high polymers. A short time after the initial color was gone, alkali was added to bring back the color, stirring was continued, and a small portion of diacid chloride in solution was added. These steps were repeated two or three times. (See procedure with phosgene gas.) The molecular weights of the products were greatly enhanced.

The same procedure was applied successfully to polymers from bisphenol A and aliphatic diacid chlorides (Table III). In this case the initial mixing was completed, a trace of phenolphthalein was added then the needed alkali. A pH meter can be used but is more cumbersome.

### Polymer Structure

The easy solubility of most of the polymers and the high viscosity of the solutions, both dilute and concentrated, indicates the essential linearity of their structure. Most of the polymers in pure form were colorless and, therefore, do not contain quinone structure which would yield a yellow coloration. They are not soluble in bases or acids and, therefore, no large proportion of the lactone or lactam rings are open.

Infrared spectra were obtained on several polymers and phenolphthalein dibenzoate, diacetate, and dimethyl ether (Figs. 1-8). These spectra showed no carboxyl or carboxylate ion. The spectrum for the dimethyl

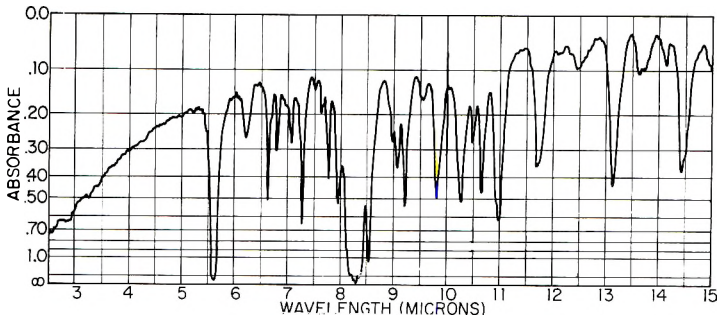


Fig. 1. Infrared spectrum of phenolphthalein dibenzoate.

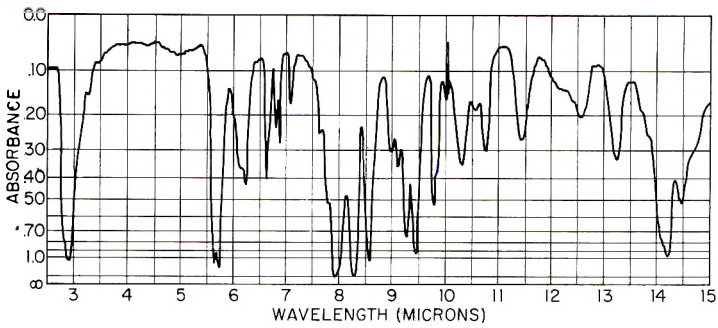


Fig. 2. Infrared spectrum of phenolphthalein diacetate.

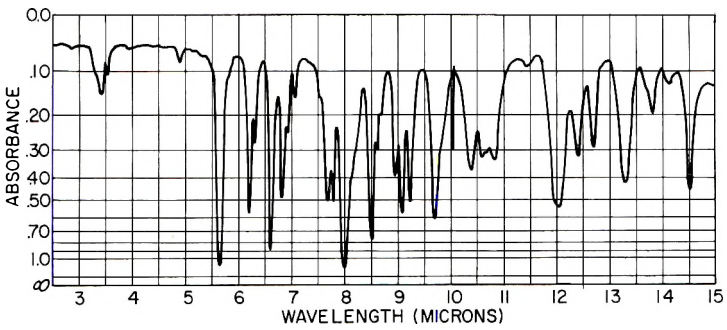


Fig. 3. Infrared spectrum of phenolphthalein dimethyl ether.

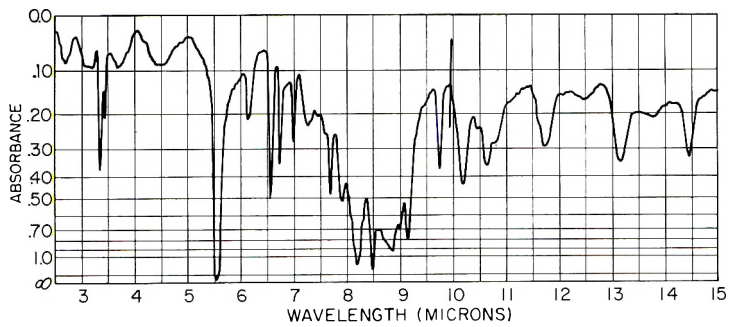


Fig. 4. Infrared spectrum of poly(phenolphthalein isophthalate).

ether showed a single carbonyl absorption band at  $5.65 \mu$ , whereas the monomeric and polymeric esters of phenolphthalein showed a split carbonyl absorption. From a comparison of the spectra of the sebacate and the isophthalate, it was possible to assign the shoulder at  $5.6 \mu$  in the sebacate spectrum to the lactone carbonyl and the band at  $5.66 \mu$  to the aliphatic ester carbonyl. The corresponding bands for the isophthalate are at  $5.62$

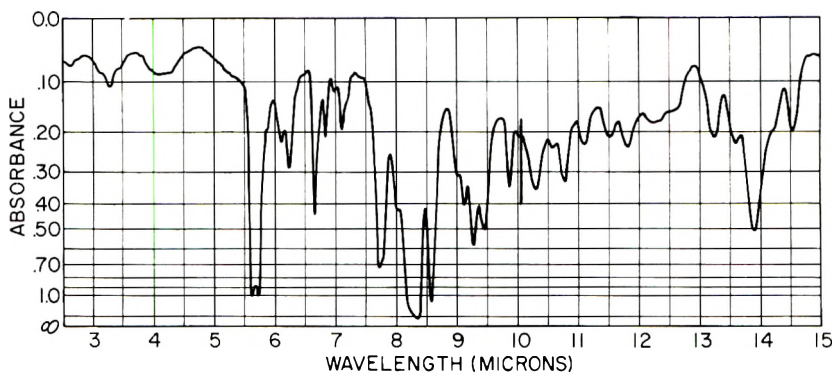


Fig. 5. Infrared spectrum of poly(phenolphthalein sebacate).

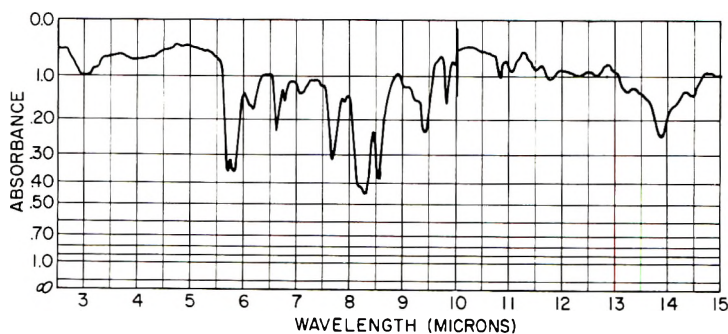


Fig. 6. Infrared spectrum of poly(phenolphthalimidine isophthalate).

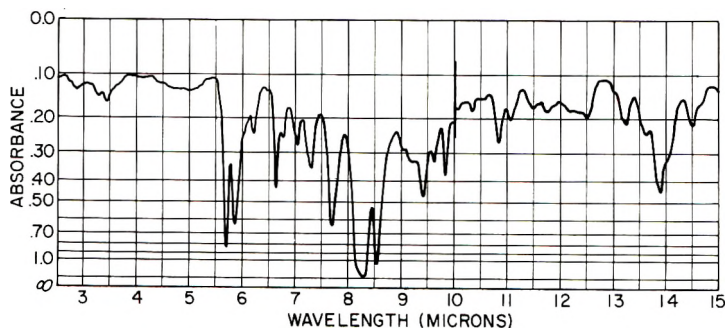


Fig. 7. Infrared spectrum of poly(*N*-methylphenolphthalimidine isophthalate).

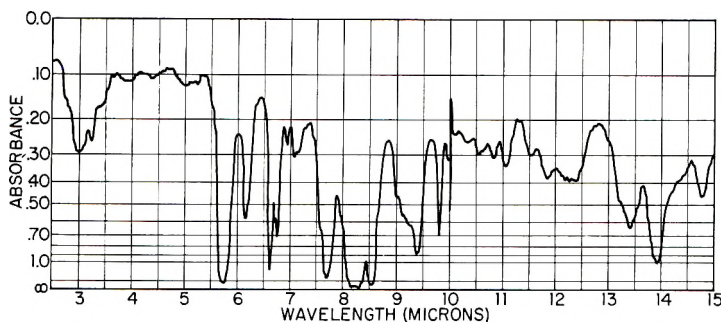


Fig. 8. Infrared spectrum of poly(phenolisatin isophthalate).

and  $5.72 \mu$ . Assignments for *ortho* ( $13.2$  and  $14.5 \mu$ ), *meta* ( $13.6$  and  $13.85 \mu$ ), and *para* ( $11.8 \mu$ ) substitution can be made from a comparison of sebacate and isophthalate spectra.

### Polymer Solubility

All of the polymers as prepared were essentially noncrystalline. It is well known that amorphous regions of polymers are more readily accessible to and swollen by solvents than the crystalline areas. It is also true that many polymers show a greater range of solubility in the amorphous form than in the crystalline state. Furthermore, the solubility of an amorphous polymer is often increased by lowering the molecular weight, whereas the solubility of a highly crystalline polymer will be little affected. The solubility of the polymers with inherent viscosity values below 0.4 should be regarded with these effects in mind.

Nearly all of the polymers showed solubility in a wide range of solvent types (Tables I-V). They were not soluble in aliphatic hydrocarbons, fully chlorinated hydrocarbons, acyclic ethers, alcohols, acetone (some were swollen), or weak organic acids (a few dissolved in formic acid).

The high solubility of the three isophthalates having unsubstituted phthalide, phthalimidine, and oxindole structures is undoubtedly due to both the affinity of these structures for the solvents and to a bulking or opening of the structure. When the phthalimidine nitrogen was substituted with a methyl group, solubility was lost except in phenolic and strongly acid solvents. The latter solubility is characteristic of poly[(2,2-bisphenylene)propane isophthalate] and related polyesters.

In general, ring substituents in the bisphenol or diacid increased solubility. The greatest effect was produced by a *5-tert*-butyl group in isophthalic acid. Although chlorosubstituents usually increased solubility, tetrachloroterephthalates were less soluble than unsubstituted esters. Poly(phenolphthalein isophthalate) was soluble in formic acid, whereas the terephthalate was not. On the other hand, the terephthalate was more soluble than the isophthalate in many other solvents. This is the opposite of experience with most esters of these two acids.

Chloro-substituents (3',3'',5',5'') in poly(phenolphthalein isophthalate) destroyed solubility in formic acid but increased solubility in the other test solvents. The corresponding bromo- and iodo-substituted polymers had decreased solubility in ketone solvents. The phenolphthalein esters of aliphatic acids were less soluble than the bisphenol A polyesters in benzene and methyl ethyl ketone.

In addition to these observations a number of interesting solubility peculiarities were found.

**Amide Solvents.** Poly(phenolphthalein isophthalate) formed solutions in amide solvents which were unusually thin at 20% solids for the measured inherent viscosity and in comparison with solutions in other solvents. In addition the polymers were degraded in the hot solvents. For example, a 20 wt.-% solution in dimethylformamide was heated 4 hr. at 100°C. and the polymer recovered. Initially the  $\eta_{inh}$  was 0.97, and after recovery it was 0.77. A solution of another sample with  $\eta_{inh}$  of 0.73 was heated in dimethylacetamide for 2 hr. at 120°C. Upon isolation the polymer had an  $\eta_{inh}$  of 0.48. The nature of this degradation reaction is not known, although it may be a hydrolysis catalyzed by traces of base. No color developed in the solution or upon precipitation in water.

**Partial Solubility.** These polymers frequently formed oily or viscous phases with several solvents. That is, they would associate with a certain amount of solvent in a liquid state but additional solvent was excluded. The effect was encountered most often with benzene and methyl ethyl ketone. A similar effect with tetrahydrofuran was examined briefly.

The solubility of poly(phenolphthalein isophthalate) in tetrahydrofuran was dependent on temperature and molecular weight. When about 3% of high polymer was placed in the solvent at 30°C., the low fraction (below an  $\eta_{inh}$  of about 0.5) dissolved, and the remainder formed an oily phase. By cooling the system below 15°C., polymer with  $\eta_{inh}$  up to 1.0 could be dissolved, whereas raising the temperature would cause even the low polymer to oil out. The effect was reversible and is believed to be somewhat concentration-dependent. The solubility range of a given polymer was increased by small amounts of water if the polymer concentration was high. The above behavior has similarities to the separation of polyamide 66 solution into liquid phases in phenol-water mixtures, which was used by Taylor<sup>28</sup> to fractionate the polyamide.

**Synergistic Solvents.** Synergistic solubility effects are well known in the polymer field. Instances were encountered in the present group of polymers. As an example poly(phenolphthalimidine isophthalate) was insoluble in tetrahydrofuran, but upon the addition of water a solution was formed. This solution gelled reversibly upon warming, in the same manner as solutions of poly(phenolphthalein isophthalate).

**Antagonistic Solvents.** Many of the polymers exhibited a rare solubility effect, of which only three other examples in the polymer field are known to the author;<sup>29,30</sup> that is, certain pairs of solvents which independently would readily dissolve a polymer would not dissolve it in combina-

tion. Or if a polymer solution were first made in one of the solvents, the addition of the opposing solvent, even in small amounts, would cause precipitation. Solutions of the polymer in the two solvents would likewise not mix, but yielded a precipitate. The precipitate was usually stringy and white, but in a few cases was gummy and still plasticized by the solvents.

Antagonistic pairs were obtained by combining any Group 1 solvent with a Group 2 solvent listed in Table VI.

TABLE VI  
Antagonistic Solvents

Group 1 solvents	Group 2 solvents
Dichloromethane	Dimethylformamide
Chloroform	Dimethylacetamide
1,2-Dichloroethane	Dimethyl sulfoxide
1,1,2-Trichloroethane	Tetrahydrofuran
<i>sym</i> -Tetrachloroethane	Dioxolane
	Dioxane
	2-Butanone
	Cyclohexanone

The lists of the two classes of solvents shows that group 1 consists of hydrogen donors and group 2 of hydrogen acceptors or electron donors. The peculiar solubility effect presumably is due to a much stronger affinity between the solvent pairs than between either type of solvent and the polymer. Suitable solvent pairs are characterized by exhibiting a negative deviation from Raoult's law and, when the boiling points are near together, they form maximum boiling point azeotropes. Numerous mixtures of this type were studied by Elwell and Welch,<sup>31</sup> and others are to be found in the compilations of Horsley.<sup>32</sup> Synergistic solvents for polymers are found among the pairs which show minimum boiling point azeotropes or positive deviations in vapor pressure.

Some of the polymers upon which the antagonistic effect was observed are phenolphthalein with isophthalic, 5-chloroisophthalic, sebacic, and carbonic acids; phenolphthalimidine with isophthalic and carbonic acids; and tetraiodophenolphthalein with isophthalic acid.

The antagonistic solubility effect was not shown by aromatic polyesters, such as the carbonate or 5-*tert*-butyl isophthalate of bisphenol A and others, which were soluble in the solvent pairs needed for a test. The reason for the difference is that, although the polyesters of the phthaleins and related structures are soluble in many solvents, they have interacted less strongly with the solvents or they retain or possess a greater polymer-polymer interaction than the polymers having nonpolar substituents. As a result the energy balance is such that very little disturbance is needed to cause precipitation.

The cases described by Fuchs were poly(vinyl pyrrolidone) in nitromethane-water and polyacrylonitrile in dimethylformamide-cyanoacetic



acid. Beaman found an interesting combination of synergistic and antagonistic effects. Nitromethane–water (90–10) dissolved polyacrylonitrile, although neither liquid alone is a solvent for the polymer.<sup>31</sup> The addition of 10% of dimethylformamide, a solvent for the polymer, caused the polymer to precipitate.<sup>33</sup> In these instances, as in the case of the phthalein polyesters, the polymers bear polar substituents and have borderline solubility.

**Solubility of Polymers from 3,3-Bis(4-hydroxyphenyl)oxindole.** This compound (VIII), also known as phenolisatin, is isomeric with phenolphthalimidine (VII), made from phenolphthalein and ammonia. Soluble polymers were readily prepared from phenolphthalimidine, but only insoluble or partially soluble polymers could be obtained from the oxindole by interfacial and high temperature solution methods. By solution polycondensation with triethylamine as the acid acceptor, soluble polymers with inherent viscosities of 0.3–0.4 were obtained.

The insolubility is believed to result from crosslinking by acylation of some of the amide groups under the conditions of high heat or strong aqueous alkali. The crosslinking reaction was not dependent upon the initial formation of a polymer precipitate, since the potentially soluble *tert*-butylisophthaloyl and 5-chloroisophthaloyl esters were also insoluble when made by the interfacial polycondensation process. Sumpter<sup>34</sup> has reported the preparation of a triacetate of phenolisatin. There was no indication that the lactam ring was opened.

Phenolisatin with halogen substituents in position 7 were reported to form only normal diesters or to yield triesters only under severe conditions.<sup>23,34</sup> Therefore, 3,3-bis(4-hydroxyphenyl)-5,7-dichlorooxindole was synthesized. This yielded as expected by interfacial polycondensation soluble, linear polymers with isophthaloyl or terephthaloyl chlorides. The more reactive sebacyl chloride produced an insoluble polymer.

The insoluble polymers from diphenoloxindole (phenolisatin) dissolved in the strong base piperidine. This could mean that there was a large number of carboxyl groups in the structure. No carboxyl groups or ions were evident in infrared spectra. Possibly piperidine cleaves the side chains starting with the amide nitrogen. A more likely situation is that the ester groups are rapidly aminolyzed. This appears to be the case with poly-(phenolphthalein isophthalate), for immediately after solution of this polymer, the addition of water gave a dark red coloration. Deep colors were likewise produced with piperidine solutions of phenoloxindole and phenoldichlorooxindole polymers and more slowly with the phthalimidine derivatives.

### Polymer Melting Characteristics and Glass Transition Temperatures

Since the polymers were amorphous, melting temperatures were usually rather broad. The polymer melt temperature (PMT), i.e., the temperature at which the polymers would stick on the temperature gradient bar under moderate pressure, was reasonably sharp and reproducible. This tempera-

ture is appreciably dependent upon molecular weight and is usually changed by crystallization of the polymer. All comparisons then must be made at the same molecular weight range. In the tables any additional noteworthy behavior has been recorded briefly.

TABLE VII  
Glass Transition and Softening Temperatures of Polyesters

Polymer		$T_g$ , °C. <sup>a</sup>	PMT, °C.
Bisphenol	Acid		
2,2-Bis(4-hydroxyphenyl)propane	Isophthalic	180	280
	Terephthalic		350 <sup>b</sup>
	Carbonic	149	230
1,1-Bis(4-hydroxyphenyl)cyclohexane	Isophthalic	127	240
	Carbonic	175 <sup>c</sup>	250
Bis(4-hydroxyphenyl)phenylmethane	Isophthalic	160 <sup>d</sup>	
	Terephthalic	200 <sup>d</sup>	
	Carbonic	121 <sup>c</sup>	205 <sup>c</sup>
Phenolphthalein	Isophthalic	318	355
	Terephthalic		>400
	Carbonic	240	>350 (dec.)
	5-Chloroisophthalic	313	390
	5-tertiary-Butyl-isophthalic	279	343
3',3'-Dimethylphenolphthalein	Isophthalic	273 <sup>e</sup>	295
Phenolphthalimidine	Isophthalic	325	>400
	Terephthalic	327	>400
<i>N</i> -Methylphenolphthalimidine	Isophthalic	285 <sup>f</sup>	395
	Terephthalic	282 <sup>f</sup>	>400
Phenol; satin	Isophthalic	256	320
Phenol-5,7-dichloroisatin	Isophthalic	270	>400
Fluorescein	Isophthalic	276	335

<sup>a</sup> Determined by a modified method of differential thermal analysis.

<sup>b</sup> Determined on polymer with  $\eta_{inh}$  of 1.5; Eareckson<sup>5</sup> reports a PMT of 315°C. at an  $\eta_{inh}$  of 0.51.

<sup>c</sup> Data of Schnell.<sup>2</sup>

<sup>d</sup> Data of Conix.<sup>4</sup>

<sup>e</sup> Shows an exotherm rather than endotherm.

<sup>f</sup> Transition indistinct.

The polymers and copolymers as a whole were high melting. All of the polymers from phenolphthaleins melted at higher temperatures than corresponding polymers from bisphenol A and the polymers from phthalimides melted in an even higher range. As is the case with other bisphenols, the terephthalates softened at higher temperatures than the isophthalates. Presumably, the effect is due to the more rodlike structure of the polyterephthalate chain. A similar effect is seen in the polysulfonates (Table V) having 1,3-phenylene and 4,4'-biphenylene structures. The phenolphthalein esters of aliphatic diacids are noteworthy for melting in a range acceptable for melt-spinning (200–250°C.), while the aliphatic esters from bis-

phenol A, except the carbonate and oxalate, melted below 150°C. (Table III).

Most of the polyesters were thermally stable for short periods up to 300°C., and some did not rapidly decompose at higher temperatures.

The glass transition temperatures  $T_g$  (Table VII) are parallel to the high softening temperatures<sup>4</sup> and, like the latter, are higher than the values for similar polymers of the bisphenol A type. The exceptionally high  $T_g$  values probably indicate both greater interchain bonding and lower flexibility in these structures.

Poly(phenolphthalimidine isophthalate) has a  $T_g$  value as high as the poly(phenolphthalein isophthalate), but the oxindole polymer has a value 70°C. lower. This lowering may be due to the change from aliphatic to aromatic substitution on the N-H group and a consequent lowering in the strength of hydrogen bonding. The replacement of hydrogen by a methyl group on the amide of the phthalimidine nucleus produced a similar drop in  $T_g$ .

### Discoloration by Ultraviolet Light

Eareckson<sup>5</sup> reported that the aromatic polyesters of bisphenol A yellowed very rapidly when exposed to ultraviolet light from a carbon arc. The polyesters from phenolphthalein were found to be color-stable to prolonged exposures, and when discoloration finally occurred, it increased at a slow rate. Phthalimidine and isatin derivatives discolored rapidly with the formation of brownish tints.

### Water Absorption

The water absorptions of solvent-cast films of polyesters from phenolphthalein, phenolphthalimidine, and phenolisatin are appreciably higher than those of other all-aromatic polyesters without polar substituents (Table VIII). These values would be reduced some if the polymers were crystalline. Increased water permeability can have utility such as providing increased rate of permeation by dyes. However, it is also usually accompanied in polyesters by an increased sensitivity to hydrolysis.

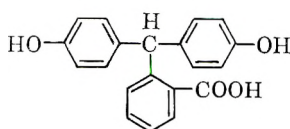
TABLE VIII  
Water Absorption in Polyester Films

Polymer		Water absorption, %
Bisphenol	Diacid	
2,2-Bis(4-hydroxyphenyl)propane	Isophthalic	0.2
Phenolphthalein	Isophthalic	1.7
Phenolphthalimidine	Isophthalic	2.9
2,2-Bis(4-hydroxyphenyl)propane	Carbonic	0.4
Phenolphthalein	Carbonic	4.4
2,2-Bis(4-hydroxyphenyl)propane	Adipic	2.7
Phenolphthalein	Adipic	2.0
	Sebacic	0.4

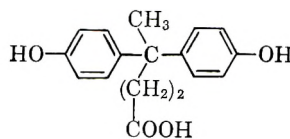
Although poly(phenolphthalein carbonate) has a high water absorption, the adipate and sebacate have successively lower values, as would be expected from the greater amount of hydrocarbon structure. The value for the adipate of bisphenol A is relatively high. This effect is probably related to a lack of crystallinity and to the low melting temperatures of the aliphatic esters of bisphenol A (Table III).

### Polyesters Bearing Carboxyl Groups

Phenolphthalein can be reduced to phenolphthalin, which is a bisphenol containing a carboxyphenyl group (IX).



Phenolphthalin (IX)



Diphenolic Acid (X)

Another somewhat related bisphenol and several derivatives are available from the Johnson Wax Co. under the name of diphenolic acid (X).

Polyisophthalates were made from these bisphenols (Table IX). They had low molecular weights and, therefore, the properties must be judged with this in mind. Solubility in benzene and chloroform was reduced. As would be expected, these polymers were soluble in dilute aqueous alkali.

### Fibers from Poly(phenolphthalein Isophthalate)

Polymer with an inherent viscosity of 0.8 was dry-spun from cyclohexanone into lustrous, colorless fibers having a peanut-shaped cross section. Some finishing steps and a few properties are given in Table X.

TABLE IX  
Polyisophthalates from Bisphenols Bearing Carboxyl Groups

Bisphenol <sup>a</sup>	$\eta_{inh}$	Yield, %	PMT, °C.	Solubility <sup>b</sup>
Phenolphthalin	0.17 <sup>c</sup>	79	>350 (dec.)	1, 2s, 3s, 4, 8s
Diphenolic acid	0.19	80	192	1-5o-10
3,3',5,5'-Tetrachloro- diphenolic acid	0.15	72	213	1-5o-10
3,3',5,5'-Tetrabromo- diphenolic acid	0.23	73	228	1-5g-10
3,3'-Dinitrodiphenolic acid	0.17	78 <sup>d</sup>	168	1-5g-10
Diphenolic acid ethyl ester	0.30	68	170	1-5s, 6s, 7s, 8s, 9

<sup>a</sup> See structural formulas IX and X.

<sup>b</sup> See notes to Table I for explanation.

<sup>c</sup> Determined in 1,2-dichloroethane/trifluoroacetic acid (70/30 by weight).

<sup>d</sup> Bright yellow.

TABLE X  
Poly(phenolphthalein Isophthalate) Fibers

Processing		Physical properties <sup>a</sup>			
Extraction	Drawing	Denier	Tenacity, g./den.	Break elonga- tion, %	Initial modulus, g./den.
Water	2.1 × at 115°C.	9.7	1.95	38.0	24.0
75% Aqueous ethanol	2.0 × at 235°C.	7.5	2.41	27.0	27.3

<sup>a</sup> After boiling relaxed in water and conditioning at 21°C. and 65% R.H.

The drawn fibers showed low crystallinity and orientation by x-ray diffraction pattern. The zero strength temperature was 318°C., and the fiber sticking temperature on a hot brass surface under light pressure was 225°C.

Thanks are due to W. F. Dryden and J. Sparks for excellent technical assistance, to W. R. Brandt for the absorption spectra and their interpretation, and to C. R. Smullen for the preparation of fibers.

### References

- Baeyer, A., *Ber.*, **4**, 659 (1871); *Ber.*, **9**, 1230 (1876); *Ann.*, **202**, 36 (1880).
- Schnell, H., *Angew. Chem.*, **68**, 633 (1956); *Ind. Eng. Chem.*, **51**, 157 (1959).
- Schnell, H., *Trans. Plastics Inst.*, **28**, No. 75, 143 (1960).
- Conix, A., *Ind. Eng. Chem.*, **51**, 147 (1959).
- Eareckson, W. M., *J. Polymer Sci.*, **40**, 399 (1959).
- Chopey, N. P., *Chem. Eng.*, **67**, No. 23, 174 (1960).
- Bistrzycki, A., and K. Nencki, *Ber.*, **29**, 131 (1896).
- Meyer, R., and H. Meyer, *Ber.*, **28**, 2962 (1895).
- Swiss Pat. 292,453 (11/2/53); assigned to Ciba Ltd.; *Chem. Abstr.*, **48**, 6326 (1954).
- Bafna, S. L., and H. A. Shah, *J. Sci. Ind. Res. (India)*, **13B**, 48 (1954).
- Lo, E. S., *Ind. Eng. Chem.*, **52**, 319 (1960).
- Korshak, V. V., S. V. Vinogradova, and S. N. Salazkin, *Vysokomol. Soedin.*, **4**, 339 (1962).
- Howe, J. H., U. S. Pats. 3,035,021 (5/15/62) and 3,036,036-9 (5/22/62), assigned to Dow Chemical Co.
- Underwood, H. W., and G. E. Barker, *J. Am. Chem. Soc.*, **52**, 4082 (1930).
- Beaman, R. G., and F. B. Cramer, *J. Polymer Sci.*, **21**, 223 (1956).
- Orndorff, W. R., and S. A. Mahood, *J. Am. Chem. Soc.*, **40**, 942 (1918).
- Blicke, F. F., F. D. Smith, and J. L. Powers, *J. Am. Chem. Soc.*, **54**, 1470 (1932).
- Whiting, E. T., *J. Am. Chem. Soc.*, **42**, 2366 (1920).
- Orndorff, W. R., and J. J. Kennedy, *J. Am. Chem. Soc.*, **38**, 2487 (1916).
- Copissarow, M., *J. Chem. Soc.*, **117**, 209 (1920).
- Meyer, H., *Monatsh.*, **20**, 361 (1899).
- Christensen, E. V., *Arch. Pharm. Chem.*, **88**, 47, 69 (1931).
- Liebermann, C., and N. Danaila, *Ber.*, **40**, 3588 (1907).
- Morgan, P. W., and S. L. Kwolek, *J. Polymer Chem.*, **40**, 299 (1959) and following papers.
- Schwarwin, W., and Kusnezof, *Ber.*, **36**, 2023 (1903).
- Alphen, J. van, *Chem. Weekblad*, **42**, 42 (1946).

27. Fischer, E., *Ber.*, **7**, 1212 (1874).
28. Taylor, G. B., *J. Am. Chem. Soc.*, **69**, 635 (1947).
29. Fuchs, O., *Kunststoffe*, **43**, 409 (1953).
30. Beaman, R. G., this laboratory, private communication.
31. Elwell, R. H., and L. M. Welch, *J. Am. Chem. Soc.*, **63**, 2474 (1941).
32. Horsley, L. H., *Anal. Chem.*, **19**, 508 (1947); *ibid.*, **21**, 831 (1949).
33. Beaman, R. G., U. S. Pat. 2,658,879 (11/10/53), assigned E. I. du Pont de Nemours & Co., Inc.
34. Sumpter, W. C., *J. Am. Chem. Soc.*, **54**, 3766 (1932).

### Résumé

On a trouvé que la phénolphthaléine, la phénolphthalimidine, la phénolisatine et des composés analogues réagissaient comme des bisphénols avec les chlorures de diacides aliphatique et aromatique, les bischloroformiates, et le phosgène pour former des produits linéaires de haut poids moléculaire. On a employé les procédés de polycondensation interfaciale et en solution à basse et haute températures. Les polymères étaient incolores et formaient facilement des films et des fibres à partir de nombreux solvants. On a rencontré plusieurs particularités dans les propriétés de solubilité. Les températures de transition vitreuse et de fusion de tous les polymères étaient beaucoup plus élevées que les valeurs pour des polymères similaires dérivés du bisphénols A. L'absorption d'eau était assez élevée et la stabilité à la décoloration par la lumière U.V. était bonne. La majorité des substances ne cristallisait pas facilement.

### Zusammenfassung

Phenolphthalein, Phenolphthalimidin, Phenolisatin und ähnliche Verbindungen reagieren als Bisphenole mit aliphatischen und aromatischen Dikarbonsäurechloriden, Bischloroformiaten und Phosgen unter Bildung linearer, hochmolekularer Produkte. Die Reaktion wurde als Grenzflächenpolykondensation sowie als Lösungspolykondensation bei niedriger und hoher Temperatur durchgeführt. Die Polymeren waren farblos und bildeten aus einer Vielfalt von Lösungsmitteln Filme oder Fasern. Das Löslichkeitsverhalten wies einige Besonderheiten auf. Die Glasumwandlungs- und Schmelztemperatur aller Polymeren lag bedeutend höher als bei ähnlichen, von Bisphenol A abgeleiteten Polymeren. Die Wasserabsorption war verhältnismässig hoch und die Beständigkeit gegen Verfärbung durch ultraviolettes Licht gut. Die Mehrzahl der Produkte kristallisierte nicht leicht.

Received November 13, 1962

## X-Ray Diffraction and Infrared Spectra Studies on the Fine Structure of Rayon Improved by High Temperature Steaming

SABURO OKAJIMA and KIMIO INOUE, *Faculty of Technology, Tokyo Metropolitan University, Tokyo, Japan*

### Synopsis

Five samples of rayon containing two high tenacity rayons and three textile rayons of viscose and Bemberg types were heat-treated with high temperature water or steam (110–210°C.) for a few minutes or seconds, and the change in the fine structure was investigated by means of x-ray diffraction and small-angle scattering. An additional study by infrared spectra was carried out on cellulose films similarly heat-treated. The crystallinity increased with increasing temperature and extension of the treating time within the range of less than 10%. Crystallites thicken laterally and grow into those of a higher order. Newly formed crystallites are of cellulose IV. The change is more striking in the high tenacity rayon than in the textile rayons. The remarkable reduction in the degree of swelling is considered to be due partially to such development of crystallinity. No clear conclusion could be drawn as to the contribution of junction points in the amorphous region.

### 1. INTRODUCTION

As described previously,<sup>1</sup> the quality of rayon can be improved by continuous high temperature steaming at 150–190°C. for 15 sec. with negligible depolymerization. The degree of swelling is reduced to the order of that of natural cotton or commercially mercerized cotton. Rayon having such a reduced degree of swelling resists hot water (up to 180°C.) or dilute alkaline solution.

Studies on the heat treatment of rayon in the presence of water have been conducted by many authors<sup>2</sup> since Preston first made such a study, and generally it has been inferred that the decrease in the degree of swelling is due to crosslink formation between cellulose chain segments in the amorphous region and not to crystallization, because it is generally interpreted that the x-ray diffraction pattern of the yarn does not change on heat treatment.

But later, Okajima and Kikuchi<sup>3</sup> found that a slight extent of crystallization does occur, while Ingersoll<sup>4</sup> and Yurugi<sup>5</sup> also showed that cellulose IV appears in heat-treated yarn.

Recently, the present authors<sup>6</sup> have succeeded in constructing an apparatus which makes possible continuous flash steaming of rayon tow or

sliver on an industrial scale. Studies on the fine structure of the heat-treated rayon have thus become more important and more interesting not only from a theoretical point of view but from the practical standpoint of the upgrading of rayon. Thus the present authors, by making continuous studies of this problem by means of x-ray diffraction and infrared spectral studies, have obtained evidence that the structural change takes place not only in the amorphous region but in the crystalline region also. The details are reported in the present paper.

## 2. EXPERIMENTAL

### 2.1 Samples

Three commercially available products along with two laboratory-spun rayons were used as samples.

**Viscose Rayon.** The viscose rayon samples were tire-cord rayon C, 1650  $\times$  2 den.; textile rayon NR-B, 120/26 den.; and high-tenacity rayons TH<sub>3</sub> and TH<sub>1</sub> (tow manufactured for trial in the laboratory). The TH<sub>1</sub> monofilament is of 1.6 den. TH<sub>3</sub> is more highly stretched at spinning than TH<sub>1</sub>.

**Bemberg Rayon.** The Bemberg rayon used was Tow BFK, a 1.3 den. monofilament.

Except for NR-B, the samples are identical with those used in the previous study.<sup>1</sup>

### 2.2 Heat Treatment of Rayon

The samples were heat-treated with steam or hot water by the batch (BS and BW types) or continuous (CS and CW types) method at 110–210°C. as described in detail in the previous paper.<sup>1</sup> (Letters B and C refer to batch and continuous and W and S refer to treated with water and treated with steam, respectively.) The moisture content of the rayon to be BS-treated was adjusted to 30% (optimum water content) by leaving the sample for some days in an atmosphere of 100% R.H. at room temperature.

### 2.3. X-Ray Examination

A recording x-ray diffractometer, Geigerflex, made by Rigaku Denki Ltd. was used. X-ray radiation, Cu K $\alpha$ , was monochromatized by passing through a nickel filter.

### 2.4. Infrared Examination

Infrared spectra were obtained with a Hitachi Model EPI-2 double-beam spectrometer equipped with a sodium chloride prism. For convenience in the experiment, thin cellulose film was used as sample instead of rayon. For this purpose, a 1% cellulose triacetate solution in methylene chloride-methanol cosolvent was cast into a thin film, which was saponified into regenerated cellulose by a 0.7N NaOH methanolic solution. The



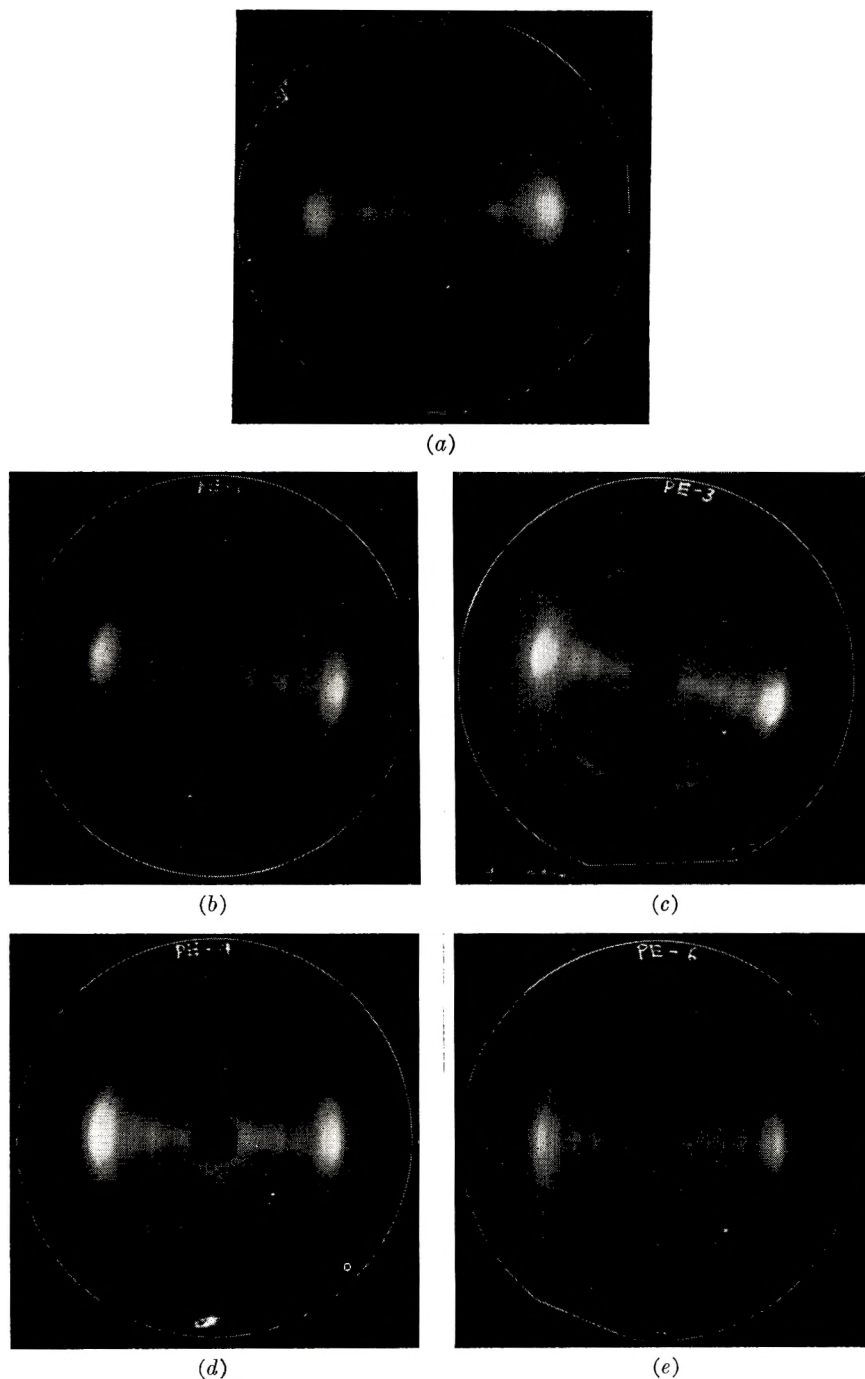


Fig. 1. X-ray diffraction patterns of tire-cord rayon C, BW-treated with top water for 2 min.: (a) untreated unstretched; (b) treated at 130°C, stretched 5%; (c) treated at 170°C, stretched 5%; (d) treated at 130°C, stretched 10%; (e) treated at 170°C, stretched 10%.

cellulose film was washed thoroughly, boiled in water for 1 hr., air-dried, and stored in a desiccator. The complete saponification of the film was proved by the disappearance of the C=O stretching band.

### 3. X-RAY DIFFRACTION STUDY

#### 3.1. X-Ray Diffraction Diagram

Figure 1 shows the x-ray diffraction diagrams of tire-cord rayon C, untreated and CW-treated with tap water at 130–170°C. for 2 min. They indicate that the diffraction of the treated yarns becomes so sharp as compared to that of the untreated yarns, that on samples treated at 170°C., the (020) interference can be clearly seen. At the same time it can be seen that the treated yarns contain the patterns of cellulose IV.

Figure 1 shows two series of the samples treated at 5% and 10% elongation, but almost no difference is detected between these two groups of samples.

The effect of CS treatment (15 sec.), on the x-ray diffraction diagram is very similar to that for the CW treatment described above. This is very noteworthy because there was found to be a pronounced difference in the effect of reduction in swelling between the two types of heat treatment.<sup>1</sup>

#### 3.2. Equatorial Scanning

As shown above, crystallization is likely to occur during the heat treatments, so now equatorial scanning was carried out in order to investigate this in greater detail. The parameters were as follows: 35 k.v., 15 ma., divergency 2 mm. diameter, receiving slit  $2^\circ \times 1^\circ$ , scanning speed  $1^\circ/\text{min.}$ , chart speed 1 cm./min. Each specimen was prepared by placing 70 mg.

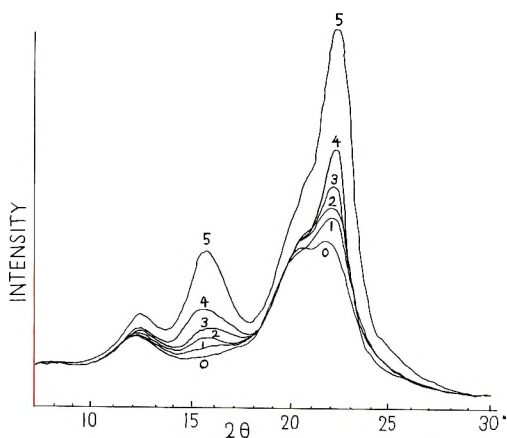


Fig. 2. Equatorial scanning curves of high-tenacity rayon TH<sub>13</sub>, BS-treated at 130–210°C. for 2.5 min.: (0) untreated; (1) 130°C., (2) 150°C.; (3) 170°C.; (4) 190°C.; (5) 210°C.

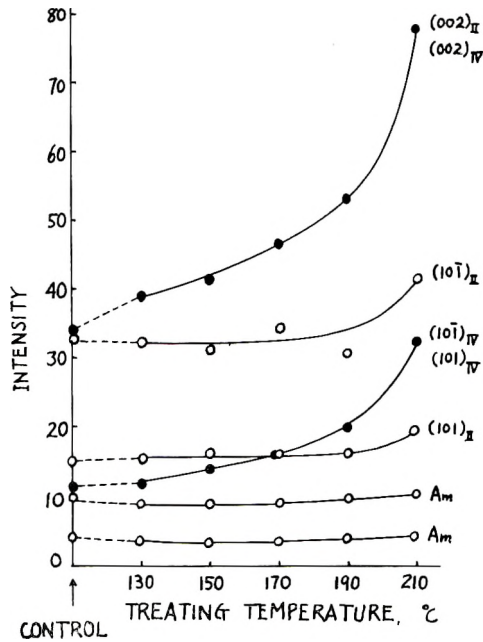


Fig. 3. X-ray diffraction intensity of the high-tenacity rayon TH1<sub>3</sub>, BS-treated at 130–210°C. for 2.5 min.

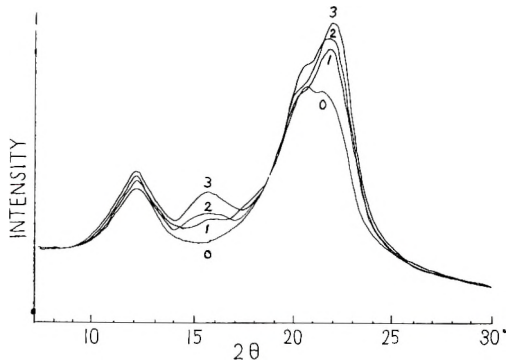


Fig. 4. Equatorial scanning curves of textile rayon NR-B, CS-treated for 15 sec.: (0) untreated; (1) 5 kg./cm.<sup>2</sup>; (2) 9 kg./cm.<sup>2</sup>; (3) 12 kg./cm.<sup>2</sup>.

of yarn in parallel in a groove,  $1 \times 3 \times 30$  mm., made on a bronze plate and solidifying both ends of the yarn with collodion.

The results obtained on TH1<sub>3</sub>, BS-treated at 130–210°C. for 2.5 min. are shown in Figure 2. The diffraction intensity  $I$  at  $2\theta = 15.5^\circ$  of the untreated yarn, corresponding to the diffraction range of  $(10\bar{1})_{IV} + (101)_{IV}$ , is not sufficiently low and, therefore, it is inferred that the untreated yarn already contains a small quantity of cellulose IV as is usually the case in ordinary high-tenacity rayon.<sup>7</sup>

In Figure 3,  $I$  at  $2\theta = 10^\circ, 12.5^\circ, 15.5^\circ, 20^\circ, 22^\circ,$  and  $30^\circ$  are plotted against the temperature of BS treatment. The diffractions at  $2\theta = 10^\circ$  and  $30^\circ$  relate principally to the amorphous phase and it seems their intensities do not change upon treatment. This is reasonable because the sample weight is taken at a constant value. The other four peaks are crystalline diffractions and the  $I$  increases as the treating temperatures rise; especially those at  $15.5^\circ$  and  $22^\circ$ , corresponding to  $(10\bar{1})_{IV} + (101)_{IV}$  and  $(002)_{II} + (002)_{IV}$ , increase more strikingly.

Therefore it can be concluded that the amounts of both crystalline phases, especially cellulose IV, increase during the treatment, and cellulose IV may probably be formed from the amorphous cellulose and may not be converted from cellulose II.

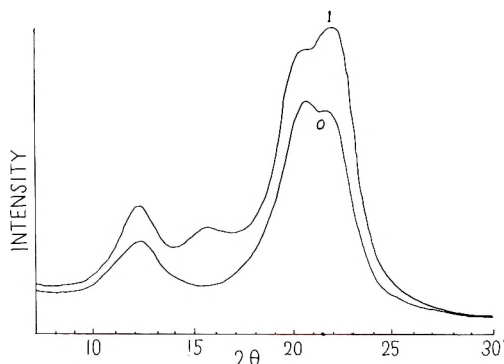


Fig. 5. Equatorial scanning curves of Bemberg rayon BFK, CS-treated with steam at 12 kg./cm.<sup>2</sup> pressure (gauge) for 15 sec.: (0) untreated; (1) treated.

Figure 4 gives the results for textile rayon CS-treated with steam at 5, 9, and 12 kg./cm.<sup>2</sup> each for 15 sec.; the peaks of  $(101)_{II}$  and  $(002)_{II}$  grow higher in this order. Cellulose IV also appears, although it is difficultly detectable on the untreated yarn. A similar phenomenon occurs in the case of Bemberg rayon, as shown in Figure 5. A comparison of these three types of rayon shows clearly that the change is more striking in the case of  $THI_3$  than in the other two cases. This agrees well with the results obtained by Yurugi et al.,<sup>5</sup> where the yarn was heat-treated in a glycerin bath at up to  $250^\circ\text{C}$ .

It is known<sup>8</sup> that the  $(002)$  interference of the cellulose IV derived from cellulose I or III is located at  $2\theta = 22.3^\circ$ , while that derived from cellulose II is located at  $2\theta = 22.0^\circ$ . In the studies made by the present authors, the  $2\theta$  is  $22.0^\circ$ , which is in perfect agreement with this generalization.

As described already, the swelling thus reduced recovers gradually in a caustic alkaline solution of increasing concentration; therefore the x-ray study was conducted as follows. A  $THI_3$  sample which had been CS-treated at 12 kg./cm.<sup>2</sup> for 15 sec. was immersed in solutions of 3 and 5% NaOH at room temperature for 10 min., washed, air-dried, and examined.

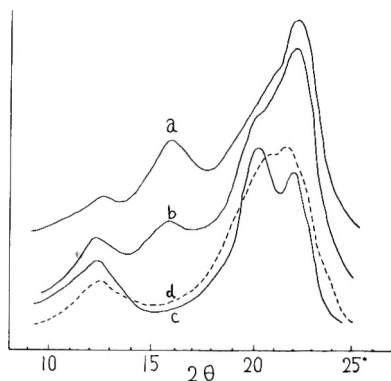


Fig. 6. Equatorial scanning curves of high-tenacity rayon TH1, CS-treated with steam at 12 kg./cm.<sup>2</sup> pressure for 15 sec. and the change after alkaline treatment: (a) before alkaline treatment; (b) after treatment with 3% NaOH solution for 10 min. at room temperature; (c) after treatment with 5% NaOH solution for 10 min. at room temperature; (d) original rayon before CS treatment.

The patterns of cellulose IV still remain after treatment with a 3% alkaline solution but disappear after treatment with a 5% solution as shown in Figure 6. Comparison of the scanning curves of *c* and *d* at  $2\theta = 15.5^\circ$  and  $20-23^\circ$  indicates that *c* is completely of cellulose II, and even the small quantity of cellulose IV which was formed in the original yarn at the time of spinning, disappears after treatment with a 5% NaOH solution. It is interesting to note that the amount of cellulose IV remaining in the yarn is likely to be parallel to the degree of swelling of yarn.<sup>1</sup>

### 3.3. Meridional Scanning

In the meridional scanning, each specimen was mounted on the sample holder at an inclination of  $90^\circ - \theta$  against the x-ray beam, where  $\theta$  is the Bragg angle. Then as shown in Figure 7, the (020) and (040) patterns gradually become sharper and at the same time the intensity ratio of (020)

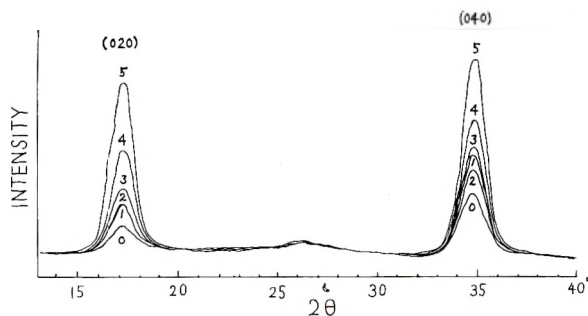


Fig. 7. Meridional scanning curves of high-tenacity rayon TH1, BS-treated at 130–210°C. for 2.5 min.: (0) untreated; (1) 130°C.; (2) 150°C.; (3) 170°C.; (4) 190°C.; (5) 210°C.

to (040) approaches unity asymptotically as the temperature of heat treatment increases. This phenomenon is most noticeable in the high tenacity rayon and least significant in the textile rayon.

Now by measuring the half-value width  $B$  of the (020) or (040) peak, the crystallite size  $L$  perpendicular to the (020) or (040) plane can be estimated by the Scherrer formula:

$$L = K\lambda/\beta \cos \theta \quad (1)$$

where  $K = 0.9$ ,  $\lambda$  is the wavelength of the x-ray,  $\beta = (B^2 - B_0^2)^{1/2}$  and  $B_0 = B$  for (111) of the silicon crystallite =  $0.85 \times 10^{-2}$  radian.

The results are listed in Table I;  $L_{(020)}$  is nearly equal to  $L_{(040)}$  and increases a little during the heat treatment. The estimated length of the crystallite coincides well with the values recently reported by Nukushina<sup>9</sup> and Hermans.<sup>10</sup>

TABLE I  
Crystallite Length of Rayon

Sample	Steam pressure (gauge), Kg./cm. <sup>2</sup>	Treatment conditions			Half-value width, °		Crystallite length, A.	
		Temp., °C.	Time, min.	Type	$B_{(020)}$	$B_{(040)}$	$L_{(020)}$	$L_{(040)}$
High tenacity rayon, TH1 <sub>3</sub>		Untreated	—	—	1.50	1.50	56.6	58.8
		130	5 <sup>a</sup>	BS	1.50	1.40	56.6	63.4
		150	"	"	1.40	1.40	61.2	63.4
		170	"	"	1.50	1.45	56.6	61.0
		190	"	"	1.40	1.45	61.2	61.0
		210	"	"	1.40	1.35	61.2	66.0
Bemberg rayon, BFK		Untreated	—	—	1.35	1.45	63.9	61.0
	3		0.25	CS	1.30	1.35	66.7	66.0
	7		"	"	1.35	1.35	63.9	66.0
	12		"	"	1.35	1.35	63.9	66.0

<sup>a</sup> Approximately 2.5 min. is required to warm the content of the autoclave to the temperature of the oil bath.

### 3.4. X-Ray Crystallinity

As is well known, the method of separation of crystalline diffraction from the amorphous diffraction to estimate crystallinity is somewhat arbitrary and the obtained figure varies according to the method of separation. A precise description of the experiment in the present study is omitted; suffice it to say that the crystallinity increases definitely on heat treatment but the increment is only a few per cent and unexpectedly small.

Some data have already been given in Table Xb of the previous paper.<sup>1</sup>

## 4. SMALL-ANGLE SCATTERING

Small-angle scattering on heat-treated rayon has been reported previously only by Kiessig,<sup>11</sup> who reported that a viscose rayon sample heated

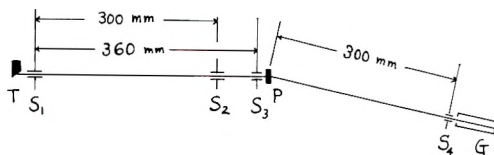


Fig. 8. Schematic diagram of the x-ray small-angle scattering apparatus: (T) target; (P) sample; (G) Geiger counter; (S<sub>1</sub>) first slit,  $0.3 \times 12$  mm.; (S<sub>2</sub>) second slit,  $0.2 \times 12$  mm.; (S<sub>3</sub>) third slit;  $0.3 \times 12$  mm.; (S<sub>4</sub>) fourth slit,  $0.4 \times 15$  mm.

in water at  $200^\circ\text{C}$ . shows a long meridional periodicity. It is, therefore, interesting to examine our samples by this method.

However, there remain some questions<sup>12</sup> as to the application of small-angle scattering theories to rayon for calculation of the periodic length, so the following estimation is of semiquantitative significance, but it is helpful to discuss the wide-angle diffraction data.

The specimen was prepared as described in section 3 and, especially for the equatorial scanning, it was soaked in water for 10 min., blotted with filter paper, covered with a thin polymethyl methacrylate film and mounted on a holder. The parameters were as follows: 35 k.v., 15 ma., scanning speed  $2^\circ/\text{hr}$ . A schematic diagram of the apparatus is shown in Figure 8.

#### 4.1. Equatorial Scattering

The intensity distribution curves ( $I$  versus  $\epsilon$ ) and the effect of the heat treatment upon them are characteristic of the type of rayon, as shown in Figures 9–11.  $I$  for the high tenacity rayon is low but becomes higher after BW or BS treatment (the case of BW treatment is akin to the change in BS treatment, so the former case was omitted from Fig. 9). This may be because there are many small junctions in the amorphous region of this type of rayon, and, therefore, the electron density of the amorphous phase does

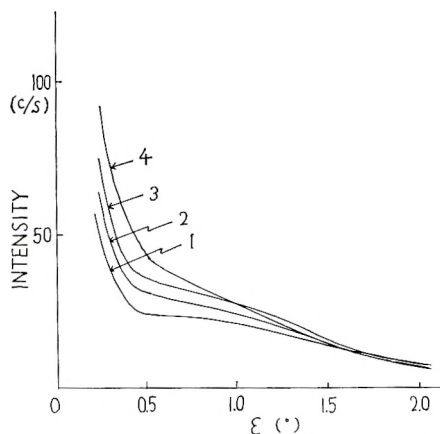


Fig. 9. Equatorial scattering curves of high-tenacity rayon TH1<sub>3</sub>, BS-treated at 110–190°C. for 2.5 min.: (1) untreated; (2) 110°C.; (3) 150°C.; (4) 190°C.

not differ much from that of the crystalline part, even in the swollen state, but the difference increases on treatment because the crystalline part grows into more complete lattices, while, on the contrary, the amorphous part relaxes.

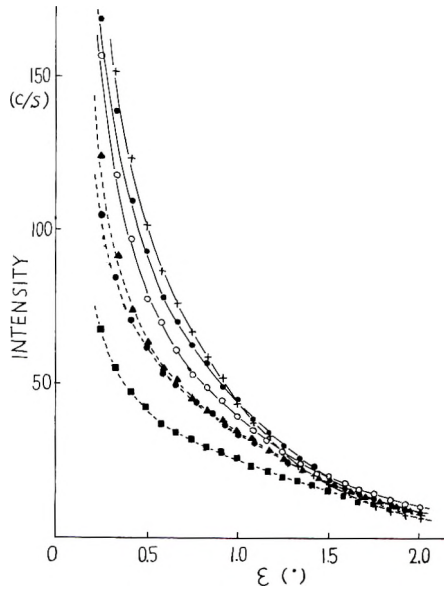


Fig. 10. Equatorial scattering curves of the textile rayon NR-B, treated variously for 2.5 min.: (-O-) untreated; (-●-) BW-treated, 150°C.; (-+-) BW-treated, 210°C.; (-▲-) BS-treated, 110°C.; (-●-) BS-treated, 150°C.; (-■-) BS-treated, 190°C.

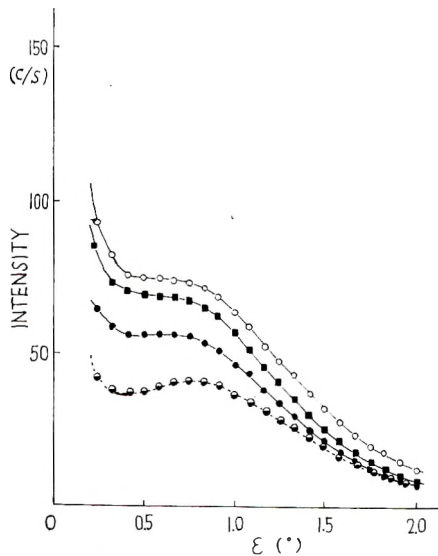


Fig. 11. Equatorial scattering of the Bemberg rayon BFK-B, variously treated: (-O-) untreated; (-●-) BS-treated, 150°C., 2.5 min.; (-■-) BW-treated, 190°C., 2.5 min.; (-○-) CS-treated, 12 kg./cm.<sup>2</sup>, 15 sec.



TABLE II  
Diameter of Fibril, Distance between Micelles, and Degree of Swelling of High Tenacity Rayon TH<sub>3</sub>

Treatment conditions			Diameter of fibril, A.	Distance between micelles, A.	Degree of swelling, Q <sup>b</sup>
Temp., °C.	Time, min. <sup>a</sup>	Type			
Untreated			30.1	56.3	1.87
110	5	BW	35.6	61.6	1.86
150	"	"	37.2	61.6	1.72
190	"	"	43.0	68.5	1.62
110	"	BS	33.5	61.6	1.84
150	"	"	37.2	61.6	1.62
190	"	"	40.3	61.6	1.62

<sup>a</sup> Approximately 2.5 min. is required to warm the content of the autoclave to the temperature of the oil bath.

<sup>b</sup> Q = centrifuged weight/bone dry weight.

When the  $I$  versus  $\epsilon$  curves are transformed to a log  $I$  versus  $\epsilon^2$  relation, the plot curves slightly; on calculating the diameter of the fibrils from the initial slope by assuming that the Guinier formula is applicable, the diameter increases with increasing treating temperature and, consequently, with decreasing degree of swelling as listed in Table II. Therefore, a relaxation, i.e., melting of the small-sized and more unstable crystallites and crystallization to larger-sized and more stable crystallites, seems to occur.

The scattering of the textile rayon (Fig. 10) is of higher intensity than that of TH<sub>3</sub> and the intensity increases further as the temperature rises

TABLE III  
Diameter of Fibril 2R, Distance between Micelles D, and Degree of Swelling Q of Bemberg Rayon BFK

Treatment conditions			Diameter of fibril, A.	Distance between micelles, A.	Degree of swelling, Q
Temp., °C.	Time, min. <sup>a</sup>	Type			
A. Untreated			50.8	77.0	1.94
150	5	BW	—	—	1.80
190	"	"	—	78.0	1.81
210	3	"	—	78.0	—
110	5	BS	—	68.4	1.66
150	"	"	—	68.4	1.59
190	"	"	—	68.4	1.60
B. Untreated			—	65.5	1.83
150	5	BW	—	70.0	—
190	"	"	—	70.0	—
<sup>b</sup>	0.25	CS	—	63.0	—

<sup>a</sup> Approx. 2.5 min. is required to warm the content of the autoclave to the temperature of the oil bath.

<sup>b</sup> Steam pressure, 12 kg./cm.<sup>2</sup> (gauge).

in the BW treatment but decreases, on the contrary, in the BS treatment. The change in the latter case may be due to the predominant formation of many junctions in the amorphous region, which causes the decrease in the difference in electron density between the amorphous and crystalline regions.

Bemberg rayon, too, is of similar type in respect to the effect of the treatment, but a small shoulder appears on each  $I-\epsilon$  curve; Figure 11 is an example of such a curve for BHK-B. In Table III the period  $D$  is shown, which is obtained by substituting  $\epsilon$  at the peak of the  $\epsilon^2 I-\epsilon$  curve into the Bragg formula, providing, of course, that the system is composed of plate-like micelles. The assumption of a dilute system and the application of the Guinier formula are not correct for this rayon.

TABLE IV  
Distance between Micelles and Degree of Swelling of Textile Rayon NR-B

Treatment conditions			Distance between micelles, A.	Degree of swelling, $Q$
Temp., °C.	Time, min. <sup>a</sup>	Type		
Untreated			61.5	1.97
110	5	BW	62.9	1.93
150	"	"	68.5	1.94
190	"	"	—	1.88
210	3	"	73.3	—
110	5	BS	61.5	1.79
150	"	"	59.2	1.65
190	"	"	56.0	1.55

<sup>a</sup> Approximately 2.5 min. is required to warm the content of the autoclave to the temperature of the oil bath.

$D$  decreases on BS or CS treatment, while it increases on BW treatment. The former change relates predominantly to the reduction in the degree of swelling, while the latter change relates predominantly to the loose packing due to relaxing; the actual crystallite width is considered to increase in every case. The textile rayon behaves similarly as the Bemberg rayon does, as shown in Table IV.

#### 4.2. Meridional Scattering

Figures 12 and 13 show the  $I-\epsilon$  plots of the air-dried textile rayon and Bemberg rayon, respectively. Although the  $I-\epsilon$  curve of the untreated yarn changes monotonically, a peak appears on each curve of the treated yarn which disappears again on being soaked in water. In the case of the high tenacity rayon this peak rarely appears after the heat treatment.

On calculating the long period  $L_s$  from this peak angle (Fig. 13) by using the Bragg formula, 212 Å. was obtained for all of the specimens tested; thus no effect of the treatment on  $L_s$  can be detected. Therefore, it is inferred

that the crystallites gain higher regularity and elongate. Upon hydrolysis of the treated yarn with a 2.5*N* HCl solution at 60°C. for 1 hr.,  $L_s$  decreased to 189 Å. This may be because the specimen was treated in a relaxed state and shrank a little.

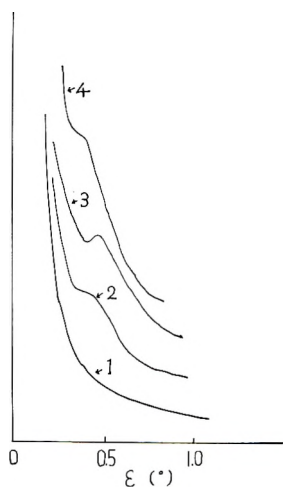


Fig. 12. Meridional scattering of Bemberg rayon BFK-B, variously treated: (1) untreated; (2) BW-treated, 210°C., 0.5 min.; (3) hydrolyzed in 2.5*N* HCl at 60°C. for 1 hr.; (4) high-tenacity rayon TH1<sub>s</sub>, BW-treated, 190°C., 2.5 min.

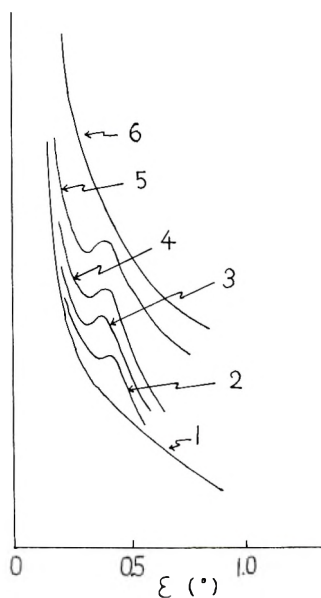


Fig. 13. Meridional scattering of textile rayon NR-B, BW-treated at 130–190°C.: (1) untreated; (2) 130°C., 2.5 min.; (3) 150°C., 2.5 min.; (4) 170°C., 2.5 min.; (5) 190°C., 1.5 min.; (6) sample 5 in swollen state.

## 5. INFRARED SPECTRA

### 5.1. Heat Treatment of Cellulose Film

**BW Treatment with Heavy Water.** Approximately 0.1 g. of cellulose film, which was protected from mechanical damage by being rolled with a fine mesh stainless steel gauze, was placed in F (glass tube 7.5 mm. diameter  $\times$  120 mm.) as shown in Figure 14 and vacuum-dried by continuous pumping through tap 1. On closing tap 1 and opening tap 2, a small quantity of  $D_2O$  (99.7%) was vaporized from G to F through tap 2, and after 2 hr. deuteration tap 2 was closed and the film was vacuum-dried. This deuteration and drying cycle was repeated three times and finally about 1 cm.<sup>3</sup> of  $D_2O$  was transferred from G to F by distillation and F was cut at the stem using flame; 1 cm.<sup>3</sup> of water was sufficient to wet the film thoroughly.

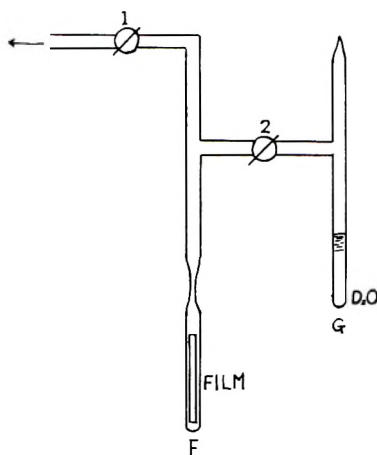


Fig. 14. Apparatus for deuteration of cellulose film.

The tube F was now put directly into an oil bath adjusted to the desired temperature, and the wet film was heated for a desired time. When the treating temperature was above 190°C. the tube was put into a small stainless steel autoclave containing a small quantity of water and indirectly heated. The time of treatment was referred to the instant at which a sample was immersed in the oil bath.

In the case of the heat treatment with  $H_2O$ , the cellulose film protected by a stainless steel gauze was placed in a small Titan autoclave (capacity 11 cm.<sup>3</sup>) and heated as above.

**BS Treatment with  $D_2O$ .** A cellulose film placed in a glass tube was first thoroughly dried by passing over it dry  $N_2$  gas; then moist  $N_2$  gas which had been bubbled through 99.7%  $D_2O$ , for 6 hr. at 25°C. was passed over it. The tube was closed and heating was carried out as similarly as in the BW treatment.

**Measurement of the Amount of Resistant OD.** The experiment was carried out according to the method of Mann and Marrinan.<sup>13</sup> Rehydrogena-

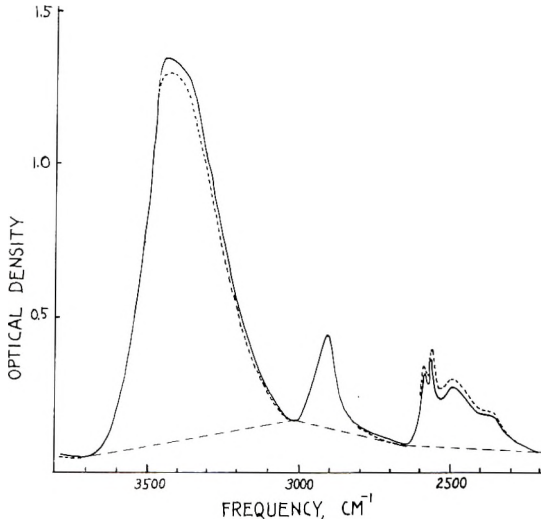


Fig. 15. Infrared spectra of cellulose film deuterated and BS-treated at 170°C. for 7.5 min. in the presence of  $D_2O$ : (---) deuterated; (—) rehydrogenated in liquid  $H_2O$  for 3 hr.; (-·-) base line.

tion was carried out for 3 hr. at room temperature; extension of the soaking time in  $H_2O$  to 24 hr. had a negligible effect on the amount of resistant OD. Figure 15 is an example of infrared spectra of film BS-treated at 170°C. for 10 min.

## 5.2. Results

When the deuterated film is treated in the presence of heavy water, partial crystallization is expected to occur (from the results obtained in sections 3 and 4) and the degree of crystallization is to be estimated by the amount of resistant OD, providing that water cannot penetrate into the

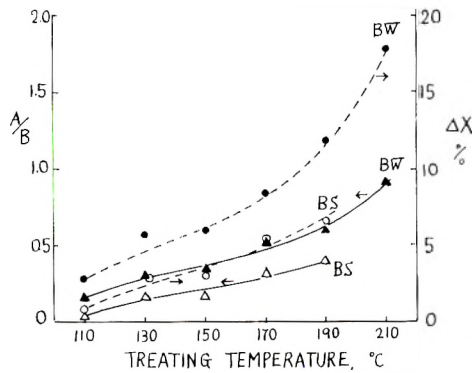


Fig. 16. Relation between (—) the resistant OD or (- -) increase in crystallinity and the treatment temperature (5 min.): (▲, ●) BW-treatment; (Δ, O) BS-treatment.

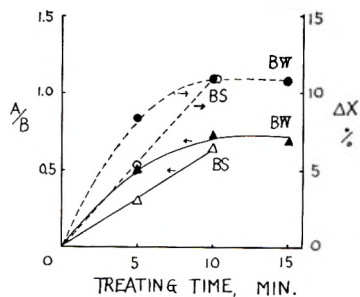


Fig. 17. Relation between (—) the resistant OD or (---) increase in crystallinity and the treating time at 170°C.

TABLE V  
Change in the Amount of Resistant Crystallinity on BW-Treatment

Treatment conditions		Absorption					A/B	C/B	$\Delta X$ , % <sup>a</sup>
Temp., °C.	Time, (min.)	A 2490 cm. <sup>-1</sup>	B 2900 cm. <sup>-1</sup>	C 3440 cm. <sup>-1</sup>	D 2530 cm. <sup>-1</sup>	E 3360 cm. <sup>-1</sup>			
110	5 <sup>b</sup>	0.045	0.275	1.320	0.038	1.188	0.164	4.80	2.8
130	"	0.089	0.295	1.339	0.073	1.103	0.302	4.54	5.7
150	"	0.101	0.291	1.301	0.082	1.180	0.347	4.47	5.9
170	"	0.220	0.427	1.991	0.173	1.722	0.515	4.07	8.4
170	10 <sup>b</sup>	0.223	0.301	1.253	0.161	1.155	0.740	4.16	11.2
170	15 <sup>b</sup>	0.140	0.205	0.892	0.123	0.806	0.683	4.35	10.8
190	7 <sup>c</sup>	0.155	0.262	1.008	0.140	0.946	0.591	3.85	11.8
210	7 <sup>c</sup>	0.185	0.204	0.801	0.174	0.720	0.907	3.93	17.8

<sup>a</sup> Calculated by eq. (2) for  $K_{OD}/K_{OH} = 1.11$ .

<sup>b</sup> Approximately 2.5 min. is required to warm the content of the autoclave to the temperature of the oil bath.

<sup>c</sup> Approximately 5 min. is required to warm the content of the autoclave to the temperature of the oil bath.

TABLE VI  
Change in the Amount of Resistant OD and Crystallinity on BS Treatment

Treatment conditions		Absorption					A/B	C/B	$\Delta X$ % <sup>b</sup>
Temp., °C.	Time, min. <sup>a</sup>	A 2490 cm. <sup>-1</sup>	B 2900 cm. <sup>-1</sup>	C 3440 cm. <sup>-1</sup>	D 2530 cm. <sup>-1</sup>	E 3360 cm. <sup>-1</sup>			
110	5	0.014	0.345	1.895	0.015	1.649	0.041	5.49	0.8
130	"	0.044	0.279	1.338	0.038	1.213	0.158	4.79	2.9
150	"	0.061	0.358	1.781	0.053	1.538	0.171	4.97	3.0
170	"	0.112	0.360	1.682	0.088	1.578	0.311	4.67	5.3
170	10	0.199	0.304	1.256	0.163	1.155	0.655	4.13	11.3
190	5	0.100	0.251	1.085	0.076	0.981	0.399	4.32	6.5

<sup>a</sup> Approximately 2.5 min. is required to warm the content of the autoclave of the temperature of the oil bath.

<sup>b</sup> Calculated by eq. (2) for  $K_{OD}/K_{OH} = 1.11$ .

crystalline region. Use of a D<sub>2</sub>O tracer for such a high temperature treatment of cellulose has not previously been made, so the results obtained by the present authors will be reported in detail.

As shown in Figures 16 and 17 and Tables V and VI, the amount of resistant OD groups increases clearly with increasing treatment temperature. The thickness of cellulose film varied a little from specimen to specimen, so the ratio  $A/B$  of the optical density at 2490 cm.<sup>-1</sup> ( $\nu_{OD}$ ), divided by the optical density at 2900 cm.<sup>-1</sup> ( $\nu_{OH}$ ), was determined. Beer's law was valid in the relation between the optical density of 2490 cm.<sup>-1</sup> or 2900 cm.<sup>-1</sup> and the film thickness.

As a measure of the fraction of the crystallized OD groups by the heat treatment,  $\Delta X$  was calculated from eq. (2):

$$\begin{aligned}\Delta X &= 100C_{OD}/(C_{OD} + C_{OH}) \\ &= 100(1 + C_{OH}/C_{OD})^{-1} \\ &= 100\{1 + (K_{OD}/K_{OH})[\log(I_0/I)_{OH}/\log(I_0/I)_{OD}]\}^{-1}\end{aligned}\quad (2)$$

where the 3360 and 2530 cm.<sup>-1</sup> bands were used and  $K_{OD}/K_{OH}$  was assumed to be 1.11 according to Mann and Marrinan.

A comparison of the two types of heat treatment (Fig. 16) shows that the BW heating appears to be more effective in increasing  $A/B$  or  $\Delta X$  than the BS treatment, but nearly equal values are obtained on 10 min. treatment, as seen in Figure 17 which shows the time effect. Any conclusion pertaining to this problem requires future study, taking into consideration the fact that the accessibility of a cellulose film to D<sub>2</sub>O is higher in liquid water than in gas phase water, which may lead to an effective crystallization of the region of higher lateral order in the BW treatment.

The curves in Figure 16 become steeper above 190°C.; this corresponds to the changes in the x-ray diffraction (section 3) and in degree of swelling<sup>1</sup> and is considered to be additional evidence for the beginning of depolymerization at that temperature as already indicated.

TABLE VII  
Change in Crystallinity on BW Treatment

Treatment conditions		Absorption		Crystallinity, % <sup>b</sup>	
Temp., °C.	Time, min. <sup>a</sup>	2530 cm. <sup>-1</sup>	3360 cm. <sup>-1</sup>	$X$	$\Delta X$
Untreated		0.533	0.161	24.5	—
110	5	0.708	0.257	28.7	4.2
130	"	0.605	0.227	29.4	4.9
150	"	0.582	0.252	32.5	8.0
170	"	0.623	0.314	35.9	11.4
190	"	0.446	0.207	35.1	10.6
210	"	0.502	0.330	42.2	17.7

<sup>a</sup> Approximately 2 min. is required to warm the content of the autoclave to the temperature of the oil bath.

<sup>b</sup> Calculated by eq. (2) for  $K_{OD}/K_{OH} = 1.11$ .

The crystallinity  $X$  of cellulose film BW-treated with  $H_2O$  was also estimated by complete deuteration of OH groups in the amorphous region (deuteration for 5–6 hr. at 25°C.) according to Mann and Marrinan.<sup>13</sup> Results are listed in Table VII, it being assumed, of course, that  $D_2O$  vapor cannot be accessible to OH groups in the crystalline region. As can be seen from Table VII, the crystallinity increases linearly with increasing temperature from 24.5% of the untreated (but boiled in water) film and amounts to 42% at 210°C. It is noteworthy that the increment  $\Delta X$  nearly coincides with the values listed in Table V, which are obtained by a separate method, because the above assumption is approved here. But further study may be necessary to obtain the absolute values of  $X$  and  $\Delta X$ .

## 6. SUMMARY AND DISCUSSION

The following conclusions are derived from the results given in sections 3–5.

(1) Crystallization occurs during the heat treatment, and the x-ray diffraction patterns sharpen even when rayon is flash steamed at 170°C. for 15 sec. The development of the crystalline region consists in the growing of small crystallites into larger ones, both longitudinally and laterally, and of conversion unstable crystallites of low regularity into stable ones of higher regularity in addition to the new formation of crystalline order in the amorphous region. These newly formed crystallites are of cellulose IV.

(2) The degree of crystallization increases linearly with increasing treating temperature within the range of less than 10% under ordinary conditions. When the temperature is above 190°C., the crystallinity develops markedly. This is because the treatment at such high temperature is followed by the depolymerization of cellulose, even on flash steaming, and the increased mobility of the cellulose chain segments near the broken ends accelerates crystallization.

(3) The crystallization of high tenacity rayon is more marked than that of textile rayon. This is considered to be related to the lower lateral order of high tenacity rayon.

(4) Junction points are formed in the amorphous region; however, some weak junctions temporarily formed at lower temperature disappear, and more stable junctions or crystallites are formed as the treating temperature rises. Such relaxation brings about a loosely packed structure in rayon, and this is likely to occur especially in the BW treatment.

(5) The degree of swelling of BS-treated rayon is much lower than that of the BW-treated rayon, as already reported. X-ray investigation indicates, however, that the crystallinity of the former is not higher than that of the latter, and the amount of resistant OD groups of BW-treated yarn is rather larger than that of the BS-treated yarn. A reason is that water can be accessible to OH groups in higher lateral order of cellulose in the liquid-phase deuteration than in the gas-phase deuteration, and these OD groups in higher lateral order easily crystallize into resistant OD groups.



In the amorphous region, a large number of junction points are formed during the heat treatment, but a junction point is composed of a few hydrogen-bonded glucose units and, therefore, it can not be detected by x-ray diffraction as crystallite. If the heat treatment is carried out in the presence of D<sub>2</sub>O, the junction points are formed by hydrogen-bonding between OD groups, but the hydrogen-bonded D may exchange slowly with H during the rehydrogenation, and transforms into hydrogen-bonded H. When the film is heat-bonded H may exchange with D, remaining as junction points. So the change in the number of junction points does not reflect the amount of resistant OD and there is no quantitative information on the junction points.

Consequently no clear conclusion can be drawn at present, and while it is likely that the BS-treated yarn has a large number of junction points compared with the BW-treated yarn, although there is no quantitative evidence for it. This explanation is probable because the BS treatment is carried out in a suitably swollen state and not excessively swollen state as in the case of the BW treatment. After all, the degree of swelling is considered to be a function of the number of crosslinks, such as crystallites and junction points, and not a simple function of the degree of crystallinity.

### References

1. Okajima, S., K. Inoue, M. Yazawa, and Y. Kuwazuka, *Textile Res. J.*, **32**, 843 (1962).
2. Preston, J. M., N. M. Nimkar, and S. P. Gundavda, *J. Soc. Dyers Colorists*, **67**, 169 (1951); J. M. Preston, and S. P. Gundavda, *ibid.*, **68**, 511 (1952); M. Yazawa and S. Okajima, *Kogyo Kagaku Zasshi*, **57**, 512 (1954); K. Schwertassek, *Faserforsch. Textiltech.*, **8**, 351 (1955); K. Kanamaru, N. Tokita, and S. Noyama, *Kogyo Kagaku Zasshi*, **60**, 624 (1957); S. Mukoyama and T. Tsuda, *Kogyo Kagaku Zasshi*, **60**, 934 (1957).
3. Okajima, S., and T. Kikuchi, *Kogyo Kagaku Zasshi*, **64**, 1665 (1961).
4. Ingersoll, H. G., *J. Appl. Phys.*, **47**, 924 (1946).
5. Yurugi, T., and T. Ogihara, *Kogyo Kagaku Zasshi*, **63**, 1457 (1960).
6. Yazawa, M., and S. Okajima, U. S. Pat. Appl. 155,324 (Nov. 28, 1961); U. S. Pat. Appl. 177,382 (March 5, 1962).
7. Ingersoll, H. G., *J. Appl. Phys.*, **17**, 924 (1946); J. A. Howsmon, and W. A. Sisson, *Cellulose and Cellulose Derivatives*, Interscience, New York, 1954, p. 241; H. Sobue, and H. Minato, *Kogyo Kagaku Zasshi*, **60**, 327 (1957); T. Yurugi, and T. Kurita, *Kogyo Kagaku Zasshi*, **60**, 1187 (1957).
8. Segal, L., *J. Polymer Sci.*, **55**, 395 (1961).
9. Nukushina, Y., *Kogyo Kagaku Zasshi*, **64**, 38 (1961).
10. Hermans, P. H., and A. Weidinger, *Textile Res. J.*, **31**, 558 (1961).
11. Kiessig, H., *Kolloid-Z.*, **157**, 62 (1957).
12. Heyn, A. N. J., *Textile Res. J.*, **19**, 163 (1949); *ibid.*, **23**, 782 (1953); *J. Appl. Phys.*, **26**, 519, 1113 (1954); D. Heikens, P. H. Hermans, and A. Weidinger, *J. Polymer Sci.*, **11**, 433 (1953); P. H. Hermans and A. Weidinger, *J. Polymer Sci.*, **14**, 397, 405 (1954); W. O. Statton, *J. Polymer Sci.*, **22**, 385 (1956).
13. Mann, J., and H. J. Marrinan, *Trans. Faraday Soc.*, **52**, 481, 487, 492 (1956).

### Résumé

On a chauffé durant quelques minutes ou quelques secondes, avec de l'eau ou de la vapeur à température élevée (110 à 210°C), cinq échantillons de rayonne: deux

rayonnes de haute résistance et trois rayonnes pour textile du type viscose et Bemberg. On a étudié le changement dans la structure fine par la diffraction des rayons-X et la diffusion sous faible angle. Une étude additionnelle par spectrométrie infrarouge a été effectuée sur des films de cellulose, chauffés de façon similaire. La cristallinité augmente avec la température et la durée du traitement sans que l'augmentation dépasse 10 %. Le changement est plus net pour la rayonne de haute résistance que pour les rayonnes de textile. On considère que la diminution remarquable du degré de gonflement est due partiellement à un tel développement de la cristallinité. Au sujet de la contribution de points de jonction dans la région amorphe, on n' a pu tirer de conclusions claires.

### Zusammenfassung

Fünf Kunstseideproben, nämlich zwei hochfeste Kunstseiden und drei Textilkunstseiden vom Viskose- und Bembergtyp wurden mit hochtemperiertem Wasser oder Dampf (110–210°C) während einiger Minuten oder Sekunden hitzebehandelt und die Feinstrukturänderungen mittels Röntgenbeugung und Kleinwinkelstreuung untersucht. Zusätzlich wurde an in ähnlicher Weise hitzebehandelten Cellulosefolien eine IR-spektroskopische Untersuchung durchgeführt. Die Kristallinität nahm mit der Temperatursteigerung und mit Verlängerung der Behandlungsdauer in einem Bereich von weniger als 10% zu. Die Kristallite verdicken sich seitlich und wachsen in solche von höherer Ordnung. Neu gebildete Kristallite bestehen aus Cellulose IV. Die Änderungen sind bei hochfester Kunstseide auffälliger als bei Textilkunstseide. Der bemerkenswerte Rückgang des Quellungsgrades wird zum Teil auf eine solche Entwicklung der Kristallinität zurückgeführt. Bezüglich des Beitrages von Vernetzungspunkten im amorphen Bereich konnte keine klare Entscheidung getroffen werden.

Received November 13, 1962

## Polymers from Sulfamide. I. Preparation\*

H. Q. SMITH and F. L. SCOTT, † *Pennsalt Chemicals Corporation, Research and Development Department, Wyndmoor, Pennsylvania*

### Synopsis

Sulfamide and formaldehyde react at pH 10 to give a polymeric white solid (A) which decomposes at 234–235°C. A similar material results at pH 7. Modification of A was achieved by inclusion of melamine in the polymeric matrix. Sulfamide–melamine–formaldehyde polymer had a melting point of 261–265°C., was insoluble in organic solvents, and formed a cohesive film on compression. The polymer was obtained when sulfamide, formaldehyde, and melamine were all allowed to react simultaneously, or when a methylol melamine derivative was first prepared and then crosslinked with sulfamide. Sulfamide appears to be a more rapid crosslinking agent than urea for this system. Other aminotriazines were used in place of melamine and some 1,3-dialkyl-sulfamides were employed in place of sulfamide, but no significant improvement in thermal stability of the polymers was achieved.

Sulfamide has been reported to condense with formaldehyde under mildly basic conditions to give a gum<sup>1</sup> and an insoluble, infusible solid.<sup>2</sup> Under strongly acidic conditions, the product was reported to be a toxic solid, characterized as tetramethylenedisulfotetramine.<sup>3</sup>

We have condensed formaldehyde and sulfamide under the conditions of a standard<sup>4</sup> recipe for melamine–urea–formaldehyde resins (pH 10) and obtained a product melting at 234–235°C. with decomposition. It was insoluble in most organic solvents except hot dimethylformamide and dimethyl sulfoxide and did not press to a film (see Experimental).

In order to improve the thermal stability of this material, some attempts were made to incorporate melamine and other aminotriazines into the polymeric structure. With equimolar amounts of melamine and sulfamide with formaldehyde, the product was a cementlike solid (m.p. 261–265°C. with decomposition), which was totally resistant to solvent attack and which pressed to a film. The use of only one-sixth the molar amount of melamine gave a similar product but with reduced melting point. With only one-sixth the molar quantity of sulfamide the product displayed a higher melting point. Under identical reaction conditions, melamine and formaldehyde alone developed no solid, nor did the addition of urea induce the development of insoluble polymers. The apparent crosslinking potency of even a relatively small molar ratio of sulfamide is evident.

In order to demonstrate further that the triazine component was not

\* Presented in part at the 136th meeting of the American Chemical Society, Atlantic City, New Jersey, September 13–18, 1959.

† Present address: Department of Chemistry, University College, Cork, Ireland.

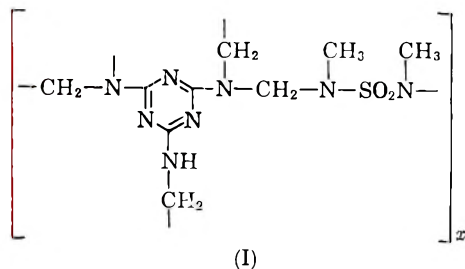
merely physically trapped in the sulfamide-formaldehyde matrix, sulfamide was added to a melamine-formaldehyde mixture which had been allowed to react for 1 hr. under the basic conditions. The resulting product was identical with that obtained when all the components were present and allowed to react simultaneously; thus, at least part of the melamine is chemically involved.

Sulfamide in aqueous solution is a neutral entity, and its crosslinking potency is therefore not an acid hardening or curing effect. The condensation of sulfamide and formaldehyde at pH 7 gave essentially the same product as that produced at pH 10, although in somewhat reduced yield. This suggests that the active moiety in the crosslinking process may be the sulfamide anion,  $\text{NH}_2\text{SO}_2\text{NH}^-$ . The sulfamide-melamine-formaldehyde condensation at pH 2 gave a product melting at 275–280°C., which did not form a film under pressure as easily as did the polymer prepared under basic conditions.

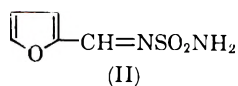
The structure of the sulfamide-formaldehyde and sulfamide-melamine-formaldehyde polymers described above is considered in further detail in Part II of this series.<sup>5</sup>

Further studies were carried out with these types of condensations by varying the aminotriazine, the sulfamide moiety, and the aldehyde employed. Benzoguanamine and ammeline were expected to reduce the extent of crosslinking compared to that developed by melamine. Benzoguanamine, sulfamide, and formaldehyde under our standardized basic conditions gave a product melting at 235–245°C. with decomposition which did not form a film. With ammeline, the products were a sulfamide-formaldehyde polymer and unchanged aminotriazine.

Replacement of sulfamide in the sulfamide-melamine-formaldehyde reaction with 1,3-dimethylsulfamide gave a product melting at about 250°C. with decomposition, whose analysis was reasonably consistent with the speculative structure I. With 1,3-di-*tert*-butylsulfamide, no sulfamide entity was incorporated into the resulting product.



Replacement of formaldehyde in the sulfamide-melamine-formaldehyde reaction with benzaldehyde failed to yield polymeric products under our conditions. With 2-furaldehyde, the only product obtained was the Schiff base, 2-furfurylidene-sulfamide (II).



## EXPERIMENTAL

Sulfamide was prepared by the method of Degering and Gross.<sup>6</sup> After recrystallization from absolute ethanol it had a melting point of 90.5–92.0°C.

The 1,3-dialkylsulfamides were prepared from the amine and sulfonyl chloride in ether according to:



*N,N'*-Dimethylsulfamide was recrystallized from benzene and had a melting point of 79–80°C.<sup>7</sup>

*N,N'*-Di-*tert*-butylsulfamide has not been reported previously. It was separated from the concurrently formed *tert*-butylamine hydrochloride by treatment with boiling ether or boiling water, from either of which the product crystallized on cooling. The yield was 38%, m.p. 142.5–145.5°C.

ANAL. Calcd. for  $C_8H_{20}N_2O_2S$ : H, 46.12%; C, 9.68%; N, 13.45%. Found: C, 46.48%; H, 9.13%; N, 13.05%.

2-Furfurylidenesulfamide (II) was prepared<sup>8</sup> by refluxing 2.0 g. (20.8 mmole) of sulfamide, 2.0 g. (20.8 mmole) of freshly distilled 2-furaldehyde, 0.64 g. of anhydrous copper sulfate, and 10 ml. of absolute ethanol for 6 hr. After cooling, the resulting solid was filtered off and extracted with three 20-ml. portions of boiling absolute ethanol which on cooling gave 1.0 g. of 2-furfurylidenesulfamide, as a yellow solid, m.p. 166–169°.

ANAL. Calcd. for  $C_8H_6N_2O_3S$ : C, 34.48%; H, 3.47%; S, 18.41%. Found: C, 34.64%; H, 3.99%; S, 18.18%.

The following is a typical example of our condensation experiments. A mixture of 5.2 g. of 37% formaldehyde solution (64 mmole  $CH_2O$ ), 1.3 ml. of 0.558*N* sodium hydroxide solution, 0.16 g. of concentrated aqueous ammonia solution, 2.0 g. (16 mmole) of melamine and 2.0 g. (16 mmole) of 1,3-dimethylsulfamide was refluxed for 1 hr. The reaction mixture became clear on reflux and then a solid gradually developed. The mixture was cooled and the solid was filtered off, washed with water, dried, and its properties determined.

ANAL. Calcd. for  $C_9H_{17}N_8O_3S$ : C, 34.06%; H, 5.40%; N, 35.31%; S, 10.10%. Found: C, 33.27%; H, 5.58%; N, 35.75%; S, 9.38%.

The other polymerizations and appropriate blank runs were carried out similarly and are described in Table I.

This work was supported in part by the Office of Naval Research. Microanalyses were carried out by Dr. P. A. Munter and associates of the Analytical Department of our laboratories.

TABLE I  
Sulfamide-Aminotriazine-Aldehyde Polymers<sup>a</sup>

No.	Reactants			Catalyst	Yield, g./2.0 g. (20.8 mmole) sulfamide	Form	Products		
	HCHO, mmole	Sulfamide, mmole	Melamine, mmole				M.p., °C.	Compression test <sup>b</sup>	Solubility
Group I: Sulfamide-Formaldehyde Polymers									
1	83	20.8	—	NaOH, NH <sub>3</sub>	1.7	White solid	234-235 (dec.)	No	°
2	42	10.4	—	KH <sub>2</sub> PO <sub>4</sub> -NaOH buffer, pH 7	1.2	White solid	235-242 (dec.)	No	°
Group II: Sulfamide-Melamine-Formaldehyde Polymers									
3	104	52 <sup>d</sup>	8.3	NaOH, NH <sub>3</sub>	0	°	—	—	—
4	104	52	8.3	NaOH, NH <sub>3</sub>	2.7	White solid	222-230 (dec.)	Yes	Insoluble <sup>f</sup>
5	104	—	8.3	NaOH, NH <sub>3</sub>	0	°	—	—	—
6	83	20.8	20.8	NaOH, NH <sub>3</sub>	6.4	White solid	261-265 (dec.)	Yes	Insoluble <sup>f</sup>
7	83	20.8 <sup>g</sup>	20.8	NaOH, NH <sub>3</sub>	7.1	White solid	246-260 (dec.)	Yes	Insoluble <sup>f</sup>
8	83	20.8	20.8	KH <sub>2</sub> PO <sub>4</sub> -NaOH buffer, pH 7	7.1	White solid	256-270 (dec.)	Yes	Insoluble <sup>f</sup>
9	104	8.3	52	NaOH, NH <sub>3</sub>	24	White solid	290 (dec.)	Yes	Insoluble <sup>f</sup>
10	83	20.8	20.8	HCl	5.5	White solid	275-280 (dec.)	Poor	Insoluble <sup>f</sup>
11	83	—	20.8	HCl	4.1 <sup>b</sup>	White solid	300 (dec.)	Poor	Insoluble <sup>f</sup>



- <sup>a</sup> All reactions were run for 1 hr. at reflux.
- <sup>b</sup> Ability to form a cohesive plaque on a Carver press at about 210°C. and 10,000 lb./in.<sup>2</sup> for 0.5–3 min.
- <sup>c</sup> Insoluble in water and common organic solvents except hot dimethylformamide and hot dimethyl sulfoxide.
- <sup>d</sup> Urea used instead of sulfamide.
- <sup>e</sup> Clear solution resulted, no solid obtained.
- <sup>f</sup> Insoluble in hot or cold water, ethanol, acetone, benzene, and dimethylformamide.
- <sup>g</sup> Sulfamide added after 1 hr. reflux of the other reactants (no solid produced), followed by another hour's reflux.
- <sup>h</sup> Based on 2.6 g. (20.8 mmole) of melamine.
- <sup>i</sup> Benzoguanamine used in place of melamine.
- <sup>j</sup> Insoluble in water and common organic solvents except hot dimethylformamide.
- <sup>k</sup> Soluble in cold dimethylformamide and in hot acetone, ethanol, and water.
- <sup>l</sup> Ammeline used instead of melamine.
- <sup>m</sup> Shown to be a mixture of ammeline and sulfamide-formaldehyde polymer.
- <sup>n</sup> Based on 2.6 g. (20.8 mmole) of ammeline.
- <sup>o</sup> Apparently *N,N'*-dimethylolammelmine (Calcd. for C<sub>5</sub>H<sub>9</sub>N<sub>4</sub>O<sub>3</sub>: C, 32.09%; H, 4.85%; N, 37.42%. Found: C, 32.01%; H, 4.87%; N, 37.40%).
- <sup>p</sup> Benzaldehyde used in place of formaldehyde.
- <sup>q</sup> Shown to be a mixture of melamine and benzoic acid.
- <sup>r</sup> 2-Furaldehyde used in place of formaldehyde.
- <sup>s</sup> Shown to be a mixture of melamine and 2-furfurylidenesulfamide.
- <sup>t</sup> 1,3-Di-*tert*-butylsulfamide.
- <sup>u</sup> Yield expressed in grams of product obtained from 2.1 g. (10 mmole) of 1,3-di-*tert*-butylsulfamide.
- <sup>v</sup> Shown to be a mixture of 1,3-di-*tert*-butylsulfamide and probably melamine-formaldehyde polymer.
- <sup>w</sup> Recovered 1,3-di-*tert*-butylsulfamide.
- <sup>x</sup> 1,3-Dimethylsulfamide.
- <sup>y</sup> Yield expressed in grams of product obtained from 2.0 g. (64 mmole) of 1,3-dimethylsulfamide.

## References

1. Wood, F. C., and A. E. Battye, *J. Soc. Chem. Ind.*, **52**, 346T (1933).
2. Paquin, A., *Angew. Chem.*, **A60**, 316 (1948).
3. Hecht, G., and H. Henecka, *Angew. Chem.*, **61**, 365 (1949).
4. D'Alelio, G. F., *Experimental Plastics and Synthetic Resins*, Wiley, New York, 1946, p. 43.
5. Florentine R. A., G. Barth-Wehrenalp, I. Mockrin, I. Popoff, and R. Riordan, *J. Polymer Sci.*, **A2**, 489 (1964).
6. Degering, E. F., and G. C. Gross, *Ind. Eng. Chem.*, **35**, 751 (1943).
7. Franchimont, A. P. N., *Rec. Trav. Chim.*, **3**, 418 (1884).
8. Traube, W., and E. Reubke, *Ber.*, **56**, 1660 (1923).

## Résumé

Le sulfamide et le formaldéhyde réagissent à un pH 10 pour donner un polymère solide blanc (A) qui se décompose à 234–235°C. Un produit semblable se produit à pH 7. Une modification de A était obtenu par inclusion de mélamine dans la matrice polymérique. Le polymère sulfamide-mélamine-formaldéhyde a un point de fusion de 261–265°C, il était insoluble dans les solvants organiques et formait un film adhérent par compression. Le polymère était obtenu lorsque le sulfamide, le formaldéhyde et la



mélatamine réagissent ensemble ou quand un dérivé méthylol-mélatamine était d'abord préparé et ensuite ponté avec la sulfamide. Le sulfamide semble être un agent de pontage plus rapide que l'urée pour un tel système. D'autres aminotriazines ont été employés à la place de la mélatamine et plusieurs 1,3-dialcoylsulfamidés furent utilisés à la place du sulfamide, mais on n'a pas atteint d'amélioration sensible de la stabilité thermique.

### Zusammenfassung

Sulfamid und Formaldehyde reagieren bei pH 10 unter Bildung eines polymeren, weissen Festkörpers (A), der sich bei 234–235°C zersetzt. Ein ähnlicher Stoff entsteht bei pH 7. Eine Modifizierung von A wurde durch Einbau von Melamin in die Polymermatrix erreicht. Das Sulfamid-Melamin-Formaldehyd-Polymere besass einen Schmelzpunkt von 261–265°C, war unlöslich in organischen Lösungsmitteln und bildete bei der Kompression einen zusammenhängenden Film. Das Polymere entstand bei der simultanen Reaktion von Sulfamid, Formaldehyd und Melamin oder bei der Vernetzung eines vorgebildeten Methylolmelamins mit Sulfamid. Sulfamid scheint für dieses System ein rascher wirkender Vernetzer zu sein als Harnstoff. An Stelle von Melamin wurden andere Aminotriazine und an Stelle von Sulfamid einige 1,3-Dialkylsulfamide verwendet, es wurde jedoch keine nennenswerte Verbesserung der thermischen Stabilität der Polymeren erreicht.

Received November 13, 1962

## Polymers from Sulfamide. II. Evaluation and Structure\*

R. A. FLORENTINE,† G. BARTH-WEHRENALP, I. MOCKRIN,‡  
I. POPOFF, and R. RIORDAN, *Pennsalt Chemicals Corporation, Research and Development Department, Wyndmoor, Pennsylvania*

### Synopsis

Acid- and base-catalyzed polymers involving sulfamide, melamine, and formaldehyde have been prepared and investigated. The products are insoluble and their thermal stability does not exceed 225°C. in N<sub>2</sub>.

The preparation of polymers by condensation of sulfamide, melamine, and formaldehyde was described in Part I.<sup>1</sup> Samples of the more promising materials were synthesized for structure and evaluation purposes. The results of this investigation, as well as the results of additional studies on the related sulfamide-formaldehyde 1:4 polymers, are discussed. (Here and throughout this paper 1:4, etc., indicates the molar ratio of reactants.) Data on solubility, thermal stability, infrared and x-ray structure analysis of these materials are included.

### EXPERIMENTAL

Some of the more promising compositions described in Part I<sup>1</sup> were selected for evaluation, and their preparations were also examined somewhat more closely than previously.

#### Preparations

**Acid-Catalyzed Sulfamide-Melamine-Formaldehyde 1:1:4 (IA).** (Preparation 10, Table I, Part I.) A mixture of 6.0 g. (62.4 mmoles) of sulfamide, 7.8 g. (62.4 mmoles) of melamine, 20.4 g. of 37% aqueous formaldehyde solution [7.54 g. (249 mmoles) CH<sub>2</sub>O], and 4.5 ml. of 0.558*N* hydrochloric acid (2.51 mmoles) was refluxed for 1 hr. at about 85° C. The pH of the resulting suspension was 2. Two phases remained throughout the course of the reaction. The product was a porous, tough, white solid, which was powdered and washed with 133 ml. of water, filtered,

\* Paper presented at the 140th meeting of the American Chemical Society, Chicago, Ill., September 3-8, 1961.

† Present address: Robert Florentine Associates, Philadelphia Pennsylvania.

‡ Present address: Kawecki Chemical Company, Boyertown, Pennsylvania.

and then dried for 18 hr. at 70°C. The filtrate had a pH of 6. The crude product obtained weighed 17.2 g. The solid was refluxed for 2–3 min. with 100 ml. of water, filtered hot, and dried to constant weight, 15.3 g. It had a melting point of 275–280°C. (decomposes with red foaming).

ANAL. Calcd. for structure I,  $C_7H_{13}N_8SO_3$ : C, 29.06%; H, 4.53%; N, 38.74%; S, 11.08%; O, 16.59%. Found: C, 28.60%; H, 4.26%; N, 39.59%; S, 12.24%; O, 15.31% (by difference).

**Base-Catalyzed Sulfamide–Melamine–Formaldehyde 1:1:4 (IB).** (Preparation 6, Table I, Part I.) A mixture of 12.0 g. (124.8 mmoles) of sulfamide, 15.6 g. (124.8 mmoles) of melamine, 40.8 g. of 37% aqueous formaldehyde solution [15.08 g. (498 mmoles)  $CH_2O$ ], 9.6 ml. of 0.523*N* aqueous sodium hydroxide, (5.02 mmoles NaOH) and 1.2 g. of 29% aqueous ammonia (21 mmoles  $NH_3$ ) was refluxed for 1 hr. at about 87–92°C. The two-phase reaction mixture became homogeneous on reaching 87°C. After 7 min. at this temperature, however, the solution became turbid, and after an additional 10 min. refluxing, a solid was formed. The product was filtered, washed with water, ground, and dried to constant weight (30.8 g.) at 70°C. It had a melting point of 261–265°C. (decomposes with red foaming).

ANAL. Calcd. for structure I,  $C_7H_{13}N_8SO_3$ : C, 29.06%; H, 4.53%; N, 38.74%; S, 11.08%; O, 16.59%. Found: C, 28.55%; H, 4.41%; N, 40.21%; S, 11.06%; O, 16.93% (analyzed); water, 0.51%.

**Acid-Catalyzed Sulfamide–Formaldehyde (1:4A).** (Not previously prepared.) A solution of 2.0 g. (20.8 mmoles) of sulfamide in 6.82 g. of 37% aqueous formaldehyde solution [2.52 g. (83 mmoles) of  $CH_2O$ ] and 1.5 ml. of 0.558*N* hydrochloric acid (0.82 mmoles HCl) was refluxed for 1 hr. at 85–91°C. After the mixture was refluxed for 17 min. a precipitate formed. The reaction mixture was filtered at room temperature, the filtrate had a pH of 2. The solid was washed with 30 ml. of water and dried to constant weight (0.12 g.) at 70°C. The product had a melting point of 225–256°C. (decomposes with red foaming).

ANAL. Found: C, 26.63%; H, 4.37%; N, 25.37%; S, 23.26%. Empirical formula:  $C_{3.0}H_{6.0}N_{2.5}S_{1.0}O_{1.8}$ .

**Base-Catalyzed Sulfamide–Formaldehyde (1:4B).** (Preparation 1, Table I, Part I.) A solution of 2.0 g. (20.8 mmoles) of sulfamide in 6.82 g. of 37% aqueous formaldehyde solution, [2.52 g. (83 mmoles) of  $CH_2O$ ], 1.69 ml. of 0.494*N* aqueous sodium hydroxide (0.83 mmoles NaOH) and 0.18 g. of 29% aqueous ammonia [0.05 g. (3 mmoles)  $NH_3$ ] almost immediately formed a precipitate. The reaction mixture was refluxed for 1 hr. at 82–93°C. and filtered at room temperature. The filtrate had a pH of 2 (the pH of the original solution was 10). The solid product was

washed with 9 ml. of water and dried to constant weight at 70°C. to obtain 1.57 g. of a solid with a melting point of 234–235°C. (decomposes with red foaming).

ANAL. Found: C, 21.46%; H, 3.82%; N, 22.20%; S, 24.90%. Empirical formula:  $C_{2.3}H_{4.9}N_{2.0}S_{1.0}O_{2.2}$ .

### Evaluation Techniques

**Thermogravimetric Analysis (TGA).** All thermogravimetric data were obtained with the use of a Chevenard thermobalance, whose description and operation were previously reported.<sup>2</sup> A dry nitrogen atmosphere was used throughout. The heating rate used for all runs was 2.5°C./min.

**Constant Temperature Pyrolysis.** To study the long-term thermal stability and to investigate the products of pyrolysis, constant temperature runs were made. Samples were heated (2.5°C./min.) in a nitrogen atmosphere to a given temperature level. Heating was then continued until weight loss was less than 0.1%/hr. The residues were then removed and placed in a nitrogen-filled desiccator at room temperature.

**Solubility.** Solubility measurements with IB were made at 30 and 80°C. in closed tubes; the solutions were removed and weighed portions were evaporated with infrared heat to determine the weight of solute.

**Infrared Analysis.** Infrared spectra of the solids, which were run as Nujol mulls, were obtained on a Perkin-Elmer infrared spectrometer, Model 21.

**Infrared-Monitored Thermal Decomposition.** The thermal decomposition of IA was studied with a technique that permitted continuous monitoring of the pyrolyzing sample by infrared. A Nujol mull of the material was spread on a NaCl plate inserted in a small disk heater. This heater-sample assembly was placed in an infrared gas cell with heater leads attached. A thermocouple inserted in the cell touched a face of one of the NaCl plates. The entire cell assembly was evacuated and placed in the spectrometer. The sample was heated to appropriate temperatures. Spectra were obtained before, during, and after each heating cycle. Only qualitative information was obtained concerning the specific group instabilities as a function of temperature. These changes were all observed on a single polymer sample.

**X-Ray Diffraction.** Powder diagrams were made on capillary-filled samples on a General Electric x-ray spectrometer, Model XRD-1.

## RESULTS

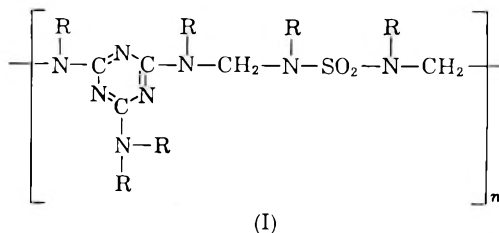
### Composition of Polymers

**Sulfamide–Melamine–Formaldehyde 1:1:4.** In Table I the elemental analyses of products IA and IB are compared with the calculated composition for Structure I.

TABLE I  
Sulfamide-Melamine-Formaldehyde 1:1:4

Element	Weight-%		
	IA	IB	Structure I
C	28.60	28.55	29.06
H	4.26	4.41	4.53
N	39.59	40.21	38.74
S	12.24	11.06	11.08
O	15.31 (by difference)	16.93 (analyzed)	16.59
Total	100.00	101.16	100.00
H <sub>2</sub> O	Not det.	0.51	0.00

Structure I, one of a number of possible structures, has the empirical formula  $C_7H_{13}N_8SO_3$ :



In structure I, one R can be  $-\text{CH}_2-$ , one  $-\text{CH}_2\text{OH}$ , and the rest, H. No specific position can be assigned to the R groups.

**Sulfamide-Formaldehyde 1:4A and 1:4B.** Table II lists the analyses of the acid- and base-catalyzed sulfamide-formaldehyde 1:4 polymers prepared for this evaluation.

TABLE II  
Sulfamide-Formaldehyde 1:4

Element	Weight-%	
	1:4 A	1:4 B
C	26.63	21.46
H	4.37	3.82
N	25.37	22.20
S	23.26	24.90
O (by difference)	20.37	27.62
Total	100.00	100.00

The analyses in Table II do not correspond unequivocally to any single sulfamide-formaldehyde polymer composition. The stability of these compositions is pertinent to the discussion of the structures of IA and IB. Of significance here is the variation in the oxygen analysis (by difference).

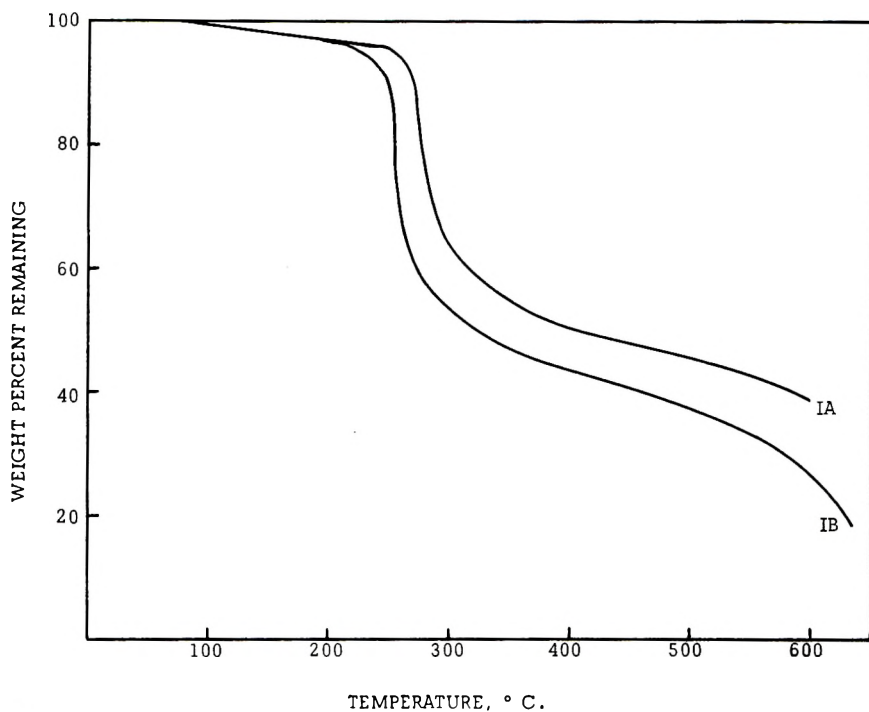


Fig. 1. TGA of sulfamide-melamine-formaldehyde, 1:1:4 (2.5° C./min., dry nitrogen atmosphere): (IA) acid-catalyzed; (IB) base-catalyzed.

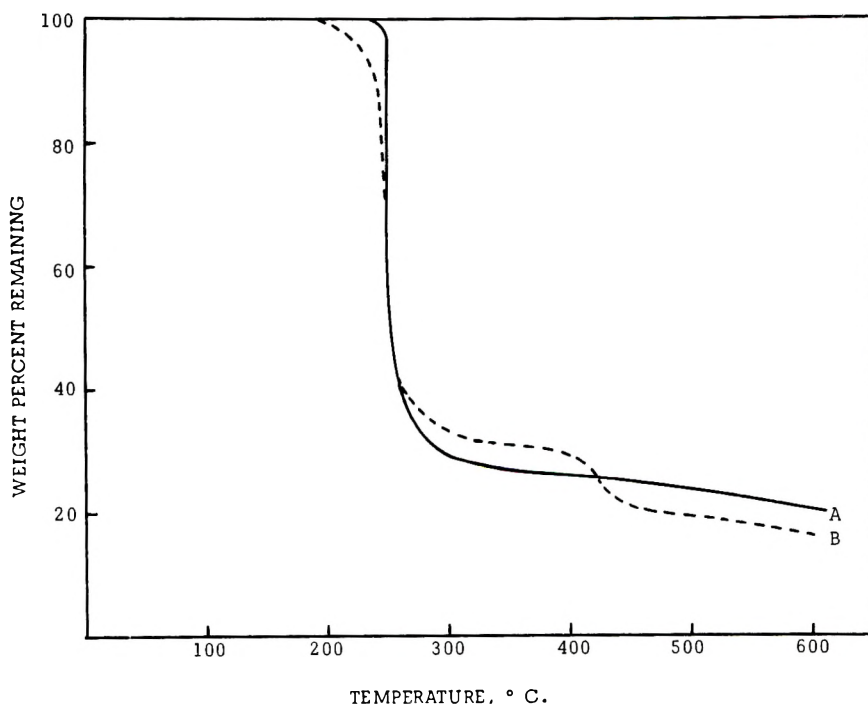


Fig. 2. TGA of sulfamide-formaldehyde, 1:4 (2.5°C./min., dry nitrogen atmosphere): (A) acid-catalyzed; (B) base-catalyzed.

For 1:4A, the S content exceeds the O content; in 1:4B, S is less than O by almost exactly the same amount. For a polymer involving  $-\text{SO}_2-$ , the weight percentage of S should exactly equal that of oxygen. The excess of oxygen is considered as indicative of the presence of  $-\text{CH}_2\text{OH}$  groups in the base-catalyzed system, involving sulfamide and formaldehyde.

### Thermogravimetric Analysis

The thermogravimetric (TGA) curves for IA and IB appear in Figure 1. IA shows greater stability in the range 300–600°C. in nitrogen.

The TGA curves for 1:4A and 1:4B appear in Figure 2, both compositions showing comparable thermal behavior in nitrogen.

### Constant-Temperature Pyrolysis

**Sulfamide-Melamine-Formaldehyde (IA and IB).** Constant temperature pyrolyses were made for IA and IB at 225°C. The curves appear in Figure 3. The acid-catalyzed material (IA) shows considerably greater stability at 225°C., losing only 15% of its original weight compared with a corresponding 32% weight loss of IB in nitrogen.

**Sulfamide-Formaldehyde (1:4A and 1:4B).** The TGA curves for

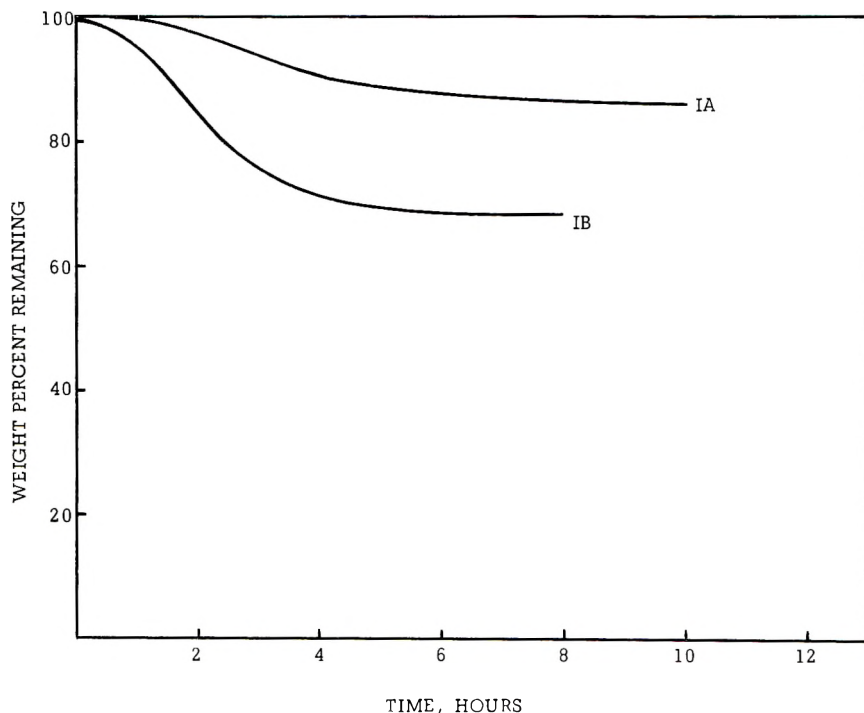


Fig. 3. Stability of sulfamide-melamine-formaldehyde, 1:1:4. (225°C., nitrogen atmosphere): (IA) acid-catalyzed; (IB) base-catalyzed. Weight per cent remaining is corrected for weight loss below 225° C.

1:4A and 1:4B at 225°C. in nitrogen, given in Figure 4, indicate 1:4B to be somewhat more stable than 1:4A.

**Mixtures of 1:4A and 1:4B with Melamine.** A mixture (A + M) consisting of 50% of 1:4A and 50% of melamine (M) was heated at 225°C. in nitrogen until the weight of residue remained approximately constant with time. If melamine is considered as an inert diluent, a corrected curve can be plotted. These TGA curves for 1:4A, for A + M, and for A + M, corrected, are given in Figure 5, along with the corresponding

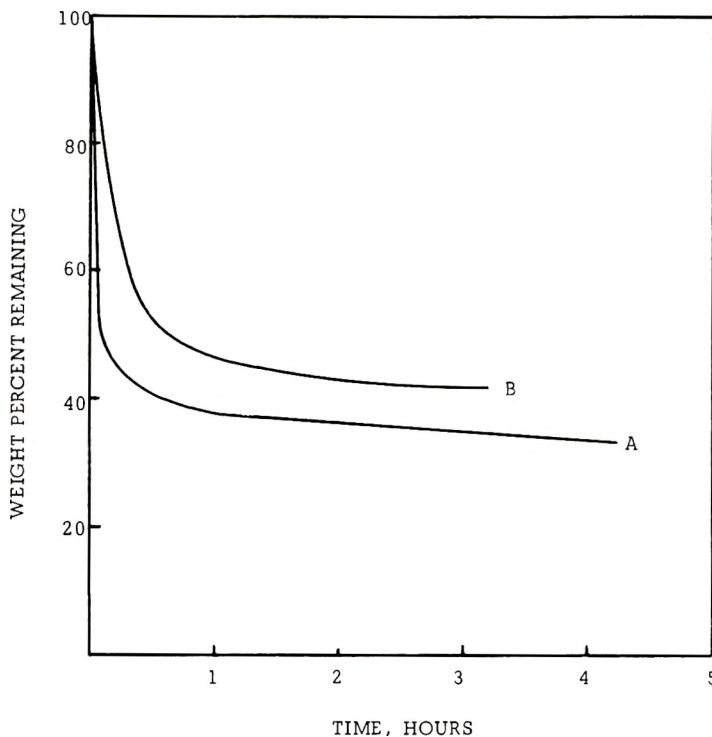


Fig. 4. Stability of sulfamide-formaldehyde, 1:4 (225°C., nitrogen atmosphere): (A) acid-catalyzed; (B) base-catalyzed. Weight per cent remaining is corrected for weight loss below 225°C.

curve for IA. The corrected curve (A, M OUT) indicates a small increase in stability of 1:4A + M over 1:4A. A slight reaction between 1:4A and melamine may have occurred.

Figure 6 consists of similar curves obtained by using 1:4B instead of 1:4A. Here, a significant increase in stability apparently results from mixing 1:4B with melamine, indicating reaction between the two.

The inference can be drawn that the role of melamine in the 1:1:4 composition is not well established on the basis of the TGA curves and that in IB at least some of the melamine has remained uncombined and has left sites for further combination.



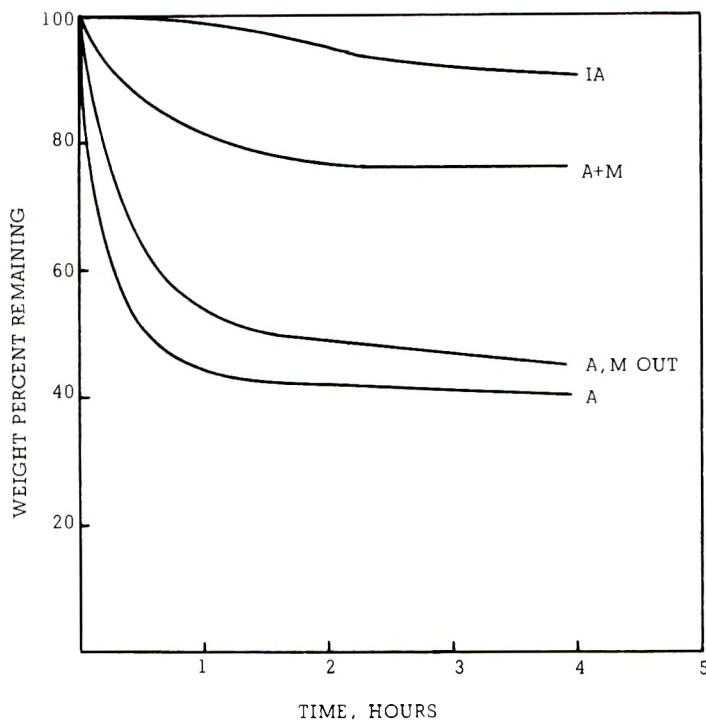


Fig. 5. Stability of acid-catalyzed sulfur-nitrogen polymers (225° C., nitrogen atmosphere): (IA) sulfamide-melamine-formaldehyde, 1:1:4; (A + M) 50-50 mixture of melamine with sulfamide-formaldehyde, 1:4; (A, M OUT) A + M corrected for presence of melamine as a diluent; (A) sulfamide-formaldehyde, 1:4. Weight per cent remaining is corrected for weight loss below 225°C.

Some selected data on the stability runs at 225°C. are given in Table III.

TABLE III  
Stability of Compositions at 225°C. in  $N_2$

Composition	Time at 225°C., hr.	Wt.-% remaining	Figure No.
IA	14	85	3
IB	8	68	3
1:4A	4	34	4
1:4B	3	41	4
1:4A-Melamine (50/50)	4	76	5
1:4B-Melamine (50/50)	4	81	6

### Solubility

The solubility of IB was determined at 30 and 80°C., in xylene, toluene, *n*-heptane, pyridine, aniline, dichloromethane, trichloroethylene, *o*-dichlorobenzene, Isotron 113, nitrobenzene, 2-nitropropane, dimethyl sul-

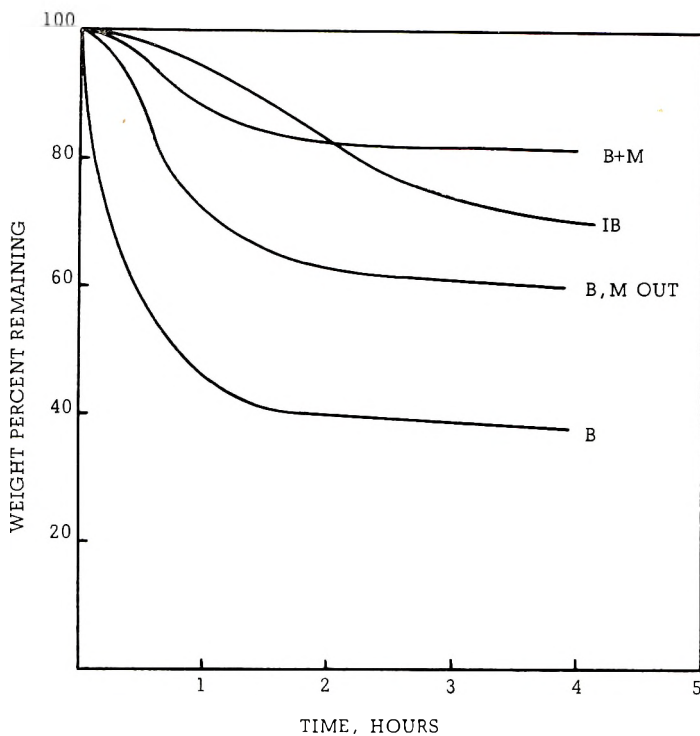


Fig. 6. Stability of base-catalyzed sulfur-nitrogen polymers (225°C., nitrogen atmosphere): (IB) sulfamide-melamine-formaldehyde, 1:1:4; (B + M) 50-50 mixture of melamine with sulfamide-formaldehyde, 1:4; (B, M OUT) B + M corrected for presence of melamine as a diluent; (B) sulfamide-formaldehyde, 1:4. Weight per cent remaining is corrected for weight loss below 225°C.

foxide, methyl ethyl ketone, dimethylformamide, cyclohexanone, *n*-butyl ether, methyl cellosolve, *n*-butyl acetate, and *n*-butyl alcohol. In all cases the solubility was less than 0.05%. This insolubility is typical of a highly crosslinked polymer.

### Infrared Spectra

Infrared spectra were obtained for melamine, melamine-formaldehyde, sulfamide-melamine-formaldehyde (1:1:4), and sulfamide-formaldehyde (1:4).

The characteristic absorptions<sup>3,4</sup> of the functional groups present are given in Table IV.

TABLE IV

Band	Wavelength, $\mu$
N-H and/or OH	3.0-3.1
SO <sub>2</sub> -N	7.5, 8.7
Triazine ring	12.3

### Infrared-Monitored Thermal Decomposition Study

IA was studied with the technique described under Experimental. Infrared curves run at 30, 225, 250, and 300°C. permit the following generalizations to be made for the thermal decomposition of base-catalyzed sulfamide-melamine-formaldehyde, 1:1:4.

The N—H group absorbs at 3  $\mu$ ; the absorption appears to decrease in intensity at 200°C., some indication that free —NH remains up to 225°C.

SO<sub>2</sub>—N absorbs at 7.5 and 8.7  $\mu$ ; the group is stable up to 225°C., when its bands disappear.

The triazine ring absorbs at 12.3  $\mu$ ; this absorption persists to 300°C., at which temperature it largely disappears.

At 9.7  $\mu$  an unidentified band in the original spectrum increases in intensity up to 300°C. when it disappears; this band is somewhat removed from the region usually associated with C—O—C absorption.

At 300°C. a band appears at 9.0  $\mu$ , which is probably due to C—O—C.

A band originally present at 12.7  $\mu$  persists until 300°C., when it disappears. This band has appeared strongly in other samples in this study, but has not been assigned. Possibly, it is due to an impurity stable to 300°C.

### X-Ray Diffraction

Exposures of IA and IB (for 4 hr.) show identical weak patterns; *d* spacings and relative intensities are listed in Table V.

TABLE V  
Sulfamide-Melamine-Formaldehyde (1:1:4 IA and IB) X-Ray *d* Spacings  
(Cu Radiation)

<i>d</i> , A.	Intensity
2.05	100
2.01	75
1.26	50
1.259	75
1.189	2
1.164	25
1.074	2
1.029	2

The *d* spacings for IA and IB do not correspond to any spacings for the parent materials.

### DISCUSSION

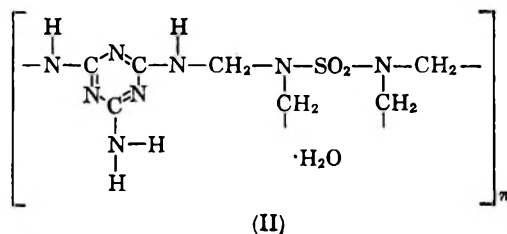
Sulfamide, melamine, and formaldehyde may condense to form polymers of the generalized structure I, where R in a given composition may include —CH<sub>3</sub> and —CH<sub>2</sub>OH (as terminating groups) or —CH<sub>2</sub>— where branching and crosslinking occur.

### The Presence of Oxygen

In structure I, two oxygen atoms accompany each sulfur, thus, equal weights of sulfur and oxygen are anticipated in the polymer structure where sulfamide is involved. This weight of oxygen may not account for the total oxygen found by analysis. In the discussion following, we denote oxygen combined with S in  $\text{SO}_2$  as  $\text{O}_\text{S}$  and oxygen as terminal  $-\text{OH}$  as  $\text{O}_\text{H}$ .

In sulfamide-melamine-formaldehyde 1:1:4 (I), for example, the calculated oxygen content can be broken down as follows: sulfur, 11.1%; Total oxygen, 16.6%;  $\text{O}_\text{S}$ , 11.1%;  $\text{O}_\text{H}$ , 5.5%.

**Oxygen in Water of Hydration.** It was possible that part of the oxygen was present as water of hydration, as, for example, in structure II:



Analysis of the base-catalyzed sulfamide-melamine-formaldehyde 1:1:4 revealed only 0.51% water, about one-tenth of the value required for this structure.

**Oxygen as Terminal  $-\text{OH}$ .** To establish the presence of terminal  $-\text{OH}$  in structure I, a standard active hydrogen analysis was made, with negative results. Since the technique applied would not only detect quantitatively the  $-\text{OH}$ , but also incompletely substituted  $-\text{NH}$  groups, which both the preparation and the analysis suggest, this negative result may be the consequence of the extreme insolubility of the polymer in the reagents used in the analysis.

Of these two hypotheses, that of terminal  $-\text{OH}$  to account for the excess oxygen is the more reasonable. In condensations of amines with formaldehyde, a first intermediate is  $\text{RNHCH}_2\text{OH}$ .<sup>5a</sup> Ureas and formaldehyde form stable methylol ureas as end-products in basic and neutral media.<sup>5b,6</sup>

In the sulfamide-formaldehyde (1:4) polymers, the acid-catalyzed material shows no evidence of  $-\text{OH}$  or  $-\text{NH}$  absorption. The base-catalyzed material does show absorptions ascribable to the presence of terminal hydroxyl or unsubstituted  $\text{NH}$  groups.

Additional significant evidence for the existence of terminal  $-\text{OH}$  in the base-catalyzed compositions is the thermal behavior of the acid- and base-catalyzed condensation products of sulfamide and formaldehyde when these polymers are separately mixed with melamine.

**Oxygen in Sulfamide-Formaldehyde 1:4 Polymer.** The analyses of acid and base-catalyzed sulfamide-formaldehyde 1:4 are compared in Table VI.





### **Résumé**

Des polymères, préparés par catalyse acide et basique, contenant du sulfamide, de la mélamine et du formaldéhyde, ont été préparés et étudiés. Les produits sont insolubles et leur stabilité thermique ne dépasse pas 225°C sous azote.

### **Zusammenfassung**

Säure- und basenkatalysierte Polymere auf Grundlage von Sulfamid, Melamin und Formaldehyd, wurden dargestellt und untersucht. Die Produkte sind unlöslich und ihre thermische Stabilität geht über 225°C unter Stickstoff nicht hinaus.

Received November 13, 1962

## Preparation and Reactions of *p*-Cyanostyrene-Styrene Copolymers\*

RICHARD BECKERBAUER and HENRY E. BAUMGARTEN,  
*Avery Laboratory, University of Nebraska, Lincoln, Nebraska*

### Synopsis

Copolymers of *p*-cyanostyrene and styrene were prepared by heating *p*-iodostyrene-styrene copolymers with cuprous cyanide in *N*-methylpyrrolidinone. The *p*-cyanostyrene copolymers could not be hydrolyzed to the benzoic acid derivative but were converted to the methyl *p*-vinylbenzoate-styrene copolymer by reaction with methanol and hydrogen chloride. This methyl ester copolymer was partially hydrolyzed to the free acid. A *p*-cyanostyrene(11%)-styrene copolymer was treated with *n*-butyl and methyl Grignard reagents to yield the corresponding *n*-butyl- and methyl-*p*-styrylketone copolymers. In the reaction with *n*-butylmagnesium chloride, the intermediate *n*-butyl-*p*-styrylketimine copolymer was isolated.

### INTRODUCTION

The procedures for the bromination and chlorination of polystyrene<sup>1</sup> have been known for many years, but only recently has Braun<sup>2</sup> been able to iodinate polystyrene. The availability of the iodinated polymer would appear to make possible a number of polymer reactions that proceed sluggishly or not at all with chloro or bromo polystyrenes. For example, Newman and Boden<sup>3</sup> have recently reported the preparation of aromatic nitriles from aromatic halides by the use of cuprous cyanide in *N*-methylpyrrolidinone solutions. Inasmuch as polystyrene polymers are usually reasonably soluble in *N*-methylpyrrolidone, it appeared feasible to apply the Newman technique to iodinated polystyrene if not to brominated or chlorinated polystyrenes. Therefore, as a part of our study of the modification of polymers and copolymers of styrene derivatives by chemical reactions, we investigated the preparation of *p*-cyanostyrene polymers and copolymers from *p*-halostyrene polymers. In addition, a few characteristic reactions of *p*-cyanostyrene copolymers were studied.

### EXPERIMENTAL RESULTS

#### Preparation of Iodinated Polystyrenes

Copolymers of styrene and *p*-iodostyrene containing ca. 65% (I), 43.5% (II) ( $\eta_{inh} = 0.33$ , chloroform), and 11% (III) iodostyrene units were pre-

\* This work was supported in part by grants G-11339 and G-21405 of the National Science Foundation.



pared by partial iodination of polystyrene ( $\eta_{inh} = 0.45$ , chloroform) with iodine and iodic acid in nitrobenzene by using the procedure of Braun.<sup>2</sup>

ANAL. (I) Composition estimated from yield data and infrared analysis.

(II) Calcd. for  $C_8H_7I$  (43.5%)– $C_8H_8$  (56.5%): C, 60.43%; H, 4.79%; I, 34.77%. Found: C, 60.45%; H, 4.79%; I, 34.77%.

(III) Calcd. for  $C_8H_7I$  (11%)– $C_8H_8$  (89%): C, 81.65%; H, 6.76%; I, 11.58%. Found: C, 81.11%; H, 6.77%; I, 11.93%.

### Preparation of *p*-Cyanostyrene–Styrene Copolymers

A solution of 1.15 g. (0.005 mole) of the 65% *p*-iodostyrene copolymer (I) and 0.74 g. (0.0075 mole) of freshly prepared cuprous cyanide<sup>4</sup> in 30 ml. of *N*-methylpyrrolidinone was refluxed for 4 hr., cooled, and added to a solution of 6 g. of  $FeCl_3 \cdot 6H_2O$  in 100 ml. of 6% aqueous hydrochloric acid. The resulting mixture was heated on a steam bath for 30 min., cooled, and filtered. The solid product obtained was dark grey and rubbery. It was soluble in ketone solvents but insoluble in chloroform, benzene, and tetrahydrofuran. The product gave a negative Beilstein test for halogen. A brittle fiber could be pulled from a melt of this polymer.

The reaction was carried out as above with 5 g. (0.013 mole) of the 43.5% iodinated polymer (II) and 3 g. (0.03 mole) of cuprous cyanide in 100 ml. of *N*-methylpyrrolidinone to yield 3.1 g. of a grey polymer (IV) ( $\eta_{inh} = 0.50$ , chloroform). This product was soluble not only in ketone solvents but also in chloroform, benzene, and tetrahydrofuran.

ANAL. Calcd. for  $C_9H_7N$  (43.5%)– $C_8H_8$  (56.5%): C, 87.97%; H, 6.62%; N, 5.36%; I, 0.00%. Found: C, 87.74%; H, 6.13%; N, 5.75%; I, 0.00%.

The reaction was carried out as above with 9.5 g. of the 11% iodinated polystyrene (III) and 1.5 g. of cuprous cyanide in 180 ml. of *N*-methylpyrrolidinone to yield 7.8 g. of a light grey polymer (V).

ANAL. Calcd. for  $C_8H_7N$  (11%)– $C_8H_8$  (89%): C, 91.10%; H, 7.43%; N, 1.46%; I, 0.00%. Found: C, 90.27%; H, 7.39%; N, 1.98%; I, 0.00%.

### Cuprous Cyanide Reaction with Brominated Polystyrenes

Poly(*p*-bromostyrene) and *p*-bromostyrene (30%)–styrene copolymer were prepared by bromination of polystyrene in chloroform with an iron catalyst.<sup>1</sup> The reaction products of these polymers with cuprous cyanide as above had similar physical properties to those from the iodinated derivatives, but they contained unaltered *p*-bromostyrene units as indicated by infrared analysis and chemical tests. Reaction times exceeding 4 hr. were accompanied by a large amount of gel formation.

### Attempted Hydrolysis of the Cyanostyrene Copolymers

No hydrolysis of the cyano groups of IV and V could be detected when the polymers were treated with (a) potassium hydroxide in aqueous dimethylacetamide at 25° for 14 hr., (b) potassium hydroxide in *N*-methylpyrrolidinone at 60° for 2 hr., (c) concentrated hydrochloric acid in tetra-

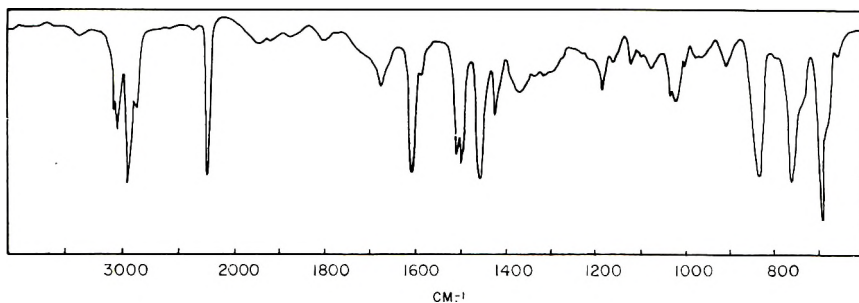


Fig. 1. Infrared spectrum of polymer IV (43.5% *p*-cyanostyrene units).

hydrofuran at reflux for 4 hr. or (d) cold, concentrated sulfuric acid for 2 weeks. Treatment with concentrated sulfuric acid at 90°C. for 4 hr. gave conversion to the acid as indicated by a strong band in the infrared spectrum at 1685  $\text{cm}^{-1}$  but also gave sulfonation of the styrene rings and accompanying solubilization of the polymer.

#### Preparation of a Methyl *p*-Vinylbenzoate Copolymer

To a solution of 1 g. of the 43.5% cyano copolymer (IV) in 40 ml. of tetrahydrofuran was added anhydrous methanol (30 ml. required) until a precipitate formed. Tetrahydrofuran (5 ml.) was added to solubilize the polymer and then dry hydrogen chloride was passed into the solution for 30 min. with stirring. The solution was refluxed for 2 hr., cooled, and added to 200 ml. of methanol. The crude polymer was collected, reprecipitated from chloroform into methanol, collected, and dried to yield 1 g. of a light grey polymer (VI), ( $\eta_{\text{inh}} = 0.51$ , chloroform).

ANAL. Calcd. for  $\text{C}_{10}\text{H}_{10}\text{O}_2$  (40%)– $\text{C}_9\text{H}_7\text{N}$  (3.5%)– $\text{C}_8\text{H}_8$  (56.5%): C, 81.89%; H, 6.92%; O, 9.86%. Found: C, 81.67%; H, 6.68%; O, 9.47%.

#### Hydrolysis of the Methyl *p*-Vinylbenzoate Copolymer

A solution of 0.1 g. of the ester polymer (VI) in 10 ml. of tetrahydrofuran and 10 ml. of 20% potassium hydroxide solution was refluxed for 21 hr. The two-phase reaction mixture was poured into 200 ml. of water, and this

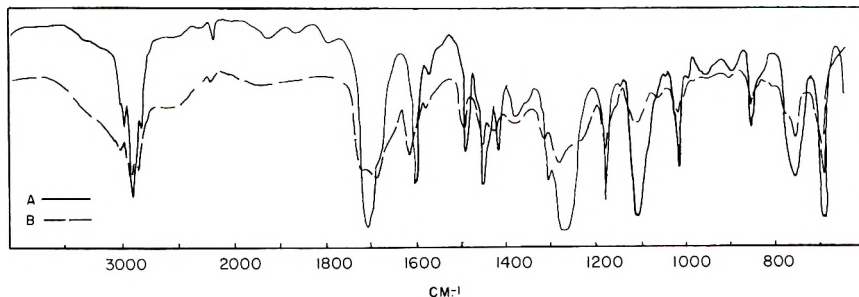


Fig. 2. Infrared spectra of (A) polymer VI (40% methyl *p*-vinylbenzoate units, 3.4% *p*-cyanostyrene units) and (B) polymer VII (*p*-vinylbenzoic acid polymer from VI).

solution was made just acidic with dilute hydrochloric acid. The white polymer which formed was removed by filtration, washed with water, and dried to 0.13 g. of solid. This product was insoluble in all common organic solvents tested except pyridine. The solid was reprecipitated from pyridine into acidic methanol, but the product (VII) was a dark, rubbery polymer. Only a poorly resolved infrared spectrum could be obtained and this suggested that complete hydrolysis had not occurred.

### Preparation of a *n*-Butyl-*p*-styrylketimine Copolymer

To a solution of 5 ml. of *n*-butylmagnesium chloride (Arapahoe, 3*M* in ether) and 5 ml. of dry tetrahydrofuran was added a solution of 0.5 g. (0.0003 mole) of the 11% cyanostyrene copolymer (V) in 20 ml. of tetrahydrofuran. The solution was stirred for 20 min. and then refluxed for 1 hr. The solution was cooled in an ice bath and then decomposed with a solu-

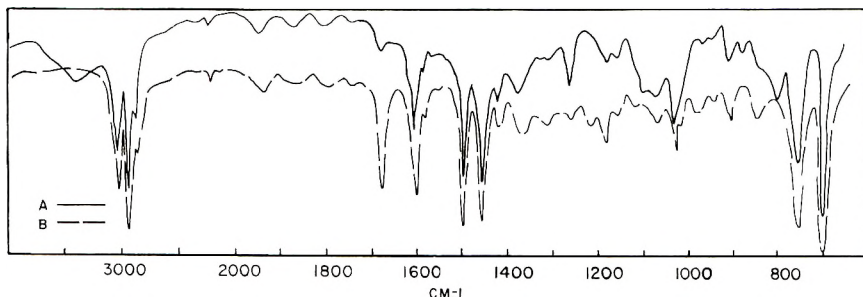


Fig. 3. Infrared spectra of (A) polymer VIII (11% *n*-butyl *p*-styryl ketimine units) and (B) polymer IX (11% *n*-butyl *p*-styryl ketone units).

tion of 3 ml. of anhydrous methanol in 10 ml. of tetrahydrofuran. The mixture was stirred for 12 hr., chilled, and filtered to remove the white solid. The filtrate was poured into anhydrous methanol and the resulting grey solid was removed by filtration. It was dried to 0.5 g. of a nearly white polymer (VIII).

ANAL. Calcd. for  $C_{13}H_{17}N(11\%)-C_8H_8(89\%)$ : C, 90.65; H, 7.97%; N, 1.32%. Found: C, 87.59%; H, 7.93%; N, 1.30%; adjusted for 2.24% ash.

Attempted further purification of this product led to partial hydrolysis to the ketone as indicated by the infrared spectrum.

### Hydrolysis of the Ketimine Copolymer

A solution of 0.1 g. of the ketimine copolymer VIII and 20 drops of concentrated hydrochloric acid in 15 ml. of tetrahydrofuran was stirred for 1 hr. The solution was poured into 80 ml. of methanol, filtered, washed with methanol, and dried to give 0.1 g. of ketone copolymer (IX).

ANAL. Calcd. for  $C_{13}H_{16}O(11\%)-C_8H_8(89\%)$ : C, 90.55%; H, 7.96%. Found: C, 89.93%; H, 7.60%.